Mining Optimization Laboratory

Report Two – 2009/2010

Directed by Hooman Askari-Nasab

School of Mining and Petroleum Engineering
Department of Civil & Environmental Engineering,
University of Alberta, Edmonton, Alberta, CANADA

Hooman Askari-Nasab, Ph.D., P.Eng.
Director of Mining Optimization Laboratory
Assistant Professor of Mining Engineering
3-044 Markin/CNRL NREF Building
Department of Civil & Environmental Engineering
University of Alberta, Edmonton, AB,
Canada T6G 2W2
Phone: (780) 492 4053
Fax: (780) 492-0249
Email: hooman@ualberta.ca
Webpage: www.ualberta.ca/~hooman
MOL Hompage: www.ualberta.ca/mol

Executive Summary

As promised, research and training has been conducted and documented in two main categories, mine planning and design and simulation optimization of mining systems. This report is a deliverable that would rationalize sponsorship of the *MOL* research. I would like to thank MOL sponsors for their support: (1) Newmont Mining Corporation, (2) Maptek Pty Ltd, (3) Iron Ore of Canada, (4) Suncor Energy Inc, and (5) Shell Canada Limited. I am sure the tangible research results generated this year will create more industrial awareness and excitement to support the MOL for the long haul.

Three PhD students joined our team in September 2009 (Hesam, Mahdi, and Mohammad) and a new PhD student (Elmira) joined MOL in September 2010. I firmly believe that with the increase in the number of high quality researchers, you will see an increase in productivity and quality of contributions in the near future. Our goal is to align the research directions at the MOL with our industry sponsors' interests.

This year, we have prepared a hardcopy report, a CD-ROM containing all the papers in PDF format, PowerPoint presentations, and software source code. The prototype software code is documented and is available through HTML links in the appendix section of the papers. We have launched the MOL webpage for members and non-members (www.ualberta.ca/mol). All member companies would have access to the members' section. All papers from all reports, presentations, and source code are available on line. Limited information is available to non-members, hopefully just enough for them to seriously consider membership. Let's review the contributions in the MOL Report Two (2009/2010) by considering some of the main contributors.

Hooman has continued working on large-scale long-term open pit production scheduling using mixed integer linear programming (MILP) techniques. We are working towards development of an open pit production scheduler based on MILP which will seamlessly connect the long-term plans to the short-term planning horizons. The initial results towards this prototype software are very promising. In paper 101 we verify and validate the MILP production scheduler by a comparative case study against Whittle strategic mine planning software. The difference between the cumulative discounted cash flow of the MILP schedule and the Whittle Milawa Balanced schedule is $50.4 million dollars. The considerable difference between the two methods, demonstrates the importance of production scheduling optimization and the necessity for scheduling optimization to turn into a common practice in mining industry.

One of the main obstacles in using MILP models in practice for open pit production scheduling is the inability to solve large-scale real-size mining problems at the block level. In practice, the current commercial software use an aggregated block model as the input into their optimizers. The aggregation is usually done manually by the mine planner by creating polygons in the general mine planning software. How mining-cut polygons are created directly affects the quality of the solution of the MILP based schedulers in terms of dollar values and practicality of the schedules. In paper 103**,** we tackle the automatic mining-cut generation using clustering algorithms. ***Mohammad*** has taken solid steps towards development of a meta-heuristic approach based on Tabu Search (TS) and hierarchical clustering, which aggregates the blocks into larger clusters in each mining bench representing a selective mining unit. The definition of similarity among blocks is based on rock types, grade ranges, location, and the dependency of extraction of a mining-cut to the mining-cuts located above it. The algorithm is developed and tested on synthetic and real mine data.

Hesam has been working towards development of a multi-ramp, multi-destination MILP formulation for short-term open pit planning (papers 104 and 202). The main goal of the study is to develop a framework for monthly mine plans with the objective function of costs minimization. The costs taken into account include mining, haulage, processing, waste rehabilitation, and rehandling costs. The major advantage of this model is its comprehensiveness in considering different processes, stockpiles, waste dumps, and routes for haulage of mined materials. The scheduler decides the route (ramp) and the destination of all materials in a short-term horizon to minimize the haulage costs. The model has been developed, verified, and validated by an iron ore case study.

Behrang has continued working on the transfer of grade uncertainty into mine planning. In paper 105 two methodologies are presented: (i) the kriged block model of an oil sands deposit is used to generate an optimal final pit limit. Then, Sequential Gaussian Simulation is used to generate fifty realizations. An optimum final pit limits design is carried out for each SGS realization based on the same input parameters as the kriged model. Afterwards, the long-term schedule of each final pit shell is generated; and (ii) the kriged schedule is followed for all the each SGS realizations. Uncertainty in the final pit outline, net present value, production targets, and the head grade are assessed and presented.

Eugene has been carrying out research on oil sands mine planning and waste management using goal programming (paper 106). In oil sands mining, due to the limitation of lease area, the pit phase advancement is carried out simultaneously with the construction of tailings dykes in the mined out areas of the pit. Most of the materials used in constructing these dykes come from the oil sands mining operation (overburden and interburden). The research problem here is determining the order of extraction of ore, dyke materials, and waste to be removed from a predefined ultimate pit limit over the mine life. A mixed integer goal programming (MIGP) theoretical framework for oil sands open pit production scheduling with multiple material types has been developed, implemented and tested. The developed model proved to be able to generate a uniform schedule for ore and dyke material. This is in accordance with the requirements of Directive 074 issued by the Alberta Energy and Resource Conservation Board on tailings performance and criteria for oil sands mining schemes.

Samira has been working on the disposal planning of the oil sands composite tailings (CT) (paper 107). The long-term mine plan should assist in minimization of the storage of fluid tailings in the reclamation landscape. Also the mine plan should assist in creating a trafficable landscape at the earliest opportunity to facilitate progressive reclamation. Paper 107 focuses on development of the formulations required to link oil sands mine production schedules to the respective amount of composite tailings produced downstream. The yearly production schedule of the oil sands mine is the input for the CT calculations.

Yashar has been working on long-term block cave mine production scheduling using mixed integer linear programming (MILP) (papers 108-109). In the case of a block cave mine, the production schedule mainly defines the amount of ore and waste to be mined from the drawpoints in every period of production to achieve a given planning objective. The mine plan also defines the number of new drawpoints that need to be constructed and their sequence to support a given production target. Another aspect of this study is integration of geotechnical constraints into real-scale production scheduling of block cave mines. The developed MILP model has the capability of dealing with the important geomechanical parameters as a part of production scheduling.

Mohammad Mahdi has taken important steps in theoretical developments of solving the large scale mine planning problems, using Lagrangian relaxation technique. He has developed an algorithm to solve open pit production scheduling MILP models using the concept of Lagrangian relaxation. The proposed algorithm has resulted in a very tight gap between upper and lower bounds of the

MILP formulation (paper 110). Focused research is underway to continue this work in the future. ***Mohammad Mahdi*** has also started research in the optimization coal supply chain. The study focuses on designing a proper coal logistic network among coal mines, coal terminals and the steel manufacturing plants. The study simulates the input and output rates of a typical coal terminal to estimate the required stockyard capacity of the terminal (paper 205).

Kwame has worked on linear programming (LP) optimization models (paper 203) and attendant solution procedures, that minimize the hot-mix asphalt (HMA) aggregate cost while producing high quality HMA. The models have been validated with real-life examples. The results indicate that the models can be used to replicate HMA mixes during field modifications to reduce the aggregate cost in a mixture and manage stockpile inventory. It is believed that the application of optimization models will increase the application of the Bailey method in the United States.

Eugene, ***Samira,*** **and** ***Yashar*** have done a research in hierarchical mine production scheduling using discrete-event simulation (paper 201). The goal of this study is to develop a discrete-event simulation model to link long-term predictive mine plans with short-term production schedules in the presence of uncertainty. We have developed, verified and validated a discrete-event simulation model for open pit production scheduling with the SLAM simulation language. The simulation model has proved to bridge the gap between a deterministic long-term yearly plan and a daily dynamic short-term schedule. The simulation model takes into consideration the constraints and uncertainties associated with mining and processing capacities, crusher availability, stockpiling strategy and blending requirements.

September 2010

Hooman Askari

Second Annual Research Report of the Mining Optimization Laboratory (MOL) 2009/2010

Table of Contents

Mining Optimization Laboratory (MOL) Sponsors:

Newmont USA Limited
10101 E. Dry Creek Road
Englwood, CO 80112, USA
Contact: Xiaolin Wu

Suncor Energy Inc. (Oilsands)
P.O. Box 4001, Tar Island Drive
Fort McMurray, AB, Canada,
T9H 3E3, Mine Planning & Projects
Contact: Ross McElroy

Maptek Pty Ltd.
165 S. Union Blvd. Suite 888
Lakewood, CO, USA 80228
Contact: Eric Gonzalez

Shell Canada Limited
Heavy Oil-Upstream Americas
400 4th Avenue S.W.,
PO Box 100, Station M,
Calgary, Alberta T2P 2H5, Canada
Contact: Jeffery Roberts

Iron Ore Company of Canada
1000 Sherbrooke Street West, Suite 1920
Montreal, Qubec, H3A 3G4, Canada
Contact: Matt Simpson

Mining Optimization Laboratory (MOL) Researchers / Graduate Students

Following are researchers and students affiliated with Mining Optimization Laboratory in September 2010.

1. **Hooman Askari-Nasab**	Assistant Professor and Director of MOL
2. **Kwame Awuah-Offei**	Assistant Professor of Mining Engineering
3. **Mohammad Mahdi Badiozamani**	PhD Student - 2009/09
4. **Eugene Ben-Awuah**	PhD Student - 2009/01
5. **Hesameddin Eivazy**	PhD Student - 2009/09
6. **Yashar Pourrahimian**	PhD Student - 2008/09
7. **Samira Kalantari**	Msc Student - 2009/01
8. **Behrang Koushavand**	PhD Student (CCG) - 2007/09
9. **Mohammad Tabesh**	PhD Student - 2009/09
10. **Elmira Torkamani**	PhD Student - (new) - 2010/09

Applications of MILP long-term open pit production scheduler

Hooman Askari-Nasab
Mining Optimization Laboratory (MOL)
University of Alberta, Edmonton, Canada

Abstract

A number of mixed integer linear programming (MILP) formulations have been introduced for production scheduling of open pit mines. One of the main obstacles in using MILP formulations for open pit production scheduling is the size of the problem. The number of integer and continuous decision variables, as well as the number of constraints required to formulate a real-size mine will set up a computationally intractable problem. The main objective of this paper is to present a practical MILP formulation for open pit production scheduling problem. Also, we highlight the achievable economic gains that are possible through production scheduling optimization. We present an application of using mixed integer linear programming formulations for the open pit long-term production scheduling problem. We verify and validate the MILP production scheduler by a comparative case study against Whittle strategic mine planning software. An iron ore deposit with 427 million tonnes of rock and 116 million tonnes of iron ore in the final pit limit at an average grade of 72.9% magnetic weight recovery is studied. The difference between the cumulative discounted cash flow of the MILP schedule and the Whittle Milawa Balanced schedule is $50.4 million dollars. The considerable difference between the two methods, demonstrates the importance of production scheduling optimization and the necessity for scheduling optimization to turn into a common practice in industry.

1. Introduction

The life-of-mine production schedule defines the strategy of displacement of ore, waste, and overburden over the mine life. The objective of long-term production scheduling is to determine the sequence of extraction and displacement of material in order to maximize or minimize an objective function. Commonly, the goal is to maximize the net present value of mining operation within the existing economic, technical, and environmental constraints. However, other objectives such as cost minimization or reserve maximization could be considered too. Long-term production schedules are the backbone of short-term planning and day to day mining operations. The long-term production schedules determine mine and processing plant capacity and their expansion potential. The production schedule also defines the management investment strategy. Deviations from optimal plans in mega mining projects will result in enormous financial losses, delayed reclamation, and resource sterilization. Current open pit production scheduling methods in the literature and industry are not limited to, but can be divided into two main categories: heuristics and exact algorithms. The main motivation of this paper is to demonstrate that the economic difference between a practical optimal production schedule, generated by exact mathematical methods and production schedules generated by common techniques used in industry is substantial. Optimization practice is becoming more common in well-built mining companies, but still it is a long way until it becomes a common practice in mining industry.

Mixed integer linear programming (MILP) mathematical programming has been used by various researchers to tackle the long-term open-pit scheduling problem. The MILP models theoretically have the capability to model diverse mining constraints such as multiple ore processors, multiple material stockpiles, and blending strategies. However, current MILP formulations developed for open pit production scheduling have two major shortcomings: (i) the inability to generate the global optimal large-scale life-of-mine production schedule within a reasonable timeframe, and (ii) the inability to quantify the geological uncertainty inherent within the problem and as a result, the associated risk with the mine plans. As the first step, we focus on development of a deterministic MILP formulation for large-scale open pit production scheduling problem. We will address the stochastic case in our future research.

The objective of this study is to (i) develop a deterministic MILP formulation for long-term open pit production scheduling problem, (ii) implement and document the details of the MILP numerical models in TOMLAB/CPLEX (Holmström, 2009) environment, (iii) verify and validate the MILP production scheduler by a comparative case study against one of the standard industry tools — Whittle strategic mine planning software (Gemcom Software International, 2008), and (iv) demonstrate the importance of production scheduling optimization to become a common practice industry wide.

In a typical open pit long-term scheduling problem, the number of blocks is in the order of a couple of hundred thousand to millions, and the number of scheduling periods is in the order of twenty periods and more. Evidently, the number of integer and continuous decision variables, and the number of constraints formulating a problem of this size would exceed the capacity of current state of hardware and software. The MILP formulation of open pit production scheduling becomes intractable because of the size of the problem. To overcome the size problem, we aggregate blocks into larger units, we refer to these units as mining-cuts. We present two MILP formulations at two different levels of granularity: (i) processing at block level and mining at mining-cut level; and (ii) processing and mining both at mining-cut level.

The next section of the paper covers the relevant literature to open pit production scheduling problem. Section three presents problem definition, notations of variables, and the mixed integer linear programming formulations of the problem, while the fourth section presents the numerical modeling techniques. The next section represents the verification of the MILP models by a comparative mining case study against the Whittle software (Gemcom Software International, 2008) results. Finally, the last section presents the conclusions and future work followed by the list of references.

2. Literature review

Current production scheduling methods in the literature are not just limited to, but can be divided into two main categories: heuristic and exact algorithms. Some of these algorithms are embedded into available commercial software packages.

Various models based on a combination of artificial intelligence techniques have been developed (Askari-Nasab, 2006; Askari-Nasab, et al., 2009; Denby, et al., 1996; Tolwinski, et al., 1996). Some of the artificial intelligence techniques such as intelligent open pit simulator (Askari-Nasab, 2006) are based on frameworks that theoretically will converge to the optimal solution, given sufficient number of simulation iterations. The main disadvantage of artificial intelligence and heuristic methods however, is that there is no quality measure to solutions provided comparing against the optimum. In addition most of the results are not reproducible.

A variety of operations research approaches including linear programming (LP) and mixed integer linear programming (MILP) have been applied to the mine production scheduling problem. The pioneer work of Johnson (1969) used an LP model, which led to the MIP formulations by Gershon

(1983) for the production scheduling problem. Every orebody is different, but for a typical open pit long-term scheduling problem, the number of blocks is in the order of a couple of hundred thousand to millions, and the number of scheduling periods could vary in the order of twenty and more periods for a life-of-mine production schedule. Evidently, the number of integer and linear decision variables, and the number of constraints formulating a problem of this size would become intractable.

Various models based on mixed integer linear programming mathematical optimisation have been used to solve the long-term open-pit scheduling problem (Boland, et al., 2009; Caccetta, et al., 2003; Dagdelen, et al., 2007; S. Ramazan, et al., 2004). In practice, formulating a real size mine production planning problem by including all the blocks as integer variables will become computationally intractable. Various methods of aggregation have been used to reduce the number of integer variables that are required to formulate the production scheduling problem with MILP techniques. Ramazan and Dimitrakopoulos (2004) illustrated a method to reduce the number of binary integer variables by setting waste blocks as continuous variables instead of integer variables. Ramazan and Dimitrakopoulos (2004) reported a case study on a small single level nickel laterite block model with 2,030 blocks over three periods.

Ramazan et al. (2005) presented an aggregation method based on fundamental tree concepts to reduce the number of decision variables in the MILP formulation. The fundamental tree algorithm has been used in a case study with 38,457 blocks within the final pit limits. Whittle strategic mine planning software (Gemcom Software International, 2008) has been used to decompose the overall problem into four push-backs. Subsequently, the blocks within the push-backs were aggregated into 5,512 fundamental trees and scheduled over eight periods using the formulation presented in Ramazan and Dimitrakopoulos (2004). Information about the run-time of the MILP models are not presented in Ramazan (2007); also the breakdown of the problem into four push-backs based on the nested pit approach and formulating each push-back as a separate MILP would not generate a global optimum solution to the problem. On the other hand the size of the problem of around thirty thousand blocks over eight periods is more a mid-range planning problem rather than a long-term life-of-mine schedule.

Caccetta and Hill (2003) presented a formulation that only used binary integer variables; they developed and implemented a personalized branch-and-cut (Horst, et al., 1996) method in C++ using CPLEX (ILOG Inc, 2007) to solve the relaxed LP sub-problems. Boland et al. (2009) have demonstrated an iterative disaggregation approach to using a finer spatial resolution for processing decisions to be made based on the small blocks, while allowing the order of extraction decisions to be made at an aggregate level. Boland et al. (2009) reported notable improvements on the convergence time of their algorithm for a model with 96,821 blocks and 125 aggregates over 25 periods. However, combining 96,821 blocks into only 125 aggregates would reduce the freedom of decision variables and the schedule generated could not be considered as an optimal solution in comparison to the case that 96,821 blocks had a decision variable defined for them. Moreover, in Boland et al. (2009) there is no representation of the generated schedules in terms of annual ore and waste production, average grade of ore processed, cross sections, and plan views of the schedules to assess the practicality of the solutions from mining operational point of view.

MineMax (Minemax Pty Ltd, 2009) is a commercially available strategic mine scheduling software, which uses MILP formulation solved by ILOG CPLEX (ILOG Inc, 2007) solver. Given that, MineMax is a commercial software we couldn't find detailed information about the approach and formulation, but our understanding from the evaluation of the demo tutorial version of MineMax is that it initially decomposes the final pit into nested pit shells based on parametric analysis concepts represented by Lerchs and Grossmann (1965). The pit shells define a pit to pit precedence constrained by the minimum and maximum number of benches by which the mining of one specified pit shell is to lag behind the previous one. The other option to define rules for

precedence of extraction is either by proportions mined on each bench or by block precedence based on the overall pit slopes. Then, each pit shell is formulated as a separate MILP model which can contribute to the overall quantity of mining and processing targets within the grade and precedence constraints; this approach results in MILP formulations for each pit shell with smaller size which will converge faster, but it could not be considered a global optimization of the problem since the pit shells are defined by the parametric analysis initially. Another optimization strategy is using sliding windows which are sub-problems tackled on a period by period basis. Other well known proprietary software which tackle the strategic mine production scheduling by MILP techniques are Blasor (Stone, et al., 2007), Prober (Whittle, 2007), and OptiMine (Dagdelen, et al., 2007).

Production scheduling optimization techniques are still not widely used in the mining industry. There is a need to improve the practicality and performance of the current production scheduling optimization tools used in mining industry. Also, to gain more common recognition in industry, there is a need to highlight the considerable achievable economic gains that are possible through production scheduling optimization.

3. Mixed integer linear programming model for open pit production scheduling

The basic problem of concern in its simplest form is finding a sequence in which ore and waste blocks should be removed from the predefined open pit outline and their respective destinations over the mine life, so the net present value of the operation is maximized. The production schedule is subject to a variety of physical and economic constraints. The constraints enforce the mining extraction sequence, overall pit slopes, mining, milling, and refining capacities, blending requirements, and minimum mining width. The problem presented here involves scheduling of N different ore and waste blocks within a predetermined final pit outline over T different periods of extraction. Blocks within the same mining bench are aggregated into clusters. Aggregation is based on the block attributes such as, location, rock type, and grade distribution. We refer to these clusters of blocks as mining-cuts. Similar to blocks, each mining-cut has coordinates representing the centre of the cut and its location.

As a general assumption for our formulation we define that a parameter f can take four indices in the format of $f_{k,n}^{e,t}$. Where:

$t \in \{1,....,T\}$ index for scheduling periods.

$k \in \{1,...,K\}$ index for mining-cuts.

$n \in \{1,...,N\}$ index for blocks.

$e \in \{1,...,E\}$ index for elements of interest in each block.

The objective function of the MILP formulation is to maximize the net present value of the mining operation. Hence, we need to define a clear concept of economic block value based on ore parcels which could be mined selectively. The profit from mining a block depends on the value of that block and the costs incurred in mining and processing the block. The cost of mining a block is a function of its location, which characterizes how deep the block is located relative to the surface and how far it is relative to its final dump. The spatial factor can be applied as a mining cost adjustment factor for each block according to its location to the surface. The discounted profit from block n is equal to the discounted revenue generated by selling the final product contained in block n minus all the discounted costs involved in extracting block n, this is presented by Eqs. (1) and (2).

discounted profit = discounted revenue - discounted costs (1)

$$d_n^t = [\underbrace{\sum_{e=1}^{E} o_n \times g_n^e \times r^{e,t} \times (p^{e,t} - cs^{e,t})}_{discounted\ revenues}] - [\underbrace{\sum_{e=1}^{E} o_n \times cp^{e,t}] - [(o_n + w_n) \times cm^t]}_{discounted\ costs}] \quad (2)$$

Where

- d_n^t is the discounted profit generated by extracting block n in period t,
- o_n is the ore tonnage in block n,
- w_n is the waste tonnage in block n,
- g_n^e is the average grade of element e in ore portion of block n,
- $r^{e,t}$ is the processing recovery, which is the proportion of element e recovered in time period t,
- $p^{e,t}$ is the price in present value terms obtainable per unit of product (element e),
- $cs^{e,t}$ is the selling cost in present value terms per unit of product (element e),
- $cp^{e,t}$ is the extra cost in present value terms per tonne of ore for mining and processing,
- cm^t is the cost in present value terms of mining a tonne of waste in period t.

For simplification purposes we denote:

$$v_n^t = [\sum_{e=1}^{E} o_n \times g_n^e \times r^{e,t} \times (p^{e,t} - cs^{e,t}) - \sum_{e=1}^{E} o_n \times cp^{e,t}] \quad (3)$$

$$q_n^t = (o_n + w_n) \times cm^t \quad (4)$$

Where

- v_n^t is the discounted revenue generated by selling the final product within block n in period t minus the extra discounted cost of mining all the material in block n as ore and processing it; and
- q_n^t is the discounted cost of mining all the material in block n as waste.

We present two different formulations for the open pit production scheduling problem. The objective function is to maximize the NPV of the mining operation. We used the concepts presented in Boland et al. (2009) as the starting point of our development. We have developed, implemented, and tested a new MILP formulation taking into account practical shovel movements by controlling the maximum number of extraction periods for a mining-cut.

3.1. MILP formulation one - extraction at mining-cut level and processing at block level

In the proposed model, processing is controlled at block level, whereas the extraction is controlled at mining-cut level. The amount of ore processed is controlled by the continuous variable x_n^t, and the amount of material mined is controlled by the continuous variable y_k^t. Using continuous decision variables allows fractional extraction of mining-cuts in different periods. $b_k^t \in \{0,1\}$ is the binary integer variable controlling the precedence of extraction of mining-cuts. $b_k^t \in \{0,1\}$ is equal to one, if extraction of mining-cut has started by or in period t; otherwise it is zero. The objective function is to maximize the net present value of mining operation.

Objective function:

$$\max \sum_{t=1}^{T}\sum_{k=1}^{K}\left(\sum_{n\in c_k} v_n^t \times x_n^t - (\sum_{n\in c_k} q_n^t)\times y_k^t\right) \tag{5}$$

Where

- T is the maximum number of scheduling periods, where $\mathcal{T} = \{1,...,T\}$ is the set of all the scheduling time periods in the model,
- K is the total number of mining-cuts to be scheduled, where $\mathcal{K} = \{1,...,K\}$ is the set of all the mining-cuts in the model,
- c_k represents set of blocks within mining-cut k,
- $x_n^t \in [0,1]$ is a continuous decision variable, representing the portion of block n to be extracted as ore and processed in period t,
- $y_k^t \in [0,1]$ is a continuous decision variable, representing the portion of mining-cut k to be mined in period t, fraction of y characterizes both ore and waste included in the mining-cut.

It should be mentioned that in the objective function given by Eq. (5), mining is controlled at the mining-cut level, whereas the processing is at the higher resolution of block level. The objective function is subject to the following constraints.

Mining capacity constraints:

$$\sum_{k=1}^{K}\left(\sum_{n\in c_k}(o_n + w_n)\right)\times y_k^t \le mu^t \qquad \forall t \in \{1,...,T\} \tag{6}$$

$$\sum_{k=1}^{K}\left(\sum_{n\in c_k}(o_n + w_n)\right)\times y_k^t \ge ml^t \qquad \forall t \in \{1,...,T\} \tag{7}$$

Where

- mu^t is the upper bound on mining capacity in period t (tonnes),
- ml^t is the lower bound on mining capacity in period t (tonnes).

Eq. (6) ensures that the total amount of ore and waste mined in each period is equal to or less than the targeted maximum mining capacity of equipment. The constraints are controlled by the continuous variable y_k^t at the mining-cut level. Eq. (7) on the other hand, ensures that the minimum amount of material that needs to be mined is achieved; Eq. (7) is useful in achieving a constant stripping ratio over the mine life. A production schedule with an invariable stripping ratio would have significant savings potential by ensuring that fleet size required is matched to targets for material movement. The decision of the proper production rate which leads to the boundaries on mining capacity is an important stage of the production scheduling of open pit mines. Different scenarios of annual ore production rates must be examined and the one with highest NPV and uniform mill feed must be chosen. The mining capacity boundaries are a function of the ore reserve, overall stripping ratio, designed processing capacity, targeted mine-life, and the capital investment available for purchasing equipment. The upper and lower bounds of mining capacity could vary by scheduling periods, allowing the designer to use variable mining capacities throughout the mine life. The shortage of equipment in specific periods could be compensated with contract mining. Eqs. (6) and (7) will generate one constraint per period.

Processing capacity constraints:

$$\sum_{n=1}^{N} o_n \times x_n^t \le pu^t \qquad \forall t \in \{1,...,T\} \qquad (8)$$

$$\sum_{n=1}^{N} o_n \times x_n^t \ge pl^t \qquad \forall t \in \{1,...,T\} \qquad (9)$$

Where

- N is the number of blocks in the block model, where $\mathcal{N} = \{1,...,N\}$ is a set of all the blocks in the model,
- pu^t is the upper bound on processing capacity of ore in period t (tonnes),
- pl^t is the lower bound on processing capacity of ore in period t (tonnes).

Eqs. (8) and (9) represent inequality constraints controlling the mill feed or processing capacity; These constraints assist the mine planners to achieve an overall mine-to-mill integration by providing a uniform feed throughout the mine-life. Constraints (8) and (9) are at block level, which means the decisions are made based upon the tonnage of ore above the cut-off grade within individual blocks. In practice, the processing capacity constraints must be set within a tight upper and lower bounds to provide a uniform feed to the mill. Based on the shape of the orebody and distribution of ore grades, these constraints might not be honoured under some circumstances, which will lead to an infeasible problem. Pre-stripping could be achieved by setting the upper and lower bounds of processing capacity constraints equal to zero for the desired periods. This approach would enforce the optimizer to only mine waste blocks in the early periods. Eqs. (8) and (9) will generate one constraint per period per processing path.

Grade blending constraints:

$$\sum_{n=1}^{N} g_n^e \times o_n \times x_n^t \Big/ \sum_{n=1}^{N} o_n \times x_n^t \le gu^{e,t} \qquad \forall t \in \{1,...,T\}, \quad e \in \{1,...,E\} \qquad (10)$$

$$\sum_{n=1}^{N} g_n^e \times o_n \times x_n^t \Big/ \sum_{n=1}^{N} o_n \times x_n^t \ge gl^{e,t} \qquad \forall t \in \{1,...,T\}, \quad e \in \{1,...,E\} \qquad (11)$$

Where

- g_n^e is the average grade of element e in ore portion of block n, where $\mathcal{E} = \{1,...,E\}$ is the set of all the elements of interest in the model,
- $gu^{e,t}$, is the upper bound of acceptable average head grade of element e in period t,
- $gl^{e,t}$, is the lower bound of acceptable average head grade of element e in period t.

Production scheduling is concerned with the inherent task of blending the run-of-mine materials before processing. The objective is to mine in such a way that the resulting mix meets the quality specifications of the processing plant. The blending problem becomes more important as the design moves towards mid-range to short-range planning, where the planner is concerned with reducing the grade variability. Constraints (10) and (11) are at block level and there would be one equation per element per scheduling period for both upper and lower bounds.

Ore processed and material mined constraints:

$$x_n^t \le y_k^t \qquad \forall n \in \{1,...,N\}, \quad n \in c_k, \quad t \in \{1,...,T\} \qquad (12)$$

Where x_n^t is the portion of block n to be extracted as ore and processed in period t, and y_k^t is representing the portion of mining-cut k to be mined in period t, where fraction of y characterizes both ore and waste included in the mining-cut. Eq. (12) demonstrates inequalities that ensure the amount of ore in any block which is processed in any given period is less than or equal to the amount of rock extracted from the mining-cut k in any given scheduling period. A very important assumption in the formulation is that each mining-cut is extracted homogeneously; this means that y_k^t illustrates the fraction of mining-cut k to be extracted in time period t and all the blocks within the cut $n \in c_k$ are extracted with the same proportion of y_k^t. Eq. (12) generates one equation per block per period.

Precedence of mining-cuts extraction and slope constraints

$$b_k^t - \sum_{i=1}^{t} y_s^i \le 0 \qquad \forall k \in \{1,...,K\}, \quad t \in \{1,...,T\}, \quad s \in H(S) \qquad (13)$$

$$\sum_{i=1}^{t} y_k^i - b_k^t \le 0 \qquad \forall k \in \{1,...,K\}, \quad t \in \{1,...,T\} \qquad (14)$$

$$b_k^t - b_k^{t+1} \le 0 \qquad \forall k \in \{1,...,K\}, \quad t \in \{1,...,T-1\} \qquad (15)$$

Where

- $b_k^t \in \{0,1\}$ is a binary integer decision variable controlling the precedence of extraction of mining- cuts. b_k^t is equal to one if extraction of mining-cut k has started by or in period t, otherwise it is zero,
- $H_k(S)$ is a set $H_k(S) \subset \mathcal{K}$ for each mining-cut k, defining the immediate predecessor cuts that must be extracted prior to extracting mining-cut k, where S is the total number of cuts in set $H_k(S)$.

For each mining-cut k, Eqs. (13) to (15) check the set of immediate predecessor cuts that must be extracted prior to mining-cut k. This precedence relationship ensures that all the blocks above the current mining-cut are extracted prior to extraction of mining-cut. As it could be deduced from Eq. (15), the formulation is based on the temporal sequence of extraction rather than checking for all the periods. Eqs. (13) to (15), represent one equation per mining-cut per period.

For each block n there is a set $C_n(L) \subset \mathcal{N}$, which includes all the blocks that must be extracted prior to mining block n to ensure that block n is exposed for mining with the desired overall pit slopes, where L is the total number of blocks in set $C_n(L)$. We use a directed graph to model the precedence of extraction between blocks. We define a directed graph $G_b(\mathcal{N}, \mathcal{A})$ by the set of vertices, $\mathcal{N}$ (blocks); connected by ordered pairs of elements called arcs, $\mathcal{A}$. More detailed information about directed graphs could be reviewed in (Siek, et al., 2002).

During the clustering of blocks into mining-cuts, another directed graph at mining-cut level is constructed capturing the precedence relationship of mining-cuts. This directed graph is denoted by $G_c(\mathcal{K}, \mathcal{B})$ where $\mathcal{B} = \{1,...,B\}$ is the set of all edges in the mining-cuts precedence directed graph. The directed graph $G_c(\mathcal{K}, \mathcal{B})$ is constructed in a way that while satisfying the order of extraction at mining-cut level, it would also satisfy the relationships defined by the graph $G_b(\mathcal{N}, \mathcal{A})$ at block level. This approach of defining two directed graphs at mining-cut and block level enables us to model variable pit slopes with small acceptable slope errors in the different regions of the open pit. In other words, mining is controlled at the mining-cut level, while the slopes are modelled at the block level.

3.2. Alternative MILP formulation

Eqs. (5) to (15) represent the MILP formulation for long-term open pit production scheduling. The proposed formulation requires $(2\times K+N)\times T$ number of decision variables, where $K\times T$ of these variables are binary integers. One of the major obstacles in using the MILP formulations for mine production scheduling is the sheer size of the problem. The number of blocks, N, in the model is usually between tens of thousands to millions. Moreover, the main physical constraint in open pit mining is the block extraction precedence relationship modelled by binary integer variables. The most common problem in the MILP formulation is size of the branch and cut tree. The tree becomes so large that insufficient memory remains to solve an LP sub-problem. The number of binary integer variables in the formulation determines the size of the branch and cut tree. As a general strategy in our formulations we aimed at reducing the number of binary integer variables. We have reduced the number of binary integer variables to $K\times T$, where to some extent we have control over the number of mining-cuts K created during the clustering algorithm.

We investigated the effect of using continuous decision variables (x_n^t *and* y_k^t), which leads to fractional block extraction on the quality and practicality of the generated schedules. There is a possibility that block $n\in c_k$ get extracted over multiple periods. Our computational experiments on different models using the formulation presented by Eqs. (5) to (15) shows that block fractions are usually scheduled over consecutive periods and in the worst case examined, some blocks were extracted over three periods. However, this could not be extended as a general rule. We should also emphasize again that blocks are uniformly extracted as part of mining-cuts. The total tonnage of ore processed in the MILP formulation presented by Eqs. (5) to (15) is related to how mining and processing capacities are set in accordance with the ore reserve total tonnage. There is the possibility that quantities of ore above the cut-off grade would not get processed due to the processing capacity limitations. It is feasible to overcome the abovementioned problems by adding reserve and maximum number of fractions constraints to the MILP formulation presented by Eqs. (5) to (15).

Maximum number of fractions and reserve constraints

$$\sum_{t=1}^{T} x_n^t = 1 \qquad \forall n\in\{1,...,N\} \qquad (16)$$

$$\sum_{t=1}^{T} y_k^t = 1 \qquad \forall k\in\{1,...,K\} \qquad (17)$$

$$\sum_{t=1}^{T} u_k^t \le m \qquad \forall k\in\{1,...,K\} \qquad (18)$$

$$\sum_{t=1}^{T} u_k^t \times y_k^t = 1 \qquad \forall k\in\{1,...,K\} \qquad (19)$$

Where

- $u_k^t\in\{0,1\}$ is a binary integer decision variable equal to one if mining-cut k is scheduled to be extracted in period t, otherwise zero,
- m is an integer number representing the maximum number of fractions that mining-cuts are allowed to be extracted over and the previously defined terms apply.

Equality constraints presented by Eq. (16) ensures that all the ore within the predefined pit limits or the targeted push-back is processed during the optimization. Eq. (16) adds one constraint per block. Eq. (17) ensures that all the material within the predefined pit outline is to be mined; this adds one

constraint per mining-cut. Eq. (18) and (19) guarantee that the maximum number of fractions of mining-cuts in the solution for y_k^t is not going to exceed the integer number m. For large-scale models with many scheduling periods m is set equal to two or three. This would ensure that the generated schedule is practical from the equipment movement point of view. Eq. (19) is a set of non-linear constraints, which introduces a mixed integer non-linear programming (MINLP) problem. MINLP problems are very difficult, if not possible, to solve. We linearize Eq. (19) by introducing a new continuous variable, a_k^t, to replace the product $a_k^t = u_k^t \times y_k^t$. Eq. (19) is replaced by $\sum_{t=1}^{T} a_k^t = 1$ and linear constraints represented by Eqs. (20) to (23) are added to force a_k^t to take the value of $u_k^t \times y_k^t$.

$$a_k^t \le u_k^t \qquad \forall k \in \{1,...,K\}, \quad t \in \{1,...,T\} \qquad (20)$$

$$a_k^t \le y_k^t \qquad \forall k \in \{1,...,K\}, \quad t \in \{1,...,T\} \qquad (21)$$

$$a_k^t \ge y_k^t - (1 - u_k^t) \qquad \forall k \in \{1,...,K\}, \quad t \in \{1,...,T\} \qquad (22)$$

$$a_t^k \ge 0 \qquad \forall k \in \{1,...,K\}, \quad t \in \{1,...,T\} \qquad (23)$$

4. Results and discussion

A production scheduling case study is carried out to verify and validate the MILP models. An iron ore deposit is considered with three types of ore classified as top magnetite, oxide, and bottom magnetite. The block model contains the estimated magnetic weight recovery (MWT%) of iron ore. The contaminants are phosphor (P%) and sulphur (S%). Blocks in the geological model represent a volume of rock equal to $25m \times 25m \times 15m$. We compare our model against Whittle strategic mine planning software (Gemcom Software International, 2008). Whittle is one of the tools extensively used in industry for open pit optimization and long-term production scheduling. The input parameters and the mining strategies in Whittle and MILP scheduler are scrutinized carefully to make sure an unbiased comparative study is undertaken. The goal is to maximize the NPV at a discount rate of 10%, while assuring a constant uniform feed to the processing plant through a 21year mine-life. We aimed at generating a practical schedule taking into account the minimum operational room required, the number of active benches in each period, the number of benches added to the pit in each period, uniformity of processing plant feed, and variability of the stripping ratio. The pit includes 427.33 Mt of rock where, 116.29 Mt is iron ore with an average magnetic weight recovery grade of 72.9%. Initially a capacity of 26 Mt/yr was considered as the upper bound on mining capacity, subsequently it was reduced to 25 Mt/yr from year 6 to the end of the mine life. We use Milawa Balanced scheduling algorithm in Whittle, with minimum lead of 3 and maximum lead of 6 benches. The maximum number of active benches is set to 6. In the pit limit optimization process a minimum mining width of 100 meters is used for intermediate pits. Examination of the orebody and cross sections of the open pit reveals that (Figure 2a) due to the shape of the deposit providing a uniform feed to the processing plant is a challenging task. Five years of pre-stripping is considered to ensure the deposit is exposed for open pit mining with adequate operating room in the future. Table 1 summarizes the information related to the comparative case study.

Table 1. Final pit and production scheduling information.

Description	Value	Description	Value
Number of mining-cuts	895	Minimum mining width (m)	100
Total tonnage of rock (Mt)	427.33	Number of periods (years)	21
Total ore tonnage (Mt)	116.29	Maximum number of active benches	6
Total tonnage of recovered Fe (Mt)	76.33	MILP sulphur grade constraint (%)	$0 \leq S \leq 1.9$
Average grade of MWT%	72.9%	MILP phosphor grade constraint (%)	$0 \leq P \leq 0.2$
Mining capacity (Mt/year) (years 1 to 5)	26	MILP MWT grade constraint (%)	$60 \leq MWT \leq 80$
(years 6 to 21)	25	Minimum lead between benches	3
Processing (Mt/year) (years 1 to 5)	0	Maximum lead between benches	6
(years 6 to 21)	8	Total number of blocks in the pit	19,492

In the MILP model, the mining and processing are both set at mining-cut level. The total number of blocks within the final pit limit is 19,492. We use fuzzy logic clustering to aggregate blocks into 895 mining-cuts to reduce the number of variables required in the MILP model. The clustering algorithm, aggregates blocks based on three main criteria: location, rock type, and grade distribution. Blocks that have a higher order of similarity are aggregated into mining-cuts. Figure 1a illustrates the plan view of bench at 1575m elevation; the magnetic weight recovery and rock-types are shown in Figure 1a. Magnetic weight recovery (MWT%), rock-type code, and location of each block is used to aggregate the blocks into mining-cuts, representing a selective mining unit. Figure 1b illustrates the result of the clustering at the 1575m bench. The total tonnage (quantity) of ore, waste, iron ore (MWT), phosphor, and sulphur are calculated for each mining-cut. The aggregated mining-cut model is the input into the MILP scheduler. Aggregation of blocks into mining-cuts, also impose the MILP scheduler to generate a mining schedule at the mining selective unit (SMU). This is very important in generating a practical production schedule from mining operation point of view. Grade blending constraints are set for magnetic weight recovery, sulphur, and phosphor as described in Table 1.

The scheduling of the open pit is carried out using Whittle and the MILP scheduler under the same input data and similar mining strategies. Figure 1c shows bench 1575m scheduled with the MILP scheduler, the periods of extraction are labelled on each block. Figure 1d illustrates bench 1575m scheduled with Whittle Milawa Balanced strategy. Figure2a to 2c demonstrates cross section 98500m looking east. Figure 2a illustrates the orebody, MWT grade distribution, and rock-types. Figure 2b shows the MILP production schedule with periods labelled and Figure 2c demonstrates Whittle Milawa Balanced production schedule with periods numbered accordingly.

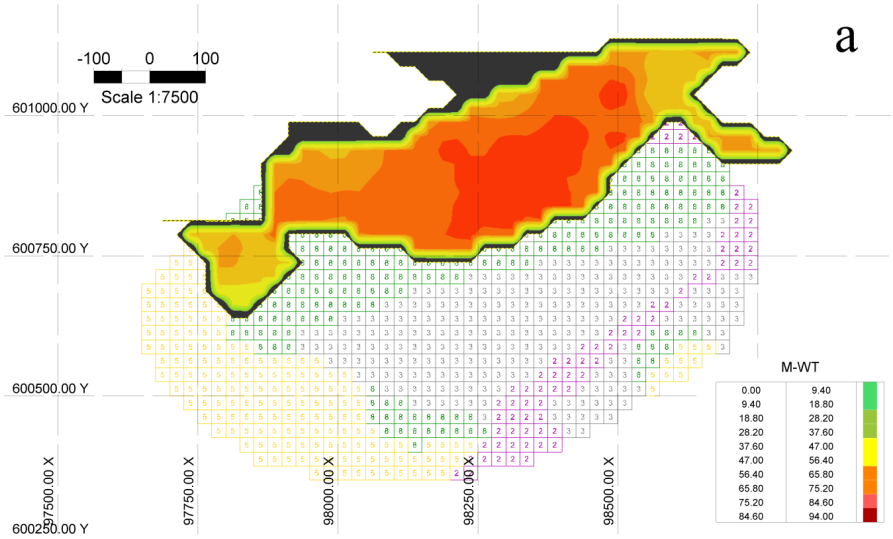

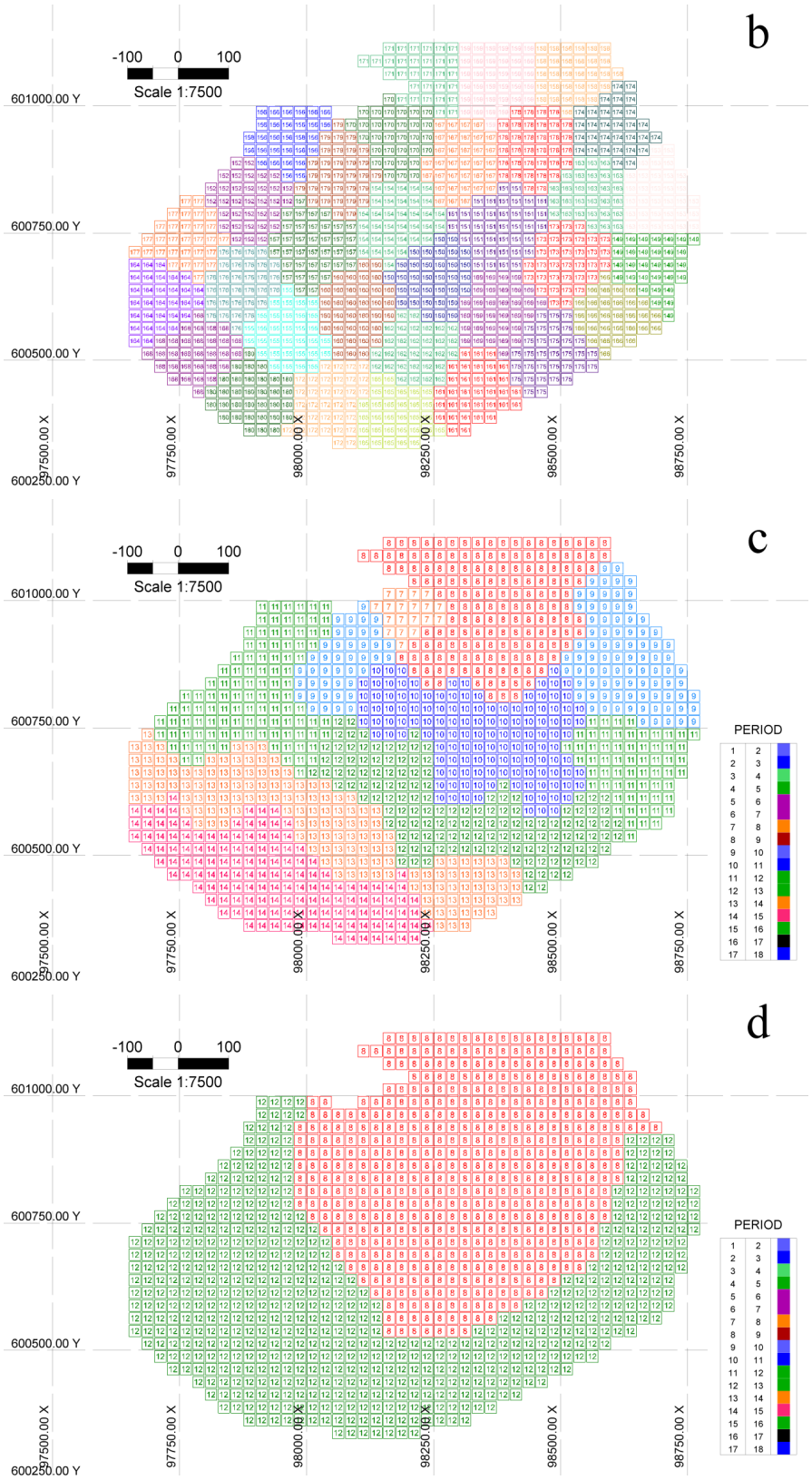

Figure 1. Bench plan view at elevation 1575m. (a) orebody outline and grade distribution with rock-types labelled; (b) clustering results aggregating blocks into mining-cuts; (c) MILP production schedule; (d) Whittle production schedule.

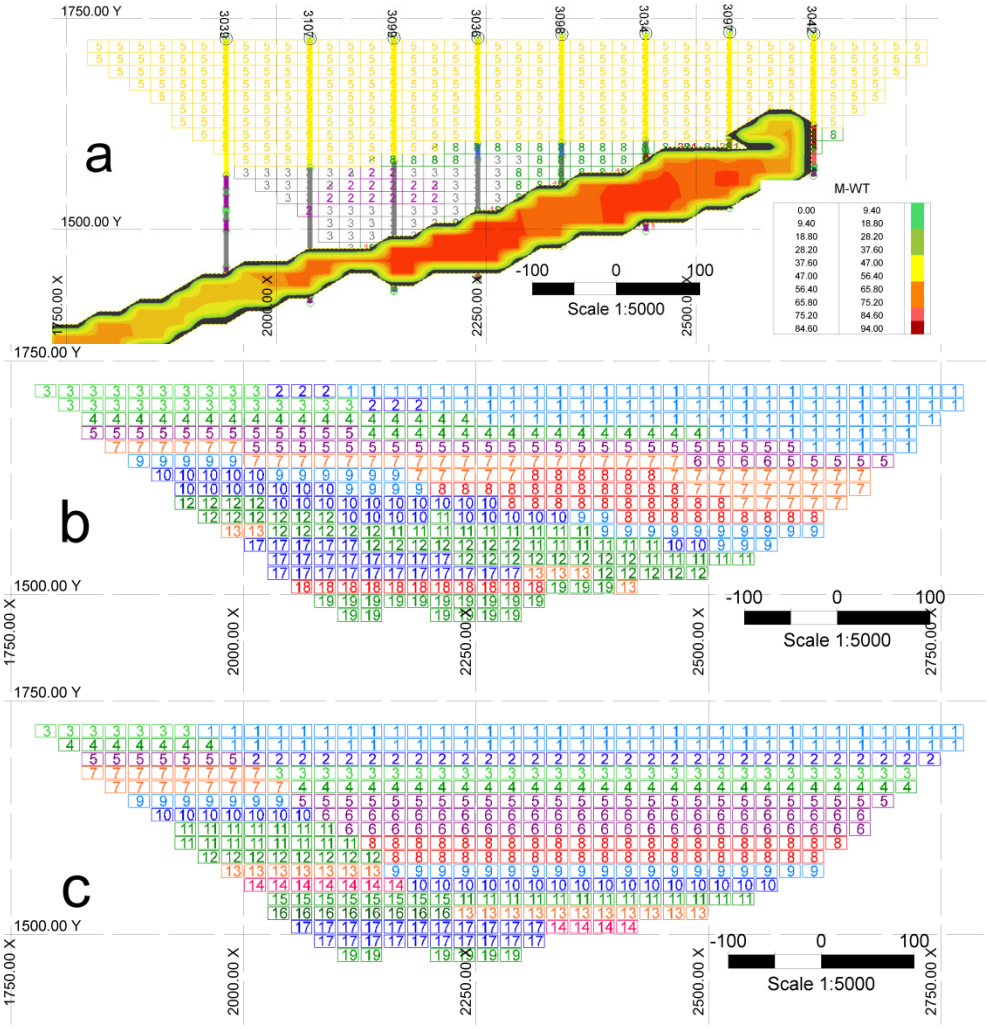

Figure 2. Cross section 98500m looking east ; (a) orebody, grade distribution, and rock-types; (b) MILP production schedule with periods labelled; (c) Whittle production schedule with periods labelled.

Figure 3a illustrates the yearly ore and waste production generated by MILP scheduler and Whittle software. There are 5 years of pre-stripping in both cases. A processing maximum capacity of 8Mt/yr is set from year 6 to 21. We have tried different scenarios and options with Whittle Milawa Balanced strategy and Whittle Milawa NPV strategy to generate a reasonable schedule with the least amount of deviation from target production. Figure 3b illustrates that there is a shortfall of ore feed in years 6 and 7; this shortfall does not occur in the MILP schedule (Figure 3a), since a minimum processing requirement of 6Mt/yr is set for years 6 to 9. The lower bound on processing requirements will ensure that ore is going to be delivered to the processing plant in the schedule.

Figure 4a and 4b illustrate the sulphur and phosphor average grade at the processing plant. The contaminant grade constraints for sulphur and phosphor as set up in Table 1 are met in both schedules. Figure 5 illustrates the head grade of magnetic weight recovery of iron ore. Comparison of Whittle and MILP schedule head grades in Figure 5 illustrates a higher average head grade by the MILP schedule. This is especially notable in the starting years of processing (years 6 to 9), which has a higher impact on the NPV of the operation. The higher average head-grade and less deviation from the 8 Mt/yr target production, translates into higher cash flows in the early years by the MILP schedule. Figure 6 illustrates the annual cash flow generated by MILP scheduler and

Whittle software. It is evident that the cash flows generated in years 6 and 7 by the MILP scheduler are substantially greater than the Whittle results. In Whittle the mine planner does not have control over the lower boundary constraints for mining and processing. Figure 7 illustrates the cumulative discounted cash flow of the MILP and Whittle schedule; it also demonstrates the difference between the cumulative discounted cash flow at the end of each period.

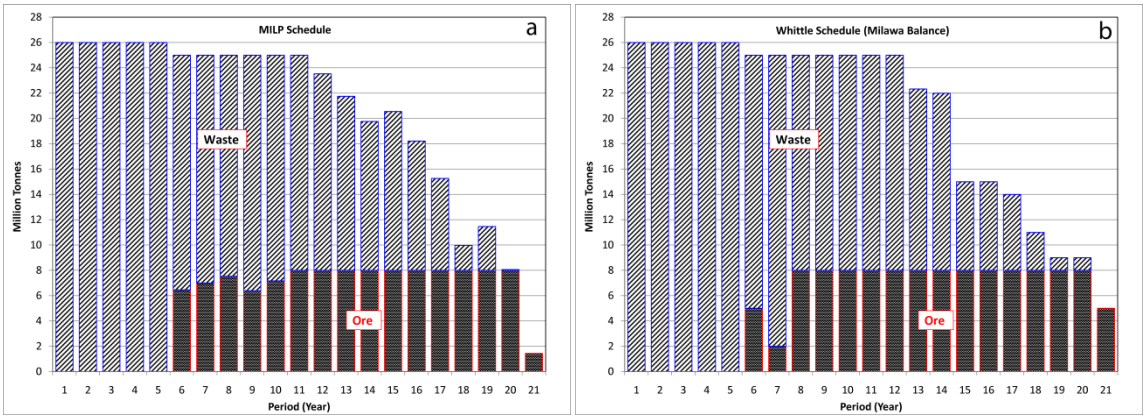

Figure 3. Yearly production schedule of ore and waste; (a) MILP schedule; (b) Whittle schedule.

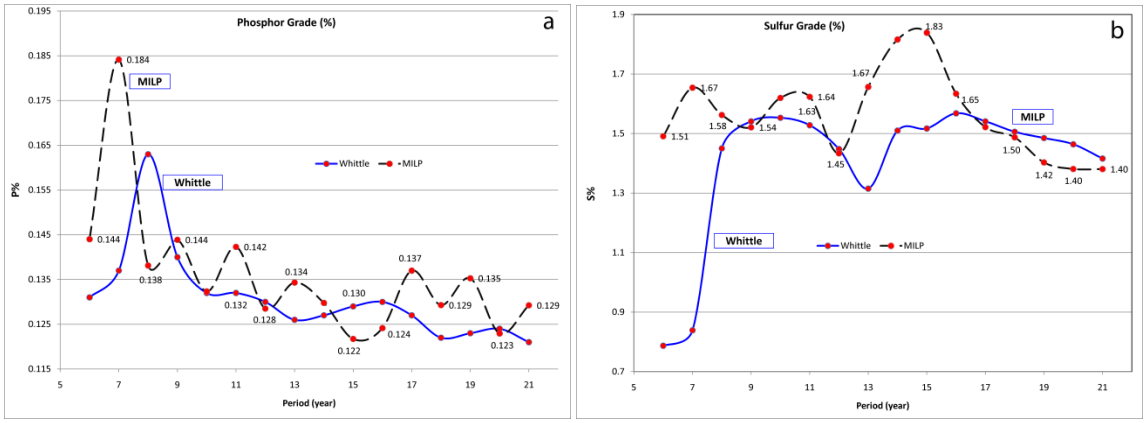

Figure 4. Contaminants grade over the mine life for MILP and Whittle schedule; (a) phosphor grade in percent; (b) sulphur grade in percent.

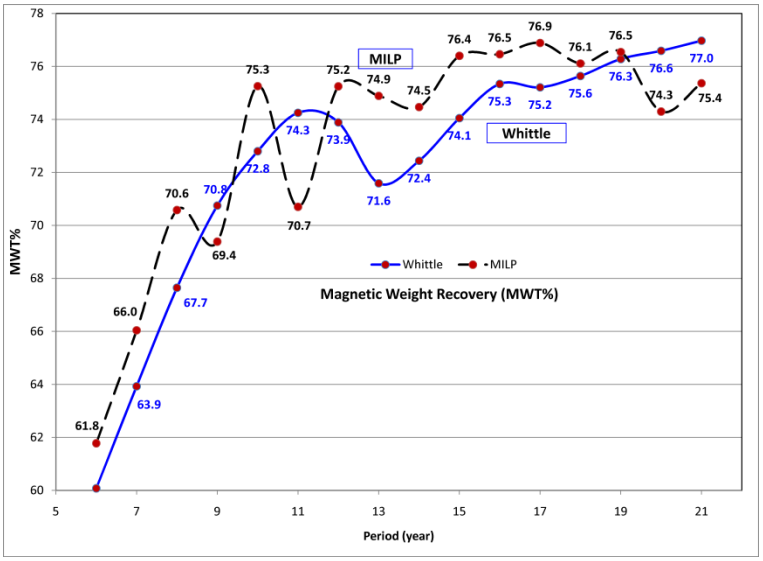

Figure 5. Magnetic weight recovery head grade for the MILP and Whittle schedule.

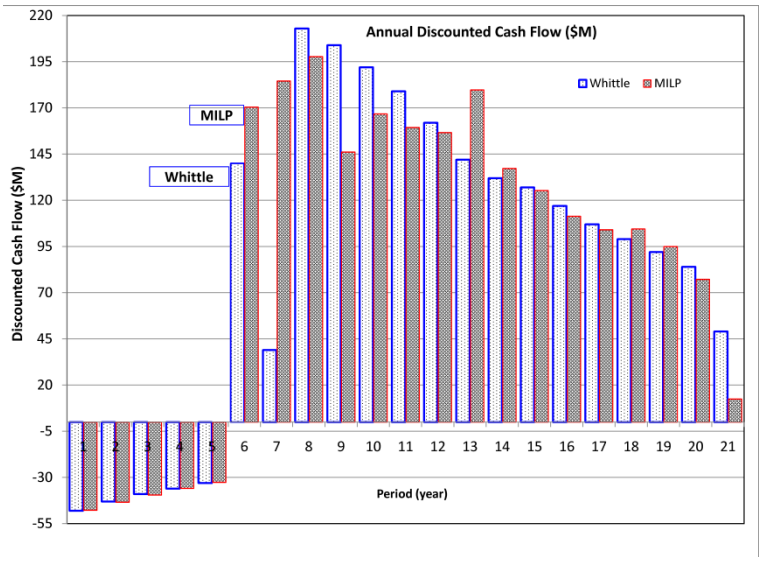

Figure 6. Annual cash flow of the MILP and Whittle schedule in million dollars.

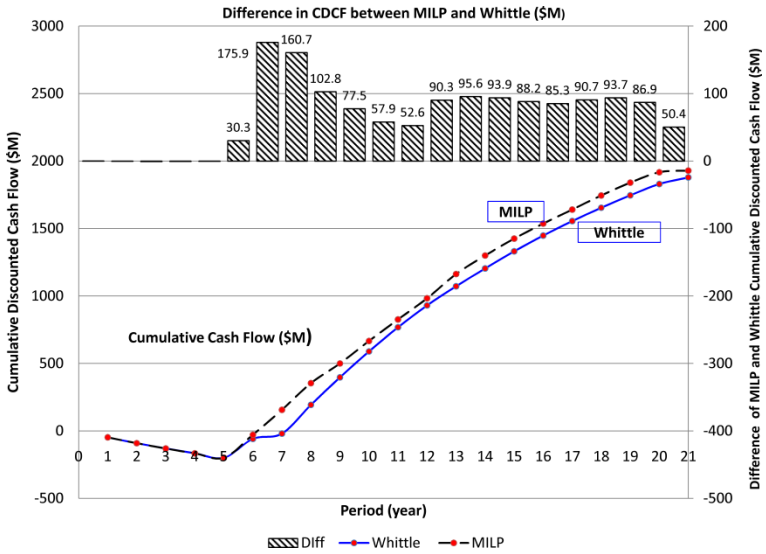

Figure 7. Cumulative discounted cash flow of the MILP and Whittle schedule- the difference between the cumulative discounted cash flows are illustrated on top.

The discounted cash flow of the MILP scheduler is $1929.4 million dollars; whereas the discounted cash flow generated by Whittle Milawa Balanced is $1879.0 million dollars. The discounted cash flow is compared over the same mine-life of 21 years and at a discount rate of 10%. We also kept all the input scheduling variables and strategies with both models the same. The difference between the cumulative discounted cash flow of the MILP scheduler and the Whittle Milawa Balanced results is $50.4 million dollars. This is a substantial amount considering the relatively small size of the open pit. We emphasize again that our goal was to compare the results under the same mining strategies, such as minimum mining width, minimum and maximum lead number, and maximum active benches in each period. We examined generating the schedule with Whittle Milawa NPV under the exact same input parameters. The cumulative discounted cash flow by Whittle Milawa NPV is equal to $1896.3 million dollars over similar mine-life. The generated schedule had a very variable stripping ratio through the mine life which makes it almost impossible to implement in practice.

5. Conclusions and future work

This paper investigated the development of a mixed integer linear programming (MILP) formulation for open pit production scheduling optimization. We developed, implemented, and tested practical MILP models for open pit production scheduling in TOMLAB/CPLEX (Holmström, 2009) environment. The MILP formulation of open pit production scheduling becomes intractable because of the size of the problem. To reduce the number of continuous and binary variables in the model, we aggregated blocks into larger units, referred to as mining-cuts using clustering algorithms.

The main objective of this paper was to highlight the considerable achievable economic gains that are possible through production scheduling optimization. Also, we aimed at improving the practicality and performance of the MILP production scheduling formulations. We verified and validated the MILP production scheduler by a comparative case study against one of the standard industry tools — Whittle strategic mine planning software (Gemcom Software International, 2008). The input parameters and the mining strategies in Whittle and MILP scheduler were inspected cautiously to make sure an unbiased comparative study was undertaken. The goal was to maximize the NPV at a discount rate of 10%, while assuring a constant uniform feed to the processing plant. We aimed at generating a practical schedule taking into account the minimum operational room required, the number of active benches in each period, the number of benches added to the pit in each period, uniformity of processing plant feed, and variability of the stripping ratio. The pit includes 427.33 Mt of rock where, 116.29 Mt is iron ore with an average magnetic weight recovery grade of 72.9%. The discounted cash flow of the MILP scheduler was $1929.4 million dollars; whereas the discounted cash flow generated by Whittle Milawa Balanced is $1879.0 million dollars. The difference between the cumulative discounted cash flow of the MILP scheduler and the Whittle Milawa balanced results is $50.4 million dollars. This is a substantial amount considering the relatively small size of the open pit.

Production scheduling optimization techniques are still not widely used in the mining industry. There is a need to improve the practicality and performance of the current production scheduling optimization tools used in mining industry. Also, to gain more common recognition in industry, there is a need to highlight the considerable achievable economic gains that are possible through production scheduling optimization. Further focused research is underway to develop and test different clustering techniques that would generate an optimized clustering approach for the mining-cuts. Also the next step is to extend the mixed integer linear programming framework into stochastic mathematical programming domain to address the grade uncertainty issue.

6. References

[1] Askari-Nasab, H. (2006). *Intelligent 3D interactive open pit mine planning and optimization.* Unpublished PhD Thesis, University of Alberta, Edmonton, Canada.

[2] Askari-Nasab, H., & Awuah-Offei, K. (2009). Open pit optimisation using discounted economic block values. *Transactions of the Institutions of Mining and Metallurgy, Section A: Mining Technology, 118*(1), 1-12.

[3] Boland, N., Dumitrescu, I., Froyland, G., & Gleixner, A.M. (2009). LP-based disaggregation approaches to solving the open pit mining production scheduling problem with block processing selectivity. *Computers and Operations Research, 36*(4), 1064-1089.

[4] Caccetta, Louis, & Hill, Stephen P. (2003). An application of branch and cut to open pit mine scheduling. *Journal of Global Optimization, 27*(November), 349 - 365.

[5] Dagdelen, K., & Kawahata, K. (2007, April 24- 27). *Opportunities in Multi-Mine Planning through Large Scale Mixed Integer Linear Programming Optimization.* Paper presented at the 33rd International Symposium on Computer Application in the Minerals Industry (APCOM), Santiago, Chile.

[6] Denby, B., Schofield, D., & Hunter, G. (1996). *Genetic algorithms for open pit scheduling - extension into 3-dimensions.* Paper presented at the 5th International Symposium on Mine Planning and Equipment Selection, Sao Paulo, Brazil.

[7] Gemcom Software International, Inc. (2008). Whittle strategic mine planning software (Version 4.2). Vancouver, B.C.: Gemcom Software International.

[8] Gershon, M.E. (1983). Mine scheduling optimization with mixed integer programming. *Mining Engineering, 35*(4), 351-354.

[9] Holmström, Kenneth. (2009). TOMLAB /CPLEX - v11.2. Pullman, WA, USA: Tomlab Optimization.

[10] Horst, Reiner, & Hoang, Tuy. (1996). *Global optimization : deterministic approaches* (3rd ed.). Berlin ; New York: Springer.

[11] ILOG Inc. (2007). ILOG CPLEX 11.0 User's Manual September (Version 11.0): ILOG S.A. and ILOG, Inc.

[12] Johnson, T.B. (1969, September 17 to 19). *Optimum Open-Pit Mine Production Scheduling.* Paper presented at the Proceedings, 8th International Symposium on Computers and Operations Research, Salt Lake City, Utah, USA.

[13] Lerchs, Helmut, & Grossmann, I.F. (1965). Optimum design of open-pit mines. *The Canadian Mining and Metallurgical Bulletin, Transactions, LXVIII*, 17-24.

[14] Minemax Pty Ltd. (2009). MineMax Scheduler (Version 4.2). West Perth, Western Australia: Minemax Pty Ltd.

[15] Ramazan, S., Dagdelen, K., & Johnson, T.B. (2005). Fundamental tree algorithm in optimising production scheduling for open pit mine design. *Mining Technology : IMM Transactions section A, 114*(1), 45-54.

[16] Ramazan, S., & Dimitrakopoulos, R. (2004). Traditional and new MIP models for production scheduling with in-situ grade variability. *International Journal of Surface Mining, Reclamation & Environment, 18*(2), 85-98.

[17] Ramazan, Salih. (2007). *Large-scale production scheduling with the fundamental tree algorithm - model, case study and comparisons.* Paper presented at the Orebody Modelling and Strategic Mine Planning, Perth, Western Australia.

[18] Siek, Jeremy, Lee, Lie-Quan, & Lumsdaine, Andrew. (2002). *The boost graph library : user guide and reference manual*. Boston: Addison-Wesley.

[19] Stone, P., Froyland, G., Menabde, M., Law, B., Pasyar, R., & Monkhouse, P. H. L. (2007). *Blasor - Blended Iron ore mine planning optimization at Yandi, Western Australia.* Paper presented at the Orebody Modelling and Strategic Mine Planning, Perth, Western Australia.

[20] Tolwinski, B., & Underwood, R. (1996). A scheduling algorithm for open pit mines. *IMA Journal of Mathematics Applied in Business & Industry*(7), 247-270.

[21] Whittle, G. (2007). *Global asset optimization.* Paper presented at the Orebody Modelling and Strategic Mine Planning, Perth, Western Australia.

MILP formulation for open pit scheduling with multiple materials destinations

Hooman Askari-Nasab
Mining Optimization Laboratory (MOL)
University of Alberta, Edmonton, Canada

Abstract

A mixed integer linear programming formulation for open pit production scheduling with multiple material destinations is presented.

1. Notation

We will present an MILP formulation for the open pit production scheduling problem with multiple materials destinations. The notation of decision variables, parameters, sets, and constraints are as follows:

1.1. Sets

$\mathcal{K} = \{1,...,K\}$	set of all the mining-cuts in the model.
$\mathcal{P} = \{1,...,P\}$	set of all the phases (push-backs) in the model.
$\mathcal{D} = \{1,...,D\}$	set of all the possible destinations for materials in the model.
$\mathcal{A}_k = \{1,...,A_k\}$	set of all the directed arcs in the mining-cuts' precedence directed graph denoted by $G_k(\mathcal{K}, \mathcal{A}_k)$.
$C_k(L)$	for each mining-cut k, there is a set $C_k(L) \subset \mathcal{K}$ defining the immediate predecessor mining-cuts that must be extracted prior to extracting mining-cut k. Where L is an integer number presenting the total number of blocks in the set C_k.
$B_p(M)$	for each phase p there is a set $B_p(M) \subset \mathcal{K}$ defining the mining-cuts constructing phase p. Phases are constructed to be sets of mining-cuts partitioning $\mathcal{K}$. where M is an integer number denoting the total number of blocks in the set B_p.
$H_P(R)$	for each phase p, there is a set $H_p(R) \subset \mathcal{K}$ defining the mining-cuts within the immediate predecessor pit phases (push-backs) that must be extracted prior to extracting phase p. Where R is an integer number presenting the total number of blocks in the set H_p.

1.2. Indices

A general parameter can take the following indices in the format of $f_{k,p}^{d,t,e}$. Where:

$k \in \{1,...,K\}$	index for mining-cuts.
$p \in \{1,...,P\}$	index for phases.
$d \in \{1,...,D\}$	index for possible destinations for materials.
$t \in \{1,....,T\}$	index for scheduling periods.
$e \in \{1,...,E\}$	index for elements of interest in each block.

1.3. Parameters

$u_k^{d,t}$	the discounted dollar value generated by extracting mining-cut k and sending it to destination d in period t.
$v_k^{d,t}$	the discounted revenue generated by selling the final products within mining-cut k in period t, if it is sent to destination d, minus the extra discounted cost of mining all the material in mining-cut k as ore and processing at destination d.
$q_k^{d,t}$	the discounted cost of mining the material in mining-cut k in period t as waste and sending it to destination d.
g_k^e	average grade of element e in ore portion of mining-cut k.
$\overline{g}^{d,t,e}$	upper bound on acceptable average head grade of element e, in period t, at processing destination d.
$\underline{g}^{d,t,e}$	lower bound on acceptable average head grade of element e, in period t, at processing destination d.
o_k	ore tonnage in mining-cut k.
w_k	waste tonnage in mining-cut k.
$\overline{p}^{d,t}$	upper bound on processing capacity of ore in period t at destination d (tonnes).
$\underline{p}^{d,t}$	lower bound on processing capacity of ore in period t at destination d (tonnes).
$\overline{m}^{t}$	upper bound on mining capacity in period t (tonnes).
$\underline{m}^{t}$	lower bound on mining capacity in period t (tonnes).
$r^{d,e}$	processing recovery, is the proportion of element e recovered if it is processed at destination d.
$s^{t,e}$	price in present value terms obtainable per unit of product (element e).
$cs^{t,e}$	selling cost in present value terms per unit of product (element e).
$cp^{d,t,e}$	extra cost in present value terms per tonne of ore for mining and processing at destination d.
$cm^{d,t}$	cost in present value terms of mining a tonne of waste in period t sending it to destination d.

h_k bench number corresponding to mining-cut k, benches are numbered from the top of the pit towards the bottom accordingly.

$\overline{h}_p$ maximum acceptable lead between phase p and $p+1$. Where the lead is the number of benches by which the mining of a specified phase must be ahead of the next one.

$\underline{h}_p$ minimum acceptable lead required between phase p and $p+1$.

M the total number of mining-cuts in the set $B_p(M)$.

R the total number of mining-cuts in the set $H_p(R)$.

L the total number of mining-cuts in the set $C_k(L)$.

1.4. Decision Variables

$x_k^{d,t} \in [0,1]$ continuous variable, representing the portion of mining-cut k sent to processing destination d, in period t.

$y_k^{d,t} \in [0,1]$ continuous variable, representing the portion of mining-cut k mined in period t, and sent to destination d.

$b_k^t \in \{0,1\}$ binary integer variable controlling the precedence of extraction of mining-cuts. b_k^t is equal to one if extraction of mining-cut k has started by or in period t, otherwise it is zero.

$z_p^t \in \{0,1\}$ binary integer variable controlling the precedence of mining phases. z_p^t is equal to one if extraction of phase p has started by or in period t, otherwise it is zero.

2. Economic block value modeling

The objective function of the MILP formulation is to maximize the net present value of the mining operation. Hence, we need to define a clear concept of economic value based on the amount of ore within mining-cuts, which can be mined selectively. The profit from mining depends on the value of the mining-cut based on its processing destination and the costs incurred in mining and processing it. The cost of mining a cut is a function of its location, which characterizes how deep the mining-cut is located relative to the surface and how far it is relative to its final dump. The spatial factor can be applied as a mining cost adjustment factor for each mining-cut according to its location to the surface. The discounted profit from mining-cut k is equal to the discounted revenue generated by selling the final product contained in mining-cut k minus all the discounted costs involved in extracting mining-cut k, this is presented by Eq. (1).

$$u_k^{d,t} = [\underbrace{\sum_{e=1}^{E} o_k \times g_k^e \times r^{d,e} \times (s^{t,e} - cs^{t,e})}_{discounted\ revenues}] - \underbrace{\sum_{e=1}^{E} o_k \times cp^{d,t,e}}_{discounted\ costs}] - [(o_k + w_k) \times cm^{d,t}] \qquad \forall d \in \{1,...,D\} \qquad (1)$$

For simplification purposes we denote:

$$v_k^{d,t} = \sum_{e=1}^{E} o_k \times g_k^e \times r^{d,e} \times (s^{t,e} - cs^{t,e}) - \sum_{e=1}^{E} o_k \times cp^{d,t,e} \qquad \forall d \in \{1,...,D\}, \quad k \in \{1,...,K\} \qquad (2)$$

$$q_k^{d,t} = (o_k + w_k) \times cm^{d,t} \qquad \forall d \in \{1,...,D\}, \quad k \in \{1,...,K\} \tag{3}$$

3. Model

Objective function:

$$\max \sum_{d=1}^{D} \sum_{t=1}^{T} \sum_{p=1}^{P} \left(\sum_{k \in B_p} (v_k^{d,t} x_k^{d,t} - q_k^{d,t} y_k^{d,t}) \right) \tag{4}$$

Subject to:

$$\underline{g}^{d,t,e} \le \sum_{p=1}^{P} \left((\sum_{k \in B_p} g_k^e o_k \Big/ \sum_{k \in B_p} o_k) x_k^{d,t} \right) \le \overline{g}^{d,t,e} \quad \forall t \in \{1,...,T\}, \quad d \in \{1,...,D\}, \quad e \in \{1,...,E\} \tag{5}$$

$$\underline{p}^{d,t} \le \sum_{p=1}^{P} \left(\sum_{k \in B_p} o_k x_k^{d,t} \right) \le \overline{p}^{d,t} \qquad \forall t \in \{1,...,T\}, \quad d \in \{1,...,D\} \tag{6}$$

$$\underline{m}^{t} \le \sum_{p=1}^{P} \left(\sum_{k \in B_p} (o_k + w_k) y_k^{d,t} \right) \le \overline{m}^{t} \qquad \forall t \in \{1,...,T\}, \quad d \in \{1,...,D\} \tag{7}$$

$$\sum_{d=1}^{D} x_k^{d,t} \le \sum_{d=1}^{D} y_k^{d,t} \qquad \forall k \in \{1,...,K\}, \quad t \in \{1,...,T\} \tag{8}$$

$$b_k^t - \sum_{d=1}^{D} \sum_{i=1}^{t} y_s^{d,i} \le 0 \qquad \forall k \in \{1,...,K\}, \quad t \in \{1,...,T\}, \quad s \in C_k(L) \tag{9}$$

$$\sum_{d=1}^{D} \sum_{i=1}^{t} y_k^{d,i} - b_k^t \le 0 \qquad \forall k \in \{1,...,K\}, \quad t \in \{1,...,T\} \tag{10}$$

$$b_k^t - b_k^{t+1} \le 0 \qquad \forall k \in \{1,...,K\}, \quad t \in \{1,...,T-1\} \tag{11}$$

$$\underline{h}_p \ge h_l b_l^t - h_j b_j^t \ge \overline{h}_p \qquad \forall p \in \{1,...,P\}, \quad t \in \{1,...,T\}, \quad l \in B_p, \quad j \in B_{p+1} \tag{12}$$

$$R.z_p^t - \sum_{r=1}^{R} \sum_{d=1}^{D} \sum_{i=1}^{t} y_r^{d,i} \le 0 \qquad \forall p \in \{1,...,P\}, \quad t \in \{1,...,T\}, \quad r \in H_p(R) \tag{13}$$

$$\sum_{m=1}^{M} \sum_{d=1}^{D} \sum_{i=1}^{t} y_m^{d,i} - M.z_p^t \le 0 \qquad \forall p \in \{1,...,P\}, \quad t \in \{1,...,T\}, \quad m \in B_p(M) \tag{14}$$

$$z_p^t - z_p^{t+1} \le 0 \qquad \forall p \in \{1,...,P\}, \quad t \in \{1,...,T-1\} \tag{15}$$

Creating mining-cuts using hierarchical clustering and tabu search algorithms

Hooman Askari-Nasab, Mohammad Tabesh, and
Mohammad M. Badiozamani
Mining Optimization Laboratory (MOL)
University of Alberta, Edmonton, Canada

Abstract

Open pit mine plans define the complex strategy of displacement of ore and waste over the mine life. Various mixed integer linear programming (MILP) formulations have been used for production scheduling of open pit mines. The main problem with the MILP models is the inability to solve real size mining problems. The main objective of this study is to develop a clustering algorithm, which reduces the number of binary integer variables in the MILP formulation of open pit production scheduling. To achieve this goal, the blocks are aggregated into larger units referred to as mining-cuts. A meta-heuristic approach is proposed, based on Tabu Search (TS), to aggregate the individual blocks to larger clusters in each mining bench, representing a selective mining unit. The definition of similarity among blocks is based on rock types, grade ranges, spatial location, and the dependency of extraction of each mining-cut to the mining-cuts located above it. The proposed algorithm is tested on synthetic data.

1. Introduction

There are different approaches in solving optimization problems which are classified into three main categories: exact, heuristics, and meta-heuristics. In all three approaches the size of the problem and its complication is a key feature. Exact algorithms are based on mathematical programming which will find the optimal solution using different methods introduced in literature. Since most of the real world problems are large scale and complicated, non-exact algorithms have come into existence. Instead of looking for optimal solution, these algorithms just try to find a good solution within a reasonable time and resource usage. This resource usage has been of great concern when using both exact and non-exact algorithms. Different methods have been proposed for reducing the amount of resources required to solve optimization problems.

One known large-scale problem which cannot be solved using the exact optimization procedures is the open pit production scheduling. The number of variables and constraints in this problem is related to the size of the deposit and the number of blocks in the model. Open pit mine block models usually include millions of blocks, which makes the exact optimization method intractable for the open pit production scheduling problem. For the planning step the open pit mine production scheduling block models are used as the input. There will be variables, parameters and constraints regarding extraction and processing of these blocks in production scheduling formulations. The

typical mathematical model used to optimize the open pit mine production scheduling problem is Mixed Integer Programming (MIP).

If blocks are considered to be large in size in order to reduce the number of blocks, the precision required to model the overall pit slopes is lost. On the other hand, smaller blocks may result in more variables and constraints which make the problem unsolvable in a reasonable time. Therefore, methods have been proposed in the literature trying to introduce new modeling and solution procedures being able of creating the production plan and overcoming the curse of dimensionality in aforementioned MIPs.

The objective of this study is to develop an algorithm based on hierarchical clustering and Tabu Search to aggregate blocks into larger formations referred to as mining-cuts. Blocks within the same level or mining bench are grouped into clusters based on their attributes, spatial location, rock type, and grade distribution. Similar to blocks, each mining-cut has coordinates representing the center of the cut and its spatial location. Introduction of mining-cuts into mixed integer linear programming production scheduling models will reduce the number of variables and constraints and as a result, the production scheduling problem could be solved using current optimizers.

In the next section, the literature of production scheduling is reviewed. In the second section, the development of the clustering methodology based on hierarchical clustering and Tabu Search is presented, followed by an illustrative example from implementing the proposed algorithm. Then, the proposed algorithm is applied to a case study and the results are reported, followed by the conclusion.

2. Literature review

Martinez (2006) has worked on improving the performance of a mixed integer production scheduling model and has implemented his findings on a case study in Sweden. He has studied on an underground Iron ore mine and presents a combined (short and long-term) resolution model, using mixed integer programming. In order to decrease the solution time, he develops a heuristic consisting of two steps: (1) solving five sub problems and (2) solving a modified version of the original model based upon information gained from the sub problem solutions. His presented heuristic method, results in a better solution in less time comparing to solving the original MILP problem.

Newman (2007) performed another study on the same case study with Martinez (2006) on an underground Iron ore mine. They have designed a heuristic algorithm based on solving a smaller and more tractable model than the original model, by aggregating time periods and reducing the number of variables. Then, they solve the original model using information gained from the aggregated model. For the worst case performance of this heuristic, they compute a bound and show that their presented procedure produces good quality results while reducing the computation time.

Ramezan (2007) uses an algorithm entitled ‘Fundamental Tree Algorithm’ which is developed based on linear programming. This algorithm aggregates blocks of material to clusters and as a result, decreases the number of integer variables as well as the number of constraints in MIP formulation. The author proposes a new Fundamental Tree algorithm in optimizing production scheduling of open pit mine. The economic benefit of the proposed algorithm compared to existing methods is demonstrated through a case study.

Gaupp (2008) presents three approaches to make the MILP more tractable: (1) reducing the number of deterministic variables to eliminate blocks from consideration in the model; (2) strengthening the model’s formulation by producing cuts and (3) using Lagrangian techniques to relax some constraints and simplify the model. By using these three techniques, he determines an optimal (or near-optimal) solution more quickly than solving the original problem.

Askari-Nasab (2008) have proposed two MILP formulations for long-term large-scale open pit mine production scheduling problem. They have used the fuzzy C-means clustering to aggregate the blocks in each elevation and reduce the number of blocks to smaller number of aggregated blocks. As a result, they have reduced the number of variables in the proposed MILP. They have implemented the proposed MILP theoretical frameworks for large-scale open-pit production scheduling.

Amaya (2009) uses the concept of local-search based algorithm in order to obtain near optimal solutions to large problems in a reasonable time. They describe a heuristic methodology to solve very large scheduling problems with millions of blocks. They start from a known feasible solution, which they call "incumbent". Their proposed algorithm seeks to find a similar solution to the current solution with an improved objective function value. To do that, the algorithm, by means of a random search, looks for solutions that partially coincide with the incumbent. Whenever any improvement in objective function is found, the incumbent is updated and the process is repeated to reach its stopping criteria.

Boland (2009) propose a method in which the mining and processing decisions are made based on different decision variables. They use aggregates of blocks in scheduling the mining process. Then, an iterative disaggregation method is used which refines the aggregates up to the point where the refined aggregates result in the same optimal solution to the relaxed LP, considering individual blocks. Then, their proposed algorithm uses individual blocks for making decision on processing. They have proposed several strategies to create refined aggregates. These refined aggregates provide high quality solutions in terms of net present value (NPV) in reasonable time.

Through a literature review, it can be inferred that most of researchers have focused on heuristic and meta-heuristic approaches to solve the mine production planning problem which do not guarantee the optimality of the solution. Also, there are some publications on penalty function and Lagrangian relaxation methods to scale down the problem and make it solvable with mathematical programming approaches. Only few studies are done to aggregate the blocks and reduce the number of variables to make the problem tractable. Among the latest aggregation approaches employed to solve the problem is what Askari-Nasab (2008) proposed using Fuzzy C-means clustering to create mining cuts. In the next section the theoretical framework, used in developing the algorithm, is reviewed.

3. Theoretical framework and models

3.1. Clustering

According to the handbook of applied algorithms "Clustering is the process of grouping together objects that are similar. The groups formed by clustering are referred to as clusters" (Stojmenovi´c, 2008). This process is usually performed by calculating a measure of similarity (or dissimilarity) between different pairs of data. In addition to this measure, our purpose of clustering may also affect the result of the clustering process. In other words, the same set of data can be clustered in different ways when they are to be used for different purposes. Different characteristics of data which are taken into account in calculating similarity measure can be the cause of having different results as well as the clustering method used.

There have been many clustering algorithms proposed in the literature which are based on grouping data according to their different characteristics. Some of these groups are mentioned in this section.

Exclusive vs. Non-exclusive: an exclusive clustering technique ensures the resulting clusters to be disjoint in contrast with non-exclusive algorithms which result in clusters having overlaps. Most of the current famous algorithms belong to the first group.

Intrinsic vs. Extrinsic: when external effective parameters matter, clustering techniques are divided into another two categories. Intrinsic algorithms are the one which are unsupervised activities and

create the clusters based on the data itself. On the other hand, where clustering is done based on external sources of data such as predetermined objects which should or should not be clustered together the process is said to be extrinsic. Intrinsic clustering algorithms are more common.

Hierarchical vs. Partitional: hierarchical algorithms are the ones which create a sequence of partitions on the data and are divided into two groups. *Hierarchical agglomerative algorithms* are the one which start creating clusters with a single object and combine them together in order to find the final clusters. The opposite direction is used in *hierarchical divisive algorithm* where the big cluster containing all the objects is created first and it is segmented to smaller clusters in each step. Partitional clustering methods create partitions based on the similarity and dissimilarities being defined between objects such that more similar objects, according to the pre determined properties, are grouped together. A common example of these algorithms is the k-means algorithm and its many extensions.

Since in this paper, the focus is on a hierarchical clustering algorithm, a review of this algorithm is presented here. According to Johnson (1967), hierarchical clustering has the following steps:

1. Start by assigning each item to a cluster, so that if you have N items, you now have N clusters, each containing just one item. Let the distances (similarities) between the clusters be the same as the distances (similarities) between the items they contain.
2. Find the closest (most similar) pair of clusters and merge them into a single cluster, so that now you have one cluster less.
3. Compute distances (similarities) between the new cluster and each of the old clusters.
4. Repeat steps 2 and 3 until all items are clustered into a single cluster of size N.

3.2. Penalty Function

Despite clustering which reduces the number of decision variables, the penalty function commonly eliminates some or all of the constraints from a problem. Penalty functions are defined as follows: “Penalty functions, a technique used in solving constrained optimization problems, are often used to restrict the solution search to designs that meet all criteria. As the name implies, a penalty is assigned to the figure of merit or merit function if a constraint is violated during optimization” (Organization, 2009) If you consider a normal objective function to be a cost minimization function, a penalty value is the amount which is determined as the cost being applied because of violation of each constraint.

Two different kinds of constraints can be defined. The first group is called the “hard” constraints which cannot be violated during optimization procedure. The second group, which can be violated in order to have better results, are called “soft” constraints. In contrary with soft constraints, the amount of penalty for hard constraints is set so large that the solution procedure never violates the constraint.

The simplest way of representing the penalty function is a normalized weighted sum of deviations from design values of each constraint. These weights can be determined for both hard and soft constraints. This can be shown as a definition of Figure of Merit represented by Eq. (1).

$$FOM = \frac{\sum_{i=1}^{N} w_i \left(d_i - c_i \right)^2}{\sum_{i=1}^{N} w_i} \tag{1}$$

Where:

d_i is the design objective of constraint

c_i is the current value of constraint

w_i is the weight

N is the number of constraints

Although it seems to be easy and generic to implement penalty functions, it is practically difficult to use because different penalty functions for different problems should be determined.

4. Methodology

The mixed integer formulation of the open pit mine planning problem consists of different integer and continuous variables and different sets of constraints. One of these sets which are making the problem large in size is the order of extraction constraints. In order to reduce the number of constraints in this set, a clustering procedure based on fuzzy c-means algorithm is proposed in Askari-Nasab (2008). Developing these clusters is done based on similarities between blocks regarding physical location of the block and its grade which is taken into account as a (zero-one) ore-waste categorization.

In the proposed method in this study the main idea is to create clusters in a way that the number of constraints regarding order of extraction is reduced in the MILP formulation. The number of constraints for each mining-cut is equal to the number of clusters in the upper level which are supposed to be extracted prior to extraction of the current mining-cut. Therefore, the algorithm has a look on the lower level and the dependencies between clusters while creating clusters in each bench.

The clustering procedure is a two step algorithm. In the first step an initial clustering is provided based on a similarity factor representing the spatial distance between blocks, the similarity of rock types, grades, and also the clusters in the lower bench. In this step, the hierarchical clustering approach is employed. In the next step a Tabu Search procedure is applied to modify clusters in a way that the number of dependencies between the two levels and accordingly the number of constraints is reduced.

The idea of using penalty values has been borrowed from Marcos Dósea (2008) where a clustering algorithm called “Adaptive Mean-Linkage with Penalty” is introduced. In proposing this algorithm object oriented characteristics have been considered. In this concept each object is supposed to have different properties. These properties can vary from simple spatial locations to complicated computational problem specific values. These values can be divided into two main groups: categorical and numerical values. The only important point in comparing categorical properties is to see whether the properties are equal or not, opposed to numerical properties where the amount of difference is of importance. While calculating dissimilarity measure in Adaptive Mean-Linkage with Penalty algorithm, both of these types are considered and a penalty value regarding difference is assigned to each comparing property.

In the proposed algorithm, two numerical and two categorical properties are defined for each block. Spatial location and grade values are the properties where the amount of difference matters in contrast to rock type and the lower bench cluster.

The final clusters created using this procedure have to have four main characteristics:

1. Each cluster has to be spatially united which means if two blocks are the members of a cluster there should be a set of blocks in the same cluster connecting these together.
2. Ore and waste blocks should be grouped together for further planning and decision making.
3. Clusters consisting of one rock type are easier to deal with in scheduling phases.

4. One of the most important goals of the proposed clustering algorithm is to create clusters having a look at the lower bench in order to reduce the number of technical extraction dependencies. This is satisfied by defining a property called "beneath cluster" for each block. In addition, in the Tabu Search, the concept of "beneath cluster" is taken into account in measuring the goodness of each state.

At the first step of the procedure one of the parameters considered in defining the similarity measure is the similarity between the clusters beneath each block. This will make the algorithm to group the blocks at the top of one cluster together. This will reduce the number of technical extraction constraints between clusters. In the next step the Tabu Search also tries to modify boundaries of the clusters in a way that the overlap between clusters is reduced.

In order to use Tabu Search (TS) algorithm to find a good solution for clustering in each bench, an initial state solution is required to feed into the algorithm. The initial solution can be found via several means. In this paper, Hierarchical clustering algorithm is used to generate the initial state solution. In order to use the clustering algorithm, the similarity between each pair of blocks should be defined first. To do so, the following steps are considered.

4.1. Similarity definition

1. Calculate the distance matrix between all blocks in the active bench. Distance between blocks is calculated by Eq.(2):

$$D_{ij} = \sqrt{\left(x_i - x_j\right)^2 + \left(y_i - y_j\right)^2} \tag{2}$$

2. Calculate the rock type similarity matrix for all pairs of blocks in the active bench. Rock type similarity is calculated by Eq. (3) as assigning zero as the similarity between two blocks with different rock type and one, as the similarity between two blocks with same rock types.

$$R_{ij} = \begin{cases} 1 & \textit{if blocks } i \textit{ and } j \textit{ are from the same rock type} \\ r & \textit{otherwise} \end{cases} \tag{3}$$

3. Calculate the grade similarity matrix for all pairs of blocks in the active bench by Eq. (4).

$$G_{ij} = (G_i - G_j)^2 \tag{4}$$

Where G_i &G_j are grades of blocks i and j and G_{ij} is the grade similarity between these two blocks.

4. Calculate the beneath cluster similarity matrix for all pairs of blocks in the active bench. Beneath cluster similarity is calculated by assigning a number (less than one) as the similarity between two blocks which are above different clusters (in beneath bench) and one, as the similarity between two blocks which are above the same cluster. This is represented by Eq. (5).

$$C_{ij} = \begin{cases} 1 & \textit{if blocks } i \textit{ and } j \textit{ are above the same cluster} \\ c & \textit{otherwise} \end{cases} \tag{5}$$

5. Calculate the similarity matrix between all pairs of blocks in the active bench. Similarity between blocks i and j is defined by Eq. (6).

$$S_{ij} = \frac{R_{ij}^{W_R} \times C_{ij}^{W_C}}{G_{ij}^{W_G} \times D_{ij}^{W_D}} \quad (6)$$

As a result, the farther the blocks are from each other, the less similarity they have. In addition, the similarity between rock types, grades and beneath clusters of two blocks results in higher similarity between those blocks. By having the similarity matrix, it is possible to move forward to find out the initial state solution.

4.2. Hierarchical clustering algorithm:

Using the similarity matrix, the hierarchical algorithm can be described as:

1. Start by assigning each block to a cluster, so that if there are N blocks in the bench, there are N clusters, each containing just one block. Let the similarities between the clusters be the same as the similarities between the blocks they contain.
2. Find the most similar pair of clusters.
3. If clusters resulted from step 2 are neighbor (have common borders), then merge them into a single cluster, so that the number of clusters becomes one less and go to step 4. If not, ignore these clusters and return to step 2.
4. Compute similarities between the new cluster and each of the old clusters by considering the least similarity of new cluster members.
5. Repeat steps 2 and 3 until all blocks are clustered into a pre defined number of clusters.

The maximum number of blocks in each cluster is controlled in order not to have unequal sizes for clusters. The Hierarchical algorithm to find an initial state solution is presented as a flow chart in Fig. 1 (left).

4.3. Tabu search (TS)

Having the initial state solution, now the solution can be improved by applying the Tabu Search (TS). The following steps define our solution algorithm based on TS:

1. Determine the neighbors of each state through the following steps:
   1.1. Calculate the number of arcs each cluster has produced/caused (it is determined by looking at previous bench clusters (level 0) and counting the number of arcs each cluster at current bench (active level) has produced in respect to clusters of level 0). Sort the clusters in respect to the mentioned number of arcs.

   Choose m clusters which have produced more arcs (m first clusters from the sorted list of step 1.1).

   1.2. For each block in those m clusters selected in step 1.2, calculate the number of arcs that are caused by the block and sort the blocks with respect to this number.

   1.3. From top of the sorted list of step 1.3, choose n blocks which are on borders of the cluster.

   1.4. Consider all situations in which these n blocks are disconnected from previous clusters and connected to other neighbor clusters (there are at most 3 neighbor clusters for each of bordering blocks of a cluster). As the result, the maximum number of neighbors in each state is $m \times n \times 3$.

2. Update the goodness measure for all new clusters in new situation as defined by Eq. (7). This is the intra-cluster similarity measure:

$$ICM_i = \frac{1}{n_i^2} \sum_{i=1}^{n_i} \sum_{k=1}^{n_i} S_{jk} \quad (7)$$

Where

n_i : The number of block in cluster i

S_{ij} : The similarity between blocks j and k.

State measure is presented by Eq. (8).

$$SM_i = \frac{\overline{ICM}^{W_S}}{N^{W_N}} \tag{8}$$

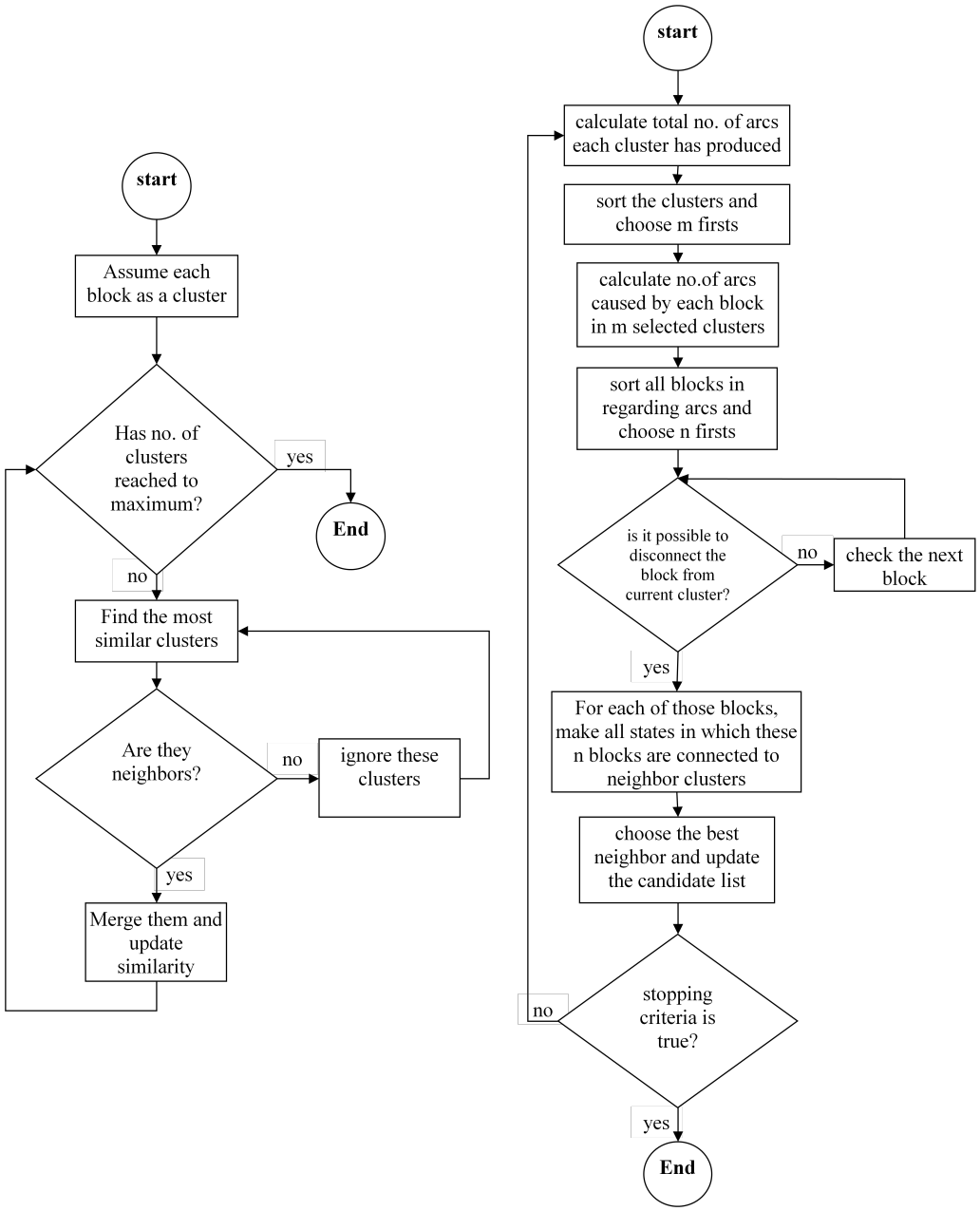

Fig. 1. Algorithm flow charts.

Where

$\overline{ICM}$: Average of all intra-cluster similarities

N : Total number of arcs

W_S : Weight of similarity

W_N : Weight of number of arcs

3. Update the candidate list by choosing the state with the maximum measure as the new member.
4. Repeat steps 1 to 3 until the stopping criteria happen.

Stopping criteria: number of candidate list members reaches to a pre-determined number or in *s* consecutive states, the best solution remains unchanged. The proposed TS algorithm is presented as a flow chart in Fig. 1 (right).

5. Numerical example

In order to show how the proposed algorithm works, the hierarchical clustering algorithm is applied to find the initial state solution to a simple example. The block model data is as presented in Table 1.

Table 1: Sample of block model data base

Block ID	X coordinate	Y coordinate	Rock type	Average grade	Beneath block
A	1	1	1	5.00%	1
B	2	1	1	4.00%	1
C	3	1	1	1.00%	2
D	4	1	2	0.50%	2
E	5	1	2	0.00%	2
F	1	2	1	4.50%	1
G	2	2	2	3.00%	1
H	3	2	2	2.00%	1
I	4	2	2	1.00%	2
J	5	2	3	0.90%	2
K	1	3	2	4.00%	1
L	2	3	3	5.20%	1
M	3	3	3	3.00%	1
N	4	3	2	2.00%	4
O	5	3	3	0.90%	2
P	1	4	2	3.00%	3
Q	2	4	1	4.00%	3
R	3	4	3	5.50%	4
S	4	4	2	5.10%	4
T	5	4	3	4.50%	4
U	1	5	2	1.00%	3
V	2	5	1	1.50%	3
W	3	5	1	2.00%	3
X	4	5	1	2.70%	4
Y	5	5	3	3.00%	4

For the sake of this problem, the beneath bench (level 0) is assumed to be clustered as presented in Figure 2(a). It is assumed that this level has 25 blocks on a regular grid of size 5×5. According to the data presented in Table 1, there are 25 blocks in the active bench, labeled 1 to 25. Furthermore, like the lower bench, they are assumed to be aligned in a regular 5×5 grid on the active bench. The sketches of grade distribution and rock types are presented in Fig. 2(b) and 2(c) respectively.

As it was mentioned in previous sections, some parameters are required in hierarchical clustering algorithm. These parameters are r, c, W_D, W_G, W_R and W_C. The parameters used in this example are presented in Table 2.

Table 2: Paremeters

W_D	W_G	W_R	W_C	r	c
1	1	1	1	0.8	0.2

The similarity matrix used in hierarchical clustering algorithm is presented in appendix A. The following sketch presented in Fig. 3(a) shows the initial state solution from hierarchical clustering algorithm. As the result of applying the hierarchical algorithm, five clusters are made in the last iteration. Applying the Tabu Search to improve the initial state solution has resulted in Fig. 3(b). After 8 Tabu Search iterations, the total number of arcs is reduced from 20 (as result of hierarchical) to 17.

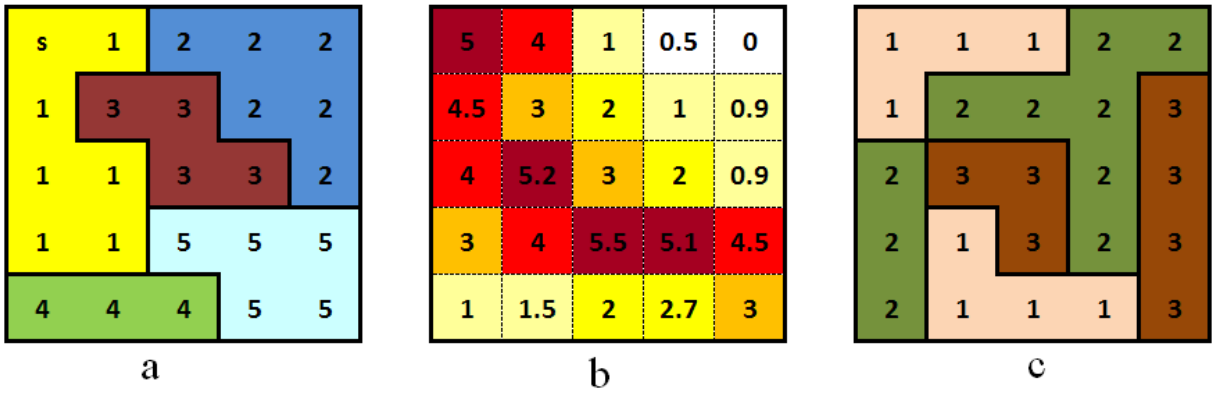

Fig. 2. (a): beneath clusters, (b): grade distribution, (c): rock types.

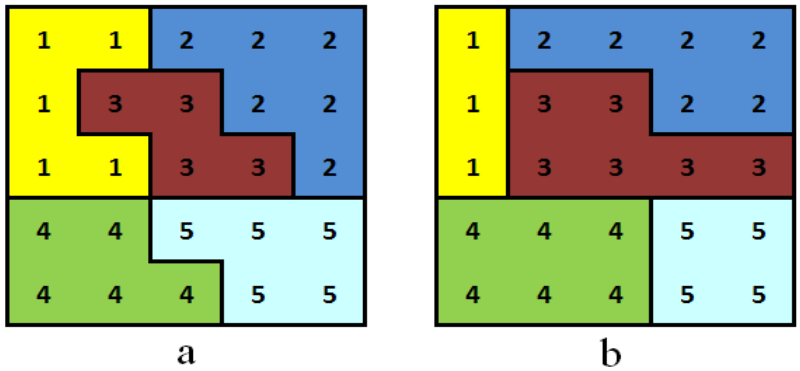

Fig. 3. (a): before Tabu Search, (b): after Tabu Search.

6. Illustrative examples

The proposed algorithm is applied to different data sets. Fig. 4 and Fig. 5 illustrate a gold, silver, and copper deposit. The blue section shows waste material and the red blocks illustrate ore. Another case is illustrated with an iron ore deposit, there are 2598 blocks in seven benches. The size of blocks is $50\times25\times25$ meters. The algorithm is executed by a MATLAB code. The plan views of the benches 13 and 14 showing the orebody and clusters created by hierarchical clustering and tabu search illustrated in Fig. 6 and Fig. 7.

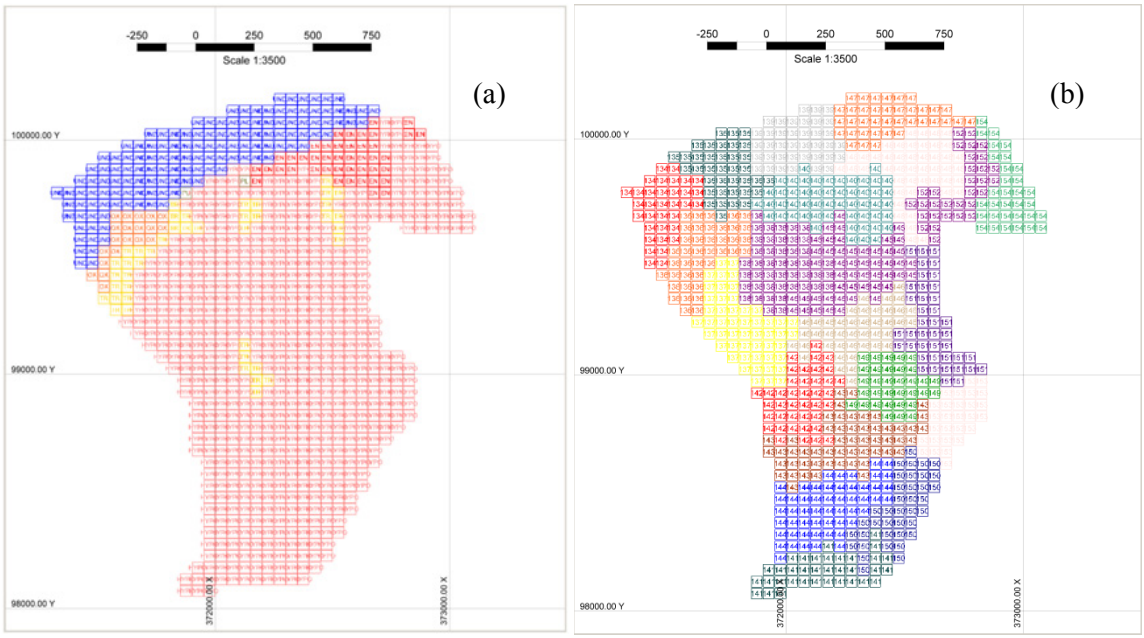

Fig. 4. Gold, Silver, Copper deposit, (a) rock type (b) mining-cuts.

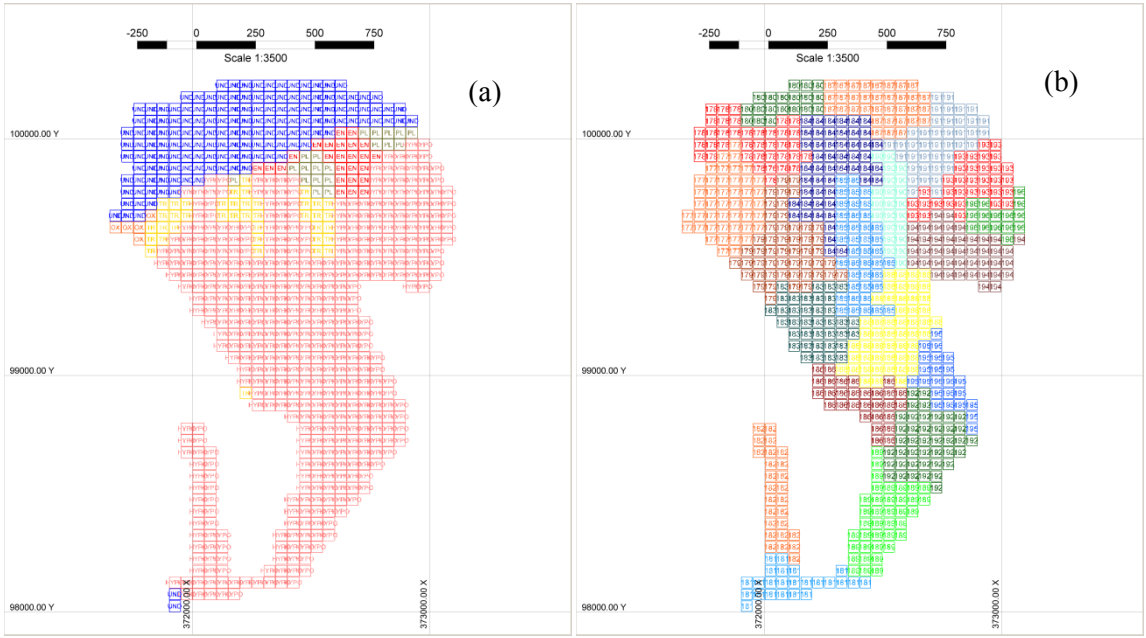

Fig. 5. Gold, Silver, Copper deposit, (a) rock type (b) mining-cuts.

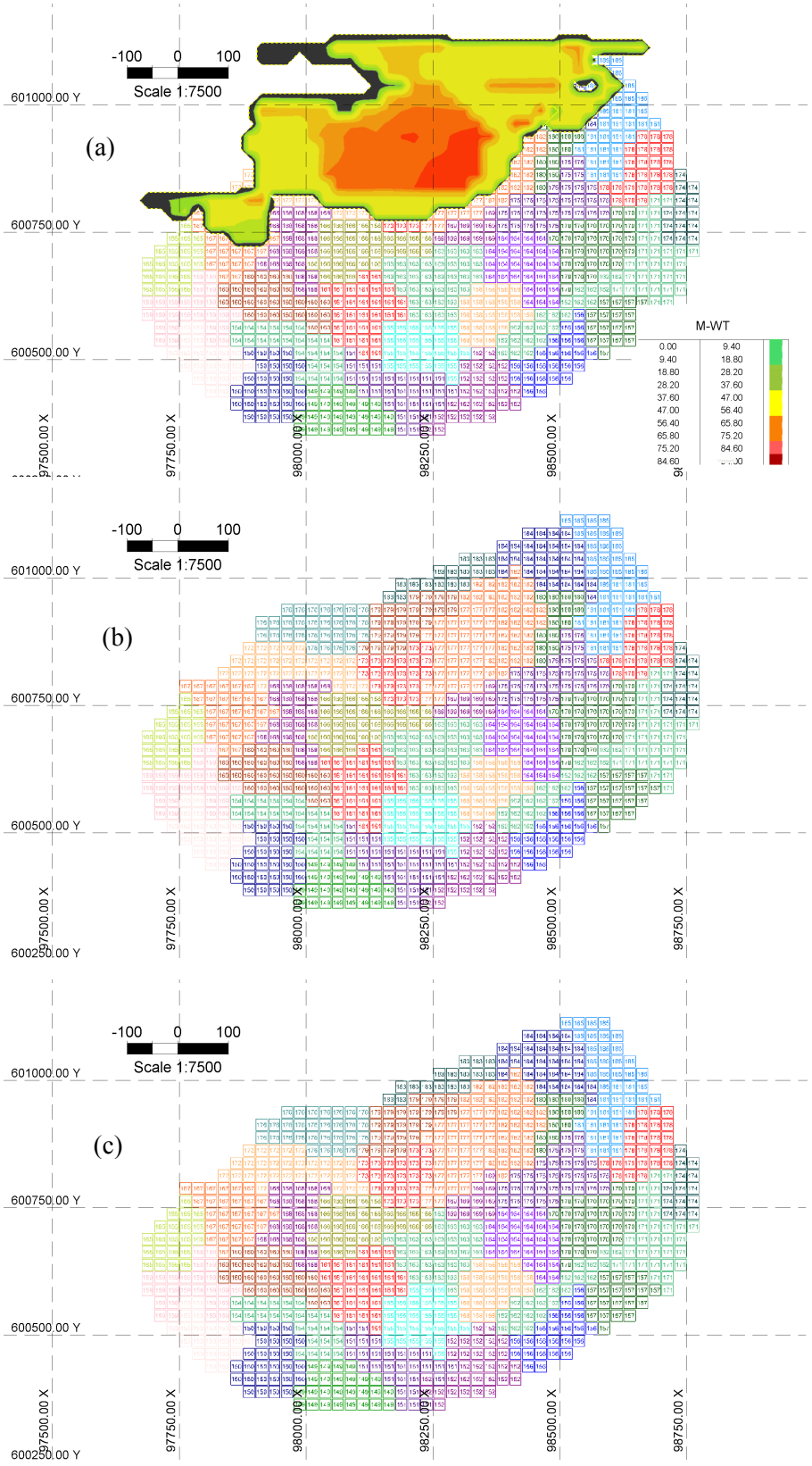

Fig. 6. Plan view of aggregated mining-cuts, bench 13,
(a) orebody, (b) hierarchical clustering, and (c) tabu search.

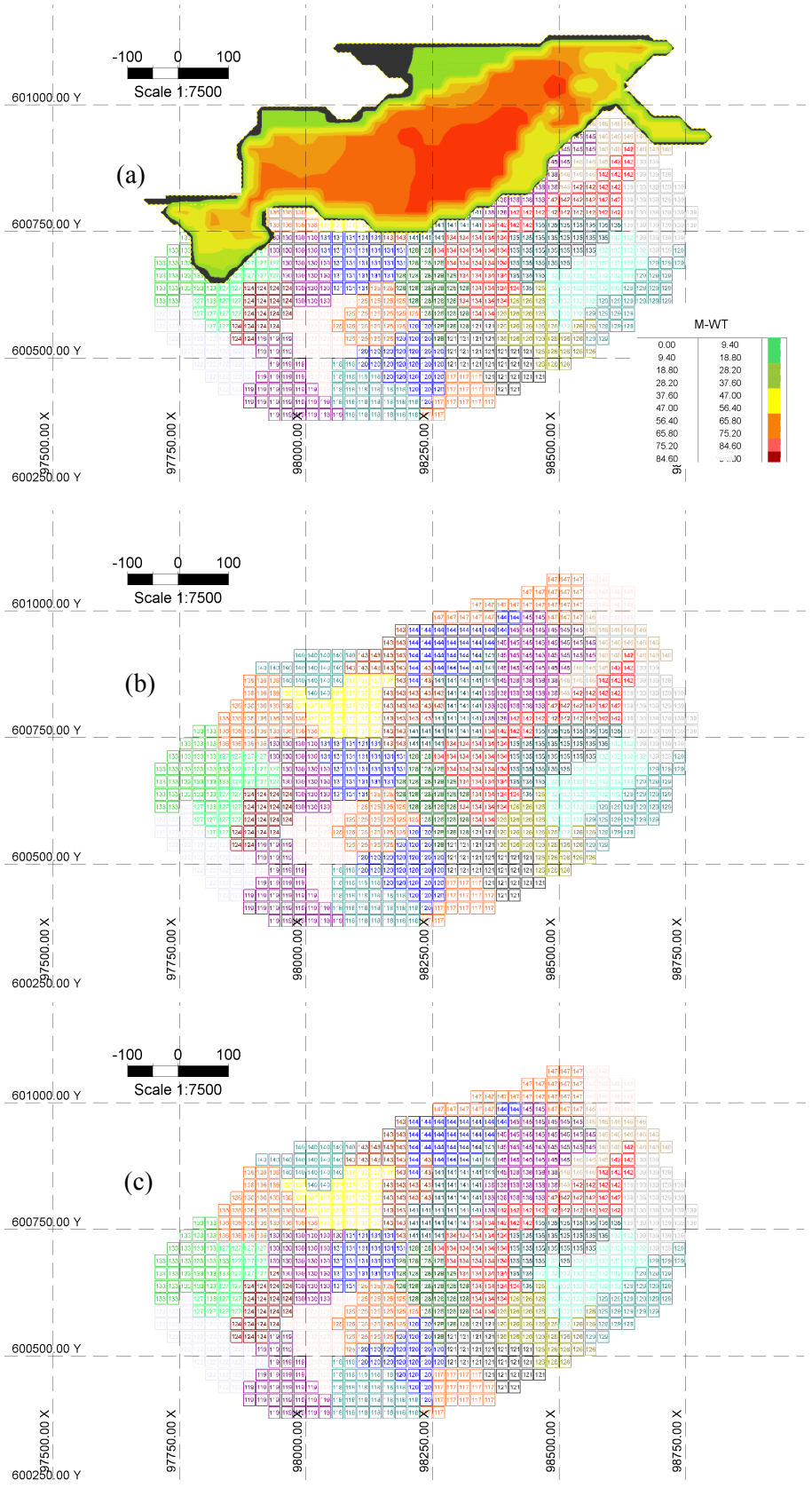

Fig. 7. Plan view of aggregated mining-cuts, bench 14,
(a) orebody, (b) hierarchical clustering, and (c) tabu search.

7. Conclusions

A meta-heuristic approach is developed, based on Tabu Search (TS), which aggregates the blocks into larger clusters in each mining bench representing a selective mining unit. The main objective of the developed clustering algorithm is to reduce the number of binary integer variables in the mixed integer linear programming formulation of open pit production scheduling problem. To achieve this goal, the blocks are aggregated into larger units referred to as mining-cuts. The definition of similarity among blocks is based on rock types, grade ranges, spatial location, and the dependency of extraction of a mining-cut to the mining-cuts located above it. The algorithm is developed and tested on synthetic data. As future work it seems relevant to fully integrate this clustering algorithm into an MILP mine production scheduling framework. The efficiency of the new platform can also be evaluated through case studies on large-scale open pit mines.

8. References

[1] Amaya, J. e. a. (2009). A scalable approach to optimal block scheduling.

[2] Askari-Nasab, H., & Awuah-offei, K. (2008). Mixed integer linear programming formulations for open-pit production scheduling. *Mining optimization laboratory (MOL)*,

[3] Boland, N., et al. (2009). LP-based disaggregation approaches to solving the open pit mining production scheduling problem with block processing selectivity. *Computers & Operations Research*, *36*,(4), 1064 - 1089.

[4] Gaupp, M. (2008). Methods for improving the tractability of the block sequencing problem for open-pit mining. PhD thesis Thesis, Colorado school of Mines, Golden,

[5] Johnson, S. C. (1967). Hierarchical Clustering Schemes. *Psychometrika*, *32*,(3), 241-254.

[6] Marcos Dósea, L. S., Maria A. Silva, Sócrates C.H. Cavalcanti (2008). Adaptive Mean-Linkage with Penalty: A new algorithm for cluster analysis. *Chemometrics and Intelligent Laboratory Systems*, *94*,(1), 1-8.

[7] Martinez, M. A. (2006). Improving the Performance of a Mixed-Integer Production Scheduling Model for LKAB's Iron Ore Mine, Kiruna, Sweden.Thesis, Colorado school of Mines, Golden, Pages 70.

[8] Newman, A. M., Kuchta, M. (2007). Using aggregation to optimize long-term production planning at an underground mine. *European Journal of Operational Research*, *176*,(2), 1205-1218.

[9] Organization, B. R. (2009). Optimization - Penalty Functions, Solving constrained optimization problems. ASAP TECHNICAL, Retrieved from: http://www.breault.com/k-base.php?kbaseID=252&catID=44

[10] Ramezan, S. (2007). The new Fundamental Tree Algorithm for production scheduling of open pit mines. *European Journal of Operational Research*, *177*,(2), 1153-1166.

[11] Stojmenovi´c, A. N. I. (2008). *Handbook of Applied Algorithms: Solving Scientific, Engineering and Practical Problems*. John Wiley & Sons, Inc.

9. Appendix

MATLAB code and documentation for hierarchical clustering and tabu search algorithms

A mathematical model for short-term open pit mine planning

Hesameddin Eivazy and Hooman Askari-Nasab
Mining Optimization Laboratory (MOL)
University of Alberta, Edmonton, Canada

Abstract

In this paper, a mixed integer model for the short-term scheduling of an open pit mine is formulated. The model includes a number of buffer stockpiles, waste dumps, and processes. The buffer stockpiles assist to smooth the process plant feed. Also, as blocks have different rock types, various processes and waste dumps are considered. In other words, extracted materials of blocks are sent to different destinations (waste dumps, processes, and stockpiles) based on their rock types. For validation of proposed formulation, a case study including 150 cuts are solved by CPLEX.

1. Introduction

One of the most important aspects of mine production planning is the short-term production planning/scheduling (Dimitrakopoulos and Ramazan, 2004). The objective of the short-term production scheduling is to determine the optimum sequence of extraction of blocks to meet the goals imposed by the long-term scheduling in each short-term period (output of long-term scheduling). In fact, the mine short-term production scheduling problem is the sequencing of each block's removal from the mine with respect to a variety of physical and economic constraints. Typically, these limitations are about to: the mining extraction sequence, mining, milling and refinery capacities, grades of mill feed and concentrates, and different operational requirements like minimum mining width (Caccetta and Hill, 2003).

On the other hand, one of the most challenging issues in the mine scheduling problems is the choice of solution methods. Typically, the short-term mine scheduling problems are complex. The complexities arise from the involvement of several continuous and binary variables and the large number of blocks to be extracted in the real-world problems. There are many research related to solution methods of the mine scheduling problems in the literature. These methods are not limited to but include:

1. Heuristics: Caccetta & Hill (2003) developed and implemented a graph-theoretic technique originally proposed by Lerchs and Grossman. They implemented a strategy including the application of a dynamic programming technique to "bound" the optimum. Also, Gershon (1987) proposed two heuristic methods; the first method is applicable in surface and underground mining with decisions on blending issues. Another method is applicable in general situations but mostly efficient in open pit mining problem.
2. Dynamic programming techniques: Tolwinski & Underwood (1996) proposed a model for the mine scheduling problem as a sequential optimization. Tolwinski & Underwood (1996) developed an algorithm for its solution. To overcome the difficulty related to large number states in the problem, they used a method based on the dynamic programming.

3. Mixed integer linear programming: Caccetta & Hill (2003) proposed a mix integer programming model for open pit mine scheduling problem. Also, Gershon (1983) developed a mixed-integer formulation, modeling the mine scheduling problem to optimize both the mine production sequencing and the mill blending and processing problems, simultaneously. Carlyle & Eaves (2001) formulated a maximization integer programming model for mining platinum and palladium at Stillwater Mining Company, which is able to reach near-optimal solutions without applying any special methods to lessen solution time.
4. And the applications of artificial intelligence algorithms: these algorithms include simulated annealing, genetic algorithms, and neural networks. For example, (Denby & Schefield (1995) applied the neural network algorithm in the mining context. Also, Denby et al. (1991) implemented the genetic algorithm in the underground mine scheduling.

Smith et al. (2003) created a production scheduling model for a copper and zinc underground mine at Mount Isa, Australia. The decision variables in Smith et al. (2003) model represent the time at which to mine each extractable production block with the objective of net present value maximization. The constraints were the operational constraints, e.g., ore availability, concentrator capacity, mine infrastructure production capacity, grade (mineral quality) limits, continuous production rules, and precedence relationships between production blocks. Also, Shu-xing and Peter (2009) surveyed the application of real options in the mining industry and proposed a framework developed at the University of Queensland, Australia, for integrating real options into medium/short-term mine planning and production scheduling. Their work introduced a new form of real option or mine planning flexibility, into medium/short-term mine planning and production scheduling processes. Also, Shu-xing and Peter (2009) demonstrated the method for valuation of these flexibilities based on the concept of real options. Basically, the uncertainty parameter considered in their paper is fuel price uncertainty. In addition, they used the approaches to estimate the values of the real options.

Classical methods are not successful to consider the risk of not meeting production targets caused by the uncertainty in estimated grades. Gap between planned expectations and actual production may occur in any steps of mining (Dimitrakopoulos and Ramazan, 2004). Vallee (2000) reported that 60% of the examined mines had an average rate of production that was less than 70% of the nominal capacity in early years. Rossi and Parker (1994) reported shortcomings against predictions of mine production in the later years of production. Dimitrakopoulos and Ramazan (2004) propose a method to integrate the grade uncertainties in optimization models. Their integrated model considers quantification of risk, equipment access, and other operational requirements. These operational requirements are blending, mill capacity, and mine production capacity. Godoy and Dimitrakopoulos (2004) proposed a method for risk-inclusive cutback designs, which yield fundamental NPV increases.

The organization of current paper is as follows: in section 2, the problem is defined in details. The theoretical framework of the proposed formulation, including definition of parameters, variables, and mathematical models are explained in section 3. In section 4 and 5, the proposed model is implemented and a case study for a year of mine production with 3089 blocks which have been clustered in 150 mining-cuts is presented. The conclusions and future work directions are presented in the section 6.

2. Problem definition

As mentioned in the introduction section, the problem is the short-term scheduling of an open pit mine. Fig. 1 shows the general schematic view of the problem. The problem is defined for an open pit mine including S buffer stockpiles, P processes, and W waste dumps. The mine has E elements, which one of them is considered as the major product. The role of buffer stockpiles is to hold

excess amount of ore extracted from the mine. The shortage of feed for the processes in different periods is balanced by reclaiming ore from buffer stockpiles, whenever required. In fact, in each period, an amount of ore is extracted from the mine with respect to the mining capacity and precedence limitations. A portion of this extracted ore is delivered to the processes directly. But, all processes cannot accept ore with all rock types. The remaining ore is delivered to the stockpiles. Also, the same procedure is valid for the waste dumps. Each waste dump accepts waste materials with specific rock-types. Therefore, the short-term scheduling of the open pit mine is making a decision about: (i) the amount of material (ore and waste) that must be extracted from the mine in each period, (ii) the destinations (waste dumps, stockpiles, and processes) that the mined materials are sent to, and (iii) also, the decision about the amount of ore reclaimed from the stockpiles to the processes in each period.

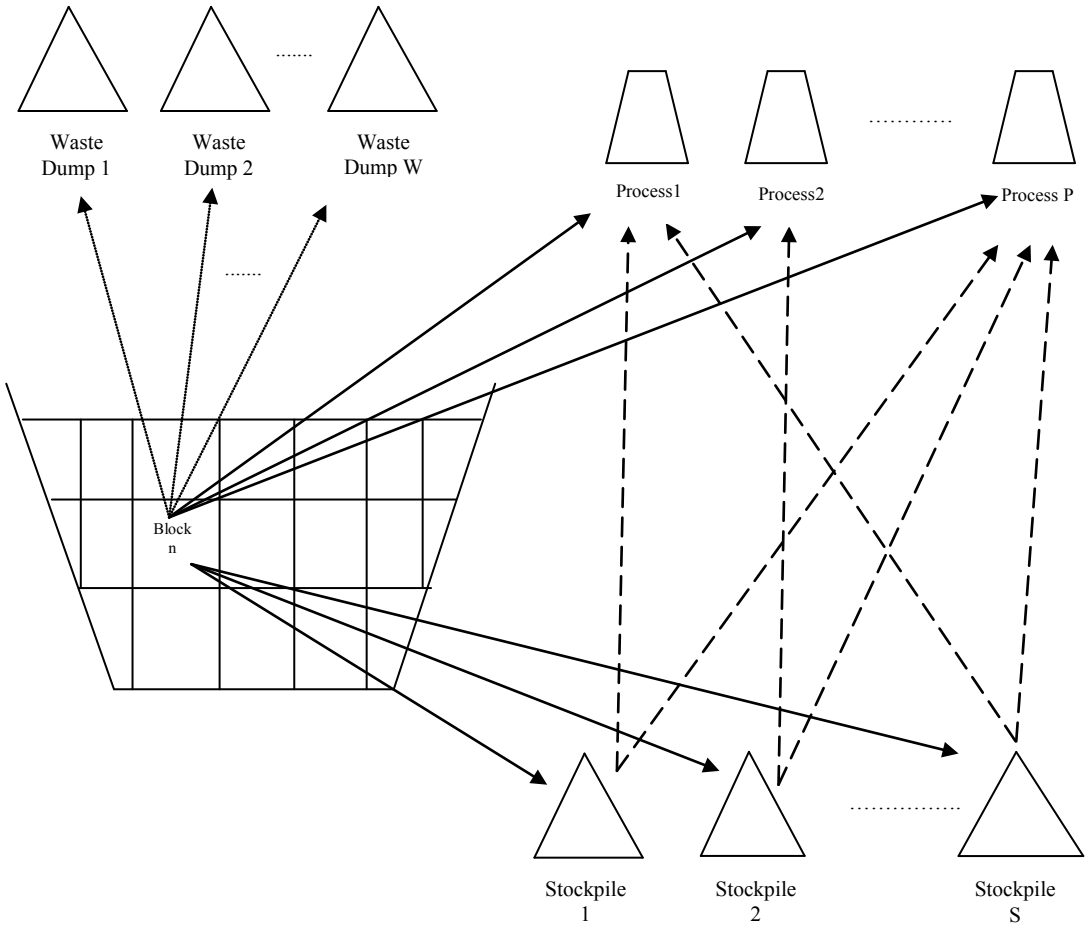

Fig. 1. Schematic view of the problem.

We assume that in the short-term horizon we have K periods with span of t. Also, from the long-term scheduling it has been determined that during K periods which blocks should be extracted from the mine. In the short-term scheduling we should decide about the amount and the time of extraction of each block in each period. There are some main assumptions in the problem. Briefly, these imposed assumptions are as follows:

- Each stockpile accepts ore from the mine with certain ranges of grade for different elements. In other words, the ore sent to each stockpile must have grades of elements within predefined ranges for that stockpile. We define stockpiles based on grade range bins.

- The grade of ore reclaimed from each stockpile is equal to the average grade of each element in that stockpile.
- Depending on the rock type of each block, the waste material of that block is sent to a certain waste dump.
- It is possible that some processes accept ore from specific stockpiles not from all of them.
- Stockpiles are classified based on rock types and grade ranges.

3. Theoretical framework and models

The proposed model is a short-term scheduling model with the objective of costs minimization with respect to physical and economic constraints. There are many parameters and variables in the model. Before presenting the formulation of the proposed model, it would be better to define these parameters and decision variables.

3.1. Parameters and decision variables

3.1.1 Parameters

1- t : period of scheduling ($t=1,\ldots,K$)
2- e : element e ($e=1,..,E$)
3- J(n) : set of blocks that must be extracted during the short-term time horizon
4- P(n) : set of processes that can receive ore from block *n*
5- SP(n) : set of stockpiles that can receive ore from block *n*
6- W(n) : set of waste dumps that can receive waste from block *n*
7- N : number of blocks in *J(n)*
8- C_m^t : unit mining cost in period *t*
9- $C_{wr}^{t,i}$: unit waste rehabilitation cost in period t for waste dump *i*
10- $C_p^{t,i}$: unit processing cost in period *t* for plant *i*
11- $RH_{SP,i}^t$: unit rehandling cost of stockpile *i* in period *t*
12- MU^t : upper bound of mining capacity use in period *t*
13- ML^t : lower bound of mining capacity use in period *t*
14- PU_i^t : upper bound of capacity of process *i* in period *t*
15- PL_i^t : upper bound of capacity of process *i* in period *t*
16- O_n : mineral zone tonnage of block *n*
17- R_n : rock tonnage of block *n*
18- g_n^e : grade of element e in block *n*
19- dE_n^i : distance of block n to exit passing from ramp *i*
20- $gu_e^{t,i}$: upper bound on acceptable grade of element e for process i in period *t*
21- $gl_e^{t,i}$: lower bound on acceptable grade of element e for process i in period *t*
22- PB(n) : set of precedent blocks of block *n*
23- $N_{PB(n)}$: number of blocks in set *PB(n)*

24- $R(n)$: set of ramps for block *n*

25- ME^t : minimum extraction of blocks in period *t*

26- $OG^e_{SP,i}$: grade of element e in the output ore of stockpile *i*

27- $UG^e_{SP,i}$: upper bound of grade of element e in received ore from mine for stockpile *i*

28- $LG^e_{SP,i}$: lower bound of grade of element e in received ore from mine for stockpile *i*

29- $C_{SP,i}$: Capacity of stockpile *i*

30- P(SP(i)) : set of processes that receive ore from stockpile *i* (destination for stockpile *i)*

31- SP(P(j)) : set of stockpile that send ore to process *j* (source for process *j)*

3.1.2 Decision variables

Decision variables are as follows:

1- u^t_n : fraction of block *n* extracted in period *t* ($n \in J(n)$)

2- $u^{t,i}_{n,W}$: fraction of block *n* extracted in period *t* and sent to waste dump *i* ($i \in W(n)$)

3- $u^{t,i}_{n,SP}$: fraction of block *n* extracted in period *t* and sent to stockpile *i* ($i \in SP(n)$)

4- $u^{t,i}_{n,P}$: fraction of block *n* extracted in period *t* and sent to process *i* ($i \in P(n)$)

5- b^t_n : binary variable, if block *n* is extracted in period *t* it gets value of 1 otherwise 0

6- $x^{t,i}_{n,r}$: amount of extracted material of block *n* in period *t* exit from ramp *i*

7- $b^{t,i}_{n,r}$: binary variable, if ramp *i* is selected for handling of amount of extracted material from block *n* in period *t*, it gets value of 1, otherwise 0

8- $y^{t,P,j}_{SP,i}$: amount of ore sent from stockpile *i* to process *j* in period *t* ($i \in SP(P(j))$ which is the set of stockpiles that send ore to process *j*)

9- $I^t_{SP,i}$: Inventory of stockpile *i* in period *t*

3.2. Formulation

After defining the parameters and variables of the model, the mathematical formulation of the proposed model is presented.

$$\begin{aligned} \text{Min } Z = & \underbrace{\sum_{t=1}^{k}\sum_{n=1}^{N} R_n \cdot u^t_n \cdot C^t_m}_{\text{total mining cost}} + \underbrace{\sum_{t=1}^{k}\sum_{n=1}^{N}\sum_{i\in P(n)} u^{t,i}_{n,p} \cdot R_n \cdot C^{t,i}_p + \sum_{t=1}^{k}\sum_{j=1}^{P}\sum_{i\in SP(P(j))} y^{t,p,j}_{SP,i} \cdot C^{t,j}_p}_{\text{total processing cost}} + \\ & \underbrace{\sum_{t=1}^{k}\sum_{n=1}^{N}\sum_{i\in W(n)} u^{t,i}_{n,w} \cdot R_n \cdot C^{t,i}_{wr}}_{\text{total waste rehabilitation cost}} + \underbrace{\sum_{t=1}^{k}\sum_{i=1}^{S}\sum_{j\in P(SP(i))} y^{t,p,j}_{SP,i} \cdot RH^{t,j}_{SP,i}}_{\text{total rehandling cost}} \\ & + \underbrace{\sum_{t=1}^{k}\sum_{n=1}^{N}\sum_{i\in R(n)} x^{t,i}_{n,r} \cdot dE^i_n \cdot H^t}_{\text{total haulage cost}} \end{aligned} \quad (1)$$

Subject to:

$$\sum_{t=1}^{k} u_n^t = 1,\ \forall n = 1...N \tag{2}$$

$$\sum_{i\in P(n)} u_{n,P}^{t,i} + \sum_{i\in SP(n)} u_{n,SP}^{t,i} + \sum_{i\in W(n)} u_{n,w}^{t,i} = u_n^t,\ \forall n = 1...N, \forall t = 1...k \tag{3}$$

$$R_n \cdot \sum_{t=1}^{k} \left(\sum_{i\in P(n)} u_{n,P}^{t,i} + \sum_{i\in SP(n)} u_{n,SP}^{t,i} \right) = O_n,\ \forall n = 1...N \tag{4}$$

$$u_n^t \le b_n^t,\ \forall n = 1...N, \forall t = 1...k \tag{5}$$

$$ME^t \cdot b_n^t \le u_n^t,\ \forall n = 1...N, \forall t = 1...k \tag{6}$$

$$ML^t \le \sum_{n=1}^{N} R_n \cdot u_n^t \le MU^t,\ \forall t = 1...k \tag{7}$$

$$PL_j^t \le \sum_{\forall n:P(n)=j}^{N} R_n \cdot u_{n,P}^{t,j} + \sum_{i\in SP(P(j))} y_{SP,i}^{t,P,j} \le PU_j^t,\ \forall t = 1...k, \forall j = 1...P \tag{8}$$

$$N_{PB(n)} \cdot b_n^t \le \sum_{\tau=1}^{t} \sum_{i\in PB(n)} u_i^\tau,\ \forall n = 1...N, \forall t = 1...k \tag{9}$$

$$gl_{e,P}^{t,j} \le \frac{\sum_{i\in SP(P(j))} y_{SP,i}^{t,P,j} \cdot OG_{SP,i}^e + \sum_{\forall n:P(n)=j} u_{n,p}^{t,j} \cdot R_n \cdot g_n^e}{\sum_{i\in SP(P(j))} y_{SP,i}^{t,P,j} + \sum_{\forall n:P(n)=j} u_{n,p}^{t,j} \cdot R_n} \le gu_{e,P}^{t,j},\ \forall t = 1...k, \forall j = 1...P, \forall e = 1...E \tag{10}$$

$$\sum_{\forall n:SP(n)=i} R_n \cdot u_{n,SP}^{t,i} - \sum_{j\in P(SP(i))} y_{SP,i}^{t,P,j} + I_{SP,i}^{t-1} = I_{SP,i}^t,\ \forall t = 1...k, \forall i = 1...S \tag{11}$$

$$\sum_{j\in P(SP(i))} y_{SP,i}^{t,P,j} \le I_{SP,i}^{t-1},\ \forall t = 1...k, \forall i = 1...S \tag{12}$$

$$LG_{SP,i}^e \le \frac{\sum_{\forall n:SP(n)=i} u_{n,SP}^{t,i} \cdot R_n \cdot g_n^e}{\sum_{\forall n:SP(n)=i} u_{n,SP}^{t,i} \cdot R_n} \le UG_{SP,i}^e,\ \forall t = 1...k, \forall i = 1...S, \forall e = 1...E \tag{13}$$

$$\sum_{j\in P(SP(i))} y_{SP,i}^{t,P,j} \le \frac{N_{SP,i}^{e,t-1} - LG_{SP,i}^e \cdot I_{SP,i}^{t-1}}{OG_{SP,i}^e - LG_{SP,i}^e},\ \forall t = 1...k, \forall i = 1...S, \forall e = 1...E \tag{14}$$

$$\sum_{j\in P(SP(i))} y_{SP,i}^{t,P,j} \le \frac{-N_{SP,i}^{e,t-1} + UG_{SP,i}^e \cdot I_{SP,i}^{t-1}}{-OG_{SP,i}^e + UG_{SP,i}^e},\ \forall t = 1...k, \forall i = 1...S, \forall e = 1...E \tag{15}$$

$$\sum_{i\in R(n)} x_{n,r}^{t,i} = R_n \cdot u_n^t,\ \forall n = 1...N, \forall t = 1...k \tag{16}$$

$$x_{n,r}^{t,i} \le M.b_{n,r}^{t,i},\ \forall n = 1...N, \forall t = 1...k, \forall i = 1...R(n) \quad (M \text{ is a large number}) \tag{17}$$

$$\sum_{i\in R(n)} b_{n,r}^{t,i} = b_n^t, \ \forall n = 1...N, \forall t = 1...k \tag{18}$$

$$0 \le u_n^t \le 1, \forall n = 1...N, \forall t = 1...k \tag{19}$$

$$0 \le u_{n,W}^{t,i} \le 1, \forall n = 1...N, \forall t = 1...k, \forall i \in W(n) \tag{20}$$

$$0 \le u_{n,P}^{t,i} \le 1, \forall n = 1...N, \forall t = 1...k, \forall i \in P(n) \tag{21}$$

$$0 \le u_{n,SP}^{t,i} \le 1, \forall n = 1...N, \forall t = 1...k, \forall i \in SP(n) \tag{22}$$

$$0 \le x_{n,r}^{t,i}, \quad \forall n = 1...N, \forall t = 1...k, \forall i \in R(n) \tag{23}$$

$$0 \le y_{SP,i}^{t,P,j}, \quad \forall t = 1...k, \forall i = 1...S, \forall j \in P(SP(i)) \tag{24}$$

$$0 \le I_{SP,i}^t \le C_{SP,i} \quad \forall t = 1...k, \forall i = 1...S \tag{25}$$

$$b_n^t \text{ and } b_{n,r}^{t,i} = 0/1, \forall n = 1...N, \forall t = 1...k, \forall i \in R(n) \tag{26}$$

Eq. (1) indicates the minimization objective function. This function includes the cost terms as follows:

1. Total mining cost: this cost contains the mining costs such as drilling, blasting and loading of material throughout *K* periods.
2. Total processing cost: this cost is the summation of processing costs of ore sent from mine directly or from stockpiles indirectly throughout *K* periods.
3. Total waste rehabilitation cost: this cost indicates the summation of costs for rehabilitation of waste dumps during *K* periods.
4. Total rehandling cost: this is the total cost incurred for handling of ore from stockpiles to different processes.
5. Total haulage cost: this is the total cost of haulage of materials from blocks to the exit of the mine.

Minimization of the abovementioned costs is under some constraints. These constraints have been reflected in Eqs. (2) to (26). Eq. (2) shows the constraints regarding to the complete extraction of all blocks. All blocks should be mined during *K* periods. Eq. (3) refers to this fact that the fraction of each block that is mined in each period is sent to different destinations. In other words, total extracted material from block *n* in each period goes to processes, stockpiles, and waste dumps. So far, decision variables u_n^t, $u_{n,w}^{t,i}$, $u_{n,SP}^{t,i}$ and $u_{n,P}^{t,i}$ can get every value. Constraint 3 imposes the relationship between these decision variables. Eq. (4) indicates that at the end of *K* periods, all of the mineralized material and waste material of each block should be mined completely. Eq. (5) defines the relation between the binary variable b_n^t and the continuous variable u_n^t. Whenever a portion of a typical block *n* is going to be mined, the respected binary variable b_n^t is set to 1. Eq. (6) refers to minimum extraction of blocks in each period. Based on this constraint, when the shovel extracts a block, it cannot extract a small portion of the block. In fact, it is not practical to extract a small fraction of a block. Thus, to avoid the very small extraction amounts, constraint 5 is used. Eq. (7) indicates the mining capacity limitation in each period. In each period the total mined rock tonnage should be in an acceptable certain range of values. This range reflects the capacity of mining by available equipments. Eq. (8) is the constraint of process capacity in each period.

According to this constraint, total ore sent to each process from mine and stockpiles should be in a certain range. Like mining constraint, this range is assigned by available capacity of processes in each period. Eq. (9) forces the precedence or slope constraints in which the extraction of each block can be start only when all blocks which are placed above that block directly are mined completely. To explain this constraint, suppose block (x) with 9 blocks above. According to precedence constraint concept, in each period the extraction of block x can be performed only when all of these 9 blocks have been extracted completely through the previous periods and current period. The right-hand side of Eq. (9) shows the summation of portions of all of these 9 blocks through the previous periods and current period. The value of this summation can equal to a value less than 9 or exactly 9. Less than 9 value means that all of 9 blocks above are not mined completely. Therefore, the extraction of block x cannot be started. By dividing the value of summation by 9, a value less than 1 would be obtained. This less than 1 value forces b_n^t to be 0. On the other hand, if the value of summation equals to 9, by dividing by 9, the value of 1 would be obtained which indicates that mining of block x can be start from this period. Eq. (10) indicates the head grade constraint of each process in each period. Based on this constraint, the average grade of each element in ore sent to each process in each period should be in a certain range which is determined by processes. Eq. (11) is the balancing of stockpiles inventory during time horizon. Total material that each stockpile receives in each period plus the current inventory minus the ore tonnage it sends to processes determines the inventory for the next period. Eq. (12) shows that the total ore sent from each stockpile in each period should be less than the inventory of that stockpile at the beginning of that period. Here, the assumption is that the ore is going to be sent from each stockpile to processes at the beginning of each period. As each stockpile stores ore with a certain grade for each element, Eq. (13) is the constraint on the values of grade of elements in ore sent to each stockpile. Eqs. (14) and (15) guarantee that after sending ore from each stockpile, the average grade of elements of ore inside that stockpile remains in the acceptable range. The following theorem shows that Eqs. (14) and (15) result in keeping the grade of elements in stockpiles between lower and upper bounds.

Theorem 1:

Fig. 2 indicates the procedure of reclaiming ore from a typical stockpile *i* in period *t*. As mentioned, the assumption is that reclaiming ore from stockpiles is done at the beginning of each period. Suppose the metal content for element *e* in stockpile *i* at the beginning of period *t* (or at the end of period *t*-1) is $N_{SP,i}^{e,t-1}$. Since the ore is sent with average grade $OG_{SP,i}^{e}$, the remaining metal content for element *e* is as follows:

$$N_{SP,i}^{e,t-1} - OG_{SP,i}^{e} \cdot \sum_{j \in P(SP(i))} y_{SP,i}^{t,P,j}, \quad \forall e = 1...E \tag{27}$$

Also, the remaining ore in stockpile *i* is as follows:

$$I_{SP,i}^{t-1} - \sum_{j \in P(SP(i))} y_{SP,i}^{t,P,j} \tag{28}$$

As the average grade of element *e* in ore stored inside the stockpile *i* should be between its predefined lower and upper bound, then

$$LG_{SP,i}^{e} \le \frac{N_{SP,i}^{e,t-1} - OG_{SP,i}^{e} \cdot \sum_{j \in P(SP(i))} y_{SP,i}^{t,P,j}}{I_{SP,i}^{t-1} - \sum_{j \in P(SP(i))} y_{SP,i}^{t,P,j}} \le UG_{SP,i}^{e}, \ \forall e = 1...E \tag{29}$$

After reorganization of Eq. (29), Eqs.(14) and (15) are obtained. It should be mentioned that the metal content of element *e* in stockpile *i* is calculated by Eq. (30).

$$N_{SP,i}^{e,t-1} = \sum_{\tau=1}^{t-1} \sum_{\forall n:SP(n)=i} u_{n,SP}^{\tau,i} \cdot R_n \cdot g_n^e + IMC_{SP,i}^e - \sum_{\tau=1}^{t-1} \sum_{j \in P(SP(i))} y_{SP,i}^{\tau,P,j} \cdot OG_{SP,i}^e \,, \quad \forall e = 1...E, \forall t = 1...K, \forall i = 1...S \tag{30}$$

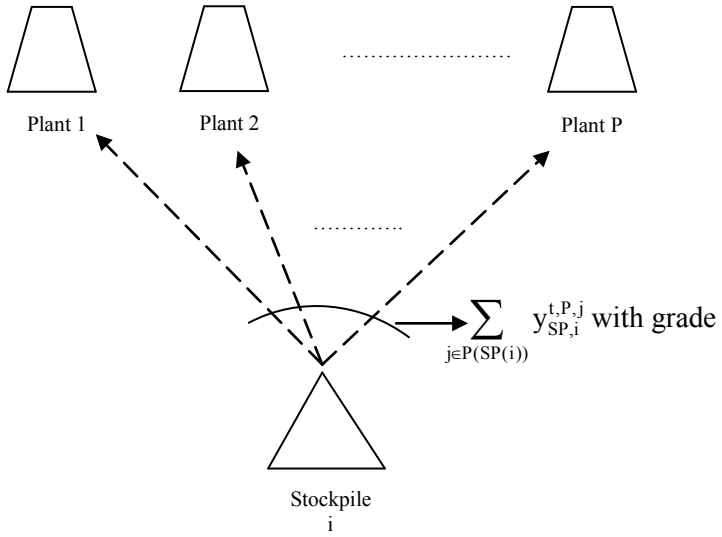

Fig. 2. Procedure of sending ore from stockpile *i* to processes.

In Eq. (30) the metal content of element *e* in period *t* for stockpile *i* is calculated by the summation of all received ore tonnages in the previous periods and the initial metal content of element *e,* minus the total ore tonnages that the stockpile have sent to the processes through the previous periods.

Eqs. (16) to (18) indicate that total extracted material from each block in period *t* is handled to one of the possible ramps. In other words, just one of possible ramp is selected for handling the material of each block. Eq. (16) means summation of material sent from block *n* to different ramps in each period equals to total extracted material from that block in that period. Eqs. (17) and (18) indicate the extracted material can be sent to only one of the possible ramps. Eqs. (19) to (26) represent the sign constraints regarding to decision variables. Among these constraints, Eq. (25) shows the limitation of storage for stockpiles.

4. Discussion and results

In this section, an illustrative example for short-term planning of an open pit mine is presented. The example refers to Gol-E-Gohar mines in south of Iran. The main element of this mine is Iron (Fe). The contaminants present are phosphor and sulfur. Fig. 3 shows the 3D view of one of the designed pit. The open pit has 20 benches. Only blocks of benches 14, 15, 16, and 17 are used for the purpose of short-term planning. These benches are scheduled over 12 months. The total number of blocks in these benches is 3089. These 3089 blocks are clustered into 150 mining-cuts using fuzzy C-mean method. We aggregate blocks for two reasons: (i) to reduce the number of variables in the MILP formulation, and (ii) to generate a schedule that follows a selective mining unit. For this pit, only one exit has been designed. Also, on average, two ramp accesses have been designed for each bench. For the four benches considered in this study, there are 7 ramp accesses. Table 1 represents the general information of the problem. All the blocks can be sent to all destinations. Stockpile 1 only feeds process 1 and Stockpile 2 feeds process 2.

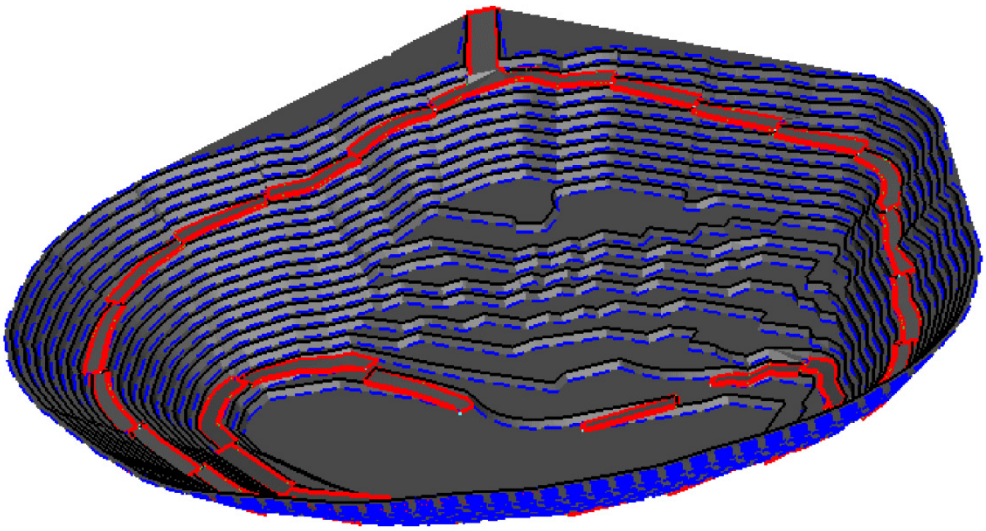

Fig. 3. 3D view of the open pit mine.

Table 1. General information of the problem.

	Bench Number			
	1	2	3	4
Number of blocks	614	726	820	929
Number of Cuts	30	35	40	45
Ramp access #	1 ,2	3, 4	5, 6	7
Total number of blocks	3089			
Total number of cuts	150			
Block size	25×25×15 ( )			
Total rock tonnage	93.8544 Million Tonnes			
Total mineral tonnage	47.4898 Million Tonnes			

For implementation of the proposed mathematical model, 6 destinations including 2 processes, 2 stockpiles, and 2 waste dumps are considered. Table 2 and Table 3 indicate the main specifications of these destinations. Material could be sent to any of the waste dumps.

Table 2. Processes main features.

Process	Lower grade			Upper grade			Min. capacity (tonne)	Max. capacity (tonne)
	MWT	S	P	MWT	S	P		
Process 1	0	0	0	1	1	1	1,000,000	2,000,000
Process 2	0	0	0	1	1	1	1,000,000	1,750,000

Table 3. Stockpiles main features.

Stockpile	Lower grade			Upper grade			Output grade			Max. capacity (tonne)	Initial inventory (tonne)
	MWT	S	P	MWT	S	P	MWT	S	P		
Stockpile 1	0.55	0	0	0.65	0.3	0.3	0.6	0.04	0.035	2,000,000	0
Stockpile 2	0.651	0	0	0.78	0.3	0.3	0.71	0.04	0.035	2,000,000	0

Unit costs are shown in Table 4. Fig. 5 to Fig. 8 illustrate sample plan views and cross sections of the generated schedule. Fig. 5 shows the plan view of the top level of the considered blocks while Fig. 6 illustrates the plan view of bench 17. Fig. 7 and Fig. 8 show the cross sections looking East and North, respectively. The values inside of these figures indicate the period that the maximum amount of extraction of blocks has occurred. For plan views, each cell has a size of 25m×25m and for Figs. 7 and 8, each cell has a size of 25m×15m. The optimum objective function shows the total costs including mining, haulage, processing, rehandling, and rehabilitation.

Table 4. Unit costs.

Processing 1 ($/tonne)	Processing 2 ($/tonne)	Rehandling 1 ($/tonne.m)	Rehandling 2 ($/tonne.m)	Waste rehabilitation 1 ($/tonne)	Waste rehabilitation 2 ($/tonne)
5.5	5.75	0.5	0.25	1.75	2

Fig. 4 shows the schedule of extraction during 12 periods. Based on this figure, almost the maximum capacities of mining equipments and processes are used with a small deviations.

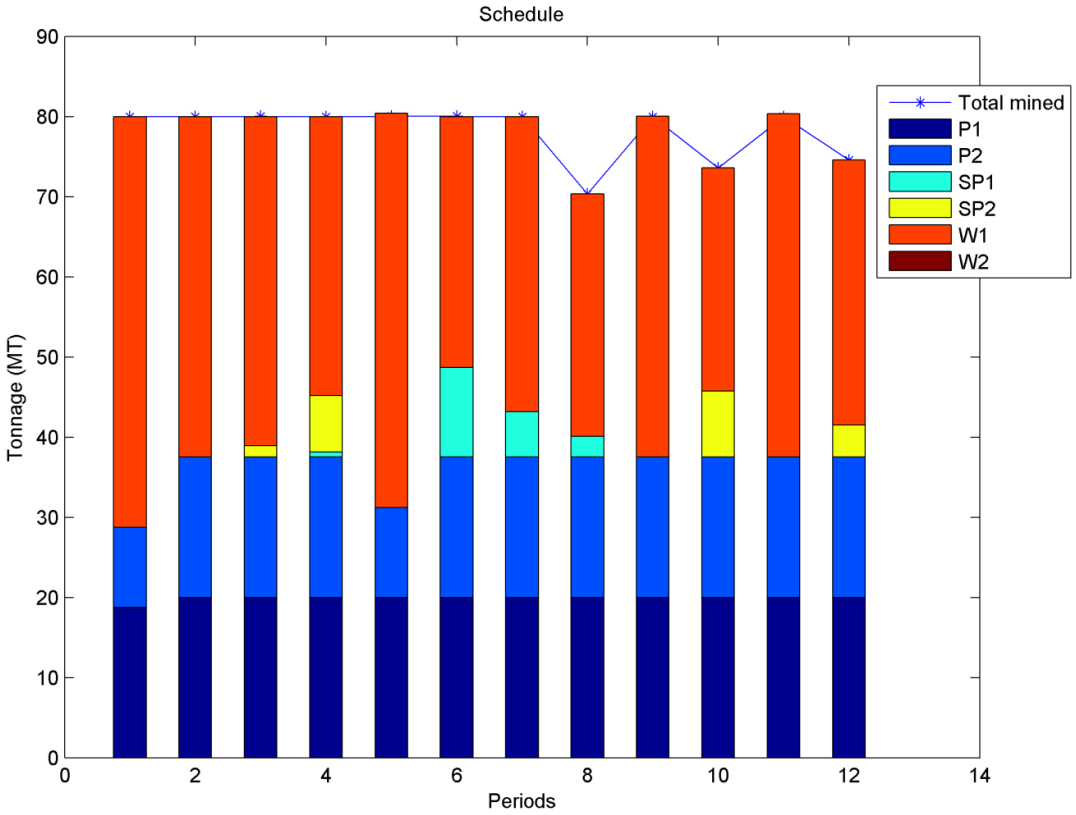

Fig. 4. Schedule of mine production during 12 periods.

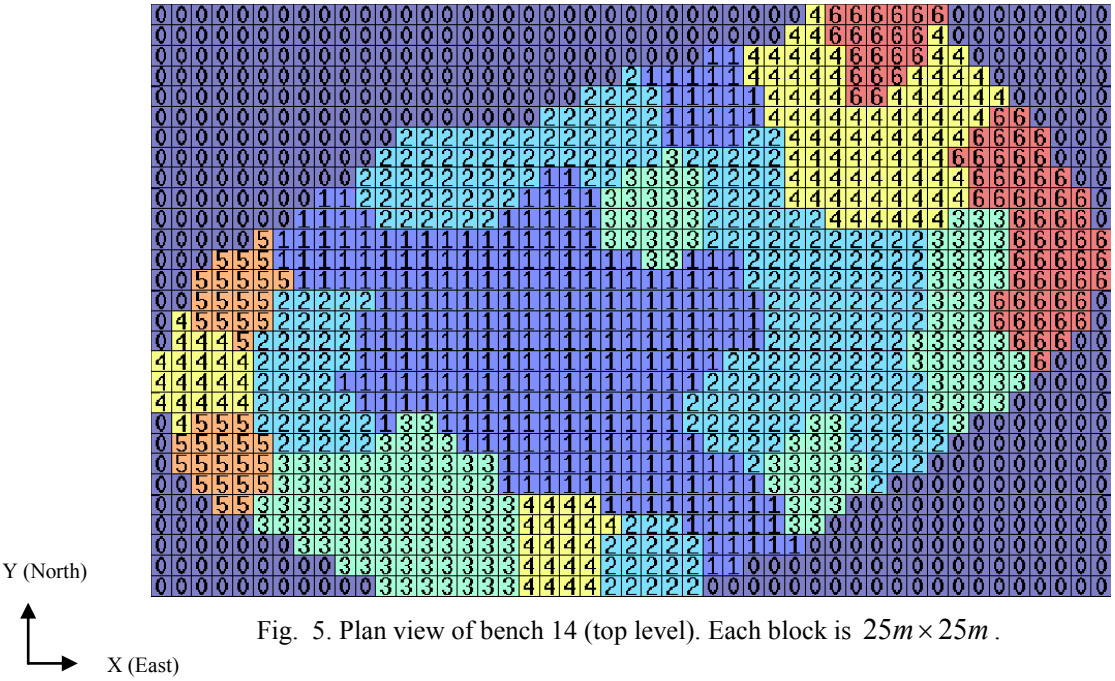

Fig. 5. Plan view of bench 14 (top level). Each block is $25m \times 25m$.

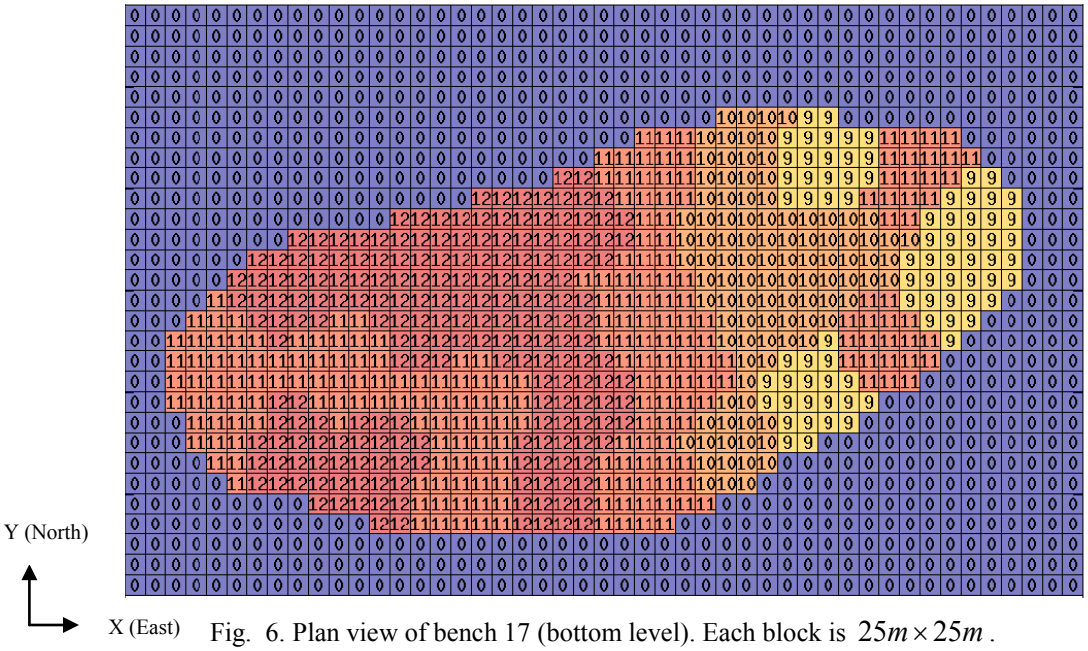

Fig. 6. Plan view of bench 17 (bottom level). Each block is $25m \times 25m$.

Fig. 7. Sample cross section looking East. Each block is $25m \times 15m$.

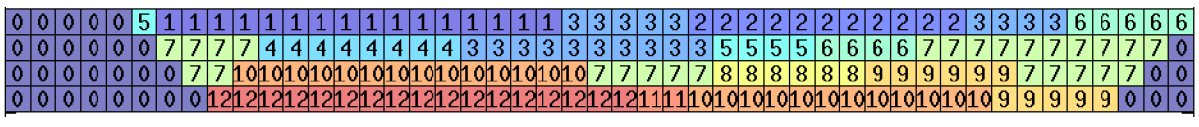

Fig. 8. Sample cross section looking North. Each block is $25m \times 15m$.

5. Conclusions and future work

Mine scheduling is a challenging problem in the mining industry. In this paper, a mixed integer model for the short-term scheduling of open pit mines is formulated and solved. The proposed model includes different destinations, processes, stockpiles, and waste dumps. Each process plant processes the received ore to produce the final product. The stockpiles are considered to keep extra mined ore for using in the next periods. The objective function of model aims to minimize the total costs incurred by mining and haulage, processing, rehandling, and waste rehabilitation. This function is subject to different mining operational constraints such as head grade blending, precedence constraints, etc. The proposed model is solved by CPLEX for a typical set of blocks in 4 benches.

6. References

[1] Caccetta, L. and Hill, S. P. (2003). An Application of Branch and Cut to Open Pit Mine Scheduling. *Journal of Global Optimization*, *27*, 349-365.

[2] Carlyle, M. and Eaves, B. (2001). Underground planning at stillwater mining company. *Interfaces*, *31*,(4), 50-60.

[3] Denby, B. and Schefield, D. (1995). *The Use of Genetic Algorithms in Underground Mine Scheduling*, in Proceedings of 25th APCOM Symposium of the Society of Mining Engineers, New York, pp. 389-394.

[4] Denby, B., Schefield, D., and Bradford, S. (1991). Neural Network Applications in Mining Engineering. in *Department of Mineral Resources Engineering Magazine,University of Nottingham*, pp. 13-23.

[5] Dimitrakopoulos, R. and Ramazan, S. (2004). Uncertainty based production scheduling in open pit mining. *SME Transactions*, *316*, 1-9.

[6] Gershon, M. (1983). Mine Scheduling Optimization with Mixed Integer Programming. *Mining Engineering*, *35*, 351-354.

[7] Gershon, M. (1987). Heuristic Approaches for Mine Planning and Production Scheduling. *International Journal of Mining and Geological Engineering*, *5*, 1-13.

[8] Godoy, M. C. and Dimitrakopoulos, R. (2004). Managing risk and waste mining in long-term production scheduling. *Transaction of SME*, *316*, 43-50.

[9] Rossi, M. and Parker, H. M. (1994). Estimating recoverable reserves - Is it Hopeless? in Geostatistics for the Next Century. in *Kluwer Academic*, pp. 259-276.

[10] Shu-xing, L. and Peter, K. (2009). Integration of real options into short-term mine planning and production scheduling. *Mining Science and Technology*, *19*, 0674-0678.

[11] Smith, M., Sheppard, I., and Karunatillake, G. (2003). *Using MIP for strategic life-of-mine planning of the lead/zinc stream at Mount Isa Mines*, in Proceedings of 31st International APCOM Symposium, Capetown, South Africa, pp. 465-474.

[12] Tolwinski, B. and Underwood, R. (1996). A Scheduling Algorithm for Open Pit Mines. *IMA Journal of Mathematics Applied in Business and Industry*, *7*, 247-270.

[13] Vallee, M. (2000). Mineral resource + engineering, economic and legal feasibility = ore reserve. in *CIM Bulletin*, vol. 90, pp. 53-61.

7. Appendix

MATLAB and CPLEX Code Documentation

Transfer of grade uncertainty into mine planning

Behrang Koushavand and Hooman Askari-Nasab
Mining Optimization Laboratory (MOL)
University of Alberta, Edmonton, Canada

Abstract

Uncertainty is always present because of sparse geological data. Conditional simulation algorithms such as Sequential Gaussian Simulation (SGS) and Sequential Indicator Simulation (SIS) are used to assess uncertainty in the spatial distribution of grades. Long-term mine planning and the management of future cash flows are vital for surface mining operations. Traditionally the long-term mine plans are generated based on an estimated input geological block model. Estimated or kriged models do not capture uncertainty and must be tuned to avoid biases. Mine plans that are generated based on one input block model fail to account for the uncertainty and its impact on the future cash flows and production targets. A method is presented to transfer grade uncertainty into mine planning. First, Sequential Gaussian Simulation is used to generate fifty realizations of an oil sands deposit. An optimum final pit limits design is carried out for each SGS realization while fixing all other technical and economic input parameters. Afterwards, the long-term schedule of each final pit shell is generated. Uncertainty in the final pit outline, net present value, production targets, and the head grade are assessed and presented. The results show that there is significant uncertainty in the long-term production schedules. In addition, the long-term schedule based on one particular simulated ore body model is not optimal for other simulated geological models. The mine planning procedure is not a linear process and the mine plan generated based on the krig estimate is not the expected result from all of the simulated realizations. The probability of each block being extracted in each planning period and the probability that the block would be treated as ore or waste in the respective period are calculated and can be used to assist in long range mine planning. Finally a stochastic linear programming model is presented to use all simulation realization in mine planning. This model tries to minimize negative effects of geological uncertainty and maximize the NPV simultaneously.

1. Introduction

Open pit production scheduling is the process of defining a feasible block extraction sequence that maximizes the net present value (NPV) of mining operation while meeting technical and economic constraints. There are three time ranges for production scheduling: long-term, medium-term and short-term. Long-term can be in the range of 20 – 30 years. This period is divided into several medium-term periods between 1 to 5 years. Medium-term schedules provide detailed information that allows for an accurate design of ore extraction from a special area of the mine, or information that would allow for necessary equipment substitution or the purchase of essential equipment. The medium-term schedule is also divided into 1 to 6 month periods (Osanloo *et al.*, 2008).

In this paper, the main focus will be on long-term production planning (LTPP) in open pit mines. LTPP determines the distribution of cash flow over the mine life, the feasibility of the project, and also it is a prerequisite for medium and short-term scheduling.

Uncertainty is inevitable with sparse geological data. Geostatistical simulation algorithms are widely used to quantify and assess this uncertainty. The generated realizations are equally probable and represent plausible geological outcomes (Journel and Huijbregts, 1981; Deutsch and Journel, 1998). Choosing one or some of these realizations does not realistically account for what might happen in the future. In addition, the uncertainty of ore grade in block models may cause discrepancies between planning expectations and actual production. Traditional production scheduling methods that use an estimated block model as the input into the scheduling process cannot capture the risk associated with production schedules caused by the grade variability. The majority of the current production scheduling methods used in industry have two major shortcomings: (i) the production scheduling methods are either heuristic based, or derived from the mine planner's experience; most of the current scheduling tools do not use global optimization methods, therefore the generated schedules are not necessarily optimal; and (ii) the inability to account for the grade uncertainty inherent within the production scheduling problem and as a result, there is no measure of the associated risk with the generated mine plans.

Effective open pit design and production scheduling is a critical stage of mine planning. The effects of pit design and scheduling and related predictions have major consequences on cash flows, which are typically on the order of millions of dollars. Open pit push-back design is commonly based on the well known Nested Lerchs-Grossman algorithm. This algorithm provides an optimal scenario of how an orebody should be mined given a set of geological, mining and economic considerations. Since 1965, several types of mathematical formulations have been considered for the LTPP problem: Linear programming (LP), mixed integer programming (MIP), pure integer programming (IP), dynamic programming (DP) and Meta-heuristic techniques.

All of these deterministic algorithms try to solve the LTPP problem without considering grade uncertainty.

Vallee (2000) reported that 60% of the mines surveyed had 70% less production than designed capacity in the early years. Rossi and Parker (1994) reported shortfalls against predictions of mine production in later stages of production. Traditional production scheduling methods that do not consider the risk of not meeting production targets caused by grade variability, cannot produce optimal results. Therefore, the common drawback of all deterministic algorithms is that they do not consider any type of uncertainty during the optimization process.

Dimitrakopoulos et al. (2001) show that there are substantial conceptual and economic differences between risk-based frameworks and traditional approaches. Some authors tried to use stochastic orebody models sequentially in traditional optimization methods. Dowd (1994) proposed a framework for risk integration in surface mine planning. Ravenscroft (1992) discussed risk analysis in mine production scheduling. He used simulated orebodies to show the impact of grade uncertainty on production scheduling. He concluded that conventional mathematical programming models cannot accommodate quantified risk. Dowd (1994) and Ravenscroft (1992) used stochastic orebody models sequentially in traditional optimization methods. However the traditional process cannot produce an optimal schedule considering uncertainty.

Godoy and Dimitrakopoulos (2003) and Leite and Dimitrakopoulos (2007) presented a new risk inclusive LTPP approach based on simulated annealing. A multistage heuristic framework is presented to generate a final schedule, which considers geological uncertainty so as to minimize the risk of deviations from production targets. A basic input to this framework is a set of equally probable scenarios of the orebody, generated by the technique of conditional simulation. They reported significant improvement on NPV in presence of uncertainty.

Leite and Dimitrakopoulos (2007) presented a proposed technique that for each of conditional simulation realizations, an optimum schedule is generated. Afterwards, using simulated annealing technique, a single schedule is generated based on all schedules, such that deviation from target production is minimized. The main drawback of simulated annealing method is that it merely finds an acceptably good solution in a fixed amount of time, rather than the optimum solution.

Dimitrakopoulos and Ramazan (2004) proposed a probabilistic method for long-term mine planning based on linear programming. This method uses probabilities of being above or below a cut-off to deal with uncertainty. The LP model is used to minimize the deviation from target production. This method does not directly and explicitly account for grade uncertainty and also does not maximize the NPV.

Dimitrakopoulos and Ramazan (2008) presented a stochastic integer programming (SIP) model to generate the optimal production schedule using equally probable simulated orebody models as input, without averaging the related grades. This model has a penalty function that is the cost of deviation from the target production and is calculated from geological risk discount rate (GDR) that is discounted unit cost of deviation from a target production. They use linear programming to maximize a function equal to NPV minus penalty costs. They concluded that the generated production schedule is the optimum solution that can produce the maximum achievable discounted total value from the project, given the available orebody uncertainty described through a set of stochastically simulated orebody models. The proposed scheduling approach considers multiple simulated orebody models without increasing the required number of binary variables and thus computational complexity.

The objective of this study is to: (i) present two methodologies to quantify the grade uncertainty transferred into production schedules; (ii) assess the impact of grade uncertainty on output parameters of mine production scheduling such as: NPV, ore tonnage, head grade, stripping ratio, amount of final product, and annual targeted production; and (iii) propose a mixed integer linear programming (MILP) formulation for optimal production scheduling that aims at maximizing the net present value while minimizing the deviations from targeted production, caused by grade uncertainty.

Kriging (Goovaerts, 1997; Deutsch and Journel, 1998) is used to estimate grades and construct the block model. Next, a final pit limit optimization study is performed using Lerchs and Grossmann (LG) (Lerchs and Grossmann, 1965) algorithm. Afterwards, a long-term life-of-mine production schedule is generated using Whittle software (Gemcom Software International, 1998-2008); this is referred to as the krig schedule throughout the paper.

Method 1- We use Sequential Gaussian Simulation (SGS) (Journel and Huijbregts, 1981; Goovaerts, 1997; Deutsch and Journel, 1998) is used to generate equally probable realizations of the orebody. An optimum final pit limit design is carried out for each SGS realization with the same technical and economic input parameters as used for the kriged model. Next, the long-term schedule of each final pit shell is generated. Uncertainty in the final pit outline, net present value, production targets, and the head grade are assessed and compared against the krig schedule. This process is labelled as method number one in Fig. 1.

Method 2- The optimal final pit limit and the krig production schedule are the basis of this approach. The same ultimate pit limit and the same krig schedule are applied to all the SGS realizations. This provides an assessment of the uncertainty in the production schedule. This process is labelled as method number two in Fig. 1.

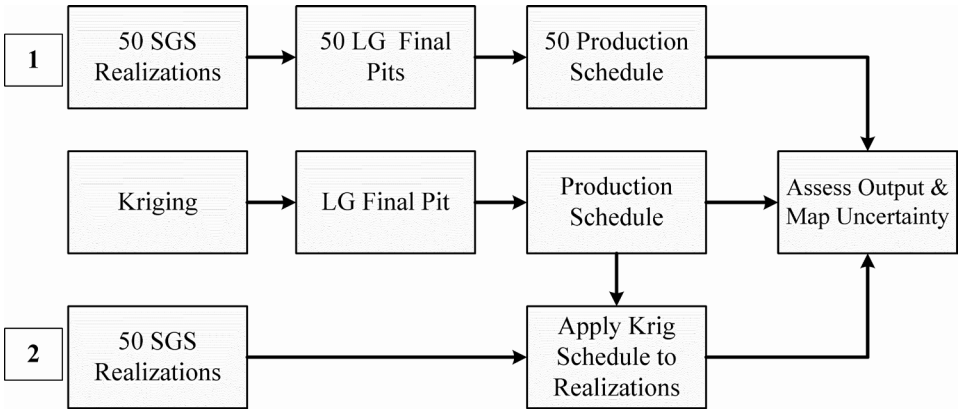

Fig. 1. Flow diagram of the study.

The results show that there is significant uncertainty in the long-term production schedules. In addition, the long-term schedule based on one particular simulated ore body model is not optimal for other simulated geological models. The mine planning procedure is not a linear process and the mine plan generated based on the krig estimate is not the expected result from all of the simulated realizations. The probability of each block being extracted in each planning period and the probability that the block would be treated as ore or waste in the respective period are calculated and can be used to assist in long range mine planning.

2. Methodology

The comparison of Method 1 and 2 and the respective results will be illustrated through a case study corresponding to an oil sands deposit in Fort McMurray, Alberta, Canada. In order to quantify the grade uncertainty transferred into the mine plans using Methods 1 and 2 the following steps are followed:

2.1. Geostatistical Modeling

A sufficient number of realizations must be considered for the purpose of mine planing; otherwise, there may be undue reliance on some stochastic features. The steps presented by Leuangthong *et al.* (2004) are followed for geostatistical modelling of an oil sand deposit using GSLIB (Deutsch and Journel, 1998) software catalogue to create conditional simulated realizations. The steps presented by Leuangthong et al. (2004) (see Fig. 2) are:

1. Analyze of correlation structure- This investigates whether a transformation of the vertical coordinate system is required, in order to determine the true continuity structure of the deposit. Determination of the correct grid is dependent on the correlation grid that yields the maximum horizontal continuity.
2. *Decluster drillhole data distribution*- The relevant statistics must be deemed representative of the deposit prior to modelling. Declustering may be employed to determine the summary statistics that are representative of the field.
3. *Variography*- Model the spatial continuity of the normal scores of the bitumen grade using variograms. Directional experimental variograms are calculated and fit. The Azimuths of major and minor directions are 50 and 140 degrees. Figure 3 shows the experimental and the fitted variogram models in major (Fig. 3a), minor (Fig. 3b) and vertical (Fig. 3c) directions.

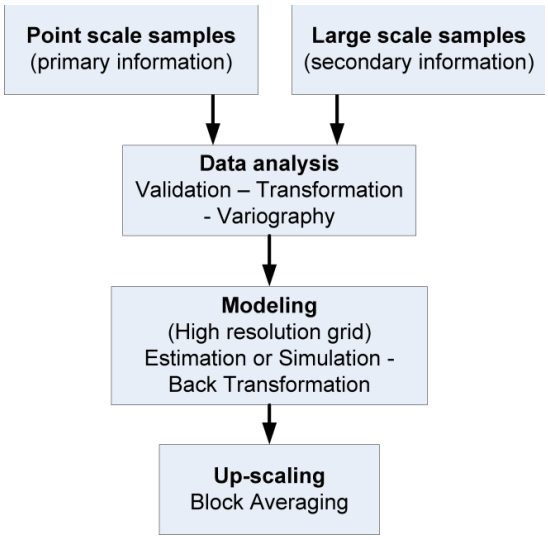

Fig. 2. Geostatistical modeling stages.

4. *Estimation*- Perform estimation and cross validation using kriging as checks against simulation results. Ordinary kriging is used to estimate the bitumen grade (with no normal score transform) at each block location.
5. Fig. 4a and 4b illustrate the map of the bitumen grade for the kriged and the E-type models. As expected, the E-type model is smoother than the kriged model. Multiple realizations of the bitumen grade are generated using Sequential Gaussian Simulation (SGS) (Isaaks and Srivastava, 1989) at a very high resolution three-dimensional grid at the point scale, this method is the means of constructing uncertainty models of bitumen grades.

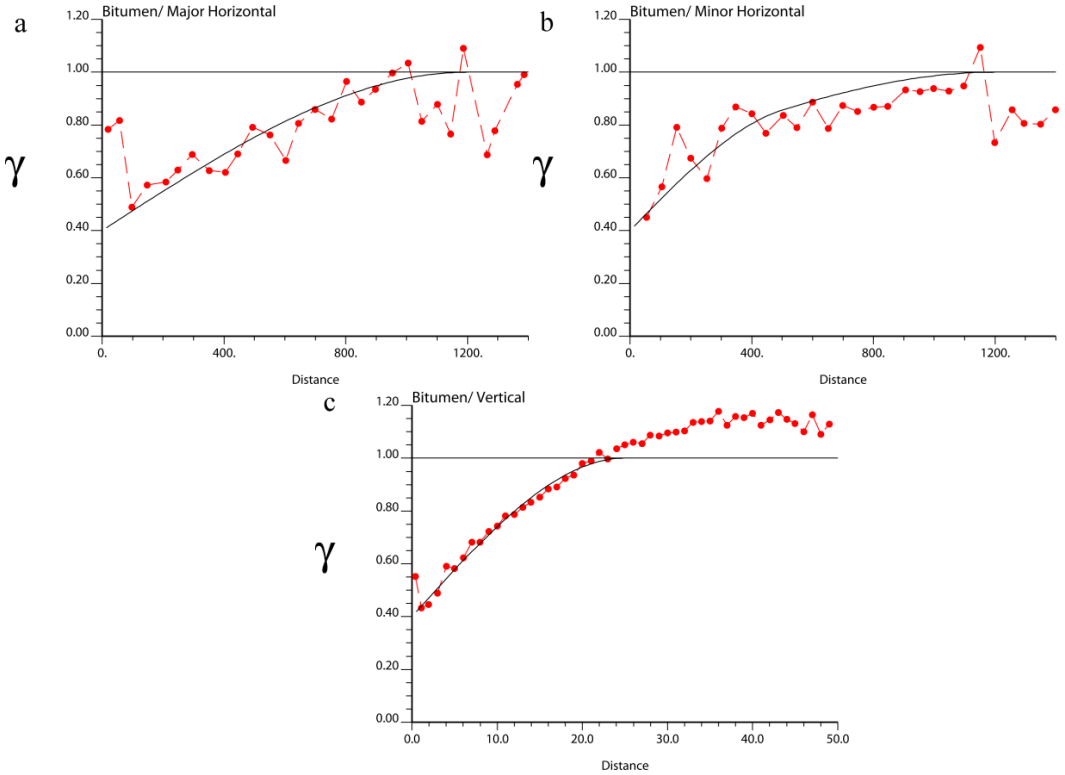

Fig. 3. Experimental directional variograms (dots) and the fitted variogram models (solid lines), distance units in meters.

6. Check simulation results against the input data and compare results against the Kriging model. We check the quality of geo-model by histogram and variogram reproduction. Fig. 5a to 5c show the variogram reproduction at major and minor horizontal, and vertical directions.
7. The block dimensions for mine planning are selected according to the exploration drilling pattern, ore body geology, mine equipment and anticipated operating conditions. The sizes of the blocks used in mine planning are a function of the selective mining unit (SMU). The high resolution grid is up-scaled to get the correct block scale values. Arithmetic averaging of point scale grades provides the up-scaled SMU grades (Fig. 2).

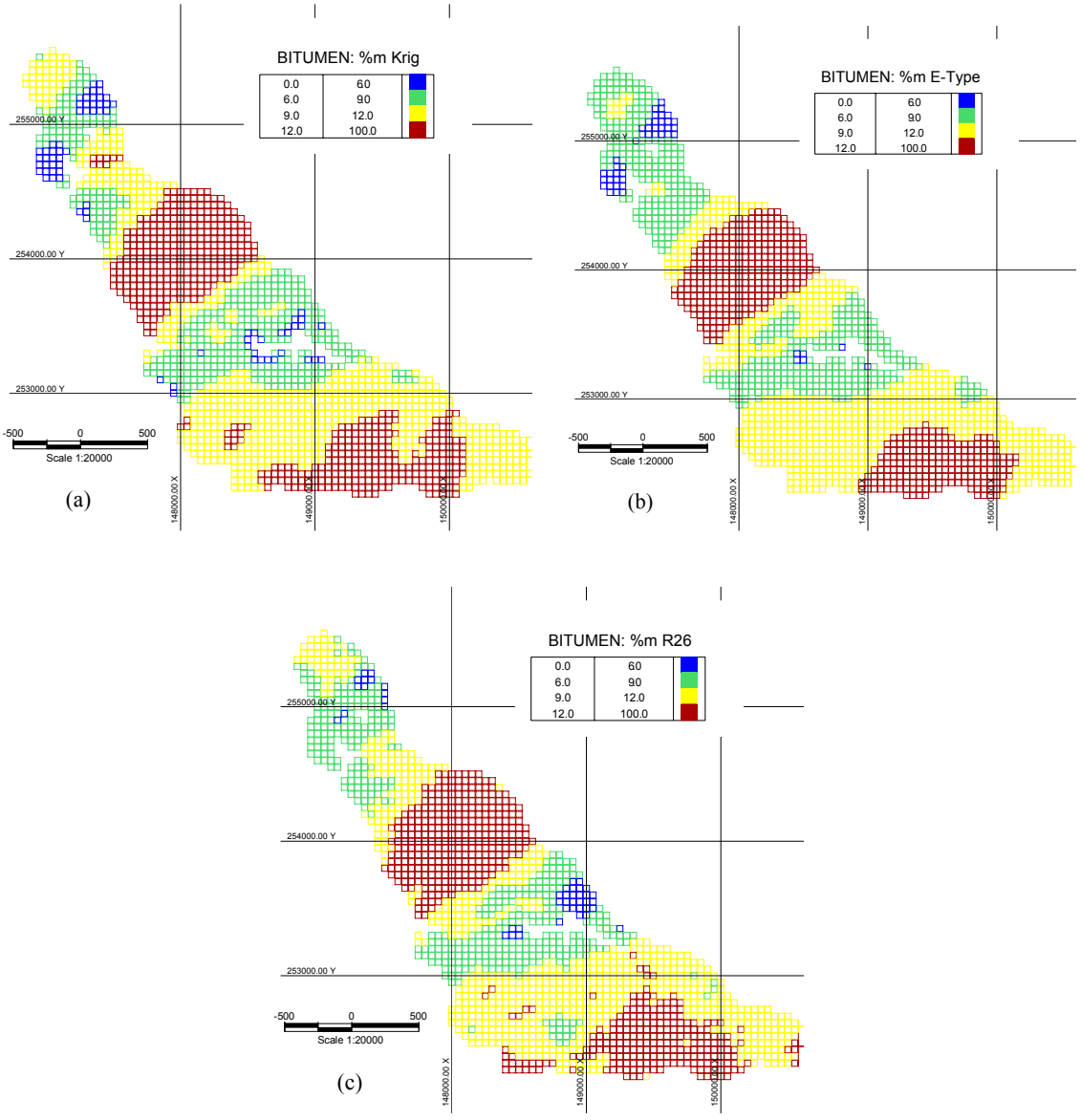

Fig. 4. Plan view at 260m; (a) Kriging model, (b) E-type model, (c) realization 26.

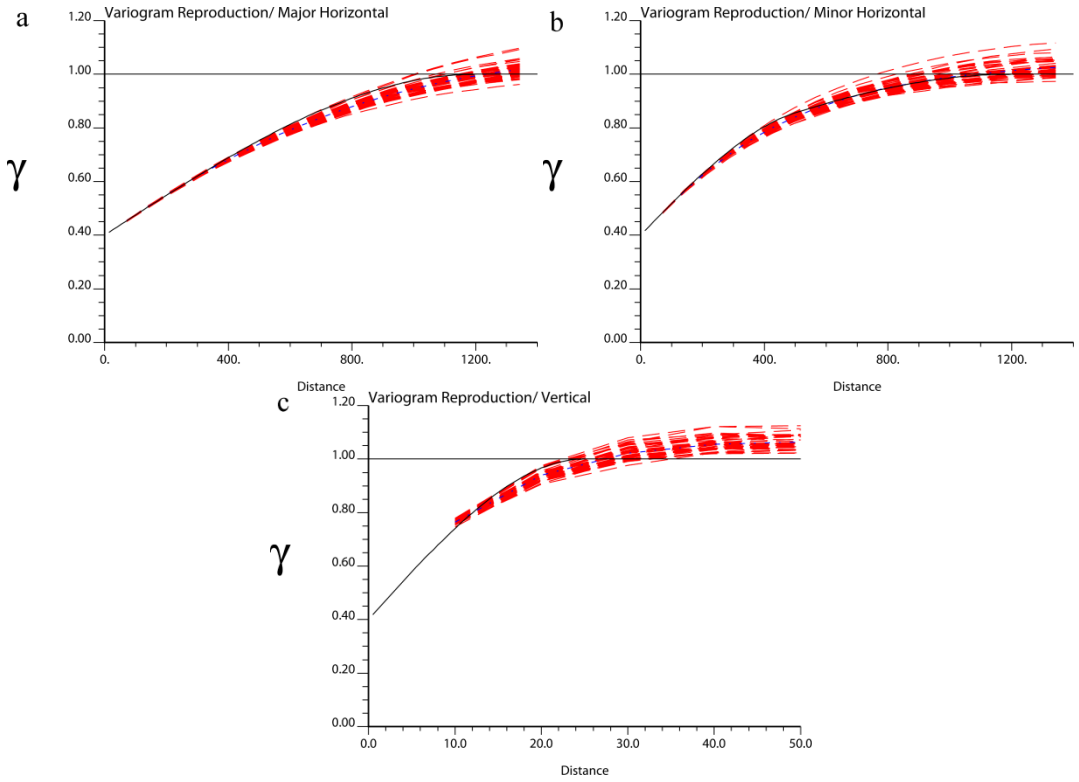

Fig. 5. Variogram reproduction of simulation realizations (red dash lines) and reference variogram model (black line).

2.2. Optimal final pit outline design

The final pit limit design is carried out based on the industry standard Lerchs and Grossmann algorithm (Lerchs and Grossmann, 1965) using the Whittle strategic mine planning software (Gemcom Software International, 1998-2008). The kriged, E-type, and fifty SGS realizations models are imported into the Whittle software. The ultimate pit limit design is carried out based on the Syncrude's costs in CAN$/bbl of sweet blend for the third quarter of 2008 (Jaremko 2009). Price of oil was considered US$45 with an exchange rate of 1.25:1 equal to CAN $56.25/bbl SSB for the same time period. We assume that every two tonnes of oil sands with an average grade of 10% mass will produce one barrel of sweet blend, which is approximately 200 kg. We also assume a density of 2.16 tonne/m³ for oil sands, and a density of 2.1 tonne/m³ for waste material, including clay and sand. Table 1 summarizes the costs used in the pit limit design. The mining cost of $12.18 is per tonne of oil sands ore, we assumed a stripping ratio of 1.8:1, and this would lead to a cost of $4.6/tonne of extracted material (ore and waste).

Table 1. Summary of costs used in pit limit design.

Description	Value	Description	Value
Mining Costs (CAN $/ bbl SSB)	24.35	Mining Costs (CAN $/tonne)	12.18
Upgrading Costs (CAN $/ bbl SSB)	10.05	Upgrading Costs (CAN $/tonne)	5.025
Others (CAN $/bbl SSB)	1.5	Others (CAN $/tonne)	0.75
Total Costs (CAN $/ bbl SSB)	35.9	Total Costs (CAN $/tonne)	17.28

Table 2. Final pit limit and mine planning input parameters.

Description	Value	Description	Value
Cutoff grade (%mass bitumen)	6	Processing limit (M tonne/year)	20
Mining recovery fraction	0.88	Mining limit (M tonne/year)	35
Processing recovery factor	0.95	Overall slope (degrees)	20
Minimum mining width (m)	150	Pre-stripping (years)	5

Table 2 shows the pit design and production scheduling input parameters. Thirty three pit shells are generated using 49 fixed revenue factors ranging between 0.1 to 2.5, based on the Kriging block model. The number of pit shells is reduced to 14 after applying the minimum mining width of 150 meters for the final pit and the intermediate pits. Table 3 summarizes the information related to the Kriging final pit limit at 6% bitumen cut-off grade. Fig. 6 illustrates the histogram of total tonnage of material within the optimal final pit limits. Ultimate pits are generated for each SGS realization. E-type and Kriging results are marked by a solid circle and a hollow circle respectively.

Table 3. Material in the final pit using the Kriging block model.

Description	Value
Total tonnage of material (M tonne)	653.61
Tonnage of ore (M tonne)	280.5
Tonnage of material below cutoff (M tonne)	37.4
Tonnage of waste (M tonne)	335.71
Bitumen recovered (M tonne)	27.52
Stripping ratio (waste:ore)	1.33

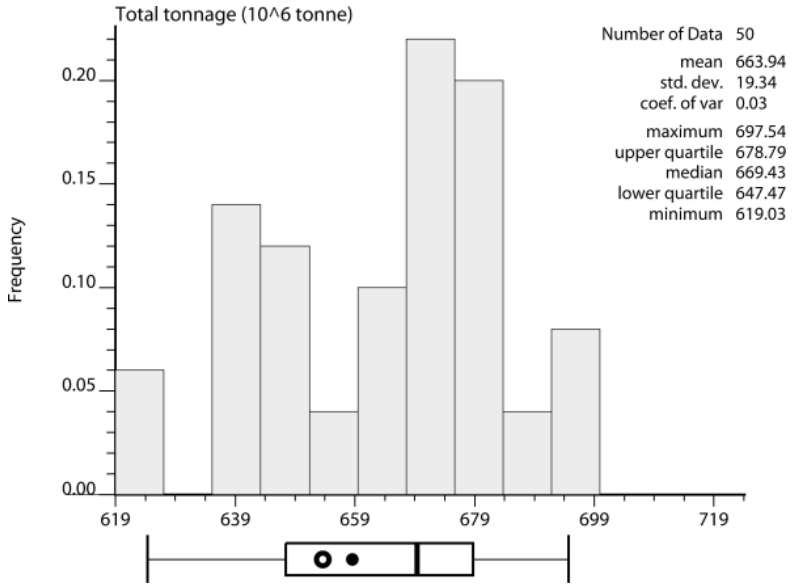

Fig. 6. Histogram of total tonnage of material within the final pit limits.

2.3. Production Scheduling

The kriged model is the basis for production scheduling. The aim is to maintain a uniform processing feed throughout the mine life. Four push backs are defined with a fixed lead of three benches between pushbacks. Five years of pre-stripping is considered to provide enough operating space and ore availability. No stockpile is defined and the target production is set to 20 million tonnes of ore per year with a mining capacity of 35 million tonnes per year. Figure 8 illustrates the kriged block model schedule over 21 years of mine-life. This schedule is the basis of Method 2. The schedule is applied to all the 50 SGS realizations within the krig fixed optimal pit limit. In Method 1, the final pit limits is designed for E-type model and all the fifty realizations with the exact same input variables.

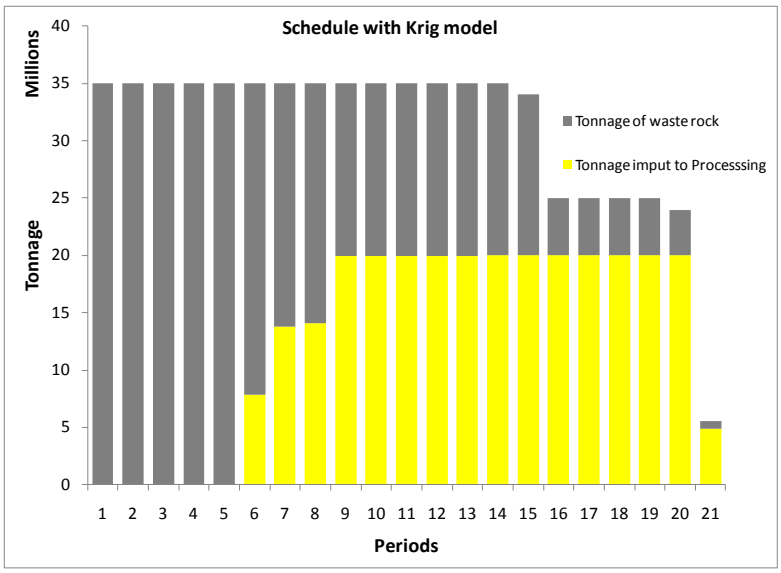

Fig. 7. Production schedule based on the Kriging block model.

3. Discussion of results

Conditional simulation enables us to provide a set of production scenarios, which capture and asses the uncertainty in the final pit outline, net present value, production targets, and the head grades. The realizations provide equally probable scenarios to calculate different outcomes in terms of NPV and production. The probability of each block being extracted in each planning period and the probability that the block would be treated as ore or waste in the respective period is calculated. The histograms and box plots for the following production schedule output variables are presented and discussed for Methods 1 and 2:

1. Overall stripping ratio.
2. Total tonnage of ore.
3. Average grade of ore.
4. Net present value.

Fig. 6 illustrates the uncertainty within the final pit limits. The krig final pit (the hollow circle) has 653 million tonnes, which is less than the average amount of 663 million tonnes, recorded for the simulation realizations. The inter quartile limits are 647 and 678 million tonnes. The stripping ratio of the krig pit is 1.33 (Fig. 8b), which is near the 1.35 stripping ratio of the lower quartile of the simulation realizations. As expected, Method 1 has a larger standard deviation compared against Method 2 (Fig. 8).

Fig. 9 shows the histogram and box plot of ore at final pit. The amount of ore in the kriged and Etype models is close when different schedules are generated for each of them (Fig. 9a). The tonnage of ore in the kriged model is almost the same as Etype where the same schedule is followed (Fig. 9b).

The histogram of average input grade to the mill for kiging (solid circle), Etype (hollow circle) and SGS realizations are presented in Fig. 10. The average grade of the kriged model is more than the Etype model and also it is higher than the third quartile of the realizations of both methods. The grade uncertainty is clearly illustrated in this figure. The average grade of the Etype is less than kriged model and even less than lower quartile of average grade of realizations.

Fig. 11 Figure 12 shows the input average head grade for each period. Kriged model (bold solid line), Etype model (bold dashed line) and the simulation realizations (dashed lines). As expected, the grade fluctuations of the first method (Fig. 11a) are greater than second method (Fig. 11b).

Histogram and box plot of produced ore is showed in Figure 13. 27.52 million tonnes of bitumen is produced by kriged block model. 26.86 and 26.97 million tonnes of bitumen was produced by Etype model for method 1 and 2 respectively. The kriged block model produced more bitumen than third quartile of realizations at both method.

Fig. 13 shows the tonnage of feed to the plant. The deviation from target production is also presented in Fig. 14. There are under productions at first years for each of two methods. In addition, in first method, we have hard constraint for upper limit of plant feed, there is no over production for each of realizations (Fig. 13a). When the same schedule is followed for each of realizations, at some realizations, there are overproduction between years 8 to 16 (Fig. 13b). One should take into account that the shortfall in production has happened although we have used five years of pre-stripping. The effect of the grade uncertainty on the production targets would be more severe if the pre-stripping strategy was not adopted.

Fig. 14 illustrates the box plot for the plant feed, the percentage deviation from the target production, and the probability that we would not meet the target production. There is a relatively high probability to not meeting the target production at first and last years of mine life. If the krig schedule would be followed, the probability of not meeting the target production for some middle age of mine life will be increase. There is a 1.2 and 2.1 percent probability of not meeting the target production for years 13 and 14 respectively.

Fig. 15 shows the histogram of cumulated discounted cash flow. E-type and krig results are marked by solid circle and hollow circle respectively. NPV of kriged block model is 847 million dollars, where the NPV of Etype method is 724 and 780 million dollars for method 1 and 2 respectively. The NPV of kriged model is also more that third quartile of realizations.

Fig. 16 illustrates the discounted cash flow over the years. Cumulative discounted cash flow for 50 realizations and the kriged and Etype models are showed by dashed lines, solid line and dashed blue line respectively. The optimum final pit limit is calculated for each realization; therefore, there are some realizations that the mine life is 22 years, where for most realizations, kriged and the Etype model the mine life is 21 years (Fig. 16a). In method 2, the same schedule as kriged model is followed. Therefore the mine life is 21 years for all realizations and Etype model (Fig. 16b).

Fig. 17 shows the box plot of discounted cash flow for all realizations. Kriging model is showed by solid line and dashed line is used for E-type model. The probability of meeting the NPV from Kriging model is also presented. As it is clearly illustrated, based on 50 realizations, there is very low chance to reach the NPV of Kriging model for each period. There is not any realization at first method to exceed the NPV of Kriging model. Where, there is only one realization (2%) that exceeds the final NPV of Kriging model for second method (Fig. 17b). This graph shows generated schedule based on the kriging model and generally based on only one block model can produce unrealistic and unachievable NPV in present of grade uncertainty.

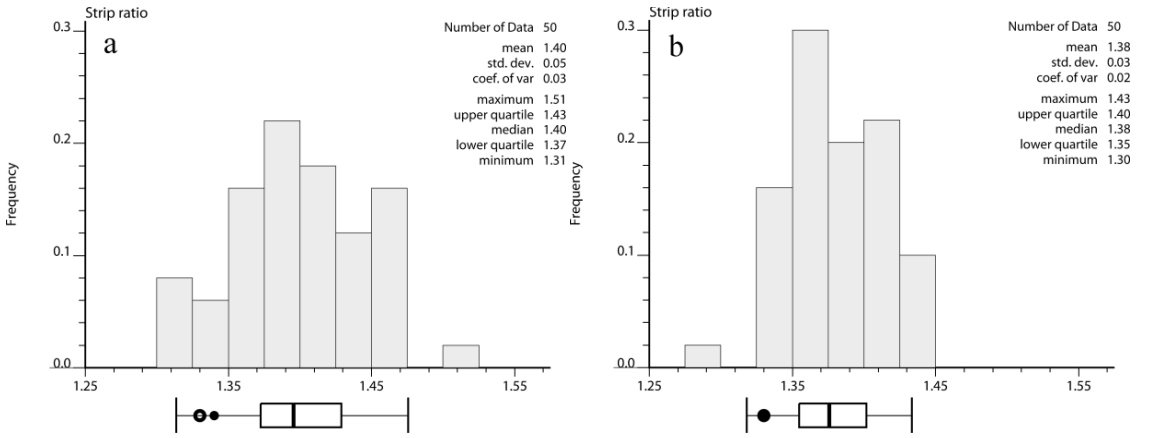

Fig. 8. Histograms and box plots of overall stripping ratio. (a) schedules are generated for each block model separately. (b) Kriging schedule applied to all realizations. E-type and Kriging results are marked by solid circle and hollow circle respectively.

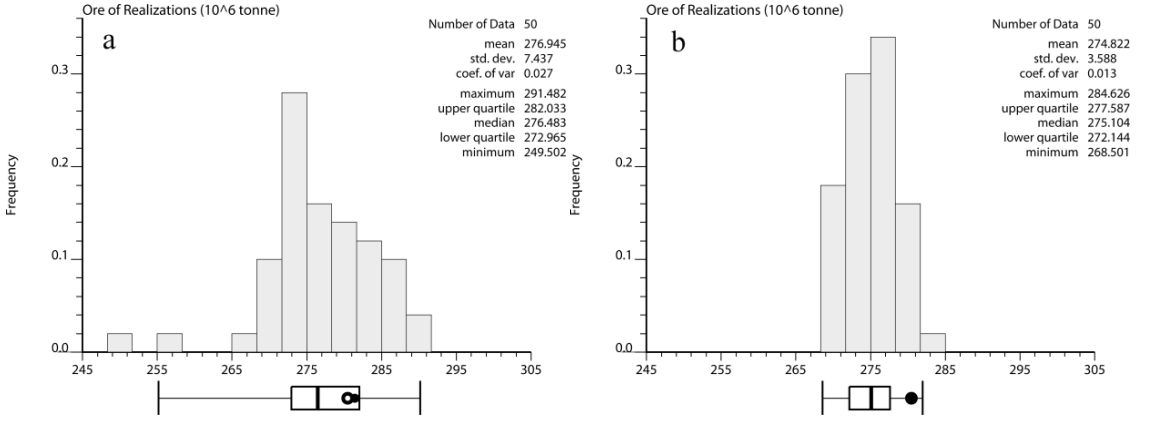

Fig. 9. Histograms and box plots of total tonnage of ore. (a) schedules are generated for each block model separately. (b) Kriging schedule applied to all realizations. E-type and Kriging results are marked by solid circle and hollow circle respectively.

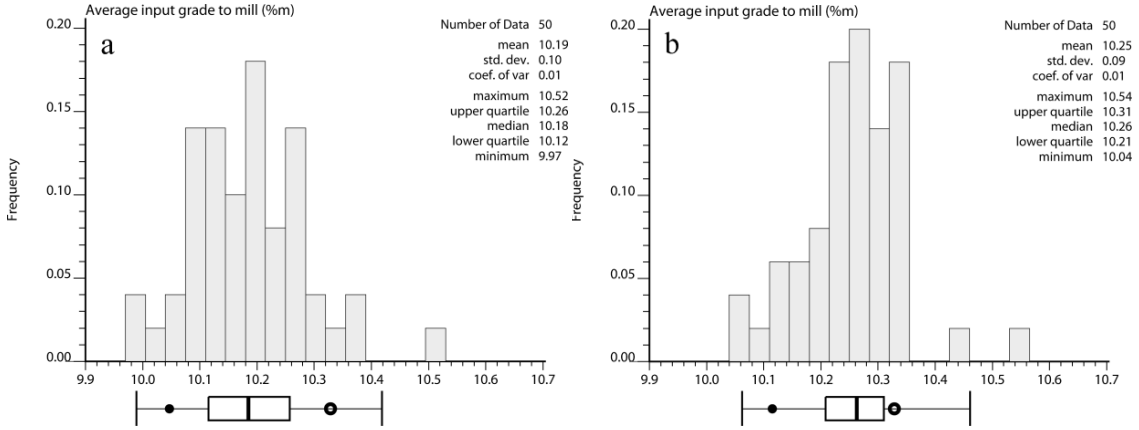

Fig. 10. Histograms and box plots of average head grade in bitumen %mass. (a) schedules are generated for each block model separately. (b) Kriging schedule applied to all realizations. E-type and Kriging results are marked by solid circle and hollow circle respectively.

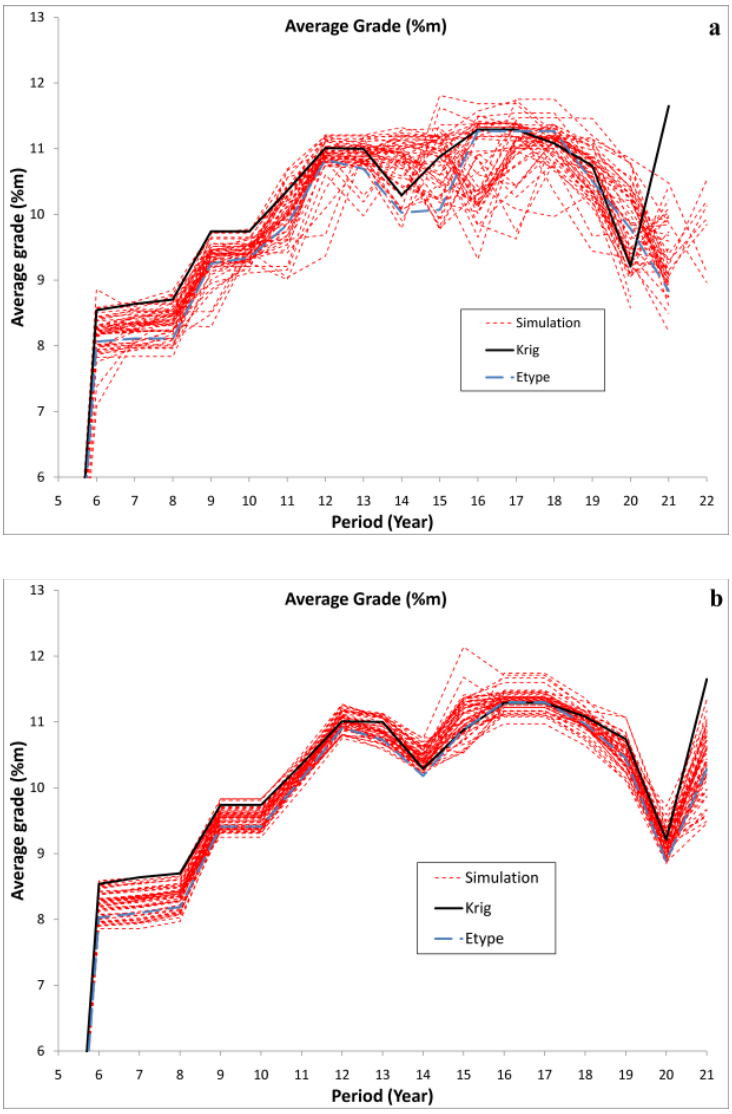

Fig. 11. Head grade simulation realizations, Kriging, and E-type models. (a) schedules are generated for each block model separately. (b) Kriging schedule applied to all realizations. Kriging result is marked by solid line.

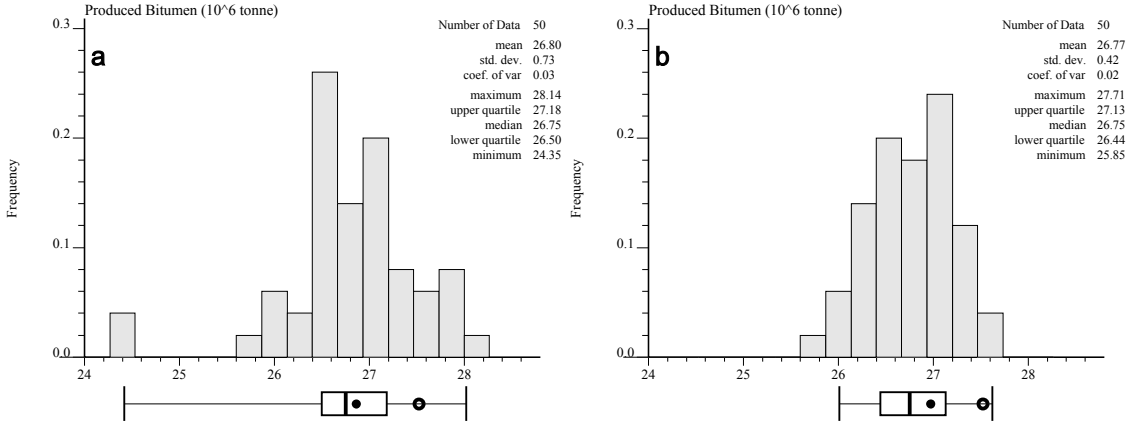

Fig. 12. Histograms and box plots of tonnage of bitumen produced. (a) schedules are generated for each block model separately. (b) Kriging schedule applied to all realizations. E-type and Kriging results are marked by solid circle and hollow circle respectively.

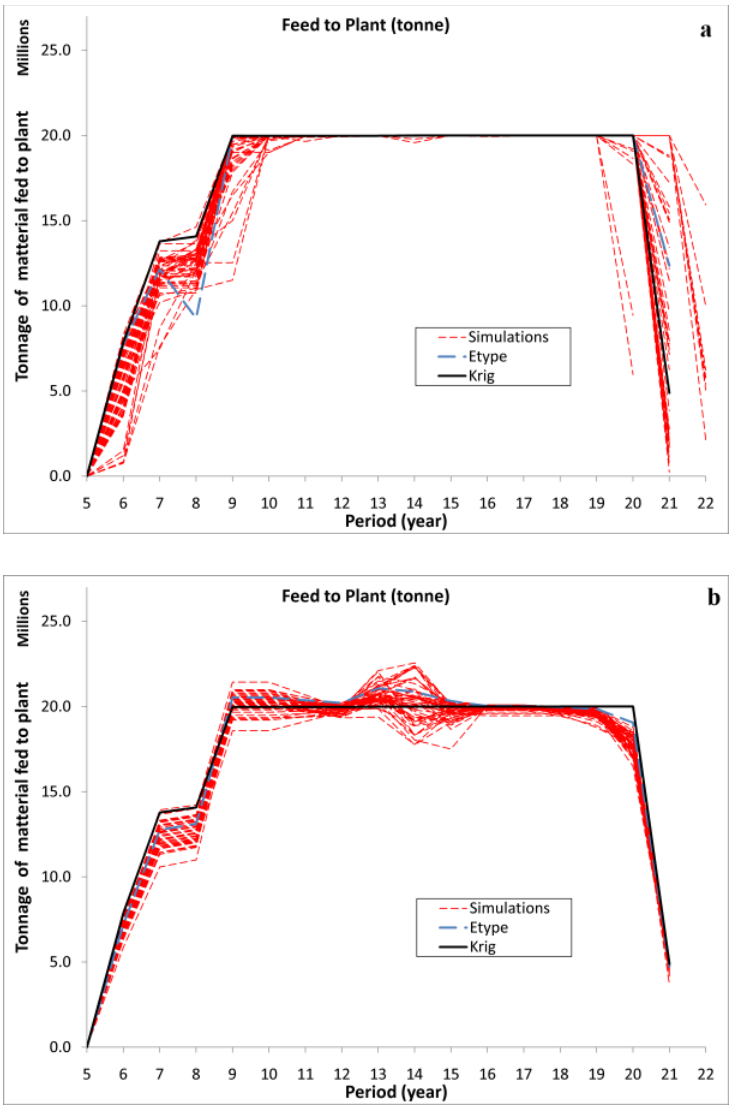

Fig. 13. Plant feed (realizations dash lines), Kriging Model (solid line) and E-type (blue dash line). (a) schedules are generated for each block model separately. (b) Kriging schedule applied to all realizations.

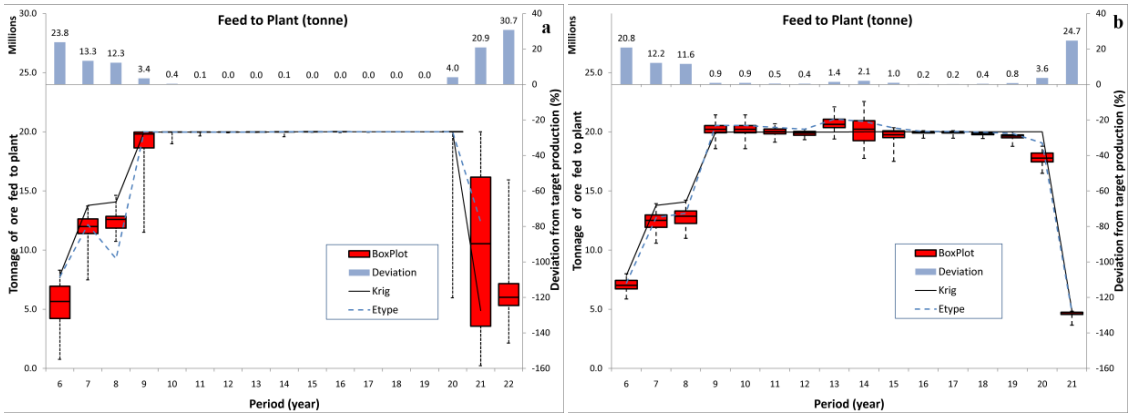

Fig. 14. Box plot of the simulation plant feed, Kriging schedule (solid line) and E-type (blue dash line). Deviations from target production are reported in percentage. (a) schedules are generated for each block model separately. (b) Kriging schedule applied to all realizations.

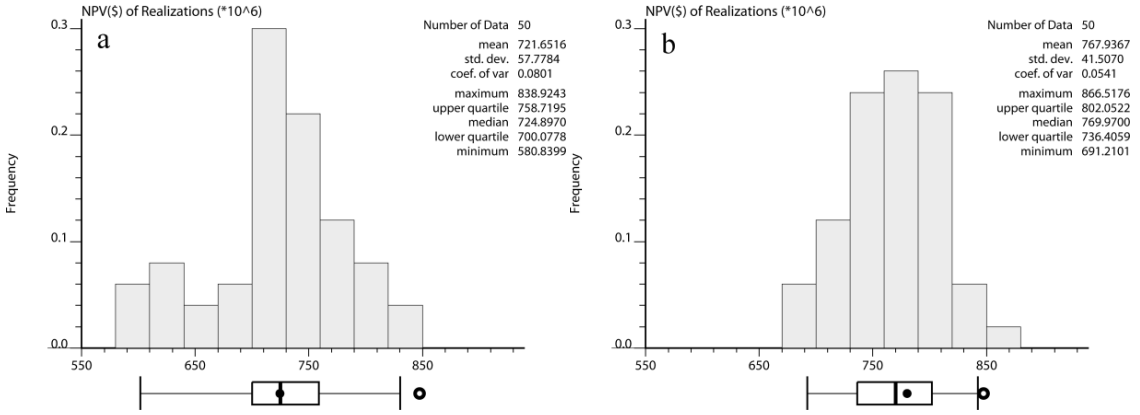

Fig. 15. Histograms and box plots of NPV in billion dollars. (a) schedules are generated for each block model separately. (b) Kriging schedule applied to all realizations. E-type and Kriging results are marked by solid circle and hollow circle respectively.

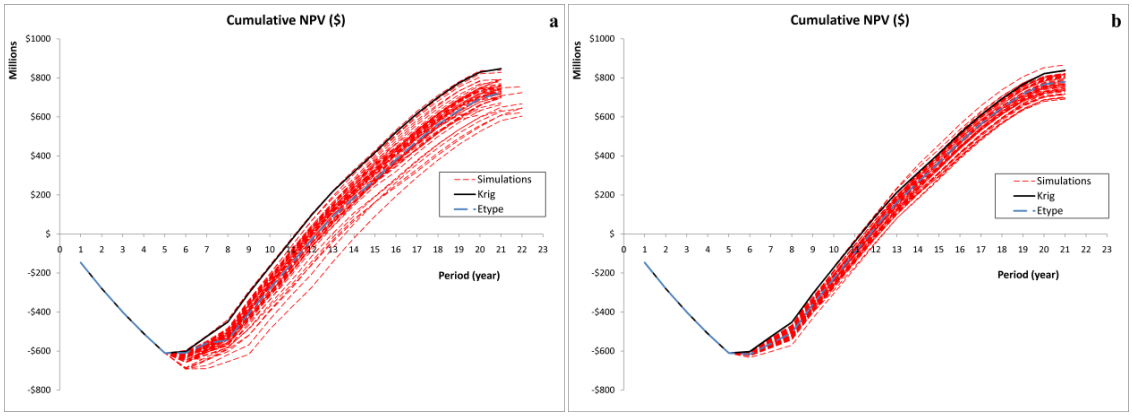

Fig. 16. Cumulative discounted cash flow for 50 realizations (dashed lines) and Kriging model (solid line). (a) schedules are generated for each block model separately. (b) Kriging schedule applied to all realizations.

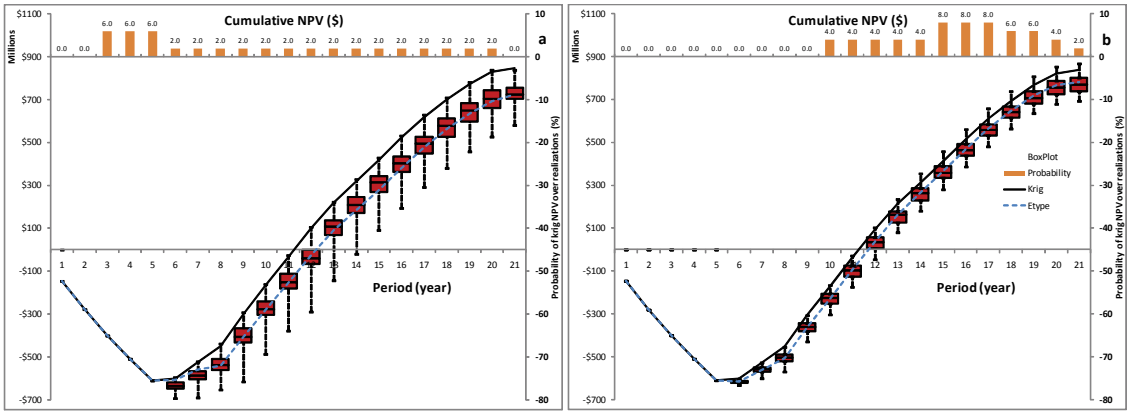

Fig. 17. Box plot of the Cumulative discounted cash flow for 50 realizations (dashed lines) and Kriging model (solid line). Probabilities of reaching the Kriging NPV over realizations are presented in percentage. (a) schedules are generated for each block model separately. (b) Kriging schedule applied to all realizations.

4. MILP formulation

The discounted profit of mining a block is represented by Eq. (1).

$$\text{discountedprofit} = \text{discounted revenue} - \text{discounted costs} \tag{1}$$

Askari-Nasab and Awuah-Offeri (2009) present four mixed integer linear programming models without taking into account the grade uncertainty. The proposed model in this paper uses Askari-Nasab and Awuah-Offeri (2009) fourth model as the starting point.

The profit from mining a block depends on the value of the block and the costs incurred in mining and processing. The cost of mining a block is a function of its location, which characterizes how deep the block is located relative to the surface and how far it is relative to its final dump. The spatial factor can be applied as a mining cost adjustment factor for each block according to its location to the surface. The discounted profit from a block is equal to the discounted revenue generated by selling the final product contained in block n minus all the discounted costs involved in extracting block.

Grade uncertainty causes shortfalls from target production levels. Therefore, to obtain an optimum schedule, NPV must be maximized and the deviation from target productions must be minimized simultaneously among all simulation realizations.

$$\begin{cases} \text{Max. NPV} \\ \text{Min. Deviationfrom target production} \end{cases}$$

A new profit function is defined by Eq. (2).

New discounted profit = discounted profit – penalty cost for over and under production (2)

The objective function of the mathematical programming formulation is presented by Eq (3), All notations are defined in the appendix.

$$Max \sum_{t=1}^{T}\left\{\sum_{n=1}^{N}\left(V_n^t \times z_n^t - Q_{l,n}^t \times y_n^t\right) - \frac{1}{L}\sum_{l=1}^{L}\left(c_{op}^t \times op_l^t + c_{up}^t \times up_l^t\right)\right\} \tag{3}$$

Subject to:

$$g_l^{t,e} \le \left(\sum_{n=1}^{N} g_n^e \times o_n \Big/ \sum_{n=1}^{N} o_n\right) \times z_n^t \le g_u^{t,e} \qquad \forall t = 1,2,\ldots,T \ , \ e = 1,2,\ldots,E \tag{4}$$

$$\sum_{n=1}^{N}\left(o_{n,l} \times z_n^t - op_l^t\right) \le P_u^t \qquad \forall t = 1,2,\ldots,T \ , \ l = 1,2,\ldots,L \tag{5}$$

$$\sum_{n=1}^{N}\left(o_{n,l} \times z_n^t - up_l^t\right) \ge P_l^t \qquad \forall t = 1,2,\ldots,T \ , \ l = 1,2,\ldots,L \tag{6}$$

$$m_l^t \le \sum_{n=1}^{N}\left(o_n + w_n\right) \times z_n^t \le m_u^t \qquad \forall t = 1,2,\ldots,T \tag{7}$$

$$z_n^t \le y_n^t \qquad \forall t = 1,2,\ldots,T \ , \ n = 1,2,\ldots,N \tag{8}$$

$$a_n^t - \sum_{i=1}^{t} y_l^i \le 0 \qquad \forall t = 1,2,\ldots,T; \ n = 1,2,\ldots,N; \ l = 1,2,\ldots,C_n\left(L\right) \tag{9}$$

$$\sum_{i=1}^{t} y_n^i - a_n^t \le 0 \qquad \forall\, t = 1,2,\ldots,T \;\;,\; n = 1,2,\ldots,N \tag{10}$$

Where V_n^t is the expected discounted revenue over all simulation realizations and $Q_{l,n}^t$ is the expected discounted cost over all simulation realizations as is shown by Eq. (11):

$$\begin{aligned} V_n^t &= \frac{1}{L}\sum_{l=1}^{L} v_{n,l}^t \\ Q_n^t &= \frac{1}{L}\sum_{l=1}^{L} q_{n,l}^t \end{aligned} \tag{11}$$

The discounted revenue and discounted cost can be rewritten as Eq. (12) and Eq.(13).

$$v_{l,n}^t = \sum_{e=1}^{E} o_{l,n} \times g_n^e \times r^{e,t} \times \left(p^{e,t} - cs^{e,t}\right) - \sum_{e=1}^{E} o_{l,n} \times cp^{e,t} \qquad \forall l = 1,\ldots,L \;\; t = 1,\ldots,T \;\; n = 1,\ldots,N \tag{12}$$

$$q_{l,n}^t = \left(o_{l,n} + w_{l,n}\right) \times cm^t \qquad \forall l = 1,\ldots,L \;\; t = 1,\ldots,T \;\; n = 1,\ldots,N \tag{13}$$

Eq. (4) is grade blending constraints; these inequalities ensure that the head grade of the elements of interest and contaminants are within the desired range in each period. There are two equations (upper bound and lower bound) per element per scheduling period in Eq.(4). Eqs. (5) and (6) are processing capacity constraints; these inequalities ensure that the total ore processed in each period is within the acceptable range of processing plant capacity. There are two equations (upper bound and lower) per period per ore type. Eq. (7) is mining constraints; these inequalities ensure that the total tonnage of material mined (ore, waste, overburden, and undefined waste) in each period is within the acceptable range of mining equipment capacity in that period. There are two equations (upper bound and lower bound) per period. Eq. (8) represents inequalities that ensure the amount of ore of any block which is processed in any given period is less than or equal to the amount of rock extracted in the considered time period.

Eqs. (9) and (10) control the relationship of block extraction precedence by binary integer variables at block level. This model only requires the set of immediate predecessors' blocks on top of each block to model the order of block extraction relationship. This is presented by set $C_n(L)$ in Eq.(9).

In this model, the number of variables is equal to the number of blocks multiplied by the number of periods. Boland *et al.* (2009) and Askari-Nasab and Awuah-Offeri (2009) tried to solve this problem with clustering the blocks into aggregates to reduce the number of variables. Using grade aggregation methodology similar blocks are clustered into one group. Clustering blocks into mining-cuts is done without sacrificing the accuracy of the estimated (or simulated) values. The mining-cut clustering algorithm developed uses fuzzy logic clustering (Kaufman and Rousseeuw, 1990). Coordinates of each mining-cut has been represented by the center of the cut and its location.

5. Conclusion

We used two methods to show the impact of grade uncertainty at mine planning. First, using the kriged model for an oil sand deposit, an optimal final pit limit is generated. Sequential Gaussian Simulation is used to generate fifty realizations. An optimum final pit limits design is carried out for each SGS realization based on same parameters and technique that are fixed with kriged block model. Afterwards, the long-term schedule of each final pit shell is generated. Uncertainty in the final pit outline, net present value, production targets, and the head grade are assessed and presented.

In the second method, for each SGS realization, schedule that generated from kriged model was followed. The results show that there is significant uncertainty in the long-term production schedules. In addition, the long-term schedule based on one particular simulated ore body model is not optimal for other simulated geological models. The mine planning procedure is not a linear process and the mine plan generated based on the kriged estimate is not the expected result from all of the simulated realizations.

One of the main aspects of this study is to show the impact of grade uncertainty on mine planning. The study is not aimed to compare the simulation with kriging, because it is well-known that kriging is conditionally biased (Isaaks, 2005) and on the other hand "there is no conditional bias of simulation when the simulation results are used correctly" (McLennan and Deutsch, 2004). Conditional biasness of kriging can be reduced by tuning estimation parameter but it cannot be eliminated. Grade-Tonnage curve is the good tool to check the impact of kriging biasness. Fig. 18 shows the grade tonnage curve of simulation realization (dashed lines), krig (bold solid line) and Etype (bold dashed line). The systematic biasness of kriging was tried to be minimized but still the there are differences between kriging and simulation results. Also Etype is slightly different than kriging; Theoretically Etype model is identical with simple kriging result at Gaussian space (Journel and Huijbregts, 1981).

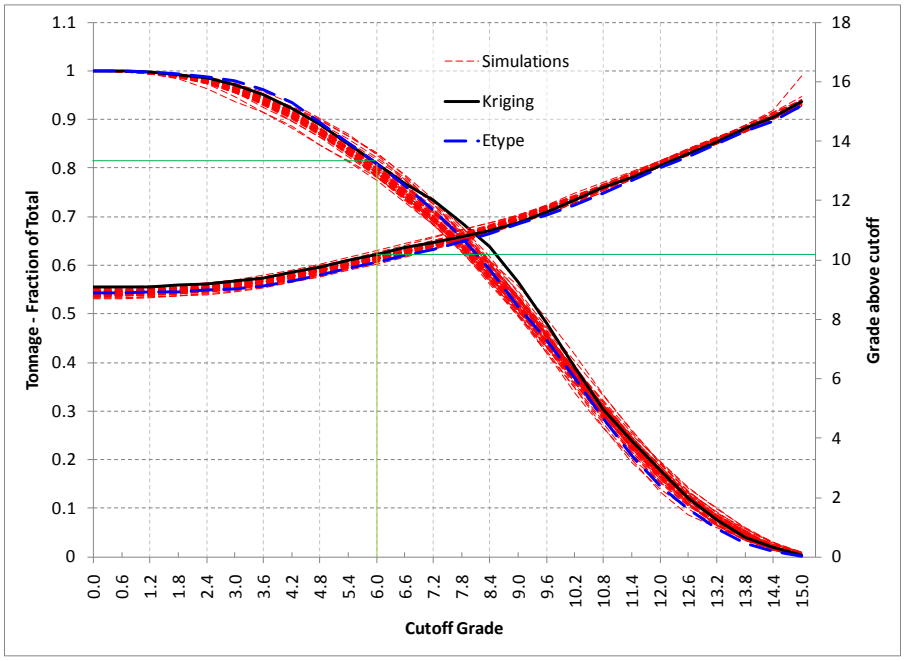

Fig. 18. Grade tonnage curve of Kriging, simulation realizations and E-type

6. Reference:

[1] Askari-Nasab, H. and Awuah-Offeri, K. (2009). Mixed integer programming formulations for open pit production scheduling. *MOL Report one*, *1*, 1-31.

[2] Boland, N., Dumitrescu, I., Froyland, G., and Gleixner, A. M. (2009). LP-based disaggregation approaches to solving the open pit mining production scheduling problem with block processing selectivity. *Comput.Oper.Res.*, *36*,(4), 1064-1089.

[3] Deutsch, C. V. and Journel, A. G. (1998). GSLIB : geostatistical software library and user's guide. in *Applied geostatistics series*, vol. 2. New York: Oxford University Press, pp. 369.

[4] Deutsch, C. V. and Journel, A. G. (1998). *GSLIB geostatistical software library and user's guide.* Oxford University Press, New York.

[5] Dimitrakopoulos, R., Farrelly, C. T., and Godoy, M. (2001). Moving forward from traditional optimization: Grade uncertainty and risk effects in open-pit design. *Transactions of the Institution of Mining and Metallurgy, Section A: Mining Industry*, *111*, 82-88.

[6] Dimitrakopoulos, R. and Ramazan, S. (2004). Uncertainty based production scheduling in open pit mining. 106-112.

[7] Dimitrakopoulos, R. and Ramazan, S. (2008). Stochastic integer programming for optimising long term production schedules of open pit mines: methods, application and value of stochastic solutions. *Mining Technology : IMM Transactions section A*, *117*, 155-160.

[8] Dowd, P. A. (1994). Risk assessment in reserve estimation and open-pit planning. *Transactions of the Institution of Mining and Metallurgy Section a-Mining Industry*, *103*, A148-A154.

[9] Gemcom Software International, I. (1998-2008). Whittle strategic mine planning software. 4.2 ed. Vancouver, B.C.: Gemcom Software International.

[10] Godoy, M. and Dimitrakopoulos, R. (2003). Managing risk and waste mining in long-term production scheduling of open pit mine. *SME Annual Meeting & Exhibition*, *316*, 43-50.

[11] Goovaerts, P. (1997). *Geostatistics for natural resources evaluation.* Oxford University Press, New York, Pages 483.

[12] Isaaks, E. (2005). The Kriging Oxymoron: A conditionally unbiased and accurate predictor (2nd edition). *Geostatistics Banff 2004, Vols 1 and 2*, *14*, 363-374.

[13] Isaaks, E. H. and Srivastava, R. M. (1989). *Applied geostatistics.* Oxford University Press, New York, N.Y. ; Oxford, England, Pages 561.

[14] Journel, A. G. and Huijbregts, C. J. (1981). *Mining geostatistics.* Academic Press, London, Pages 600.

[15] Kaufman, L. and Rousseeuw, P. J. (1990). *Finding groups in data : an introduction to cluster analysis.* Wiley, New York, Pages 342.

[16] Leite, A. and Dimitrakopoulos, R. (2007). Stochastic optimisation model for open pit mine planning: Application and risk analysis at copper deposit. *Transactions of the Institutions of Mining and Metallurgy, Section A: Mining Technology*, *116*,(3), 109-118.

[17] Lerchs, H. and Grossmann, I. F. (1965). Optimum design of open-pit mines. *The Canadian Mining and Metallurgical Bulletin, Transactions*, *LXVIII*, 17-24.

[18] Leuangthong, O., Schnetzler, E., and Deutsch, C. V. (2004). Geostatistical modeling of mcmurray oil sands deposits. 2004 CCG annual report papers, Centre for Computational Geostatistics, Edmonton, September 2004, 309-1 to 309-10.

[19] McLennan, J. A. and Deutsch, C. V. (2004). Conditional non-bias of geostatistical simulation for estimation of recoverable reserves. *CIM bulletin*, *97*,(1080).

[20] Osanloo, M., Gholamnejad, J., and Karimi, B. (2008). Long-term open pit mine production planning: a review of models and algorithms. *International Journal of Mining, Reclamation and Environment*, *22*,(1), 3-35.

[21] Ravenscroft, P. J. (1992). Risk analysis for mine scheduling by conditional simulation. *The Canadian Mining and metallurgical Bulletin, Transactions.(Sec. A: Min. Industry)*, *101*, 82-88.

[22] Rossi, M. E. and Parker, H. M. (1994). *Estimating recoverable reserves: Is it hopeless?, Geostatistics for the Next Century*, in Proceedings of Kluwer Academic, Dordrecht ; Boston.

[23] Vallee, M. (2000). Mineral resource + engineering, economic and legal feasibility = ore reserve. *CIM bulletin*, *90*, 53-61.

7. Appendix

$v_{l,n}^{t}$	the discounted revenue generated by selling the final product within block n in period t at realization number l minus the extra discounted cost of mining all the material in block n as ore and processing.
$q_{l,n}^{t}$	the discounted cost of mining all the material as waste in block n in period t at realization number l.
E	number of element of interests in each block.
T	Total number of periods.
L	Total number of simulation realizations.
$o_{l,n}$	Ore tonnage in block n at realization l.
$g_{l,n}^{e}$	Average grade of element e in one portion of block n at realization l.
$r^{e,t}$	processing recovery, the proportion of element e recovered in time period t.
$p^{e,t}$	Price in present value terms obtainable per unit of product, element e.
$cs^{e,t}$	Selling cost in present value terms obtainable per unit of product, element e.
$cp^{e,t}$	Extra cost in present value terms per unit of production, element e.
$w_{l,n}$	Waste tonnage in block n at realization l.
cm^{t}	Cost in present value terms of mining a tone of waste in period t.
$a_{n}^{t} \in \{0,1\}$	Binary integer variable controlling the precedence of extraction of blocks. It is equal to one if extraction of block n has started by or in period t, otherwise it is zero.
$z_{n}^{t} \in [0,1]$	continues variable, representing the portion of bock n to be extracted as ore and processed in period t.
$y_{n}^{t} \in [0,1]$	continues variable, representing the portion of bock n to be mined in period in period t, fraction of y characterizes both ore and waste.
op_{l}^{t}	is the over produced amount of ore tonnage above a desired tonnage, or upper limit, in period t and realization number l.
up_{l}^{t}	is the under produced amount of ore tonnage bellow a desired tonnage, or upper limit, in period t and realization number l.
c_{op}^{t}	is the discounted unit cost of op^{t} at period t.
c_{up}^{t}	is the discounted unit cost of up_{l}^{t} at period t.
V_{n}^{t}	is the expected discounted revenue over all simulation realizations.
$Q_{l,n}^{t}$	is the expected discounted cost over all simulation realizations.

Oil sands mine planning and waste management using goal programming

Eugene Ben-Awuah and Hooman Askari-Nasab
Mining Optimization Laboratory (MOL)
University of Alberta, Edmonton, Canada

Abstract

Strategic mine planning and waste management is an important aspect of surface mining operations. Recent environmental and regulatory requirements makes waste management an integral part of mine planning in the oil sands industry. In oil sands mining, due to the limitation of lease area, the pit phase advancement is carried out simultaneously with the construction of tailings dykes in the mined out areas of the pit. These dykes are constructed to hold tailings that are produced during the processing of the oil sands. Most of the materials used in constructing these dykes come from the oil sands mining operation (overburden and interburden) making it necessary to have a plan for supplying the dyke material. The research problem here is determining the order of extraction of ore, dyke material and waste to be removed from a predefined ultimate pit limit over the mine life that maximizes the net present value of the operation – a strategic schedule. The strategic schedule to be developed is subject to a variety of economic, technical and physical constraints.

We have developed, implemented, and tested a proposed mixed integer goal programming theoretical framework for oil sands open pit production scheduling with multiple material types. The formulation uses binary integer variables to control mining precedence and continuous variables to control mining of ore and dyke material. There are also goal deviational variables and penalty costs and priorities that must be set up by the planner. The optimization model was implemented in TOMLAB/CPLEX environment.

The developed model proved to be able to generate a uniform schedule for ore and dyke material. It also provides the planner the flexibility of choosing goal deviational variables, penalty costs and priorities to achieve a uniform schedule. These parameters can also be used to set priorities for goals thereby leading to improved NPV. Similarly, tradeoffs between achieving a goal and maximizing NPV can be made.

1. Introduction

Mining is the process of extracting a beneficial natural resource from the earth (Newman et al., 2010). The extraction process can be an underground or open pit mining operation and this research will be restricted to the latter. An important aspect of mining engineering is mine planning. Whittle (1989) defined open pit mine planning as the process of finding a feasible block extraction schedule that generates the highest net present value (NPV) subject to some operational and technical constraints. Depending on the size of the deposit, the mine plan can be divided into short-term, medium-term and long-term with planning durations ranging from 1 month to 30 years.

Long-term production schedules are the main backbone that drives the activities of the mine throughout its life. The main focus of this research will be on long-term production scheduling

optimization process. The process attempts to maximize the net present value of the overall profit to be generated from the mining operation within some operational and technical constraints such as mining and ore processing capacities, grade blending and block extraction sequencing.

Oil sands mining comprise the mining of overburden material and the McMurray formation. The overburden material is barren and the McMurray formation contains bitumen which is the desirable mineral. About 80% of the oil sands ore after processing finds its way to the tailings dam, making the tailings facility and waste management important aspects of this operation. Due to lack of lease area, these tailings facilities are sited mostly in-pit and embankments or dykes are constructed to contain the tailings. Most of the materials used in constructing these dykes come from the mining operation which makes it necessary to have a plan for supplying the dyke material.

Depending on the dykes' designs, they have different configurations at different locations within the dyke and hence require different material types. Some of the dyke construction methods shown in Fig. 1 are: 1) upstream construction, 2) downstream construction, and 3) centerline construction. More literature that provides details on dyke construction methods for tailings facilities are provided by Vick (1983) and Sego (2010). These dykes are constructed simultaneously as the mine phase advances and the dyke footprints are released. Fig. 2 shows a mining phase advancement schedule at Syncrude Canada Ltd. and this schedule is used to decide the in-pit dyke construction schedule (Syncrude, 2009). This emphasizes the need for a simultaneous development of a life of mine ore and dyke material schedule that can support the mining operation and this will be the main focus of this research.

Currently, scheduling of dyke material is done after mining has started and this may result in inconsistent production of dyke material at different periods during the mine life. It is also a regulatory requirement that life of mine schedules for tailings management strategies are documented and reported annually resulting in the need for a more systematic approach towards oil sands waste management (McFadyen, 2008).

The oil sands mine long-term production planning problem will be modeled numerically as an optimization problem using a mixed integer goal programming model. The optimization problem will be coded using MATLAB (Mathworks Inc., 2009) and solved with TOMLAB/CPLEX which is a large scale mixed integer programming solver. This solver uses a branch and cut algorithm (Holmström, 2009).

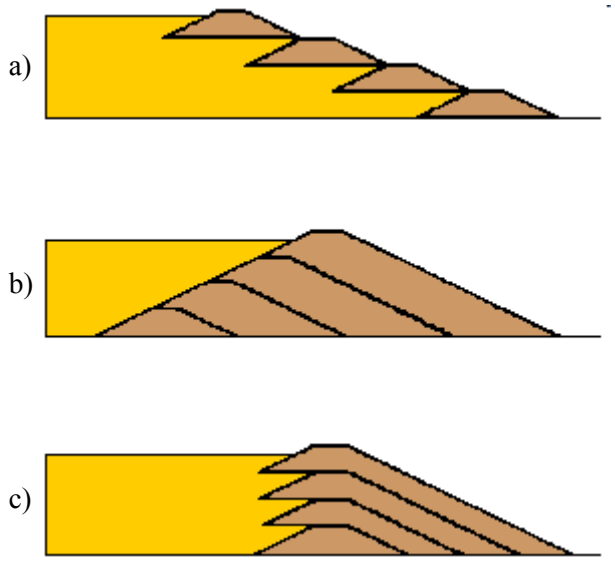

Fig. 1. a) Upstream construction, b) downstream construction, and c) centerline construction (after Vick, 1983)

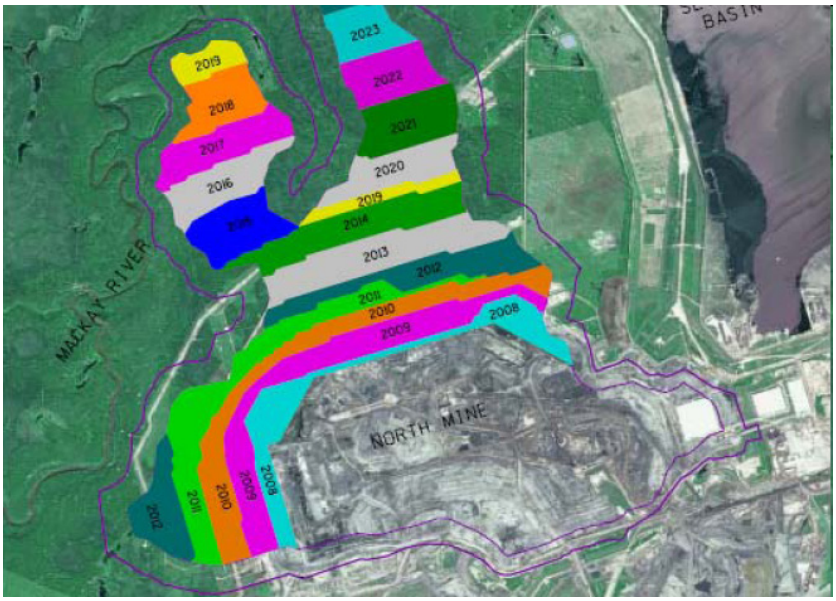

Fig. 2. Syncrude Canada Ltd: North mine development sequence
(after Syncrude, 2009)

1.1. Oil sands formation

The mineral deposit under consideration is oil sands in the McMurray formation. There are five main soils or rock types associated with this deposit namely:

1) Muskeg/Peat 2) Pleistocene Unit 3) Clearwater Formation 4) McMurray Formation and 5) Devonian carbonates. The oil bearing rock type is the McMurray formation (MMF) which is also made up of three rock types. These are the Upper McMurray (UKM), the Middle McMurray (MKM) and the Lower McMurray (LKM). The main element of interest is bitumen which exists in various grades across the formation. Details of the five rock types associated with the oil sands deposit are:

1. Muskeg/Peat – this is the topmost overburden material that contains the seeds and roots of native plants and is used for the topmost layer of the reclaimed land. Before mining, this layer is removed and stockpiled and later used for reclamation works.
2. Pleistocene Unit (PLU) and Clearwater Formation (CWF) – the next rock profiles are the PLU followed by the CWF. These are considered as waste rocks lying above the bitumen bearing McMurray formation. Materials from these profiles are used for road and dyke construction in the mine depending on the soil properties and its mineral content.
3. McMurray Formation (UKM, MKM, LKM) – the bulk of the bitumen and gas reserves are contained within the McMurray interval in the oil sands area. The McMurray formation rests with profound unconformity on the Devonian carbonates and is unconformably overlain by the Clearwater formation. The McMurray formation ranges between 0 – 130m thick from Devonian highs to bitumount basins. The LKM is comprised of gravel, coarse sand, silt and clay with siderite as cement. The UKM and MKM comprises of micaceous, fine-to-medium-grained sand, silt and clay, with rare siderite as cement and intraclasts and pyrite nodules up to 10cm in diameter (Hein et al., 2000).
4. Devonian Carbonates (DVN) – this is the rock type which lies beneath the McMurray formation and is made up of numerous limestone outcrops. It marks the end of the oil sands deposit on a vertical profile.

To obtain details of the oil sands deposit, it is required that a detailed exploration programme is undertaken where drilling is carried out and the resulting data logged for further analysis and modeling. Fig. 3 shows a sketch of the vertical soil profile of an oil sands formation.

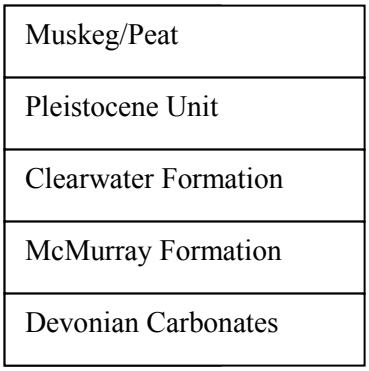

Fig. 3. Sketch of the vertical soil profile of an oil sands formation

1.2. Oil sands mining and material classification system

The oil sands mining system comprises of the removal of the overburden material and the mining of the McMurray formation. The overburden material comprises of muskeg/peat, the Pleistocene unit and the Clearwater formation. The muskeg/peat, which is barren, is very wet in nature and therefore once it is stripped, it is left for about 2 to 3 years to get it dry, making it easier to handle. This material is stockpiled for future reclamation works which is required for all disturbed landscapes.

The mining of the Pleistocene and Clearwater formation, which is classified as waste, is to enable the exposure of the ore bearing McMurray formation. Some of this material is also used in the construction of dykes and roads required for the operation. The dyke construction is for the development of the tailings dam constructed either in the pit or elsewhere. About 80% of the oil sands mined find its way to the tailings dam after processing. The development of the tailings facility is therefore very important and strategic for the entire oil sands operation.

The classification of the oil sands material is basically driven by economic, technical and regulatory requirements (Dilay, 2001). The geotechnical requirement for dyke construction material varies depending on the dyke design configuration and location of the material within the dyke. The dyke construction material required from the oil sands mining operation (overburden and interburden) must have fines content less than approximately 50%. This type of material contains some amount of clays such as kaolinite, illite, chlorite and smectite (Wik et al., 2007) required as a binding material for improving the stability of the dykes. The waste from the Pleistocene and Clearwater formation is therefore classified based on the fines content. Material with percentage fines less than 50% is classified as dyke material which is required for dyke construction and that with fines more than 50% is classified as waste.

The mining of the oil bearing McMurray formation follows after the mining of the overburden material. By the regulatory and technical requirements, the mineable oil sand grade should be about 7% bitumen content (Dilay, 2001; Masliyah, 2010). All material satisfying this requirement is classified as ore and otherwise as waste. The ore is sent directly to the processing plant for bitumen extraction. This class of waste also known as interburden is reclassified based on the fines content. The material with fines content less than 50% is classified as dyke material and that with fines more than 50% is classified as waste. It is important to note that this material classification system is dynamic and can vary from one mine to another. The criteria may change depending on the grade distribution of the orebody under consideration. Cash flow analysis can also be used to classify the different material types.

The next section of this paper covers a summary of the literature review on mine planning, goal programming, mixed integer programming, oil sands mining, and waste management. Section 3 gives details of the problem definition. The theoretical framework of the proposed formulation is highlighted in section 4. The application of the formulation to an oil sands case with two examples is explained in sections 5 and 6. Conclusions and future research work are outlined in section 7.

2. Summary of literature review

The problem of long-term production planning (LTPP) has been a major research area for quite some time now and though tremendous improvements have been made, the current challenging mining environment poses new sophisticated problems. Effective LTPP is critical in the profitability of surface mining ventures and can increase the life of mine considerably. Recent production scheduling algorithms and formulations in literature have been developed along two main research areas: 1) heuristic methods and 2) exact optimization methods (Askari-Nasab and Awuah-Offei, 2009).

Commercial mine scheduling software such as XPAC AutoScheduler (Runge Limited, 2009), WHITTLE (Gemcom Software International, 2008), and NPV Scheduler (Datamine Corporate Limited, 2008) use heuristic methods to generate long-term production schedules. Heuristic methods iterate over different alternatives leading to the generation of the ultimate pit limit with each alternative having a different discounted cash flow and hence NPV of the operation. Due to this, the solution generated may be sub-optimal in terms of NPV.

Authors like Denby and Schofield (1995) and Askari-Nasab (2006) have done extensive research using artificial intelligence techniques to solve the problem of LTPP. Denby and Schofield (1995) used multi-objective optimization to deal with ore grade variance. Using genetic algorithm, Denby and Schofield (1995) tried to maximize value and minimize risk in open pit production planning. Askari-Nasab (2006) also developed and implemented an intelligent-based theoretical framework for open pit production planning. The drawback in the application of these techniques is the non reproducibility of the solution and a measure of the extent of optimality of the solution.

Exact optimization methods have proved to be robust in solving the LTPP problem. They have the capability of considering multiple material types and multiple elements during optimization. This flexibility of mathematical programming models leads to the generation of production schedules with higher NPV than heuristic methods. Goal programming (GP) is an exact optimization technique that has been used for production scheduling in the industry. The advantage of this technique is that it allows for flexible formulation and the specification of priorities among goals or targets. This formulation also allows some form of interaction between the decision maker and the optimization process (Zeleny, 1980; Hannan, 1985). Depending on its use, some alterations are made to the formulation structure. Goal programming was applied to the mine scheduling problem using multiple criteria decision making formulation by Zhang et al. (1993). Multiple goals were considered based on their priorities. The model was tested for a surface coal mine production scheduling and implemented using a branch-and-bound method in ‘C’ programming language environment. This model was developed for a single ore type process. Chanda and Dagdelen (1995) used goal programming and an interactive graphics system for optimal blending in mine production. Their model sets up the blending problem with multiple goals and attempts to minimize the deviation from the goals using a Fortran 77 computer program based on simplex method of linear programming. The model was tested for a coal mine deposit, but due to some interactions involved in solving the problem, optimal solution cannot be always guaranteed. A mineral dressing criteria was defined by Esfandiri et al. (2004) and used in the optimization of an iron ore mine. A 0-1 non-linear goal programming model was defined based on multiple criteria decision making and the deviations for economics, mining and mineral dressing functions were minimized. This

formulation was solved using LINGO software. The model was found to have limitations and constraints that are numerous for practical application.

Other mine and production related problems have been solved using goal programming with some modifications. Oraee and Asi (2004) used a fuzzy goal programming model for optimizing haulage system in an open pit mine. Due to the variations in operating conditions caused by technical, operational, and environmental factors for a mechanical shovel, their model use fuzzy numbers to represent parameters for these operating conditions in optimization. They argue that, their model generates a more realistic results than those based on random numbers derived from probability distributions. A 0-1 goal programming model was developed by Chen (1994) for scheduling multiple maintenance projects for a mineral processing equipment at a copper mine. Using 0-1 decision variables and multiple scheduling periods, the model scheduled for four projects, 40 jobs and nine types of resources. In comparison to a heuristic method that was already used by the mine, the goal programming model reduced the project duration, total project cost and overall workload. Many industrial production planning and project selection decision making problems have been solved making use of the advantages of goal programming formulations (Jääskeläinen, 1969; Mukherjee and Bera, 1995; Leung et al., 2003; Lee et al., 2010).

Other exact optimization techniques that have been used for mine production scheduling are mixed integer programming (MIP) and linear programming (LP). Initial works that was carried out by Johnson (1969), Gershon (1983) and Dagdelen (1985) developed linear programming (LP) and mixed integer programming (MIP) formulations that uses integer variables for optimizing mine schedules. Their formulations could not ensure feasible solutions for all cases and could not overcome the issue of solving large integer programming problems. An integer programming formulation that was developed by Dagdelen and Johnson (1986) uses Lagrangian relaxation and subgradient optimization algorithm to solve the LTPP problem. This formulation could not be implemented on large scale problems and could not handle dynamic cut off grades. Subsequent integer programming models developed by Akaike and Dagdelen (1999) and Caccetta and Hill (2003) use 4D-network relaxation, subgradient optimization algorithm, and branch and cut algorithm respectively to solve the LTPP optimization problem but these models also could not be implemented on large scale problems or handle dynamic cutoff grades.

MIP formulations that was developed by Ramazan and Dimitrakopoulos (2004) attempt to reduce the number of binary variables and solution times by setting certain variables as binary and others as continuous. This resulted in partial mining of blocks that have the same ore value affecting the NPV generated. Ramazan et al. (2005) and Ramazan (2007) developed an MIP model that uses an aggregation method to reduce the number of integer variables in scheduling. This formulation was solved based on fundamental tree algorithm and was used in scheduling a case with 38,457 blocks within the final pit limit. The problem was broken down into four push-backs based on the nested pit approach using WHITTLE (Gemcom Software International, 2008) and formulated as separate MIP models. This would not guarantee a global optimum solution of the problem. Boland et al. (2009) presented an LP approach to generate mine production schedules with block processing selectivity. They however did not present enough information on the generated schedules to enable an assessment of the practicality of the solutions from mining operation point of view.

Recent research work by Askari-Nasab and Awuah-Offei (2009) on the application of exact optimization methods to the LTPP problem has lead to the development of mixed integer linear programming (MILP) models that use block clustering techniques to solve the problem of having large number of decision variables. With a combination of their MILP models and a block clustering algorithm, Askari-Nasab and Awuah-Offei (2009) applied their models to a large scale problem. The formulations use a combination of continuous and binary integer variables. The continuous variables control the portion of a block to be extracted in each period and binary integer variables control the order of block extraction or precedence of mining-cuts through a dependency directed graph using depth-first-search algorithm. The concept of mining-cuts using clustering

techniques is reinforced as an option for solving MILP problems for large scale deposits. The formulation was successfully implemented on an iron ore mine intermediate scheduling case study over twelve periods in TOMLAB/CPLEX (Holmström, 2009) environment. This model does not consider multiple material types.

Due to the advantages that are presented by GP and MILP, some efforts have been made to combine these two techniques and used together for solving industrial problems. This hybrid termed as mixed integer goal programming (MIGP) has been used for scheduling and budgeting problems in nursing, business administration and manufacturing industries (Selen and Hott, 1986; Ferland et al., 2001; Liang and Lawrence, 2007; Nja and Udofia, 2010). MIGP formulation is the proposed model in this paper for application to the oil sands mine LTPP problem.

Oil sands also known as bituminous sands are sedimentary deposits that contain high molar mass viscous petroleum. The largest sources of crude bitumen in the world are Canada and Venezuela (Masliyah, 2010). The origin of the oil that is trapped in the sands to form the oil sands are; marine animals die and sink to the ocean bottom and become embedded by sedimentary minerals. Major alterations caused by aerobic and anaerobic processes, high temperatures and pressures and decomposition produce liquid petroleum. The liquid petroleum flows through the pores of the rock in which it was formed and migrates until it becomes trapped and cannot flow any further, thus forming an oil reservoir (Masliyah, 2010). In the case of the Alberta oil sands, the oil was trapped in the McMurray formation. Oil sands mining started in the 1960s with a surface mining operation that used hot water extraction to recover bitumen from the oil sands and an upgrading complex to upgrade the extracted bitumen to a light synthetic crude (Morgan, 2001). This mining operation involves the movement of huge amount of bituminous sands to the processing plant with over 80% being sent to the tailings dam after processing. The remaining waste material mined from the pits are sent to waste dumps or used for dyke construction. This makes waste management an important integral part of the oil sands mining process.

An issue that can bring a mine to its knees within the shortest possible time is the management of its waste. Waste management issues can also result in future unbearable financial liabilities. Strategies for managing oil sands mine waste in an environmentally acceptable manner, in the short and long-term, are a responsibility that cut across a wide range of disciplines. This includes geologists, geotechnical and mine planning engineers, tailings planners, operations and project teams (Fauquier et al., 2009). The team works towards the goal of building tailings dam dykes on time, within budget and design specifications. This involves managing tailings and the general mine waste. Tailings dams that are constructed to store tailings are usually constructed in-pit due to the lack of lease area and the large amount of storage space required. The tailings are stored behind dykes that are constructed in the pit one section at a time as the mining advances. The tailings storage plan requires the in-pit dykes to be designed, constructed and operated on a continual basis throughout the mine life. The in-pit dyke construction materials are derived from the overburden and interburden seams of the deposit (Fauquier et al., 2009). The dyke construction materials are predicted using the geologic block model. This makes it necessary that during the long-term production planning process, schedules for ore and dyke material are generated simultaneously to enable the consistent material supply to the plant and for dyke construction. The nature of dyke material required at any time depends on the dyke configuration and the location of the material within the dyke. A robust oil sands long-term plan should be able to supply ore for the plant and appropriate dyke material throughout the mine life. Fig. 4 shows a typical ore, waste, in-pit dyke and tailings plan for an oil sands mine.

After carefully reviewing the literature on GP, MILP, and MIGP formulations, and oil sands mining and waste management, a formulation has been developed to attempt solving the problem of LTPP for oil sands mining operations. The model has been used to generate a long-term production schedule for ore, dyke material and waste.

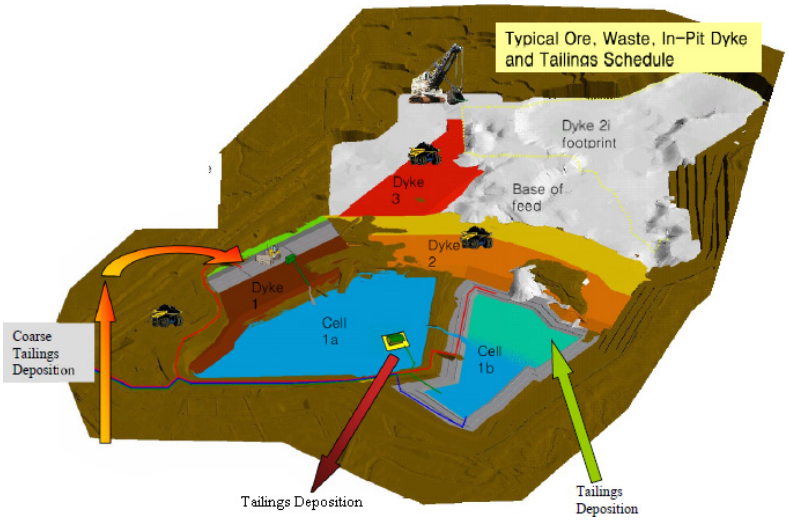

Fig. 4. Dyke construction planning at Shell Canada Ltd. – long to medium term (Fauquier et al., 2009)

3. Problem definition

Mine management is always faced with the problem of achieving multiple goals with the available limited resources. In oil sands mining, due to the limitation of lease area, the pit phase advancement is carried out simultaneously with the construction of tailings dykes in the mined out areas of the pit, one section at a time. These dykes are constructed to hold tailings that are produced during the processing of the oil sands. Dykes with different configurations are required during the construction. Most of the materials used in constructing these dykes come from the oil sands mining operation (overburden and interburden). It is assumed that the material sent to the processing plant (ore) must have a specified amount of bitumen and percentage fines as well as the material sent for dyke construction (dyke material). Any other material that does not meet the requirements of ore or dyke material is sent to the waste dump.

The main problem here is determining the order of extraction of ore, dyke material and waste to be removed from a predefined ultimate pit limit over the mine life that maximizes the net present value of the operation – a strategic schedule. Fig. 5 shows a schematic representation of the problem definition. Fig. 5 illustrates the scheduling of an oil sands ultimate pit block model containing N blocks. Each block n, is made up of ore o_n, dyke material d_n, and waste w_n. The material in each block is to be scheduled over T periods depending on the goals and constraints associated with the mining operation. For period t_1, the ore material scheduled is o_n^1, the dyke material scheduled is d_n^1, and the waste material scheduled is w_n^1.

The strategic schedule to be developed is subject to a variety of economic, technical and physical constraints. The constraints control the mining extraction sequence, ore and dyke material blending requirements and mining, processing and dyke material goals. The mining, processing, and dyke material goals specifies the quantities of material allowed for the mining operation, processing plant and dyke construction respectively.

The strategic schedule is the main driver for the profitability of the oil sands mining operation. The schedule controls the NPV of the operation and enables a robust waste management planning strategy. Improper waste management planning can lead to environmental issues causing immediate mine closure by regulatory agencies and major financial liabilities.

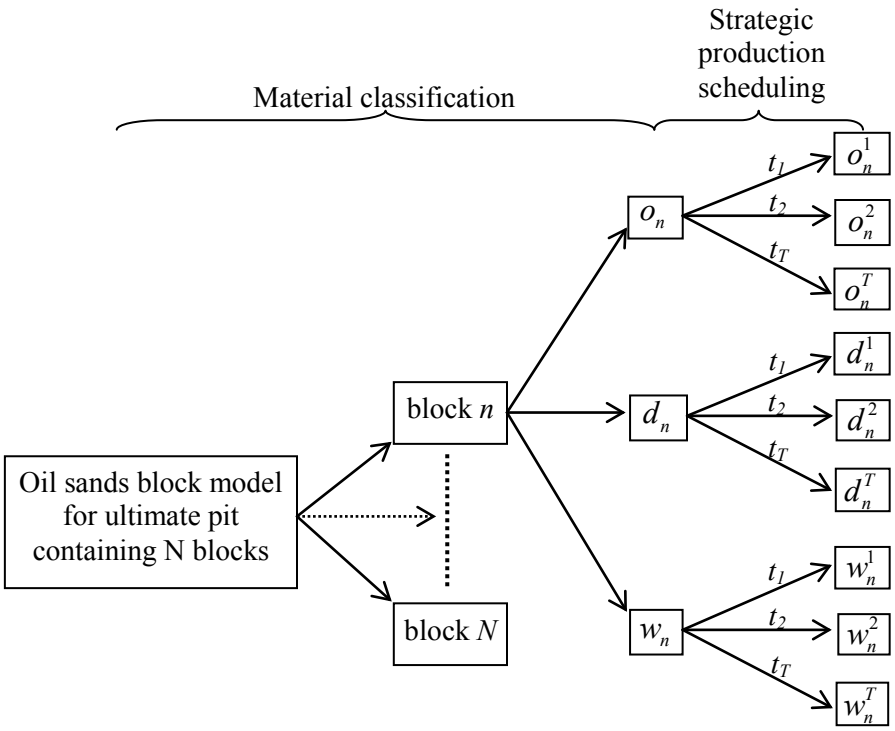

Fig. 5 Schematic representation of the problem definition

4. Theoretical framework and models

4.1. Orebody block modeling, ultimate pit limit, and some assumptions

In long-term mine planning, one of the significant steps in the planning process is orebody block modeling. This is made up of the geologic and economic block models which serve as the backbone that drives the activities of the mine throughout its life. It is used for assessing the cash flow of the entire mining operation and then further exploited in subsequent mine planning processes such as optimization, pit design, production scheduling, waste management, equipment selection and plant design. Block models are three-dimensional arrays of rectangular blocks used to model orebodies. Each attribute in a block model represents one characteristic of the volume of material. These attributes include but are not limited to rock types, grades, density and dollar value. These attributes are stored in individual models, which have the same number of rows, columns and levels (Hustrulid and Kuchta, 2006). To determine the size of the block model needed to define the orebody, attributes like the shape and size of the orebody, the mining method, the mining bench height, and mining equipment selection need to be taken into consideration.

The source data for the geologic block model is the information from the drill holes logged from the exploration of the orebody. It is also required that the modeler understands the basic geology of the formation of the orebody and its country or host rock. Cost and revenue information such as mining cost, processing cost and mineral selling price are used in generating the economic block model (Askari-Nasab, 2009).

In geologic modeling, reliable estimation or simulation techniques are provided by Geostatistics to generate block attributes at locations where no data is available. A common estimation technique described as the “workhorse” in Geostatistics is Kriging (Deutsch, 2002). Inverse distance weighting (IDW) is another spatial interpolation algorithm that has been used over the years (ArcGIS, 2010) for geologic modeling. IDW is used for building the geologic model of the

synthetic and real case data used for this initial analysis and Kriging will be used for other real case data in future.

It is assumed that the blocks within the block model are made of smaller regions known as parcels. A parcel is part of a block for which the rock-type, tonnage and element content are known. A block can be made up of zero or more parcels and the total tonnage of the parcels may sum up to the block tonnage or it may be less. The difference, which is waste of unknown rock-type, is known as undefined waste. Neither the location nor the shape of a parcel within a block is defined but the spatial location of each block is defined by the coordinates of its center. Based on the ore tonnage and the grade in each block, the quantity of contained mineral are calculated (Gemcom Software International, 2008; Askari-Nasab and Awuah-Offei, 2009).

It is assumed that the orebody will be extracted using open pit mining techniques and a classical ultimate pit limit design will be generated based on the graph algorithm (Lerchs and Grossmann, 1965; Hustrulid and Kuchta, 2006). This pit outline contains reserves that maximize the profit. As demonstrated by Askari-Nasab and Awuah-Offei (2009), the ultimate pit limit generated directly when an optimal long-term scheduling algorithm is used will become a subset of the conventional ultimate pit limit that is generated using the Lerchs and Grossman's algorithm (Lerchs and Grossmann, 1965). With this basis, the process of finding the optimal long-term strategic and operational schedule will be divided into two steps: 1) determine the ultimate pit limits, and 2) generate a production schedule within the ultimate pit limit.

4.2. Clustering

One of the main problems associated with finding the optimal long-term production schedule is that, the size of the problem grows exponentially as the number of blocks increases (Askari-Nasab and Awuah-Offei, 2009) resulting in insufficient computer memory during optimization. This is caused by an increase in the number of decision variables and constraints resulting mainly from the block mining precedence. An efficient way of dealing with this problem is by applying a clustering technique. Clustering is a technique used for aggregating blocks in a block model. In the clustering algorithm to be used in this research, blocks within the same level or mining bench are grouped into clusters based on the attributes: location, rock-type, and grade distribution. These clusters of blocks are referred to as mining-cuts and they have similar attribute definitions to that of the blocks such as coordinates representing the spatial location of the mining-cut.

This block aggregation approach will summarize ore data as well as maintain an important separation of lithology. The total quantity of contained elements in the blocks will be modeled for the mining-cuts to ensure the accuracy of the estimated values. This approach also ensures the planning of a practical equipment movement strategy based on the contained elements and tonnages in the mining-cuts. The clustering algorithm to be used for this research is a fuzzy logic clustering algorithm (Kaufman and Rousseeuw, 1990; Askari-Nasab and Awuah-Offei, 2009).

It is important to note that, clustering of blocks in a block model to mining-cuts reduces the degree of freedom of variables or resolution of the problem when finding the mining sequence that maximizes the NPV of the operation. This may lead to reduced NPV values as compared to a high resolution block level optimization (Askari-Nasab and Awuah-Offei, 2009).

For this paper, since the block model data used has small number of blocks, no clustering was done. Clustering will be done in subsequent implementation of the MIGP model to be conducted on large scale problems.

4.3. The goal programming model

The long-term mine production scheduling problem will be formulated using a combination of mixed integer and goal programming formulation. Using goal programming is appropriate in this context because the structure enables the optimization solution to try achieving a set of goals where some goals can be traded off against one another depending on their priority. Hard constraints can

also be converted to soft constraints which otherwise could lead to infeasible solutions. In simple terms, goal programming allows for flexible formulation and the specification of priorities among goals (Liang and Lawrence, 2007).

The formulated model for the strategic scheduling problem has an objective function, goal function and constraints. The goal objectives are mining, processing and dyke construction. These goals will be prioritized according to the impact of a deviation from their targets on the entire mining operation. The general form of goal programming as applied in multiple criteria decision making optimization can be mathematically expressed as in Eqs. (1) to (4) (Ferland et al., 2001; Esfandiri et al., 2004; Liang and Lawrence, 2007):

Objective function

$$Z = \sum \left(P_i \left(d_i^+ + d_i^- \right) \right) \qquad P_1 > P_2 > .....P_i \tag{1}$$

Goal function

$$\sum C_{ij} X_j + d_i^- + d_i^+ = G_i \tag{2}$$

Constraints

$$\sum D_{ij} X_j = T_i \tag{3}$$

$$\sum E_{ij} X_j \le M_i$$

Limitations

$$\forall X_i,\ d_i^+,\ d_i^- \ge 0 \tag{4}$$

where P_i = i-th priority

X_j = decision variable

G_i = target level of i-th goal

T_i, M_i = mining and technological constraints

C_{ij} = unit contribution of activity j-th to goal

D_{ij}, E_{ij} = unit contribution of activity j-th to system constraint

d_i^+ = positive deviation

d_i^- = negative deviation

4.3.1 Application of mixed integer goal programming (MIGP) model

4.3.1.1. Notation

The notations used in the formulation of the oil sands strategic production scheduling problem has been classified as sets, indices, subscripts, parameters and decision variables.

4.3.1.2. Sets

N= {1,…..,N}	set of all blocks in the model.
$D_n(J)$	for each block, *n*, there is a set $D_n(J) \subset N$ which includes all the blocks that must be extracted prior to mining block *n* to ensure that block *n* is

exposed for mining with safe slopes, where J is the total number of blocks in the set $D_n(J)$.

$C_n(L)$ for each block, *n*, there is a set $C_n(L) \subset D_n(J)$ defining the immediate predecessor blocks that must be extracted prior to extraction of block *n*, where L is the total number of blocks in the set $C_n(L)$.

4.3.1.3. Indices and subscripts

A parameter, *f*, can take three indices and a subscript in the format $f_{n,l}^{e,t}$. Where:

$t \in \{1,.....,T\}$ index for scheduling periods.

$n \in \{1,.....,N\}$ index for blocks.

$e \in \{1,.....,E\}$ index for element of interest in each block.

$l = \{m,\ p,\ d\}$ subscripts for mining, processing or dyke construction respectively.

4.3.1.4. Parameters

d_n^t the discounted profit obtained by extracting block *n* in period t.

v_n^t the discounted revenue obtained by selling the final product within block *n* in period *t* minus the discounted processing cost of all the ore material in block *n*.

p_n^t the extra discounted cost of mining all the material in block *n* as dyke material for construction.

q_n^t the discounted cost of mining all the material in block *n* as waste.

g_n^e the average grade of element *e* in ore portion of block *n.*

$\underline{g}^{t,e}$ the lower bound on the required average head grade of element *e* in period *t.*

$\overline{g}^{t,e}$ the upper bound on the required average head grade of element *e* in period *t*.

f_n^e the average percent of fines in ore portion of block *n*.

$\underline{f}^{t,e}$ the lower bound on the required average fines percent of ore in period *t.*

$\overline{f}^{t,e}$ the upper bound on the required average fines percent of ore in period *t*.

f_n^d the average percent of fines in dyke material portion of block *n*.

$\underline{f}^{t,d}$ the lower bound on the required average fines percent of dyke material in period *t.*

$\overline{f}^{t,d}$ the upper bound on the required average fines percent of dyke material in period *t*.

o_n the ore tonnage in block *n*.

w_n the waste tonnage in block *n*.

d_n the dyke material tonnage in block *n*.

T_m^t the mining goal in period *t* (tonnes).

$d_1^{-,t}$ the negative deviation from the mining goal in period *t* (tonnes).

$d_1^{+,t}$ the positive deviation from the mining goal in period *t* (tonnes).

T_p^t the processing goal in period *t* (tonnes).

$d_2^{-,t}$ the negative deviation from the processing goal in period *t* (tonnes).

$d_2^{+,t}$ the positive deviation from the processing goal in period *t* (tonnes).

T_d^t the dyke material goal in period *t* (tonnes).

$d_3^{-,t}$ the negative deviation from the dyke material goal in period *t* (tonnes).

$d_3^{+,t}$ the positive deviation from the dyke material goal in period *t* (tonnes).

P_1 the priority level associated with minimizing the deviations from the mining goal.

P_2 the priority level associated with minimizing the deviations from the processing goal.

P_3 the priority level associated with minimizing the deviations from the dyke material goal.

$r^{e,t}$ the proportion of element *e* recovered in time period t (processing recovery).

$p^{e,t}$ the price of element *e* in present value terms per unit of product.

$s^{e,t}$ the selling cost of element *e* in present value terms per unit of product.

$c^{e,t}$ the cost in present value terms per tonne of ore for processing.

k^t the cost in present value terms per tonne of dyke material for dyke construction.

m^t the cost in present value terms of mining a tonne of waste in period *t*.

a_1 the penalty paid per tonne in deviating from the mining goal.

a_2 the penalty paid per tonne in deviating from the processing goal.

a_3 the penalty paid per tonne in deviating from the dyke material goal.

4.3.1.5. Decision variables

$x_n^t \in [0,1]$ a continuous variable representing the portion of block *n* to be extracted as ore and processed in period *t*.

$z_n^t \in [0,1]$ a continuous variable representing the portion of block *n* to be extracted as dyke material and used for dyke construction in period *t*.

$y_n^t \in [0,1]$ a continuous variable representing the portion of block *n* to be mined in period *t*, which includes both ore, dyke material and waste.

$b_n^t \in [0,1]$ a binary integer variable controlling the precedence of extraction of blocks. b_n^t is equal to one if the extraction of block *n* has started in period t, otherwise it is zero.

4.3.1.6. Modeling of economic block value

The objective function of the MIGP model for strategic LTPP is to maximize the net present value of the mining operation and minimize the deviations from the mining goal, processing goal and dyke material goal. The concept of economic block value is based on ore parcels which could be mined selectively. The profit from mining a block is a function of the value of the block and the cost incurred in mining, processing and dyke construction. The discounted profit from block *n* is equal to the discounted revenue obtained by selling the final product contained in block *n* minus the discounted cost involved in mining block *n* minus the extra discounted cost of mining dyke material (Askari-Nasab and Awuah-Offei, 2009). This has been simplified into Eqs. (5) to (8).

$$d_n^t = v_n^t - q_n^t - p_n^t \tag{5}$$

Where:

$$v_n^t = \sum_{e=1}^{E} o_n \times g_n^e \times r^{e,t} \times \left(p^{e,t} - s^{e,t} \right) - \sum_{e=1}^{E} o_n \times c^{e,t} \tag{6}$$

$$q_n^t = \left(o_n + d_n + w_n \right) \times m^t \tag{7}$$

$$p_n^t = d_n \times k^t \tag{8}$$

4.3.1.7. The mixed integer goal programming model

Using multiple criteria decision making analysis, the objective functions of the MIGP model for strategic LTPP as applied in oil sands mining, can be formulated as maximizing the NPV and minimizing deviations from the goals. These are represented by Eqs. (9) and (10).

$$Max \sum_{t=1}^{T} \sum_{n=1}^{N} \left(v_n^t \times x_n^t - p_n^t \times z_n^t - q_n^t \times y_n^t \right) \tag{9}$$

$$Min \sum_{t=1}^{T} \sum_{n=1}^{N} \left[P_1 \left(a_1 d_1^{-,t} \right),\ P_2 \left(a_2 d_2^{-,t} \right),\ P_3 \left(a_3 d_3^{-,t} + a_3 d_3^{+,t} \right) \right] \tag{10}$$

Eqs. (9) and (10) can be combined as a single objective function formulated as in Eq. (11).

$$Max \sum_{t=1}^{T} \sum_{n=1}^{N} \left[\left(v_n^t \times x_n^t - p_n^t \times z_n^t - q_n^t \times y_n^t \right) - \left(P_1 \left(a_1 d_1^{-,t} \right) + P_2 \left(a_2 d_2^{-,t} \right) + P_3 \left(a_3 d_3^{-,t} + a_3 d_3^{+,t} \right) \right) \right] \tag{11}$$

The complete MIGP model comprising of the objective function, goal function and constraints can be formulated as:

Objective function:

$$Max \sum_{t=1}^{T} \sum_{n=1}^{N} \left[\left(v_n^t \times x_n^t - p_n^t \times z_n^t - q_n^t \times y_n^t \right) - \left(P_1 \left(a_1 d_1^{-,t} \right) + P_2 \left(a_2 d_2^{-,t} \right) + P_3 \left(a_3 d_3^{-,t} + a_3 d_3^{+,t} \right) \right) \right] \tag{12}$$

Goal functions:

$$\sum_{n=1}^{N}\left(\left(o_n + w_n + d_n\right)\times y_n^t\right) + d_1^{-,t} = T_m^t \qquad \forall t \in \{1,...,T\} \tag{13}$$

$$\sum_{n=1}^{N}\left(o_n \times x_n^t\right) + d_2^{-,t} = T_p^t \qquad \forall t \in \{1,...,T\} \tag{14}$$

$$\sum_{n=1}^{N}\left(d_n \times z_n^t\right) + d_3^{-,t} - d_3^{+,t} = T_d^t \qquad \forall t \in \{1,...,T\} \tag{15}$$

Constraints:

$$\underline{g}^{t,e} \le \sum_{n=1}^{N} g_n^e \times o_n \times x_n^t \Big/ \sum_{n=1}^{N} o_n \times x_n^t \le \overline{g}^{t,e} \qquad \forall t \in \{1,...,T\},\quad e \in \{1,...,E\} \tag{16}$$

$$\underline{f}^{t,e} \le \sum_{n=1}^{N} f_n^e \times o_n \times x_n^t \Big/ \sum_{n=1}^{N} o_n \times x_n^t \le \overline{f}^{t,e} \qquad \forall t \in \{1,...,T\},\quad e \in \{1,...,E\} \tag{17}$$

$$\underline{f}^{t,d} \le \sum_{n=1}^{N} f_n^d \times d_n \times z_n^t \Big/ \sum_{n=1}^{N} d_n \times z_n^t \le \overline{f}^{t,d} \qquad \forall t \in \{1,...,T\},\quad d \in \{1,...,D\} \tag{18}$$

$$x_n^t + z_n^t \le y_n^t \qquad \forall t \in \{1,...,T\},\quad n \in \{1,...,N\} \tag{19}$$

$$b_n^t - \sum_{i=1}^{t} y_s^i \le 0 \qquad \forall t \in \{1,...,T\},\ n \in \{1,...,N\},\ s \in C(L) \tag{20}$$

$$\sum_{i=1}^{t} y_n^i - b_n^t \le 0 \qquad \forall t \in \{1,...,T\},\quad n \in \{1,...,N\} \tag{21}$$

$$b_n^t - b_n^{t+1} \le 0 \qquad \forall t \in \{1,...,T-1\},\quad n \in \{1,...,N\} \tag{22}$$

$$d_1^{-,t},\ d_2^{-,t},\ d_3^{-,t},\ d_3^{+,t} \ge 0 \qquad \forall t \in \{1,...,T\} \tag{23}$$

$$P_1 > P_2 > P_3 \tag{24}$$

Eq. (12) is the objective function of the formulation which seeks to maximize the net present value and minimize the deviations from the mining, processing and dyke construction material goals. Eqs. (13), (14), and (15) are the goal functions which define the mining, processing and dyke material goals that are required to be achieved. Eqs. (16), (17), and (18) specify the limiting requirements for ore bitumen grade, ore fines and dyke material fines. Eq. (19) ensures that the total material mined in each period does not exceed the sum of the ore and dyke material mined. Eqs. (20), (21) and (22) check the set of immediate predecessor blocks that must be mined prior to mining block *n*. Eq. (23) ensures that the negative and positive deviations from the targeted mining, processing and dyke material goals are always positive. Eq. (24) states the order of prioritization associated with achieving the goals. The model assumes that there exists a pre-emptive priority structure among the goals and this can be changed depending on the aim of optimization.

5. Application of the MIGP model for strategic production scheduling

The problem being looked at here is finding the sequence of extracting ore, dyke material and waste blocks from a predefined ultimate pit over the mine life so that the NPV of the operation is

maximized. The production schedule is subject to some physical, technical and economic constraints such as mining extraction sequence and mining and processing capacities.

The formulation presented here for open pit strategic production scheduling has the objective of maximizing the NPV of the mining operation and minimizing the goal deviations whilst achieving the multiple goals of ore and dyke material requirements. The block sizes used for production scheduling must be similar to the selective mining units; otherwise, the generated schedule may not be feasible in practice. The formulation has been implemented and tested with different sets of parameters for calibration. The proposed MIGP model uses binary integer decision variables, b_n^t to control precedence of block or mining-cut extraction and continuous variables, y_n^t, x_n^t, and z_n^t are used to model extraction, processing and dyke material requirements respectively at block or mining-cut level. Continuous deviational variables, $d_1^{-,t}$, $d_2^{-,t}$, $d_3^{-,t}$, and $d_3^{+,t}$ have been defined to support the goal functions that control extraction, processing and dyke material. These deviational variables provide a continuous range of units (tonnes) that the optimizer chooses from to satisfy the defined goals. The deviational variables are minimized in the objective function. Within the objective function, deviational penalty cost parameters have been defined by a_1, a_2, and a_3 which penalizes the NPV for any deviation from the set goals. This is a significant component of this formulation in that, the optimizer is forced to meet the set goals in order to avoid being penalized resulting in an improved NPV value. To be able to place more emphasis on the goals which are more important, priority parameters P_1, P_2, and P_3 have been defined in the objective function which also penalize the NPV more if the most important set goal is not met. This ensures that goals such as processing are prioritized above dyke material requirements to improve the NPV.

5.1. Precedence of block/mining-cut extraction

The mining precedence constraints are the main reason for the increase in the number of constraints and the complexity of the scheduling problem. Previous mining precedence constraint set-ups enforces that, before a block is mined all blocks on top of it must be mined first. For the example shown in Fig. 6, before block 1 is mined, the 24 blocks above it must be mined first. This results in 24 mining precedence constraint equations in each period for block 1. This increases the size of the problem quickly making the optimization intractable (Askari-Nasab and Awuah-Offei, 2009).

The mining precedence constraint in the MIGP formulation has been modeled using the directed graph theory (Askari-Nasab and Awuah-Offei, 2009). Eqs. (20) to (22) in the model control the relationship of block extraction precedence by the binary integer variable, b_n^t. Specifically, Eq. (20) ensures that only the set of immediate predecessor blocks on the top of a block need to be extracted prior to extracting the block. This is represented by the set $C_n(L)$ in the formulation. Eq. (21) ensures that if extraction of block *n* is started in period *t,* then block *n* has not been extracted before. Eq. (22) ensures that b_n^t is equal to one if extraction of block *n* has started by or in period *t*, otherwise it is zero. This means once the extraction of a block starts in period *t*, this block is available for extraction during the subsequent periods. Fig. 6 shows the set that has to be mined for extracting block 1: $C_1(L) = \{2, 3, 4\}$. This results in 3 mining precedence constraint equations in each period for block 1 as compared to 24 in previous formulations. This decreases the size of the mine production scheduling optimization problem considerably.

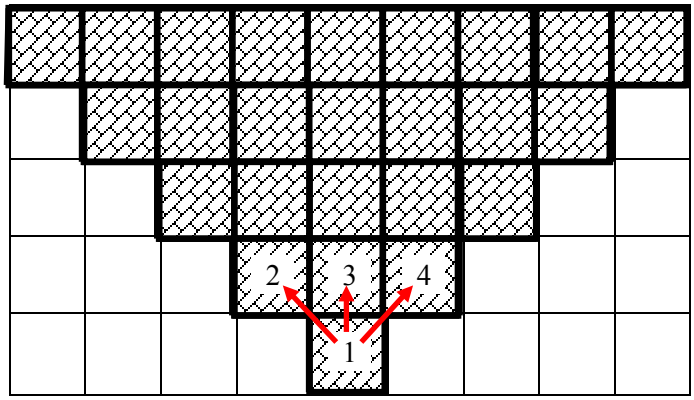

Fig. 6. Block extraction precedence in the MIGP formulation

5.2. Selecting deviational, penalty and priority parameters in the model

To select the appropriate goal deviational parameters for a given problem, the modeler is required to first select a large continuous variable range starting from zero. This is to ensure that the optimizer can find an initial solution for the problem at hand and to give the modeler an idea of which periods certain types of material are available subject to the physical, technical and economic constraints imposed on the schedule. With this background knowledge, the modeler can start tightening the range of the deviational variables for specific goals in some periods. This is to ensure that the solution of the optimization problem is found with as little deviation as possible from the set goals.

The initial penalty cost for deviating from the set goals are set to zero. This literally means that, no penalties are being applied initially for deviating from the set goals. The NPV of the operation generated at this point serves as the baseline NPV which can be improved upon. The next step is to set penalty cost for deviating from the ore and dyke material goals. No penalty cost should be set for deviating from the mining goal because after mining ore and dyke material, the optimizer will be forced to mine waste to make up for the mining goal thereby reducing the NPV of the mining operation. The deviational penalty cost for ore and dyke material should be set below the average cash flow for mining a unit (tonne) of ore or dyke material. This ensures that the optimizer avoids going in for a deviational variable to make up the set goals unless it has no other option under the prevailing constraints. This stems from the fact that in the objective function, the deviation from the goals are being minimized and any deviation from the goals will have a negative impact on the NPV as a result of the penalty cost associated with the deviations. This makes deviational variables chosen by the optimizer in each period as low as can guarantee a feasible solution. If the deviational penalty cost for ore or dyke material are set above the average cash flow for mining ore or dyke material, the optimizer may in some periods choose to go in for deviational variables to make up the set goals since it sees that as a less expensive option to have a greater NPV than mining the required material to get the set goals. The subsequent deviational penalty cost for ore and dyke material should be increased further and the schedule re-optimized to see its impact on the NPV. An increase in the NPV resulting from mining more ore is expected. Subsequent increase in the deviational penalty cost may also result in a decrease in NPV if the optimizer has to mine more waste before mining the ore required to make up the goal; resulting in a negative cash flow for that additional ore block.

The element of goal priority setting in the formulation was introduced to enforce the priority of one goal over the other. This is introduced in the formulation in a similar way to that of penalty cost. Deviational variables of goals with higher priorities are made to carry a heavier negative impact on the NPV of the operation than goals with lower priorities. This forces the optimizer to ensure that goals with higher priorities deviate least from the set goals to avoid higher negative impacts on the

NPV of the operation. For example, it is obvious that in oil sands mining, the priority for achieving goals for processing will be set higher than dyke material.

Whilst setting up these parameters, the modeler needs to keep an eye on the NPV to become aware of the impact of any parameter change on the NPV. It is interesting to note that in some cases the extent of setting the penalty cost below the average cash flow of mining ore or dyke material depends on the extent to which the modeler is ready to trade off NPV to meet the set goals. For example, placing a much higher penalty on ore goal deviational variable may result in a negative cash flow, depending on how many waste or dyke material blocks need to be mined before getting access to an ore block to make up the set goal. In such a case, a higher penalty may enforce the ore goal to be met whilst reducing the NPV of the operation.

In summary, the relationship between penalty cost and priority variable for ore and NPV of the operation is not linear. A general value function plot of NPV of the operation versus penalty cost and priority variable for ore shows an initial direct relationship which later becomes an inverse relationship. This is shown in Fig. 7. The details for the value function plot vary according to the problem setup. It can also be seen from Fig. 7 that the demand for ore in relation to the NPV is not open ended. This is in line with the statement made by Hannan (1985) that in goal programming "more is not always better despite the fact that it is represented that way in the objective function".

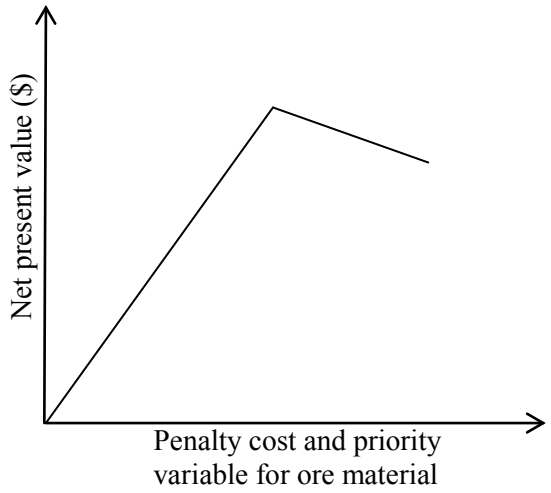

Fig. 7. A general value function plot of NPV of the operation versus penalty cost and priority variable for ore

5.3. Solving the optimization problem

The use of the MIGP formulation for an orebody model usually results in a large scale optimization problem. One of the recent optimization solvers capable in handling such problems is the ILOG CPLEX (ILOG Inc., 2007). This optimizer was developed based on branch and cut algorithm and makes the solving of MIGP models possible for large scale problems. Branch and cut is an algorithm which combines different optimization techniques for solving integer programming problems. This algorithm is a hybrid of branch-and-bound and cutting plane methods (Horst and Hoang, 1996; Wolsey, 1998).

This research uses TOMLAB/CPLEX (Holmström, 2009) as the MIGP model solver. The CPLEX solver engine (ILOG Inc., 2007) has been successfully integrated with MATLAB (Mathworks Inc., 2009) working environment by TOMLAB/CPLEX. An optimization termination criterion that the user set in CPLEX is the gap tolerance (EPGAP). The gap tolerance sets an absolute tolerance on the gap between the best integer objective and the objective of the best node remaining. It instructs CPLEX to stop as soon as it has found a feasible integer solution proved to be within the set EPGAP.

6. Results and discussions

We have developed, implemented, and tested the proposed MIGP model presented in section 4.3 in TOMLAB/CPLEX environment (Holmström, 2009). The performance of the proposed model is analyzed based on net present value, mining production goals and smoothness of the generated schedules. The model is verified by numerical experiments on a synthetic data set containing 120 blocks on four mining benches and a real mining ultimate pit containing 555 blocks on five mining benches. This was for an oil sand deposit and scheduling was done for ore, dyke material and waste over 15 periods. The model was tested on a Dell Precision T3500 computer at 2.4GHz, with 3GB of RAM. A relative tolerance of 1% and 5% on the gap between the best integer objective and the feasible integer solution was set for the 120 blocks and 555 blocks respectively.

Table 1 and Table 2 show the inputs and numerical results of the test of the MIGP model with the data set containing 120 blocks over five periods of extraction. The initial goal deviational variables were set at 20,000 tonnes. This was subsequently modified and the final goal deviational variables were set at 20,000 tonnes for mining and processing goals and 300 tonnes for dyke material goal for all the runs. In setting the deviational variables, among other things the smoothness of the schedule should be monitored. Initially, the model was run with no penalty cost and goal priorities to get the baseline NPV which is subject to further improvement. Subsequent penalty cost and priorities placed on the goals did not bring any further NPV improvements. This was because all the 120 blocks were mined either with or without penalty cost and priorities. The average runtime was 4 seconds. The required ore and dyke material goals were met within the set deviational variables as well as the grade of each material. Figs. 8, 10, and 11 show the schedules for ore, dyke material and waste over the five periods for run 3. Fig. 9 shows the average ore grade over the five periods.

Table 1. Inputs for the synthetic data containing 120 blocks scheduled over 5 periods

Run	Penalty cost ($/tonne) and priority			Goals (Million tonnes)		
	Mining	Processing	Dyke material	Mining	Processing	Dyke material
1	0	0	0	1.95	1.35	0.52
2	0	3	2	1.95	1.35	0.52
3	0	6	4	1.95	1.35	0.52

Table 2. Results for the synthetic data containing 120 blocks scheduled over 5 periods

Run	Root Node Gap %	NPV ($M)
1	0.45	1.21
2	5.53	1.21
3	7.91	1.21

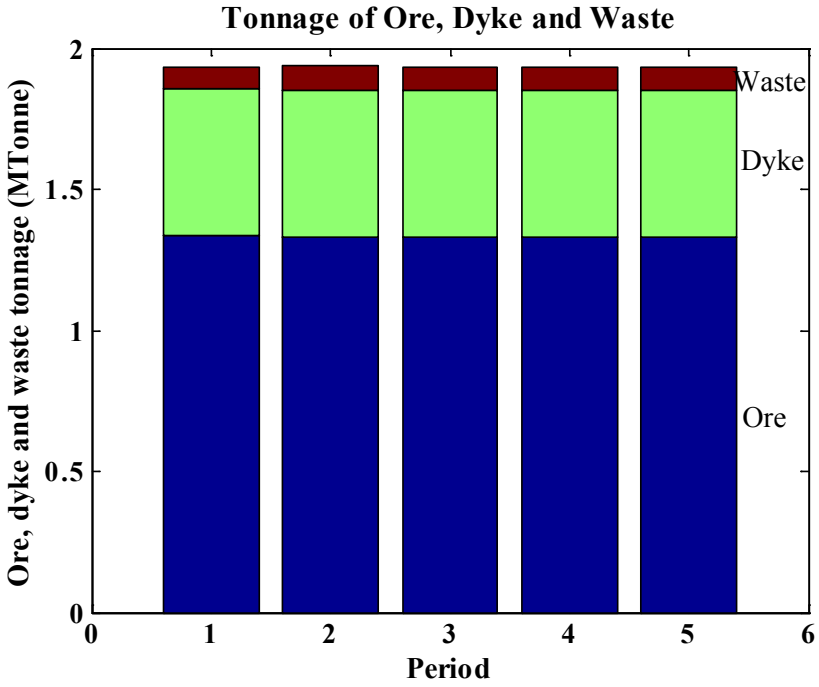

Fig. 8. Tonnage of ore, dyke material and waste per period

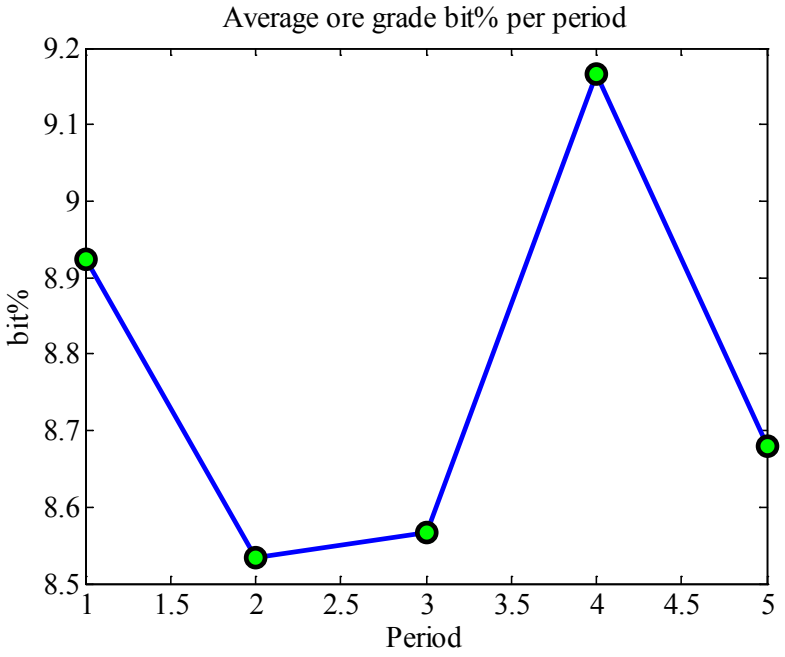

Fig. 9. Average ore grade (bitumen %) per period

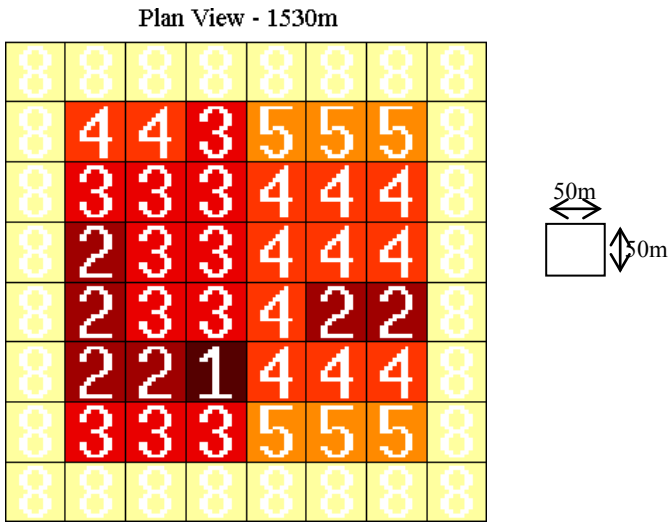

Fig. 10. Plan view of bench 1575m showing periods of block extraction

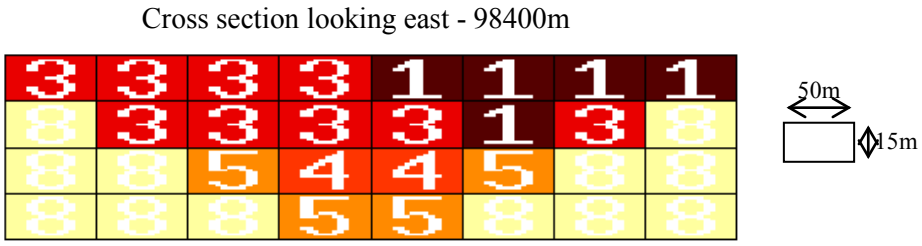

Fig. 11. Cross section 98400m looking east showing periods of block extraction

Table 3 shows inputs and numerical results from the MIGP model for an oil sands ultimate pit data set containing 555 blocks over 15 scheduling periods. The ultimate pit contains five 15m benches from elevation 312.5m to 237.5m. The ultimate pit was obtained using WHITTLE (Gemcom Software International, 2008). Each block represents a volume of 100m x 100m x 15m of rock. The original block model was reblocked by putting four blocks into one, thereby resulting in 555 blocks with four parcels each in the ultimate pit. The model contains 178 million tonnes of material with 94 million tonnes of ore. The ore bitumen grade ranges from 7 to 15.5% with an average grade of 10.8%. The ore fines grade ranges from 0 to 30.0% with an average grade of 6.8%. It also contains 70 million tonnes of dyke material. The dyke material fines grade ranges from 0 to 47.2% with an average grade of 1.1%. Bitumen and fines grades need to be controlled within an acceptable range for processing plant feed and dyke construction.

Table 3. Inputs and results for the oil sands data set containing 555 blocks scheduled over 15 periods

Run	Penalty cost ($/tonne) and priority			Root Node Gap %	NPV ($M)
	Mining	Processing	Dyke material		
1	0	0	0	2.60	336.93
2	0	4	2	2.32	337.91
3	0	10	6	2.67	$339.49
4	0	16	8	4.78	331.80

Table 4. Inputs for the oil sands data set containing 555 blocks scheduled over 15 periods

Run	Mining goals (Million tonnes)			Processing goals (Million tonnes)			Dyke material goals (Million tonnes)		
	P1-P3	P4-P9	P10-P15	P1-P3	P4-P9	P10-P15	P1-P3	P4-P9	P10-P15
1, 2, 3, 4	10.5	10.5	13.9	0	6.5	8.5	10.5	3.8	2.6

Table 5. Inputs for the oil sands data set containing 555 blocks scheduled over 15 periods

Run	Mining deviation (Million tonnes)			Processing deviation (Million tonnes)			Dyke material deviation (Million tonnes)		
	P1-P3	P4-P9	P10-P15	P1-P3	P4-P9	P10-P15	P1-P3	P4-P9	P10-P15
1, 2, 3, 4	1.0	1.0	1.0	0	0.05	0.5	0.1	0.1	0.1

Table 6. Inputs for the oil sands data set containing 555 blocks scheduled over 15 periods

Run	Ore bitumen grade (wt%)		Ore fines grade (wt%)		Dyke material fines grade (wt%)	
	$\overline{g}^{t,e}$	$\underline{g}^{t,e}$	$\overline{f}^{t,e}$	$\underline{f}^{t,e}$	$\overline{f}^{t,d}$	$\underline{f}^{t,d}$
1, 2, 3, 4	12	7	23	0	50	0

It is desired to keep an average processing plant head grade with bitumen content between 7 and 12% and fines content less than 23%. The dyke material is required to have bitumen content less than 7% and fines content less than 50%. Our goal is to generate a uniform schedule based on the availability of material, the plant processing and dyke construction requirements. Further to this, we intend to keep a steady stripping ratio of about 1.6 when the mining of ore starts. This would ensure that the mining equipment capacity will be uniform over some time. Table 6 shows the input grade limits set for ore and dyke material.

To schedule the 555 blocks over 15 periods, the initial deviational variables chosen were 1M tonnes for all the goals. These were further reduced based on the availability of material to enable a uniform and smooth supply of plant feed and dyke construction material and maintain a uniform mining capacity. The mining, processing and dyke material goals were also modified accordingly. The final goal deviational variables used for the runs are shown in Table 5. The associated goals are shown in Table 4.

The initial penalty cost and priority were set to zero to establish the baseline NPV. These were subsequently increased and the NPV recalculated whilst monitoring the uniformity and smoothness of the resulting schedule. The NPV starts to increase due to the deviational penalty cost and priority placed on the ore material. The NPV reaches some threshold value under the set goals and constraints and any further increase in the deviational penalty cost and priority results in a decrease in the NPV. This happens when the penalty cost and priority placed on the ore material is so high that, whilst forcing the optimizer to mine more ore to achieve the goal, the cash flow from any

additional ore block is negative. This may result from an ore block being overlain by lots of waste or dyke material which must be mined before mining the ore block. This drives the overall value of mining the additional ore block negative. From Table 3, run 3 generated the maximum NPV and a uniform schedule and the results that follow are based on this run.

An important feature of this MIGP formulation, that makes it a robust and flexible platform for mine planning, is that apart from the NPV maximization, the planner has control over the setting of goals and their deviational variables, upper and lower limits of grades and the deviational penalty cost and priority of goals. The planner can also decide on tradeoffs between NPV maximization and goal achievement.

The results from run 3 shows that during the first three years, due to the formation of the oil sands deposit, dyke material was the most abundant as a result of the presence of the overburden material which must be stripped. Once the overburden material is mined, ore becomes available in period 4 and was again ramped up in period 10. The dyke material was ramped down after period 3 and reduced further in period 10 due to the dwindling reserves of interburden dyke material. The mining capacity was uniform for the first 9 periods and then increased for the remaining periods. Figs. 12, 13, 14, and 15 show the schedules for ore, dyke material, and waste mined over the 15 scheduling periods. The total amount of material mined was 176 million tonnes. This is made up of 87 million tonnes of ore, 68 million tonnes of dyke material and the rest being waste. It can be seen from the schedule that the mining of waste was delayed until later years. This phenomenon is in accordance with the objective of maximizing the NPV of the operation.

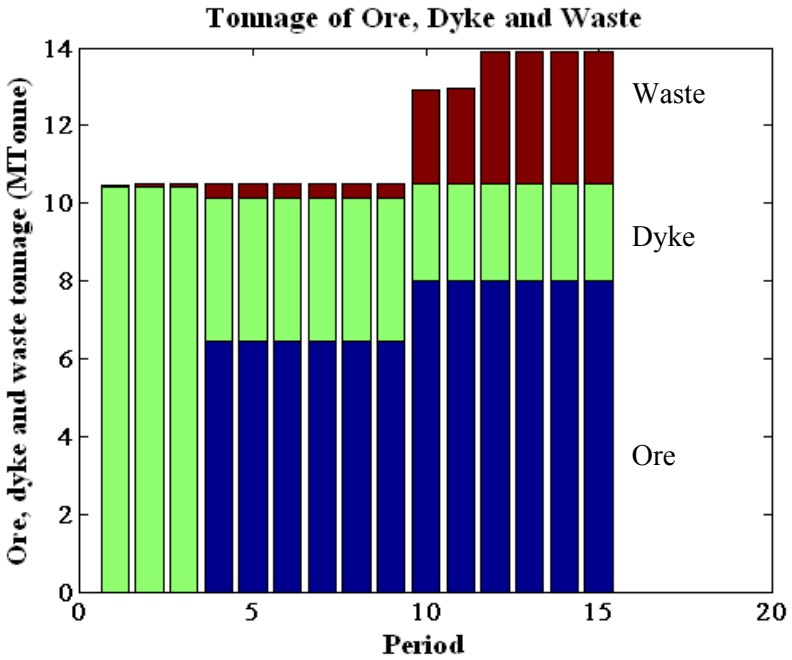

Fig. 12. Tonnage of ore, dyke material and waste per period

Plan view - 297.5m

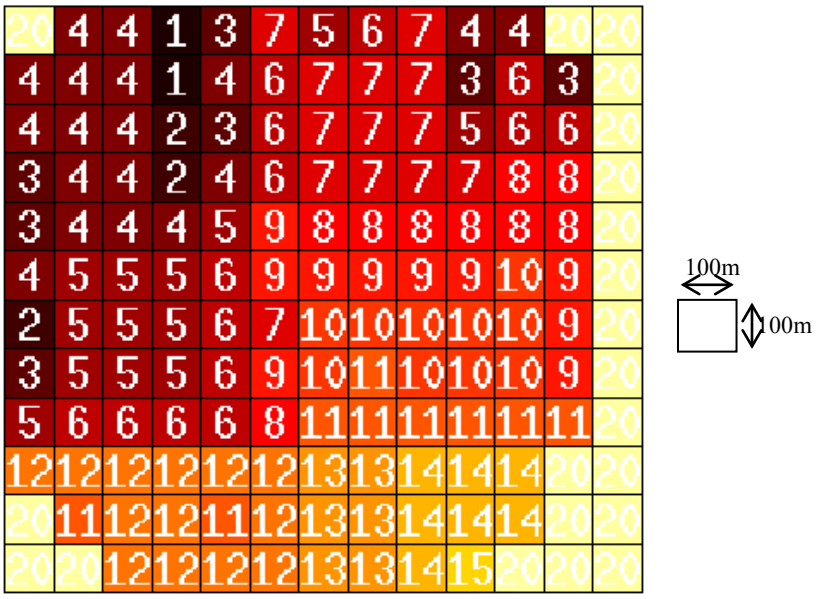

Fig. 13. Plan view of bench 297.5m showing periods of block extraction

Cross section looking east – 47800m

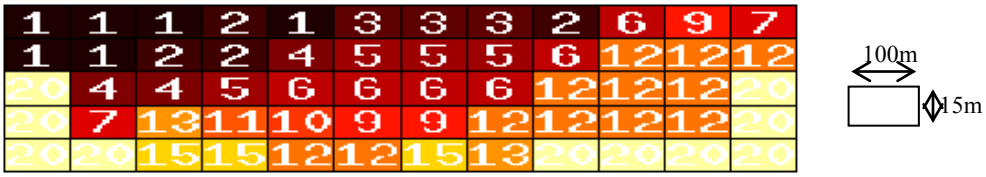

Fig. 14. Cross section 47800m looking east showing periods of block extraction

Cross section looking north – 50800m

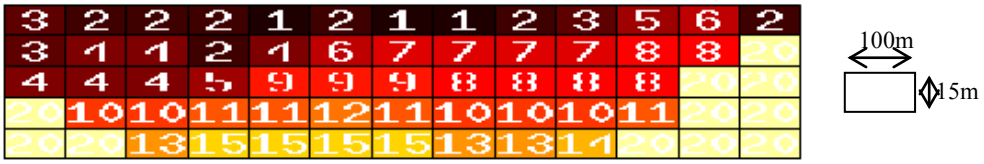

Fig. 15. Cross section 50800m looking north showing periods of block extraction

It is our target to blend the run-of-mine ore to meet the quality and quantity specification of the processing plant and dyke construction. As more detailed planning is done in the short and medium term, the blending problem becomes more prominent. The plant head grade and the dyke material grade that was set were successfully achieved in all the periods. The ore material bitumen grade was between 9.5 and 12% with fines grade between 5% and 17%. The dyke material fines grade was also between 0 and 50%. These can be seen in Figs. 16, 17, and 18. It can be seen in the graphs that there is a general trend of decreasing bitumen grade for ore over the periods. This high grading phenomenon in the early periods is in accordance with the objective of maximizing the NPV of the operation.

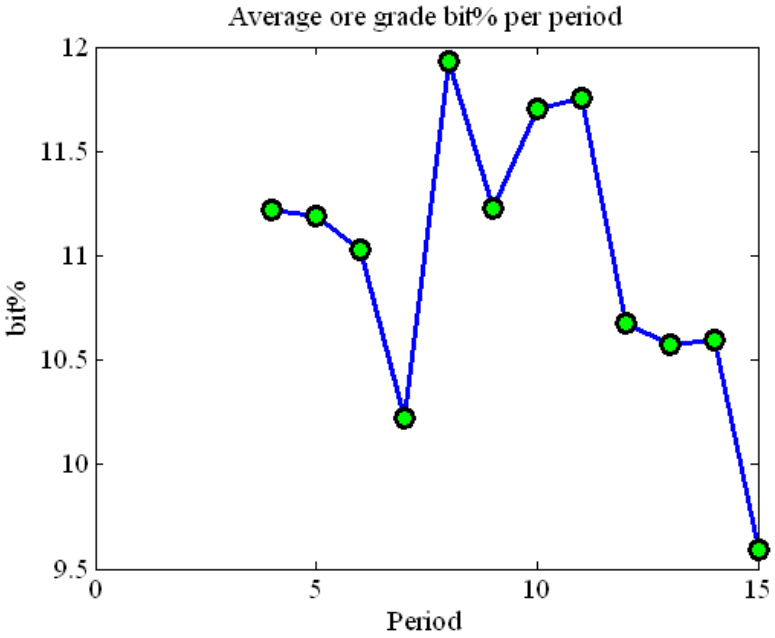

Fig. 16. Average bitumen grade of ore per period

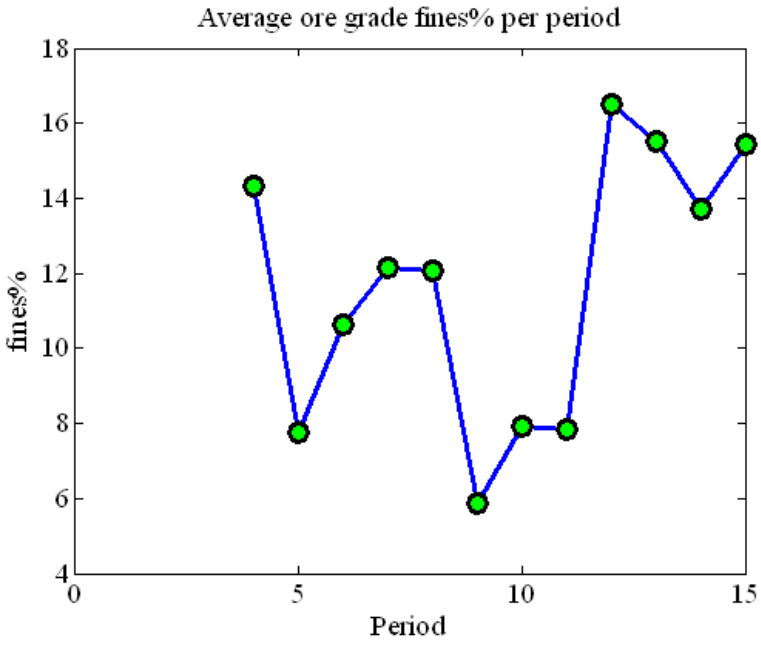

Fig. 17. Average fines grade of ore per period

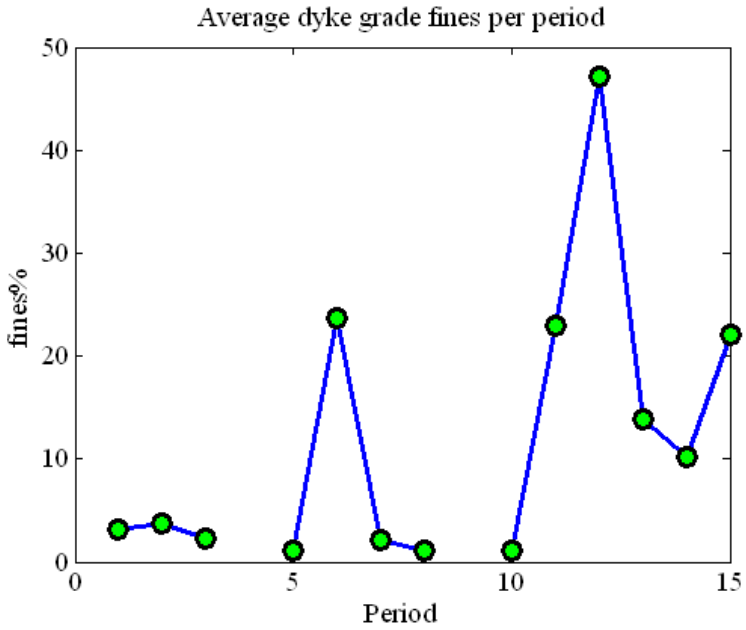

Fig. 18. Average fines grade of dyke material per period

7. Conclusions and future research work

This paper discussed the current application of mixed integer programming and goal programming to the open pit long-term production scheduling problem and some of the limitations. Further to this, we looked at the use of mixed integer goal programming formulations in solving industrial problems due to the advantages derived from this hybrid formulation. In this paper, we have developed, implemented and tested a MIGP optimization formulation for open pit production scheduling of multiple material types. The oil sands mining case was used. This requires that a production schedule is generated for ore, dyke material and waste. These schedules ensure that whilst ore is fed to the plant, there is enough material available for dyke construction. This enables adequate space for the in-pit storage of tailings from the plant.

The formulation uses binary integer variables to control mining precedence and continuous variables to control mining of ore and dyke material. There are also goal deviational variables and penalty costs and priorities that must be set up by the planner. The optimization model was implemented in TOMLAB/CPLEX environment.

The developed model proved to be able to generate a uniform schedule for ore and dyke material. It also provides the planner the flexibility of choosing goal deviational variables, penalty costs and priorities to achieve a uniform schedule. These parameters can also be used to set priorities for goals thereby leading to improved NPV. Similarly, tradeoffs between achieving a goal and maximizing NPV can be made.

From the results of the schedule, there is a problem where the block extraction sequence, especially for the first bench, does not follow a practical mining sequence. This is due to the degree of freedom for the first bench blocks which are not constrained in any way during optimization in terms of mining precedence thereby leading to a schedule that is less smooth. Further research will focus on developing a horizontal direction block extraction sequence constraint that will enforce a more systematic way of mining especially for the first bench. This becomes more significant in the short term due to the equipment maneuverability requirements in oil sands mining. Clustering will also be done for large scale deposits.

8. Appendix

Matlab code developed to define and implement the proposed MIGP formulation for oil sands production scheduling optimization.

9. References

[1] Akaike, A. and Dagdelen, K. (1999). *A strategic production scheduling method for an open pit mine*. Paper presented at 28th International Symposium on the Application of Computers and Operations Research in the Mineral Industry, pp. 729-738.

[2] ArcGIS (2010). How inverse distance weighted interpolation works. *ArcGIS Resource Center,* Retrieved July 19, 2010 from: http://help.arcgis.com/en/arcgisdesktop/10.0/help/index.html#//00310000002m000000.htm

[3] Askari-Nasab, H. (2006). Intelligent 3D interactive open pit mine planning and optimization. PhD Thesis, University of Alberta, Edmonton, Pages 167.

[4] Askari-Nasab, H. (2009). *Surface mine design and optimization.* University of Alberta, Edmonton. Pages C7-15.

[5] Askari-Nasab, H. and Awuah-Offei, K. (2009). Mixed integer linear programming formulations for open pit production scheduling. Mining Optimization Laboratory, University of Alberta, Edmonton, 335.

[6] Askari-Nasab, H. and Awuah-Offei, K. (2009). Mixed integer linear programming formulations for open pit production scheduling. University of Alberta, Mining Optimization Laboratory Report One, Edmonton, 1-31.

[7] Askari-Nasab, H. and Awuah-Offei, K. (2009). Open pit optimization using discounted economic block value. *Transactions of the Institution of Mining and Metallurgy, Section A, Mining Industry*, *118*,(1), 1-12.

[8] Boland, N., Dumitrescu, I., Froyland, G., and Gleixner, A. M. (2009). LP-based disaggregation approaches to solving the open pit mining production scheduling problem with block processing selectivity. *Computers and Operations Research*, *36*,(4), 1064-89.

[9] Caccetta, L. and Hill, S. P. (2003). An application of branch and cut to open pit mine scheduling. *Journal of Global Optimization*, *27*, 349-365.

[10] Chanda, E. K. C. and Dagdelen, K. (1995). Optimal blending of mine production using goal programming and interactive graphics systems. *International Journal of Mining, Reclamation and Environment*, *9*,(4), 203-208.

[11] Chen, V. Y. X. (1994). A 0-1 goal programming model for scheduling multiple maintenance projects at a copper mine. *European Journal of Operational Research*, *76*, 176-191.

[12] Dagdelen, K. (1985). Optimum multi-period open pit mine production scheduling by Lagrangian parameterization. PhD Thesis, University of Colorado, Golden, Colorado, Pages 325.

[13] Dagdelen, K. and Johnson, T. B. (1986). *Optimum open pit mine production scheduling by Lagrangian parameterization*. Paper presented at 19th International Symposium on the Application of Computers and Operations Research in the Mineral Industry, Society of Mining Engineers (AIME), pp. 127-142.

[14] Datamine Corporate Limited (2008). NPV Scheduler. Ver. 4, Beckenham, UK.

[15] Denby, B. and Schofield, D. (1995). Inclusion of risk assessment in open pit design and planning. *Institution of Mining and Metallurgy*, *104*,(A), 67-71.

[16] Deutsch, C. V. (2002). *Geostatistical reservoir modeling.* Oxford University Press, New York. Pages 376.

[17] Dilay, J. D. (2001). Interim Directive ID 2001-7. Alberta Energy and Utilities Board, Calgary, 9.

[18] Esfandiri, B., Aryanezhad, M. B., and Abrishamifar, S. A. (2004). Open pit optimization including mineral dressing criteria using 0-1 non-linear goal programming. *Mining Technology, Transactions of the Institutions of Mining and Metallurgy*, *113*, A3-A13.

[19] Fauquier, R., Eaton, T., Bowie, L., Treacy, D., and Horton, J. (2009). In-pit dyke construction planning. Shell Upstream Americas, Ft. McMurray, 15.

[20] Ferland, J. A., Berrada, I., Nabli, I., Ahiod, B., Michelon, P., Gascon, V., and Gagne, E. (2001). Generalized assignment type goal programming problem: application to nurse scheduling. *Journal of Heuristics*,(7), 391-413.

[21] Gemcom Software International (2008). Whittle strategic mine planning software. Ver. 4.2, Vancouver.

[22] Gershon, M. E. (1983). Optimal mine production scheduling: evaluation of large scale mathematical programming approaches. *International Journal of Mining Engineering*, *1*, 315-329.

[23] Hannan, E. L. (1985). An assessment of some criticisms of goal programming. *Computers and Operations Research*, *12*,(6), 525-541.

[24] Hein, F. J., Cotterill, D. K., and Berhane, H. (2000). An Atlas of Lithofacies of the McMurray Formation, Athabasca Oil Sands Deposit, Northeastern Alberta: Surface and Subsurface. Alberta Geological Survey, Edmonton, Alberta, 07, June, 217.

[25] Holmström, K. (2009). TOMLAB /CPLEX (Version 11.2). Tomlab Optimization, Pullman, WA, USA.

[26] Horst, R. and Hoang, T. (1996). *Global optimization: deterministic approaches.* Springer, Berlin; New York. 3rd ed, Pages 727.

[27] Hustrulid, W. A. and Kuchta, M. (2006). *Open pit mine planning and design.* Taylor and Francis/Balkema, Second ed, Pages 735.

[28] ILOG Inc. (2007). ILOG CPLEX 11.0 User's manual September. Ver. 11.0.

[29] Jääskeläinen, V. (1969). A goal programming model of aggregate production planning. *The Swedish Journal of Economics*, *71*,(1), 14-29.

[30] Johnson, T. B. (1969). *Optimum open-pit mine production scheduling*. Paper presented at 8th International Symposium on Computers and Operations Research, Salt Lake City, Utah, USA. pp. 539-562.

[31] Kaufman, L. and Rousseeuw (1990). *Finding groups in data: an introduction to cluster analysis.* Wiley, New York. Pages 342.

[32] Lee, J., Kang, S., Rosenberger, J., and Kim, S. B. (2010). A hybrid approach of goal programming for weapons systems selection. *Computers and Industrial Engineering*, *58*, 521-527.

[33] Lerchs, H. and Grossmann, I. F. (1965). Optimum design of open-pit mines. *The Canadian Mining and Metallurgical Transaction*, *68*, 17-24.

[34] Leung, S. C. H., Wu, Y., and Lai, K. K. (2003). Multi-site aggregate production planning with multiple objectives: a goal programming approach. *Production Planning and Control*, *14*,(5), 425-436.

[35] Liang, F. and Lawrence, S. (2007). A goal programming approach to the team formation problem. Leeds School of Business, University of Colorado, 8.

[36] Masliyah, J. (2010). *Fundamentals of oilsands extraction.* University of Alberta, Edmonton. Pages C1-2.

[37] Mathworks Inc. (2009). MATLAB Software. Ver. 7.9 (R2009b).

[38] McFadyen, D. (2008). Directive 074. Energy Resources Conservation Board, Calgary, 14.

[39] Morgan, G. (2001). An energy renaissance in oil sands development. *World Energy*,(4), 46-53.

[40] Mukherjee, K. and Bera, A. (1995). Application of goal programming in project selection decision - A case study from the Indian coal mining industry. *European Journal of Operational Research*, *82*, 18-25.

[41] Newman, A. M., Rubio, E., Caro, R., Weintraub, A., and Eurek, K. (2010). A review of operations research in mine planning. *Institute for Operations Research and the Management Sciences*, *40*,(3), 222-245.

[42] Nja, M. E. and Udofia, G. A. (2010). Formulation of the mixed-integer goal programming model for flour producing companies. *Asian Journal of Mathematics and Statistics*, *3*,(3), 201-210.

[43] Oraee, K. and Asi, B. (2004). *Fuzzy model for truck allocation in surface mines*. Paper presented at 13th International Symposium on Mine Planning and Equipment Selection, Routledge Taylor and Francis Group, Wroclaw, Poland. pp. 585-593.

[44] Ramazan, S. (2007). *Large-scale production scheduling with the fundamental tree algorithm - model, case study and comparisons*. Paper presented at Orebody Modelling and Strategic Mine Planning, The Australian Institute of Mining and Metallurgy, Perth, Western Australia. pp. 121-127.

[45] Ramazan, S., Dagdelen, K., and Johnson, T. B. (2005). Fundamental tree algorithm in optimising production scheduling for open pit mine design. *Institute of Materials, Minerals and Mining and Australasian Institute of Mining and Metallurgy*, *114*,(A), 45-54.

[46] Ramazan, S. and Dimitrakopoulos, R. (2004). *Recent applications of operations research and efficient MIP formulations in open pit mining*. Paper presented at SME Annual Meeting, Society for Mining, Metallurgy, and Exploration, Cincinnati, Ohio. pp. 73-78.

[47] Runge Limited (2009). XPAC AutoScheduler. Ver. 7.8.

[48] Sego, D. C. (2010). Mine waste management. Course notes, University of Alberta, Geotechnical Center, Edmonton, 83.

[49] Selen, W. J. and Hott, D. D. (1986). A mixed-integer goal-programming formulation of the standard flow-shop scheduling problem. *Journal of the Operational Research Socitey*, *37*,(12), 1121-1128.

[50] Syncrude (2009). Annual tailings plan submission: Syncrude Mildred Lake. Syncrude Canada Ltd, Fort McMurray, 45.

[51] Vick, S. G. (1983). *Planning, design, and analysis of tailings dams.* John Wiley and Sons, New York. Pages 369.

[52] Whittle, J. (1989). The facts and fallacies of open pit design. Whittle Programming Pty Ltd.

[53] Wik, S., Sparks, B. D., Ng, S., Tu, Y., Li, Z., Chung, K. H., and Kotlyar, L. S. (2007). Effect of bitumen composition and process water chemistry on model oilsands separation using a warm slurry extraction process simulation. Science Direct, *Elsevier ltd,* Retrieved 29th November, 2009 from: www.sciencedirect.com

[54] Wolsey, L. A. (1998). *Integer programming.* J. Wiley, New York. Pages 264.

[55] Zeleny, M. (1980). Mathematical programming with multiple objectives. *Computers and Operations Research*, *7*,(1-2), iii.

[56] Zhang, Y. D., Cheng, Y. P., and Su, J. (1993). Application of goal programming in open pit planning. *International Journal of Mining, Reclamation and Environment*, *7*,(1), 41-45.

Oil Sands composite tailings disposal planning

Samira Kalantari and Hooman Askari-Nasab
Mining Optimization Laboratory (MOL)
University of Alberta, Edmonton, Canada

Abstract

Waste management is one of the critical problems in the current oil sands industry. Linking the long-term production schedule to the produced tailings at the end of the process can lead to valuable developments in the mine planning and waste management. In this paper, the formulations required to link oil sands mine production schedules to the respective amount of composite tailings produced downstream are developed and discussed.

1. Introduction

The mine and tailings long-term plans define the complex strategy of displacement of ore, waste, overburden, and tailings over the mine life. The objective of long-term mine plan is to minimize the environmental footprint and maximize the future cash flows. Limitation of space because of lease conditions, scale of the operations, and construction of external in-pit dyke impoundments adds to the complexity of planning in oil sands mining. Contrary to metal and non-metal mine planning; oil sands long-term mine plans are driven by quantity and quality of mature fine tailings and composite/consolidated tailings produced downstream.

Production scheduling is an important aspect of mine planning and design. Maximizing the net present value (NPV) and considering the sequence of the material that has to be mined over time under the defined constraints is used in order to construct a schedule for long-term production (Dimitrikopoulos et al., 2004).

Not meeting the production target in the early years of a project is one of the main problems in long-term mine planning, and it is due to the geological uncertainties which will also lead to the production shortfalls in the later years of the operation (Goody et al., 2004).

The hot water process that is being used to extract bitumen from oil sands in northern Alberta will result in producing a tailing stream which contains residual bitumen, clays, sand and small amount of soluble organic compounds (Kasperski, 1992).

In oil sands mining, every barrel of oil produces approximately three cubic meters of tailings which contains between 35 and 65% of solids content, with fines content between 8 and 25% and approximately 1% of residual bitumen (Beier et al., 2008). Due to the specific characterization of tailings, it will segregate with the sands going down the water and fines going up. Since it will be harmful for the environment and wild life to dispose tailings to the river system, MFT is stored on site. Therefore this method of tailings disposal will result in a tailings pond with a fine tails zone that will take many decades to fully consolidate (Boratynec, 2003).

In order to increase the tailings dewatering rate and reduce the formation of fine tailings zone, composite tailings (CT) is used to produce non-segregating tailings which is a mixture of coarse sand, gypsum, and MFT. The CT process reduces the storage and tailings management costs, and

will decrease the volume of mature fine tailings (MFT) on leases. In addition, the CT process will help to reclaim the distributed areas for terrestrial land use faster (Caughill, 1992).

To produce CT, using the pipelines, coarse tailings are pumped from the extraction plant to the CT plant, where they are cycloned to produce a densified coarse tailings stream. The resulting densified stream is combined with the MFT and gypsum in order to produce CT. The CT produced is transported hydraulically to the specified tailings disposal facility. After deposition of CT in the pond, the dewatering of the mixture starts rapidly which will leave a soft deposit behind (Syncrude, 2009).

The implementation of CT process has a number of benefits such as reducing the existing volumes of the MFT and increasing the percentage of dry landscape. This is a positive response to environmental and regulatory concerns regarding the long term management of fluid fine tailings and also result in reducing the tailings management and storage costs (Matthews et al., 2002).

2. Problem definition

The oil sands long-term mine plans are driven by quantity and quality of the MFT and composite/consolidated tailings produced downstream. Unfortunately, common approaches to mine planning rely on deterministic ore-body models as the basis for the mine tailings long-term plans. The geological uncertainties caused by grade variability, are not considered which may result in not reaching the targets for ore tonnage, grades and cash flow.

Oil sands production leads to the production of waste by-products including waste rock and a finer grained slurry called tailings. Management of tailings results in environmental challenges and financial burdens for operators. One of the mine waste management techniques is to create a non-segregating mixture or composite tailings that will increase the rate of dewatering process resulting in a higher consolidation rate of the fine tailings (Chalaturnyk et al., 2002).

In the oil sands mine planning, developing an optimal risk-based methodology for the oil sands mine and in-pit CT disposal planning is of good interest. The long-term mine plan should minimize and eventually eliminate long-term storage of fluid tailings in the reclamation landscape, and to create a trafficable landscape at the earliest opportunity to facilitate progressive reclamation.

The final mine schedule should relate the mine plan of the oil sands production to the amount of CT which will be produced at the end of the process. The resulting schedule should be mathematically optimal within the practical constraints and should account for the risk and uncertainties associated with the long-term schedule. The overall goal is to assist in progressive reclamation of the mined-out pits and to minimize the lead-time between mining and start of reclamation.

In finding the optimal mine plan the constraints such as production rate, the effect of different uncertainties on the oil sands production and tailings production, rate of gypsum addition to MFT, and the composite tailings production rate should be considered.

At the end of the day, the mine schedule should provide the yearly plan on the quantities of bitumen, fines, overburden and waste, and the final CT produced.

3. Assumptions & definitions of terms

3.1. Mass-volume relationships

Oil sands tailings are composed of four different phases with different characteristics. The four different phases are mineral grains, bitumen, gas and water. Since the viscosity of bitumen is higher than the viscosity of water, it has a really low mobility and can be assumed as a solid phase. The unique characteristics of oil sands tailings, lead to defining some mass-volume relationships

which are complicated due to the effects of clay contained within the tailings stream. When the mineral phase split into two phases, the oil sands tailings will become a five-phase material.

Defining the mass-volume relationships for oil sands tailing helps to increase the understanding of the material behavior. The most common mass-volume relationships for the oil sands tailing are sands fines ratio (SFR), fines water ratio (FWR), fines void ratio and sands void ratio (Boratynec, 2003). Fig. 1 shows a schematic diagram of oil sands tailings different phases.

Where:

M : *total mass of ore feed*

M_g : *mass of gas*

M_w : *mass of water*

M_b : *mass of bitumen*

M_f : *mass of fines*

M_{sd} : *mass of sand*

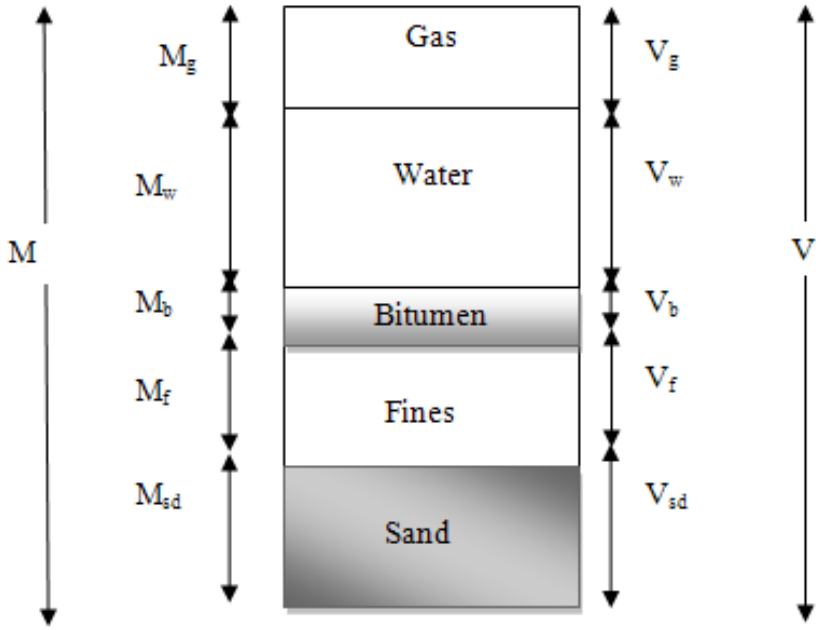

Fig. 1. Schematic diagram of oil sands tailings different phases.

3.2. Definitions of mass-volume relationships

Eqs. (1) to (6) represent the mass-volume relationships for the oil sands ore.

$$Fines\ content\ of\ \ feed\ (F_{feed}) : \frac{mass\ of\ \ fines}{total\ mass\ of\ \ feed} = \frac{M_f}{M} \qquad (1)$$

$$Sand\ content\ of\ feed\ (SD_{feed}):\frac{mass\ of\ sand}{total\ mass\ of\ feed}=\frac{M_{sd}}{M} \quad (2)$$

$$Water\ content\ of\ feed\ (W_{feed}):\frac{mass\ of\ water}{total\ mass\ of\ feed}=\frac{M_{w}}{M} \quad (3)$$

$$Solid\ content\ of\ feed\ (S_{feed})=1-B_{feed}-W_{feed} \quad (4)$$

$$Sands\ to\ fines\ ratio\ (SFR):\frac{mass\ of\ sand}{mass\ of\ fines+mass\ of\ bitumen}=\frac{M_{sd}}{M_{f}+M_{b}} \quad (5)$$

$RJ\%: reject\ percent$

$RJ_{sd}: sand\ reject$

$U/F: cyclone\ underflow$

$$FR_{sd}: sand\ in\ froth=\frac{Bitumen\ in\ froth}{SET\ bitumen}\times SET\ sand \quad (6)$$

4. Mature fine tailings (MFT)

The total tailings will tend to segregate after deposition into the tailings ponds due to its gap-graded characteristics, and high void ratio, therefore tailings is classified as a segregating mixture. In other words, after deposition of the tailings into the tailings ponds, the fines grained material tends to be separated from the coarse-grained material. Near the discharge point, the sands will fall out from the suspension, while most of the water plus approximately half of the fine material (thin tails), will flow towards the pond centre. During the first two years, the thin tails has a high tendency to release water until it reaches a solid content of approximately 30% and it will be known as MFT. As a result of high water release rate during the first two years, the thin fine tails will experience hindered sedimentation followed by consolidation. After the first two years, the dewatering rate of mature fine tailings will be decreased until it reaches zero, and due to its low hydraulic conductivity and thixotropic strength gain, even after hundreds of years, the full consolidation of tailings will not occur. One of the crucial problems in the oil sands mining is the extremely slow rate of consolidation of MFT (Boratynec, 2003).

5. Non-segregating tailings

The MFT with the solid content of more than 30% has an extremely slow rate of consolidation, therefore would take more than several decades to consolidate completely under self weight consolidation. As a result, over the production of oil sands, a large amount of the MFT will be accumulated (Tang, 1997). MFT is harmful for the environment due to its toxic behavior; therefore changing the physical properties of the MFT is required in order to form a mixture which has a low tendency to segregate. Depending upon the solid content and the gradation of the solid material, the segregation of the tailing stream will change (Boratynec, 2003). To produce consolidated tailings, the process should be able to replace the water that is found in tailings with the MFT. As a result of consolidated tailings, the strength of tailings will increase (Mikula et al., 2008).

6. Composite tailings (CT)

To produce a non-segregating tailings, research shows that a mixture of tailings cyclone underflow and MFT, with the addition of lime (CaO) or phosphogypsum ($CaSo_4.2H_2O$) produces composite tailings which is a non-segregating tailings stream (Boratynec, 2003). One important advantage of composite tailings production is that the transportation and pumping of the produced CT is easy. Using MFT to produce CT, the required sand comes directly from the extraction process. Fig. 2 shows a schematic diagram of the CT production process. The ore feed from the oil sands mine is sent to the separation cell (flotation cells) to separate bitumen from the fines using aeration (air flotation) technique. The tailings from the froth treatment will be sent to the ponds. Mature fine tailings will be formed in almost a two year period in the pond. In the hydro-cyclone, coarse solids will be simply separated from fine solids; cyclone over flow contains fine solids whilst the cyclone under flow carries the coarse solids. A portion of cyclone under flow will be sent to cell DT and the remaining portion will be used in the composite tailings production. In order to complete the CT production process, fines and water will be added from the MFT deposit with a solid content of approximately 30%. Finally, Gypsum will be added to MFT to produce the non-segregating tailings.

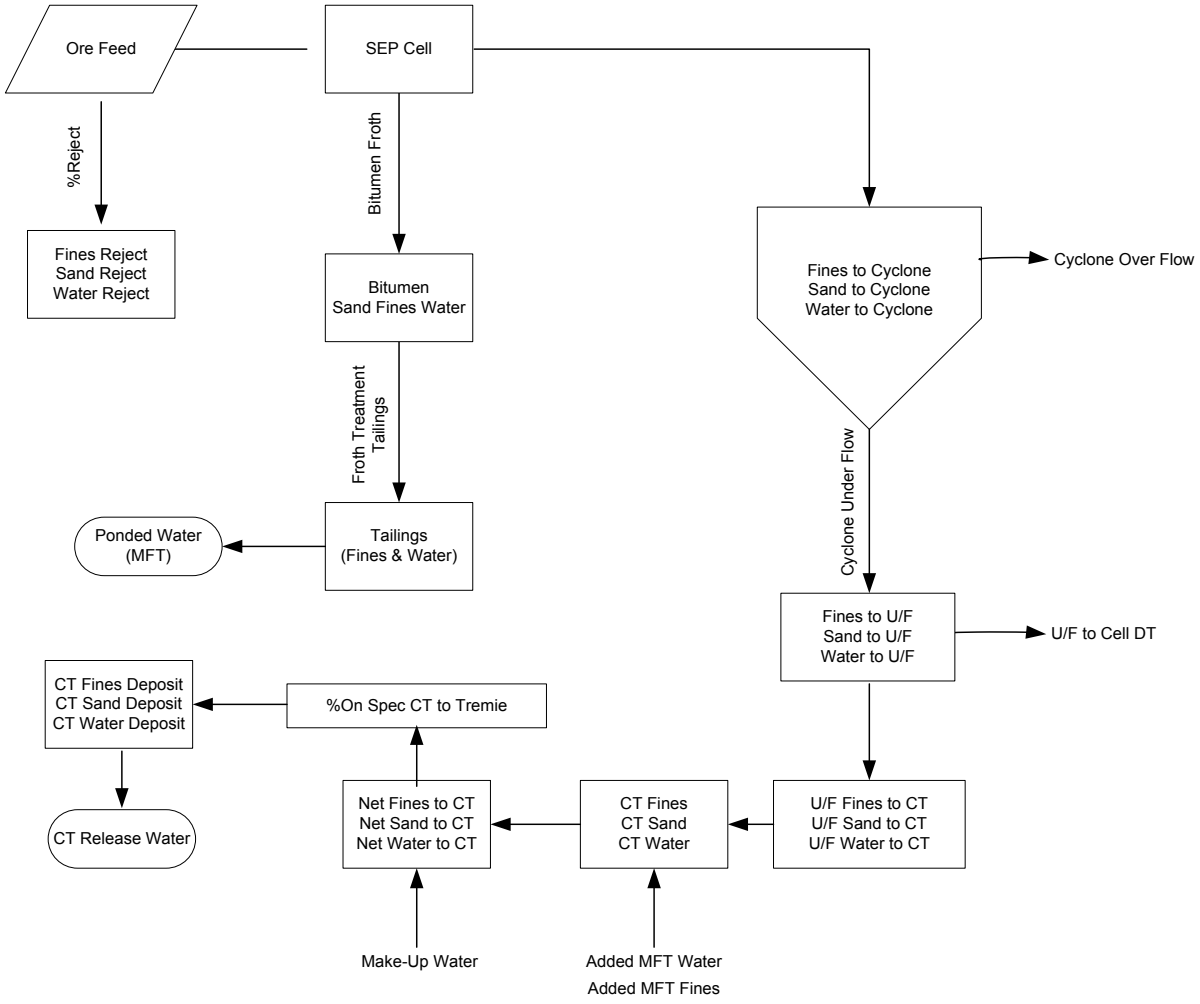

Fig. 2. Mass balance flow diagram for CT production

7. Mass relationship between CT and the ore feed

The ultimate goal of this project is to generate an oil sands mine production schedule according to the limitation of the CT required at the end of the process. In order to find the relationship between CT and the mine plan, first we should find out the relationship between the quantities of the ore tonnage and the produced CT. Eq. (7) shows that the total mass of CT can be calculated by finding the total mass of sand, fines, and water needed to produce CT. Eq. (8) controls the total mass of fines in the CT deposit for a specific ore tonnage. To calculate the CT sand and water deposits, Eqs. (9) and (10) can be used.

$$Total\ mass\ of\ CT = CT\ fines\ deposit + CT\ sand\ deposit + CT\ water\ deposit \tag{7}$$

$$CT\ fines\ deposit = \%\,on - spec\ CT\ to\ Tremie \times \left(added\ MFT\ fines + U\ /\ F\ fines\ to\ CT\right) \tag{8}$$

$$CT\ sand\ deposit = \%on - spec\ CT\ to\ Tremie \times U\ /\ F\ sand\ to\ CT \tag{9}$$

$$CT\ water\ deposit = \%\,on - spec\ CT\ to\ Tremie \times \left(make - up\ water + added\ MFT\ water + U\ /\ F\ water\ to\ CT\right) \tag{10}$$

7.1. CT fines deposit

According to Eq.(8), the total mass of fines in CT can be found by adding the total mass of added MFT fines and the mass of underflow fines to CT. In order to find the total mass of added MFT fines, Eq. (11) should be used. In order to find the total mass of U/F sand used for CT production, Eq. (12) should be used. Eqs. (13) to (17) control the sand content of the cyclone under flow.

The total mass of sand in cyclone under flow which is sent for CT production, can be found using Eqs. (18) to (26). Eqs. (27) and (28) represent the total mass of fines in cyclone under flow which is sent for CT production.

Total mass of added MFT fines is represented by Eq. (29). According to Eq.(8), the total mass of CT fines, can be found by adding the mass of added MFT fines to the mass of fines in U/F which is sent to the CT production process; therefore, using Eqs. (28) and (30), CT fines deposit could be calculated. Eq. (31) represents the total mass of fines used for CT production.

$$Added\ MFT\ fines = \frac{U\ /\ F\ sand\ to\ CT}{SFR\ in\ pipe} - U\ /\ F\ fines\ to\ CT \tag{11}$$

$$U\ /\ F\ sand\ to\ CT = sand\ to\ U\ /\ F \times \left(1 - U\ /\ F\%\ to\ cell\ DT\right) \tag{12}$$

$$Sand\ to\ U\ /\ F = sand\%\ to\ U\ /\ F \times sand\ to\ cyclones \tag{13}$$

$$Sand\ to\ cyclones = sand\ \ feed - sand\ reject - sand\ in\ froth \tag{14}$$

$$Sand\ to\ cyclones = SD_{feed} - RJ_{sd} - FR_{sd} \tag{15}$$

$$Sand\ to\ cyclones = SD_{feed} - RJ_{sd} - \left(\frac{bitumen\ in\ froth}{SET\ bitumen} \times SET\ sand \right) \tag{16}$$

$$Sand\ to\ U/F = sand\%\ to\ U/F \times \left(SD_{feed} - RJ_{sd} - \left(\frac{bitumen\ in\ froth}{SET\ bitumen} \times SET\ sand \right) \right) \tag{17}$$

$$U/F\ fines\ to\ CT = fines\ to\ U/F \times \left(1 - U/F\%\ to\ cell\ DT\right) \tag{18}$$

$$fines\ to\ U/F = \frac{sand\ to\ U/F}{sand\ in\ U/F} \times fines\ in\ U/F \tag{19}$$

$$U/F\%\ to\ cell\ \ DT = \frac{sand\ to\ DT}{sand\ to\ U/F} \tag{20}$$

$$Sand\ to\ DT = \frac{sand\ to\ cell}{physical\ capture \times cell\ efficiency} \tag{21}$$

$$Sand\ to\ cell = \left(cell\ volume \times cell\ dry\ density\right) - fines\ to\ cell \tag{22}$$

$$fines\ to\ cell = cell\ volume \times cell\ dry\ density \times fines\%\ in\ solids \tag{23}$$

$$Sand\ to\ DT = \frac{\left(cell\ volume \times cell\ dry\ density\right) \times \left(1 - fines\%\ in\ solids\right)}{physical\ capture \times cell\ efficiency} \tag{24}$$

$$U/F\%\ to\ cell\ DT = \frac{\dfrac{\left(cell\ volume \times cell\ dry\ density\right) \times \left(1 - fines\%\ in\ solids\right)}{physical\ capture \times cell\ efficiency}}{sand\%\ to\ U/F \times \left(SD_{feed} - RJ_{sd} - \left(\dfrac{bitumen\ in\ froth}{SET\ bitumen} \times SET\ sand \right) \right)} \tag{25}$$

$$U/F\ sand\ to\ CT = sand\%\ to\ U/F \times \left(SD_{feed} - RJ_{sd} - \left(\frac{bitumen\ in\ froth}{SET\ bitumen} \times SET\ sand \right) \right)$$

$$\times \left(1 - \frac{\frac{\left(cell\ volume \times cell\ dry\ density \right) \times \left(1 - fines\%\ in\ solids \right)}{physical\ capture \times cell\ efficiency}}{sand\%\ to\ U/F \times \left(SD_{feed} - RJ_{sd} - \left(\frac{bitumen\ in\ froth}{SET\ bitumen} \times SET\ sand \right) \right)} \right) \tag{26}$$

$$fines\ to\ U/F = \frac{sand\%\ to\ U/F \times \left(SD_{feed} - RJ_{sd} - \left(\frac{bitumen\ \ in\ froth}{SET\ bitumen} \times SET\ sand \right) \right)}{sand\ in\ U/F} \times fines\ in\ U/F \tag{27}$$

$$U/F\ \ fines\ to\ CT = \frac{sand\%\ to\ U/F \times \left(SD_{feed} - RJ_{sd} - \left(\frac{bitumen\ \ in\ froth}{SET\ \ bitumen} \times SET\ sand \right) \right)}{sand\ in\ U/F} \times fines\ in\ U/F$$

$$\times \left(1 - \frac{\frac{\left(cell\ volume \times cell\ dry\ density \right) \times \left(1 - fines\%\ in\ solids \right)}{physical\ capture \times cell\ efficiency}}{sand\%\ to\ U/F \times \left(SD_{feed} - RJ_{sd} - \left(\frac{bitumen\ \ in\ froth}{SET\ \ bitumen} \times SET\ sand \right) \right)} \right) \tag{28}$$

$$Added\ MFT\ fines = \frac{sand\%toU/F \times \left(SD_{feed} - RJ_{sd} - \left(\frac{bitumen\ in\ froth}{SET\ bitumen} \times SET\ sand \right) \right) \times \left(1 - \frac{\left(cell\ volume \times cell\ dry\ density \right) \times \left(1 - fines\%in\ solids \right)}{physical\ capture \times cell\ efficiency} \right)}{sand\%\ to\ U/F \times \left(SD_{feed} - RJ_{sd} - \left(\frac{bitumen\ in\ froth}{SET\ bitumen} \times SET\ sand \right) \right)}$$

$$SFR\ in\ pipe$$

$$- \frac{sand\%toU/F \times \left(SD_{feed} - RJ_{sd} - \left(\frac{bitumen\ in\ froth}{SET\ bitumen} \times SET\ sand \right) \right)}{sand\ in\ U/F} \times fines in U/F \times \left(1 - \frac{\left(cell\ volume \times cell\ dry\ density \right) \times \left(1 - fines\%in\ solids \right)}{physical\ capture \times cell\ efficiency} \right) \quad (29)$$

$$sand\%\ to\ U/F \times \left(SD_{feed} - RJ_{sd} - \left(\frac{bitumen\ in\ froth}{SET\ bitumen} \times SET\ sand \right) \right)$$

$$Added\ MFT\ fines + U/F\ fines\ to\ CT = \frac{U/F\ sand\ to\ CT}{SFR\ in\ pipe}$$

$$= \frac{sand\%toU/F \times \left(SD_{feed} - RJ_{sd} - \left(\frac{bitumen\ in\ froth}{SET\ bitumen} \times SET\ sand \right) \right) \times \left(1 - \frac{\left(cell\ volume \times cell\ dry\ density \right) \times \left(1 - fines\%in\ solids \right)}{physical\ capture \times cell\ efficiency} \right)}{SFR\ in\ pipe} \quad (30)$$

$$sand\%\ to\ U/F \times \left(SD_{feed} - RJ_{sd} - \left(\frac{bitumen\ in\ froth}{SET\ bitumen} \times SET\ sand \right) \right)$$

$$CT\ fines\ deposit = \%on - spec\ CT\ to\ Tremie$$

$$\times \frac{1}{SFR\ in\ pipe} \times sand\%toU/F \times \left(SD_{feed} - RJ_{sd} - \left(\frac{bitumen\ in\ froth}{SET\ bitumen} \times SET\ sand \right) \right) \times \left(1 - \frac{\left(cell\ volume \times cell\ dry\ density \right) \times \left(1 - fines\%in\ solids \right)}{physical\ capture \times cell\ efficiency} \right) \quad (31)$$

$$sand\%\ to\ U/F \times \left(SD_{feed} - RJ_{sd} - \left(\frac{bitumen\ in\ froth}{SET\ bitumen} \times SET\ sand \right) \right)$$

7.2. CT sand deposit

The total mass of sand used for CT production for a specific ore tonnage can be found using Eqs. (31) and (32). Eq. (33) controls the CT sand deposit.

$$CT\ sand\ deposit = CT\ \ fines\ deposit \times SFR\ in\ pipe \tag{32}$$

$$CT\ sand\ deposit = \%on - spec\ CT\ to\ Tremie \times sand\%\ to\ U/F \times \left(SD_{feed} - RJ_{sd} - \left(\frac{bitumen\ in\ froth}{SET\ bitumen} \times SET\ sand \right) \right) \times \left(1 - \frac{\frac{(cell\ volume \times cell\ dry\ density) \times (1 - fines\%\ in\ solids)}{physical\ capture \times cell\ efficiency}}{sand\%\ to\ U/F \times \left(SD_{feed} - RJ_{sd} - \left(\frac{bitumen\ in\ froth}{SET\ bitumen} \times SET\ sand \right) \right)} \right) \tag{33}$$

7.3. CT water deposit

Based on Eq. (10), added MFT water, make-up water, and mass of under flow water sent to the CT production process, are three different water deposits used in the CT production. Mass of the added MFT water can be calculated using Eqs. (34) and (35).

In order to find the total mass of under flow water sent to the CT production, Eqs. (36) to (39) should be used. Eq. (40) controls the mass of make-up water used for CT production for a specified ore tonnage.

Finally, Eq. (41) represents the total mass of water used for CT production for a specified ore tonnage.

$$Added\ MFT\ water = \frac{added\ MFT\ \ fines}{MFT\%\ solids} - added\ MFT\ \ fines = added\ MFT\ \ fines \times \left(\frac{1}{MFT\%\ solids} - 1 \right) \tag{34}$$

$$Added\ MFT\ water = \left(\frac{1 - MFT\%\ solids}{MFT\%\ solids}\right) \times \frac{1}{SFR\ in\ pipe} \times (sand\%toU/F \times \left(SD_{feed} - RJ_{sd} - \left(\frac{bitumen\ in\ froth}{SET\ bitumen} \times SET\ sand\right)\right)$$
$$\times \left(1 - \frac{\frac{(cell\ volume \times cell\ dry\ density) \times (1 - fines\%\ in\ solids)}{physical\ capture \times cell\ efficiency}}{sand\%toU/F \times \left(SD_{feed} - RJ_{sd} - \left(\frac{bitumen\ in\ froth}{SET\ bitumen} \times SET\ sand\right)\right)}\right) - \frac{sand\%toU/F \times \left(SD_{feed} - RJ_{sd} - \left(\frac{bitumen\ in\ froth}{SET\ bitumen} \times SET\ sand\right)\right)}{sand\ in U/F}$$
$$\times fines\ in U/F \times \left(1 - \frac{\frac{(cell\ volume \times cell\ \ dry\ density) \times (1 - fines\%\ in\ solids)}{physical\ capture \times cell\ efficiency}}{sand\%toU/F \times \left(SD_{feed} - RJ_{sd} - \left(\frac{bitumen\ \ in\ \ froth}{SET\ \ bitumen} \times SET\ sand\right)\right)}\right) \quad (35)$$

$$U/F\ water\ to\ CT = water\ to\ U/F \times (1 - U/F\%\ to\ cell\ DT) \quad (36)$$

$$Water\ to\ U/F = \frac{sand\ to\ U/F}{sand\ in\ U/F} \times water\ in\ U/F \quad (37)$$

$$water\ to\ U/F = \frac{sand\%toU/F \times \left(SD_{feed} - RJ_{sd} - \left(\frac{bitumen\ in\ froth}{SET\ bitumen} \times SET\ sand\right)\right)}{sand\ in U/F} \times water\ in U/F \quad (38)$$

$$U/F\ water\ to\ CT = \frac{sand\%\ to\ U/F \times \left(SD_{feed} - RJ_{sd} - \left(\frac{bitumen\ in\ froth}{SET\ bitumen} \times SET\ sand \right) \right)}{sand\ in\ U/F} \times water\ in\ U/F \times \left(1 - \frac{\frac{(cell\ volume \times cell\ dry\ density) \times (1 - fines\%\ in\ solids)}{physical\ capture \times cell\ efficiency}}{sand\%\ to\ U/F \times \left(SD_{feed} - RJ_{sd} - \left(\frac{bitumen\ in\ froth}{SET\ bitumen} \times SET\ sand \right) \right)} \right) \tag{39}$$

$$if\ \frac{CT\ fines + CT\ sand}{CT\%solids} \times (1 - CT\%solids) - CT\ water < 0 \rightarrow make - up\ water = 0 \tag{40}$$

$$if\ \frac{CT\ fines + CT\ sand}{CT\%solids} \times (1 - CT\%solids) - CT\ water \geq 0 \rightarrow make - up\ water = \frac{CT\ fines + CT\ sand}{CT\%solids} \times (1 - CT\%solids) - CT\ water$$

$$CT\ water\ deposit = \%on - spec\ CT\ to\ Tremie \times sand\%\ to\ U/F \times \left(SD_{feed} - RJ_{sd} - \left(\frac{bitumen\ in\ froth}{SET\ bitumen} \times SET\ sand \right) \right) \times \left(1 - \frac{\frac{(cell\ volume \times cell\ dry\ density) \times (1 - fines\%\ in\ solids)}{physical\ capture \times cell\ efficiency}}{sand\%\ to\ U/F \times \left(SD_{feed} - RJ_{sd} - \left(\frac{bitumen\ in\ froth}{SET\ bitumen} \times SET\ sand \right) \right)} \right) \tag{41}$$

$$\times \left\{ \left(\frac{1 - MFT\ \%\ solids}{MFT\%\ solids} \times \left(\frac{1}{SFR\ in\ pipe} - \frac{fines\ in\ U/F}{sand\ in\ U/F} \right) \right) + \frac{water\ in\ U/F}{sand\ in\ U/F} \right\} + make - up\ water$$

7.4. Total mass of CT

Based on Eqs. (7) and (40), the total mass of the composite tailings depends on whether the make-up water is required for CT production or not. Eq. (42) represents the total mass of CT when make-up water is not added to the CT production process. Finally Eq. (43) controls the total mass of CT in case of adding make-up water to the CT production process.

$$If\ \frac{CT\ \ fines + CT\ sand}{CT\ \ \%solids} \times \left(1 - CT\ \ \%solids\right) - CT\ \ water < 0 \rightarrow make - up\ water = 0$$

$$\Rightarrow Total\ \ mass\ of\ \ CT = \%On - spec\ \ CT\ \ to\ \ Tremie \times sand\%\ \ to\ \ U\ /\ F \times$$

$$\left(SD_{feed} - RJ_{sd} - \left(\frac{bitumen\ \ in\ \ froth}{SET\ \ bitumen} \times SET\ sand\right)\right) \times \left(1 - \frac{\frac{(cell\ volume \times\ cell\ \ dry\ \ density) \times (1 - fines\%\ \ in\ \ \ solids)}{physical\ \ capture \times\ cell\ \ efficiency}}{sand\%\ \ to\ \ U\ /\ F \times \left(SD_{feed} - RJ_{sd} - \left(\frac{bitumen\ \ in\ \ froth}{SET\ \ bitumen} \times SET\ sand\right)\right)}\right) \tag{42}$$

$$\times \left(\frac{1 + SFR}{SFR} + \left\{\left(\frac{1 - MFT\ \ \%\ \ solids}{MFT\%\ \ \ solids} \times \left(\frac{1}{SFR\ \ in\ \ \ pipe} - \frac{fines\ \ in\ \ U\ /\ F}{sand\ \ in\ \ U\ /\ F}\right)\right) + \frac{water\ \ in\ \ U\ /\ F}{sand\ \ in\ \ U\ /\ F}\right\}\right)$$

$$If \quad \frac{CT\ fines + CT\ sand}{CT\ \%solids} \times (1 - CT\ \%solids) - CT\ water \geq 0 \rightarrow make - up\ water = \frac{CT\ fines + CT\ sand}{CT\ \%solids} \times (1 - CT\ \%solids) - CT\ water$$

$$\Rightarrow Total\ mass\ of\ CT = \%on - spec\ CT\ to\ Tremie \times \left(\frac{1 + SFR\ in\ pipe}{SFR\ in\ pipe} \right)$$

$$\times \left(\frac{1}{CT\ \%solids} \right) \times sand\%\ to\ U\ /\ F \times \left(SD_{feed} - RJ_{sd} - \left(\frac{bitumen\ in\ froth}{SET\ bitumen} \times SET\ sand \right) \right)$$

$$\times \left(1 - \frac{\frac{\left(cell\ volume \times cell\ dry\ density \right) \times \left(1 - fines\%\ in\ solids \right)}{physical\ capture \times cell\ efficiency}}{sand\%\ to\ U\ /\ F \times \left(SD_{feed} - RJ_{sd} - \left(\frac{bitumen\ in\ froth}{SET\ bitumen} \times SET\ sand \right) \right)} \right) \tag{43}$$

8. Illustrative example

With the calculations discussed in this paper, we can find the mass relationship between the produced composite tailings (CT) and the ore tonnage. Three different blocks from a long-term mine schedule were selected to implement the CT calculations. The inputs for the calculations are represented in Table 1.

Table 1. Inputs for the CT calculations.

Cell volume (m^3)	100
Cell dry-density (kg/m^3)	1.559
Cell efficiency (%)	75
Physical capture (%)	70
SFR in pipe	4
MFT %solids (%)	30
%On-spec CT to Tremie (%)	85
CT %solids (%)	55

Table 2 represents the results of implementing CT production calculations on three different blocks. According toTable 2, the total mass of the produced CT is related to the feed tonnage.

For three blocks with the same ore tonnage, the total mass of the composite tailings depends on the sand content of the input block. As the sand content increases, the total mass of the produced CT will increase for a block with the same ore tonnage. For block #1 with the lowest sand content of 83%, the total mass of CT is 15678 tonnes, whilst for block #2 with the highest sand content of 93%, the total mass of the produced CT is 17752 tonnes.

Table 2. CT calculation results for three different blocks.

Block Number	Ore tonnage (tonne)	Bitumen grade (%)	Fines grade (%)	Water content (%)	Solid content (%)	Sand content (%)	CT produced (tonne)
Block #1	74812	1.050	12.28	4.303	94.651	83.03	15678
Block #2	74812	1.120	3.11	2.583	96.290	93.30	17752
Block #3	74812	0.321	6.83	3.281	96.397	89.81	17068

Fig. 3 shows the relation between sand content of the input blocks and the total mass of the CT which is produced at the end of the process. From this figure it can be seen that the fines content of the block has a direct impact on the total mass of CT produced at the end of the process.

Based on the information represented in Table 2, when fines grade increases in the blocks with the same ore tonnage, the total mass of the CT will decrease. According to Table 2, block #2 with the lowest fines content will lead to the maximum mass of CT produced, whilst block #1 with the

highest fines content will result in producing 15678 tonnes of CT which is the lowest amount of CT amongst three different blocks with the same ore and feed tonnage.

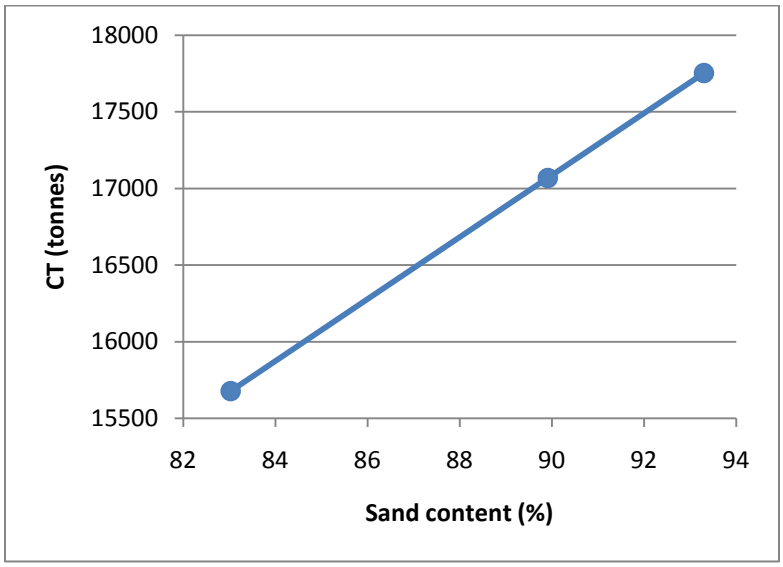

Fig. 3.Relation between sand content and CT.

Fig. 4 represents the inverse relation between fines content of the block and the total mass of composite tailings produced at the end of the process.

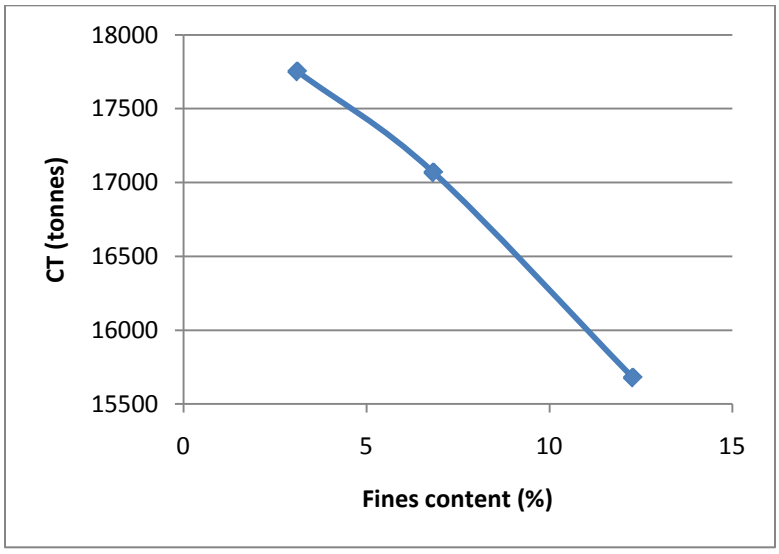

Fig. 4. Relation between fines content and CT.

9. Conclusions and future work

In this paper the mass relation between the ore feed and the quantity of the total composite tailings produced at the end of ore processing was calculated. The final equation, Eq. (43), represents the total mass of CT produced for a specified ore tonnage, and it is the linkage between the mine plan and the final product. This relationship can lead to proper tailings management. In other words, the mass relation between the final CT product and the ore feed can help in developing a disposal planning strategy for the produced composite tailing .The yearly mine plan will be the input for CT

calculations in order to link the mine plan of the oil sands production to the amount of CT which will be produced at the end of the process.

Based on these calculations, the long-term mine plan can be optimized according to the storage area limitations for the disposal of tailings. In other words, in case of having limitations on the tailings disposal areas, these calculations can lead to optimizing the long-term mine schedules based on the disposal restrictions.

In the future steps of this project, the CT calculations will be implemented on a realistic long-term mine schedule from an oil sands mine.

The main goal of this project is to consider the uncertainties associated with the long-term mine schedule in relating the mine plan to the final CT. Probability distributions which will capture the uncertainties associated with oil sands production process, will be defined as the inputs for CT calculations.

10. References

[1] Beier, N. and Sego, D. (2008). The Oil Sands Tailings Research Facility. *Geotechnical news*, 72-77.

[2] Boratynec, D. J. (2003). Fundamentals of Rapid Dewatering of Composite Tailings. Master Thesis, University of Alberta, Edmonton, Alberta, Pages 280.

[3] Caughill, D. L. (1992). Geothecnics of Non-Segregating Oil Sand Tailings. Master Thesis, University of Alberta, Edmonton, Alberta, Pages 262.

[4] Chalaturnyk, R. J., Scott, J. D., and Ozum, B. (2002). Management of oil sands tailings. *Petroleum science and technology*, *20*, 1025-1045.

[5] Dimitrikopoulos, R. and Ramazan, S. (2004). Uncertainty-based production scheduling in open pit mining. *Society for Mining, Metallurgy, and Exploration*, *316*, 106-112.

[6] Goody, M. and Dimitrikopoulos, R. (2004). Managing risk and waste mining in lokg-term production scheduling of open-pit mines. *Society for Mining, Metallurgy, and Exploration*, *316*, 43-50.

[7] Kasperski, K. L. (1992). A review of properties and treatment of oil sands tailings. *AOSTRA Journal of Research*, *8*, 11-51.

[8] Matthews, J. G., Shaw, W. H., Mackinnon, M. D., and Cuddy, R. G. (2002). Developement of Composite Tailings Technology at Syncrude. *International Journal of Mining, Reclamation and Environment*, *16*, 24-39.

[9] Mikula, R. J., Munoz, V. A., and Omotoso, O. (2008). *Water use in bitumen production: Tailing management in surface mine oil sands*. Paper presented at Canadian International Petroleum Conference, Calgary, Alberta. pp. 8.

[10] Syncrude (2009). 2009 Annual tailings plan submission Syncrude Mildred Lake (Leases 17 and 21). Syncrude Canada Ltd., Fort McMurray, Alberta, September 30, 2009, 39.

[11] Tang, J. (1997). Fundamental Behaviour of Composite Tailings. Master Thesis, University of Alberta, Edmonton, Alberta, Pages 224.

An overview of block caving operation and available methods for production scheduling of block cave mines

Yashar Pourrahimian and Hooman Askari-Nasab
Mining Optimization Laboratory (MOL)
University of Alberta, Edmonton, Canada

Abstract

Long-term mine scheduling is among one of the optimization problems. Block caving technique is a mass mining method in which gravity is used in combination with internal rock stresses to fracture and break the rock mass into pieces that can be handled by miners. This method is normally applied to large, low-grade ore-bodies because of its low production cost and high capacity.

In this paper, first, production scheduling methods for underground mining are reviewed and then, block caving method is described. Afterwards, available mathematical models of block cave scheduling and their shortcomings are described. Finally, the conclusions and future work are presented.

1. Introduction

Long-term mine scheduling is classified as complex optimization problems. A production schedule must provide a mining sequence that takes into account the physical limitations of the mine and, to the extent possible, meets the demanded quantities of each raw ore-type at each time period throughout the mine life. Mines use the schedules as long-term strategic planning tools to determine when to start mining a production area and as short-term operational guides.

Underground mining is more complex in nature than surface mining (Kuchta et al., 2004). Flexibility of underground mining is less than surface mining due to the geotechnical, equipment and space constraints (Topal, 2008).

Some of the underground mine problems that can be optimized were identified by Alford et al. (2007) and include:

- Primary development,
- Evaluation and selection from alternative stoping methods,
- Sublevel location and spacing,
- Stope envelope,
- Stope sequencing,
- Ore blending,
- Ore transportation,
- Activity scheduling, and
- Ventilation

Scheduling of underground mining operations is primarily characterized by discrete decisions to mine blocks of ore, along with complex sequencing relationships between blocks. Since linear programming (LP) models cannot capture the discrete decisions required for scheduling, mixed integer programming models (MIP) are generally the appropriate mathematical programming model for this purpose.

Williams et al. (1972) planned sublevel stoping operations for an underground copper mine over one year. They used a linear programming approximation model to determine the amount of ore to be mined per month from each stope. Jawed (1993) formulated a linear goal programming model for production planning in an underground room and pillar coal mine. In his formulation, the decision variables determine the amount of ore to be extracted and the objective function minimizes production deviations from target levels, though only for a single period. These two models compromise schedule quality and the length of the time horizon, respectively. Tang et al. (1993) integrated linear programming with simulation to address scheduling decisions, as did Winkler (1998). The linear program handled the continuous variables, which were determination of the amount of ore to be extracted; while simulation model evaluated discrete scheduling decisions. In these two examples, the applications consist of only a single time period. Solving for a single period cannot guarantee optimal solutions because the technique iteratively fixes variable values and optimizes only a portion of the scheduling problem.

Chanda (1990) employed MIP in conjunction with simulation to generate a schedule for producing finger raises in an underground block caving situation.

Trout (1995) was perhaps the first to try integer programming for optimizing underground mine production schedules. He used MIP to schedule the optimal extraction sequence for underground sublevel stoping.

Ovanic (1998) used mixed integer programming of type two special ordered sets to identify a layout of optimal stopes.

Several years later, researchers formulate more manageable MIP models. Carlyle et al. (2001) presented a model that maximized revenue from Stillwater's platinum and palladium mine, which used the sublevel stoping mining method. The problem was focused on strategic mine expansion planning, so that the integer decision variables scheduled the timing of various mining activities: development and drilling, and stope preparation.

Smith et al. (2003) incorporated a variety of features into their lead and zinc underground mine model, including sequencing relationships, capacities, and minimum production requirements. However, they significantly reduced the resolution of the model by aggregating stopes into large blocks.

Topal et al. (2003) generated a long-term production scheduling MIP model for a sub-level caving operation and successfully applied it to Kiruna Mine, one of the largest underground mine in the world. The model determined which section of the ore to mine, and when to start mining them so as to minimize deviation from the planned production quantities, while adhering to the geotechnical and machine availability constraints.

Sarin et al. (2005) scheduled a coal mining operation with the objective of net present value maximization. They expedited the solution time for their model with a Benders' decomposition-based methodology.

Ataee-Pour (2005) critically evaluated some optimization algorithms according to their capabilities, restrictions and application for use in underground mining. Based on his study, only dynamic programming, geostatistical approach and the branch and bound techniques can generate optimal results because these are considered exact algorithms, while all other remaining techniques are heuristics. In fact, optimal results can only be generated by some exact optimization techniques that evaluate the whole model over the life of mine within all the operational constraints and

parameters. Heuristic techniques proceed to a solution by a process of trial and error. They do not guarantee optimality; however, they may be used as reasonable starting point for future references (Ataee-Pour, 2004).

McIssac (2005) formulated the scheduling of underground mining of a narrow veined polymetallic deposit utilizing MIP. The deposit was divided into eleven zones and scheduled over quarterly time periods. The production schedules were generated for each zone, rather than for the individual stopes within these zones.

Nehring et al.(2007) presented a mixed integer programming formulation for production schedule optimization in underground hard rock mining. The results of his study indicated that the potential benefits of the MIP production scheduling model for the purpose of maximizing NPV were significant. He formulated a new constraint to limit multiple exposures of fill masses for being used in an existing MIP production scheduling model.

2. Block caving method

Underground mining is the planned extraction and transportation of a mineral resource from its underground location to a mill or processing plant on the surface (Alford et al., 2007).

Different methods of extraction of the economic material have been devised depending on the geometry of the ore-body and the geotechnical stability of excavation volumes and the surrounding rock.

This section is focused on block caving method. Block caving is a technique in which gravity is used in conjunction with internal rock stresses to fracture and break the rock mass into pieces that can be handled by miners. Block refers to the mining layout in which the ore-body is divided into large sections of several thousand square meters. Caving of the rock mass is induced by undercutting a block. The rock slice directly beneath the block is fractured by blasting, which destroys its ability to support the overlying rock. Gravity forces on the order of millions of tons act on the block, causing the fractures to spread until the whole block is affected. Continued pressure breaks the rock into the smaller pieces that pass through drawpoints (Hustrulid et al., 2001). The term "block caving" is used for all types of gravity caving methods. There are three major systems of block caving, and the type of production equipment used differentiates them; (1) The first system based on the original block cave system is the grizzly or gravity system and is a full gravity system wherein the ore from the drawpoints flows directly to the transfer raises after sizing at the grizzly and then is gravity loaded into ore cars, (2) The second is the slusher system which uses slusher scrapers for the main production unit, and (3) The last is the rubber-tired system which uses load-haul-dump (LHD) units for the main production unit. The general view of this method is illustrated in Fig 1 . (Hustrulid et al., 2001).

The block caving operation is non-selective, except for the high recovery of ore immediately above the undercut horizon which is virtually certain. Generally, a fairly uniform distribution of values throughout the ore-body is required to assure realization of the maximum ore potential of the deposit (Brady, 2004). The method is applicable to low-grade, massive ore bodies with the following characteristics (Hustrulid et al., 2001):

- Large vertical and horizontal dimensions,
- A rock mass that will break into pieces of manageable size, and
- A surface that is allowed to subside.

The factors to be considered in evaluating the caving potential of an ore-body include the pre-mining state of stress, the frequency of joints and other fractures in the rock medium, the mechanical properties of these features, and the mechanical properties of the rock material. It also appears that the orientations of the natural fractures are important (Brady, 2004).

Based on the undercutting sequence a block cave mine is classified into conventional undercutting, advanced undercutting or pre-undercutting (Barraza et al., 2000).

Conventional undercutting method: It consists of blasting the undercut level once the development and construction of the production level has been finalized.

Advanced undercutting method: It has been introduced to reduce the exposure of the drawpoints to the abutment stress zones induced as a result of the undercutting process. For this method just the production drifts are developed in advance of blasting of the undercut.

Pre-undercutting: It is such that no development or construction takes place on the production level before the undercut has been blasted.

Block caving method needs more detailed geotechnical investigations of the ore-body than other methods where conventional drilling and blasting are employed as part of the production of the mine. This is due to reliance of block caving on natural processes for its success. The main geotechnical parameters affecting the planning of the block cave are presented by Brown (2003) as follows:

- Cavability
- Cave initiation
- Cave propagation
- Fragmentation
- Stress performance surrounding the cave boundary

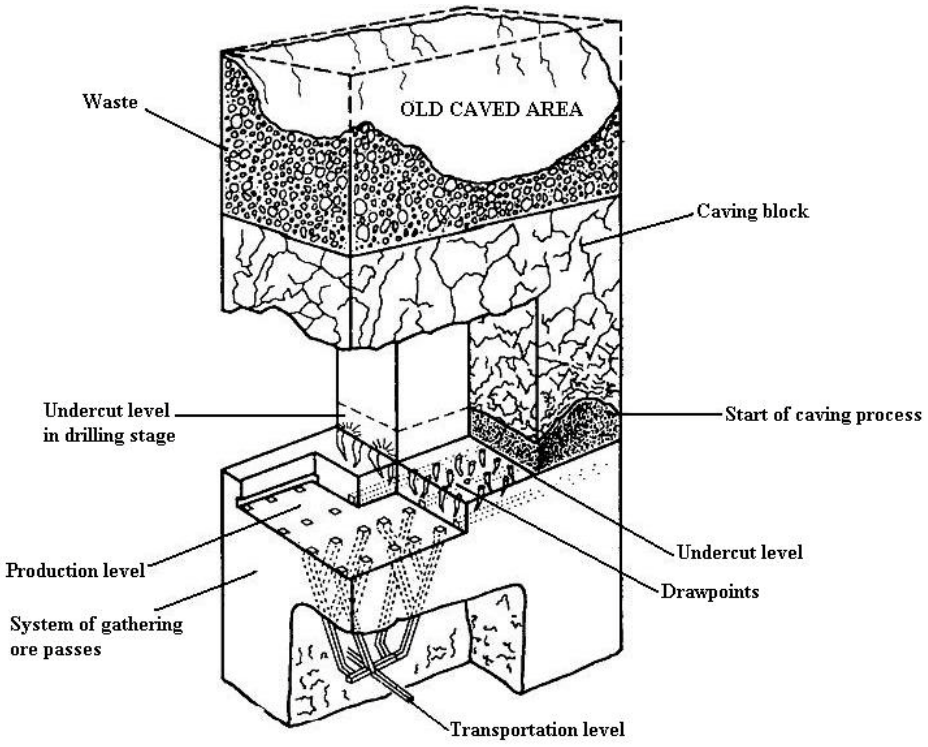

Fig 1. Schematic view of block caving operation (Brady, 2004)

Determining the cavability of an ore body is the first task to be undertaken. For a good caving action generally the ore body should have fractures in three orientations (Julin, 1992). To

investigate the cavability of the ore body, drill cores are obtained throughout the ore body using exploration openings and then rock quality designation (RQD) analysis is done. The RQD value helps to identify the caving characteristics of the rock mass.

The draw control and drawpoint spacing are the second applications of caving mechanics after determining ore cavability.

Fig 2 illustrates plan view of drawpoints arrangement (Richardson, 1981).

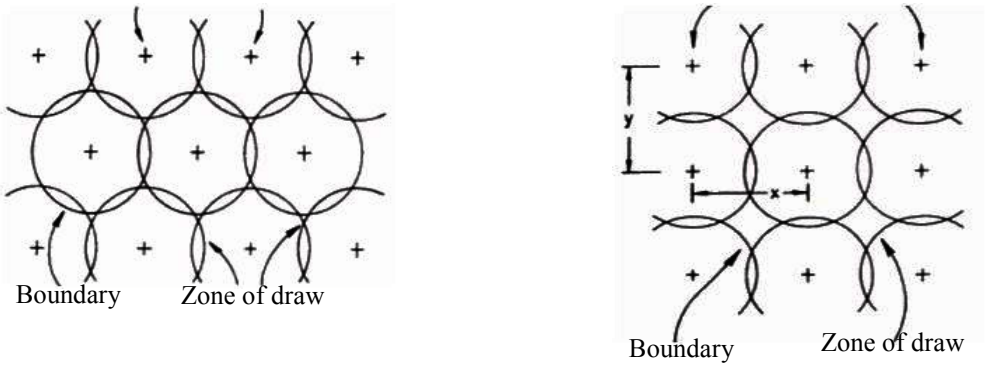

a) Suitable hexagonal spacing b) Suitable square spacing

Fig 2. Plan view of drawpoints configuration

3. Block cave production scheduling

The production rates of a mining system are defined by production planning. In underground mining, the extraction and rates of production should be scheduled during the life of the mine from feasibility through to the final production phase. In the case of a block cave mine, the production schedule mainly defines the amount of tonnage to be mined from the drawpoints in every period of the plan to achieve a given planning objective. The mine plan also defines the number of new drawpoints that need to be constructed and their sequence to support a given production target.

The planning parameters that consider computing a production schedule of a block cave mine are as follows (Rubio, 2006):

- *Development rate:* this defines the maximum feasible number of drawpoints to be opened at any given time within the scheduled horizon.
- *Drawpoint construction sequence:* this defines the order in which the drawpoints will be constructed. It is usually defined as a function of the undercut sequence.
- *Maximum opened production area at any given time:* this is an operational constraint which depends on infrastructure and equipment availability as well as on ventilation resources. A large number of active drawpoints might lead into serious operational problems such as excessive haulage distance and problems related to the movement of equipment within the active drawpoints.
- *Draw rate:* this parameter limits the production yield of a drawpoint at any given time within the production schedule. The draw rate is a function of the fragmentation and the cavability model. It should be fast enough to avoid compaction and slow enough to avoid air gaps.

- *Draw ratio:* this defines a temporary relationship in tonnage between one drawpoint and its neighbor. In fact this parameter controls the dilution entry point and the damage of the production level due to induced stress.

Period constraints: these force the mining system to achieve the desired production target usually keeping it within a range that allows flexibility for potential operational variations.

Fig 3 illustrates the planning parameters of a block cave mine. There are some fundamental models for determination of planning parameters. The modeling is normally used to estimate parameters such as stress distribution at the front cave to decide upon the mining sequence and stress re-distribution on the cave back to estimate ultimate fragmentation. These models include:

- Geomechanical model
- Fragmentation model
- Geological model
- Reconciliation model

The geomechanical model affects the following aspects of the design and planning of a block cave mine:

- Drawpoint sequence would be affected by the structural pattern. Usually, the undercut sequence is oriented perpendicular to the major structures to produce blocks than can enhance the cavability of the rock mass (Rojas et al., 2000).
- Abutment stress at the cave front would be a function of the pre-mining stresses and the angle of draw. This affects the stability of the excavation located on the undercut, production level and haulage level immediately below the front of the caving boundary (McKinnon et al., 1999). The angle of draw is commonly measured in a vertical cross section perpendicular to the mining sequence displaying the height of draw (HOD) of the drawpoints.

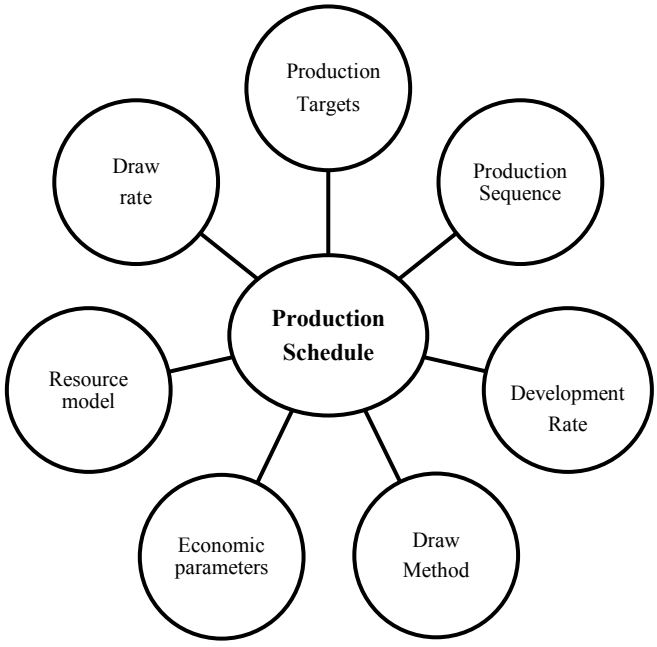

Fig 3. Planning parameters of block cave mine

- Seismicity is the response of the rock mass to the stresses developed at the cave back as the cave propagates to surface and also the response of the rock mass surrounding the excavations exposed to the abutment stress such as undercut, production, ventilation and haulage drifts and rib tunnels (Glazer et al., 2004).
- Induced stresses due to uneven draw. By performing uneven draw high stresses are transferred to the zones of low draw due to the compaction of the broken rock overlying the production level (Febrian et al., 2004).

The fragmentation model affects several aspects of the planning of a block cave mine, the most important aspects are as follows:

- Dilution entry point which is the result of mixing of fragmented material along the draw column (Heslop et al., 1981).
- Drawpoint spacing is the result of the draw column diameter which is believed to be a function of the ultimate fragmentation of the draw column (Kvapil, 1965).
- Drawpoint secondary breakage activity is the result of the frequency of oversize boulders, typically larger than $2m^3$ that cannot be handled by the LHD.
- Oversize and hang up frequency which severely affects the productivity of the mining system (Barraza et al., 2000; Moss et al., 2004).
- Drawpoint yield is the maximum productivity of a drawpoint in the free flow state. As the drawpoint matures, the fragmentation becomes finer because of secondary fragmentation. Therefore, the void ratio decreases as the drawpoint matures leading to an increase in LHD bucket capability, consequently achieving higher drawpoint productivity (Esterhuizen et al., 2004).

The geological model links data relating to structure, lithology and mineralogy with the ultimate metallurgical recovery.

The reconciliation model captures the production performance of the mine. If this model is available, it is used to feedback key performance indicators to the fundamental models to calibrate their behavior. This model is also used to check the validity of different assumptions made regarding to a production schedule. Thus this model will be used as a guide to frame the production planning of the mine based on historical performance (Rubio, 2006). This model affects the following aspects of the design and planning of a block cave mine:

- Draw rate is adjusted based on the historical production performance of drawpoints located in a given rock mass domain.
- Development rate is adjusted depending on the rock mass stress regime in which the construction will take place.
- Draw strategy is compared against the historical performance of the mine.

4. Mathematical programming in block cave production scheduling

Mathematical programming contains all the tools needed to formulate the block cave scheduling in a comprehensive manner. The block cave scheduling should always pursue a goal, which can be represented by an objective function. The actual constraints in the production schedule also can be represented explicitly as constraints to the optimization.

The methods, currently used to compute production schedule in block cave mining, can be classified in two main categories: (a) heuristic methods and (b) exact optimization methods.

Heuristic methods are particularly used to rapidly come to a solution that is hoped to be close to the best possible answer, or optimal solution. These methods are used when there is no known method to find the optimal solution under the given constraints.

The original heuristic methods were the manual draw charts used at the early days of block caving. These methods evolved to be used at Henderson mine where a way to avoid early dilution entry was described by constraining the draw profile to an angle of draw of 45 degrees (Dewolf, 1981). Heslop et al. (1981) described a volumetric algorithm to simulate the mixing along the draw column. Carew (1992) described the use of a commercial package called PC-BC (Diering, 2000) to compute production schedules at Cassiar mine. Diering (2000) showed the principles behind the commercial tool PC-BC to compute production schedules, providing several case studies where different draw methods have been applied depending on the ore body geometry and rock mass behavior.

The application of operations research methods to the planning of a block cave mines was first described by Riddle (1976). This development was intended to compute mining reserves and define the economic extent of the footprint. The final algorithm did not reflect the operational constraints of block caving described above since it worked with the block model directly instead of defining the concept of draw column as an individual entity of the optimization process.

The first attempt to use mathematical programming in block cave scheduling was made by Chanda (1990) who implemented an algorithm to write daily orders. This algorithm was developed to minimize the variance of the milling feed in a horizon of three days. Guest et al. (2000) made another application of mathematical programming in block cave long term scheduling. The objective function was explicitly defined to maximize draw control behavior. However, the author stated that the implicit objective was to optimize NPV. Two problems potentially can arise with this approach are: 1) that maximizing tonnage or mining reserves will not necessarily lead to maximum NPV, 2) that draw control is a planning constraint and not an objective function. The objective function in this case would be to maximize tonnage, minimize dilution or maximize mine life.

Rahal et al. (2003) used a dual objective mixed integer linear programming algorithm to minimize the deviation between the actual state of extraction (height of draw) and a set of surfaces that tend towards a defined draw strategy. This algorithm assumes that the optimal draw strategy is known. Nevertheless, it is postulated that by minimizing the deviation to the draw target the disturbances produced by uneven draw can be mitigated.

Diering (2004) presented a non-linear optimization method to minimize the deviation between a current draw profile and the target defined by the mine planner. Diering emphasized that this algorithm could also be used to link the short with the long-term plan. The long-term plan is represented by a set of surfaces that are used as a target to be achieved based on the current extraction profile when running the short-term plans. Rubio et al.(2004a) presented an integer programming algorithm and an iterative algorithm to optimize long-term schedules in block caving integrating the fluctuation of metal prices in time.

5. Uncertainty in Block cave production scheduling

Uncertainty in block cave production scheduling is due to the lack of formal link between the fundamental models and the planning parameters. Summers (2000) described the main source of uncertainty in block cave mining.

The treatment of uncertainty in production planning as generally being discussed by several authors such as Samis et al.(1998). Singh et al.(1991) and Kajner et al. (1992) have also looked at the flexibility needed in mineral resource industry as a function of the level of uncertainty. Commonly, simulation of the mining system has been the main tool used to assess the amount of flexibility

needed in a mine design. The main problem with this approach is that often simulation models do not integrate the fundamental models such as stress distribution, cavability and gravity flow.

Flexibility or the ability to deal with changes and upsets has often been proposed as a response to uncertainty in mine planning. Real options have been used to estimate the value of flexibility (Trigeorigs, 1990).

There are several methods developed to quantify the impact of uncertainty on the financial valuation of the mine. Often Monte Carlo simulations have been used to quantify the risk related to metal price uncertainty. The existing methods concentrate mainly in uncertainty derived from metal prices and grades. Rubio (2006) applied block cave mine infrastructure reliability to production planning.

6. Mathematical formulation for production scheduling of block cave mines

6.1. Chanda (1990)

Chanda (1990) presented a computerized model for short-term production scheduling in a typical block caving mine with a stratiform ore-body. The model combined two separate operation research techniques; mixed integer programming and simulation.

The model was based on a given layout of the mining block, which was considered fixed during the planning period. The model could be used in the selection of finger raises to put on draw in each drift in a block and to simulate in a shift.

In comparison with manual scheduling, the computerized model was faster and generated near-optimal schedules. In the mixed integer programming formulation of the problem 0/1 variables are introduced to represent decisions on whether to draw or not to draw from a particular finger raise during a shift. Fig 4 shows the block layout represented in the mathematical model. It should be noted that this formulation does not incorporate economic parameters such as costs or revenue. In this model, variables are as follows:

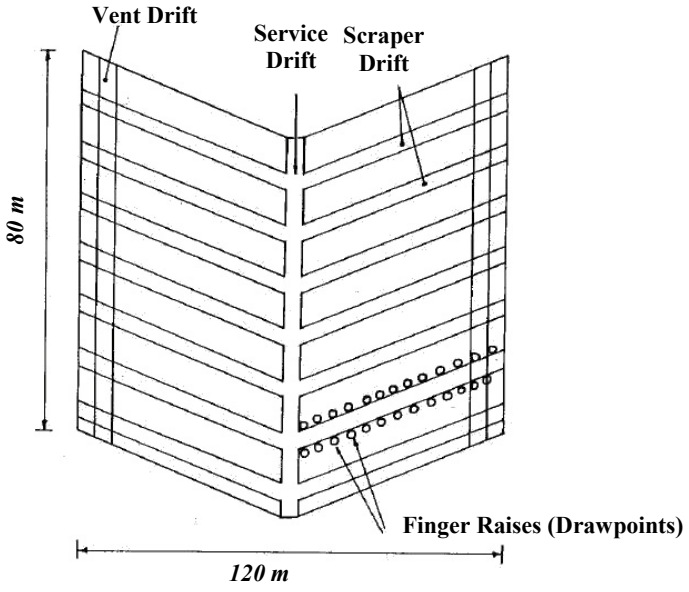

Fig 4. Block layout represented mathematical model

$d_{it} = \begin{cases} 1 & \text{if raise } i \text{ is drawn in shift } t, \\ 0 & \text{otherwise,} \end{cases}$

$y_{it} = \begin{cases} 1 & \text{if raise } i \text{ is on draw in shift } t, \\ 0 & \text{otherwise,} \end{cases}$

X_{it} = Tonnage of ore from raise *i* in shift t, (this is a continuous variable)

T_t = Tonnage of blended ore produced in shift t, (this is a continuous variable)

M_i = The maximum allowable output per shift from raise *i* based on production control considerations.

Q_t = The grade of ore from raise *i*

P_t = The required or call grade in shift t

6.1.1 Objective function

Chanda (1990) used an objective function, which would reduce as much as possible the fluctuation between shifts in the average grade drawn:

$$Minimize \sum_{i,t} \left| X_{it} \times Q_{it} - X_{it-1} \times Q_{it-1} \right| \quad (1)$$

6.1.2 Constraints

The constraints considered in the integer program are mainly quality and quantity requirements. Other constraints such as profile constraints or slushing capacity are handled by the simulation part of the model.

$$X_{it} - M_i d_{it} \le 0 \quad (2)$$

This constraint implies that if raise *i* is not drawn in shift *t*, there can be no output from it.

$$d_{it} \le N \qquad \text{for all } t \quad (3)$$

This constraint allows no more than N out of the whole raises to be on draw in a shift.

$$d_{it} - y_{it} \le 0 \qquad \text{for all } i,t \quad (4)$$

According to this constraint if raise *i* is barricaded in shift *t*, it cannot be drawn in that shift.

$$y_{it+1} - y_{it} \le 0 \qquad \text{for all } i,t \quad (5)$$

This constraint forces a raise to be declared exhausted.

$$\sum_i Q_i \times X_{it} - P_t T_t = 0 \qquad \text{for all } t \quad (6)$$

$$\sum_i X_{it} - T_t = 0 \qquad \text{for all } t \quad (7)$$

This constraint ensures that the tonnage of blended ore in each shift equals the combined tonnage of the constituents.

6.2. Rubio(2002)

Rubio (2002), proposed a methodology to compute production schedules in block caving. He used two objective functions as the main goal of mine planning. The first one was the maximization of NPV by explicitly defining the mathematical expression of NPV. The second proposed objective function was to minimize dilution entry by controlling the profile of the caving back. The second algorithm indirectly represented the maximization of the life of the mine. In this formulation there is no relation constraining the total tonnage drawn from a drawpoint. Thus, mining reserves are not included in the formulation, since it is believed that these reserves should be an output of the optimization rather than an input. This formulation is a mixed integer problem, since it contains integer and real variables. The objective function is also non-linear and the interior point algorithm has been used to solve the problem.

Assumptions which are used in his formulation are as follows:

- There is just one mine in production at the time ignoring possible blending between mines.
- The undercut sequence is known.
- The size of the layout should be fixed, and defined as part of the previous planning steps.

In this model, variables are as follows:

$P_t =$ The profit to be earned in period t.

$d_{it} =$ Tonnage to be drawn from drawpoint i in period t.

$a_{it} =$ $\begin{cases} 1 & \text{if drawpoint } i \text{ is drawn in period } t. \\ 0 & \text{otherwise,} \end{cases}$

$S_{it} =$ $\begin{cases} 1 & \text{if drawpoint } i \text{ is opened in period } t \\ 0 & \text{otherwise} \end{cases}$

$C_{it} =$ $\begin{cases} 1 & \text{if drawpoint } i \text{ is closed in period } t \\ 0 & \text{otherwise} \end{cases}$

$G_{kit} =$ The diluted grade of element k from drawpoint i in period t.

$RF_{kt} =$ The revenue factor of element k in period t.

$MR_k =$ The metallurgical recovery of element k.

$MC_{it} =$ The mining cost of drawpoint i in period t.

$PC_{it} =$ The processing cost of drawpoint i in period t.

$\delta =$ Discount rate of one period

$v_t =$ The total number of new drawpoints to open in period t.

$DV =$ The development cost of opening a new drawpoint.

$TU_{it} =$ The maximum draw rate of drawpoint i in period t.

$TL_{it} =$ The minimum draw rate of drawpoint i in period t.

$TTU_t =$ The maximum feasible production targets for the mine.

$TTL_t =$ The minimum feasible production targets for the mine.

6.2.3 Objective function

To maximize NPV, the objective function is composed of the tonnage to be drawn from the drawpoints and a binary variable that indicates whether a specific drawpoint has a production call in a particular period of the schedule or not.

The profit to be earned per period of the mine schedule is computed as follows

$$P_t = \sum_{i=1}^{l} d_{it} a_{it} \left[\sum_{k=1}^{K} \left(G_{kit} RF_{kt} MR_k \right) \right] - MC_{it} - PC_{it} \tag{8}$$

The objective function is to maximize the NPV over all periods $1 \le t \le T$

$$MAX \left[\sum_{t=1}^{T} \frac{P_t - v_t \, DV_t}{(1+\delta)^t} \right] \tag{9}$$

The objective function is non-linear since the relation between tonnage and grade along a draw column is non-linear. A draw column tonnage (V_{it}) and grade (G_{kit}) are coupled by a non-linear function given by the initial block model and the mixing process.

6.2.4 Constraints

1. Development rate

$$\sum_{i=1}^{l} S_{it} = v_t \qquad \forall t, 1 \le t \le T \tag{10}$$

$$0 \le v_t \le New_t \qquad \forall t, 1 \le t \le T \tag{11}$$

Note that v_t is an integer variable and New_t is an upper bound for the problem.

2. Undercut sequence

$$\sum_{k=1}^{t} S_{ik} \ge S_{i+lt} \tag{12}$$

This constraint guarantees that drawpoints are opened in sequence.

$$\sum_{t=1}^{T} S_{it} \le 1 \tag{13}$$

This constraint guarantees that every drawpoint is opened just once.

3. Drawpoint status

To avoid the closure of the drawpoint before it is opened the following constraint needs to be formulated

$$\sum_{k=1}^{t} S_{ik} \ge \sum_{k=1}^{t-1} C_{ik} \tag{14}$$

Also to avoid that drawpoint is opened twice the following needs to the set of constraints

$$\sum_{t=1}^{T} C_{it} \le 1 \tag{15}$$

To link a_{it} with C_{it}, the below constraint should be used

$$a_{it} = \sum_{k=1}^{t} S_{ik} \left(1 - \sum_{k=1}^{t} C_{ik} \right) \tag{16}$$

If drawpoint *i* has not been opened $a_{it} = 0$ because $\sum_{k=1}^{t} S_{ik} = 0$, thus the drawpoint *i* will not be part of the schedule in period t.

If $\sum_{k=1}^{t} S_{ik} = 1$, then a_{it} can either be 1 or 0 depending on the need to use drawpoint *i* in period t of the schedule.

If the drawpoint *i* is not drawn in period t, then this drawpoint is closed automatically ($C_{it} = 1$).

4. Maximum opened production area

$$\sum_{i=1}^{l} a_{it} \leq A_t \tag{17}$$

This constraint controls the maximum open area at any given period of the schedule. A_t should be given as an input to the algorithm.

5. Draw rate

$$d_{it} \leq TU_{it} a_{it} \tag{18}$$

$$d_{it} \geq TL_{it} a_{it} \tag{19}$$

This constraint can also be written as follows

$$TL_{it} = \frac{TU_{it}}{dcf_t} \tag{20}$$

dcf_t represents the desired draw control factor to be used in period t of the schedule. The draw control factor is an indicator of how even the draw is performed among active drawpoints at a given horizon of time. The following formula has been traditionally used to compute the draw control factor

$$dcf_t = \frac{\left[\dfrac{\sum_{k=1}^{K} \left(d_i - d_k^i \right)^2}{K} \right]^{0.5}}{\dfrac{1}{K+1} \sum_{k=1}^{K+1} d_k} \tag{21}$$

Where d_i is the tonnage drawn from drawpoint *i* in a period of time, d_k^i is the tonnage drawn from drawpoint k, a neighbor of drawpoint *i* in the same period of time and K is the number of neighbors of drawpoint *i*.

6. Period constraints

$$\sum_{i=1}^{L} d_{it} \leq TTU_i \tag{22}$$

$$\sum_{i=1}^{L} d_{it} \geq TTL_i \tag{23}$$

6.3. Diering (2004)

With production scheduling for block cave operations we want to predict or schedule the best tonnages to extract from a number of drawpoints for various periods of time (Diering, 2004). The time period can be very short, such as a day or it can extend over the life of the mine. In this model variables are as follows:

$N =$ Number of drawpoints

$M =$ Number of time periods

$i =$ The i^{th} drawpoint

$j =$ The j^{th} time period

$t_{ij} =$ Tons for drawpoint i for time period j

$T_i =$ Total tonnage allowed for drawpoint i

$T_j =$ Total tonnage allowed for time period j

$c_{ij} =$ PRC tonnage limit for drawpoint i for period j
(PRC: Production Rate Curve)

$b_{ij} =$ Minimum tonnage allowed for drawpoint i in period j. ($b_{ij} \geq 0$)

$e_{ij} =$ Allowable difference in tonnage between drawpoint and its neighbors

$m_{ij} =$ Mean tonnage of neighbors

$r_{ij} =$ Revenue from drawpoint i in period j (adjusted for mining costs)

$d_j =$ Discount fraction in period j

$g_{ij} =$ Grade of drawpoint i in time period j

6.3.5 Objective function

Diering considered the sample problem of maximizing NPV for M periods. In this function, the grades are variable and are function of t_{ij} and t_{ij} for previous period. Therefore, the objective is actually non-linear. The function is as follows:

6.3.6 Constraints

1. PRC limits per drawpoint

$$t_{ij} \leq c_{ij} \tag{24}$$

2. Lower limit per drawpoint

$$t_{ij} \geq b_{ij} \tag{25}$$

3. Total tonnage limits per drawpoint

$$\sum t_{ij} \leq T_i \tag{26}$$

4. Tonnage limits for each period

$$\sum t_{ij} = T_i \tag{27}$$

According to the above equations, the program will simply take the maximum allowable tons from the highest-grade drawpoints as soon as possible. Therefore, extra constraints, which limit how tonnages are related to neighboring drawpoints, should be added.

$$t_{ij} \leq m_{ij} + e_{ij} \tag{28}$$

$$t_{ij} \geq m_{ij} - e_{ij} \tag{29}$$

7. Conclusions

Much of the logic around the scheduling of large open pits applies to scheduling of block caves. In both cases, geotechnical constraints are very important. In both cases, the potential to add value to the overall project through careful scheduling is significant.

The methods currently used to compute production schedule in a block cave mine can be classified in two main categories: heuristic methods and exact optimization methods. Some of the main problems associated with the methods are as follows:

- They do not incorporate the variability and the dynamic behavior of the fundamental models (see section 3) throughout the ore-body.
- They do not have a rational way to link the mine planning parameters with the fundamental models which discussed in section 3.
- They do not integrate the operational upsets that affect productivity.
- They do not incorporate, in a routine basis, operational performance to adjust the medium and the long-term plans.

There are parameters in the production schedule methodology that are assumed to be constant, mainly because there are currently no planning tools to introduce the probabilistic behavior of these parameters into the process of planning a block cave mine. These parameters include draw rates, grade, undercut sequence, development rate and air gaps.

8. References

[1] Alford, C., Brazil, M., and Lee, D. H. (2007). Optimisation in Underground Mining. in *Handbook Of Operations Research In Natural Resources*, Vol. 99, *International Series in Operations Research & Management Science*, Springer US, pp. 561-577.

[2] Ataee-Pour, M. (2004). optimisation of stope limits using a heuristic approach. *Transactions of the Institutions of Mining and Metallurgy*, *113*,(2), 123-128.

[3] Ataee-Pour, M. (2005). A critical suvey of existing stope layout optimisation technique. *Journal of Mining Science*, *41*,(5), 447-466.

[4] Barraza, M. and Crorkan, P. (2000). *Esmeralda mine exploitation project*, in Proceedings of MassMin 2000, Brisbane, pp. 267-278.

[5] Brady, B. H. G. (2004). *Rock mechanics: for underground mining.* Kluwer Academic Publishers, Dordrecht ; Boston, Pages 626.

[6] Brown, E. T. (2003). *Block caving geomechanics.* Indooroopilly, Queensland : Julius Kruttschnitt Mineral Researh Centre, The University of Queensland, Pages 516.

[7] Carew, t. (1992). *The casier mine case study*, in Proceedings of MassMin 1992, Johannesburg,

[8] Carlyle, W. M. and Eaves, B. C. (2001). Underground planning at Stillwater mining company. *INTERFACES*, *31*,(4), 50-60.

[9] Chanda, E. C. K. (1990). An application of integer programming and simulation to production planning for a stratiform ore body. *Mining Science and Technology*, *11*,(1), 165-172.

[10] Dewolf, V. (1981). Draw control in principle and practice at Henderson mine. in *Design and operation of caving and sublevel stoping mines*, D. R. Steward, Ed. New York, Society of Mining Engineers of AIME., pp. 729-735.

[11] Diering, T. (2000). *PC-BC: A block cave design and draw control system*, in Proceedings of MassMin 2000, The Australasian Institute of mining and Metallurgy: melburne, brisbane, pp. 301-335.

[12] Diering, T. (2004). *Computational considerations for production scheduling of block vave mines*, in Proceedings of MassMin 2004, Santiago, Chile, pp. 135-140.

[13] Esterhuizen, G. S., Rachmad, L., Potapov, A. V., and Nordell, L. K. (2004). *Investigation of swell factor in a block cave draw column*, in Proceedings of MassMin 2004, Santiago, pp. 215-219.

[14] Febrian, I., Yudanto, W., and Rubio, E. (2004). *Application of convergence monitoring to manage induced stress by mining activities at PT Freepot Indonesia deep ore zone mine*, in Proceedings of MassMin 2004, Santiago, pp. 269-272.

[15] Glazer, S. and Hepworth, N. (2004). *Seismic monitoring of block cave crown pillar-Palabora Mining Company, RSA*, in Proceedings of MassMin 2004, Santiago, pp. 565-569.

[16] Guest, A., Van Hout, G. J., Von Johannides, A., and Scheepers, L. F. (2000). *An application of linear programming for block cave draw control*, in Proceedings of Massmin2000, The australian Institute of Mining and Metallurgy: Melbourne., Brisbane,

[17] Heslop, T. G. and Laubscher, D. H. (1981). Draw control in caving operations on Southern African Chrpsotile Asbestos mines. in *Design and operation of caving and sublevel stoping mines*, New York, Society of Mining Engineers of AIME., pp. 755-774.

[18] Hustrulid, W. A. and Bullock, R. L. (2001). *Underground mining methods : engineering fundamentals and international case studies.* Society for Mining, Metallurgy, and Exploration(SME), Pages 718.

[19] Jawed, M. (1993). *Optimal production planning in underground coal mines through goal programming-A case stydy from an Indian mine*, in Proceedings of 24th international symposium, Application of computers in the mineral industry(APCOM), Montreal,Quebec, Canada, pp. 43-50.

[20] Julin, D. E. (1992). Block caving, Chap. 20.3. in *SME Mining Engineering Handbook*, H. L. Hartman, Ed. Littleton, Colo. : Society for Mining, Metallurgy, and Exploration, Inc., pp. 1815-1836.

[21] Kajner, L. and Sparks, G. (1992). Quantifying the value of flexibility when conducting stochastic mine investment analysis. *CIM bulletin*, *85*,(964), 68-71.

[22] Kuchta, M., Newman, A., and Topal, E. (2004). Implementing a Production Schedule at LKAB 's Kiruna Mine. *Interfaces*, *34*,(2), 124-134.

[23] Kvapil, R. (1965). Gravity flow of granular materials in hoppers and bins. *International Journal of Rock Mechanics and Mining Sciences & Geomechanics Abstracts*, *2*,(1), 25-34,IN3-IN8,35-41.

[24] McIssac, G. (2005). Long term planning of an underground mine using mixed integer linear programming. in *CIM Bulletin*, vol. 98, pp. 89.

[25] McKinnon, S. D. and Lorig, L. J. (1999). Considerations for Three-Dimensional Modelling in Analysis of Underground Excavations. in *Distinct Element Modelling in Geomechanics(Ed:V.M. Sharma, K.R. Saxena, R.D. Woods)*, pp. 145-166.

[26] Moss, A., Russel, F., and Joens, C. (2004). *Caving and fragmentation at Palabora: prediction to production*, in Proceedings of MassMin 2004, Santiago, pp. 585-590.

[27] Nehring, M. and Topal, E. (2007). *Production schedule optimisation in underground hard rock mining using mixed integer programming*, in Proceedings of Project Evaluation Conference 2007, June 19, 2007 - June 20, 2007, Australasian Institute of Mining and Metallurgy, Melbourne, VIC, Australia, pp. 169-175.

[28] Ovanic, J. (1998). Economic optimization of stope geometry. PhD Thesis, Michigan Technological University, Houghton, USA, Pages 209.

[29] Rahal, D., Smith, M., Van Hout, G. J., and Von Johannides, A. (2003). *The use of mixed integer linear programming for long-term scheduling in block caving mines*, in Proceedings of 31st International Symposium on the Application of Computers and operations Research in the Minerals Industries (APCOM), Cape Town, South Africa,

[30] Richardson, M. P. (1981). Area od draw influence and drawpoint spacing for block caving mines, Chap. 13. in *Design and operation of caving and sublevel stoping mines*, D. R. Stewart, Ed. New York, SME-AIME, pp. 149-156.

[31] Riddle, J. (1976). *A dynamic programming solution of a block caving mine layout.*, in Proceedings of 14th International Symposium on the Application of Computers in the Mineral Industry(APCOM), Pennsylvania,

[32] Rojas, E., Molina, R., Bonani, A., and Constanzo, H. (2000). *The pre-undercut caving method at the E1 Teniente mine, Codelco Chile*, in Proceedings of MassMin 2000, The Australasian Institute of mining and Metallurgy:Melbourne., Brisbane, pp. 261-266.

[33] Rubio, E. (2002). Long-term planning of block caving operations using mathematical programming tools. MSc Thesis, Vancouver, Canada, Pages 116.

[34] Rubio, E. (2006). block cave mine infrastructure reliability applied to production planning.Thesis, British Columbia, Vancouver, Pages 132.

[35] Rubio, E., Caceres, C., and Scoble, M. (2004a). *Towards an integrated approach to block cave planning*, in Proceedings of MassMin 2004, Santiago, Chile, pp. 128-134.

[36] Samis, M. and Poulin, R. (1998). Valuing management flexibility : A basis to compare the standard DCF and MAP valuation frameworks. *CIM bulletin*, *91*,(1019), 69-74.

[37] Sarin, S. C. and West-Hansen, J. (2005). The long-term mine production scheduling problem. *IIE Transactions*, *37*,(2), 109-121.

[38] Singh, A. and Skibniewski, M. J. (1991). Development of flexible production systems for strip mining. *Mining Science and Technology*, *13*,(1), 75-88.

[39] Smith, M. L., Sheppard, I., and Karunatillake, G. (2003). *Using MIP for strategic life-of-mine planning of the lead/zinc stream at Mount Isa Mines*, in Proceedings of 24th international symposium, Application of computers in the mineral industry(APCOM), Cape Town, South Africa, pp. 465-474.

[40] Summers, J. (2000). *Analysis and management of mining risk*, in Proceedings of MassMin2000, The Australasian Institute of Mining and Metallurgy:Melbourne, Brisbane, Australia, pp. 63-82.

[41] Tang, X., Xiong, G., and Li, X. (1993). *An integrated approach to underground gold mine planning and sheduling optimization*, in Proceedings of 24th international symposium on the Application of computers in the mineral industry(APCOM), Montreal, Quebec, Canada, pp. 148-154.

[42] Topal, E. (2008). Early start and late start algorithms to improve the solution time for long-term underground mine production scheduling. *Journal of The South African Institute of Mining and Metallurgy*, *108*,(2), 99-107.

[43] Topal, E., Kuchta, M., and Newman, A. (2003). *Extensions to an efficient optimization model for long-term production planning at LKAB's Kiruna Mine*, in Proceedings of APCOM 2003, Cape Town, South Africa, pp. 289-294.

[44] Trigeorigs, L. (1990). A real options application in natural resource investment. *Advance in Future and Options Research*, *4*, 153-164.

[45] Trout, L. P. (1995). *Underground mine production scheduling using mixed integer programming*, in Proceedings of 25th international symposium, Application of computers in the mineral industry(APCOM), Brisbane, Australia, pp. 395-400.

[46] Williams, J., Smith, L., and Wells, M. (1972). *Planning of underground copper mining*, in Proceedings of 10th international symposium, Application of computers in the mineral industry(APCOM), Johannesburg, South Africa, pp. 251-254.

[47] Winkler, B. M. (1998). *Mine production scheduling using linear programming and virtual reality*, in Proceedings of 27th international symposium, Application of computers in the mineral industry(APCOM), Royal school of mines, London, United Kingdom, pp. 663-673.

A mathematical programming formulation for block cave production scheduling

Yashar Pourrahimian and Hooman Askari-Nasab
Mining Optimization Laboratory (MOL)
University of Alberta, Edmonton, Canada

Abstract

Caving is the lowest cost underground mining method provided that the drawpoint spacing, drawpoint size, and ore handling facilities are designed to suit the cave material. Also the drawpoint horizon must be maintained for the life of the draw for a successful operation.

This paper presents a mixed integer programming (MILP) formulation for block cave production scheduling. The objective function of the scheduler is to maximize the net present value (NPV) of operation while meeting technical and operational constraints. In development of the optimization model, in addition to the formulation of the objective function, the set of constraints that define the feasible space of solution is critical to effective mine planning solution.

In this paper, schedule optimization is carried out using six general constraints to model and control production. The constraints define: production target, draw rate, grade blending, maximum number of active drawpoints, precedence of extraction of drawpoints, and draw angle. Application of the model for production scheduling of a synthetic data shows how the constraints regulate production.

1. Introduction

Long-term mine scheduling is one of the optimization problems. A production schedule must provide a mining sequence that takes into account the physical limitations of the mine and, to the extent possible, meets the demanded quantities of each raw ore type at each period throughout the mine life. Mines use the schedules as long-term strategic planning tools to determine when to start mining a production area and as short-term operational guides.

Underground mining is more complex in nature than surface mining (Kuchta et al., 2004). Flexibility of underground mining is less than surface mining due to the geotechnical, equipment and space constraints (Topal, 2008).

In spite of the difficulties associated with the application of mathematical programming to production scheduling in underground mines, authors have attempted to develop methodologies to optimize production schedules.

Williams et al. (1972) planned sublevel stoping operations for an underground copper mine over one year using a linear programming approximation model. Jawed (1993) formulated a linear goal programming model for production planning in an underground room and pillar coal mine. Tang et al. (1993) integrated linear programming with simulation to address scheduling decisions, as did Winkler (1998). Trout (1995) used the MIP method to schedule the optimal extraction sequence for underground sublevel stoping. Ovanic (1998) used mixed integer programming of type two special ordered sets to identify a layout of optimal stopes. Carlyle et al. (2001) presented a model that

maximized revenue from Stillwater's platinum and palladium mine. Topal et al. (2003) generated a long-term production scheduling MIP model for a sub-level caving operation and successfully applied it to Kiruna Mine. Sarin et al. (2005) scheduled a coal mining operation with the objective of net present value maximization. Ataee-Pour (2005) critically evaluated some optimization algorithms according to their capabilities, restrictions and application for use in underground mining. McIssac (2005) formulated the scheduling of underground mining of a narrow veined polymetallic deposit utilizing MIP. Nehring et al.(2007) presented a mixed integer programming formulation for production schedule optimization in underground hard rock mining.

Scheduling of underground mining operations is primarily characterized by discrete decisions to mine blocks of ore, along with complex sequencing relationships between blocks. Since linear programming (LP) models cannot capture the discrete decisions required for scheduling, MIPs are generally the appropriate mathematical programming approach to scheduling.

The methods, currently used to compute production schedule in block cave mines, can be classified in two main categories: (a) heuristic methods and (b) exact optimization methods.

Heuristic methods are particularly used to rapidly come to a solution that is hoped to be close to the best possible answer, or optimal solution. These methods are used when there is no known method to find an optimal solution under the given constraints.

The original heuristic methods were the manual draw charts used at the beginning of block caving. These methods evolved through it use at Henderson mine where a way to avoid early dilution entry was described by constraining the draw profile to an angle of draw of 45 degrees (Dewolf, 1981). Heslop et al. (1981) described a volumetric algorithm to simulate the mixing along the draw cone. Carew (1992) described the use of a commercial package called PC-BC to compute production schedules at Cassiar mine. Diering (2000) showed the principles behind the commercial tool PC-BC to compute production schedules, providing several case studies where different draw methods have been applied depending on the ore body geometry and rock mass behavior.

The application of operation research methods to the planning of block cave mines was first described by Riddle (1976). This development intended to compute mining reserves and define the economic extent of the footprint. The final algorithm did not reflect the operational constraints of block caving described above since it worked with the block model directly instead of defining the concept of draw cone as an individual entity of the optimization process.

The first attempt to use mathematical programming in block cave scheduling was made by Chanda (1990) who implemented an algorithm to write daily orders. This algorithm was developed to minimize the variance of the milling feed in a horizon of three days. Guest et al. (2000) made another application of mathematical programming in block cave long term scheduling. In this case, the objective function was explicitly defined to maximize draw control behavior. However, the author stated that the implicit objective was to optimize NPV. There are two problems with this approach. The first one is that maximizing tonnage or mining reserves will not necessarily lead to maximum NPV. The second problem is the fact that draw control is a planning constraint and not an objective function. The objective function in this case would be to maximize tonnage, minimize dilution or maximize mine life.

Rubio (2002) developed a methodology that would enable mine planners to compute production schedules in block cave mining. He proposed a new production processes integration and formulated two main planning concepts as potential goals to optimize as part of the long term planning process, maximization of NPV and maximization of mine life.

Rahal et al. (2003) used a dual objective mixed integer linear programming algorithm to minimize the deviation between the actual state of extraction (height of draw) and a set of surfaces that tend towards a defined draw strategy. This algorithm assumes that the optimal draw strategy is known.

Nevertheless, it is postulated that by minimizing the deviation to the draw target the disturbances produced by uneven draw can be mitigated.

Diering (2004) presented a non-linear optimization method to minimize the deviation between a current draw profile and the target defined by the mine planner. He emphasized that this algorithm could also be used to link the short with the long-term plan. The long-term plan is represented by a set of surfaces that are used as a target to be achieved based on the current extraction profile when running the short-term plans. Rubio et al. (2004) presented an integer programming algorithm and an iterative algorithm to optimize long-term schedules in block caving integrating the fluctuation of metal prices in time.

We critically review the MILP formulations of the block cave production scheduling problem. We model the problem considering different possible directions of extraction and different draw angles. We divide the major decision variables into two categories, continuous variables representing the portion of a drawpoint that is going to be extracted in each period and binary integer variables controlling the order of extraction of drawpoints and the number of active drawpoints in each period. The MILP formulation also ensures that the angle of draw along the advance direction is 45 degree. We have implemented the optimization formulation in TOMLAB/CPLEX (Holmstrom, 1989-2009) environment. A scheduling case study with synthetic data is carried out over fifteen periods to verify the MILP model.

The next section of the paper covers the assumptions, problem definition, and the notations of variables. Section 3 presents mixed integer linear programming formulation of the problem, while section 4 presents the numerical modeling techniques. Section 5 presents an example, conclusions and future work followed by the list of references in the next section.

2. Assumptions, problem definition, and notation

We assume that a geological block model represents the orebody, which is a three-dimensional array of rectangular or cubical blocks used to model orebodies and other sub-surface structures. Numerical data are used to represent a single attribute of the orebody such as densities, grades, elevations, or economic data. The draw cones are created based on the block model. We assume that all draw cones have the same height. Average grade of all blocks inside each draw cone is presented as grade of that draw cone. Each draw cone is representative by two drawpoints (see Fig. 1). The coordinates of the center of each draw cone defines the spatial location of each drawbell. There is no selective mining and the whole material in the draw cone has to be extracted. Fig. 1 shows the flow chart from initial block model to the created draw cones.

The problem is finding a sequence of drawpoints extraction over the mine life, provided the NPV is maximized. The material in each draw cone is to be scheduled over T periods depending on the goals and constraints associated with the mining operation. To solve the problem, three decision variables are employed for each draw cone, one continuous decision variable and two binary integer variables. Continuous decision variable indicates the portion of extraction from each draw cone in each period and two binary integer variables control the number of active drawpoints and precedence of extraction. This formulation is implemented for eight advance directions to maximize the NPV. Fig 2. illustrates a schematic plan view of these directions.

According to the advance direction for each drawpoint, *d*, there is a set $C_d(K)$ which defining the predecessor drawpoints that must be started prior to extraction of drawpoint *d*, where *K* is the total number of drawpoints in set $C_d(K)$. Based on the search direction, eight different predecessor data sets can be defined for each drawpoint. Fig. 3. illustrates these data sets.

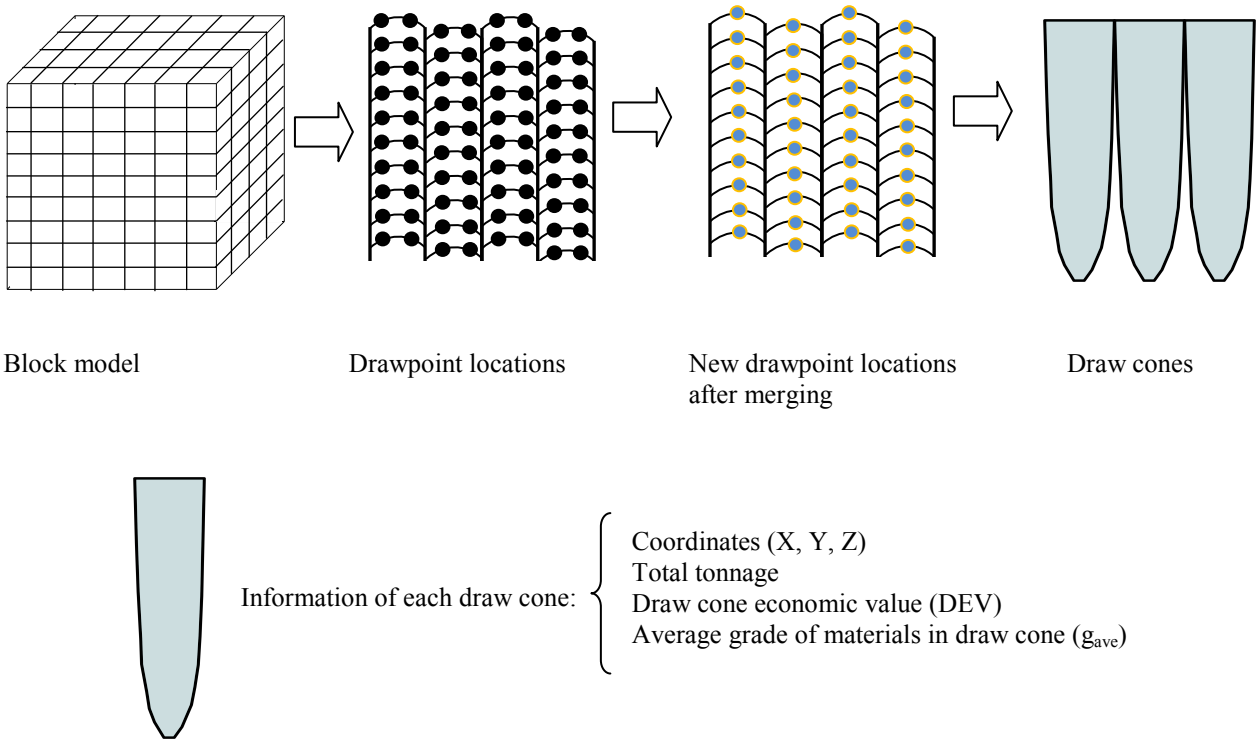

Fig. 1. Overall flowchart from initial block model to draw cones

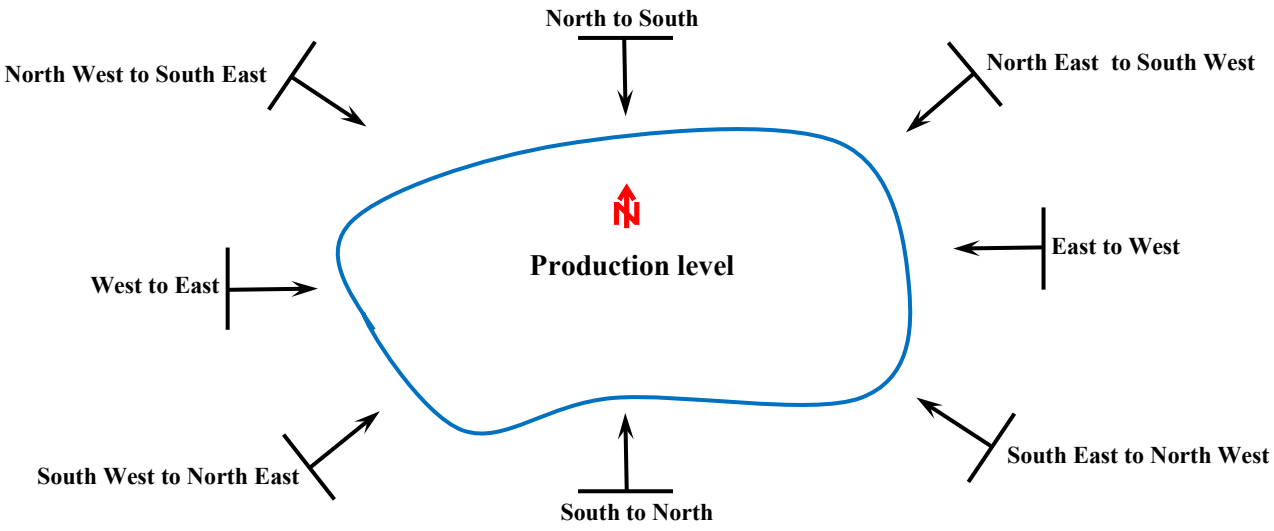

Fig. 2. Alternative cave advance directions

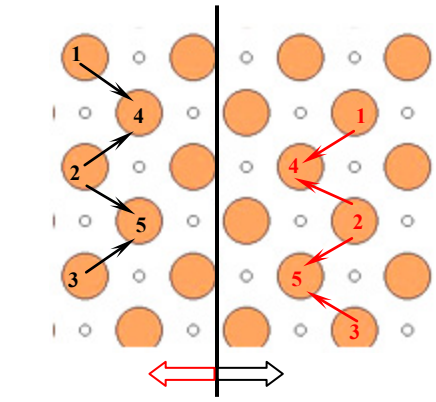

W to E or E to W

For each of the above directions, there is a set $C_d(K)$, which includes all drawpoints that must be started prior to drawpoint *d*. Set $C_4(K)$ belongs to drawpoint 4 and it has two members, drawpoints 1 and 2.

$C_4(2)=\{1,2\}$ and $C_5(2)=\{2,3\}$

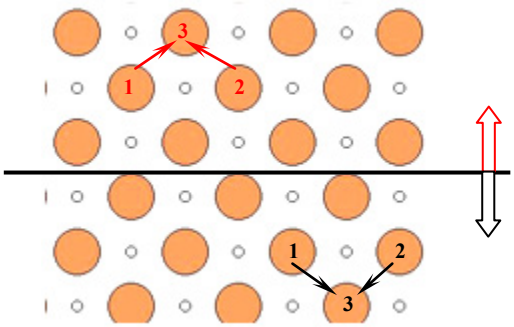

N to S or S to N

For each of the above directions, there is a set $C_d(K)$, which includes all drawpoints that must be started prior to drawpoint *d*. Set $C_3(K)$ belongs to drawpoint 3 and it has two members, drawpoints 1and 2.

$C_3(2)=\{1,2\}$

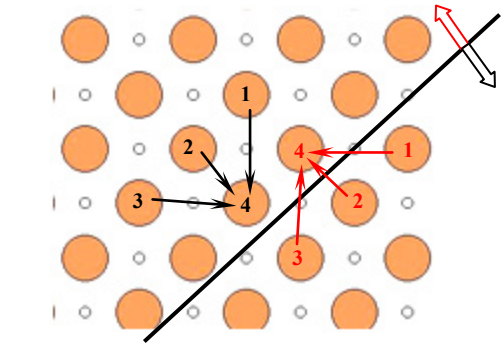

SE to NW or NW to SE

For each of the above directions, there is a set $C_d(K)$, which includes all drawpoints that must be started prior to drawpoint *d*. Set $C_4(K)$ belongs to drawpoint 4 and it has three members, drawpoints 1, 2 and 3.

$C_4(3)=\{1,2,3\}$

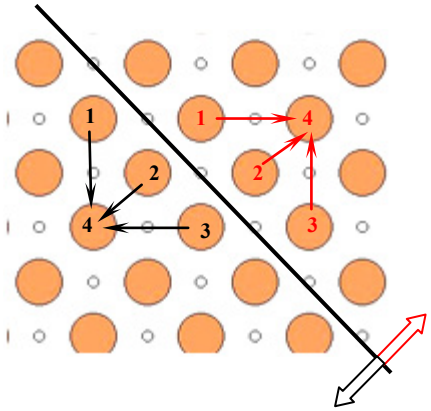

SW to NE or NE to SW

For each of the above directions, there is a set $C_d(K)$, which includes all drawpoints that must be started prior to drawpoint *d*. Set $C_4(K)$ belongs to drawpoint 4 and it has three members, drawpoints 1, 2 and 3.

$C_4(K)=\{1,2,3\}$

Fig. 3. Constructing the predecessor data set

2.1. NOTATION

The notation of decision variables, parameters, sets, and constraints are as follows:

2.1.1 Sets

$C_d(K)$ — For each drawpoint, *d*, there is a set $C_d(K)$ defining the predecessor drawpoints that must be started prior to extraction of drawpoint *d*, where *K* is the total number of drawpoints in set $C_d(K)$.

2.1.2 Indices

A general parameter *f* can take three indices in the format of $f_{d,k}^{t}$. Where:

$t \in \{1,....,T\}$ — Index for scheduling periods.

$d \in \{1,...,D\}$ — Index for drawpoints.

$k \in \{1,...,K\}$ — Index for drawpoints in the set $C_d(K)$.

2.1.3 Parameters

DEV — The drawpoint economic value.

i — The discount rate.

N^t — Maximum number of active drawpoints in period *t*.

Q_d — Total tonnage of material in draw cone associated with drawpoint *d*.

g_d — Average grade of material in draw cone associated with drawpoint *d*.

$\overline{g^t}$ — Upper bound on acceptable average head grade in period *t*.

$\underline{g^t}$ — Lower bound on acceptable average head grade in period *t*.

$\overline{R}_d^t$ — Upper bound on draw rate from drawpoint *d* in period *t*.

$\underline{R}_d^t$ — Lower bound on draw rate from drawpoint *d* in period *t*.

$\overline{M}^t$ — Upper bound on feasible production target (tonne) from the mine in period *t*.

$\underline{M}^t$ — Lower bound on feasible production target (tonne) from the mine in period *t*.

L_{dk} — The shortest distance between drawpoint *d* and drawpoint *k* from set $C_d(K)$

A_d — Cross section area between undercut level and top of extraction.

γ_d — Density of material in drawpoint *d*.

f — Extraction height factor. It is calculated by $f = \dfrac{Q_d}{A_d . \gamma_d}$

2.1.4 Decision Variables

$u_d^t \in [0,1]$ — Continuous variable, representing the portion of draw cone *d* to be extracted in period *t*.

$a_d^t \in \{0,1\}$ Binary integer variable controlling the active drawpoints. a_d^t is equal to one if drawpoint *d* is active in period *t*, otherwise it is zero.

$z_d^t \in \{0,1\}$ Binary integer variable controlling the precedence of extraction of drawpoints. z_d^t is equal to one if extraction of drawpoint *d* has started by period *t*, otherwise it is zero.

3. Mathematical formulation for NPV maximization

3.1. Objective function

The objective function is composed of the draw cone economic value, discount rate and a continuous decision variable that indicates the portion of a draw cone which is extracted in each period. The DEV value is defined based on economic block values. The profit from mining a block that is located inside the cone depends on the value of the block and the costs incurred in mining and processing. The cost of mining a block is a function of its location, which characterizes how deep the block is located relative to the surface and how far it is located relative to its final dump.

The objective function is to maximize the NPV over all periods, 1≤ t ≤ T. The objective function is expressed by Eq.(1),

$$\text{Maximize} \quad \sum_{t=1}^{T}\sum_{d=1}^{D}\left[\frac{DEV_d}{(1+i)^t}\right]u_d^t \tag{1}$$

3.2. Definition of constraints

3.2.1 Draw rate

These inequalities, Eq.(2), ensure that the draw rate from drawpoint *d* in period *t* is within the acceptable tonnage range.

$$\underline{R}_d^t \le u_d^t \times Q_d \le \overline{R}_d^t \qquad \forall t \in \{1,...,T\}, \quad d \in \{1,...,D\} \tag{2}$$

3.2.2 Target production

These inequalities, Eq.(3), ensure that the total tonnage of material extracted from drawpoints in each period is within the acceptable range of production targets for the mine.

$$\underline{M}^t \le \sum_{d=1}^{D} u_d^t \times Q_d \le \overline{M}^t \qquad \forall t \in \{1,...,T\} \tag{3}$$

3.2.3 Grade blending

These inequalities, Eq.(4), ensure that the average grade of production is within the desired range in each period.

$$\underline{g}^t \le \frac{\sum_{d=1}^{D} u_d^t \times Q_d \times g_d^t}{\sum_{d=1}^{D} u_d^t \times Q_d} \le \overline{g}^t \qquad \forall t \in \{1,...,T\} \tag{4}$$

Eq.(4) is rearranged as Eq.(4a) and Eq.(4b).

Upper bound: $\sum_{d=1}^{D} Q_d \times \left(g_d^t - \overline{g^t} \right) \times u_d^t \le 0$ (4a)

Lower bound: $\sum_{d=1}^{D} Q_d \times \left(\overline{g^t} - g_d^t \right) \times u_d^t \le 0$ (4b)

3.2.4 Maximum number of active drawpoints in each period

These constraints control the maximum number of active draw points at any given period of the schedule. N^t should be given as an input to the algorithm. u_d^t is a continuous variable and can get a value between zero and one. When it is greater than zero, it means a portion of draw cone *d* is extracted in the relevant period and the related drawpoint is active during this time. In order to control the number of active drawpoints, a binary decision variable, a_d^t, is employed. According to Eq.(5), when a portion of draw cone *d* is extracted in period *t* $(u_d^t > 0)$, the relevant binary variable to drawpoint *d*, must be equal to 1, $(a_d^t = 1)$, because of the activity of drawpoint *d* in period *t*. Eq. (6) ensures that summation of active drawpoints do not exceed the maximum number allowed in each period.

$$u_d^t - a_d^t \le 0 \qquad \forall t \in \{1,...,T\}, \quad d \in \{1,...,D\} \tag{5}$$

$$\sum_{d=1}^{D} a_d^t \le N^t \qquad \forall t \in \{1,...,T\} \tag{6}$$

3.2.5 Precedence of drawpoints

These constraints control the extraction precedence of drawpoints. Eq. (7) ensures that drawpoints belonging to the relevant set, $C_d(K)$, have been started prior to extraction of drawpoint *d*. This set is defined based on the selected mining direction (see Fig. 3). This set can be empty, which means the considered drawpoint can be extracted in any time period in the schedule. To control the precedence of extraction, a binary decision variable, z_d^t , is employed. If extraction of drawpoint *d* is started in period *t*, the variable z_d^t has to be 1. If summation of extracted portions of each draw cone from the respective set is greater than zero, then, extraction from the considered drawpoint can be started. Parameter ε in the Eq. (7) is a very small positive real number defined based on the maximum portion that can be extracted and it must be greater than zero and less than one. If this parameter is assumed zero, it means drawpoint *d* can be started before the drawpoints of set $C_d(K)$, and this leads to incorrect solution. Eqs. (7), (8) and (9) must be satisfied simultaneously to complete the precedence constraint. Eq. (8) ensures that if extraction of drawpoint *d* is started in period *t*, that drawpoint has not been extracted before. Eq. (9) ensures that extraction of drawpoint *d* is started by period *t*.

$$z_d^t - \sum_{j=1}^{t} u_k^j \le 1 - \varepsilon \qquad \forall d \in \{1,...,D\}, \quad t \in \{1,...,T\}, \quad k \in C_d(K) \tag{7}$$

$$\sum_{j=1}^{t} u_d^j - z_d^t \le 0 \qquad \forall d \in \{1,...,D\}, \quad t \in \{1,...,T\} \tag{8}$$

$$z_d^t - z_d^{t+1} \le 0 \qquad \forall d \in \{1,...,D\}, \quad t \in \{1,...,T-1\} \tag{9}$$

3.2.6 Draw angle

A uniform draw rate during the mine life will affect three aspects of design and planning of a block cave mine; (1) less dilution at the drawpoints (Laubscher, 1994), (2) reduced stresses (Barlett et al., 2000), and (3) finer fragmentation at the drawpoints.

One of the greatest dangers of block caving is the potential for excessive dilution that could significantly reduce the grade of the ore or result in a significant loss of ore. There are various methods of draw control. One that has been used successfully at the Climax and Henderson mines is to limit the draw in the drawpoints against uncaved ore to a small percentage of the ore column. The draw is increased by equal percentage increments in each line of drawpoints as they progress away from the cave line. The principle is to maintain an ore-to-waste contact of 45 to 50^o (Julin, 1992). The angle of draw affects the stress pattern at the cave front and causes over stress at this area. Fig. 4 illustrates this angle. Rubio (2006) analyzed the effect of angle of draw in a mine using historical collapses experienced at that mine. He realized that collapse of the cave front in that mine occurred under three conditions: shallow angle of draw, steep angle of draw, and sudden changes of the angle of draw between periods. Generally, range of angle of draw is site dependent and it is a function of insitu stresses, rock mass strength, and undercutting method. To control draw angle, Eq. (10) is employed. It is assumed that draw angle should be 45^o. This means difference between the remaining tonnage of draw cone, *d*, and the remaining tonnage of the relevant draw cones from set $C_d(K)$ at any given period of time should be kept in a specific range. In other words, the draw rate from set of predecessor drawpoints must be controlled in a way that the angle between the horizontal line and a line which connects the top of extraction point of drawpoints (A and B) be around 45 degrees along the advance direction (see Fig. 5). For this purpose, the extracted tonnage is converted to height using height of extraction factor (*f*). This factor can be calculated using Eq. (11). It should be noted, upper and lower bound of this equation is set based on the geomechanical condition of the study area.

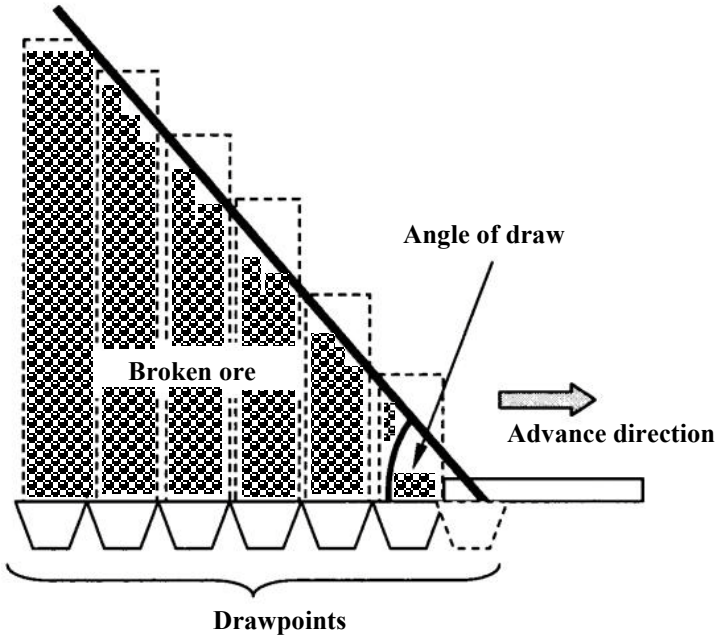

Fig. 4. Angle of draw along the advance direction

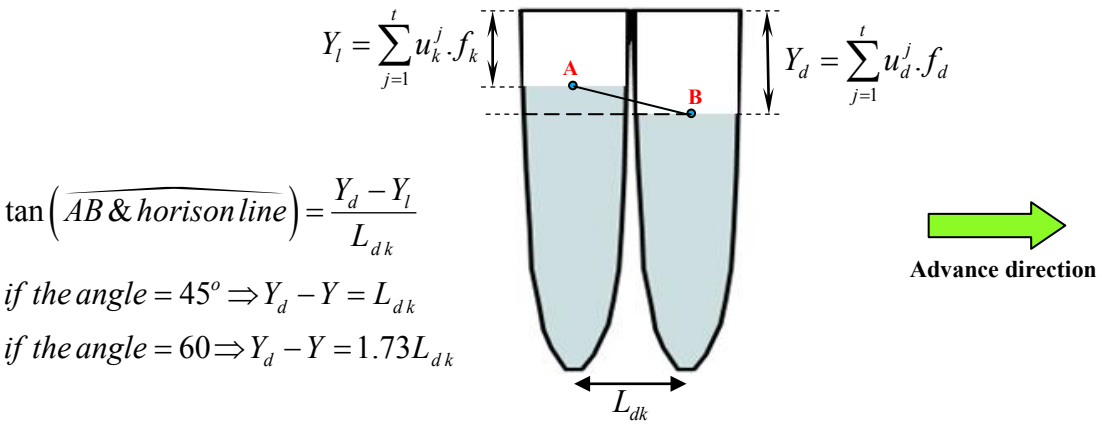

Fig. 5. Draw angle control section

$$\sum_{j=1}^{t} u_d^j . f_d - \sum_{j=1}^{t} u_k^j . f_k \le L_{dk} \qquad \forall d \in \{1,...,D\},\quad t \in \{1,...,T\},\quad k \in C_d(K) \tag{10}$$

$$f_i = \frac{Q_i}{A_i \times \gamma_i} \qquad \forall i \in \{1,...,D\} \ \ or \ \ i \in C_d(K) \tag{11}$$

3.2.7 Reserve constraint

This constraint, Eq.(12), ensures that the fractions of draw cone that are extracted over the scheduling periods are going to sum up to one, which means all the estimated draw cone tonnage is going to be scheduled.

$$\sum_{t=1}^{T} u_d^t = 1 \qquad \forall t \in \{1,...,T\},\quad d \in \{1,...,D\} \tag{12}$$

4. Numerical modeling

In most linear optimization problems, the variables of the objective function are continuous in the mathematical sense, with no gaps between real values. To solve such linear programming problems, ILOG CPLEX implements optimizers based on the simplex algorithms (Winston, 1995) (both primal and dual simplex) as well as primal-dual logarithmic barrier algorithms.

Branch and cut is a method of combinatorial optimization for solving integer linear programs. The method is a hybrid of branch and bound and cutting plane methods (Horst et al., 1996). Refer to Wolsey (1998) for a detailed explanation of the branch and cut algorithm, including cutting planes. In this study we used TOMLAB/CPLEX version 11.2 (Holmström, 1989-2009) as the MILP solver. TOMLAB/CPLEX efficiently integrates the solver package CPLEX (ILOG Inc, 2007) with MATLAB environment (MathWorks Inc., 2007).

Table 1 shows the number of decision variables and the number of binary integer variables required for the proposed MILP formulations as a function of number of drawpoints, ND, and number of scheduling periods, T.

Table 1. Number of decision variables in the presented formulation

Number of continuous variables	Number of binary integer variables
ND×T	2×ND×T

5. Illustrative example

The presented model has been implemented and tested in TOMLAB/CPLEX environment. It was verified on a synthetic data set containing 70 drawpoints. Radius of each draw cone is 15 meters. Fig. 6 shows the plan view of the center of merged drawpoints based on relevant coordinates. Average grade of drawpoints is varying between 0.65 and 0.8 percent. The tonnage of material between under cut and top of extraction for all drawpoints is same and equivalent to 26.5 MT. The top of extraction is a flat surface. To calculate the height of each drawpoint, it is assumed that (1) tonnage of each drawpoint is located between undercut level and top of extraction, (2) density of material is equal to 2.5 t/m^3, and (3) radius of each draw cone is equal to 15 m.

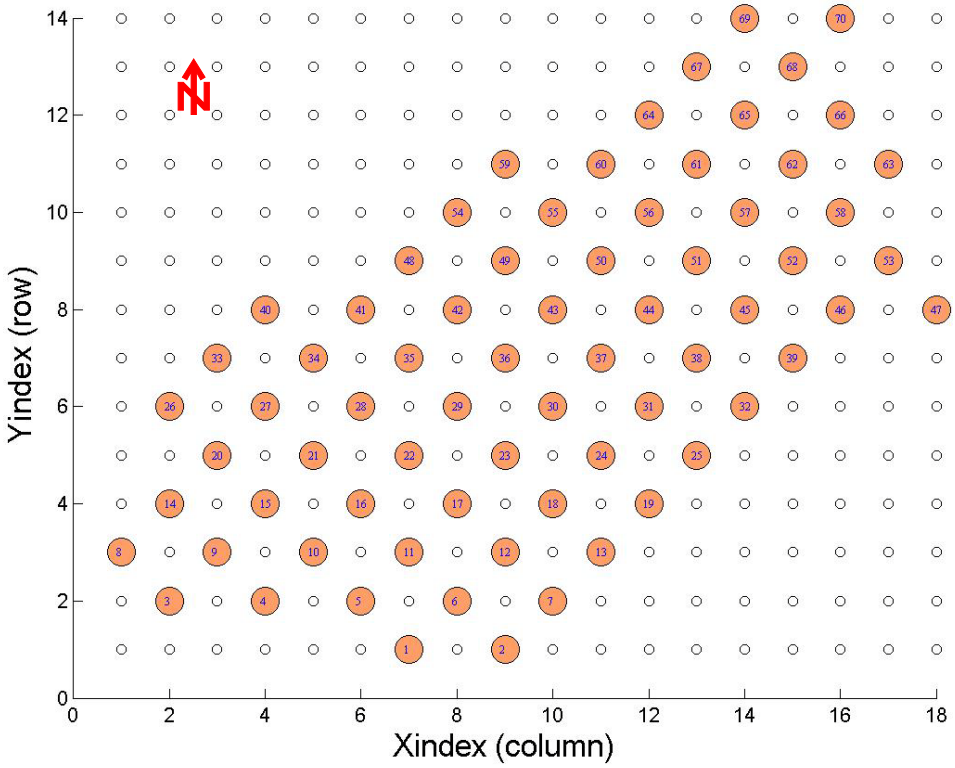

Fig. 6. Plan view of center of draws

6. Results and discussion

To find the optimum production schedule, the formulation was implemented along all the advance directions presented in section 2 over 15 periods scheduling horizon.

Table 2 shows the numerical results of the test of the MILP model with the data set containing 70 drawpoints over 15 periods of extraction. To solve the problem we set same boundaries for each advance direction (see Table 3). Table 3 shows input data and obtained results for each advance direction. The NPV for different directions is illustrated in Fig. 7. It can be seen that difference

between the highest and the lowest NPVs is more than $6.5 million. The maximum NPV is obtained in South East to North West direction. Fig. 8 shows that all constraints have been satisfied for this direction. Fig. 9 illustrates drawpoints schedule. In each period, the red color indicates that extraction of drawpoint is started in that period while the yellow color indicates that extraction of that drawpoint has been started in the previous periods and it is extracted in this period too. The blue star sign indicates that extraction of that drawpoint has been finished. It can be seen that extraction of all drawpoints is started before period 13. Recovered profiles for all drawpoints in different periods are shown in Fig. 10, which show the location of top point of each draw cone at the end of each period.

Table 2. Numerical results for the synthetic data set containing 70 drawpoints

Direction	CPU time (s)	Size of matrix A (row×col)
West to East	62.37	8865 × 3150
East to West	12.47	8865 × 3150
North to South	66.67	8865 × 3150
South to North	29.28	8865 × 3150
South East to North West	4.94	10245 × 3150
North West to South East	86.95	10245 × 3150
South West to North East	56.79	10425 × 3150
North East to South West	89.75	10425 × 3150
Necessary time to solve this problem	409.22 = 6.82 (min)	

Table 3. Inputs and NPV for the data set containing 70 drawpoints

Direction	N^t	$\underline{g^t} / \overline{g^t}$ (%)	$\underline{M^t} / \overline{M}^t$ (MT)	$\underline{DR} / \overline{DR}$ (T/day)	NPV ($M)
West to East	25	0.65 / 0.8	0 / 2	0 / 4.16	145.7
East to West	25	0.65 / 0.8	0 / 2	0 / 4.16	147.39
North to South	25	0.65 / 0.8	0 / 2	0 / 4.16	141.62(min)
South to North	25	0.65 / 0.8	0 / 2	0 / 4.16	148.04
South East to North West	25	0.65 / 0.8	0 / 2	0 / 4.16	148.24 (max)
North West to South East	25	0.65 / 0.8	0 / 2	0 / 4.16	146.27
South West to North East	25	0.65 / 0.8	0 / 2	0 / 4.16	146.99
North East to South West	25	0.65 / 0.8	0 / 2	0 / 4.16	146.51

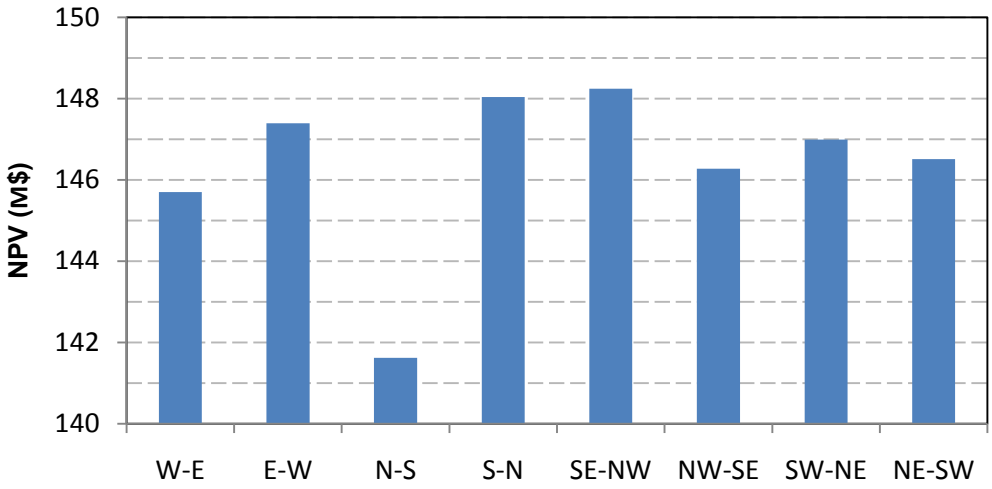

Fig. 7. Amount of NPV for different directions over 15 years scheduling horizon

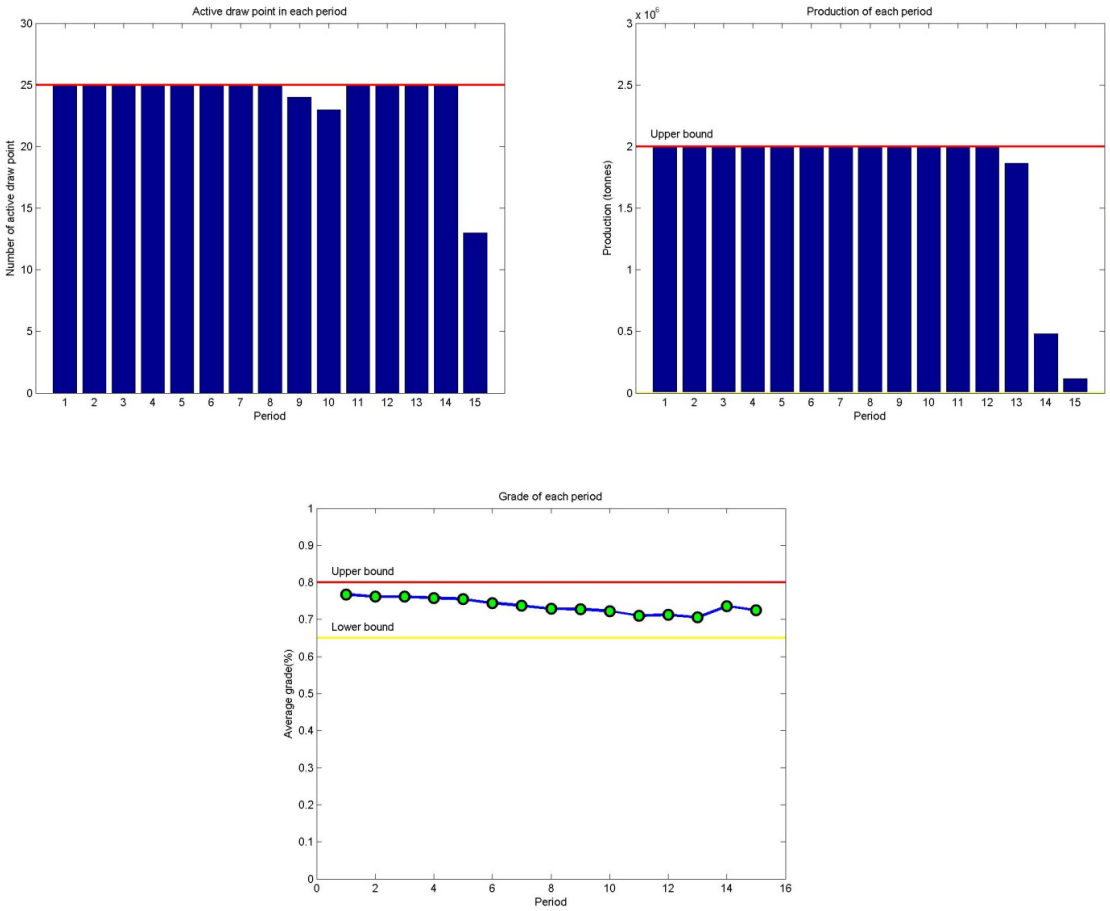

Fig. 8. Number of active drawpoints, tonnage of production and average grade for each period

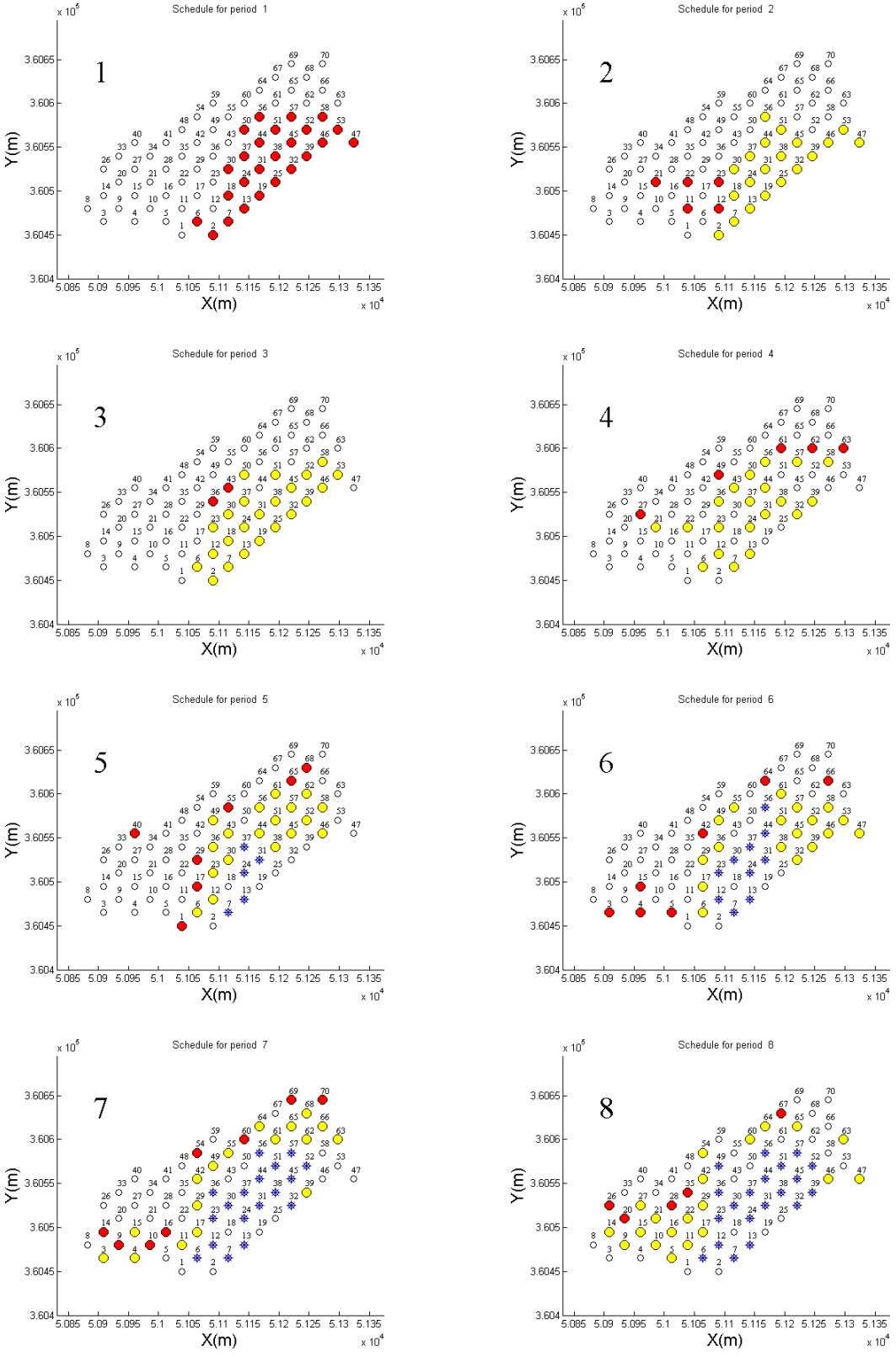

Fig. 9. Sequence of extraction

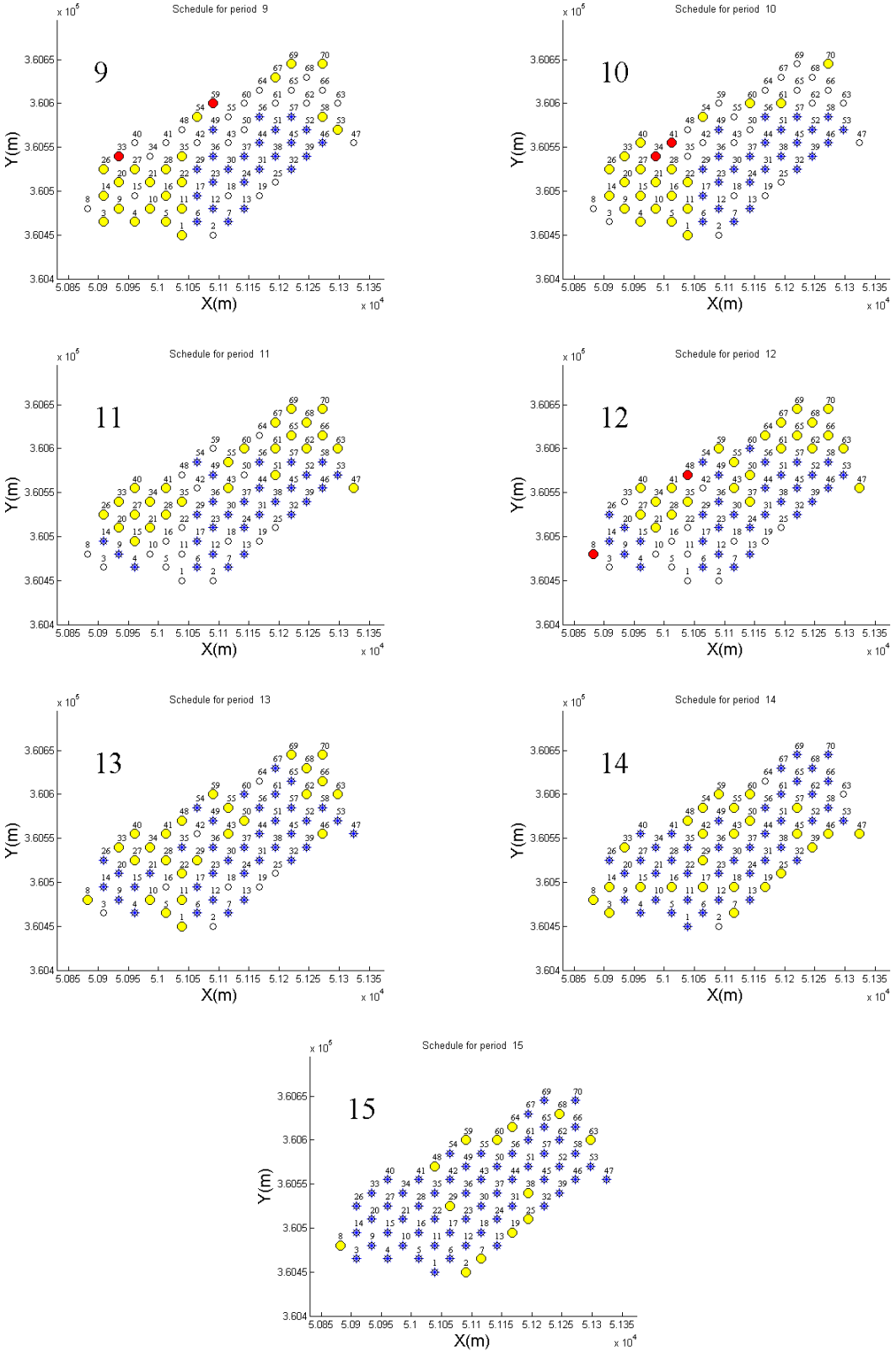

Fig. 9. Continued

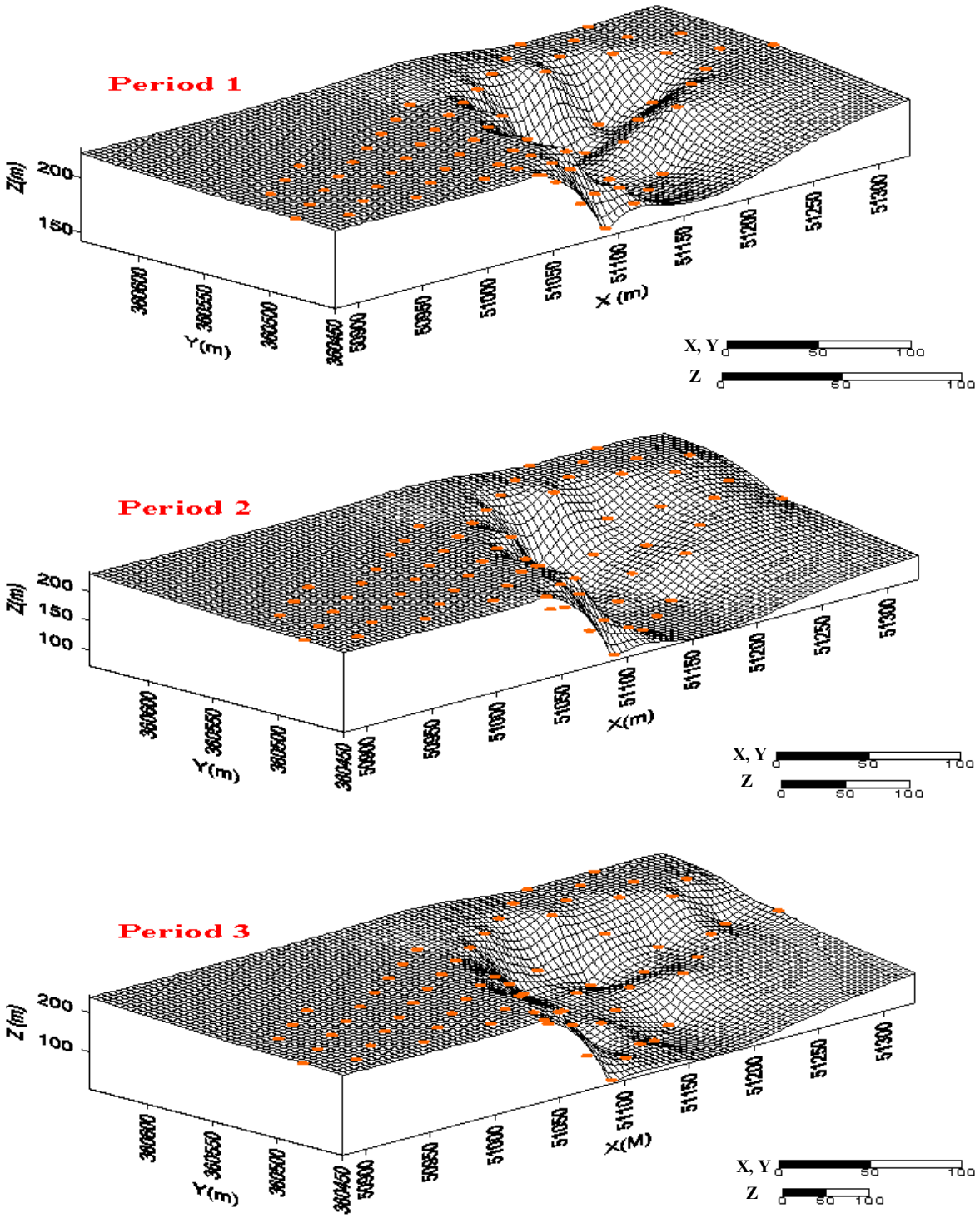

Fig. 10. Recovered drawpoints profile showing the end of the relevant period

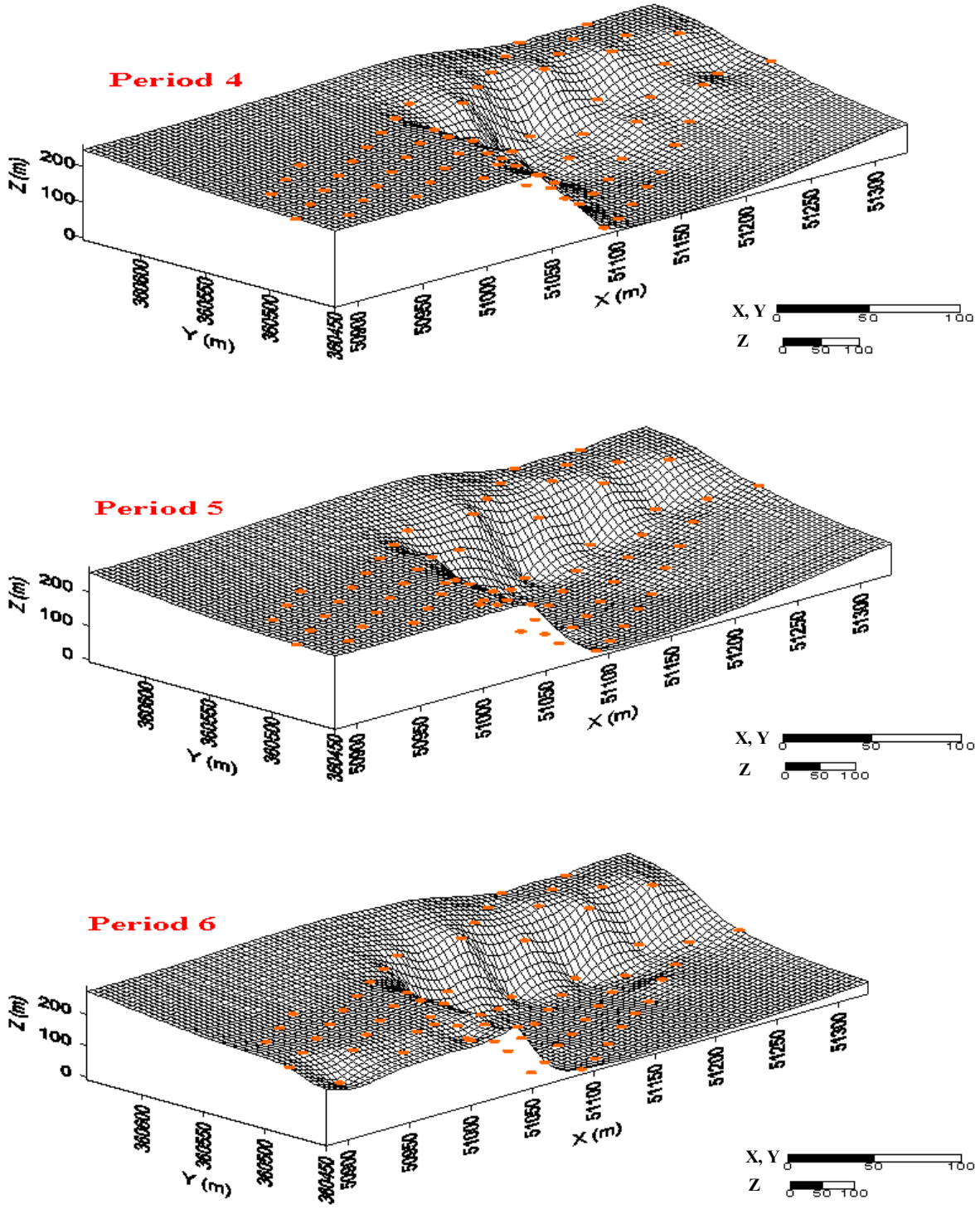

Fig. 10. Continued

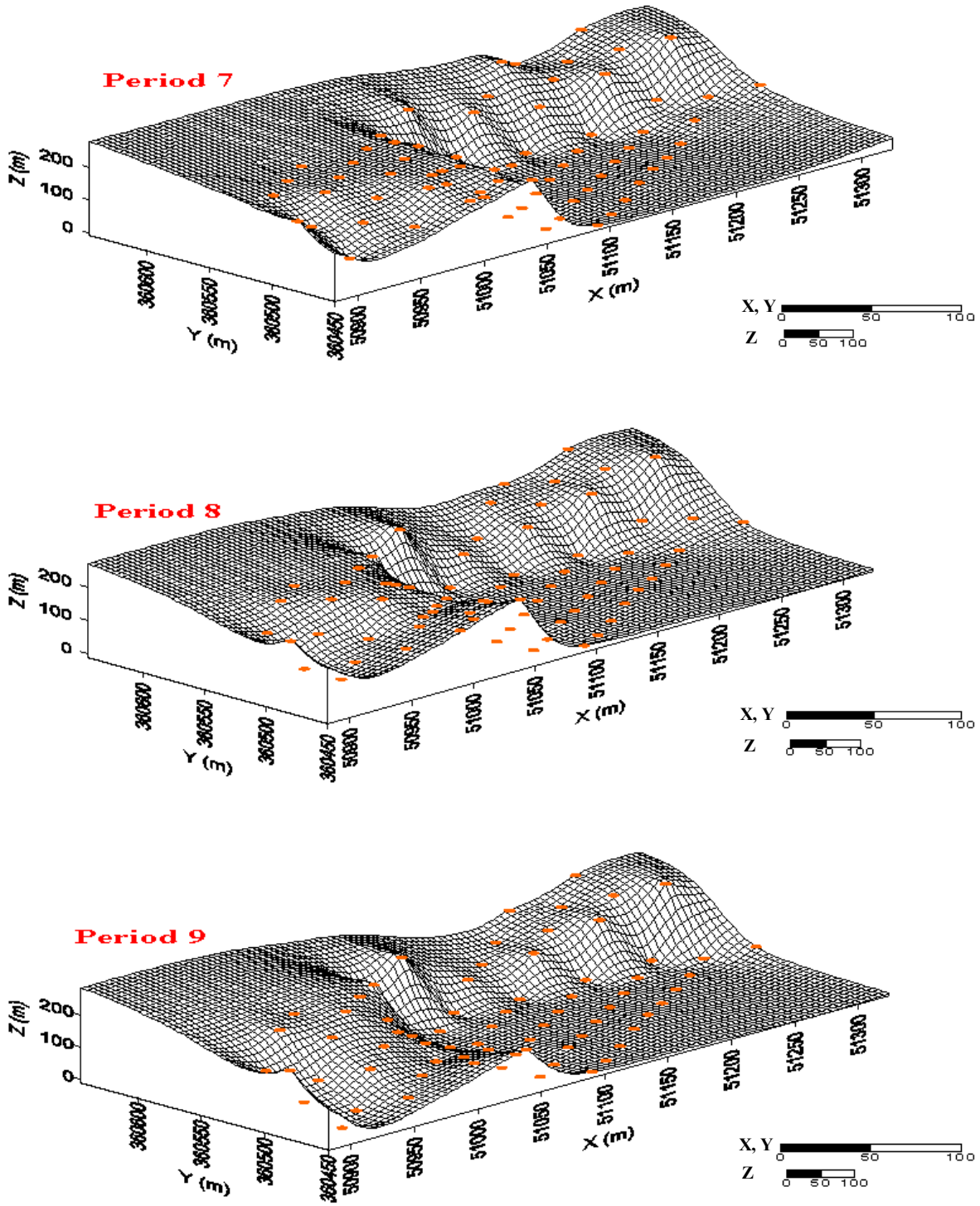

Fig. 10. Continued

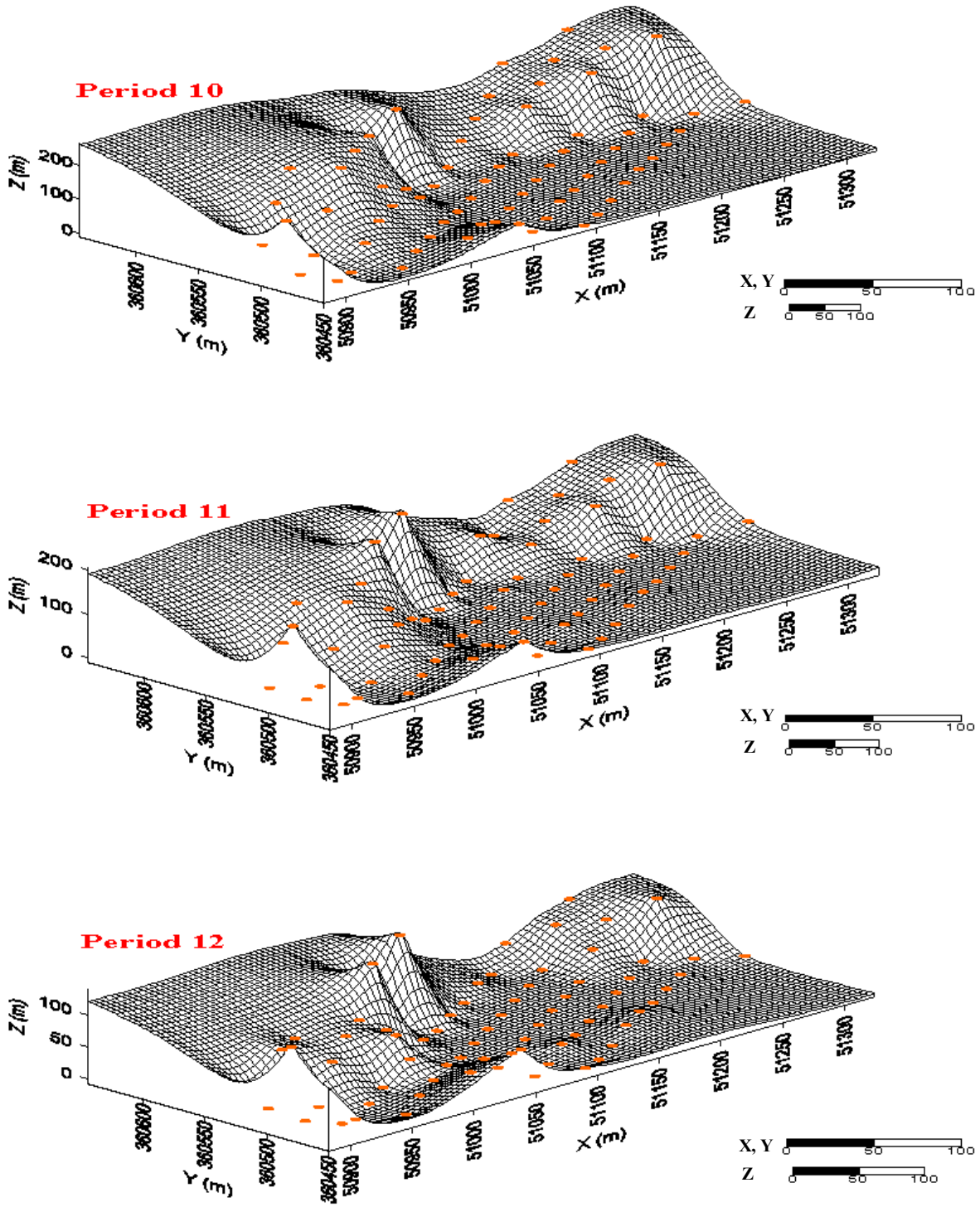

Fig. 10. Continued

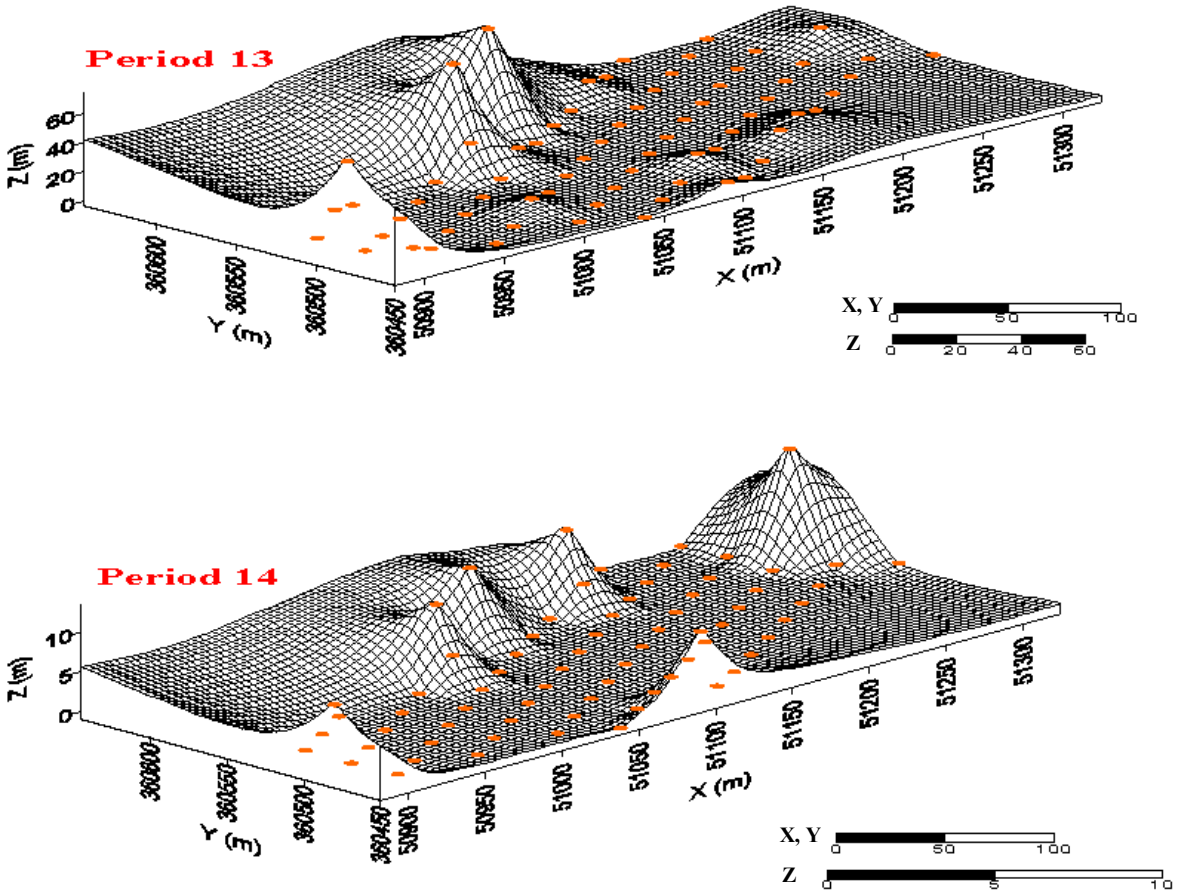

Fig. 10. Continued

7. Conclusion and future work

The paper presented an MILP formulation for block cave mines production scheduling. The formulation maximizes the NPV subject to several constraints such as draw rate, production target, grade blending, drawpoints precedence, and draw angle. We have implemented the optimization formulation in TOMLAB/CPLEX (Holmstrom, 1989-2009) environment. Further focused research is underway to add and test geomechanical constraints on the real data. There were several parameters such as grade that had been assumed to be constant; we will try to introduce probabilistic behavior of these parameters into the process of block cave mine planning.

8. References

[1] Ataee-Pour, M. (2005). A critical suvey of existing stope layout optimisation technique. *Journal of Mining Science*, *41*,(5), 447-466.

[2] Barlett, P. J. and Nesbitt, K. (2000). *Draw control at Premier diamond mine*, in Proceedings of Massmin 2000, Brisbane, pp. 227-232.

[3] Carew, t. (1992). *The casier mine case study*, in Proceedings of MassMin 1992, Johannesburg,

[4] Carlyle, W. M. and Eaves, B. C. (2001). Underground planning at Stillwater mining company. *INTERFACES*, *31*,(4), 50-60.

[5] Chanda, E. C. K. (1990). An application of integer programming and simulation to production planning for a stratiform ore body. *Mining Science and Technology*, *11*,(1), 165-172.

[6] Dewolf, V. (1981). Draw control in principle and practice at Henderson mine. in *Design and operation of caving and sublevel stoping mines*, D. R. Steward, Ed. New York, Society of Mining Engineers of AIME., pp. 729-735.

[7] Diering, T. (2000). *PC-BC: A block cave design and draw control system*, in Proceedings of MassMin 2000, The Australasian Institute of mining and Metallurgy: melburne, brisbane, pp. 301-335.

[8] Diering, T. (2004). *Computational considerations for production scheduling of block vave mines*, in Proceedings of MassMin 2004, Santiago, Chile, pp. 135-140.

[9] Guest, A., Van Hout, G. J., Von Johannides, A., and Scheepers, L. F. (2000). *An application of linear programming for block cave draw control*, in Proceedings of Massmin2000, The australian Institute of Mining and Metallurgy: Melbourne., Brisbane,

[10] Heslop, T. G. and Laubscher, D. H. (1981). Draw control in caving operations on Southern African Chrpsotile Asbestos mines. in *Design and operation of caving and sublevel stoping mines*, New York, Society of Mining Engineers of AIME., pp. 755-774.

[11] Holmstrom, K. (1989-2009). TOMLAB/CPLEX, ver. 11.2. Pullman, WA, USA: Tomlab Optimization

[12] Holmström, K. (1989-2009). TOMLAB /CPLEX - v11.2. Pullman, WA, USA: Tomlab Optimization.

[13] Horst, R. and Hoang, T. (1996). *Global optimization : deterministic approaches.* Springer, Berlin ; New York, 3rd ed, Pages xviii, 727 p.

[14] ILOG Inc. (2007). ILOG CPLEX 11.0 User's Manual September. 11.0 ed: ILOG S.A. and ILOG, Inc.

[15] Jawed, M. (1993). *Optimal production planning in underground coal mines through goal programming-A case stydy from an Indian mine*, in Proceedings of 24th international symposium, Application of computers in the mineral industry(APCOM), Montreal,Quebec, Canada, pp. 43-50.

[16] Julin, D. E. (1992). Block caving, Chap. 20.3. in *SME Mining Engineering Handbook*, H. L. Hartman, Ed. Littleton, Colo. : Society for Mining, Metallurgy, and Exploration, Inc., pp. 1815-1836.

[17] Kuchta, M., Newman, A., and Topal, E. (2004). Implementing a Production Schedule at LKAB 's Kiruna Mine. *Interfaces*, *34*,(2), 124-134.

[18] Laubscher, D. H. (1994). Cave mining - the state of the art. *Journal of The South African Institute of Mining and Metallurgy*, *94*,(10), 279-293.

[19] MathWorks Inc. (2007). MATLAB 7.4 (R2007a) Software. MathWorks, Inc.

[20] McIssac, G. (2005). Long term planning of an underground mine using mixed integer linear programming. in *CIM Bulletin*, vol. 98, pp. 89.

[21] Nehring, M. and Topal, E. (2007). *Production schedule optimisation in underground hard rock mining using mixed integer programming*, in Proceedings of Project Evaluation Conference 2007, June 19, 2007 - June 20, 2007, Australasian Institute of Mining and Metallurgy, Melbourne, VIC, Australia, pp. 169-175.

[22] Ovanic, J. (1998). Economic optimization of stope geometry. PhD Thesis, Michigan Technological University, Houghton, USA, Pages 209.

[23] Rahal, D., Smith, M., Van Hout, G. J., and Von Johannides, A. (2003). *The use of mixed integer linear programming for long-term scheduling in block caving mines*, in Proceedings of 31st International Symposium on the Application of Computers and operations Research in the Minerals Industries (APCOM), Cape Town, South Africa,

[24] Riddle, J. (1976). *A dynamic programming solution of a block caving mine layout.*, in Proceedings of 14th International Symposium on the Application of Computers in the Mineral Industry(APCOM), Pennsylvania,

[25] Rubio, E. (2002). Long-term planning of block caving operations using mathematical programming tools. MSc Thesis, Vancouver, Canada, Pages 116.

[26] Rubio, E. (2006). block cave mine infrastructure reliability applied to production planning.Thesis, British Columbia, Vancouver, Pages 132.

[27] Rubio, E., Caceres, C., and Scoble, M. (2004). *Towards an integrated approach to block cave planning*, in Proceedings of MassMin 2004, Santiago, Chile, pp. 128-134.

[28] Sarin, S. C. and West-Hansen, J. (2005). The long-term mine production scheduling problem. *IIE Transactions*, *37*,(2), 109-121.

[29] Tang, X., Xiong, G., and Li, X. (1993). *An integrated approach to underground gold mine planning and sheduling optimization*, in Proceedings of 24th international symposium on the Application of computers in the mineral industry(APCOM), Montreal, Quebec, Canada, pp. 148-154.

[30] Topal, E. (2008). Early start and late start algorithms to improve the solution time for long-term underground mine production scheduling. *Journal of The South African Institute of Mining and Metallurgy*, *108*,(2), 99-107.

[31] Topal, E., Kuchta, M., and Newman, A. (2003). *Extensions to an efficient optimization model for long-term production planning at LKAB's Kiruna Mine*, in Proceedings of APCOM 2003, Cape Town, South Africa, pp. 289-294.

[32] Trout, L. P. (1995). *Underground mine production scheduling using mixed integer programming*, in Proceedings of 25th international symposium, Application of computers in the mineral industry(APCOM), Brisbane, Australia, pp. 395-400.

[33] Williams, J., Smith, L., and Wells, M. (1972). *Planning of underground copper mining*, in Proceedings of 10th international symposium, Application of computers in the mineral industry(APCOM), Johannesburg, South Africa, pp. 251-254.

[34] Winkler, B. M. (1998). *Mine production scheduling using linear programming and virtual reality*, in Proceedings of 27th international symposium, Application of computers in the

mineral industry(APCOM), Royal school of mines, London, United Kingdom, pp. 663-673.

[35] Winston, W. L. (1995). *Introduction to mathematical programming : applications and algorithms.* Duxbury Press, Belmont, Ca., 2nd ed, Pages xv, 818, 39 p.

[36] Wolsey, L. A. (1998). *Integer programming.* J. Wiley, New York, Pages xviii, 264 p.

9. Appendix

MATLAB and TOMLAB/CPLEX documentation for block cave mines scheduling

Lagrangian relaxation of the MILP open pit production scheduling formulation

Mohammad Mahdi Badiozamani and Hooman Askari-Nasab
Mining Optimization Laboratory (MOL)
University of Alberta, Edmonton, Canada

Abstract

The optimization models for open pit mine planning have been developed in the literature under various assumptions. In a typical mathematical model, the number of variables directly relates to the number of blocks in the optimized final pit and the number of planning time periods. These variables are either integer, continuous, or a mixture of both types. However, most of the open pit mine block models consist of millions of blocks. In addition, a multi-period long-term planning time horizon over the mine-life should be considered for the optimal solution. As a result in almost all the cases, the real world problems have a large number of variables that makes the problem unsolvable with current in-hand optimization software or solvable with a very long solution time. In order to tackle such problems, two approaches are developed; (1) creating mining cuts, which reduces the number of variables by aggregating the blocks into larger clusters and reducing the problem size, and (2) defining Lagrange multipliers which decreases the number of constraints and provides an upper/lower bound for the problem. In this research, the focus is on the second group of methods, using Lagrange multipliers. The mixed integer linear programming (MILP) formulation that is presented by Askari-Nasab and Awuah-offei (2008) is considered as the basis for the mine production scheduling and is used to find the relaxed forms of the MILP. An algorithm, based on the sub-gradient method is developed to find the proper Lagrange multipliers. The algorithm is applied to a data set and the results are reported.

1. Introduction

Mine planning has been among the most dominant aspects of decision making in the mining industry. It is important, because the extraction of ore, using the expensive equipment and work force, especially in remote areas is very cost sensitive. On the other hand, the mine planning is considered as one of the branches of planning and scheduling literature that has been studied for some decades by the academia. This joint subject of interest has resulted in development of many related issues in the mining and operations research contexts and as a result, the problem is well modeled as an MILP since 1970s. The number of variables in such MILP models is directly related to the number of blocks and the number of time periods considered in planning. Since in real world problems, usually thousands of blocks are considered in the optimum pit and for long-term planning, multiple periods are taken into account, the problem has millions of variables, among them some integer and some continuous. This makes the problem NP-hard and non solvable with current in hand software or solvable, but with a very long solution time. In a brief review, the literature regarding the methodology used in finding the solution, can be classified into two main categories; (1) those based on the exact solutions, mainly relying on linear programming (LP) to find the exact optimal solution that in most cases take a very long solution time (cpu time), and (2) those based on the approximation of optimal solution, applying the heuristic and meta heuristic

algorithms to find the best solution. Using the heuristic approach, some quality solutions can be found in reasonable time, but the solutions are not necessarily optimal.

Most of researchers who have tried to find the MILP optimal solutions using exact methods have relaxed the binary nature of integer variables. For example, Tan and Romani (1992) consider the equipment capacity constraints and find the optimal extraction schedule over multiple periods, using both linear programming (LP) and dynamic programming (DP). Since they relax the integer nature of decision variables, the block sequencing constraints are not satisfied. Fytas *et al.* (1993) use different approaches for long-term and short-term decisions. They employ simulation to find those blocks that are extracted in long-term. At this stage, they consider the precedence constraints, as well as the minimum and maximum production and processing capacity constraints and the bounds on the grade of entering material to the processing plant. Then, they use LP for the short-term planning, subject to the same constraints of long-term, but they assume that the partial extraction of blocks is permitted. Finally, they propose an iterative approach to deliver a practical mining sequence.

As an example of meta heuristics application, Denby and Schofield (1994) use genetic algorithms to solve the large integer programs efficiently. They integrate two decision making problems together; determining the final open pit and extraction schedule. They consider schedules as a combination of final open pit and extraction schedule. They use a genetic algorithm, applying the concepts of mutations and crossover, to find the best schedule among mentioned combinations. Although they produce good solutions for small size problems, their algorithm does not work in reasonable time for large size problems.

Apart from meta heuristics, in order to reduce the problem size and make the large problems solvable using exact methods of operations research, some researchers have employed the idea of aggregating the blocks. The idea is to merge the blocks to create "*mining-cuts*" and hence, reduce the number of MILP variables. Askari-Nasab *et al.* (2010) propose a two stage algorithm to create mining-cuts. Their aim is to reduce the number of dependencies among the blocks/cuts in consecutive benches. They introduce a similarity index that is the basis for aggregation of neighboring blocks/cuts and continue the aggregation to reach to a predefined number of cuts in each bench (hierarchical clustering stage). Then they apply a Tabu Search algorithm to reduce the number of arcs, i.e. precedence relations, as much as possible by changing the borders of mining-cuts that are produced in previous stage (Tabu Search stage).

In 1980s, some researchers started to reduce the problem size, not by reducing the number of variables, but by relaxing some of the constraints. They used Lagrangian relaxation as an exact approach to find the optimal solution. The main idea in the Lagrangian relaxation approach is to relax some of the constraints and instead, add required penalty terms into the objective function. The constraints of the MILP can be classified into two categories: (1) hard constraints, those that define the precedence of blocks extraction and (2) soft constraints, including those constraints that are defined to satisfy the limited production and processing capacities and grade bounds for the material entering the processing plant. In most of the papers, the soft constraints are relaxed and corresponding terms are added into the objective function with a penalty multiplier. This relaxation arises another question: how much the objective function should be penalized if the corresponding constraint was not satisfied? In other words, what are the proper values for Lagrangian multipliers? Some algorithms are developed to find the answer to such question. Among them, one of non-heuristic algorithms is the sub-gradient method.

Dagdelen and Johnson (1986) use the Lagrangian relaxation to relax some of the constraints, e.g. constraints on the maximum production in each period, and placing such constraints with associated multipliers in the objective function. They apply the sub-gradient method to update the multipliers in some small examples. Their work is one of the first papers in the field of Lagrangian relaxation, using the sub-gradient method. Akaike and Dagdelen (1999) extend this work by

changing the value of the Lagrangian multipliers in an iterative procedure. The procedure continues until the relaxed problem reaches the optimal solutions that are feasible for the original problem.

Kawahata (2006) expands (Dagdelen and Johnson, 1986) work by defining a variable cut off grade that specifies the destination of extracted material, i.e. whether to go to the processing plant, to be stockpiled or to be dumped as waste. Then he uses two Lagrangian relaxation sub problems to find the bounds of the original problem; one for the most conservative case of mine sequencing and the other one for the most aggressive case. Since the solution for the relaxed problem is not necessarily feasible for the original problem, he adjusts some bounds on capacities to guarantee the feasibility of Lagrangian solution for the original problem.

Gaupp (2008) presents the MILP formulation for the open pit mine production planning problem. He proposes three approaches to make the MILP model tractable for large scale problems as (1) applying deterministic variable reduction techniques to eliminate some of the blocks, (2) producing cuts to strengthen the model formulation and (3) employing Lagrangian relaxation method using sub-gradient algorithm to reduce the problem size by eliminating some constraints. In Gaupp's (2008) proposed algorithm, to find the multiplier values corresponding to relaxed constraints, he develops a feasing routine to make the relaxed problem solution feasible for the original problem. However, Gaupp (2008) disregards the multi-element case in his model and solves the MILP model for a single element.

Newman *et al.* (2010) review those papers that have used operations research in mine planning. They specify that dynamic programming is not tractable for large size problems, while the Lagrangian approaches remain as a reliable method for solving large size problems. The Lagrangian methods also theoretically provide an optimal solution.
The structure of the paper is as follows; section 2 covers the problem definition and formulation. The theoretical framework that is the basis for the Lagrangian relaxation, in addition to the proposed algorithm is presented in section 3. A case study is described in section 4 and the results from implementation of the algorithm on the case are reported in section 5. Conclusions and future works are covered in section 6.

2. Problem definition

It is assumed that the optimal open pit has been determined previously and the block model is considered as the input to our algorithm. In addition, we use the 4th MILP model and the corresponding notation, presented by Askari-Nasab and Awuah-offei (2008) which is a long-term planning problem. In this model, it is assumed that the mining and processing are both at mining-cut level (not at block level), in order to reduce the problem size.
The notation of sets, indices, parameters and decision variables are as follows:

2.1. Sets

$\mathcal{K} = \{1,...,K\}$	set of all mining-cuts in the model.
$H(S)$	for each mining-cut c_k, there is a set $H(S) \subset \mathcal{K}$ defining the immediate predecessor cuts that must be extracted prior to extracting mining-cut k, where S is the total number of cuts in set $H(S)$.

2.2. Indices

A general parameter *f* can take three indices in the format of $f_k^{e,t}$, where:

$t \in \{1,\ldots,T\}$	index for scheduling periods.
$k \in \{1,\ldots,K\}$	index for mining-cuts.

$e \in \{1,\ldots,E\}$ index for elements of interest in each block/mining-cut.

2.3. Parameters

v_k^t the discounted revenue generated by selling the final product within mining-cut k in period t minus the extra discounted cost of mining all the material in block n as ore and processing it.

q_k^t the discounted cost of mining all the material in mining-cut k as waste.

g_k^e average grade of element e in ore portion of mining-cut k.

$gu^{e,t}$ upper bound on acceptable average head grade of element e in period t.

$gl^{e,t}$ lower bound on acceptable average head grade of element e in period t.

o_k ore tonnage in mining-cut k.

w_k waste tonnage in mining-cut k.

pu^t upper bound on processing capacity of ore in period t (tonnes).

pl^t lower bound on processing capacity of ore in period t (tonnes).

mu^t upper bound on mining capacity in period t (tonnes).

ml^t lower bound on mining capacity in period t (tonnes).

2.4. Decision Variables

$y_k^t \in [0,1]$ continuous variable, representing the portion of mining-cut c_k to be mined in period t, fraction of y characterizes both ore and waste included in the mining-cut.

$b_k^t \in \{0,1\}$ binary integer variable controlling the precedence of extraction of mining-cuts. b_k^t is equal to one if extraction of mining-cut c_k has started by or in period t, otherwise it is zero.

$s_k^t \in [0,1]$ continuous variable, representing the portion of mining-cut c_k to be extracted as ore and processed in period t.

2.5. Problem formulation

The original MILP problem, referred as the primal problem (P), is as follows:

(P):

$$\max \sum_{t=1}^{T}\sum_{k=1}^{K}(v_k^t \times s_k^t - q_k^t \times y_k^t) \quad (1)$$

Subject to:

$$gl^{t,e} \le \sum_{k=1}^{K} g_k^e \times o_k \times s_k^t \Big/ \sum_{k=1}^{K} o_k \times s_k^t \le gu^{t,e} \qquad \forall t \in \{1,...,T\}, \quad e \in \{1,...,E\} \tag{2}$$

$$pl^t \le \sum_{k=1}^{K} o_k \times s_k^t \le pu^t \qquad \forall t \in \{1,...,T\}, \quad e \in \{1,...,E\} \tag{3}$$

$$ml^t \le \sum_{k=1}^{K} (o_k + w_k) \times y_k^t \le mu^t \qquad \forall t \in \{1,...,T\} \tag{4}$$

$$s_k^t \le y_k^t \qquad \forall k \in \{1,...,K\}, \quad t \in \{1,...,T\} \tag{5}$$

$$b_k^t - \sum_{i=1}^{t} y_s^i \le 0 \qquad \forall k \in \{1,...,K\}, \quad t \in \{1,...,T\}, \quad s \in H(S) \tag{6}$$

$$\sum_{i=1}^{t} y_k^i - b_k^t \le 0 \qquad \forall k \in \{1,...,K\}, \quad t \in \{1,...,T\} \tag{7}$$

$$b_k^t - b_k^{t+1} \le 0 \qquad \forall k \in \{1,...,K\}, \quad t \in \{1,...,T-1\} \tag{8}$$

Eq. (1) presents the objective function, which is the maximization of the profit, i.e. the difference between discounted revenue and cost. Eqs. (2) to (4) control the grade blending, processing capacity, and mining capacity. Eq. (5) represents inequalities that ensure the amount of ore that is sent to the processing plant is less than or equal to the total amount of mined material. For each mining-cut k, Eqs. (6) to (8) check the set of immediate predecessor cuts that must be extracted prior to extracting mining-cut k. Fig. 1 illustrates the set $H(S) = \{B, C\}$, the predecessor mining-cuts that must be extracted prior to extraction of mining-cut A.

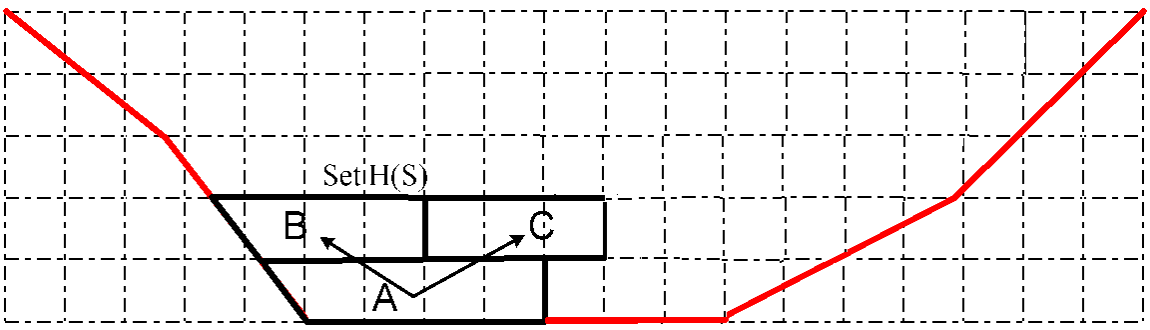

Fig. 1. Precedence of extraction in proposed MILP model.

According to Lagrangian relaxation approach, some of the constraints should be relaxed and placed in the objective function, with proper Lagrangian multipliers as the penalty for violation of relaxed constraints. The multipliers in our notation are called *lambda*, taking three indices in the format of $\lambda_n^{e,t}$ where:

$t \in \{1,....,T\}$ index for scheduling periods.

$n \in \{1,...,6\}$ index for the relaxed constraint's type.

$e \in \{1,...,E\}$ index for elements of interest in each mining-cut.

Here, we just study the relaxation of some or all of the soft constraints. As mentioned previously, soft constraints are the maximum and minimum of production capacity, processing capacity and acceptable average head grade of material entering into the processing plant in each period. This combination results in six constraint types, so $n \in \{1,...,6\}$. We have left the hard constraints, which control the precedence relationship between mining-cuts, to guarantee that the optimal solution of the relaxed problem does not violate the precedence constraints.

The six soft constraints generate 63 different relaxation combinations for the relaxed problem, in each one, just one or some of constraints out of six are relaxed. Only seven important combinations are considered as follows:

(D1) Dual problem; all soft constraints (grade, mining and processing) are relaxed.

(D2) Dual problem; grade and mining constraints are relaxed.

(D3) Dual problem; processing and mining constraints are relaxed.

(D4) Dual problem; processing and grade constraints are relaxed.

(D5) Dual problem; mining constraints are relaxed.

(D6) Dual problem; processing constraints are relaxed.

(D7) Dual problem; grade constraints are relaxed.

The first Dual MILP problem, named as (D1) is as follows:

(D1):

$$\begin{aligned}
&\max \sum_{t=1}^{T}\sum_{k=1}^{K}\left(\sum_{n\in c_k} v_k^t \times s_n^t - q_k^t \times y_k^t\right) \\
&+\sum_{t=1}^{T}\lambda_1^{e,t}(gu^{t,e}\sum_{k=1}^{K}o_k\times s_k^t - \sum_{k=1}^{K}g_k^e\times o_k\times s_k^t) + \sum_{t=1}^{T}\lambda_2^{e,t}(\sum_{k=1}^{K}g_k^e\times o_k\times s_k^t - gl^{t,e}\sum_{k=1}^{K}o_k\times s_k^t) \\
&+\sum_{t=1}^{T}\lambda_3^{t}(pu^t - \sum_{k=1}^{K}o_k\times s_k^t) + \sum_{t=1}^{T}\lambda_4^{t}(\sum_{k=1}^{K}o_k\times s_k^t - pl^t) \\
&+\sum_{t=1}^{T}\lambda_5^{t}(mu^t - \sum_{k=1}^{K}(o_k+w_k)\times y_k^t) + \sum_{t=1}^{T}\lambda_6^{t}(\sum_{k=1}^{K}(o_k+w_k)\times y_k^t - ml^t)
\end{aligned} \tag{9}$$

Subject to:

$$s_k^t \le y_k^t \qquad \forall k \in \{1,...,K\},\quad t \in \{1,...,T\} \tag{10}$$

$$b_k^t - \sum_{i=1}^{t} y_s^i \le 0 \qquad \forall k \in \{1,...,K\},\quad t \in \{1,...,T\},\quad s \in H(S) \tag{11}$$

$$\sum_{i=1}^{t} y_k^i - b_k^t \le 0 \qquad \forall k \in \{1,...,K\},\quad t \in \{1,...,T\} \tag{12}$$

$$b_k^t - b_k^{t+1} \le 0 \qquad \forall k \in \{1,...,K\},\quad t \in \{1,...,T-1\} \tag{13}$$

Since the (P) is a maximization problem, any feasible solution for the (P) is considered as a lower bound (LB) for the optimal objective function of (P). On the other hand, since we have relaxed some constraint in the formulation of (D), the optimal solution for the (D) should be considered as an upper bound (UB) for the optimal objective function of (P).

The main question is how to find the Lagrangian multipliers, $\lambda_n^{e,t}$, in a way that the corresponding UB and LB lay in a predefined desired gap interval, where gap is defined as the difference between UB and LB as (UB-LB)/UB

3. Theoretical framework and methodology

Let us assume a maximization problem with some constraints. We name this original problem as the *primal* problem. In addition, suppose that the constraints have made the primal problem so complicated that it takes a long run time to find the optimal solution. One practical way to tackle the complexity of the problem is to relax some of the constraints and consider the relaxed version of the primal problem as the *dual* problem. Since the feasible space corresponding to the dual problem is larger than the feasible space of the primal problem, the optimal solution to the dual problem always equals, or is greater than the optimal solution to the primal problem. In other words, the dual optimal solution is always considered as an upper bound to the primal optimal solution.

On the other hand, suppose that we manage to find just a feasible solution to the primal problem. Since by definition, the optimal solution to any maximization problem is greater than, or equal to any point in the feasible space of the problem, any feasible solution is considered as a lower bound to the optimal solution of the primal problem. The idea of upper bound and lower bound works for any minimization problem as well; the only difference is that any feasible solution to the primal problem is considered as an upper bound, while any optimal solution to the relaxed problem is considered as a lower bound for the optimal solution of the primal problem. This concept is illustrated in Fig. 2 for a maximization problem.

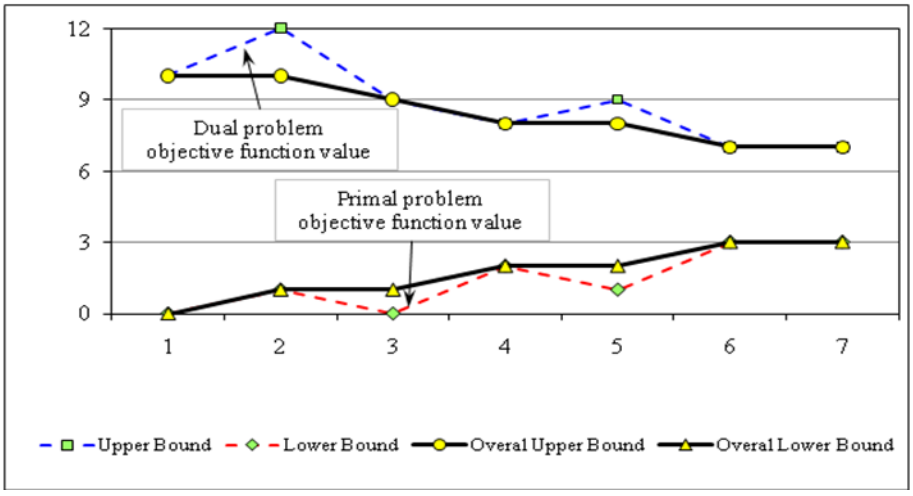

Fig. 2. Bounds for a typical maximization problem.

In Lagrangian relaxation, one or a number of constraints are relaxed to reduce the complexity of the primal problem. In return, in order to avoid the violations from relaxed constraints, proper penalty terms are added up to the objective function to penalize any violation from the corresponding constraints. For any penalty term, a penalty multiplier also called the Lagrangian multiplier, is considered and multiplied to the penalty term. One of the most well known and typical approaches used to find the multiplier values is the sub-gradient method. In the next section, a generic sub-gradient algorithm is briefly discussed.

3.1. The sub-gradient method

Fisher (1985) provides an application oriented guide to Lagrangian relaxation. He presents the following notation and formulation for typical primal and dual problems and the sub-gradient method.

The integer programming problem, called the primal is formulated as:

$$Z = \max cx \tag{14}$$

Subject to:

$$\begin{aligned} &Ax \le b \\ &Dx \le e \\ &x \ge 0, \text{int} \end{aligned} \tag{15}$$

Where x is $n \times 1$, b is $m \times 1$, e is $k \times 1$ and all other matrices have conformable dimensions. In this formulation, the constraints are partitioned into two sets, $Ax \le b$ and $Dx \le e$. It is assumed that it is easy to solve the primal problem, if the set of constraints $Ax \le b$ are relaxed. This relaxation produces the dual problem $LR_u^{\,k}$, using an *m* vector of non-negative multipliers *u,* as:

$$Z_D(u) = \max cx + u(b - Ax) \tag{16}$$

Subject to:

$$\begin{aligned} &Dx \le e \\ &x \ge 0, \text{int} \end{aligned} \tag{17}$$

Since the dual problem provides an upper bound for the primal maximization problem, ideally the vector *u* should be found in a way that $Z_D(u)$ be minimized;

$$Z_D = \min Z_D(u) \tag{18}$$

Eq. (18) is considered as the basis of the sub-gradient method. The goal is to find the proper set of Lagrangian multipliers that minimizes $Z_D(u)$. Multiplier values are updated, considering the initial value of u^0 and according to Eq. (19).

$$u^{k+1} = \max\{0, u^k - t_k(b - Ax^k)\} \tag{19}$$

Where x^k is the optimal solution to $LR_u^{\,k}$, the Lagrangian problem with dual variables set to u^k, and t_k is a scalar step size value. According to (Fisher, 1985), a formula for t_k that has been proven to be effective in practice is given by Eq. (20).

$$t_k = \frac{\lambda_k (Z_D(u^k) - Z^*)}{\sum_{i=1}^{m} (b_i - \sum_{j=1}^{n} a_{ij} x_j^{\,k})^2} \tag{20}$$

In this formula, Z^* is the objective value of the best known feasible solution to (P) and λ_k is a scalar chosen between 0 and 2. Frequently, the sequence λ_k is determined by starting with $\lambda_k = 2$

and reducing it by a factor of two whenever $Z_D(u^k)$ has failed to decrease in a specific number of iterations.

3.2. Proposed algorithm

The following algorithm is developed for implementation of the sub-gradient method to find Lagrangian multipliers for a minimization case (the objective function id multiplied by -1):

Step 1: Assign initial values for multipliers (u^0).

Step 2: Assign a (P) feasible solution as UB and a (D) optimal solution as LB.

Step 3: Update multipliers and solve (D).

Step 4: If (D) solution results in a better LB, update LB.

Step 5: If (D) solution is feasible for (P) and results in a better UB, update UB. Otherwise, do the feasing sub-routine and repeat step 5 if possible.

Step 6: If the stopping criteria are true, stop and report u^k and UB-LB gap, otherwise, go to step 3.

The flowchart of the proposed algorithm is illustrated in Fig. 3.

Since the solutions of (D), corresponding to different sets of multipliers are not necessarily feasible for (P), in most cases the UB remains unchanged, meaning that no feasible solution is found for the (P) with a better UB. This may cause the algorithm to gain no benefit from a large number of iterations. In some cases, making few changes to the (D) solution makes it feasible for (P). To do so, whenever the dual's solution is not feasible for the primal problem, the feasing sub-routine is called. However, it may happen that even after several attempts to make a solution feasible for the primal problem, the constraints still are violated and so, that specific iteration ends without any feasible solution.

Feasing sub-routine is as follows:

Step 1: sort the objective function coefficients and corresponding variable values in descending order and identify the relaxed constraint.

Step 2: select the m first ($F_i, i=1,...,m$) and n last ($L_j, j=1,...,n$) variables from the sorted list that have relaxed constraint multiplier.

Step 3: find the maximum possible change increments for each of $m+n$ variables as:

$h(F_i) = F_i / h$ and $h(L_j) = (1-L_j) / h$, where h is the change increment.

Step 4: Update $m+n$ variable values by one increment, i.e. $F_{i(revised)} = F_i - h$ and $L_{j(revised)} = L_j + h$

Step 5: Check the feasibility of revised solution. If it is feasible, send it to the main algorithm, otherwise change variable values by one more increment (if possible) and go to step 4.

The flowchart for the feasing sub-routine is illustrated in Fig. 4.

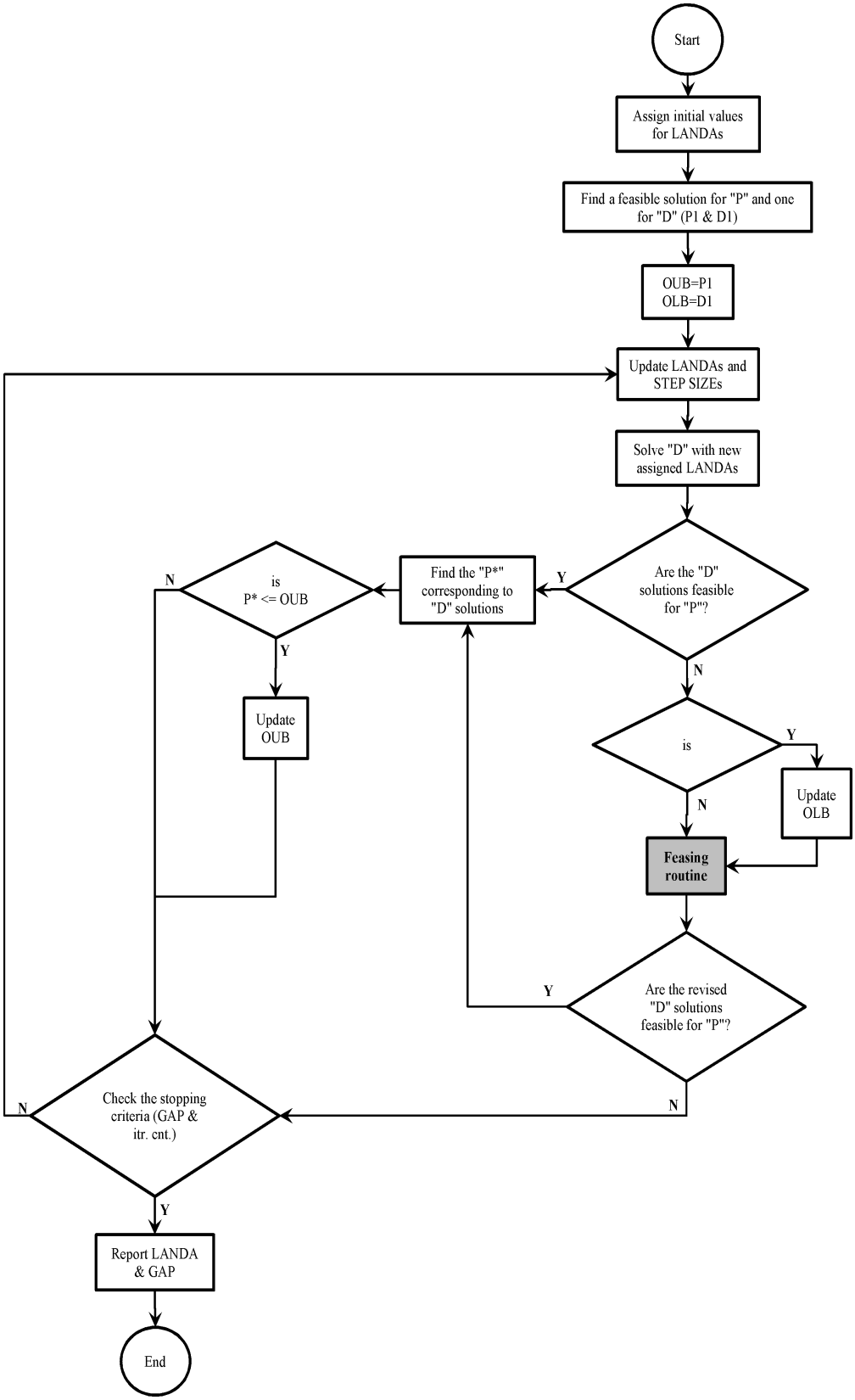

Fig. 3. Sub-gradient algorithm flowchart.

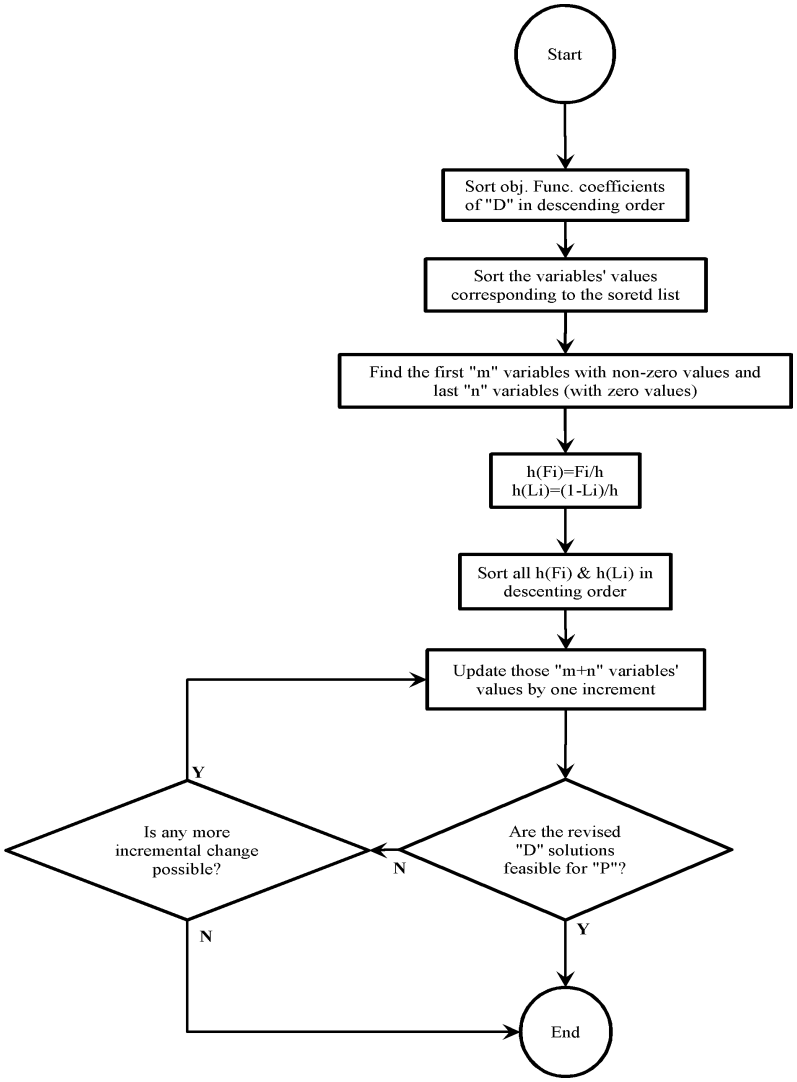

Fig. 4. Proposed feasing sub-routine flowchart.

4. Case study

To implement the proposed algorithm, a block model data set, containing 2598 blocks (aggregated into 148 miming-cuts) is considered. The mining-cuts are defined in seven mining benches. Some important specifications of the input data are presented in Table 1.

Table 1. Case study specifications.

number of blocks:	2598	max & min of mining capacity (10^6 tons):	(0.0,13.2)
number of mining-cuts:	148	max & min of processing capacity (10^6 tons):	(0.0,7.15)
interest rate:	0.1	max & min of acceptable grade for Iron ore (%):	(0.65,0.80)
number of elements:	3	max & min of acceptable grade for Sulfur (%):	(0.0,0.018)
Planning for:	12 periods	max & min of acceptable grade for Phosphor (%):	(0.0,0.014)

The algorithm is executed for 50 iterations. The detailed input parameters to the sub-gradient algorithm and the feasing sub-routine are presented in Table 2.

Table 2. Input parameters to the sub-gradient algorithm and feasing sub-routine.

Stopping criteria	UB/LB convergence: % 0.01
	maximum iterations: 50
Dual type	D5 (mining capacity constraints are relaxed)
initial multiplier values	1
initial scalar value	2 (used in step size formula)
m / n / h	500 / 500 / 0.05 (used in feasing)

5. Results and discussion

To execute the algorithm for the presented case study, a MATLAB program (MathworkInc., 2009) is developed. The code calls the TOMLAB/CPLEX (ILOGInc., 2007) in each iteration to solve the relaxed MILP problem. Fig. 5 to Fig. 8 Show two cross sections and two plan views of the resulting extraction sequence, corresponding to the relaxed problem in the last iteration. The units in figures are in meter and the size of each block is 15 by 25 by 50 cubed meters.

Fig. 5. Sample cross section, looking East. Each block 15m.

Fig. 6. Sample cross section, looking North, Each block 15m.

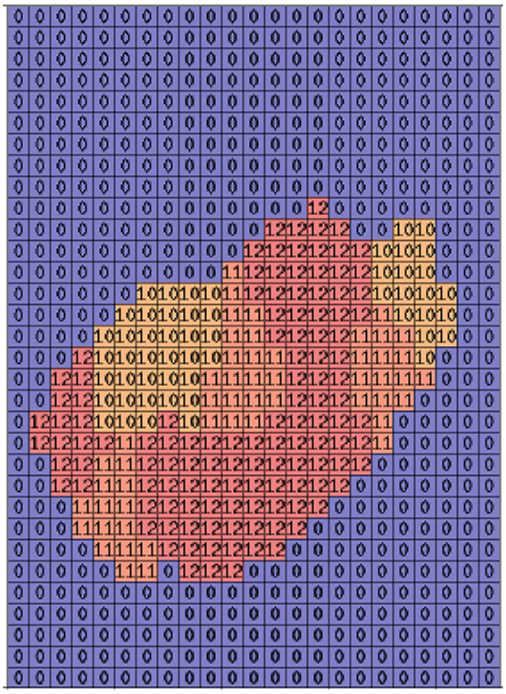

Fig. 7. Sample plan view, 1st bench.

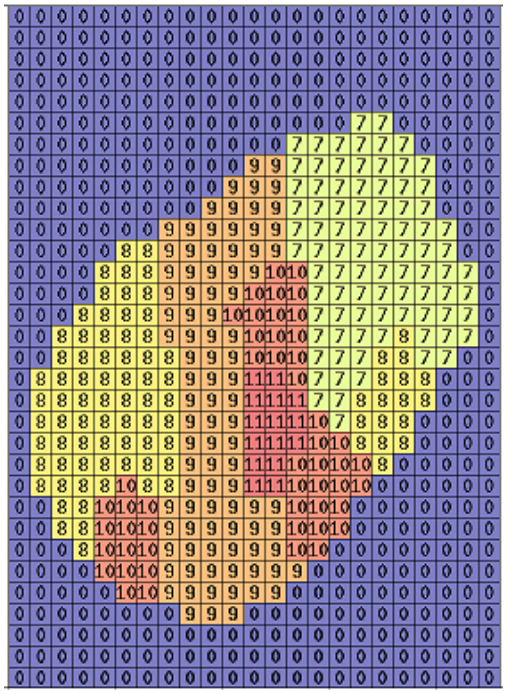

Fig. 8. Sample plan view, 3rd bench.

The extraction sequences in each iteration result in a specific amount of rock to be mined in each period and a specific amount of ore to be entered into the processing plant. Fig. 9 to Fig. 12 show the results, corresponding to four iterations. In these figures, the yellow and green lines represent the maximum processing and mining capacities, respectively. The run time for 50 iterations of algorithm on a machine with 3.00 GB of RAM and 2.40 GHz CPU is 675 seconds.

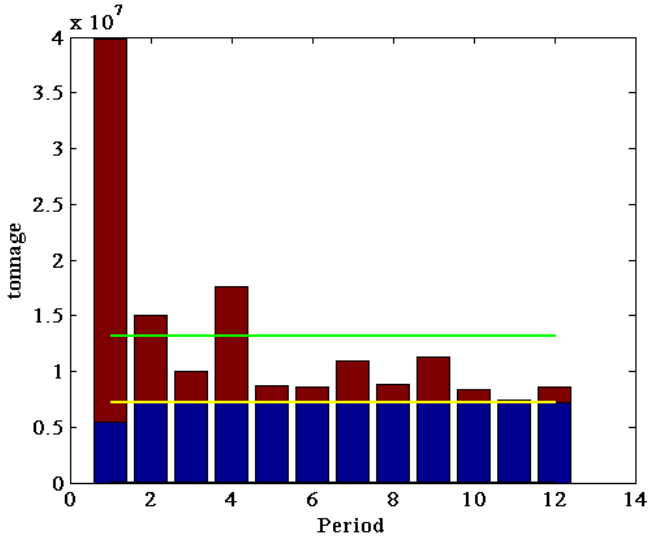

Fig. 9. Total mined and processed material, iteration 1.

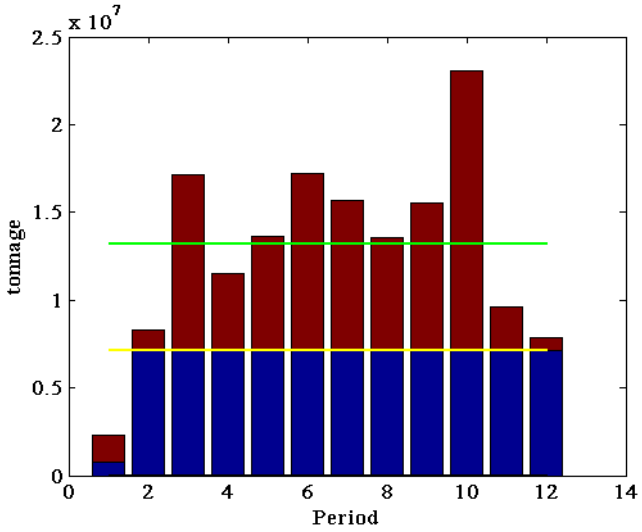

Fig. 10. Total mined and processed material, iteration 10.

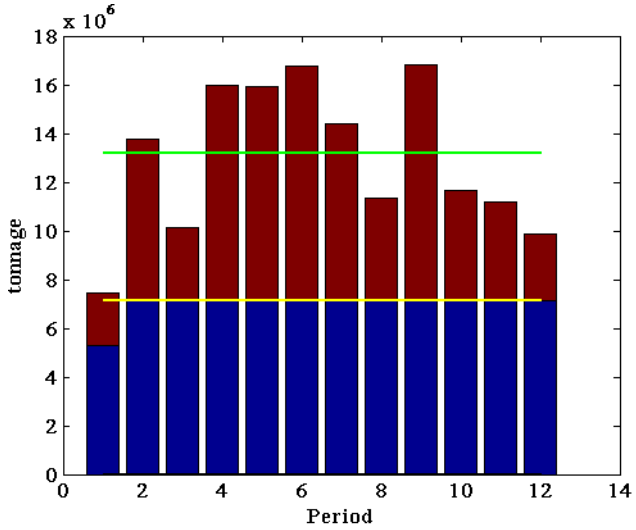

Fig. 11. Total mined and processed material, iteration 30.

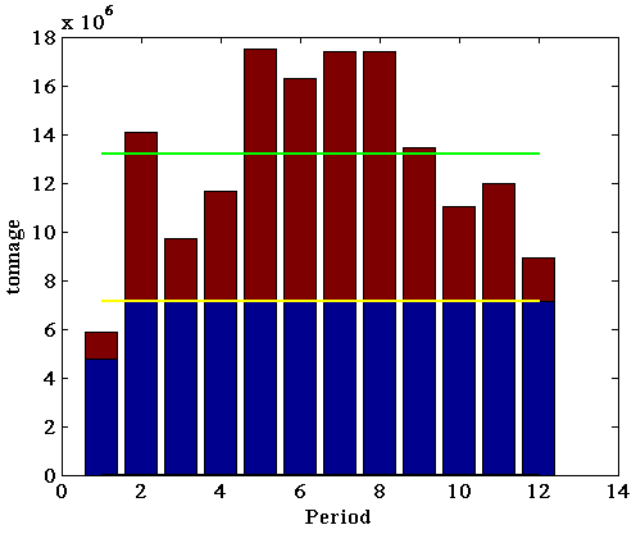

Fig. 12. Total mined and processed material, iteration 50.

Since only mining capacity constraints are relaxed in the studied case, these constraints are not satisfied, but the processing capacity constraints in all periods are satisfied and the solution has produced a uniform ore feed to the processing plant. The lower and upper bounds in each iteration, in addition to the overall lower and upper bound trends of the objective function value are illustrated in Fig. 13. Since the MILP is switched to a minimization problem by multiplying the objective function by -1, the objective function values are negative. The blue and green lines show the lower bound and upper bounds corresponding to each iteration, respectively. The red line represents the overall lower bound trend over all 50 iterations which is an increasing function.

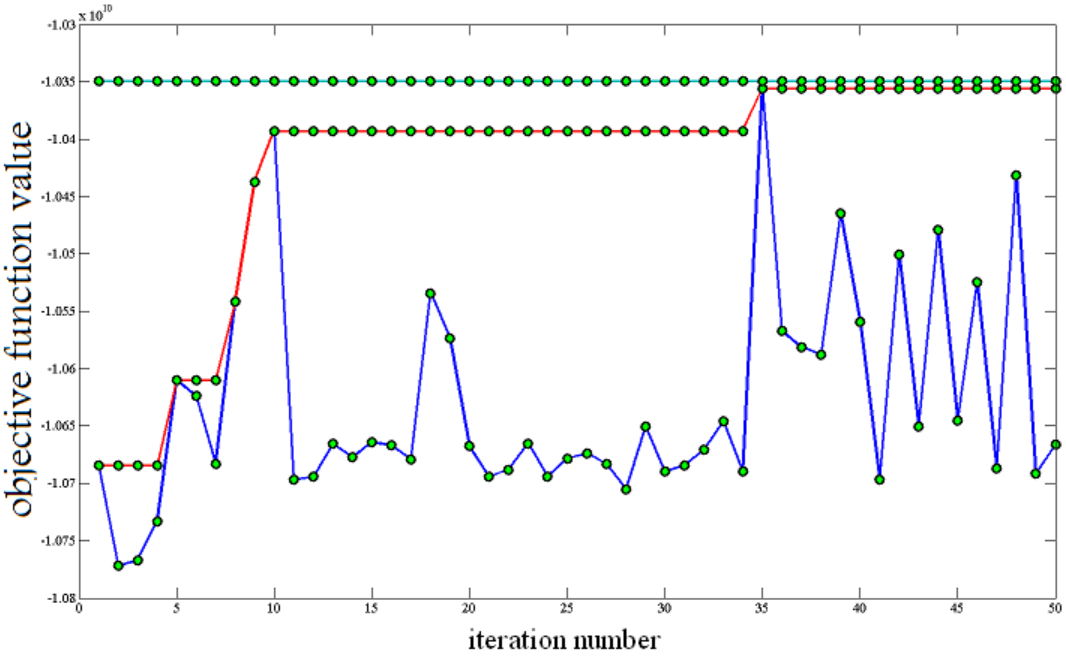

Fig. 13. Upper bound vs. lower bound.

After running the algorithm for 50 iterations, the gap between the lower and upper bounds is reached to 6.4×10^{-4}, showing a good convergence of the algorithm.
In this case, the upper bound of the problem (represented by the green line) has remained unchanged. It means either none of the dual solutions have been feasible for the primal problem, or none of those feasible solutions have been better than the first feasible solution to the primal problem and thus, could not update the upper bound.

6. Conclusions and future work

Lagrangian relaxation method is considered as a successful approach in dealing with huge and complicated LP and MILP problems. One of the well known algorithms which over the years have been used to find the Lagrangian multipliers is the sub-gradient algorithm. However in most cases, optimal solution to the relaxed (dual) problem is not feasible for the original (primal) problem. This infeasibility forces the algorithm developers to consider some additional steps (feasing) to make the solution feasible for the primal problem. In this research, we developed a heuristic feasing routine to overcome the infeasibility of solutions. Although in our studied cases, the resulting gap between the upper and lower bounds became relatively too small, but our proposed feasing routine did not overcome the infeasibility of the dual solution. Therefore, the upper bound has remained unchanged. As a future direction, it is recommended to focus on revised and more intelligent feasing heuristics.

7. References

[1] Akaike, A. and Dagdelen, K. (1999). *A strategic production scheduling method for an open pit mine*. Paper presented at 28rd Application of Computers and Operations Research in the Mineral Industries (APCOM) symposium, Littleton, Co. pp. 729-738.

[2] Askari-Nasab, H. and Awuah-offei, K. (2008). Mixed integer linear programming formulations for open-pit production scheduling. vol. 1. Edmonton, Alberta, Canada: Mining Optimization Laboratory (MOL), pp. 6-36.

[3] Askari-Nasab, H., Tabesh, M., and Badiozamani, M. M. (2010). *Creating mining cuts using hierarchical clustering and tabu search algorithms*. Paper presented at International Conference on Mining Innovation (MININ), Santiago, Chile. pp. 159-171.

[4] Dagdelen, K. and Johnson, T. (1986). *Optimum open pit mine production scheduling by Lagrangian parameterization*. Paper presented at 19th Application of Computers and Operations Research in the Mineral Industries (APCOM) symposium, Littleton, Co. pp. 127-141.

[5] Denby, B. and Schofield, D. (1994). Open pit design and scheduling by use of genetic algorithms. *Mining Technology: IMM Trans.*, Section A103, A21-A26.

[6] Fisher, M. (1985). An application oriented guide to Lagrangian relaxation. *Interfaces*, *15*,(2), 10-21.

[7] Fytas, K., Hadjigeorgiou, J., and Collins, J. L. (1993). Production scheduling optimization in open pit mines. *International journal of surface mining, reclemation and environment*, *7*,(1), 1-9.

[8] Gaupp, M. P. (2008). Methods for improving the tractability of the block sequencing problem for open pit mining.Thesis, Colorado School of Mines, Golden, Pages 150.

[9] ILOGInc. (2007). ILOG CPLEX. Ver. 11.0.

[10] Kawahata, K. (2006). A new algorithm to solve large scale mine production scheduling problems by using the Lagrangian relaxation method.Thesis, Colorado School of Mine, Golden.

[11] MathworkInc. (2009). MATLAB Software. Ver. 7.9 (R2009b).

[12] Newman, A. M., Rubio, E., Caro, R., Weintraub, A., and Eurek, K. (2010). A review of operations research in mine planning. *Interfaces*, *40*,(3), 222-245.

[13] Tan, S. and Romani, R. (1992). *Optimization models for scheduling ore and waste production in open pit mines*. Paper presented at 23rd Application of Computers and Operations Research in the Mineral Industries (APCOM) symposium, Littleton, CO. pp. 781-791.

8. Appendix

MATLAB and TOMLAB/CPLEX codes and documentation for the proposed algorithm.

The code runs the algorithm and produces the required graphs.

Production scheduling with minimum mining width constraints using mathematical programming

Yashar Pourrahimian and Hooman Askari-Nasab
Mining Optimization Laboratory (MOL)
University of Alberta, Edmonton, Canada

Abstract

The successful implementation of branch and cut algorithms for combinatorial optimization problems in mathematical optimizers has reduced the gap between theory and practice in optimization of large-scale industrial problems. Mixed integer linear programming (MILP) methods are used for optimizing production planning in open pit mines with an objective function of maximizing the net present value. Mine production schedules generated by MILP formulations occasionally create a scattered block extraction order that cannot be implemented in practice. In this paper, two alternative MILP production scheduling formulations are presented with minimum mining width integrated into the models as linear constraints. The proposed MILP formulations are implemented and tested in a TOMLAB/CPLEX optimization solver. The results show that the new formulations prevent scattering of the excavation sequence in a given scheduling period and have an acceptable computing time.

1. Introduction

Open pit mine production scheduling can be defined as specifying the sequence in which "blocks" should be removed from the mine in order to maximize the total discounted profit from the mine subject to a variety of physical and economic constraints. Typically, the constraints relate to the mining extraction sequence; mining, milling and refining capacities; mill head grades; and various operational requirements such as minimum pit bottom width. Various methods have been used for optimization of mining problems (Ramazan et al., 2003; Ramazan et al., 2004a; Ramazan et al., 2004b; Caccetta, 2007). Some examples include: linear programming and mixed integer linear programming (Caccetta et al., 2003; Ramazan et al., 2003; Ramazan et al., 2004a; Ramazan et al., 2004b), dynamic programming (Tolwinsky et al., 1996), graph and network theory (Fan et al., 2003), simulation (Dimitrakopoulos, 1998) and artificial intelligence (Denby et al., 1994; Denby et al., 1996; Tolwinsky et al., 1996; Askari-Nasab et al., 2008; Askari-Nasab et al., 2009). Among these optimization techniques, mixed integer linear programming is recognized as having significant potential to optimize production plans in large open pit mines with the objective of maximizing the total net present value.

In this paper, we will present two mixed integer linear programming (MILP) production scheduling formulations with minimum mining width integrated into the models as linear constraints.

2. MILP production scheduling formulations

2.1. Parameters

The parameters used in the mine production scheduling are listed in Table 1.

Table 1. MILP production scheduling parameters

Parameter	Description
BEV_n^t	block economic value of block n in period t
T	maximum number of scheduling periods
N	number of blocks to be scheduled
K	number of mining cuts to be scheduled
i	interest rate
X_n^t	binary integer variable controlling the sequence of extraction of blocks, equal to 1 if block n is to be mined in period t, otherwise 0
gu^t	upper bound on acceptable average head grade of ore send to the mill in period t
gl^t	lower bound on acceptable average head grade of ore send to the mill in period t
g_n	average ore grade of block n
g_k	average ore grade in mining cut k
Ot_n	ore tonnage in block n
Ot_k	ore tonnage in mining cut k
W_n	tonnage of waste material in block n
W_k	tonnage of waste material in mining cut k
$(PC_{\max})^t$	upper bound on ore processing capacity in period t
$(PC_{\min})^t$	lower bound on ore processing capacity in period t
$(MC_{\max})^t$	upper bound on ore processing capacity in period t
$(MC_{\min})^t$	lower bound on ore processing capacity in period t
Wb	working block
m	number of the blocks forced to be mined with working block (8 or 24)
v_k^t	discounted revenue generated by selling the final product within mining cut k in period t minus the extra discounted cost of mining all the material in mining cut k as ore and processing it
s_k^t	continuous variable, representing portion of mining cut c_k to be extracted as ore and processed in period t
q_n^t	discounted cost of mining all the material in block n as waste
y_k^t	continuous variable, representing portion of mining cut c_k to be mined in period t
b_k^t	binary integer variable controlling precedence of extraction of mining cuts

Each linear programming model includes an objective function and constraints. The open pit mine production schedule can be defined as specifying the sequence in which blocks should be removed from the mine to maximize the total discounted economic value, or the net present value (NPV)

from the mine, subject to a variety of physical and economic constraints. The first model is a modification of the approach used by Ramazan et al.(2004b); in this model, equipment access and mobility have been added. The second model (Askari-Nasab et al., 2009) is developed based on a combination of concepts from Caccetta et al. (2003) and Boland et al. (2009). In this model, mining and processing are both at mining-cut level. The blocks are clustered prior to schedule optimization and the ore processing and mining are controlled by two continuous variables. Blocks within the mining bench are grouped into clusters based on their attributes, spatial location, rock type, and grade distribution. Similar to blocks, each mining cut has coordinates representing the centre of the cut and its spatial location.

2.2. Model I

Objective function of model I is:

$$\text{Maximize} \quad \sum_{t=1}^{T}\sum_{n=1}^{N}\frac{BEV_n^t}{(1+i)^t}\times X_n^t \tag{1}$$

This objective function is subject to the following constraints:

$$\sum_{n=1}^{N}(g_n - gu^t)\times Ot_n \times X_n^t \le 0 \qquad \forall t \in \{1,...,T\} \tag{2}$$

$$\sum_{n=1}^{N}(g_n - gl^t)\times Ot_n \times X_n^t \ge 0 \qquad \forall t \in \{1,...,T\} \tag{3}$$

$$(PC_{\min})^t \le \sum_{n=1}^{N}(Ot_n \times X_n^t) \le (PC_{\max})^t \qquad \forall t \in \{1,...,T\} \tag{4}$$

$$(MC_{\min})^t \le \sum_{n=1}^{N}(Ot_n + W_n)\times X_n^t \le (MC_{\max})^t \qquad \forall t \in \{1,...,T\} \tag{5}$$

$$\sum_{t=1}^{T} X_n^t = 1 \qquad \forall n \in \{1,...,N\} \tag{6}$$

$$0.4\,(Int(m))\,X_{Wb}^t - \sum_{n=1}^{m} X_n^t \le 0 \qquad \forall t \in \{1,...,T\},\quad Wb \in \{1,...,N\} \tag{7}$$

Eqs. (2) and (3) are grade blending constraints; these inequalities ensure that the average grade of the material sent to the mill is within the desired range in each period. Eq. (4) imposes processing capacity constraints; these inequalities satisfy that the total tonnage of ore processed is within the acceptable range of the processing plant capacity. Eq. (5) applies mining capacity constraints; these inequalities satisfy that the total amount of material (waste, ore and overburden) mined is within the acceptable mining equipment capacity in each period. Eq. (6) is a reserve constraint; this constraint is applied to each block such that that all the blocks in the model considered have to be mined once. Eq. (7) is equipment access and mobility constraints; these constraints ensure that there is sufficient access for equipment for mining a given block and they prevent spreading of scheduling pattern over each period. Eq. (7) also minimizes equipment movement in a given period. In order to consider equipment access to each block, the optimization model should enforce extraction of a working block with a number of surrounding blocks in the same extraction period. To perform this, we define a concentric window around a working block (Fig. 1). The number of blocks in a window can be 8 or 24. The optimization model should force extraction of a working block and blocks numbered 1 to 8 or 1 to 24 in the same scheduling period, with at least *m* blocks within this window. Experience shows that it is better to use 40 percent of blocks in given window,

either 8 or 24. Using a higher percentage than 40 percent would tighten up the constraints and most of the time the MILP model will not result in a feasible solution.

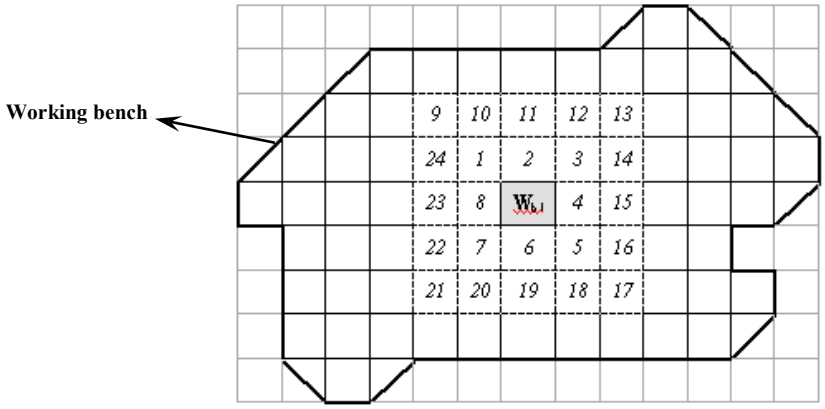

Fig. 1. Block configuration around a working block in a working bench

2.3. Model II

Objective function of model II is:

$$\text{Maximize} \quad \sum_{t=1}^{T}\sum_{n=1}^{N}(v_n^t \times s_n^t - q_n^t \times y_n^t) \tag{8}$$

This objective function is subject to the following constraints:

$$gl^t \le \sum_{k=1}^{K} g_k \times Ot_k \times s_k^t \Big/ \sum_{k=1}^{K} Ot_k \times s_k^t \le gu^t \qquad \forall t \in \{1,...,T\} \tag{9}$$

$$(PC_{\min})^t \le \sum_{k=1}^{K} Ot_k \times s_k^t \le (PC_{\max})^t \qquad \forall t \in \{1,...,T\} \tag{10}$$

$$(MC_{\min})^t \le \sum_{k=1}^{K} (Ot_k + W_k) \times y_k^t \le (MC_{\max})^t \qquad \forall t \in \{1,...,T\} \tag{11}$$

$$s_k^t \le y_k^t \qquad \forall t \in \{1,...,T\}, \quad \forall k \in \{1,...,K\} \tag{12}$$

$$\sum_{i=1}^{t} y_k^i - b_k^t \le 0 \qquad \forall t \in \{1,...,T\}, \quad \forall k \in \{1,...,K\} \tag{13}$$

$$b_k^t - b_k^{t+1} \le 0 \qquad \forall t \in \{1,...,T-1\}, \quad \forall k \in \{1,...,K\} \tag{14}$$

Eqs. (9) to (11) control grade blending, processing capacity, and mining capacity constraints at the mining-cut level with fractional extraction from mining cuts. Eq. (12) ensures that the amount of ore extracted and processed from any mining cut in any given period is going to be less than or equal to the amount of rock extracted from that mining cut. Eqs. (13) and (14) check the set of the immediate predecessor cut that must be extracted prior to extracting mining cut, *k*.

3. Application of models to production scheduling in an iron mine

A TOMLAB/CPLEX environment (Holmstrom, 1989-2009) is used to develop and test the two models. The models are then used to schedule a bench of an iron ore mine. The block model includes estimated values for percentage of sulphur, phosphor and iron ore. The main mineral considered for profit is iron ore. The bench is divided into 415 blocks with 25m×50m×15m dimension. The bench contains 11.2 million tonnes of ore, with an average grade of about 72% magnetic weight recovery (MWT) of iron ore. A production schedule for the bench is developed to maximize the total discounted economic value at a 10% discount rate. Model I and model II generated M$531.64 and M$531.21 total discounted economic value for this bench over five periods of extractions respectively. To meet the physical mining constraints we have used a mining capacity upper bound of five million tonnes per period, whereas the processing capacity is 2.5 million tonnes per period. In model II, the bench block model is divided into 30 mining cuts. Fig. 2 shows the extraction sequences of this bench for two models. Model I has created scattered block extraction order, while the schedule generated by model II is smooth and feasible to implement in practice. The yearly tonnage of ore processed, waste mined, and the total tonnage of material mined in each period of production is compared in Fig 3. Fig. 4 and Fig. 5 show average iron ore grade and cash flow per period, respectively. There are not significant differences between results from the two models, but model I has many binary integer variables and the CPU processing time is almost thirty thousand times more, comparing to model II.

4. Conclusion

Two mixed integer linear programming (MILP) models were presented. Model I only consists of binary integer decision variables. This model generates a production schedule at block level resolution. In model II, extraction, processing, and the order of block extraction are controlled at the mining-cut level. Model II reduces the size and computational time of the problem. The models were compared using block model data from a bench of an iron ore mine. Although, model I generates a higher total discounted economic value than model II, the run time for model I is 30,000 times more than model II. The results show that model II generates a practical mining schedule that includes enough space for equipment to maneuver and it prevents scattering of the excavation sequence in a given scheduling period.

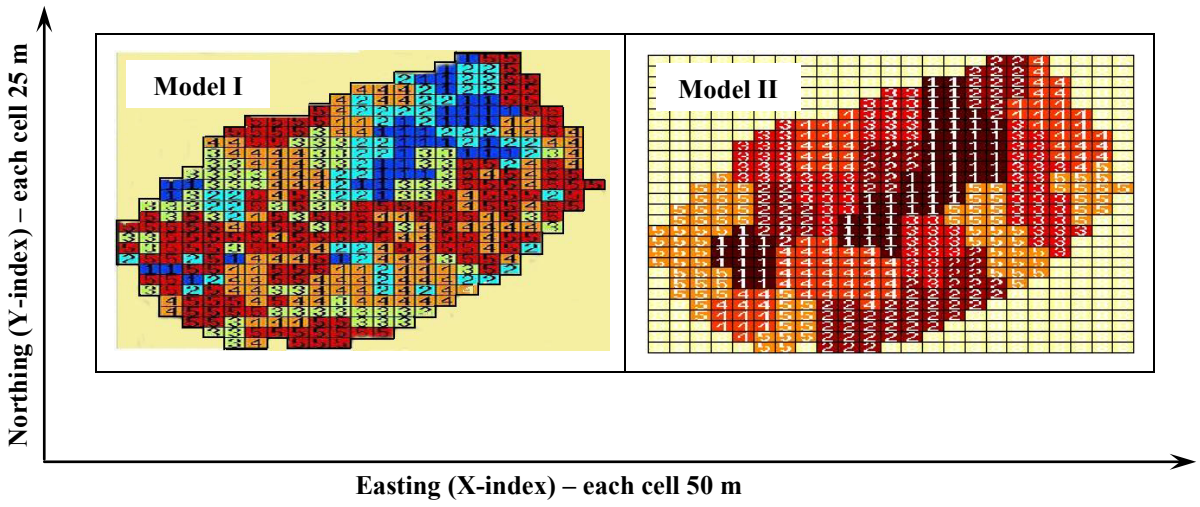

Fig. 2. Extraction sequence for the two models

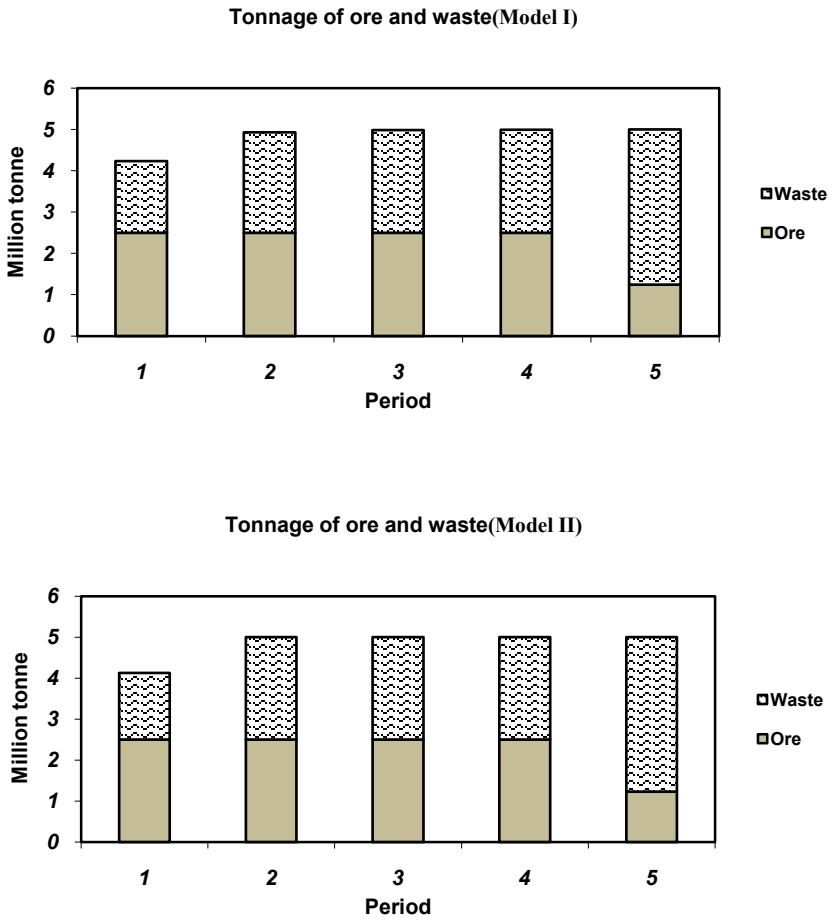

Fig 3. Tonnage of ore and waste per period

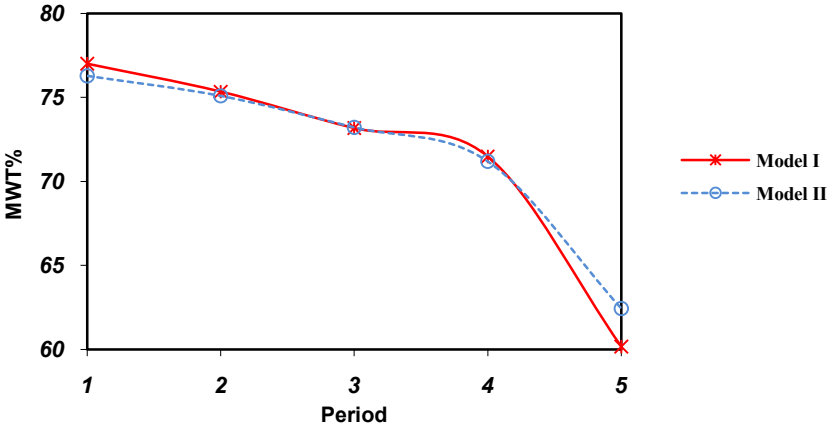

Fig. 4. Average iron ore (MWT%) grade per period

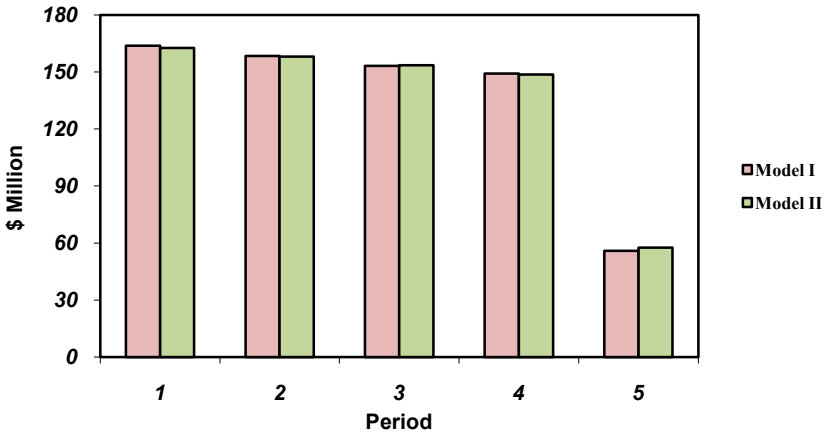

Fig. 5. Comparison between amount of cash flow

5. References

[1] Askari-Nasab, H. and Awuah-Offei, K. (2009). *Mixed integer linear programming formulations for open pit production scheduling*, in Proceedings of First report of Mining Optimization Labratory(MOL), University of Alberta, pp. 8-37.

[2] Askari-Nasab, H. and Awuah-Offei, K. (2009). Open pit optimization using discounted economic block value. *Transactions of the Institution of Mining and Metallurgy, Section A, Mining industry*, *118*,(1), 1-12.

[3] Askari-Nasab, H., Frimpong, S., and Szymanksi, J. (2008). Investigation the continuous time open pit dynamics. *The journal of the South African Institute of Mining and Metallurgy*, *108*,(2), 61-73.

[4] Boland, N., Dumitrescu, I., Froyland, G., and Gleixner, A. M. (2009). LP-based disaggregation approaches to solving the open pit mining production scheduling problem with block processing selectivity. *Computers & Operations Research*, *36*,(4), 1064-1089.

[5] Caccetta, L. (2007). Application of optimization techniques in open pit mining. *Int. Series Operate. Res. Manage. Sci.*, *29*, 547-559.

[6] Caccetta, L. and Hill, S. (2003). An application of branch and cut to open pit mine scheduling. *Journal of Global optimization*, *27*, 349-365.

[7] Denby, B. and Schofield, D. (1994). Open pit design and scheduling by use of genetic algorithms. *Transactions of the IMM, Section A*, *103*, A21-A26.

[8] Denby, B. and Schofield, D. H., G. (1996). *Genetic algorithms for open pit scheduling-extention into 3-dimensions*, in Proceedings of 5th International symposium on Mine Planning and Equipment Selection, Sao Paulo, Brazil, pp. 177-186.

[9] Dimitrakopoulos, R. (1998). Conditional simulation algorithms for modelling orebody uncertainty in open pit optimization. *International Journal of Surface Mining, Reclamation and Environment*, *12*, 173-179.

[10] Fan, Z. C., Wang, J. M., and Hao, Q. M. (2003). *Optimizing open pit mine production scheduling by graph theory*, in Proceedings of Mine Planning and Equipment Selection(MPES 2003), pp. 447-454.

[11] Holmstrom, k. (1989-2009). TOMLAB/CPLEX. 11.2 ed. WA, USA: Pullman, pp. Tomlab Optimization.

[12] Ramazan, S. and Dimitrakopoulos, R. (2003). *Production scheduling optimization in Nickel laterite deposit: MIP and LP application and in the presence of orebody variability mine*, in Proceedings of Mine Planning and Equipment Selection(MPES 2003), pp. 1-5.

[13] Ramazan, S. and Dimitrakopoulos, R. (2004a). Recent applications of operations research and efficient MIP formulation in open pit mining. *Transactions of the Society for Mining,Metallurgy and Exploration*, *316*, 73-78.

[14] Ramazan, S. and Dimitrakopoulos, R. (2004b). Traditional and new MIP models for production scheduling with in-situ grade variability. *International Journal of Surface Mining, Reclamation and Environment*, *18*, 85-98.

[15] Tolwinsky, B. and Underwood, R. (1996). A scheduling algorithm for open pit mines. *IMA J. Manage. Math.*, *7*, 247-270.

6. Appendix

MATLAB and TOMLAB/CPLEX code and documentation for Model I & Model II

Review of micro modeling and regional modeling in geostatistics with focus on McMurray data

Mohammad Mahdi Badiozamani, Yashar Pourrahimian, Mohammad Tabesh
Mining Optimization Laboratory (MOL)
University of Alberta, Edmonton, Canada

Abstract

Predicting the performance of in-situ recovery processes is required to optimize development, planning and resource management in mining and petroleum projects. In this paper, two different concepts are presented; micro modeling and regional modeling.

In the first part of this paper, vertical permeability in the McMurray formation is estimated by micro modeling and a consistent numerical modeling framework based on core data, core photographs, high resolution image logs, and detailed geological interpretation. The framework includes dividing the stratigraphic column into facies with similar spatial arrangement of sand/shale, constructing high-resolution models of sand/shale, assigning porosity and permeability to sand/shale, calibrating the models to direct measurements, solving for effective horizontal and vertical permeability at the appropriate scale and transferring the results to geomodeling.

Multiple reservoir parameters should be mapped to assess the economic viability of a particular site. Some of these parameters considered in this research are structure, gross and net thickness, amount of contained bitumen. There are others which should be taken into account in more in-depth studies. In the second part of this paper, the reservoir of McMurray formation is characterized by 2D geostatistical modeling.

1. Introduction

The McMurray formation in the Athabasca oil sands deposits of Northern Alberta is part of the world's second largest proven crude oil reserves. The formation is characterized by stratigraphic layers that correspond to three different depositional environments: Marine, Estuarine and Fluvial facies. The McMurray Formation contains a vast resource of heavy oil. The economic production of this heavy oil often makes use of thermal processes to reduce viscosity and horizontal wells that have a large contact area with the formation. Steam is often injected to introduce thermal energy. The rates of steam rise and water/oil drainage are predicted by flow simulation. A critical input parameter in that flow simulation is the vertical permeability. Accurate prediction of fluid flow would permit optimization of the recovery process and operating parameters; thus, accurate estimation of vertical permeability is of great interest in the McMurray formation.

The sands in the McMurray formation are host to the crude bitumen, in which three main lithofacies are recognized based on the depositional environments: Fluvial, Estuarine and Marine from the base to the top of the formation. Stratigraphic subdivisions for the McMurray formation include the lower, middle and upper McMurray. There are a lot of studies and historical overviews about the McMurray. Total remaining established reserves of crude bitumen in Alberta are estimated at more than 27 billion cubic meters, or imperial equivalent in excess of 175 billion barrels. This includes about 22.6 billion m^3 of in-situ bitumen, of which 0.5 billion m^3 are from

lands under active development. Surface-mineable crude bitumen reserves amount to 5.2 billion m^3 , of which 1.4 billion m^3 are from lands under active development (Hein & Cotterill, 2000).

The major bitumen reserves of Alberta are hosted within four major oil sands deposits in northern Alberta, the Athabasca, Wabasca, Cold Lake, and Peace River deposits. Some of recent studies have recommended that the informal term 'Middle McMurray' be abandoned, and what was formerly, mapped as Middle McMurray now be included as part of the Upper McMurray. What was formerly designated as 'basal' or 'lower' McMurray is called Lower McMurray. In summary, it is proposed that the two mappable informal members of the McMurray formation are the Lower McMurray and Upper McMurray, which are separated by a disconformity (Hein & Cotterill, 2000).

The ability of the reservoir formation to transmit fluids (permeability) has a large effect on the reservoir response for given operating conditions. Permeability is a constant value that relates the flow rate through a porous medium to an imposed pressure gradient. Small-scale variations in the clastic deposits of the McMurray cause permeability to be variable and direction dependent. Permeability in the vertical direction is of primary concern because operators are concerned with (1) the rise of steam through the formation, (2) the possible escape of steam and thermal energy to overlying formations, and (3) the rates at which condensed water and oil will drain to horizontal production wells (C. V. Deutsch, 2009).

The micro modeling part of this paper is concerned with absolute vertical permeability. There are important confounding effects that are not considered such as changes to permeability because of multiple fluids present in the formation and changes to permeability because of time varying geomechanical effects. This paper is primarily concerned with the influence of small scale geological heterogeneities on the estimation of vertical permeability.

Multiple reservoir parameters should be mapped to assess the economic viability of a particular site. These parameters include but are not limited to structure, gross and net thickness, amount of contained bitumen, the presence of shale and the presence of water and gas zones. In most cases, these geological variables are 2D summaries for particular productive horizons. A complete study may require the mapping of 20 to 30 variables. Hydrocarbon resources are calculated as a combination of these variables. If 2D models have a good quantitative measure of reservoir parameters, we can estimate resources without building 3D models. In addition, 2D modeling is simpler and faster than 3D modeling, and especially useful in modeling a large area where the complex 3D geostatistical models may not be practical. The regional modeling part of this paper demonstrates the reservoir characterization of the McMurray formation by 2D geostatistical modeling (Ren, Mclennan, Leuangthong, & Deutsch, 2006).

2. Installing required software

In order to do the Geostatistical modeling some software is required. It was decided to use a set of free Geostatistical tools as well as general software as mentioned in Table 1.

3. Micro modeling

For micro modeling, four steps should be done. These steps are as follows (1) process the image to create a scaled sand-shale indicator image with known spatial coordinates, (2) assign 3D sand-shale indicator, porosity and permeability values, (3) solve for the effective horizontal and vertical permeability, and (4) summarize and check the results for subsequent mini modeling.

Table 1. Required software

#	Software Name	Description	Website
1	Notepad ++	A professional open source text editor	http://Notepad-plus.sourceforge.net
2	GSView	A postscript file viewer	http://pages.cs.wisc.edu/~ghost/gsview/
3	FSViewer	An open source image viewer/editor	http://www.faststone.org/FSViewerDownload.htm
4	Cygwin	A command prompt application based on Linux syntax	http://www.cygwin.com
5	SGeMS	A free set of Geostatistical tools provided by Stanford university	http://sgems.sourceforge.net
6	GSLib	A free command based set of Geostatistical tools by Clayton Deutsch and Manu Schnetzler.	http://gslib.com
7	MS Excel	A commercial spreadsheet used for doing some statistical operations and charting	http://office.microsoft.com

3.1. Facies Modeling

In the beginning, core photographs or image logs were provided. The image must be cropped and saved as a gray scale image for processing. The scale of the image must be recorded for processing. Then, the continuous gray scale value must be converted to sand-shale indicator values (C. V. Deutsch, 2009). In this case, we have categorical variables. There are only sand and shale. The indicator variables are defined by:

$$i(u_\alpha, \mathrm{s}) = \begin{cases} 1, & \text{if sand is present at location } u_\alpha \\ 0, & \text{otherwise} \end{cases} \quad (1)$$

We have usually a set of data provided by labs or machines gathering data on the site. No matter whether the data is provided by machines or people, you have to clean some invalid records and outliers and select subsets of data for different purposes. The data provided for this project is the result of an image processing performed on the FMI data of a drill hole. The image is processed and resulted in a set of zero and ones regarding sand and shale. A set of points, which form a cylinder of 0.1m in height by 0.12m in radius, is selected for further modeling. The x and y coordinates of points are then calculated and the data required for creating the model is prepared by Clayton himself.

After gaining sand-shale indicator values for different slices, they are converted to GSLIB format and coordinates of each point with related indicator value is assigned. The sand-shale indicator data represents an annular volume. Fig. 1 shows part of preliminary data.

Fig. 2 shows part of data in GSLIB format. The columns of this figure indicate x, y, z, and facies, respectively. The annular volume has been made from 50 slices with 2 mm thickness, thus height of the cylinder is equal to 100 mm. For data visualization, Stanford Geostatistical Modeling Software (SGeMS) is used, which is a well-prepared package to visualize and manipulate the

geostatistical data. Two views of FMI data are shown in Fig. 3. Red areas and blue areas indicate sand and shale, respectively. Plan view and location of FMI data are shown in Fig. 4.

In order to have a better understanding of the data, some basic statistical operations has been done in MS Excel. The file has been imported into Excel as a space-delimited file. The zero-one values regarding sand/shale are average using subtotals in each vertical level and globally. The results can be found in Table 2. A global average of 0.6491 and a standard deviation of 0.4772 are the results of the calculation. By adding two trend lines to the chart, it can be inferred that there is an obvious downward trend in the proportion of sand in each level. As the value for z (which stands for elevation) goes up the average amount of sand goes higher with almost less standard deviation. Another trend study that seems to be useful is to do the averaging over different sectors of the cylinder. The cylinder was divided into four area based on coordinates axes. Fig. 5 shows specifications of each region. The percentages of sand and shale within each area are shown in Fig. 6. The most outstanding feature of Fig. 6 is the percentage of sand within area 1. It can be seen that only in the third area, percentage of shale is a little more than sand.

3.2. Calculate and model variograms

The variogram is function of distance and direction. Variogram inference proceeds in three main steps (Leuangthong, Khan, & Deutsch, 2008):

1. Calculate the experimental variogram in multiple directions for a number of lags that approximately correspond to the average spacing between data,
2. Interpret the experimental variogram points and supplement them with expert judgment or analogue data,
3. Fit a valid parametric model to the directional variograms in all directions.

The variogram is needed for distance up to 1m. The vertical variogram is well defined from the well logs. According to the given data, the horizontal variogram should look the same as the vertical one but with a range five times larger than the vertical one.

To calculate the vertical variogram, the normal scores of porosity within sandy IHS facies should be used; therefore, the porosity values for facies 2 are transferred to normal unit.

The variogram is usually measured in two horizontal and one vertical direction. The data we have is distributed over the lateral surface of a cylinder. Thus, calculating vertical variogram would be an ordinary job. The variogram is calculated using the "gamv" application available in GSLib (C.V. Deutsch & Journel, 1998) and the parameter file presented in Table 3.
The dip tolerance and lag tolerance values have been assumed to be small values to make sure each point is paired with only one other point. Since there is enough data and it is regularly spaced, the assumption seems to be reasonable. We usually want to have variograms for lags smaller that ¾ of the total length of the domain. Consequently, the number of lags and lag separation distance are considered 40 and 0.002, respectively ($40 * 0.002 = 0.08 \cong \frac{3}{4} * 0.1$).

```
 RADIUS 0.59999999E-01
NSLICE    1000
STHICK 0.30000000E-02
NANG       365
11111111111111000000000000000000000000001100000000000000000000000000000000
11111111111111110000000000000000000010000110000000000000000000000000000000
11111111111111110000000000000000000111111111000000000000000000000000000000
11111111111111110000000000000000000111111111000000000000000000000000000000
11111111111111110000000000000000000111111000000000000000000000000000000000
```

Fig. 1. Sand-shale indicator values

```
FMI Data for 615
4
X
Y
Z
Facies
.0600 .1200 .0010 1
.0610 .1200 .0010 1
.0621 .1200 .0010 1
.0631 .1199 .0010 1
```

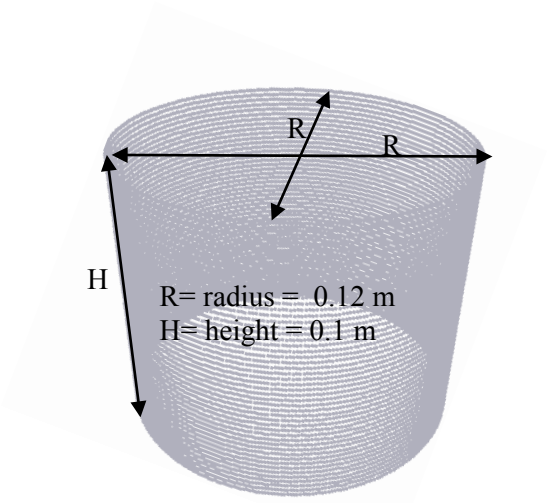

Fig. 2. Part of the created FMI.dat file and related coordinates

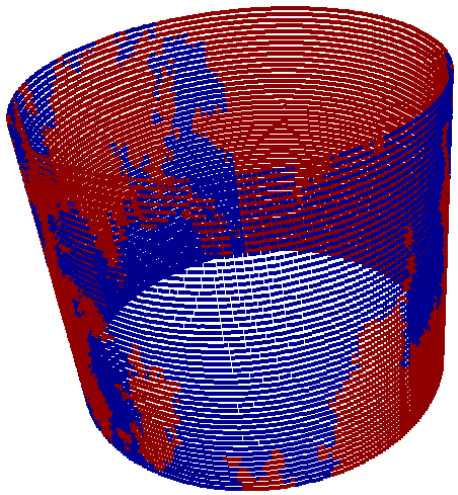

Fig. 3. 3D view of FMI data

Table 2. Level Based Averages

Z	Facies (Average)	Facies (StdDev)
0.099	0.5781	0.4945
0.097	0.6137	0.4876
0.095	0.6411	0.4803
0.093	0.6411	0.4803
0.091	0.6192	0.4863
0.089	0.6027	0.4900
0.087	0.5890	0.4927
0.085	0.5616	0.4969
0.083	0.5699	0.4958
0.081	0.5781	0.4945
0.079	0.5616	0.4969
0.077	0.5671	0.4962
0.075	0.5562	0.4975
0.073	0.5671	0.4962
0.071	0.5671	0.4962
0.069	0.5918	0.4922
0.067	0.6000	0.4906
0.065	0.6000	0.4906
0.063	0.6384	0.4811
0.061	0.6795	0.4673
0.059	0.6740	0.4694
0.057	0.6685	0.4714
0.055	0.6630	0.4733
0.053	0.6548	0.4761
0.051	0.6521	0.4770
0.049	0.6822	0.4663
0.047	0.6575	0.4752
0.045	0.6411	0.4803
0.043	0.6740	0.4694
0.041	0.6740	0.4694
0.039	0.6822	0.4663
0.037	0.6685	0.4714
0.035	0.6795	0.4673
0.033	0.7096	0.4546
0.031	0.7205	0.4493
0.029	0.7233	0.4480
0.027	0.7315	0.4438
0.025	0.7233	0.4480
0.023	0.7068	0.4558
0.021	0.7041	0.4571
0.019	0.7096	0.4546
0.017	0.7315	0.4438
0.015	0.7068	0.4558
0.013	0.7233	0.4480
0.011	0.7589	0.4283
0.009	0.7205	0.4493
0.007	0.6548	0.4761
0.005	0.6438	0.4795
0.003	0.6164	0.4869
0.001	0.5781	0.4945

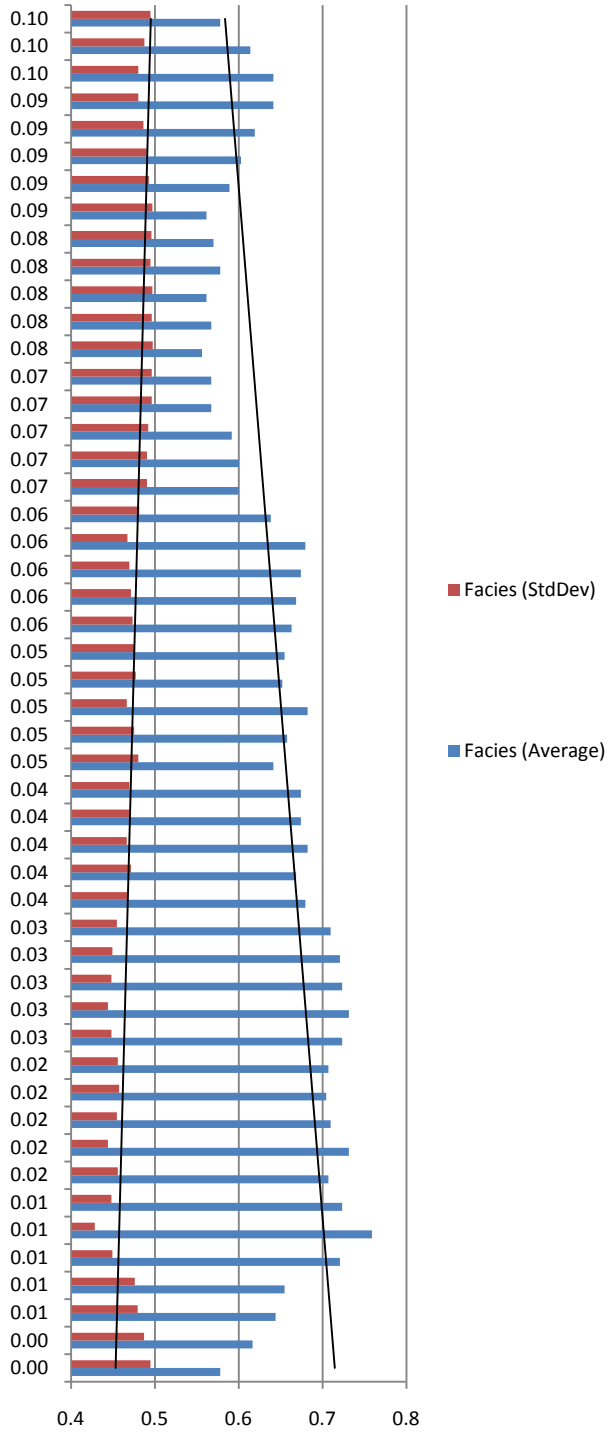

Fig. 4. Vertical trends

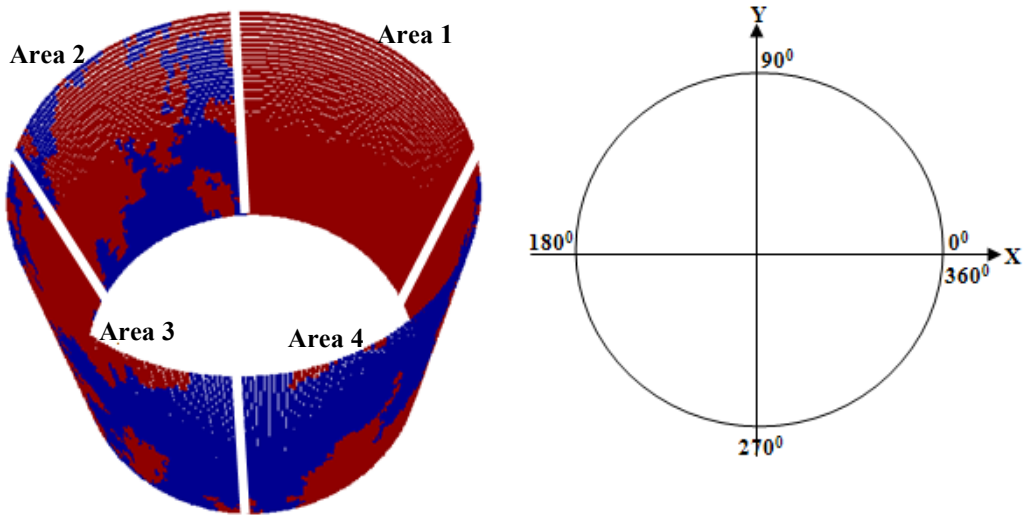

Area	Angle (β^0)	Coordinates
1	$0 \leq \beta \leq 90$	$0.06 \leq X \leq 0.12$, $0.06 \leq Y \leq 0.12$, $0.00 \leq Z \leq 0.1$
2	$90 \leq \beta \leq 180$	$0.00 \leq X \leq 0.06$, $0.06 \leq Y \leq 0.12$, $0.00 \leq Z \leq 0.1$
3	$180 \leq \beta \leq 270$	$0.00 \leq X \leq 0.06$, $0.00 \leq Y \leq 0.06$, $0.00 \leq Z \leq 0.1$
4	$270 \leq \beta \leq 360$	$0.06 \leq X \leq 0.12$, $0.00 \leq Y \leq 0.06$, $0.00 \leq Z \leq 0.1$

Fig. 5. Specified areas to determine the proportion of sand to shale

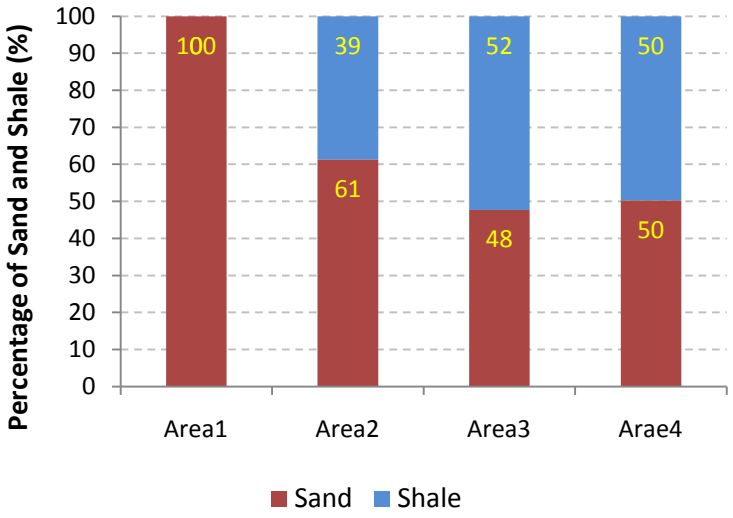

Fig. 6. Percentage of sand and shale within each area

Table 3. Parameter file used for calculating vertical variogram

Parameters for GAMV START OF PARAMETERS:	
fmi.dat	-file with data
1 2 3	-columns for X, Y, Z coordinates
1 4	-number of variables, col numbers
-1.0e21 1.0e21	-trimming limits
vgamv.out	-file for variogram output
40	-number of lags
0.002	-lag separation distance
0.0005	-lag tolerance
1	-number of directions
0.0 90.0 50.0 -90.0 0.1 50.0	-azm,atol,bandh,dip,dtol,bandv
0	-standardize sills? (0=no, 1=yes)

On the other hand, when horizontal variogram is going to be calculated, there would not be enough data to judge the maximum and minimum direction of continuity based on the available data. Therefore, an omni-directional horizontal variogram is used. The maximum distance between pairs of data in horizontal direction is 0.12 meters. Thus, we can consider 40 lags with a distance of 0.0025 ($40 * 0.0025 = 0.1 \cong \frac{3}{4} * 0.12$). Since the points are not distributed regularly, we have considered a larger lag tolerance to make sure there will be enough pairs of data to calculate the variogram. Since the FMI data points are aligned in the surface of a completely vertical cylinder, the azimuth angle for both directions is set to zero, with the azimuth tolerance equal to 90 degrees that covers the whole vertical cylinder surface. The direction of vertical cylinder also implies to set the dip angle to -90 degrees for vertical and 0 degree for horizontal directions. Because the data points are regularly spaced, a small dip tolerance, 0.1 degree, is suitable for variogram calculation.

The two experimental variograms can be found in Fig. 7. Red bullets stand for experimental vertical variogram whereas blue ones represent the experimental horizontal variogram.

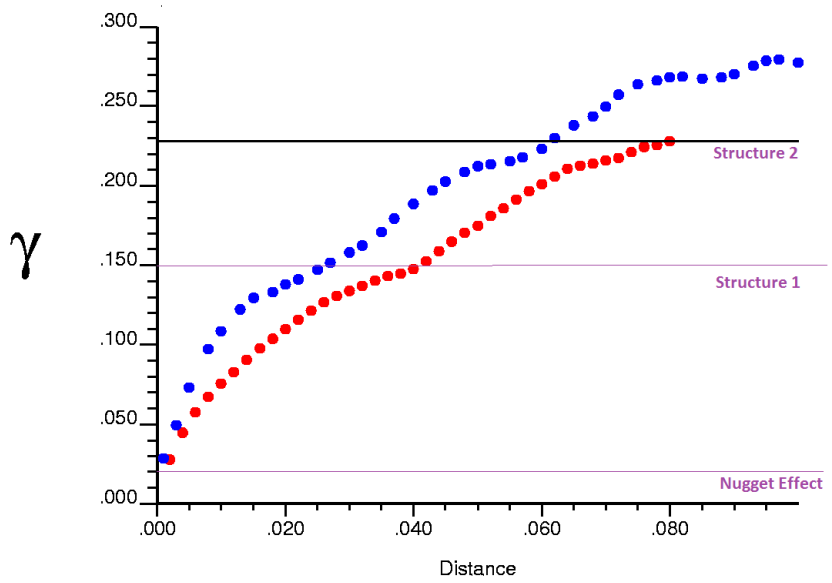

Fig. 7. Experimental variogram

Looking at variograms in two directions, using two or three nested structures seems to be reasonable. In this case, three variance regions can be defined for three horizontal and vertical variograms, the first one is a nugget effect, and the second one is exponential variogram structure. The last one is spherical variogram structure. The variogram parameters corresponding to the variogram shown in Fig. 8 have been summarized in Table 4.

$$\gamma(h) = 0.02 + 0.13\, Exp_{\substack{a_{h\max}=0.08 \\ a_{h\min}=0.08 \\ a_{vert}=0.026}}(h) + 0.078\, Sph_{\substack{a_{h\max}=0.1 \\ a_{h\min}=0.1 \\ a_{vert}=0.06}}(h) \tag{2}$$

Table 4. Variogram model corresponding to variogram shown on Fig. 8

Variance Contribution	Type of Variogram	Horizontal Range, m	Vertical Range, m
0.02	Nugget		
0.13	Exponential	0.08	0.026
0.078	Spherical	0.1	0.06

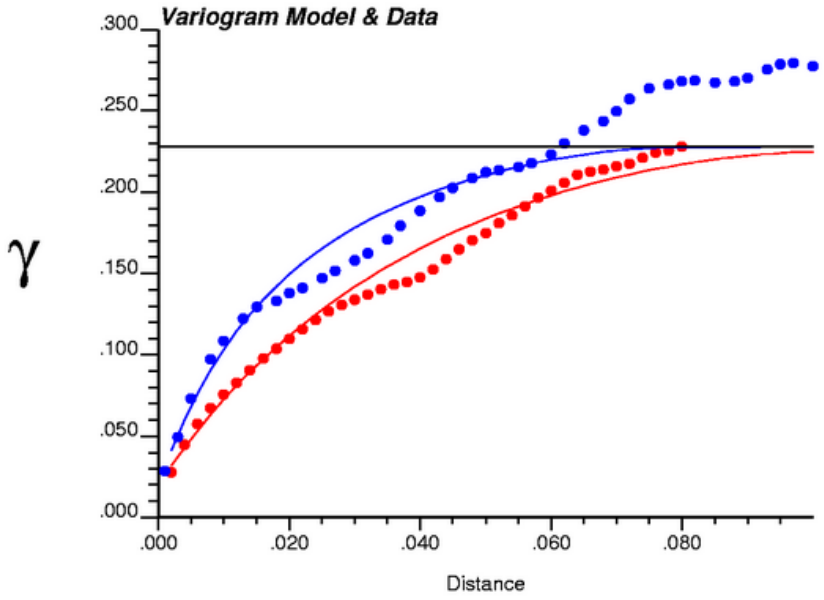

Fig. 8. Variogram models

3.3. Kriging

Kriging is the most important one among traditional mapping applications and an essential component of geostatistical simulation methods. In this section, we want to construct a model of spatial uncertainty characterizing the distribution and occurrence of the facies. There are 18250 records of data that should be used to estimate unsampled locations inside the domain. Fig. 9 shows

the domain and sampled locations. In this case, Simple Kriging (SK) is done using the variogram model provided in Eq. (2). For Kriging 50×50×50 grid nodes is used. Size of each cell in X, Y and Z directions are 2.4 mm, 2.4 mm, and 1.0 mm respectively. Fig. 9 schematically shows how the initial cylinder shape surface, containing well log data, is transferred to a cube through Kriging. In order to perform SK estimation, a search ellipsoid is defined with maximum search radius of 90 mm in all three directions and zero angles. 25 to 35 points are used to estimate the facies of each grid cell.

The result of the 3D SK operation is illustrated in 3D in Fig. 10. Three orthogonal planes in the middle of the domain are also presented in Fig. 11. Kriging has been implemented using the "kt3d.exe" application in GSLib. Simple Kriging method uses available values at sampled locations as well as variogram models to predict values at unsampled locations. In order to check if the Kriging procedure is on track, cross validation seems to be useful. In cross validation, values at some sampled locations are assumed to be unknown and are predicted using the Kriging equations. Afterwards, the difference between actual and predicted values is plotted as shown in Fig. 12. A correlation value of 0.938 shows a reasonable estimate.

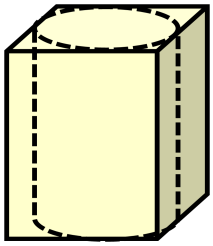

Fig. 9. Cylinder to cube transfer

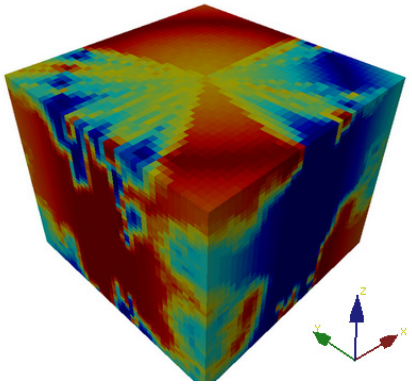

Fig. 10. Kriging 3D illustration

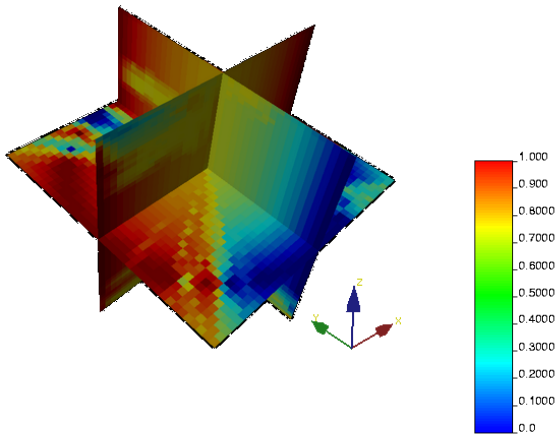

Fig. 11. Kriging planes

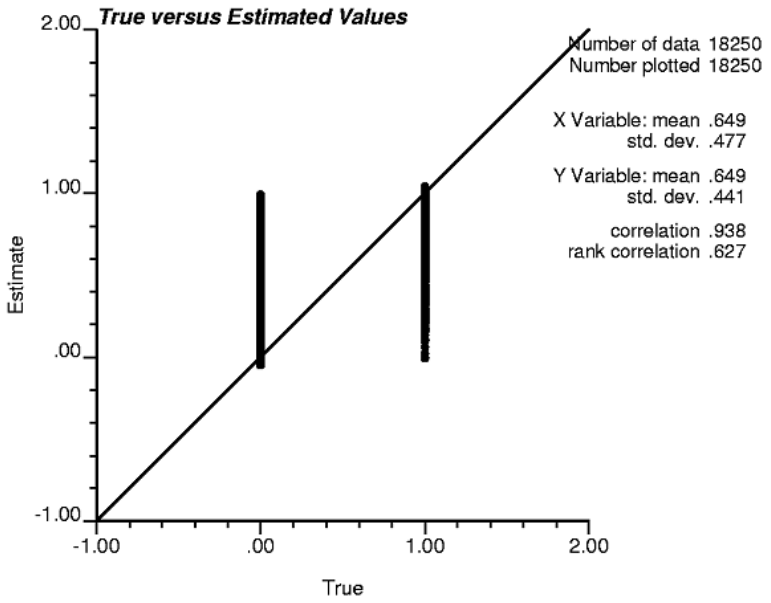

Fig. 12**.** True versus Kriged values

3.4. Simulation

3.4.1 Facies simulation

The next step is to simulate the facies in the grid. There is a drawback in Kriging which is called the smoothing effect. On the other hand, the illustrations in Fig. 3 and Fig. 4 are colored from blue to red which represent values between 0 and 1. We know that a special cell of the grid can only be zero or one (sand or shale) but these values indicate the chance of being 1 for each cell. In order to create realizations of facies values in each cell and also to overcome the smoothing effect of Kriging, simulation comes into mind.

Since the variable is a categorical variable, Gaussian simulation does not seem to be appropriate. Hence, Sequential Indicator Simulation is implemented using an application called "BlockSIS.exe". One hundred realizations are generated using this application. The first realization is illustrated in Fig. 13 and Fig. 14. Red points stand for sand whereas blue ones represent shale.

After generating 100 realizations it seems appropriate to compare the average result of the simulation with Kriging results. There is an application in GSLib which is responsible for averaging different realizations. This program which can calculate different statistics for different number of realizations is called "PostSim.exe" (see Fig. 15). In Fig. 16, some slices of Kriging and simulation are compared with each other. As it can be seen, the Kriging results are smoother than the simulation results. That is mainly because of smoothing effect of Kriging. However, by comparing the results of simulation and Kriging, it can be deduced that they are following the same pattern. In order to compare the closeness of simulation and Kriging results statistically, a scatter plot of post-simulation results and Kriging results is shown in Fig. 16. The correlation coefficient of the scattered data is 0.93. It can be inferred that the average of simulations converges to the Kriged estimates with an acceptable correlation coefficient.

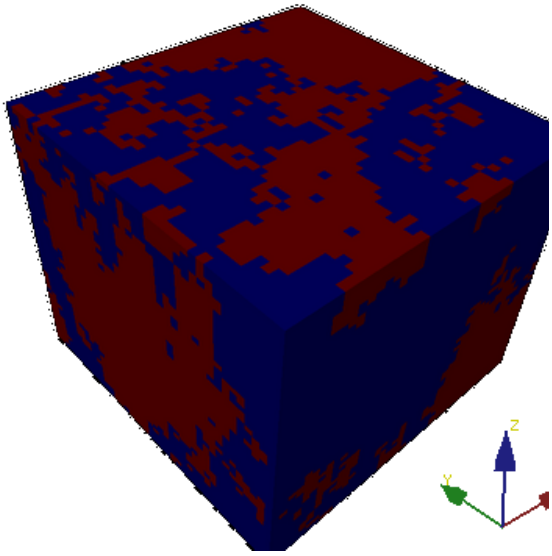

Fig. 13. Simulation result (3D)

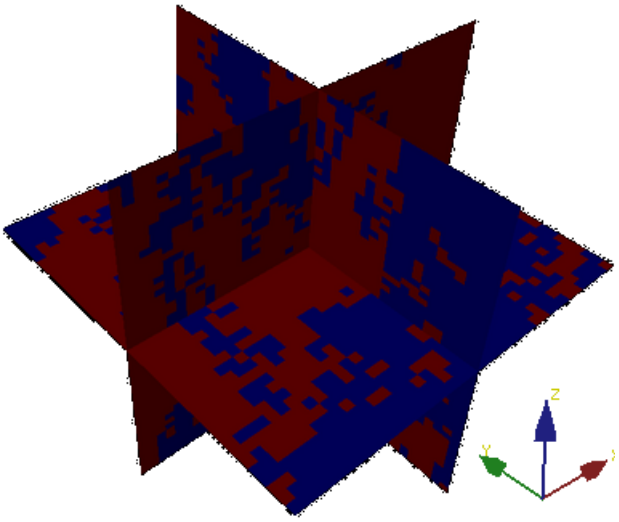

Fig. 14. Simulation result (Planes)

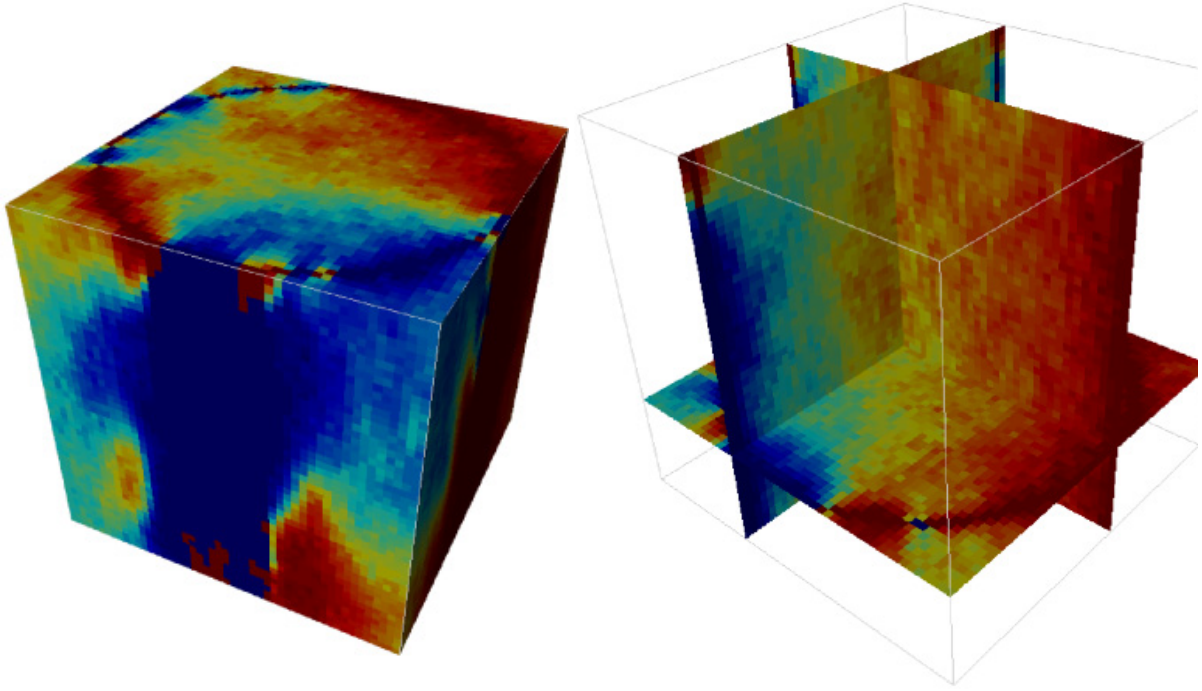

Fig. 15. 3D views of average of 100 realizations for facies (output of PostSim)

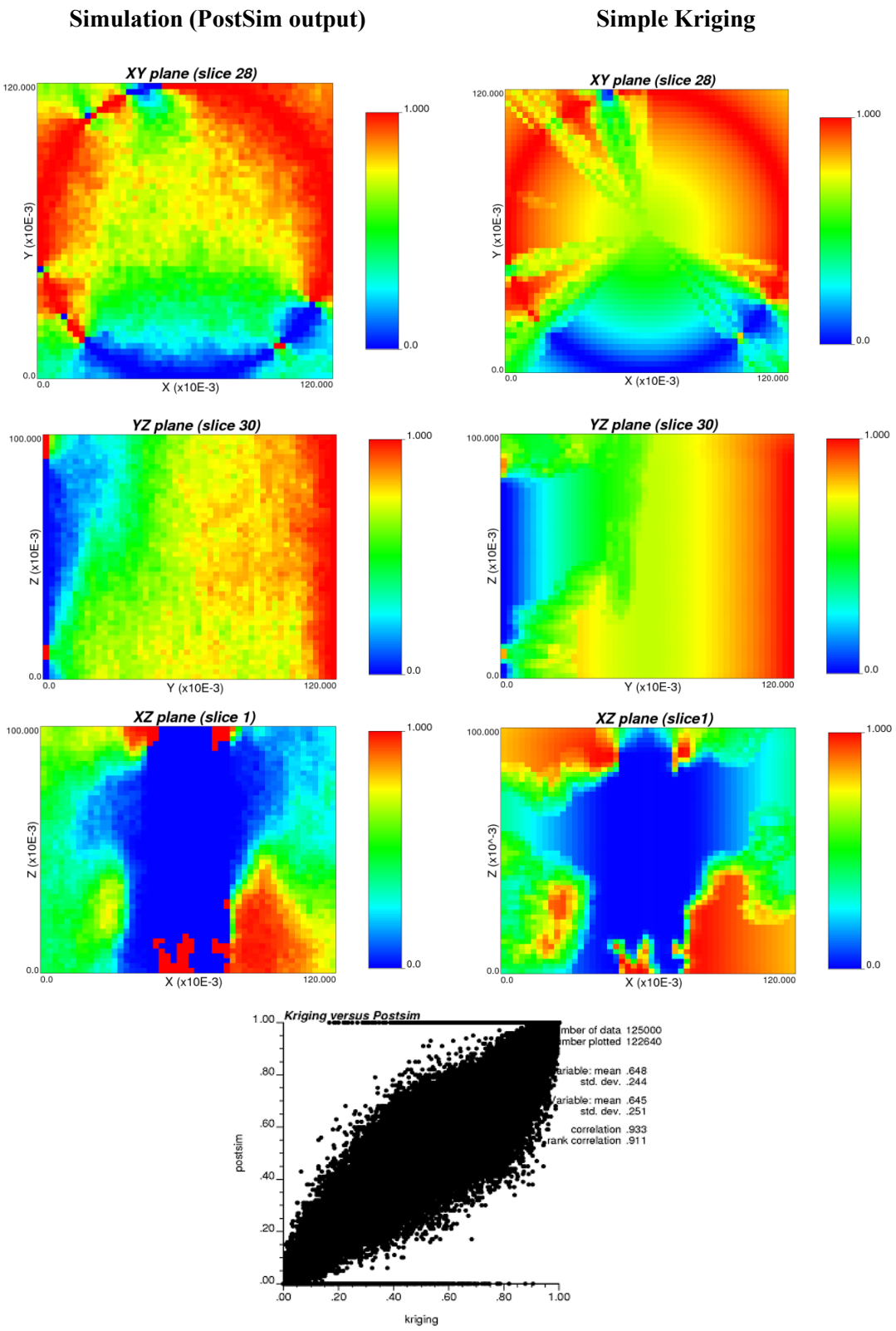

Fig. 16. Comparison between results of simple kriging and simulation of facies

3.4.2 Porosity and Permeability Simulation

In order to simulate the porosity and permeability, random Gaussian numbers are generated. The generated numbers then are transformed to the desired distribution. Permeability values are meant to have lognormal distribution with a mean and standard deviation of 4000 mD and 500 mD and 1 mD and 5 mD for sand and shale respectively. The parameters used to generate one hundred realizations for porosity and permeability are presented in Table 5.

The results of Normal generated numbers for porosity and permeability simulation are averaged two times, once before transferring to desired distribution and once after, to enable us to compare the statistics of generated data values with what it is supposed to be (Normal distribution with mean of 0 and variance of 1). The results are presented in Table 6.

The deviation of generated data from Normal (0, 1) is mainly because of the range of variogram considered in simulations. It is assumed that both porosity and permeability have the same isotropic spherical variogram with the range of 100 mm. Maybe with decreasing the range of variogram, using an anisotropic variogram or changing its type, the results could get closer to the Normal (0, 1).

The simulation results of porosity are used in permeability simulation. In other words, the permeability is simulated conditioned to the porosity, using collocated CoKriging. Correlation coefficient of 0.75 is used for collocated CoKriging. The results of simulated porosity and permeability are presented in Table 7. Fig. 17 shows the average histogram of one hundred realizations for porosity and permeability of sand and shale (Relating to Table 7). In addition to the histograms, it seems useful to check if the correlation between porosity and permeability values is respected. The scatter plot of the two sets of data is shown in Fig**.** 18.

Table 5. Parameters for porosity and permeability simulation

	distribution	particles	mean	STDev
Porosity	Normal	Sand	0.33	0.015
		Shale	0.01	0.005
Permeability(mD)	Log Normal	Sand	4000	500
		shale	1.0	5.0

Table 6. Statistics of generated data values for N (0, 1)

	distribution	particles	Mean	Std
Porosity	Normal	Sand	0.01	0.077
		Shale	0.05	0.094
Permeability(mD)	Normal	Sand	0.00	0.086
		shale	0.01	0.110

Table 7. Statistics of porosity and permeability simulation

	distribution	particles	mean	STDev
Porosity	Normal	Sand	0.33	0.001
		Shale	0.01	0.0005
Permeability(mD)	Log Normal	Sand	3999.39	43.41
		shale	0.958	0.335

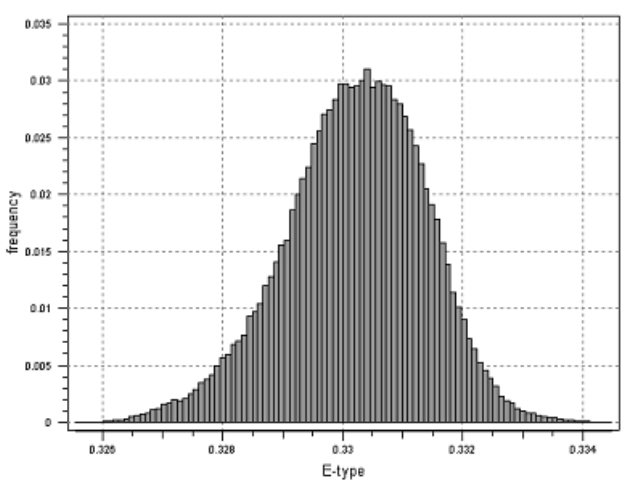

Simulation of sand porosity

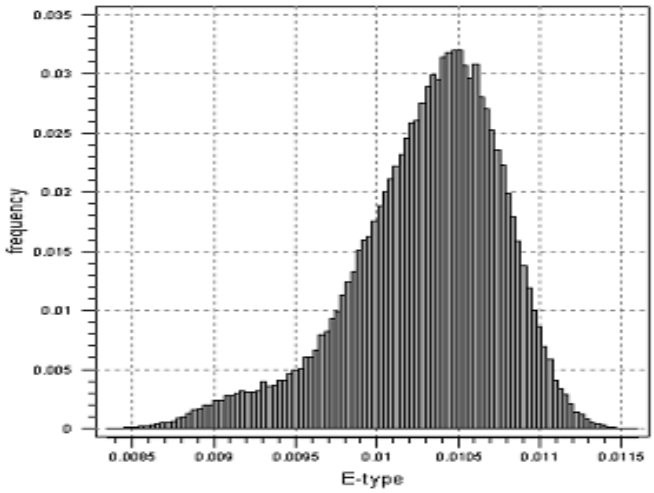

Simulation of shale porosity

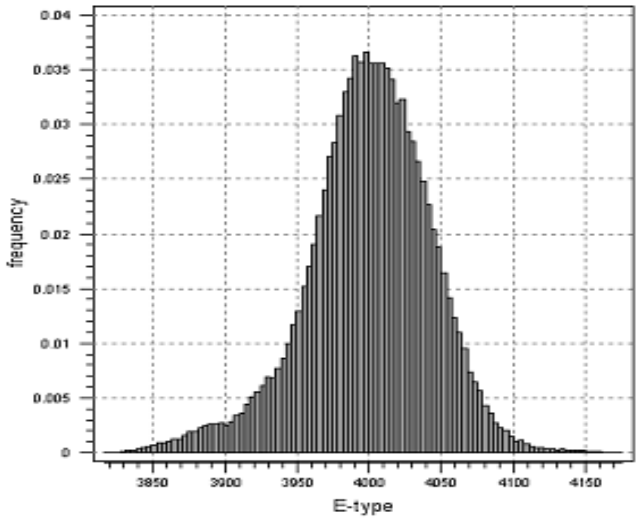

Simulation of sand permeability

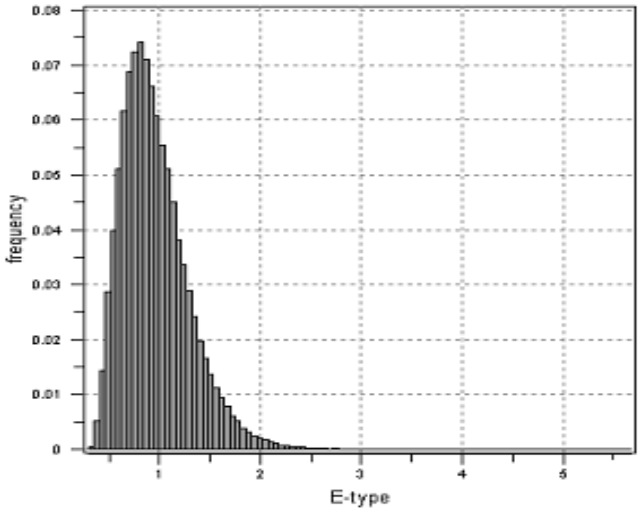

Simulation of shale permeability

Fig. 17**.** Histogram of 100 realizations for porosity and permeability of sand and shale

3.4.3 Merge porosity and permeability realizations with facies data

The domain we tend to study consists of two different facies. The first set of points is sand and the second ones are considered as shale. Each group has its own porosity and permeability values. But the final model of study consists of both groups and these values are needed to be merged before finding the porosity and permeability values for the whole block. To do so, “mergemod.exe” can help. In this application, sets of data are merged together based on different categories from another file. The categories are 0 and 1 in our case where 0 stands for shale and 1 for sand.

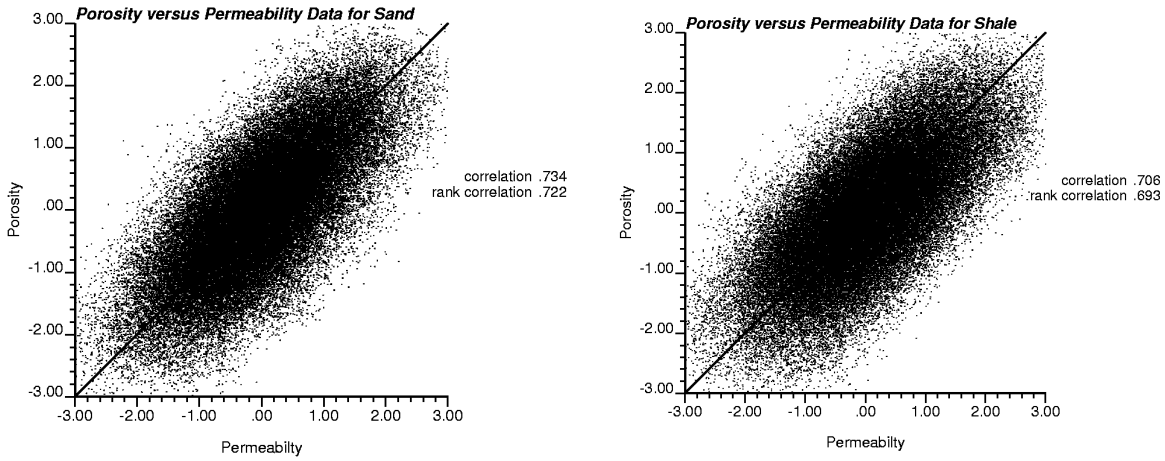

Fig. 18. Porosity versus permeability

Therefore, 100 realizations of porosity values for sand and 100 realizations of porosity values for shale are merged using 100 facies realizations. The same approach is taken for permeability values. Afterwards, the resulting datasets are averaged using "PostSim.exe" to have a better understanding of the results.

Output of BlockSIS (facies model)
Model of sand porosity (N(0.33,0.015)) } Must be merged
Model of shale porosity (N(0.01, 0.005))

Output of BlockSIS (facies model)
Model of sand permeability (lognormal(4000,500)) } Must be merged
Model of shale permeability (lognormal(1,5))

Average values for merged porosity and permeability are shown in Fig**.** 19. It can be seen that ups and downs of permeability and porosity values are correlated as expected. In addition, colors show significant similarity to average facies values. That happens because of the large difference between average porosity and permeability values for sand and shale. Wherever sand exists, higher porosity and permeability values are expected and vice versa.

3.4.4 Flow Simulation and effective permeability calculation

In order to find the porosity and permeability for the whole domain, the flow is simulated. The merged porosity and permeability are used in flow simulation. For this purpose "flowsim.exe" program is used. In the output file three directional permeability values, K_x, K_y and K_z is reported. In addition, the arithmetic, geometric and harmonic averages are also reported in output file. Histogram of effective horizontal and vertical permeabilities and arithmetic average of porosity are shown in Fig**.** 20. Table 8 represents summary of permeability results in the three principal directions. The arithmetic average of porosity is 0.215 with standard deviation of 0.016. According to the obtained results, permeability in vertical direction is higher than horizontal.

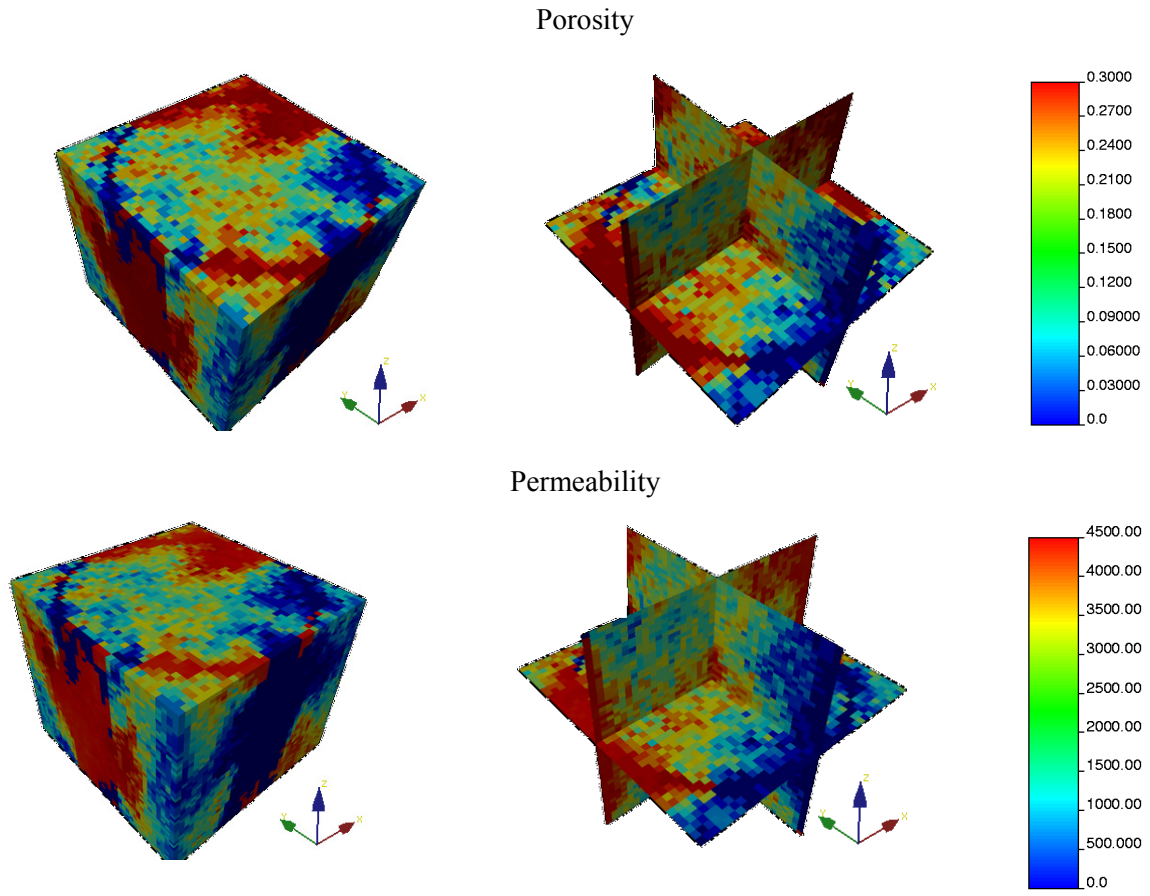

Fig. 19. Average values for merged porosity and permeability

Table 8. Results of permeability in x, y and z directions

Direction	**K_X**	**K_Y**	**K_H**	**K_Z**
Mean	1244.70	1058.28	1137.75	1885.37
Std.	383.60	180.047	249.80	258.33
Min.	377.415	589.99	527.78	13.11.46
Max	1973.68	1534.87	1645.18	2377.65

The relationship between K_H and ϕ, and the K_V/K_H ratio and K_H are the important results of the micro modeling because of their application in reservoir modeling at a large scale. These relationships are shown in Fig. 21. Correlation between K_V/K_H ratio and K_H is -0.85, that means increasing the K_V/K_H ratio, permeability in horizontal direction is reduced.

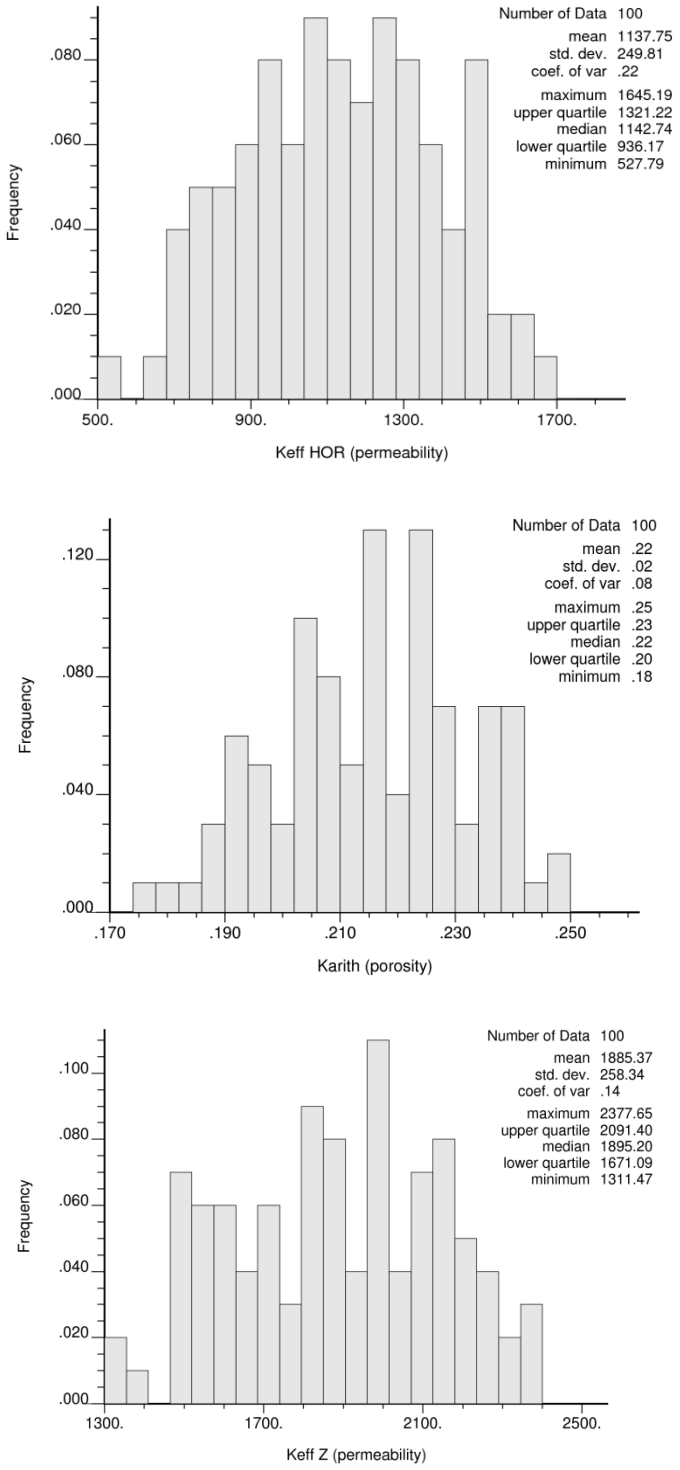

Fig. 20. Histogram of effective horizontal and vertical permeability values and arithmetic average of porosity

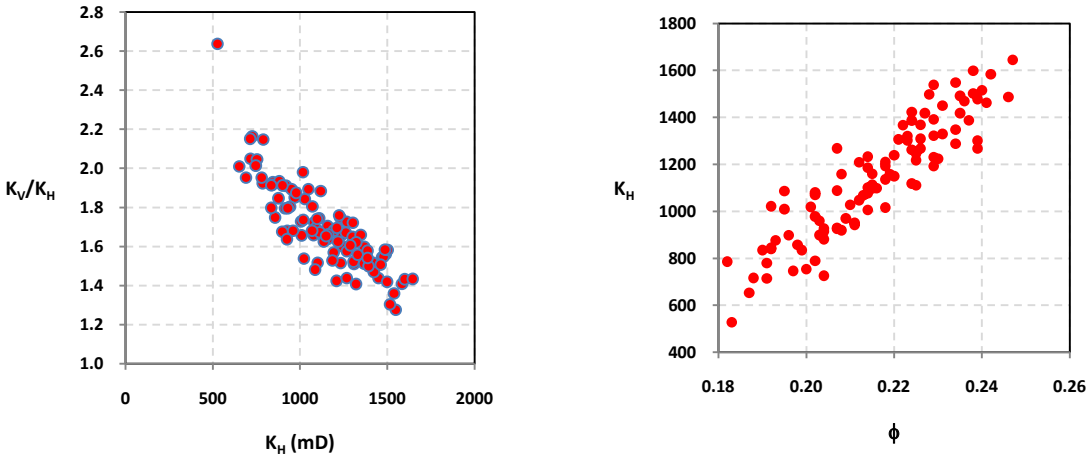

Fig. 21. Results for the K_V/K_H ratio versus the horizontal permeability (ρ=-0.85) and porosity versus horizontal permeability (ρ=0.91).

4. Regional modeling

Macro modeling is a tool for studying general properties of a reservoir or mine in macro scale. The total amount of bitumen/ore and its distribution over the region are of the great interest in macro modeling. In addition, it is interesting to know the distribution of uncertainty and to have optimistic and pessimistic estimates on the reservoir.

McMurray formation is one of the largest oil reservoirs in the world which is estimated to contain 180 billion barrels. This formation is located in north-east Alberta and covers a region of 120 by 180 kilometers approximately. Estimating the amount of bitumen in the formation and its properties and distribution over the region is the main goal of this section. This estimation can then be used for deciding on methods and requirements of the extraction and refinery processes.

The project is defined with the following steps: 1) initial data processing 2) studying preliminary stats 3) model building 4) post processing and reporting the results. .

4.1. Initial data processing

Like any other engineering practice, the available data provided by human or machines should be preprocessed. This preprocessing step contains tasks taken in order to clean the data, verify its consistency and prepare it for further studies. The data provided is obtained from a web database containing logs and histories of the wells placed in the McMurray formation. The first step is to clean data from invalid records. Duplicate values, null values and outliers are the most famous types of invalid records. Unfortunately, in our dataset null values are replaced with zeros which force us to make a decision on how to treat them. Consequently, there are two assumptions on zero values: first is that no data is collected from the well (null values) or the data was not enough reliable to be published and the second type is representing wells where no McMurray were present and the real values are zero.

In order to deal with these invalid records with zero values, the following approach has been taken. Wells with zero values where another non-zero record is present at the same location are eliminated from the set. Remaining zeros are considered as no McMurray which can be verified using location maps. There are other wells which are considered as no McMurray despite the fact that they have non-zero values. Records with a net thickness of less than or equal to 2 meters or with a mass

fraction of bitumen of less than or equal to 0.05 are considered as now McMurray present. These non-zeros are so small that it is not economical to consider them as in bitumen and also there may be some measurement errors in them. Fig. 22 shows the distribution of wells with the presence and absence of McMurray formation.. Black dots stand for well which have not shown considerable values. Table 9 represents the summary statistics of indicators. The next variable defined is calculated as multiplication of net thickness and mass fraction of bitumen used for further cross checks on the total amount of bitumen present in the region.

Table 9. Indicator variable summary

Number of 1	Number of 0	Mean	Standard deviation	Variance
2280	234	0.9069	0.2905	0.0844

Dealing with duplicates is the next step of data cleaning. An optimistic decision has been made and records with higher values are selected whenever duplicated data occurs.

The initial datasets contains 6839 records but only 2513 records remained after the data cleaning process. The other change required to be done is to clip the coordinates to be easier to work with. The UTM coordinates in the original data goes from 6095314.34 to 6417698.17m in North direction and from 375724.5 to 547494.18m in east direction. In order to have better looking coordinates, 6000000 and 300000 units have been subtracted from Y and X values respectively.

We are not usually interested in an exactly rectangular area in regional modeling. Therefore, the model is usually needed to be clipped to avoid misrepresentation of data and biased results. This clipping is done by an application called “ClipGrid.exe”. This application clips generated grids using a set of vertices provided in the parameter file. The vertices can be introduced by pairs of points. In order to find these border points easily an application called “DigXY.exe” is used. The program can open a bitmap of the region and save points selected by the user as the digitization result. In this case, the area is digitized using 100 points trying not to leave any well with McMurray formation present outside the clipped area.

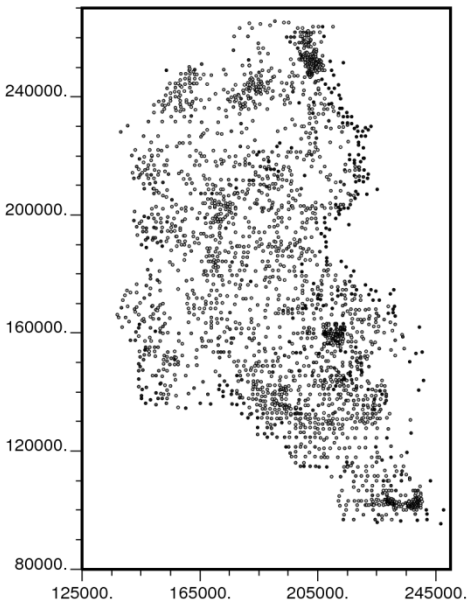

Fig. 22. Indicator map

In order to have a better understanding of the available well data, there seems to be a need to do some preliminary statistical studies on the data. There are four important variables to study. The first one is an indicator variable defined to distinguish wells with and without significant McMurray formation as defined in the previous section. This indicator has a value of 1 for 2280 records among the 2513 wells with valid data. The next variables of interest are the gross and net thickness of the formation and the mass fraction of bitumen. The histograms of these variables are shown in Fig. 23 to Fig. 25. As can be seen in the histograms there are still some zeros in different variables which show wells with no McMurray formation is present.

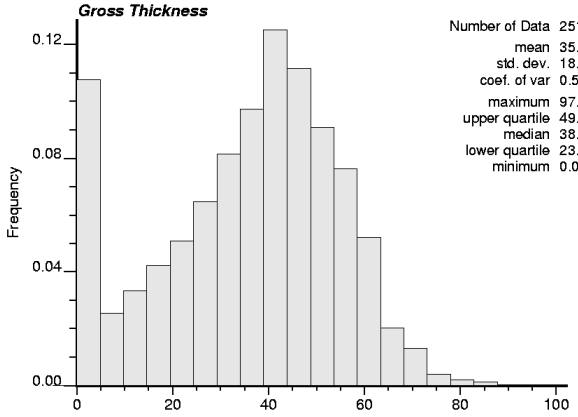

Fig. 23.Gross Thickness of Formation

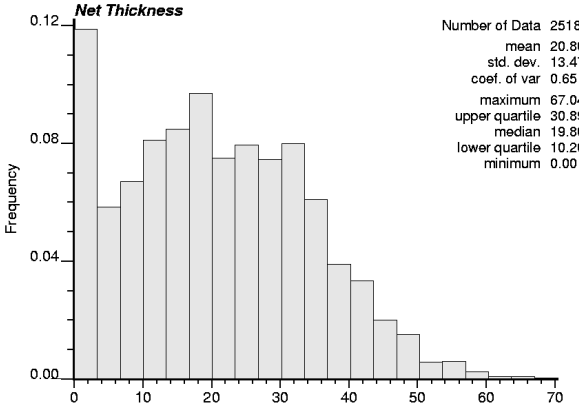

Fig. 24.Net Thickness of Formation

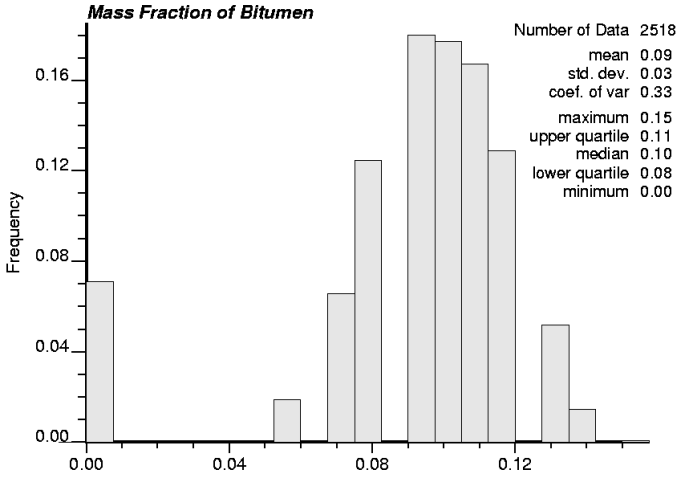

Fig. 25.Mass Fraction of Bitumen

4.1.5 Kriging indicator variable

After mapping the indicator variable and finding the borders of the area it seems reasonable to Krig the variable and clip it using the boundaries defined to examine the goodness of the borders and their relation with the probability of having bitumen inside and outside the boundaries. Kriging is one of the most important traditional mapping applications and an essential component of geostatistical simulation methods. In this part, a model of spatial uncertainty characterizing the distribution and occurrence of the indicator variables is constructed. There are 2514 data points that should be used to estimate unsampled locations that are inside the domain. In this case, the simple

Kriging was done using the given variogram model. In the given model, nugget effect is equivalent to 10 to 20 percent of sill and range is equivalent to a third of area dimension. Thus, nugget effect and range are equal to 0.017 and 70000, respectively. For Kriging 325×475 grid nodes were used. Size of each cell in X and Y directions are 400 m and 400 m, respectively. Fig. 26 shows a 2D view of Kriging result using indicators. Fig. 27 shows the Kriging result after applying the desired area.

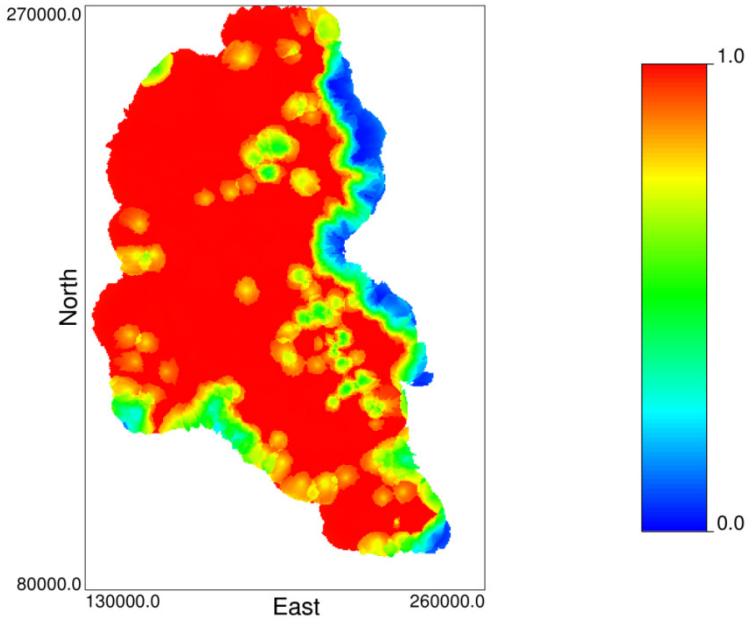

Fig. 26**.** Kriging result according to the indicators (Values less than zero has been trimmed)

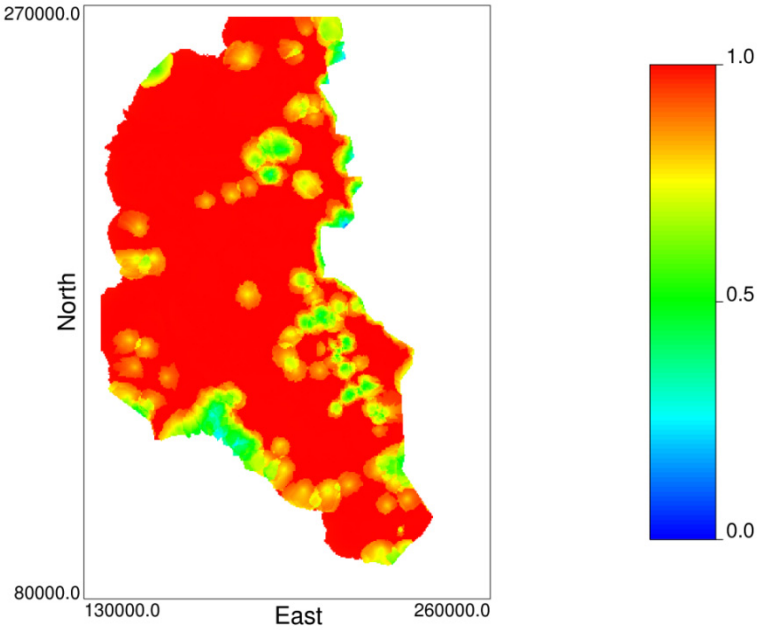

Fig. 27. Kriging result after clipping the data which are not in McMurray formation

4.1.6 Preliminary statistics

Wells are often drilled in areas with a greater probability of good reservoir rock. Closely spaced data inform fewer grid nodes and, hence, receive lesser weight. Widely spaced data inform more grid nodes and, hence, receive greater weight (C.V. Deutsch, 2002). In this project, there are clustered data in some areas. Fig. 28 shows location map of wells. It can be clearly seen in the right hand side of the map that there are three areas the wells are closer. The summary statistics were done under two different condition, equal weights and declustering weights.

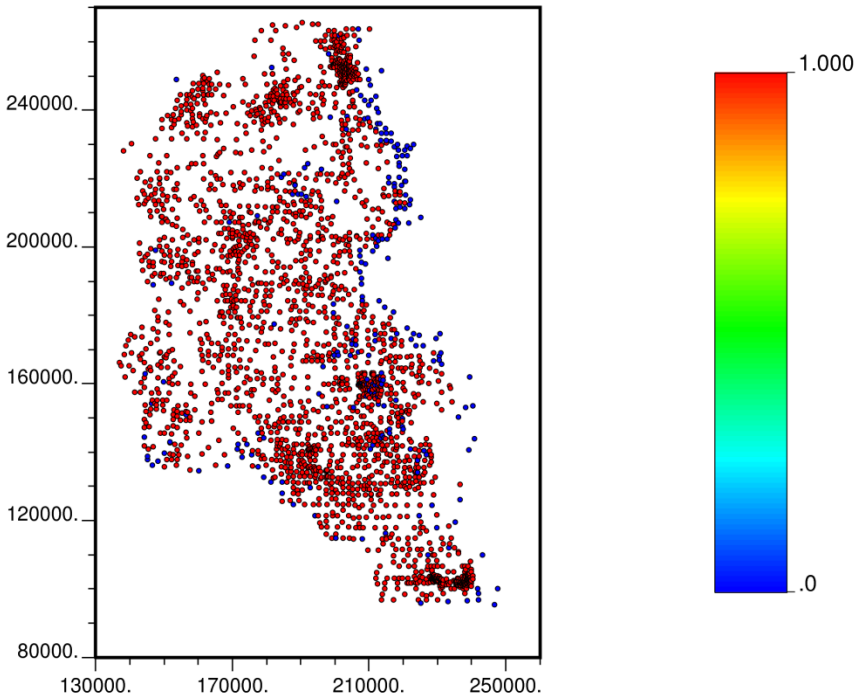

Fig. 28. Location map of the wells (The filled red circles belong to McMurray)

With declustering technique, a weight is assigned to each datum based on its closeness to surrounding data. Then the histogram and summary statistics are calculated with declustering weights. The technique of cell declustering is used in this project. For this purpose "declus.exe" program is used. The area of interest is divided into a grid of cells, then the occupied cells, and number of data in each of them is counted. Finally, weight of each data is calculated according to the number of data falling in the same cell. The summary statistics from declustering and equal weighted techniques for 2514 well data are shown in Fig. 30 and Table 10. The optimum cell size is determined automatically by "declus.exe" program. The plot of declustered mean versus cell size is shown in Fig. 29. A cell size of 16000 units with declustered mean of 16 was chosen.

The relationships between gross interval with net interval and net interval with average mass bitumen, with and without declustering were considered. Correlations between these variables have been compared in Table 11. It can be clearly seen that correlation of the cell declustering is more than equal weighted.

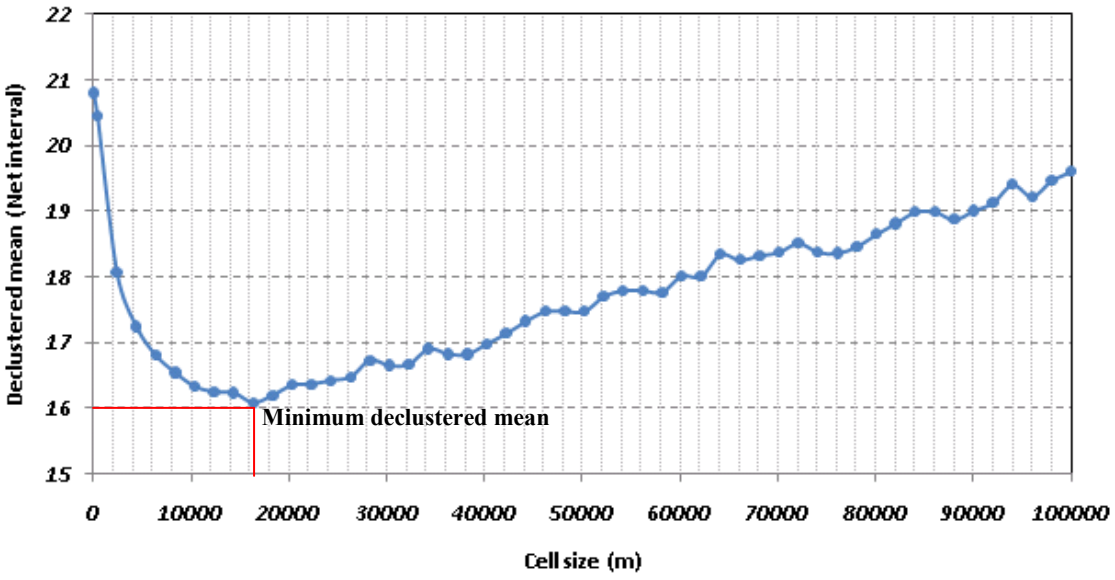

Fig. 29. Declustered mean versus cell size for Net interval

Table 10.Summary statistics of 2514 well data

	Minimum	Maximum	Mean		Standard deviation	
			Equal weighted	Cell declustering	Equal weighted	Cell declustering
Gross Interval (m)	0	97.5	35.78	29.17	18.81	19.58
Net Interval (m)	0	67.04	20.80	16.08	13.47	13.01
Average mass Bitumen (% Mass)	0	0.15	0.09	0.08	0.03	0.04

Table 11.The comparison of correlations between equal weighted and cell declustering

	Equal weighted	Cell declustering
Gross-Net (m)	0.804	0.825
Gross-Bitumen (m)	0.668	0.696

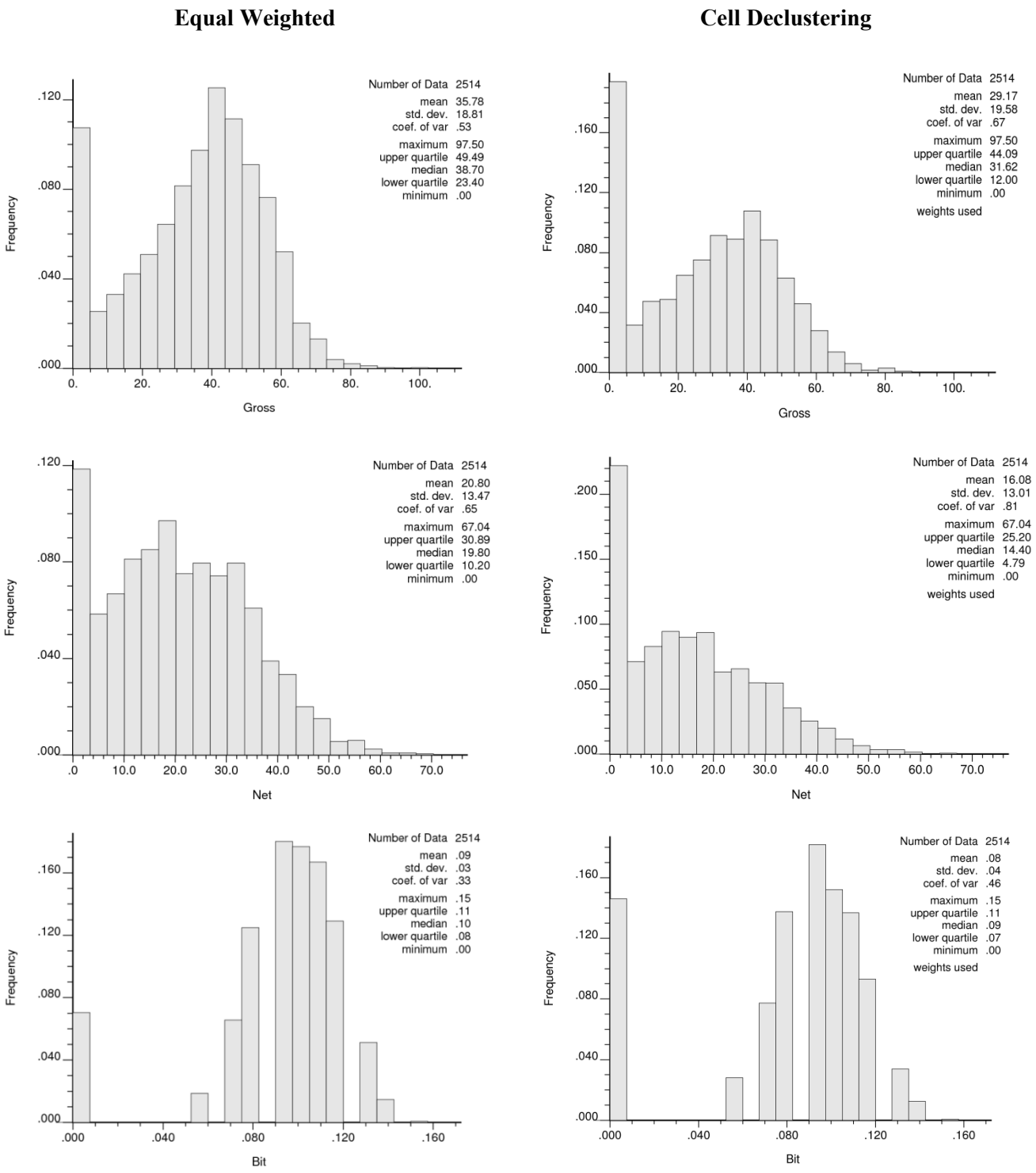

Fig. 30**.** Histogram of Gross interval, Net interval and Average mass of Bitumen with and without weight.

For estimating the amount of Bitumen in area of interest, regional area should be calculated. For this purpose, points from output of "DigXY.exe" are used and polygon area from joining the points is calculated using "Polyar.exe" program. The area of study is equal to 10.2×10^7 Km^2. To calculate the amount of Bitumen in the area of interest, Eq. (3) is used.

$$A\times\overline{T}\times\overline{B}\times C \tag{3}$$

Where A is the area of interest, $\overline{T}$ is the average net thickness of oil sand, $\overline{B}$ is the average mass of Bitumen, and C is a convergence factor. Calculation is done according to Table 12. To calculate barrels of bitumen the average net interval after declustering is used.

Table 12.Calculation of amount of Bitumen in study area

# of row	Description	Unit	formula	Value
(1)	Area	m^2	----------	10,232,151,394.4
(2)	$\overline{T}$	m	----------	16.1
(3)	$V_{Oil\,sand}$	m^3	(1)×(2)	164,532,994,421.1
(4)	$Density_{Oil\,sand}$	Kg/ m^3	----------	2,160.0
(5)	$Mass_{Oil\,sand}$	Kg	(3)×(4)	355,391,267,949,680.0
(6)	$\overline{B}$	Fraction	----------	0.0822
(7)	$Mass_{Bitumen}$	Kg	(5)×(6)	30,063,156,915,864.6000
(8)	$Density_{Bitumen}$	Kg/ m^3	----------	1,050.0
(9)	$V_{Bitumen}$	m^3	(7)/(8)	27,808,520,547.4
(10)	**Note:** 0.159 m^3 is equal to 1 bbl			
(11)	Bbl of Bitumen	------	(9)/(10)	174,910,656,515.2

4.2. Calculating the variogram

The variogram is function of distance and direction. Variogram inference proceeds in three main steps (Leuangthong, et al., 2008):

1. Calculate the experimental variogram in multiple directions for a number of lags that approximately correspond to the average spacing between data,
2. Interpret the experimental variogram points and supplement them with expert judgment or analogue data,

3. Fit a valid parametric model to the directional variograms in all directions.

Variogram maps are first generated to find the direction of continuity in the area. Variogram maps are presented in Fig. 31.

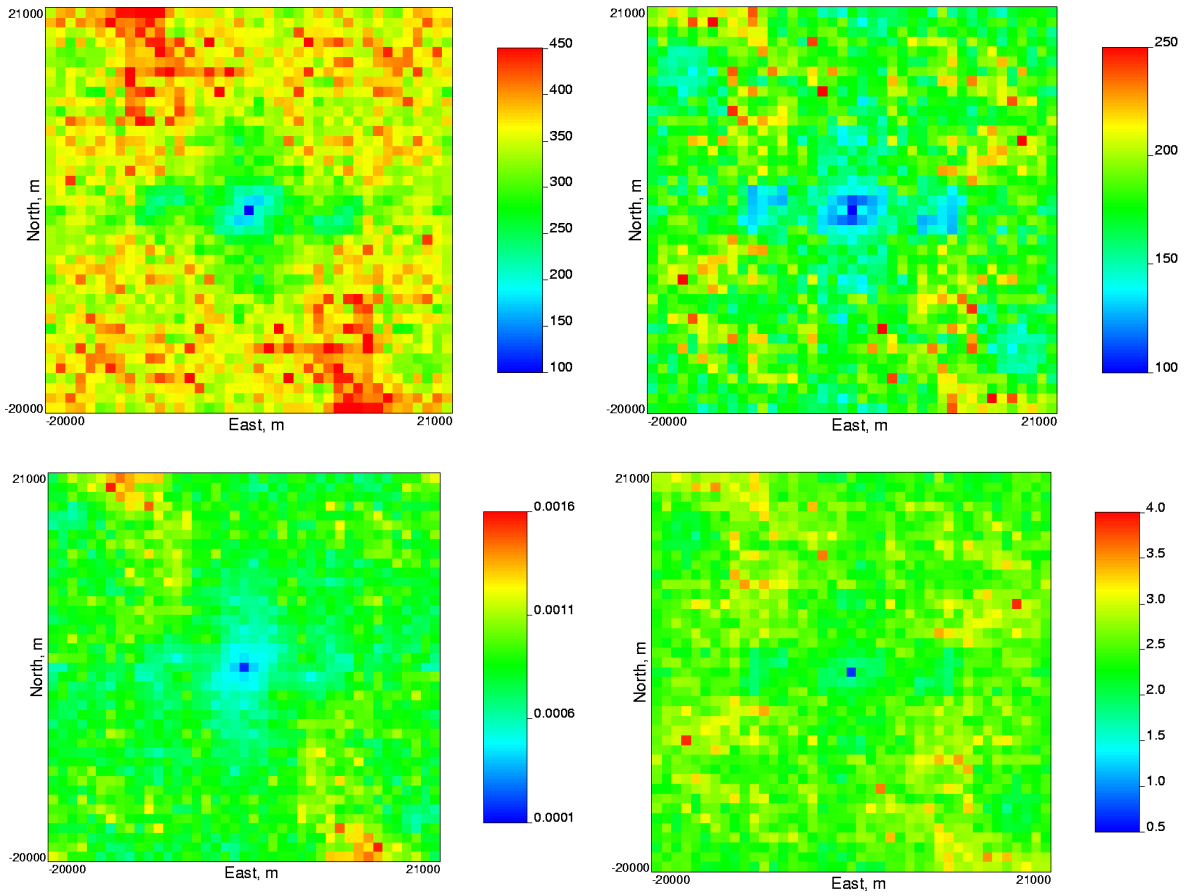

Fig. 31. Variogram maps for gross and net thickness, mass fraction of bitumen and bitumen per area

Looking at the variogram maps, an azimuth of 150 degrees south-east seems to be the direction of continuity but calculating experimental variograms they happened to have almost the same variogram range in the mentioned direction and an orthogonal one. Therefore, a horizontal variogram is used instead of a directional one for all variables.

Different variogram models have been tested by accuracy plots and cross validation in Kriging. The best resulting variogram models (based on try and error) and the corresponding accuracy plots and cross validation scatter plots are shown in the following parts.

In this part, variograms of gross interval, net interval, and bitumen were calculated. In subsequent steps such as Kriging and simulation, we need a parametric variogram model, which is fitted to the experimental points.

Gross interval

For gross interval, three variance regions can be defined as shown in Eq. (4). The first one is a nugget effect; the second one is exponential variogram structure. The last one is spherical variogram structure.

$$\gamma(h) = 0.1 + 0.87\, Exp_{\substack{a_{h\max}=10000 \\ a_{h\min}=10000}}(h) + 0.03\, Sph_{\substack{a_{h\max}=60000 \\ a_{h\min}=60000}}(h) \tag{4}$$

Net interval

For net interval, also three variance regions like as gross interval can be defined as in Eq.(5).

$$\gamma(h) = 0.1 + 0.85\, Exp_{\substack{a_{h\max}=8000 \\ a_{h\min}=8000}}(h) + 0.05\, Sph_{\substack{a_{h\max}=50000 \\ a_{h\min}=50000}}(h) \tag{5}$$

Average mass Bitumen

This variable also has variance regions as same as two other variables. Eq.(6) presents the variogram for average mass bitumen.

$$\gamma(h) = 0.3 + 0.45\, Exp_{\substack{a_{h\max}=16000 \\ a_{h\min}=16000}}(h) + 0.25\, Sph_{\substack{a_{h\max}=3200 \\ a_{h\min}=3200}}(h) \tag{6}$$

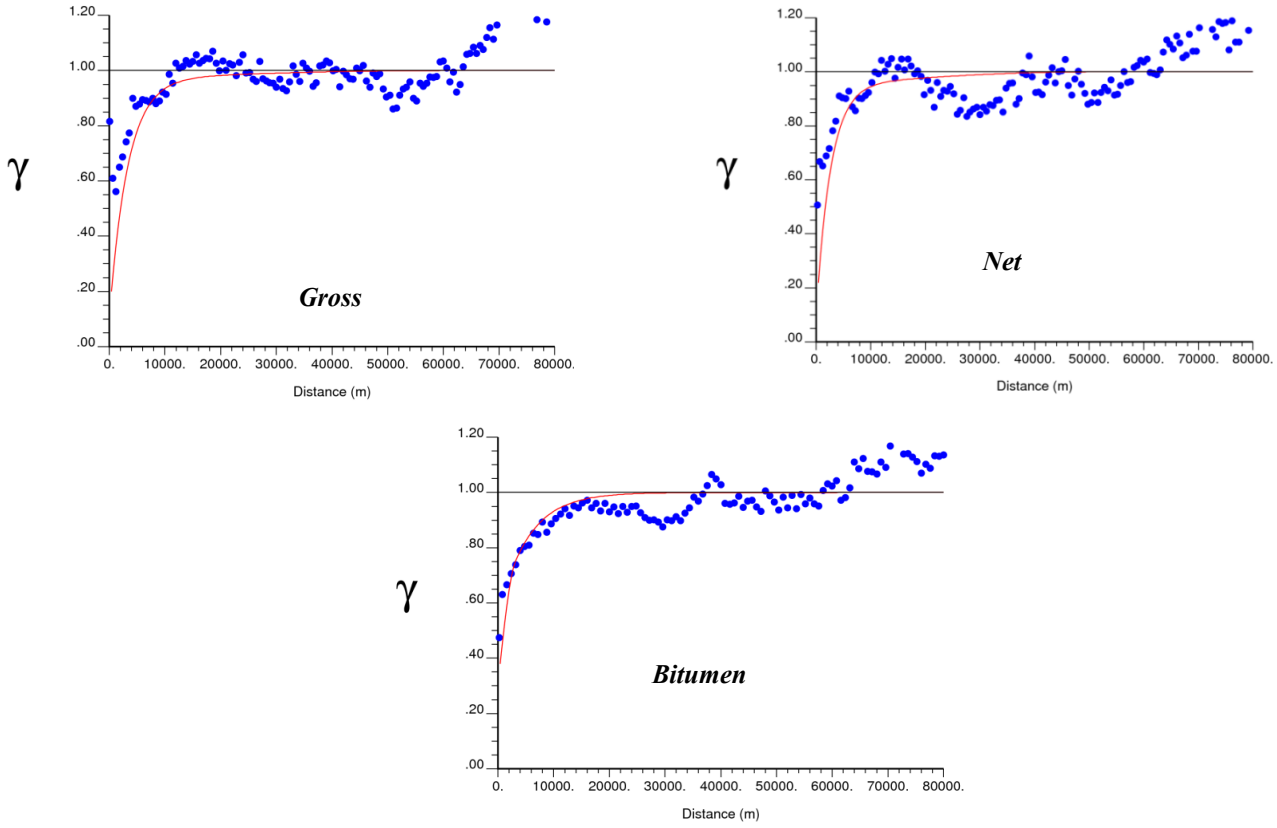

Fig. 32.The variogram models of gross interval, net interval, and average mass Bitumen

The variogram parameters corresponding to variogram shown in Fig. 31 have been summarized in Table 13.

Table 13.Variogram parameters corresponding to variograms shown on **Fig. 32**

Variable	Variance Contribution	Type of Variogram	a_{hmax}, a_{hmin}, m
Gross interval	0.1	Nugget	
	0.87	Exponential	10000
	0.03	Spherical	60000
Net interval	0.1	Nugget	
	0.85	Exponential	8000
	0.05	Spherical	50000
Average mass Bitumen	0.3	Nugget	
	0.45	Exponential	16000
	0.25	Spherical	3200

4.3. Bootstrap for uncertainty in mean

Bootstrap is a method developed by Efron. The Monte Carlo simulation is applied in this method. It is a statistical resampling technique which permits quantification of uncertainty in statistics by resampling from the original data. With this method, the uncertainty in input statistics is known. The histograms at the right hand side of Fig. 33 show the uncertainty in the mean of variables for 5000 realizations. The spatial bootstrap was applied to arrive at the distribution of uncertainty in the mean of each input variable. It can be seen that the mean of gross interval, net interval, and average mass Bitumen remain unchanged.

4.4. Trend map

The trend map is used to provide the overall trend of each variable in the entire study area. This map is created by simple Kriging with a variogram designed to reveal large scale features. Usually, a long range variogram with modest nugget effect is used (Ren, et al., 2006) .

In this case, the simple Kriging was done using the given variogram model. In the given model, nugget effect is equivalent to 30 percent of sill and range is equivalent to a third dimension area. Thus, nugget effect for gross interval, net interval, and average mass Bitumen are considered equal to 106.14, 54.43, and 0.00027, respectively. For Kriging 325×475 grid nodes was used. Size of each cell in X and Y directions are 400 m and 400 m, respectively. The trend maps of gross interval, net interval, and average mass bitumen are shown in Fig. 34. Table 14 shows comparison between the results of trend map and cell declustering. The percentage of difference between results of trend map and declustering for all variables is more than expected value. This difference should be around 5 percent, but here minimum difference is around 12.5 percent.

4.5. Model building

4.5.1 Estimation

In this step variogram models are tested to see how good they fit the data. To do so, a Kriging operation is done on the normal score transformed data. The only difference is that instead of Kriging the cell, data locations are Kriged. These values are then plotted against their true value to see how good they are. Fig. 35 shows the cross plot of true versus estimate for each variable. The

correlation of gross interval, net interval and average mass Bitumen are 0.626, 0.632 and 0.568, respectively.

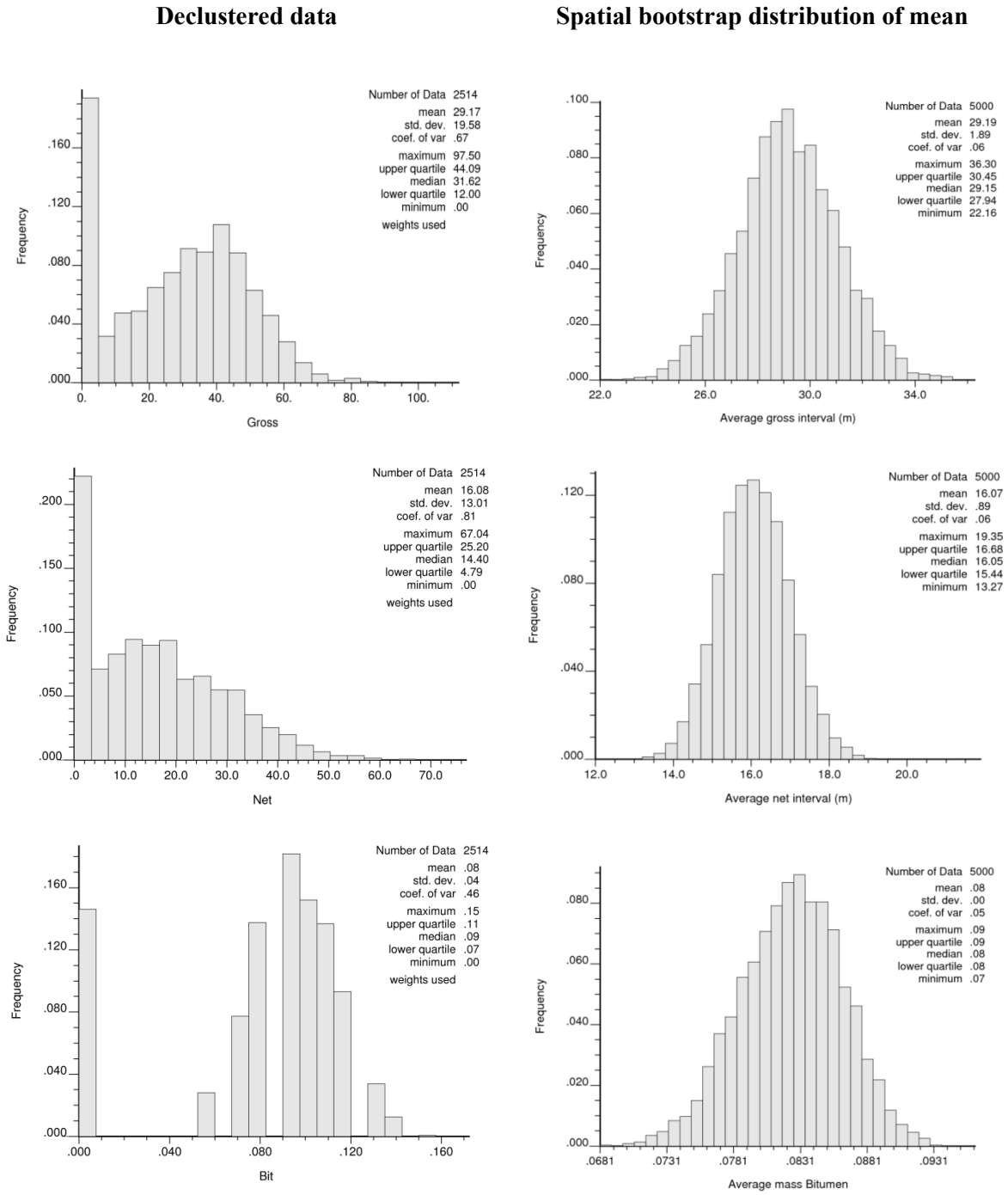

Fig. 33**.** Histogram of 2514 data for gross, net, and bit after cell declustering are shown at left hand. Histogram of spatial bootstrap results to show the distribution of uncertainty in the mean of each variable are shown at right hand.

Table 14.The comparison between average of the clipped trend model and declustered

	Average		Difference (%)
	Trend map	Cell declustering	
Gross interval (m)	33.37	29.17	14.4
Net interval (m)	18.27	16.08	13.62
Average mass Bitumen (%Mass)	0.09	0.08	12.5

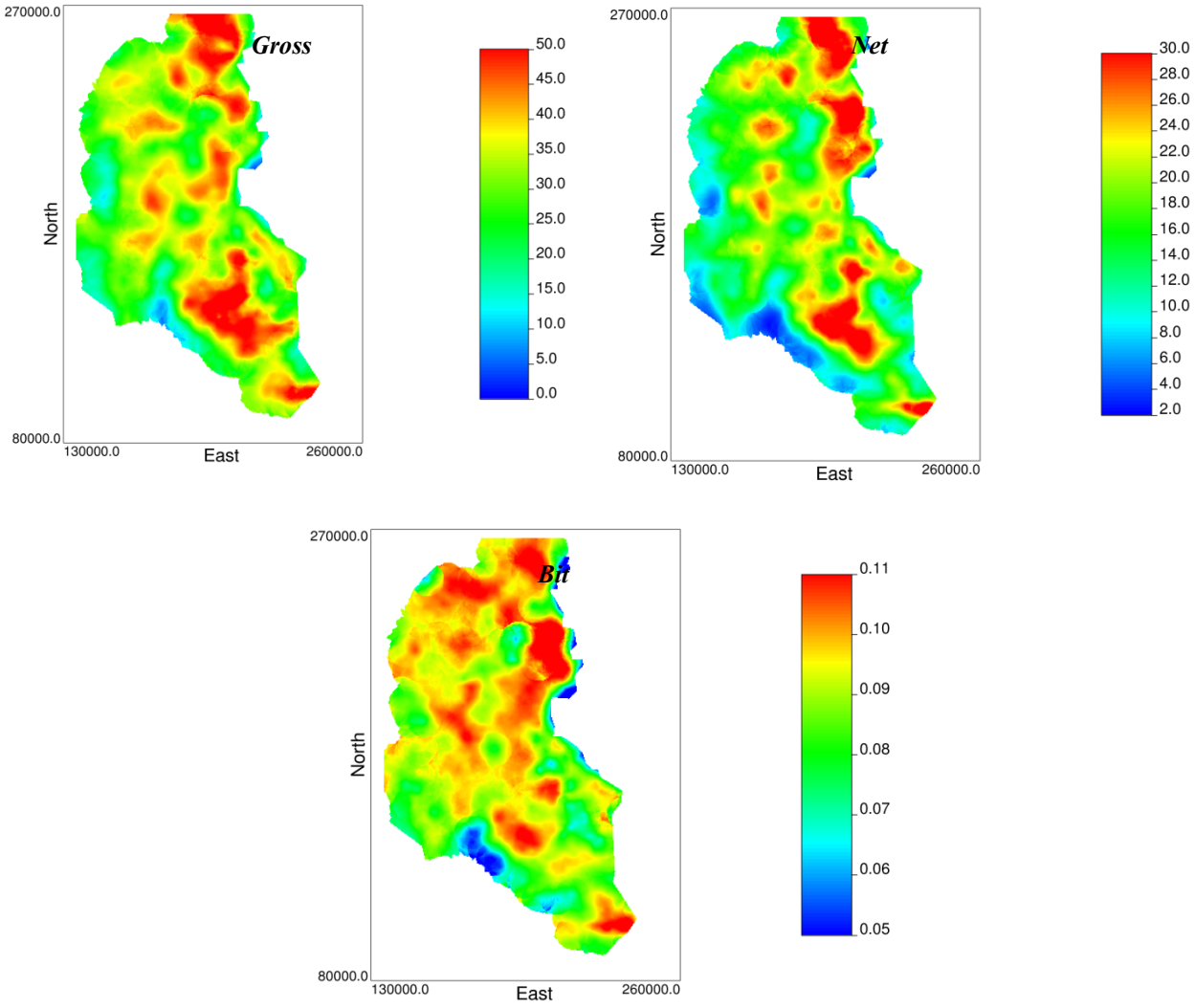

Fig. 34.The trend maps of gross interval, net interval, and average mass Bitumen

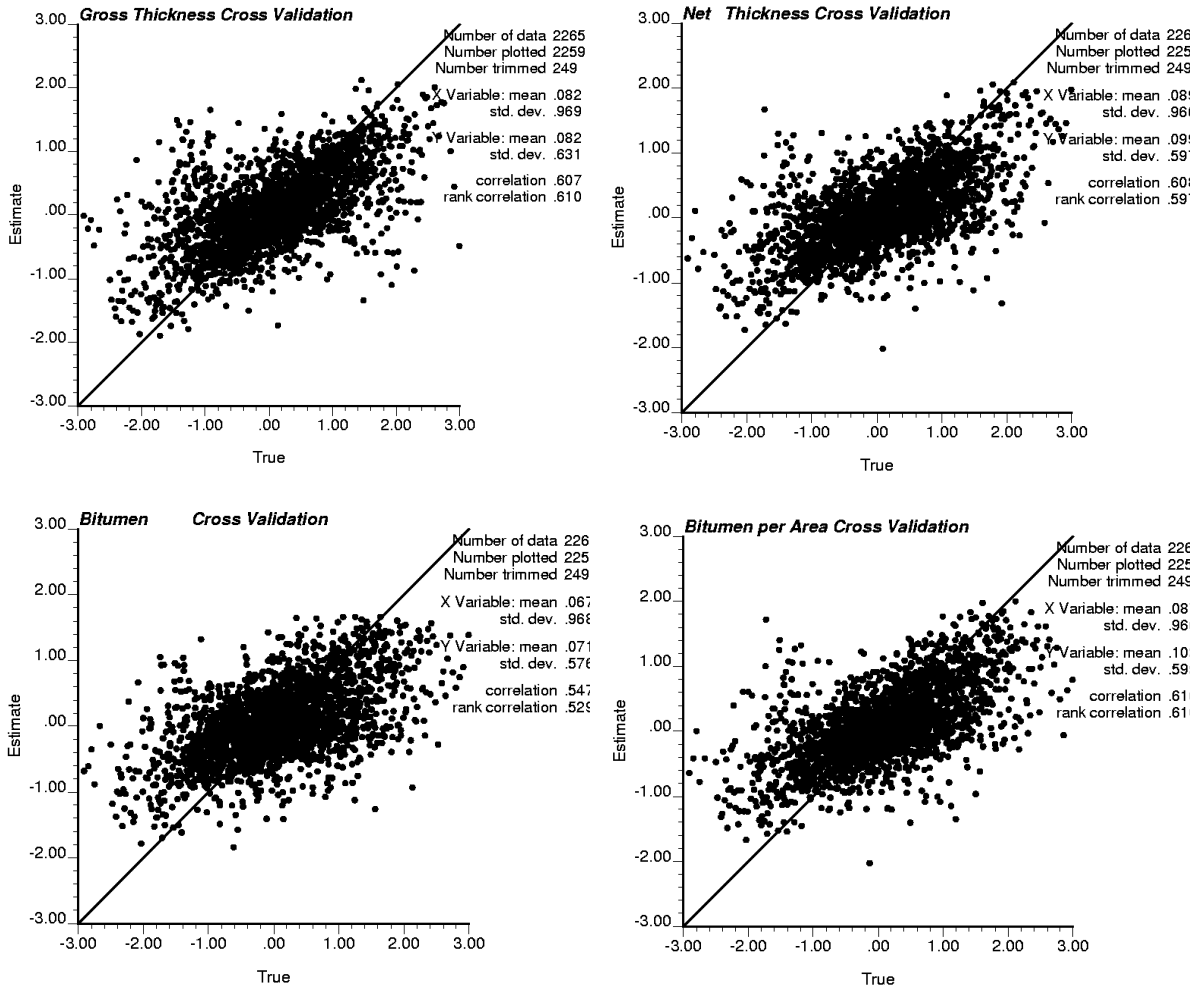

Fig. 35.Cross plot of true values versus estimated values for gross and net thickness, mass fraction of bitumen and bitumen per area

Another method used for cross validation is plotting the histogram of estimate versus true. This histogram should have a mean close to zero and a symmetric shape. Fig. 36 shows this histogram for the each variable.

Location map of error for each variable is also used for cross validation. Location map of error for gross and net intervals are shown in Fig. 37. It can be seen that the distribution of plus and minus signs approximately are same and that means there is no bias.

In the context of evaluating the goodness of a probabilistic model, specific definition of accuracy and precision are proposed. For probability distribution, accuracy and precision are based on the actual fraction of true values falling with in symmetric probability intervals of varying width *p* (C.V. Deutsch, 2002):

- A probability distribution is accurate if the fraction of true values falling in the *p* interval exceeds *p* for all *p* in [0, 1].
- The precision of an accurate probability distribution is measured by the closeness of the fraction of true values to *p* for all *p* in [0, 1].

A graphical way to check the accuracy is to cross plot actual proportion versus probability interval and see that all of the points fall above or on the 45^{o} line.

The results are ideal if the points fall close to the 45 degree line. The distribution of uncertainty are too wide when the points fall above the 45 degree line and too narrow when the points fall below the 45 degree line. The range of spatial correlation can control the spread of the distribution of uncertainty. Cross plot of actual probabilities versus the predicted probabilities for each variable are shown in Fig. 38. The closeness of the results to the 45 degree line attest to the goodness of the probabilities. As it can see in Fig. 38 the closeness of the results to the 45 degree line for net interval and average mass Bitumen are better than gross interval.

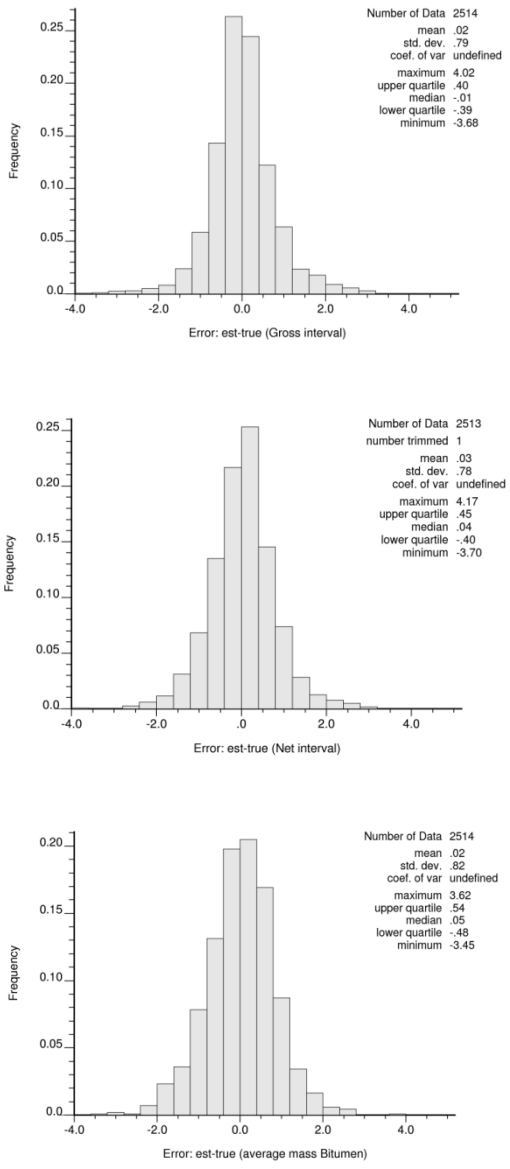

Fig. 36**.** Histogram of estimation minus true value for each variable

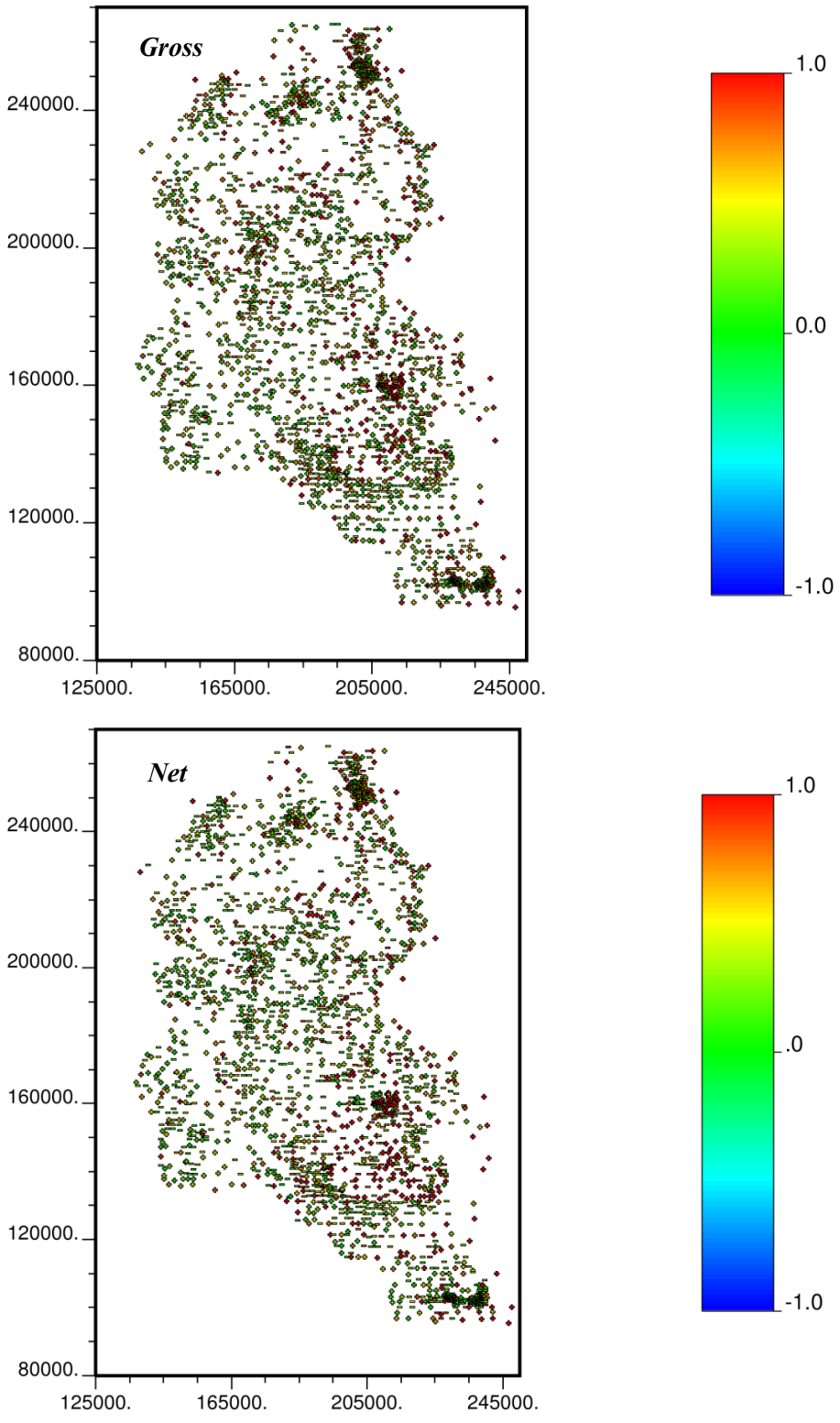

Fig. 37. Location map of estimation minus true value for gross and net intervals

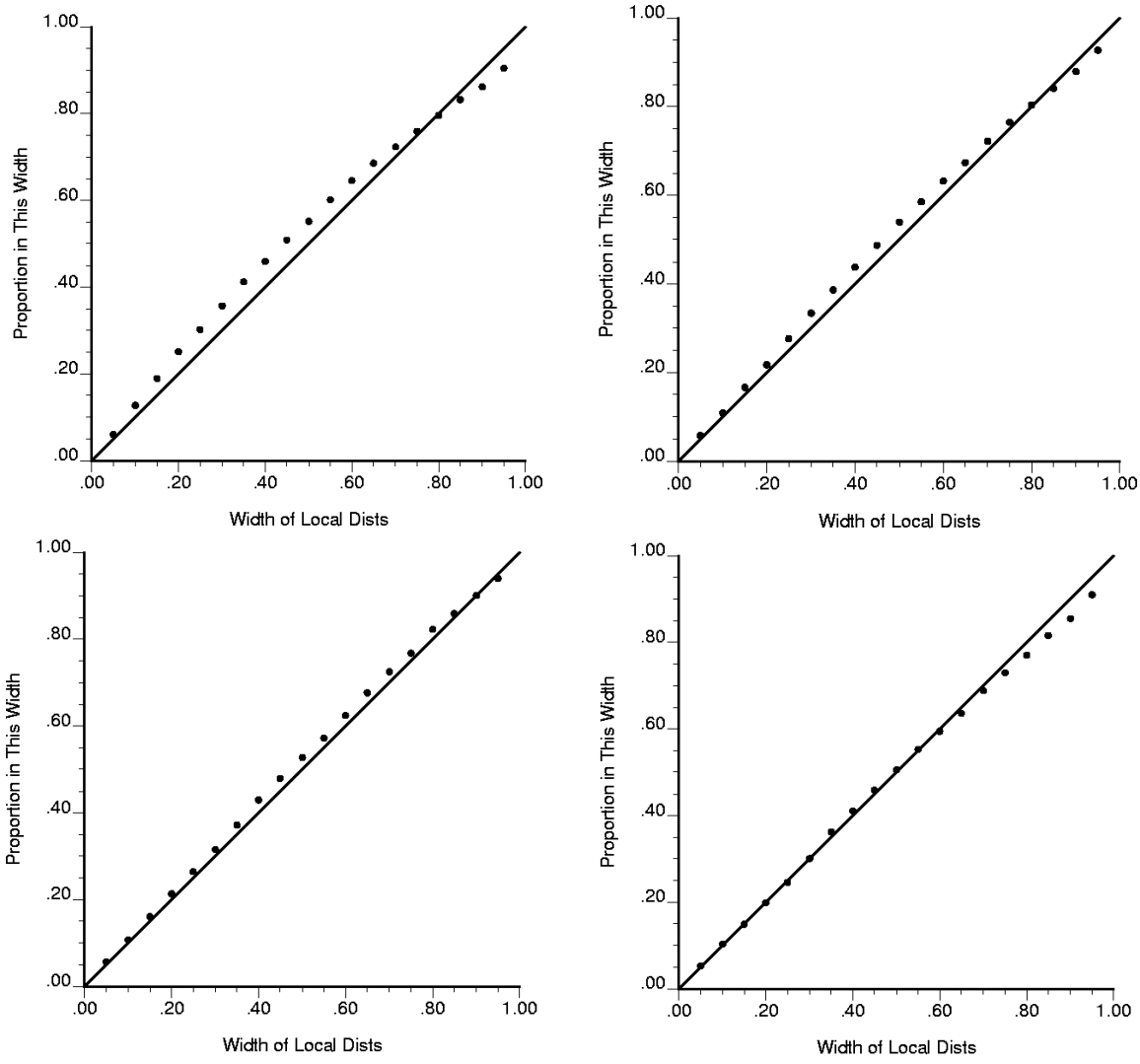

Fig. 38**.** Cross plot of actual probabilities versus the predicted probabilities for gross and net thickness, mass fraction of bitumen and bitumen per area

After cross validation, the Kriging was done for each variable. Kriging is one of the most important traditional mapping applications and an essential component of geostatistical simulation methods. In this case, Simple Kriging (SK) was done using the variogram model provided in Eqs. (4), (5), and (6). For Kriging 325×475 grid nodes was used. Fig. 39 shows the results of Kriging for each variable after clipping and transforming to the original unit.

The results of Kriging for each variable were back transformed to the original units. The results have been illustrated in Table 15.

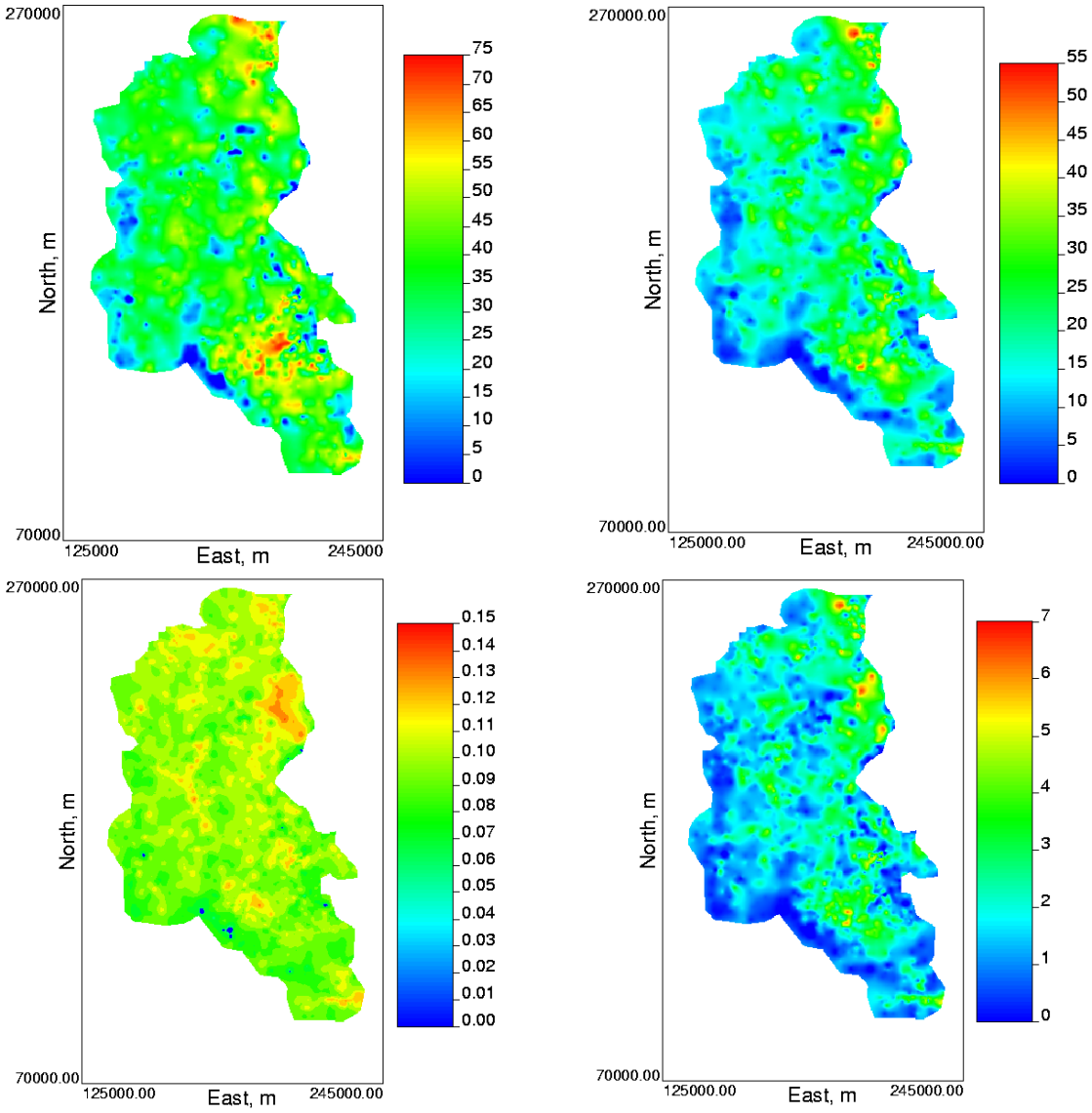

Fig. 39. Kriged map of different variables

Table 15.The results of kriging for each variable after back transforming

	Minimum	Maximum	Mean
Gross interval (m)	0	74	35.733
Net interval (m)	0	55.53	18.841
Average mass bitumen (% Mass)	0	0.14	0.0964
Bitumen per area (% Mass by m^2)	0	7.78	1.82

4.5.2 Simulation

Geostatistical realizations are being used increasingly for uncertainty quantification. In this case, for simulating, 325×475 grid nodes were used. To summarize and calculate the point-by-point average of the 100 realizations, "postsim.exe" program was used. The correlation between Kriging and simulation for gross interval, net interval, and average mass Bitumen in original units were 0.963, 0.972, and 0.853, respectively. An issue in here is the simulation of net thickness. In both simulation and Kriging there is a chance of having net thickness values higher than gross thickness. Note that in simulation it is more probable having such points. To deal with the inconsistency between net and gross thickness, net thickness is considered equal to gross thickness wherever it exceeds.

In addition to correlation between Kriging and simulation, the correlation between results of simulation and true values was calculated for each variable, all correlations were around 0.98.

The result of simulation for each variable has been illustrated in Table 16. The fluctuations of the realization variograms were also investigated. Fig. 40 shows variogram reproduction. The blue is the calculated variogram, yellow is average of simulated, and reds are 100 realizations. It can be seen that at the short distances, the variograms have been reproduced well.

To show uncertainty P_{10} and P_{90} values were used. The P_{10} represents there is a 90% probability of being larger than this value. It can also be used to identify the high value areas because when the P_{10} value is high then the value is surely high. The P_{90} represents there is a 90% probability of being less that this value. The P_{90} map can be used to identify the low valued areas because when the P_{90} value is low then the value is surely low.

The P_{10}, P_{90}, and P_{90}-P_{10} maps for gross interval, net interval and average mass Bitumen are shown in Fig. 41, Fig. 42, and Fig. 43, respectively.

Table 16.The results of simulation for each variable

	Minimum	Maximum	Mean
Gross interval (m)	0	90.6	33.49
Net interval (m)	0	67.04	18.71
Average mass bitumen (%Mass)	0	0.15	0.082
Bitumen per area (%Mass by m^2)	0	7.34	1.87

4.6. Comparison

In this section, the results of estimation and simulation are compared with true values. Fig. 44 shows comparison between true values and results of estimation and simulation. In addition, the amount of Bitumen according to the different methods has been summarized in

Table 17. It can be seen that the obtained results for amount of Bitumen from estimation and simulation are more than declustering.

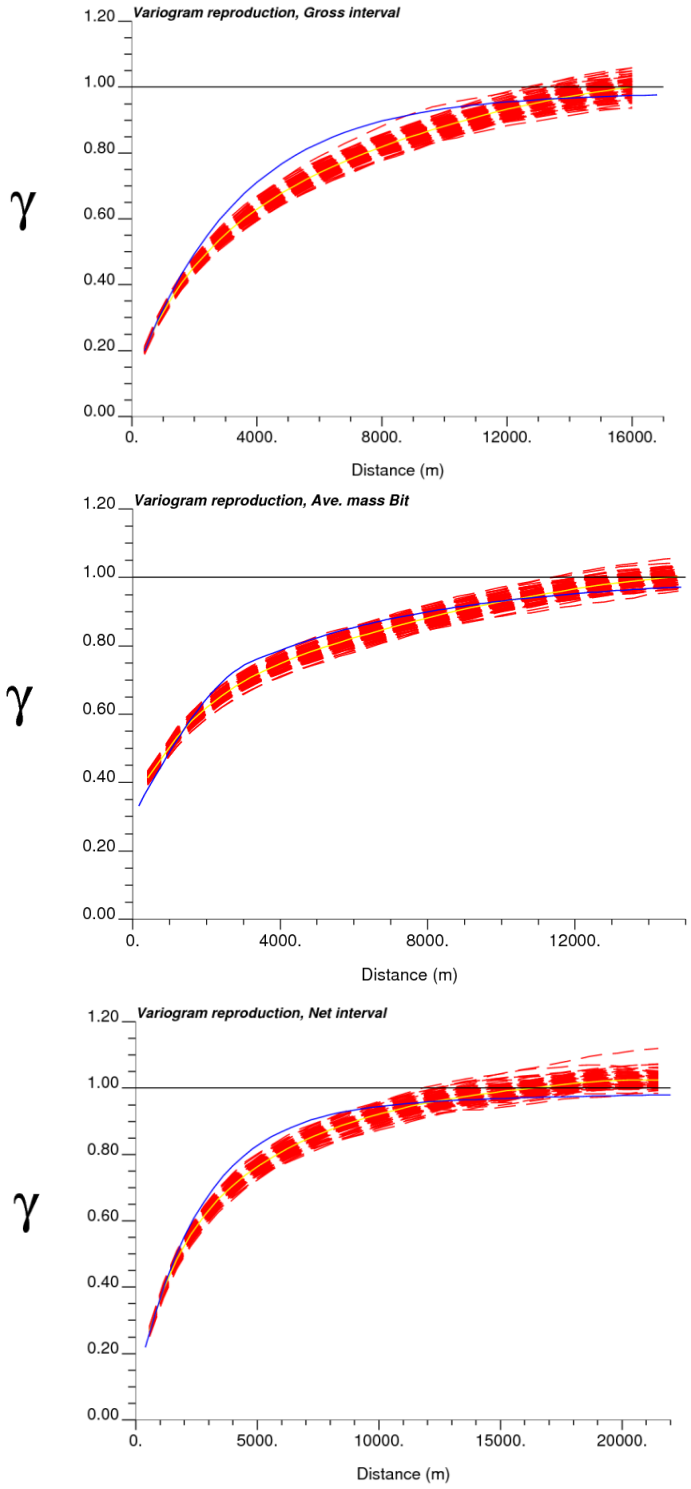

Fig. 40.Histogram and variogram reproduction (yellow line is the average variogram of 100 realizations and blue line is the calculated variogram)

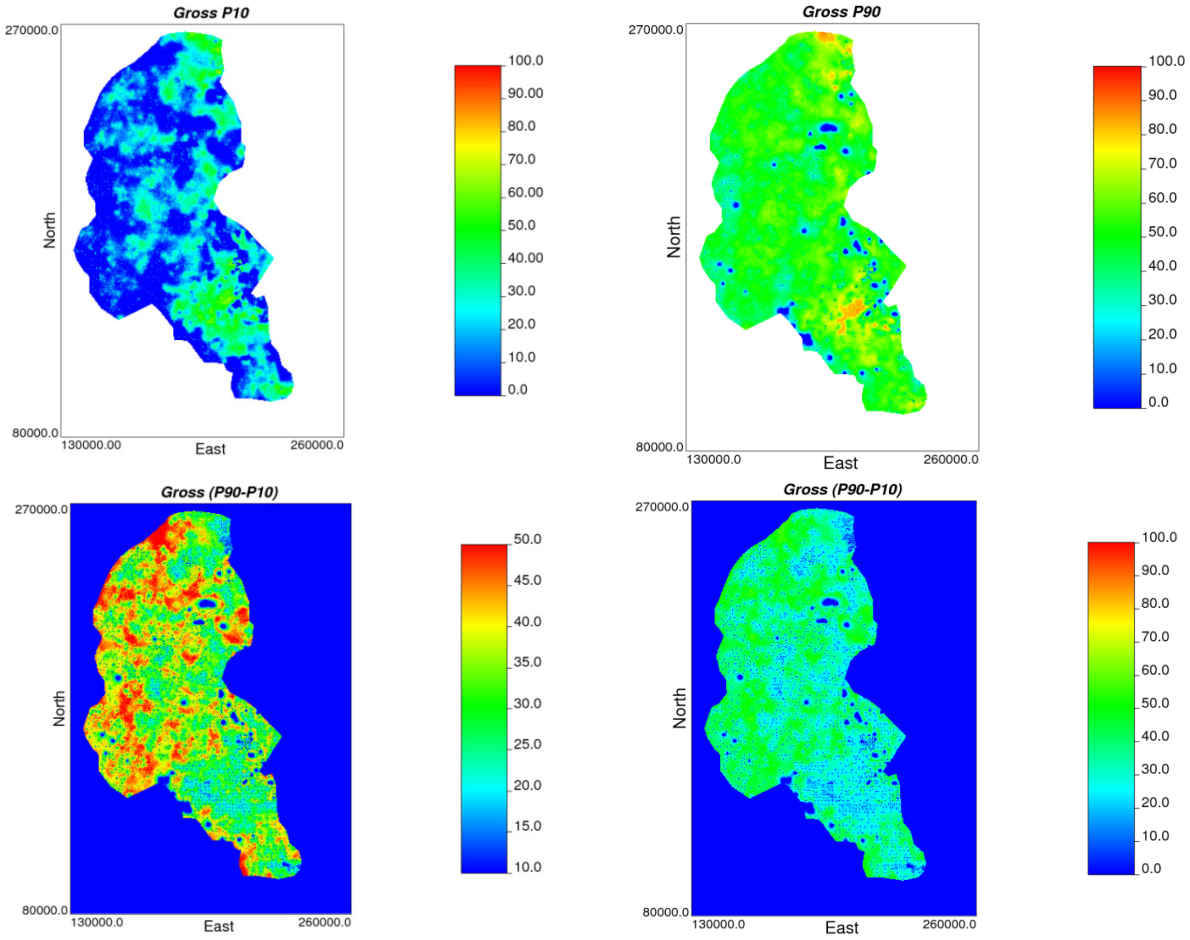

Fig. 41.The P_{10}, P_{90}, and P_{90}-P_{10} maps of gross interval

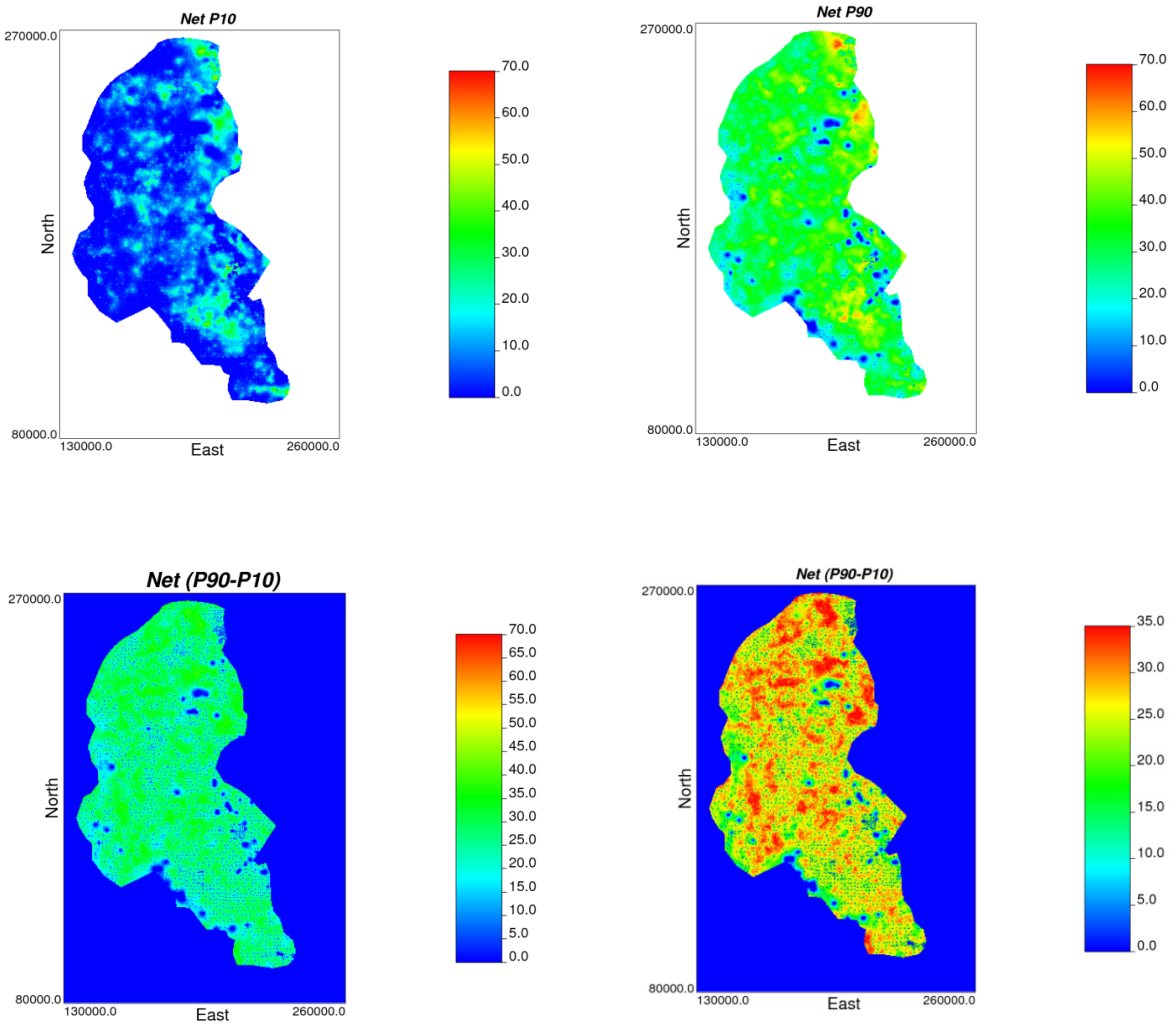

Fig. 42.The P_{10}, P_{90}, and $P_{90\text{-}P10}$ maps of net interval

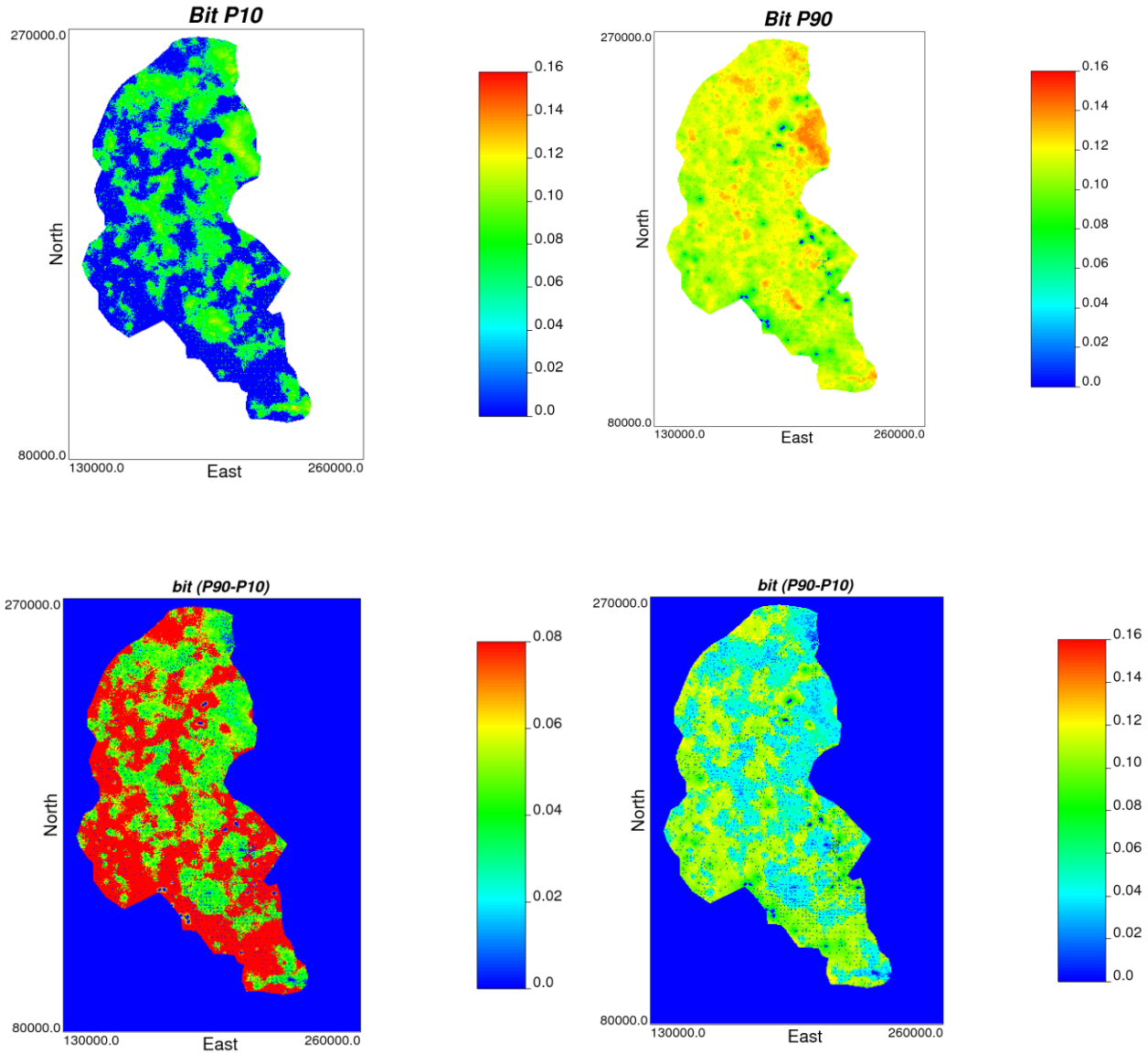

Fig. 43.The P_{10}, P_{90}, and $P_{90\text{-}P10}$ maps of average mass bitumen

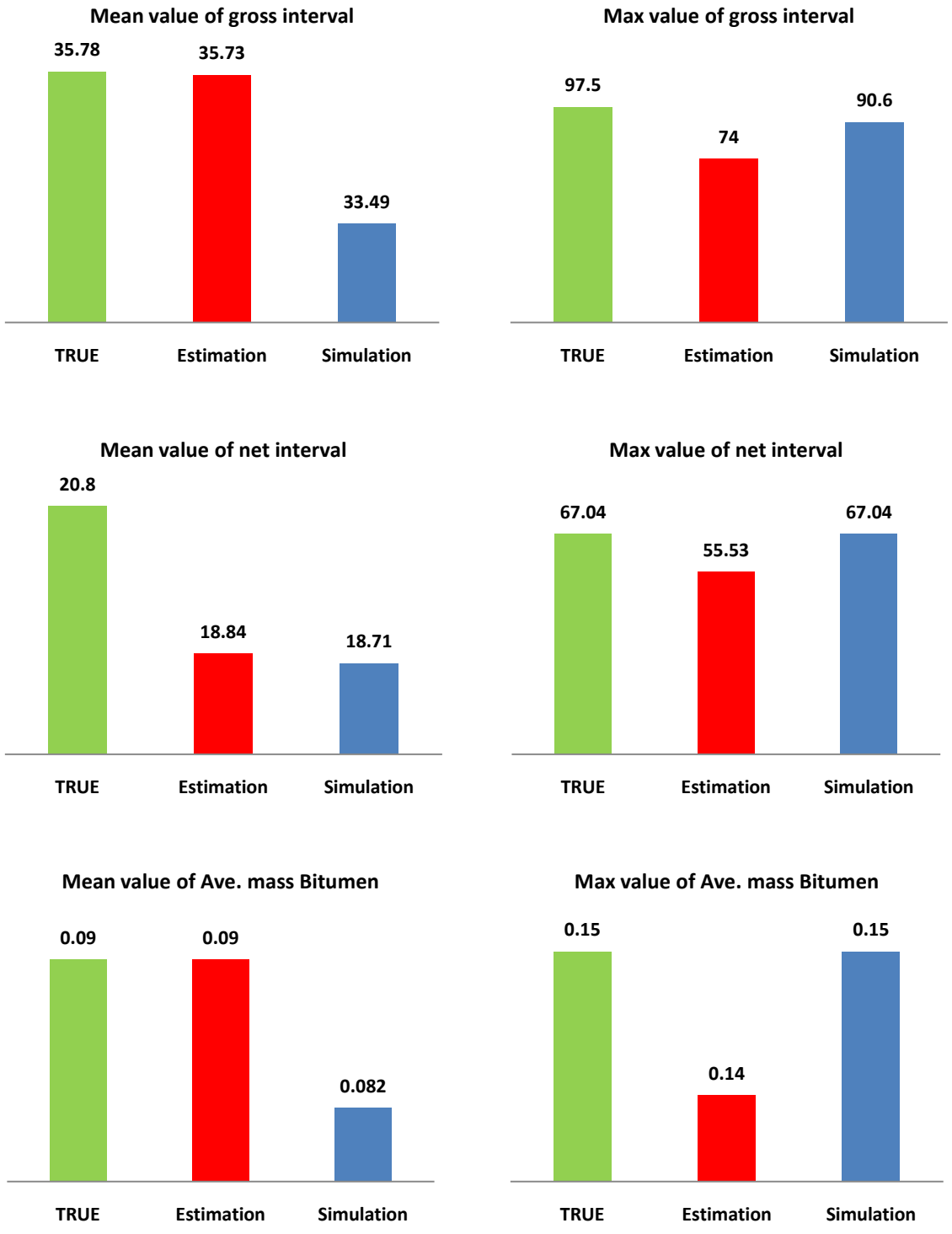

Fig. 44. Comparison of true values with the results from estimation and simulation

Table 17.of Bitumen in study area based on different methods

Method	Ave. Net interval (m)	Bbl of Bitumen $\times 10^9$	Bbl of Bitumen $\times 10^9$ (Based on fourth variable)	Difference from declustering (%)
Declustering	16.1	175	232	--------
Estimation	18.8	240	254	27
Simulation (avg)	18.7	204	260	14.2
Simulation (P10)	6.41	48	91	--------
Simulation (P90)	30.93	494	459	--------

4.7. Sensitivity analysis

To perform sensitivity analysis, the obtained results for mean uncertainty were used. For this purpose, the P_{10}, P_{50}, and P_{90} values of mean uncertainty were calculated for each variable using "quantile.exe" program. The results has been illustrate in Table 18. Afterwards, SK was done three times for each variable according to the obtained values for P_{10}, P_{50}, and $P_{90.}$ Average value of each variable after clipping has been represented in Table 19. It can be clearly seen that there is no significant difference between the results of SK with different means belong to uncertainty interval.

According to the presented value for P_{10} and P_{90} of net interval and Average mass Bitumen, amount of Bitumen for each of them was calculated. The result has been presented in Table 20. It can be seen that the amount of bitumen for estimation method and P10 and P90 values varies between 229 and 234 billion bbl.

Table 18.Obtained result from quantile program for P10, P50, and P90

	Spatial bootstrap of mean		P_{10}	P_{50}	P_{90}
	Min.	Max.			
Gross interval (m)	22.15	36.30	26.79	29.15	31.62
Net interval (m)	13.26	19.34	14.93	16.04	17.23
Ave. mass Bitumen (%Mass)	0.068	0.094	0.077	0.082	0.087

Table 19.Average of SK after clipping based on P10, P50, and P_{90} values belong to mean uncertainty interval.

	Average after cliping		
	P_{10}	P_{50}	P_{90}
Gross interval (m)	34.29	34.4	34.51
Net interval (m)	18.77	18.84	18.93
Ave. mass Bitumen (%Mass)	0.092	0.0931	0.0934

Table 20.Amount of Bitumen for estimation method according to the P_{10} and P_{90} values

	P_{10}	P_{90}
Net interval (m)	18.77	18.93
Ave. mass Bitumen (%Mass)	0.092	0.0934
Bbl of Bitumen ($\times 10^9$)	229	234

4.1. Conclusion

The predicting of porosity and permeability at unsampled locations of reservoir is one of the important problems in petroleum engineering. Micro modeling with core photograph data provides an improved understanding of porosity and permeability relationships within facies. The results of micro modeling show that in this case, the relationship between horizontal permeability, vertical permeability, and porosity are as shown in Eq. (7) to (9)

$$K_{H-effective} = 2973\ln(\phi) + 5712 \qquad (R^2 = 0.822) \tag{7}$$

$$K_V = 3099\ln(\phi) + 6653 \qquad (R^2 = 0.835) \tag{8}$$

$$K_V = 998\ln(K_{H-effective}) - 5111 \qquad (R^2 = 0.812) \tag{9}$$

For regional modeling four steps should be followed. These steps include (1) data assembly, (2) Preliminary statistics, (3) model building, and (4) post processing. In this paper reservoir of the McMurray was characterized using the regional modeling. Many different maps were created to reveal different aspects of the gross interval, net interval, average mass Bitumen and their uncertainty. P_{10} and P_{90} maps provide heterogeneity and uncertainty information on the gross interval, net interval and average mass bitumen.

As can be seen in Table 17, the calculated values are different. Some sources of errors which have caused these differences are mentioned below:

- Since wells are not distributed evenly, declustered averages are different from the original ones.

- It is not accurate to average net thickness and mass fraction of bitumen separately and multiply them in the rough estimation. Therefore, the rough estimate calculated using net and bit averages is not the same as the one calculated based on the fourth variable.
- The number of estimated points in Kriging where net thickness is larger than gross is not too high considering the total number of cells. Therefore, the average net thickness and the modified net thickness are almost the same (they are the same after rounding); but in simulation two variables vary more.
- The total estimated bitumen in place is almost the same for the two methods based on Kriging as opposed to simulation where the difference is significant.
- When simulation is applied it is more effective to use either net and bit variables or the bitnet in calculating reservoir estimates.
- P10 estimates show that at least there are 48 to 91 (using two different methods) billion barrels of oil in place by 90 percent chance.
- P90 estimates stand for 10 percent probable optimistic average which shows that there may be 459 to 494 (using two different methods) billion barrels of oil in place.
- Generally said, Kriging has resulted in higher estimate than simulation average which can be due to the smoothing effect of Kriging.

5. References

Deutsch, C. V. (2009). *Estimation of vertical permeabilty in the McMurray formation.* Paper presented at the Canadian International Petroleum Conference, Calgary, Alberta, Canada.

Deutsch, C.V. (2002). *Geostatistical Reservoir Modeling*. New York: Oxford University Press.

Deutsch, C.V. , & Journel, A. (1998). *GSLIB: geostatistical software library and user's guide* (2nd ed.): Oxford University Press.

Hein, F. J., & Cotterill, D. K. (2000). *An atlas of lithofacies of the McMurray formation, Athabasca oil sands deposit, Northeastern Alberta: surface and subsurface*: Alberta Energy and Utilities board.

Leuangthong, O., Khan, D., & Deutsch, C.V. (2008). *Solved Problems in Geostatistics*. New York: Wiley Inter science.

Ren, W., Mclennan, J.A., Leuangthong, O., & Deutsch, C.V. (2006). Reservoir Characterization of McMurray Formation by 2D Geostatistical Modeling. *Natural resource Research, 15*(2), 111-117.

Review of mini modeling and 3D conventional modeling in geostatistics with focus on McMurray data

Mohammad Mahdi Badiozamani, Yashar Pourrahimian, Mohammad Tabesh
Mining Optimization Laboratory (MOL)
University of Alberta, Edmonton, Canada

Abstract

Predicting the performance of in-situ recovery processes is required to optimize development planning and resource management in mining and petroleum projects. In this paper, two different concepts are presented; mini modeling and the 3D conventional modeling. In the first part of this paper, the mini modeling is discussed. In general, the mini modeling focuses on the porosity modeling of the formation in decimeter resolution. Then, the permeability is simulated through a number of realizations, and finally, the permeability is scaled up for the domain of interest through flow simulation. The mini modeling steps are implemented on a data set from the McMurray formation. In the second part, the steps of 3D conventional modeling are discussed and results from applying those steps to the data set from McMurray formation are illustrated. As the result of 3D conventional modeling, the porosity for different facies in the formation is both estimated and simulated through a number of realizations.

1. Introduction

This paper is divided into two parts: mini modeling and 3D conventional modeling. The mini modeling starts with section (2.1) about a survey on the characteristics of the data from McMurray formation, in terms of some statistics and histograms. Then, in section (2.2), the variogram, corresponding to each facies is calculated, followed by the variogram modeling. The simulation results for the porosity are discussed in section (2.3). Then, the permeability and flow simulation steps are discussed and the results for permeability and flow simulations are illustrated in section (2.4).

The 3D conventional modeling steps are discussed in the second part of the paper. In section (3.1), the facies proportions are calculated for each cell in the cubed grid. In section (3.2), the indicator variograms of facies are calculated, followed by the variogram modeling. After cross validating, the variogram models are used in the estimation and simulation of the facies in section (3.3). Section (3.4) starts with the declustering of the data points. Afterwards, based on the declustering weights, the variogram of porosity for each facies is calculated and modeled. The cross validation is done in order to check the goodness of variogram models as well. Estimation and simulation of porosity for each facies and the final porosity model are presented in section (3.5).The sample parameter files of GSLIB that are used in mini modeling and 3D conventional modeling are listed in the appendix section.

2. Mini Modeling

To do the geostatistical modeling some software are required. It is decided to use a set of free geostatistical tools as well as general software as mentioned in Table 1.

For mini modeling four steps should be done. These steps are as follows: (1) discussing the data characteristics, (2) calculation and modeling the porosity variogram only for one facies, the sandy IHS, (3) simulation of the porosity, and (4) simulation of the permeability and the flow.

Table 1. Required software

#	Software Name	Description	Website
1	Notepad ++	A professional open source text editor	http://Notepad-plus.sourceforge.net
2	Cygwin	A command prompt application based on Linux syntax	http://www.cygwin.com
3	SGeMS	A free set of geostatistical tools provided by Stanford university	http://sgems.sourceforge.net
4	GSLib	A free command based set of geostatistical tools by Clayton Deutsch and Manu Schnetzler.	http://gslib.com
5	MS Excel	A commercial spreadsheet used for doing some statistical operations and charting	http://office.microsoft.com

2.1. McMurray data characteristics

The data set used is a set of well logs data collected using 37 wells. Data have been measured along each well in 10 cm intervals. Wells are not distributed evenly over a large domain of 6000 by 2500 meters. Fig. 1 shows well locations. The domain of study is defined as a 6000*2500*78 m cube which is gridded by 50*50*1 m blocks. The facies parameter in the data file represents different facies. Table 2 shows the numbering scheme of the facies. The frequency of each facies is shown in Fig. 2.

Table 2. Facies numbering scheme

Number	Facies	Number	Facies
1	Sand	5	Breccia
2	Sandy IHS	6	Mud (plug)
3	Muddy IHS	7	Mud (bottom)
4	Mud (top)	9	Below or/and above the McMurray

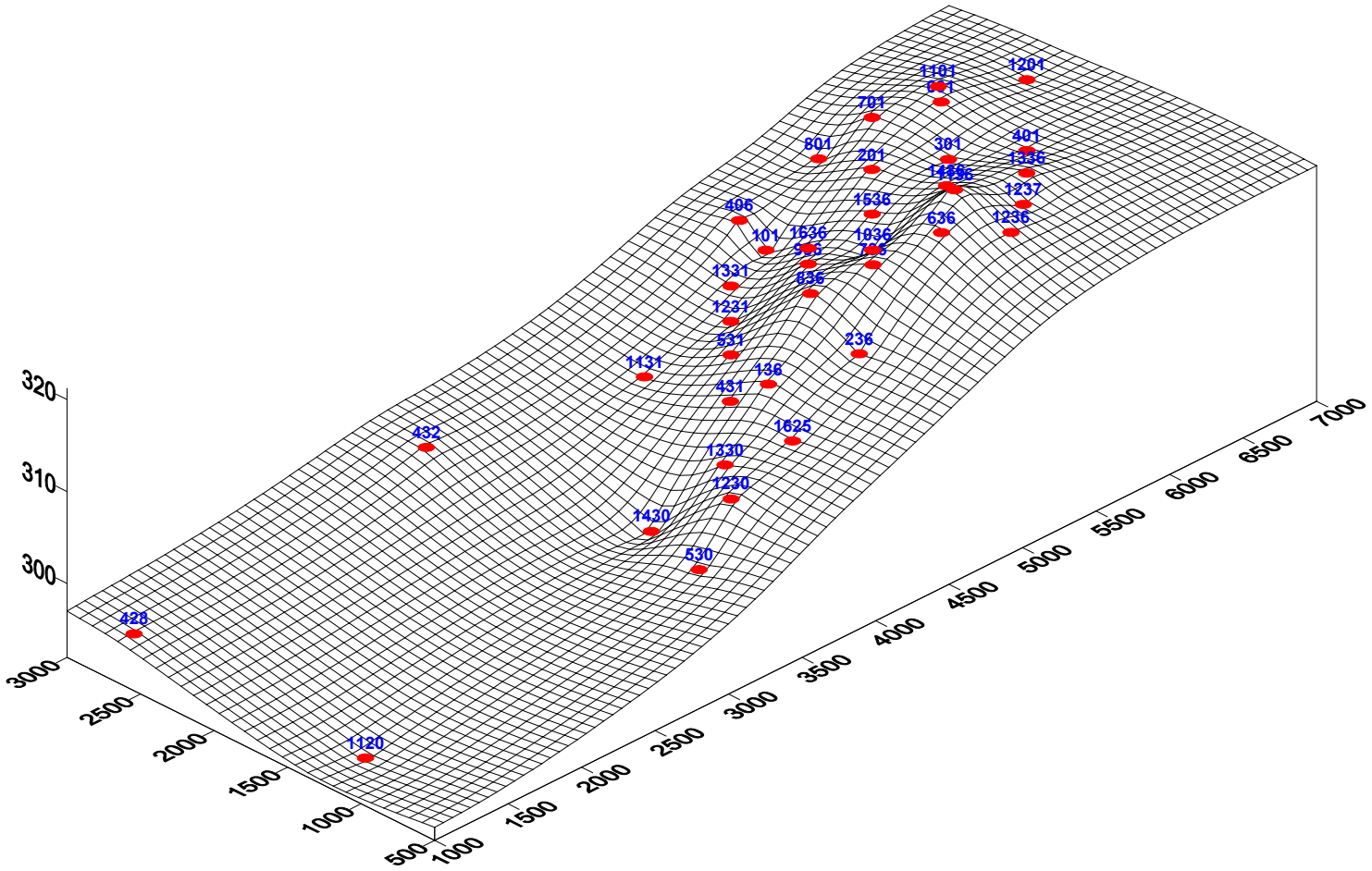

Fig. 1. Well locations and topology map of the study area

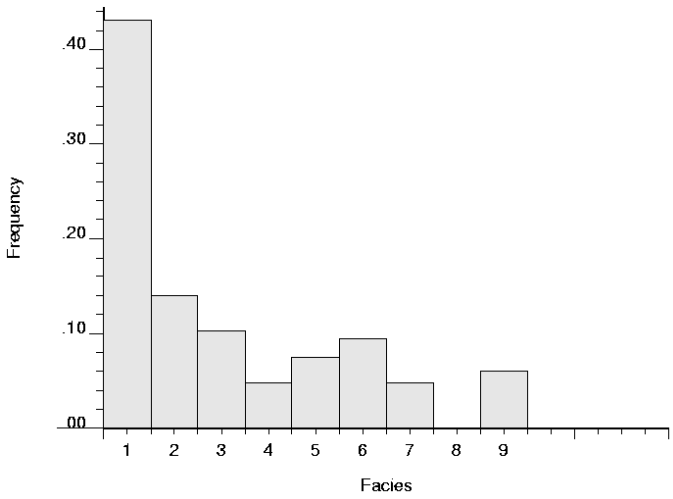

Fig. 2. Facies histogram

There are a number of fields in the database. The titles and a brief description of them are as follows:

- Well ID: the identification code of the wells.
- RX, RY and SZ: these three real numbers are the spatial coordinates of the well data in X, Y and Z orientations, respectively. The resolution of the measurements is decimeters.
- Elevation: a real number, representing the elevation from the sea level.
- Facies: an integer number, representing the code of facies Table 2. For later calculations, facies 9 is deleted, and then facies 4, 6 and 7 are all considered to be muddy shale and grouped together as a new facies, 4.
- Porosity: a real number, which represents the porosity of different facies. In the database, the points that their porosity has not been measured are reported to have the porosity of -1, which should be filtered in the calculations. Due to the precision of the measurement instruments, in some cases, the measured porosity is reported as "0".
- Oil saturation: a real number, which represents the percent of oil saturation. 0 and -1 values have the same considerations as those of the porosity field.
- The porosity frequency histograms of facies are illustrated in Fig. 3.

As we want to do mini modeling for facies 2, this facies was more considered. Fig. 4 shows the top and bottom surfaces of facies 2 in the study area. It can be seen that the top surface is smoother than the bottom. Fig. 5 shows that well 428 does not cut the facies 2 and it can be an anomaly.

2.2. Variograms

Prior to calculating the experimental variogram, the data are transformed to normal scores, using the *NSCORE* command of *GSLIB*. The transformation is required, because the variograms will be used in the sequential Gaussian simulation (SGS), which requires variogram for normal scored values.

2.2.1 Variogram Calculation

The variogram is calculated for the facies 2, the sandy IHS. As noted in the data characteristics in section 1, there are some -1 as porosity values in the data set. These values are trimmed in the

variogram calculation. Furthermore, since the trial variogram showed a very long range, only two meters is considered for variogram calculation and modeling. The variogram calculation parameters for vertical direction are presented in Table 3.

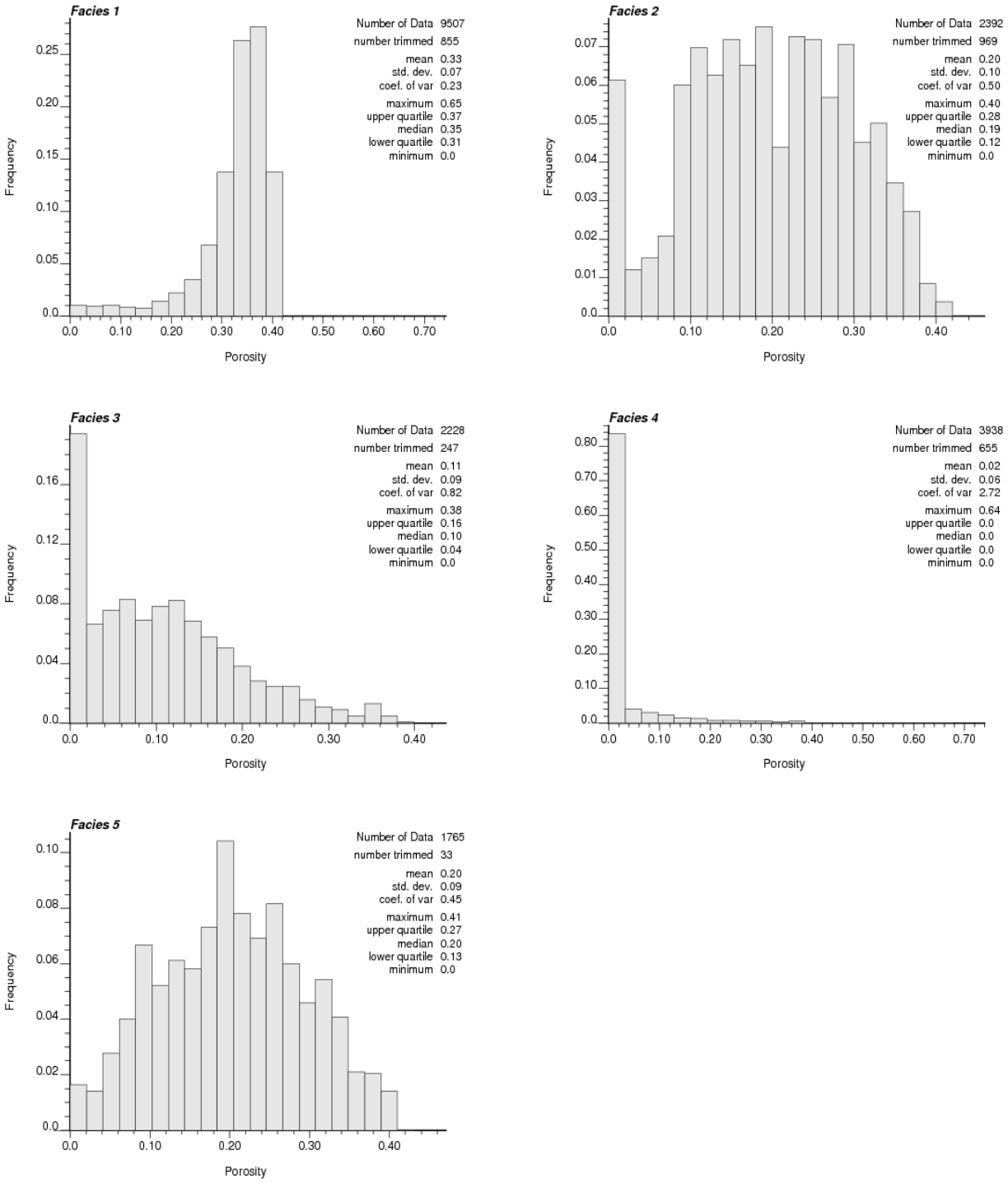

Fig. 3. Porosity distribution of facies

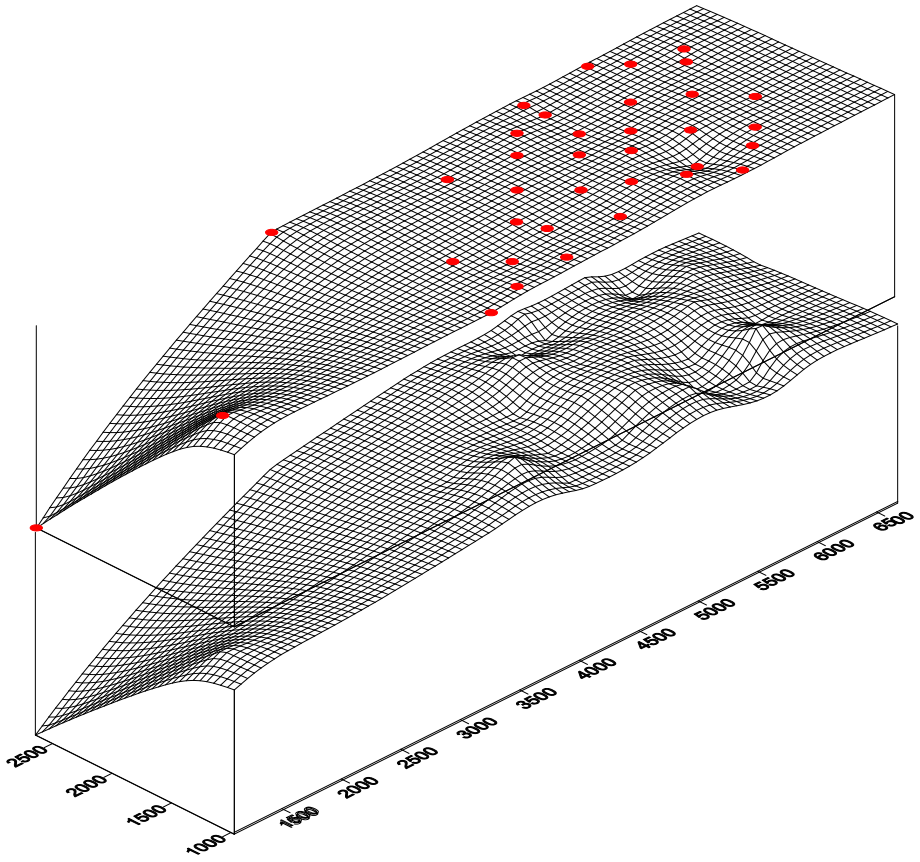

Fig. 4. top and bottom surface of facies 2 in the study area

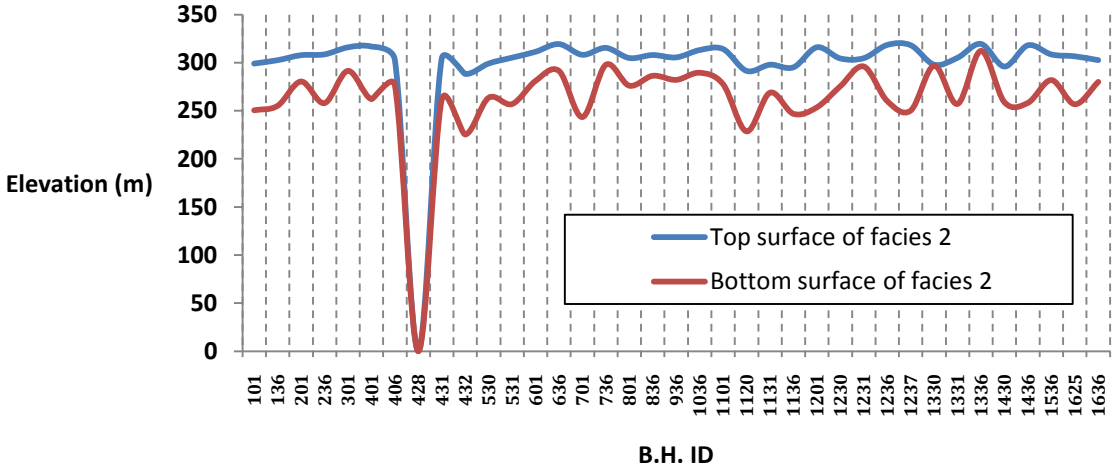

Fig. 5. Thickness of facies 2 in each well

Table 3. Variogram calculation parameters

parameter	value	parameter	value
Number of lags	200	Azimuth angle	
Lag separation	0.01m	Azimuth tolerance	
Lag tolerance	0.005m	Dip angle	
Calculation range	2 m	Dip tolerance	

2.2.2 Variogram Modeling

The nugget effect for the vertical variogram is approximately zero. In addition, since the actual range is high, the continuity of the porosity in the sandy IHS can be judged to be high.

The variogram is modeled, using the *VMODEL* command of *GSLIB*. The horizontal variogram is considered to have the same characteristics of the vertical variogram, with a range ratio of $a_{horz.} : a_{vert.} = 5:1$. It means that after modeling the vertical variogram, the horizontal variogram can be modeled only by changing the range. The variogram models are illustrated in Fig. 6. The red line represents the horizontal variogram, while the vertical variogram is illustrated with the blue line.

$$\gamma(h) = 0.39\, Sph_{\substack{a_{h\max}=3.5 \\ a_{h\min}=3.5 \\ a_{ver}=0.7}}(h) + 0.19\, Sph_{\substack{a_{h\max}=10 \\ a_{h\min}=10 \\ a_{ver}=2}}(h)$$

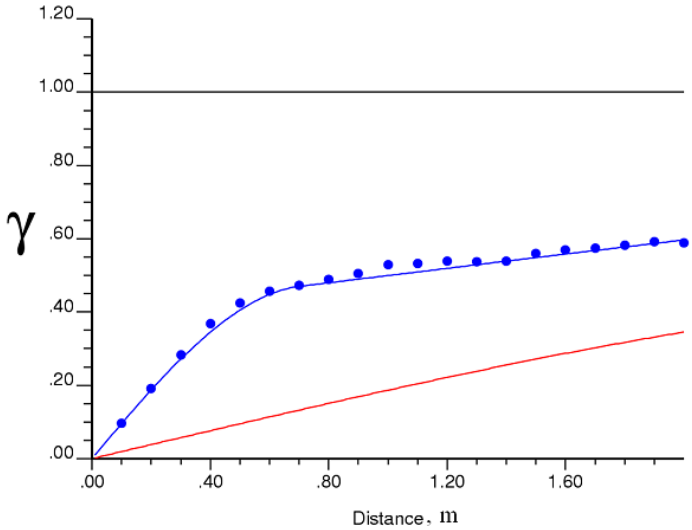

Fig. 6. Normal score variogram of well log scale porosity within the facies 2

2.3. Porosity Simulation

The porosity of the sandy IHS is simulated through 100 realizations. The horizontal and vertical variogram models are used in simulation. For simulation, the grid cells are defined $1\text{dm} \times 1\text{dm} \times 1\text{dm}$, within a cubic regular grid of $1\,m^3$. Since the simulation is done unconditionally, the results of simulation are in Gaussian units. (*SGSIM* command of *GSLIB* works this way). Therefore, the results of realizations should be back transformed to the original data units, between 0.0 and 0.4. It is done using *BACKTR* command of *GSLIB*. The back transformed results of the realizations are then averaged, using the *POSTSIM* command of *GSLIB*. The averaged result from the realizations is illustrated in Fig. 7.

In the process of averaging the simulation results, the averaged values violated the porosity limits in original data (0.0 to 0.4). That is because the *POSTSIM* command uses the first column of the input file, which is the back transformed data, but the first column of the back transform file is the original data, not the back-transformed! Therefore, first the back transform results should be refined and the first column should be omitted and then, the results should be passed to the *POSTSIM*. The results of the averaged simulations show the mean of 0.2, with the minimum and maximum of 0.18 and 0.22, respectively. The histogram of the post simulation results and histogram reproduction are shown in Fig. 8. The histogram reproduction in Fig. 8 shows that the histogram has been reproduced.

2.4. Permeability and Flow

To simulate the flow, firstly, the horizontal permeability should be simulated and then, using the $\frac{K_v}{K_h}$ ratio, the vertical permeability and the flow can be simulated.

2.4.1 Cloud Transformation; Permeability

Based on the simulation results for the porosity, the arithmetic average of porosity is calculated, using the *FLOWSIM* command of *GSLIB*. The summary statistics for the porosity are presented in Table 4.

Table 4. Statistics for porosity based on the flow simulation

statistics	value
minimum	
average	
maximum	
standard deviation	

To simulate the horizontal permeability flow, the cloud transformation and p-field simulated values are used. The p-field values are simulated through 100 realizations and unconditionally. The same variogram, as for the porosity is used for cloud transform as well. Then, for creating the bivariate distribution between porosity and horizontal permeability, the *BIMODEL* command of *GSLIB* is used. As the input, the *BIMODEL* requires the paired data points for porosity and horizontal permeability. These pairs are extracted from the results of micro modeling. The output of the *BIMODEL*, the bivariate distribution of porosity and the horizontal permeability, is illustrated in Fig. 9.

The bivariate distribution and the porosity values (simulation results that are back transformed to the original scale) are then used in cloud transformation. The cloud transformation is performed to

find the horizontal permeability values, based on the porosity values, the p-field values and the bivariate distribution of porosity and horizontal permeability.

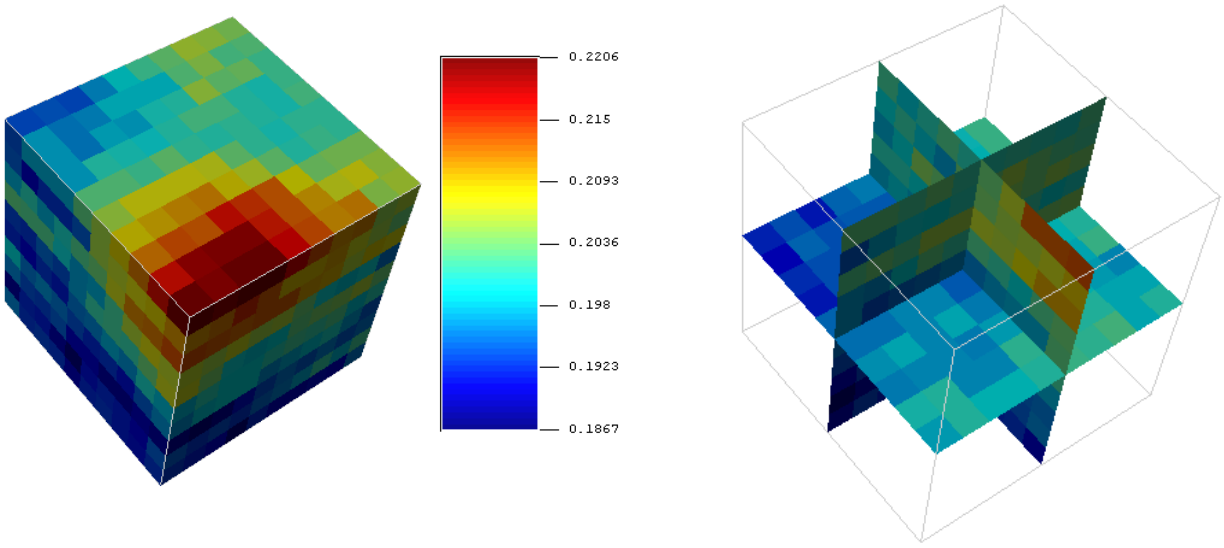

Fig. 7. simulation results for porosity, sandy IHS

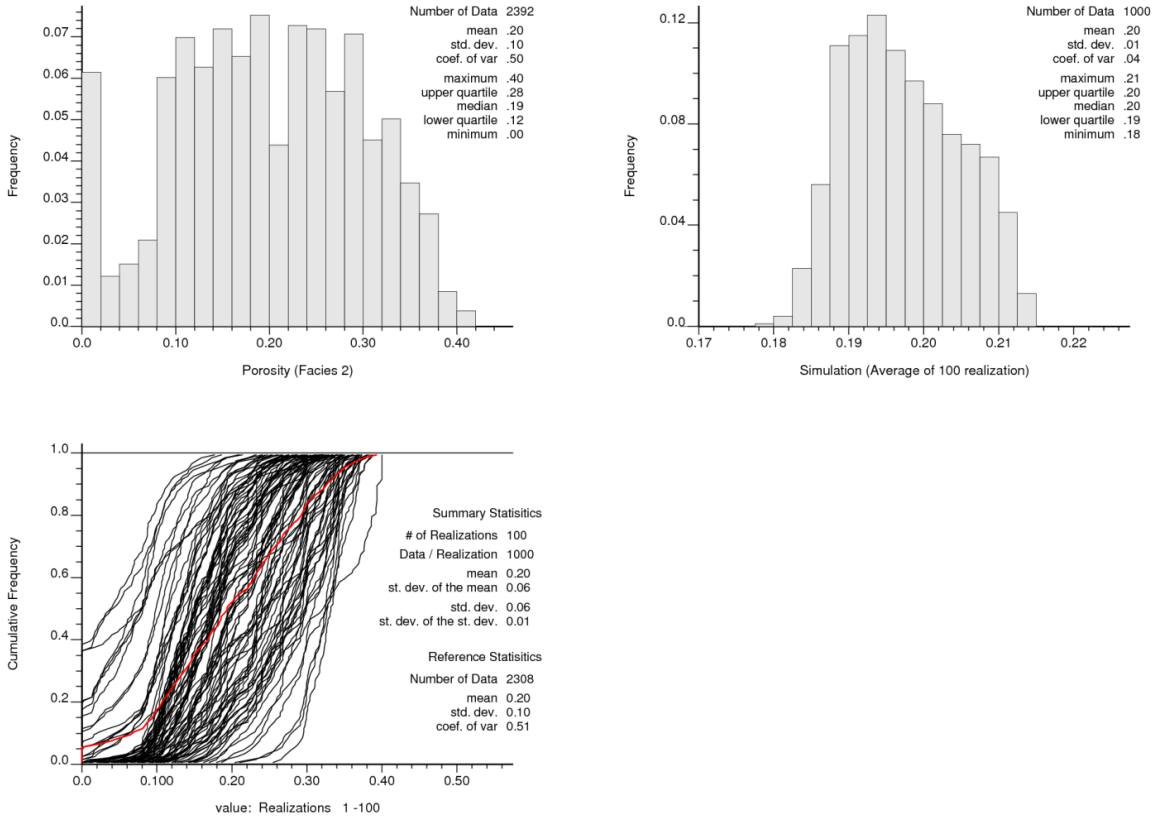

Fig. 8. Histogram of porosity for facies 2 and histogram of average of 100 realizations referenced to the distribution of porosity of facies 2

The horizontal permeability values are simulated through 100 realizations, using the *CLTRANS* command of *GSLIB*. Then, the simulated values are averaged, using the *POSTSIM* command. The average of simulated values is illustrated in Fig. 10.

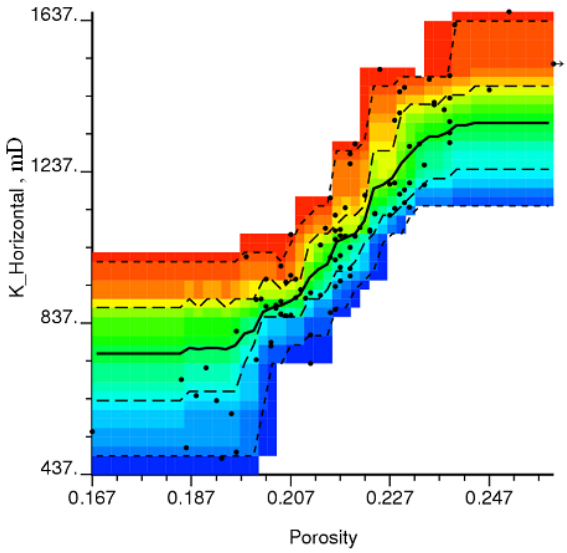

Fig. 9. The bivariate distribution of porosity and horizontal permeability

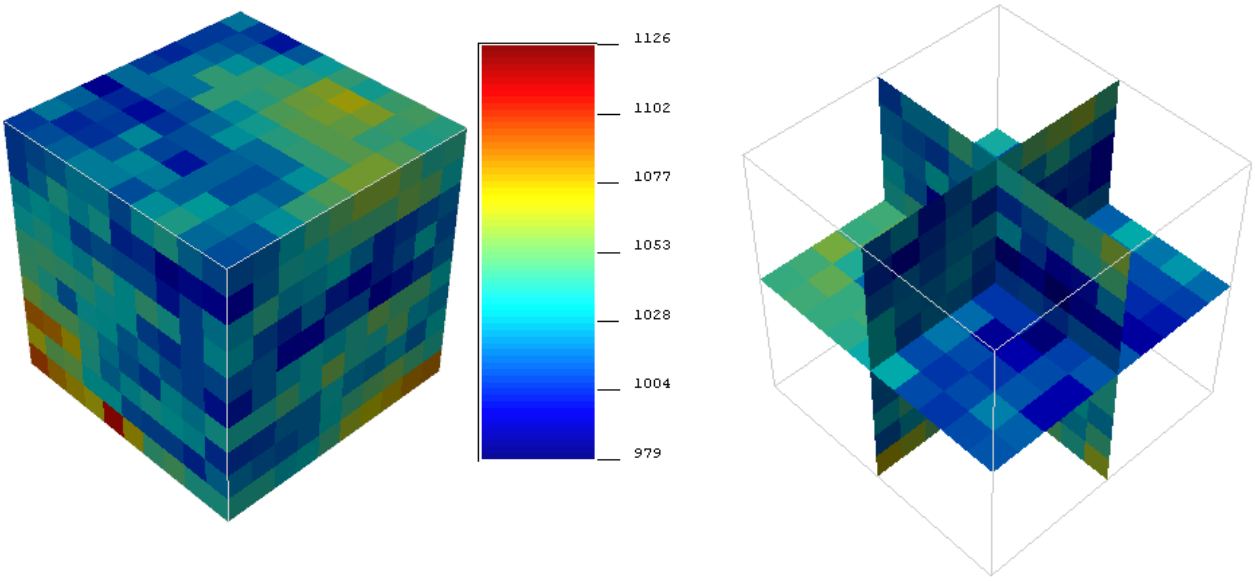

Fig. 10. Simulation result for horizontal permeability

The average of the $\frac{K_v}{K_h}$ ratio, based on the outputs of micro modeling, equals to 1.927. Using this ratio, the values for vertical permeability are calculated. The summary statistics of the permeability values is presented in Table 5.

2.4.2 Flow simulation

The simulation results for the horizontal and vertical permeability now can be used for flow simulation. The flow is simulated through 100 realizations, using the FLOWSIM command of GSLIB. The resulting values from flow simulation are illustrated as cross plots in Fig. 11. The summary statistics corresponding to the flow simulation results are presented in Table 6.

Table 5. Statistics of permeability simulation

	minimum	maximum	average	standard deviation
Vertical permeability (mD)	843	3199	1993	623
Horizontal permeability (mD)	437	1660	1034	323

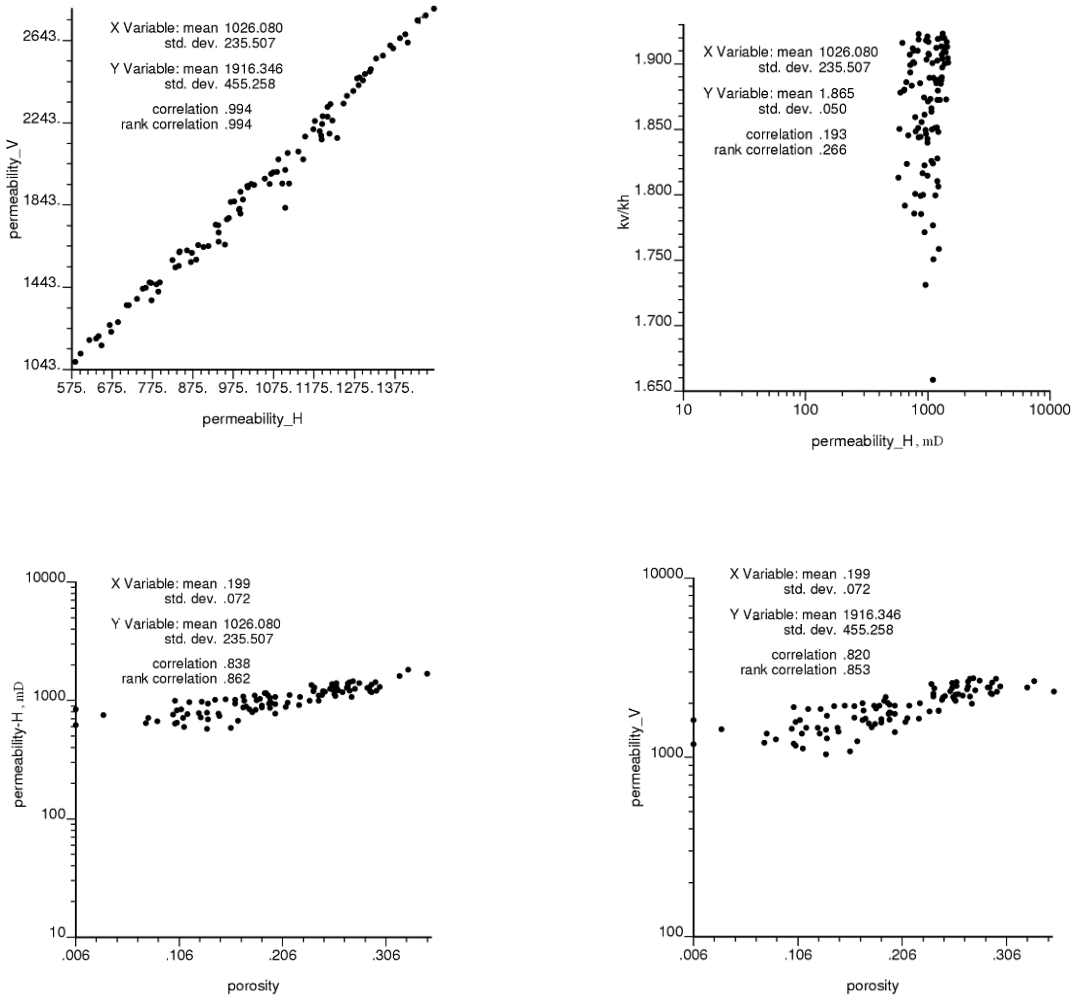

Fig. 11. Cross plot of obtained results from FLOWSIM

Table 6. Summary statistics of flow simulation results

variable	minimum	maximum	mean	Standard deviation
(mD)	1043	2798	1916	455
(mD)	575	1472	1026	236
Kv/Kh	1.65	1.93	1.87	0.05
Correlation coefficients				
vs. :	0.99	—vs. :		0.19
porosity vs. :	0.84	porosity vs. :		0.82

3. 3D Conventional Modeling

For 3D conventional modeling five steps should be done. These steps are as follows: (1) calculation of facies proportions, (2) calculation and modeling the facies indicator variograms and cross validation of the variogram models, (3) estimation and simulation of facies indicators, (4) declustering of the data points and porosity variogram calculation and modeling, and (5) estimation and simulation of porosity for each facies and building the porosity model.

3.1. 3D Proportion Cube of Facies

The facies proportions can be calculated in both vertical and areal directions. In the vertical direction, the proportions are calculated based on the values of all facies at each elevation (from 0 to -78 meter). The resulting proportion charts are illustrated in Fig. 12.

For the areal proportions, the areal trend is estimated, using the *KT3D* command of *GSLIB*. In order to estimate the trend, a variogram with a very large range, approximately equal to one third of the domain in each direction, is used. The nugget that is used for the trend model variogram is 30 percent of the sill. The grid system specifications are presented in Table 7. The areal trend maps for different facies are illustrated in Fig. 13.

Table 7. The grid specifications for the 3D conventional modeling

	Min (m)	Max (m)	specified range (m)	cell size (m)	No. of cells
X direction	1100	6679	6000	50	120
Y direction	972	2644	2500	50	50
Z direction	-78	0	78	1	78

The vertical proportions and the areal trend maps are merged together to make the "proportion cube" of facies. The theoretical background of combining proportions is based on the probability combination schemes that approximates the probability of geologic event jointly conditioned to diverse data sources through combining the calibrated probabilities conditioned to individual data source (Hong and Deutsch, 2009). Integrating the vertical and horizontal proportion that may be modeled by different data sources can be viewed as a probability combination problem. Consider the proportion of facies k in (x,y,z) location $P_k(x,y,z)$ given the areal proportion $P_k(x,y)$ and the vertical proportion $P_k(z)$, k=1,…,5. The $P_k(x,y,z)$ can be estimated as following:

$$P_K(x,y,z) = \left(\frac{P_K(x,y)}{P_K}\right).\left(\frac{P_K(z)}{P_K}\right).P_K$$

Where P_k is the global proportion of facies k. The merging is performed, using the *PCSTM* command of *GSLIB*. 3D cross sectional views of the resulting cube for each facies are illustrated in Fig. 14. For better visualization, the elevation -"Z" direction- is scaled up to 20. The global proportions are 0.46, 0.15, 0.11, 0.22 and 0.07 for facies 1 to 5.

3.2. Variogram of Facies

The indicator variogram for each facies is calculated, using *GAMV* command of *GSLIB*. Then, the variogram for each facies is modeled.

The indicator variogram in vertical direction is calculated for all five facies. Since the horizontal variograms do not show any specific behavior, it is not possible to fit a model for them. On the other hand, according to the geology of the specific domain, the ratio of variogram ranges is approximately equal to $a_{horz.} : a_{vert.} = 100:1$. Vertical variogram is modeled and then, for the horizontal variogram, the same vertical model is used with the only change in the range. Variogram calculation parameters for vertical direction are presented in Table 8.

Table 8. Facies indicator variogram calculation parameters

parameter	value	parameter	value
Number of lags	50	Azimuth angle	
Lag separation	0.4m	Azimuth tolerance	
Lag tolerance	0.05m	Dip angle	
Calculation range	20 m	Dip tolerance	

Table 9 contains the parameters used for variogram modeling in vertical direction. The variogram is modeled, using the *VMODEL* command of *GSLIB*. The horizontal variogram is considered to have the same characteristics of the vertical variogram, with a range ratio of $a_{horz.} : a_{vert.} = 100:1$. It means that after modeling the vertical variogram, the horizontal variogram can be modeled only by changing the range. The vertical variogram models are illustrated in Fig. 15.

In order to check the goodness of the variogram models, the cross validation is performed, using the *KT3D* command of *GSLIB*. For the cross validation, the 3D trend proportion cube is required. In addition, the stationary assumption should not be considered in kriging for the cross validation, because the variance changes over the domain and the homoscedastisity is not met. The results of cross validation are then compared with the original data to check the reproducibility of the data, using the variogram model. The correlation coefficients and the slope of the regression line in each case are reported in Table 10. The cross plots of original data versus the estimated data are illustrated in Fig. 16.The results show that the variogram models are acceptable.

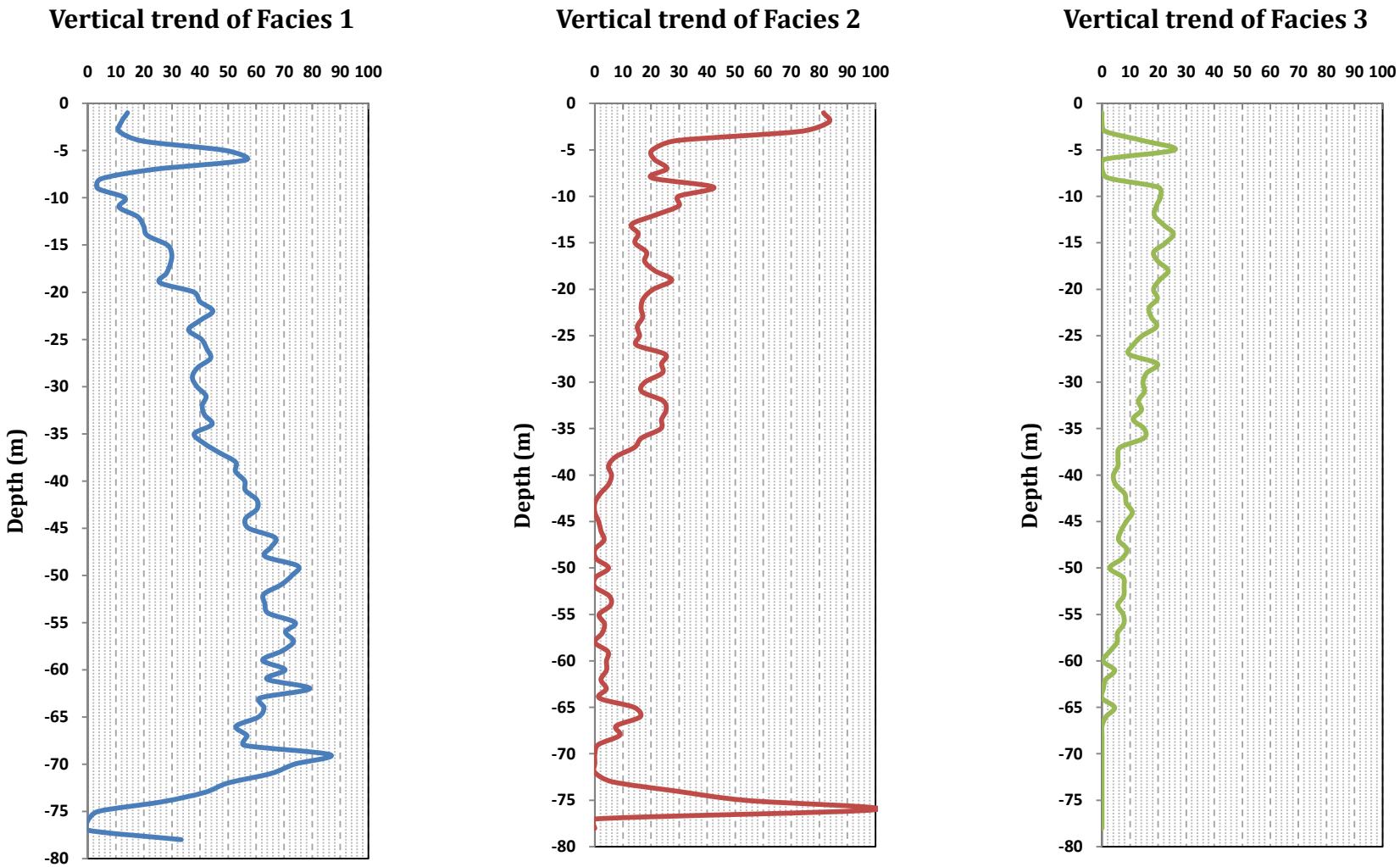

Fig. 12. Vertical trend for each facies

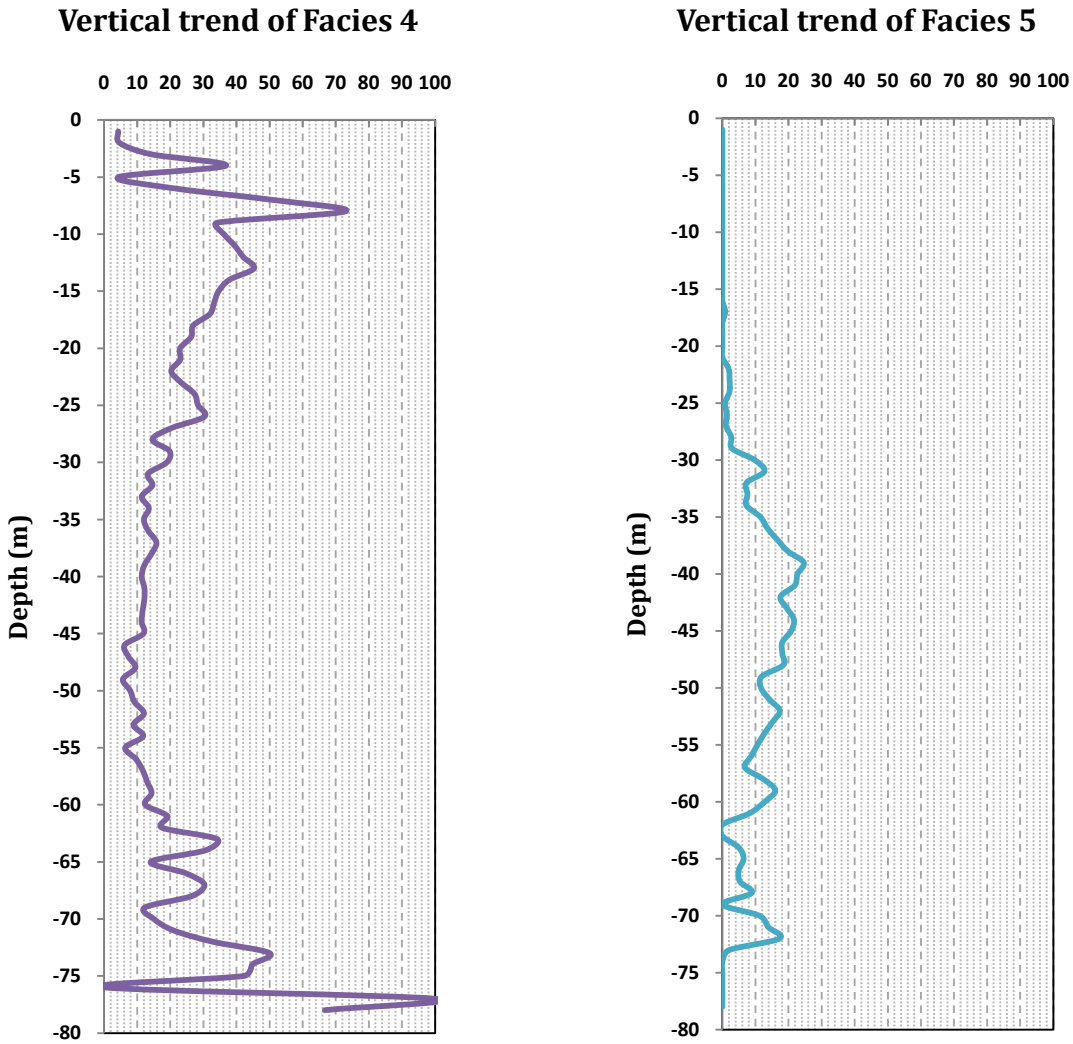

Fig. 12, Continued

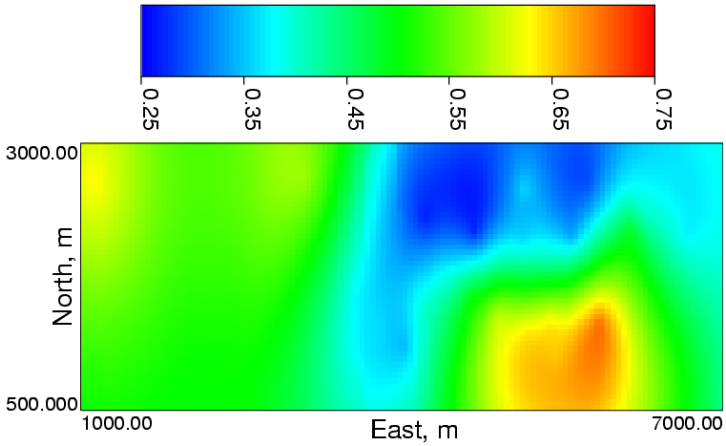

(a) facies 1

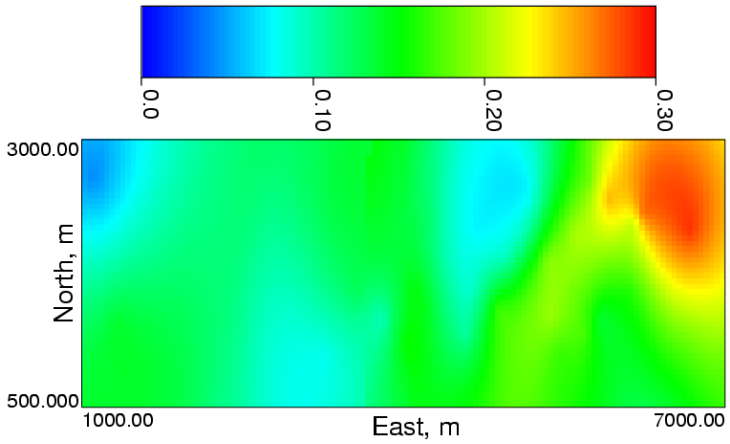

(b) facies 2

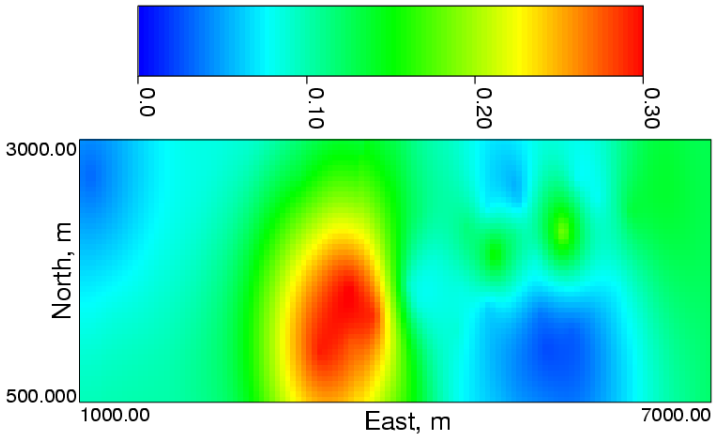

(c) facies 3

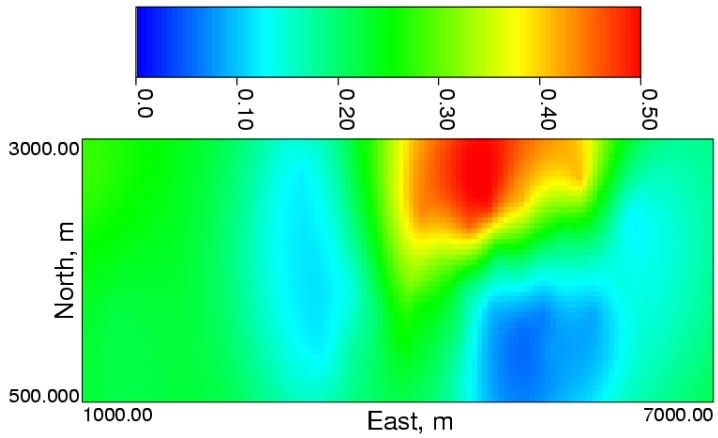

(d) facies 4

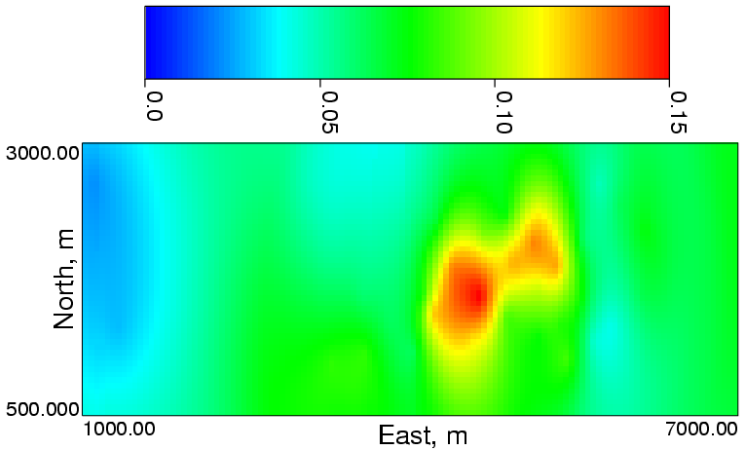

(e) facies 5

Fig. 13. The areal trend map of different facies

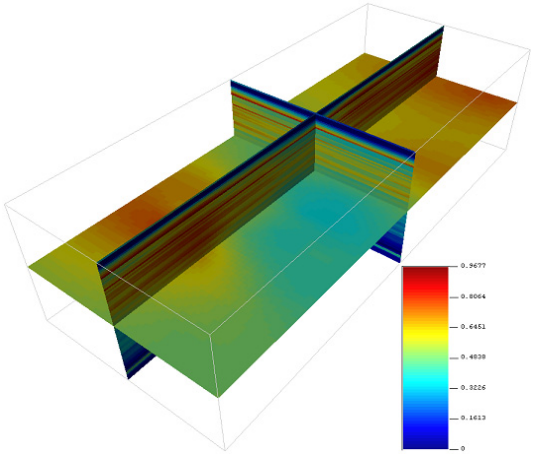

(a) facies 1 (range:0 – 0.97)

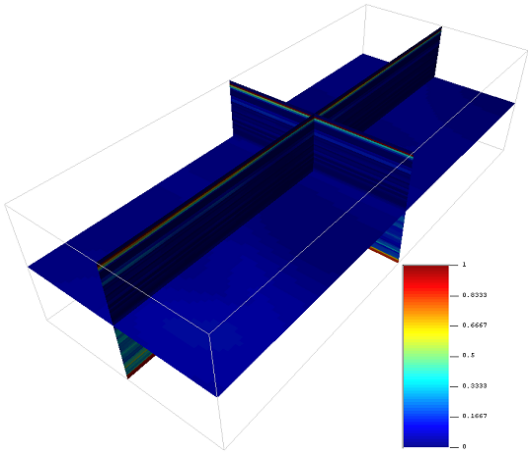

(b) facies 2 (range:0 – 1.0)

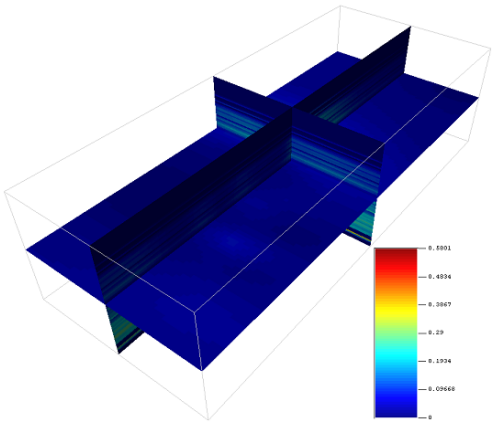

(c)facies 3 (range:0 – 0.58)

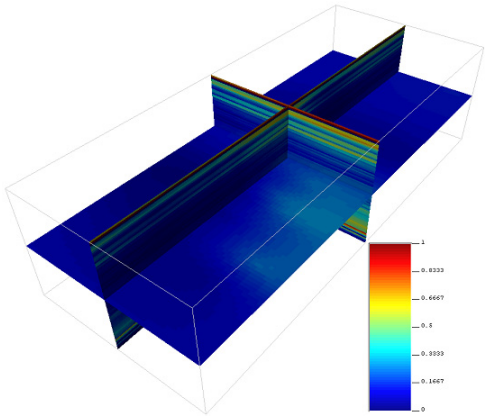

(d) facies 4 (range:0 – 1.0)

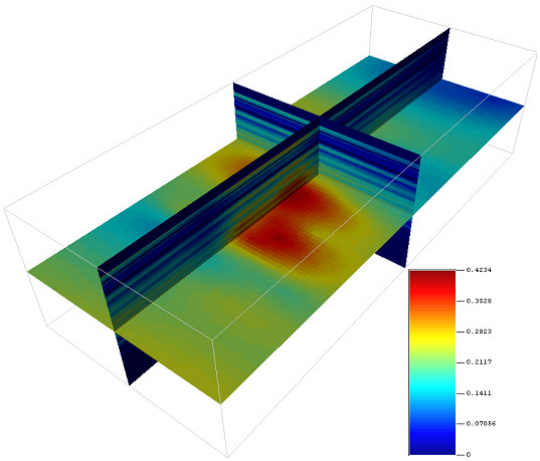

(e) facies 5 (range:0 – 0.42)

Fig. 14. The proportion cube of facies

Table 9. Parameters for facies variogram modeling

facies	Structure #	Structure type	contribution	Range (vert.), m	Range (Hor.), m
1	1	nugget	0.10	N/A	N/A
	2	spherical	0.55	6	600
	3	spherical	0.35	30	3000
2	1	nugget	0.20	N/A	N/A
	2	spherical	0.50	5	500
	3	spherical	0.30	25	2500
3	1	nugget	0.10	N/A	N/A
	2	spherical	0.80	7.5	750
	3	spherical	0.10	20	2000
4	1	nugget	0.10	N/A	N/A
	2	spherical	0.70	9	900
	3	spherical	0.20	120	12000
5	1	nugget	0.20	N/A	N/A
	2	spherical	0.78	6	600
	3	spherical	0.02	13	1300

Table 10. Cross validation summary for facies variogram

Facies	correlation coefficient	regression slope
1	0.95	1.033
2	0.94	1.059
3	0.96	1.035
4	0.95	1.034
5	0.92	1.064

3.3. Facies Estimation and Simulation

The same adjustments and configurations are considered in estimating the facies as those used in cross validation. The results from kriging are visualized, using *SGEMS* and illustrated in Fig. 17. The family of red colors represents the presence of the facies in the area.

The facies are simulated through 100 realizations, using the *BLOCKSIS* command of *GSLIB*. In order to simulate the facies, it is required to put the 3D trend proportion cube as input.

3.4. Variogram of Porosity

Prior to calculating the experimental variograms for porosity, the data is declustered, using *DECLUS* command of *GSLIB*.

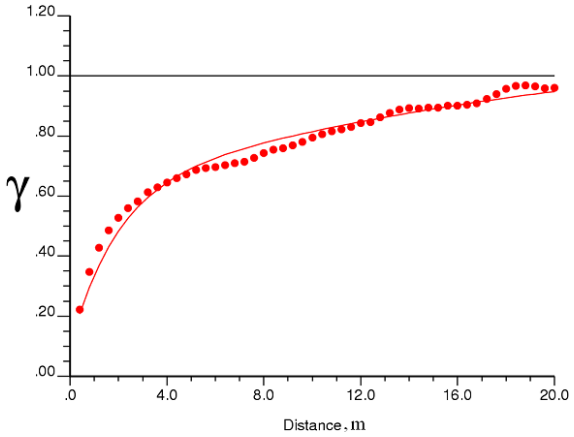

(a) facies 1

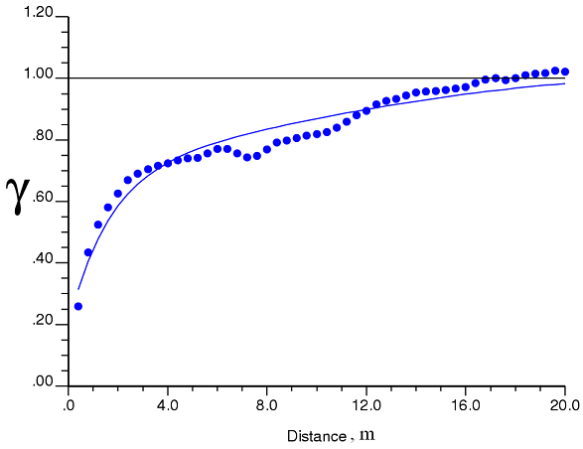

(b) facies 2

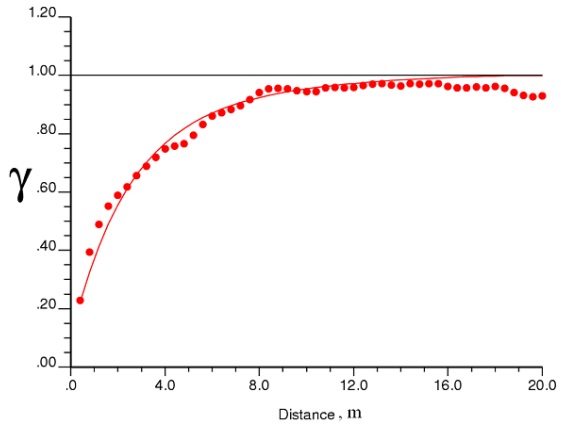

(c) facies 3

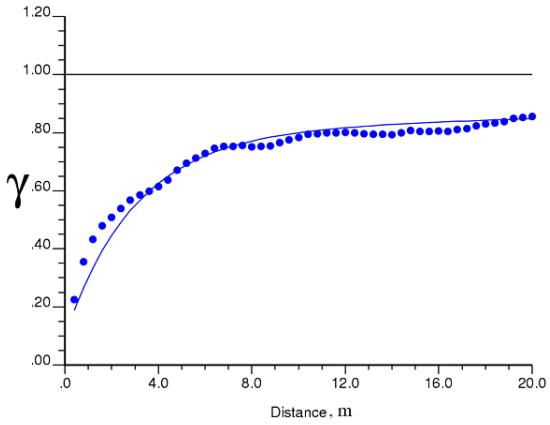

(d) facies 4

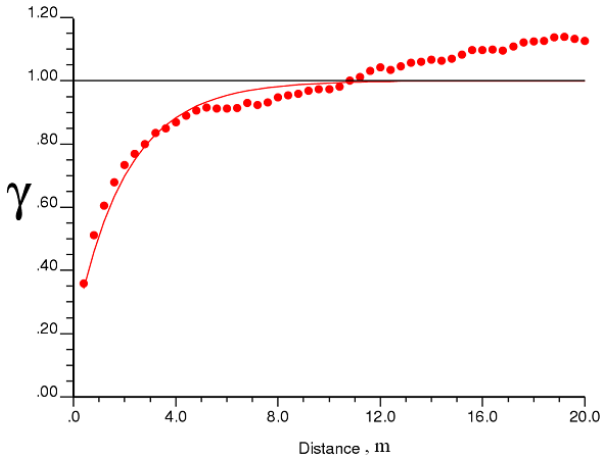

(e) facies 5

Fig. 15. Vertical variogram models for five facies

3.4.1 Declustering

Since the data points are located on a regular grid in Z direction (equal intervals of 1 m), the declustering is performed only based on X and Y coordinates. The declustering cell size is 0.211 m. The porosity frequency histograms of facies, resulted from declustering, are illustrated in Fig. 18. The summary statistics for each facies is presented in Table 11.

Then, the data are transformed to normal scores, using the *NSCORE* command of *GSLIB*. The transformation is required, because the variograms will be used in the sequential Gaussian simulation (SGS) which requires variogram for normal scored values.

3.4.2 Variogram calculation

The vertical variogram of porosity is calculated for all facies. The variogram calculation parameters for vertical direction are presented in Table 12.

3.4.3 Variogram modeling

The vertical variograms are modeled, based on the experimental variograms. For horizontal variograms, the same ratio of $a_{horz.} : a_{vert.} = 100:1$ is used, as in facies variograms.

Table 13 includes the parameters used for variogram modeling in vertical and horizontal directions. The variograms are modeled, using the *VMODEL* command of *GSLIB*. The horizontal variogram is considered to have the same characteristics of the vertical variogram, with a range ratio of $a_{horz.} : a_{vert.} = 100:1$. It means that after modeling the vertical variogram for each facies, the horizontal variogram can be modeled only by changing the range. The variogram models are illustrated in Fig. 19.

Table 11. The porosity statistics for different facies

	Facies 1 (sand)	Facies 2 (sandy IHS)	Facies 3 (muddy IHS)	Facies 4 (muddy shale)	Facies 5 (breccia)
number of data	9507	2392	2228	3938	1765
average		0.20	0.11	0.02	0.20
standard deviation	0.07	0.10	0.09	0.06	0.09
coefficient of variation	0.23	0.50	0.82	2.72	0.45
maximum	0.65	0.40	0.38	0.64	0.41

Table 12. The porosity variogram calculation parameters

parameter	value	parameter	value
Number of lags	25	Azimuth angle	
Lag separation	1 m	Azimuth tolerance	
Lag tolerance	0.5 m	Dip angle	
Calculation range	2 m	Dip tolerance	

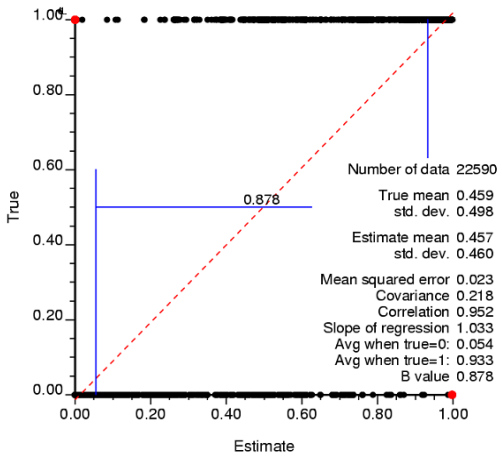

(a) facies 1

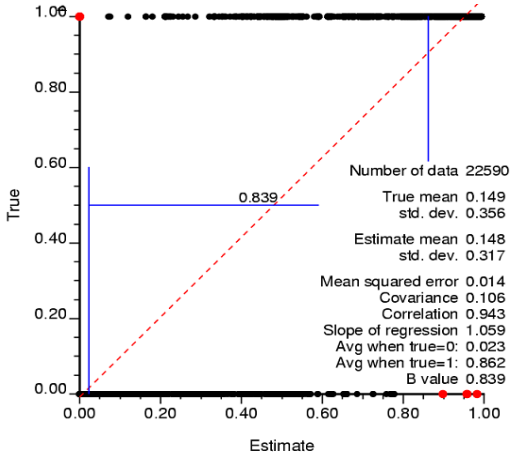

(b) facies 2

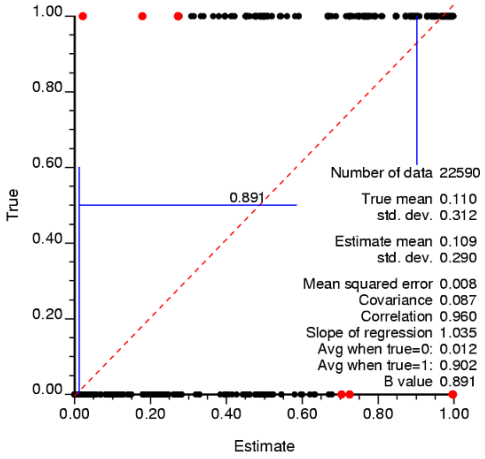

(c) facies 3

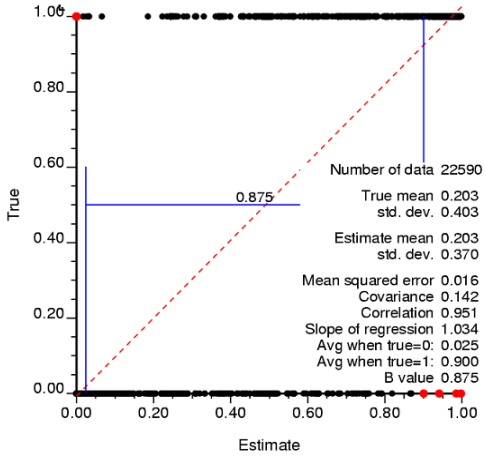

(c) facies 4

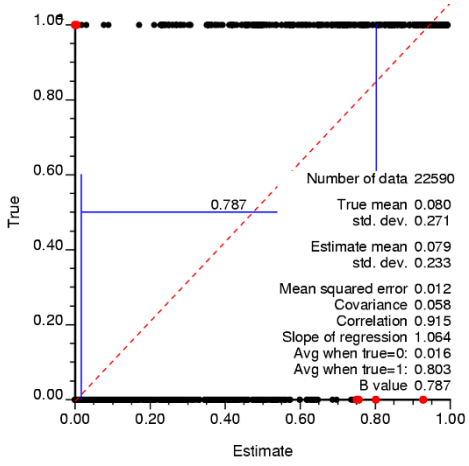

(e) facies 5

Fig. 16. Cross validation results for facies

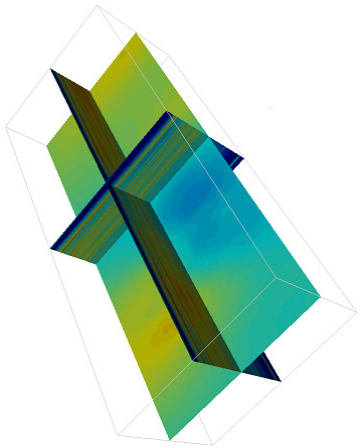

(a) facies 1

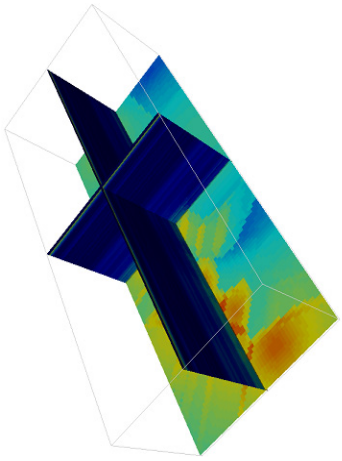

(b) facies 2

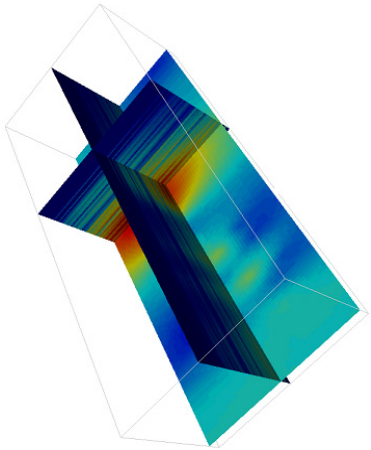

(c) facies 3

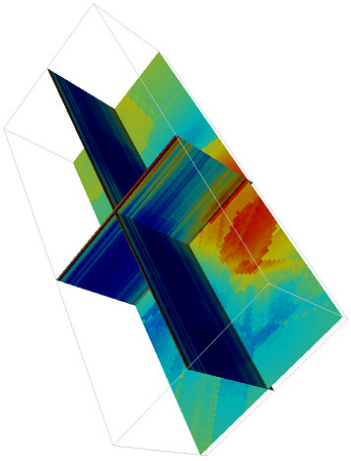

(d) facies 4

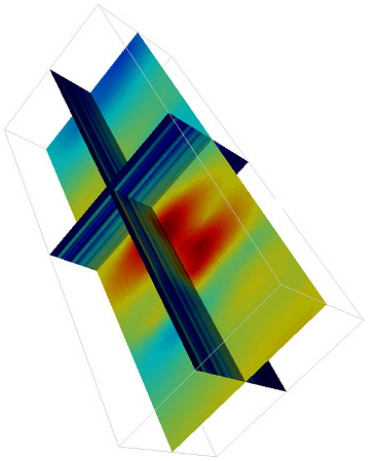

(e) facies 5

Fig. 17. The results from facies kriging

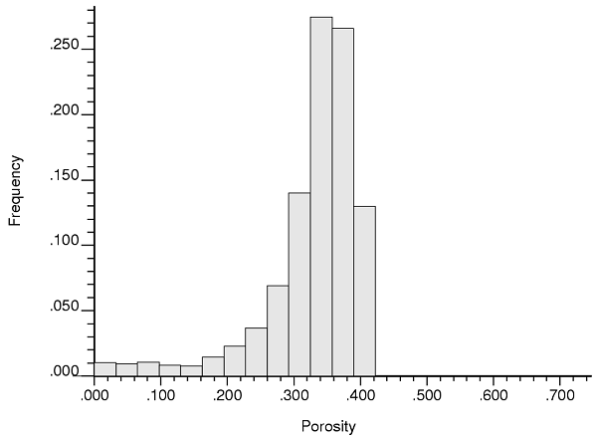

(a) facies 1

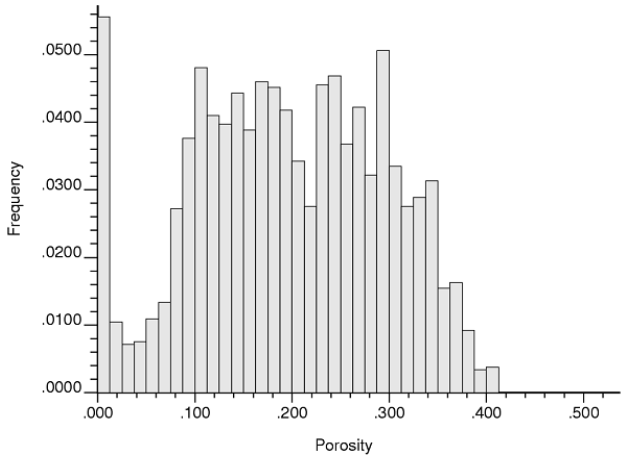

(b) facies 2

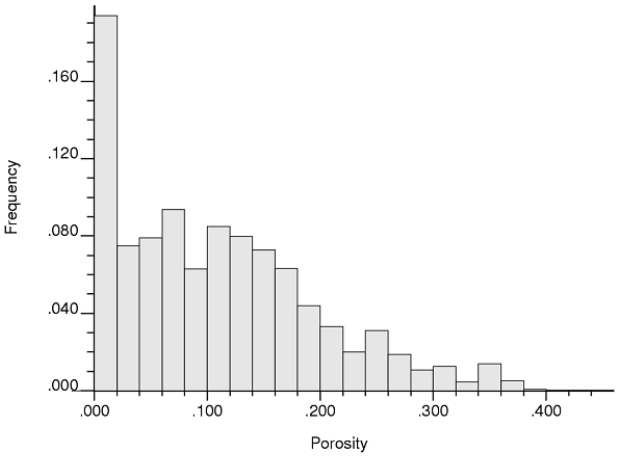

(c) facies 3

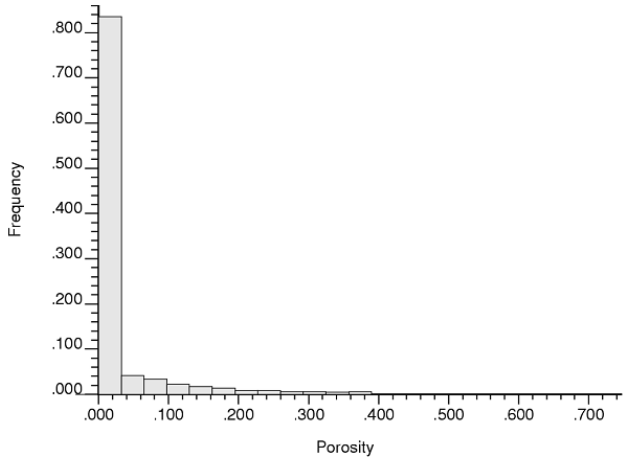

(d) facies 4

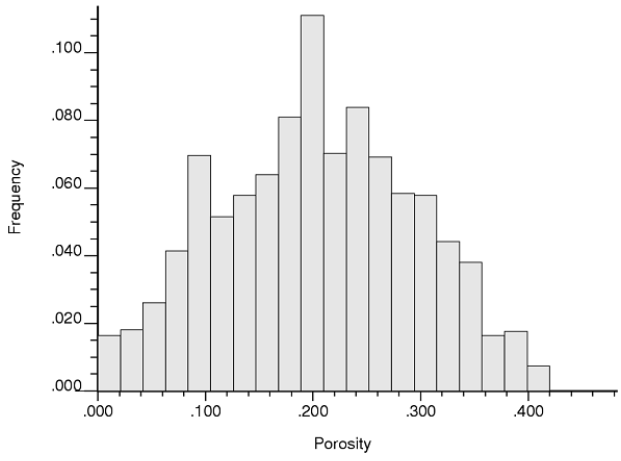

(e) facies 5

Fig. 18. Porosity distribution of the facies

Table 13. Parameters for porosity variogram modeling

facies	Structure #	Structure type	contribution	Range (vert.), m	Range (Hor.), m
1	1	nugget	0.10	N/A	N/A
	2	spherical	0.57	5	500
	3	spherical	0.33	45	4500
2	1	nugget	0.20	N/A	N/A
	2	spherical	0.47	7	700
	3	spherical	0.33	30	3000
3	1	nugget	0.10	N/A	N/A
	2	spherical	0.42	11	1100
	3	spherical	0.48	20	2000
7	1	nugget	0.52	N/A	N/A
	2	spherical	0.26	8	800
	3	spherical	0.22	50	5000
5	1	nugget	0.30	N/A	N/A
	2	spherical	0.50	7	700
	3	spherical	0.20	20	2000

In order to check the goodness of the variogram models, the cross validation is performed, using the *KT3D* command of *GSLIB*. For the cross validation, the 3D trend proportion cube is required. In addition, the stationarity assumption should not be considered in kriging for the cross validation as the variance changes over the domain, and the homoscedastisity is not met. The results of cross validation are then compared with the original data to check the reproducibility of the data, using the variogram model. The correlation coefficients and the slope of the regression line in each case are reported in Table 14. The cross plots of original data versus the estimated data are illustrated in Fig. 20.

Table 14. Cross validation summary for porosity variogram

Facies	correlation coefficient	regression slope
1	0.92	1.047
2	0.90	1.078
3	0.90	1.044
4	0.64	1.071
5	0.81	1.162

3.5. Porosity Estimation and Simulation (The Porosity Model)

The porosity is estimated for each facies, using the vertical and horizontal variogram models. As an example, the estimation results are illustrated for three facies in Fig. 21.

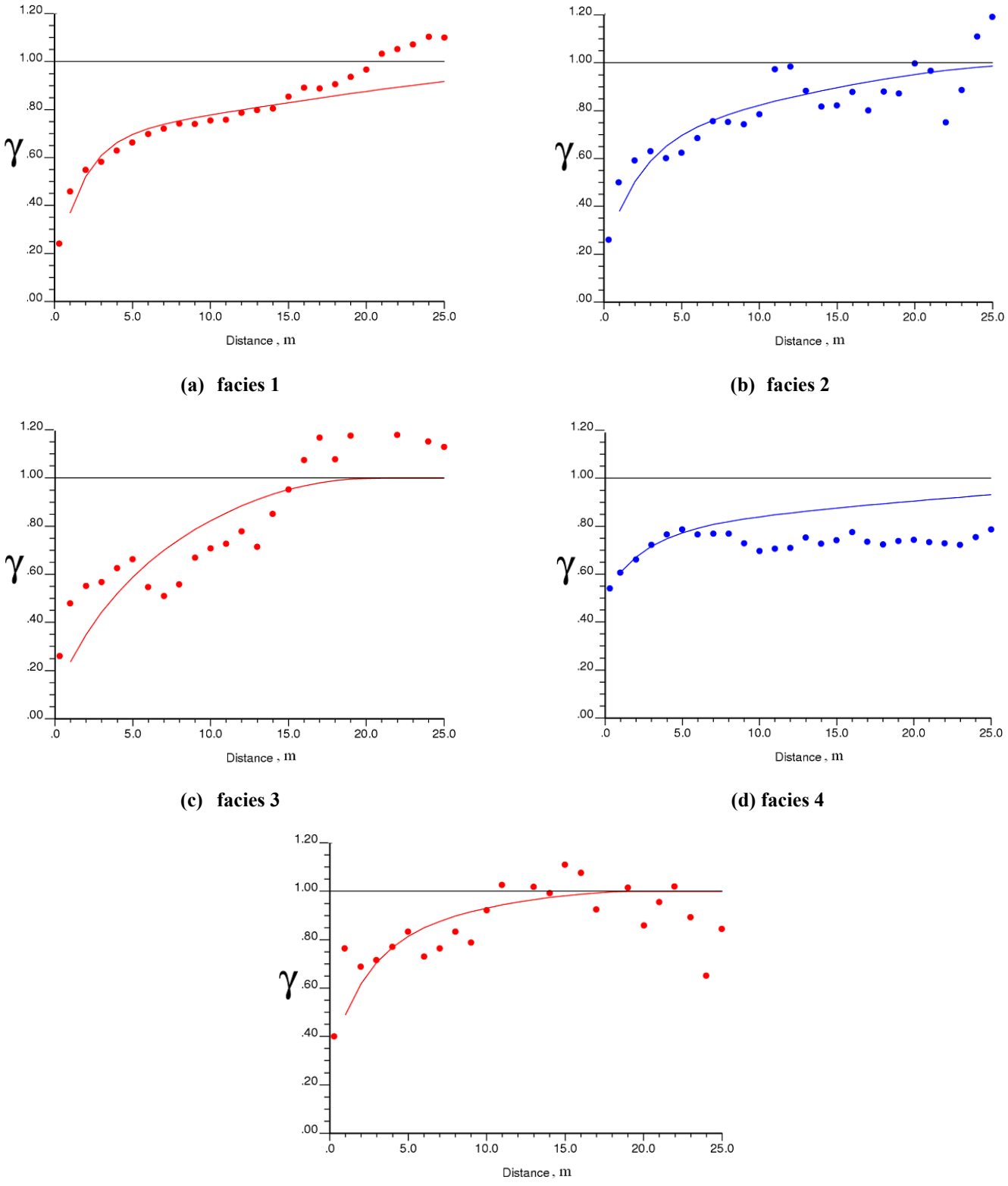

(a) facies 1

(b) facies 2

(c) facies 3

(d) facies 4

(e) facies 5

Fig. 19. Vertical variogram model for porosity of facies

The porosity is then simulated through 100 realizations for each facies. The results of simulated results are then merged together, using the facies simulation result. The averages of simulated

values for porosity are illustrated in Fig. 22. In order to take the average, the *POSTSIM* command of *GSLIB* is used.

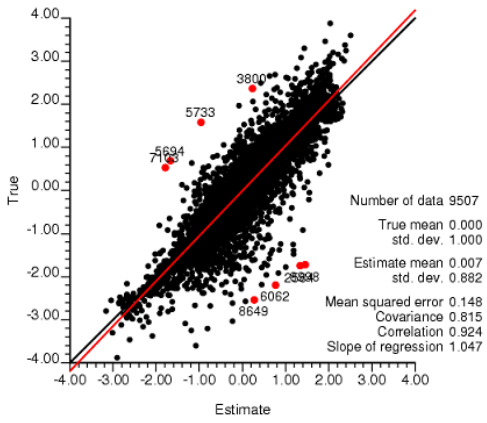

(a) facies 1

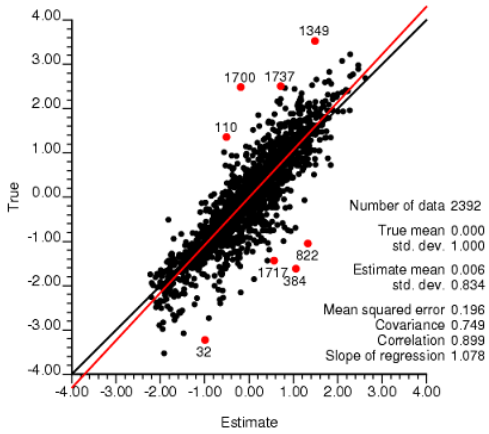

(b) facies 2

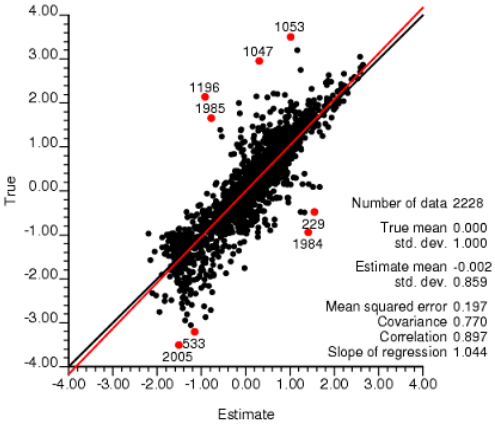

(c) facies 3

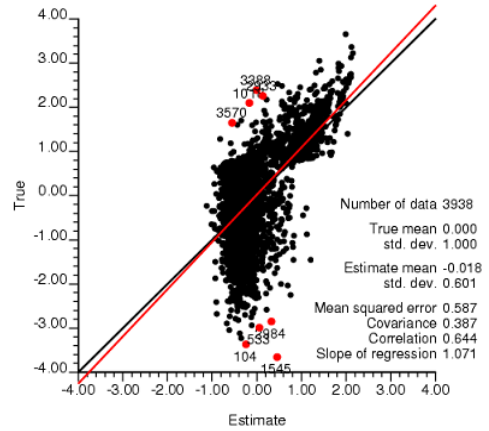

(d) facies 4

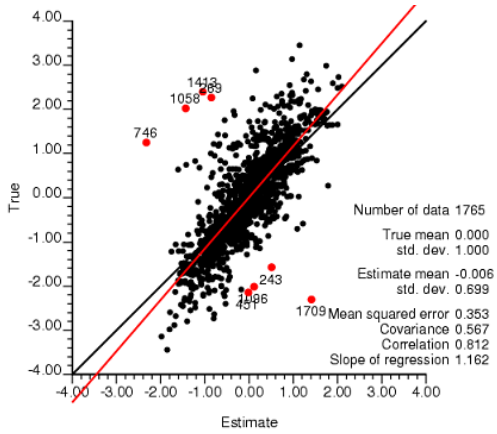

(e) facies 5

Fig. 20. Cross validation results for porosity in facies

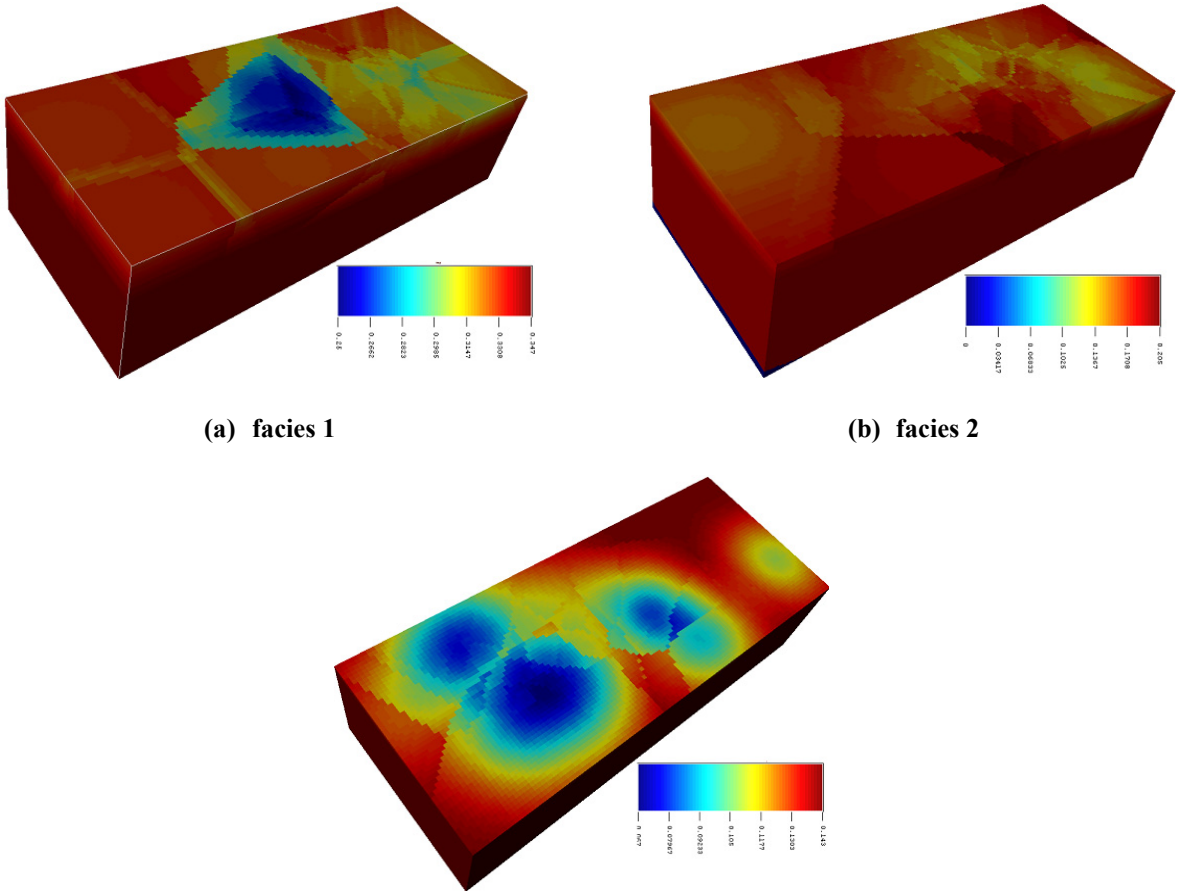

(a) facies 1 **(b) facies 2**

(c) facies 3

Fig. 21. Kriging results for porosity in facies

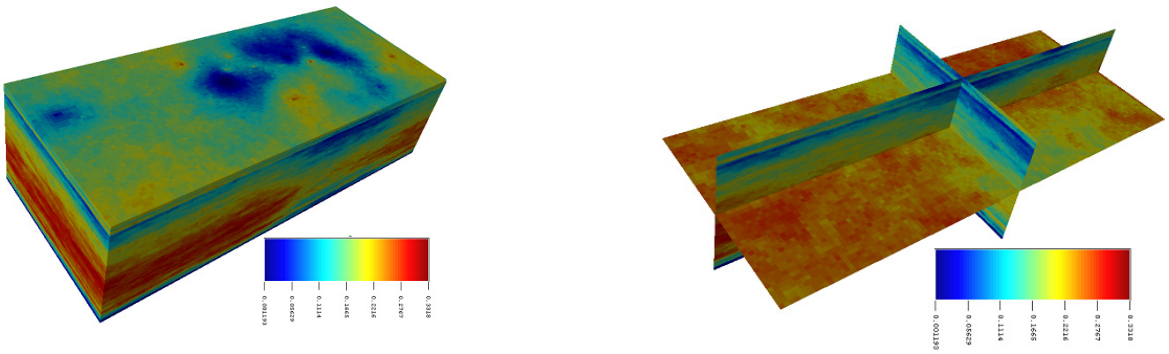

Fig. 22. The simulation results for porosity (merged) range: 0-0.34

4. Conclusion

The prediction of porosity and permeability at unsampled locations of reservoir is one of the important problems in petroleum engineering. The goal of mini modeling is to address the scale

changing from the *dm* scale to the scale of flow modeling. In this paper, all steps of mini modeling are explained. The directional permeability of each mini model is calculated with the same basic procedure as the micro models. Each mini model is summarized by an average porosity ϕ, a horizontal permeability KH, and a vertical permeability KV. The results form mini models are used directly in geological model construction.

According to the 3D conventional modeling, the porosity of deposit with resolution of dm^3 can be estimated. In this paper full 3D trend is modeled using 2D areal trend and 1D vertical trend. For this method post processing should be done after merging. For this kind of problems, reasonable sensitivity analysis and calibration are required.

5. References

[1] Hong, S. and Deutsch, C. V. (2009). 3D trend modeling by combining lower order trends. Center for Computational Geostatistics, University of Alberta, Edmonton, 130(1-14).

6. Appendix

List of GSLIB sample parameter files that are used in mini modeling and 3D conventional modeling (in alphabetical order)

backtr.par	Parameter file for back transformation to original distribution.
bimodel.par	Parameter file for calculating the bivariate distribution.
blocksis.par	Parameter file for simulating the indicator variables.
cltrans.par	Parameter file for cloud transform simulation.
declus.par	Parameter file for declustering.
flowsim.par	Parameter file for flow simulation.
gamv.par	Parameter file for variogram calculation (irregularly spaced data).
histplt.par	Parameter file for plotting histograms.
kt3d.par	Parameter file for kriging.
merge_multi.par	Parameter file for merging separated columns of data.
mergemod.par	Parameter file for merging the gridded results.
nscore.par	Parameter file for transforming to normal scores.
psctm.par	Parameter file for producing 3D maps.
sgsim.par	Parameter file for generating random numbers.
scatplt.par	Parameter file for plotting the scatter plots.

scatxval.par	Parameter file for cross plotting the results.
scatxval.par	Parameter file for cross plotting the results.
pixelplt.par	Parameter file for plotting 2D results (maps).
postsim.par	Parameter file for averaging the realizations.
vargplt.par	Parameter file for variogram plot.
vmodel.par	Parameter file for variogram modeling.

Mini-modeling and 3D conventional modeling of Fort McMurray geostatistical data

Eugene Ben-Awuah, Samira Kalantari, and Hessameddin Eivazy
Mining Optimization Laboratory (MOL)
University of Alberta, Edmonton, Canada

Abstract

In this paper, two modeling works performed on the provided geostatistical data related to Fort McMurray formation are elaborated. There are two main steps for regional modeling of reservoir known as mini-modeling and 3-D conventional data modeling. The focus of mini-modeling and 3-D conventional modeling is to model the porosity and permeability throughout the domain in 2-D and 3-D. Various steps of these modeling works are explained in great detail.

1. Introduction

The provided data is from one part of the McMurray formation and consists of 37 wells with information on X-coordinate, Y-coordinate, SZ, elevation from sea level, facies, porosity, and oil saturation for each well. There are 7 different facies (1 to 7) as follows:

- 1 for Sand
- 2 for sandy IHS
- 3 for Muddy IHS
- 4 for Mud at the top
- 5 for Breccia
- 6 for Mud plug
- 7 for Mud at the bottom

In order to visualize the data in 2D, the Locmap program of the GSLIB software is used (Deutsch and Journel, 1997). Fig. 1 shows the location map of the 37 wells in 2D. In Fig. 1, the different colors are used as the means to differentiate the various facies.

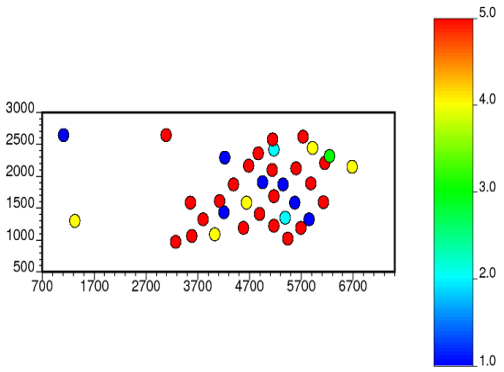

Fig. 1. Location map of the wells (separated by facies).

The organization of this paper is as follows: in section 2, different steps of mini-modeling are elaborated. Section 3 concentrates on the 3-D conventional modeling. Finally, the conclusion is presented in section 4.

2. Mini-modeling

Changing the scale from small scale (decimeter scale) to the geological scale is done by mini-modeling. Mini-modeling includes four steps: (1) finding the distribution of porosity by considering well log porosity, (2) modeling porosity-permeability relations, (3) considering the effective permeability values in horizontal and vertical direction and (4) checking the results from the previous steps for geological modeling (Deutsch, 2009). Here, the results of micro-modeling are used to build the mini models.

The main goal of mini-modeling is to establish the porosity/permeability statistics and models for sandy IHS; the resolution is 1dm by 1 dm by 1dm within a volume of 1m by 1m by 1m. Several realizations are done to simulate the porosity values for the mini-modeling grid cells. The probability field simulation and cloud transformation are done to assign the permeability values to the mini-modeling grid cells. In order to find the vertical permeability for the mini model, the K_V/K_H ratio from micro-modeling results are used. Also, to upscale the data from decimeters to meters; flow simulation is done using the simulation output of porosity values, cloud transformation outputs of horizontal and vertical permeability in order to find the effective porosity and effective horizontal and vertical permeability for the mini-modeling data.

2.1. Statistics

After the general description about the mini-modeling goals and tasks to be done, here are some statistics related to the given data, i.e. the maximum, minimum, the mean and the standard deviation (STD) of some variables, are presented in Table 1. showing their histograms.

Table 1. Statistics about the geographical information of data.

Variable	Min.	Max.	Mean	Standard deviation
X-coordinate (m)	1099.6	6678.1	4772.1	1235.66
Y-coordinate (m)	972.2	2643.5	1770.9	517.8
SZ (m)	-77.3	-6.2	-38.6	17.8
Porosity	0.0	0.647	0.208	0.146

Regarding the facies, Table 2 presents the statistics about the porosity for different facies. The following table and plots indicate a summary of statistics and histogram plots of porosity for

different facies. In addition, Figs. 2 to 6 show the histogram plots of porosity values in different facies.

Table 2. Statistics related to facies.

Variable	Facies 1 (sand)	Facies 2 (sandy IHS)	Facies 3 (muddy IHS)	Facies 5 (breccia)	Facies 4, 6 & 7 (muddy shale)
Mean		0.197	0.108	0.203	0.024
Standard deviation	0.074	0.100	0.090	0.091	0.065
Maximum	0.647	0.40	0.38	0.41	0.644
Minimum	0	0	0	0	0

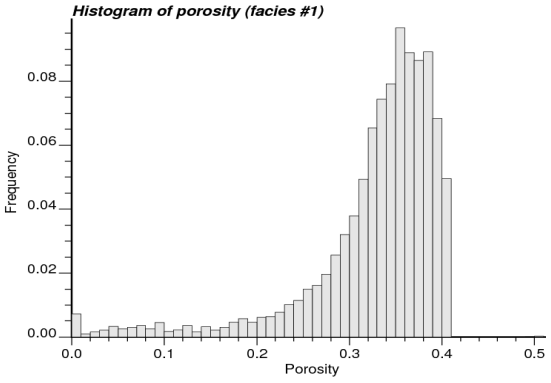

Fig. 2. Histogram plot of porosity of facies 1.

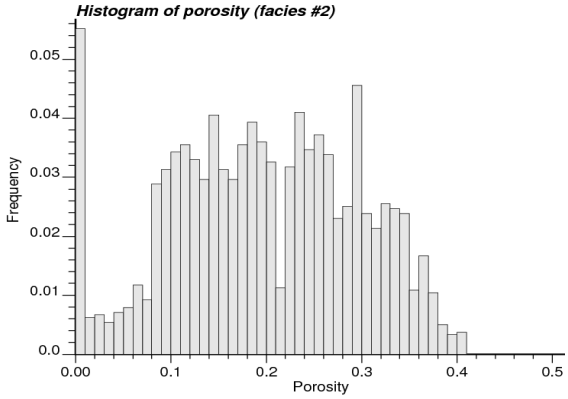

Fig. 3. Histogram plot of porosity of facies 2.

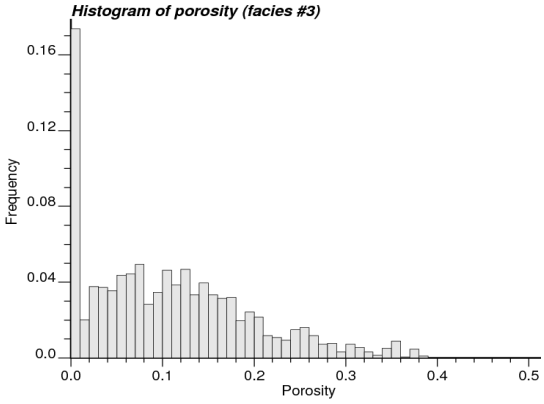

Fig. 4. Histogram plot of porosity of facies 3.

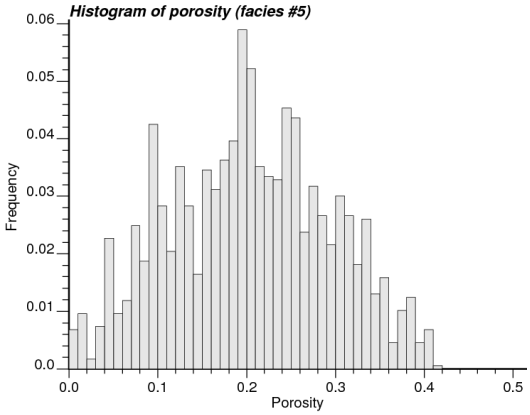

Fig. 5. Histogram plot of porosity of facies 5.

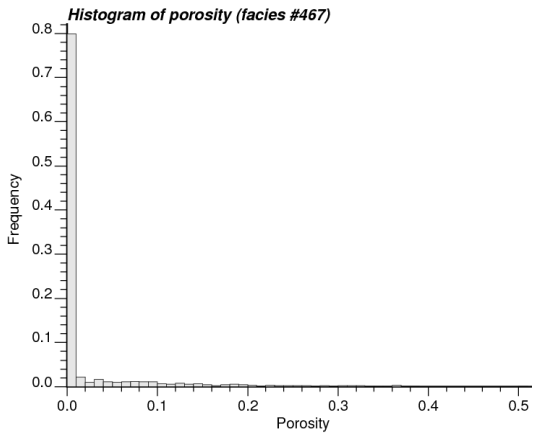

Fig. 6. Histogram plot of porosity of facies 467.

2.2. Experimental semivariogram

Experimental semivariogram shows the variability of a variable in a specific direction. To calculate the vertical semivariogram, first, the data are converted to normal score values. This is done using the NSCORE command from GSLIB (Deutsch and Journel, 1997). In this part we are interested in the semivariogram of sandy IHS facies, therefore the data for the sandy HIS facies are used to create the semivariogram. The values of porosity for facies 2 are converted to normal score values. After converting the data, the vertical semivariogram for porosity of facies 2 is calculated based on the corresponding normal score values. Table 3 indicates the parameters for vertical semivariogram calculation.

Table 3. Experimental semivariogram parameters.

Parameter	Value	Parameter	Value
Number of lags	100	Azimuth angle	
Lag separation	0.01m	Dip angle	
Lag tolerance	0.005m	Azimuth tolerance	
Calculation range	1m	Dip tolerance	

2.3. Semivariogram modeling

After calculating the experimental semivariogram, it should be modeled. The semivariogram model will be used in simulation, kriging, and other steps of mini-modeling. The specifications of vertical and horizontal semivariogram models are presented in Table 4.

Table 4. Semivariogram model parameters.

Direction	Nested Structure No.	Nested Structure type	Contribution	Range (hor.)
vertical	1	nugget	0.00	N/A
	2	spherical	0.43	0.7 m
	3	spherical	0.57	9.0 m
horizontal	1	nugget	0.00	N/A
	2	spherical	0.43	3.5 m
	3	spherical	0.57	45.0 m

The horizontal semivariogram model is considered to have the same parameters such as nested structure and nugget effect as the vertical semivariogram, but the range of the horizontal

semivariogram is considered to be 5 times the vertical one. Figs. 7 and 8 show the semivariogram models in 2 directions. Here, the value of sill is 1, because the data are normal scores.

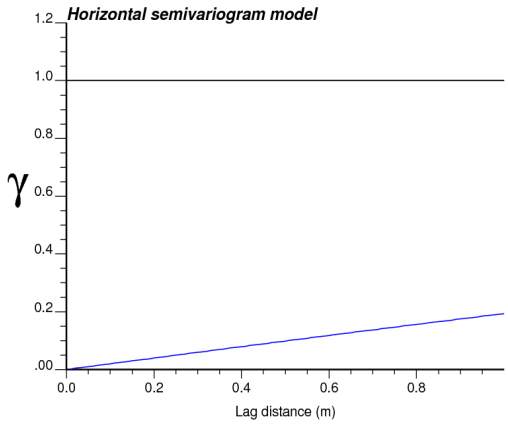

Fig. 7. Semivariogram model in the horizontal direction.

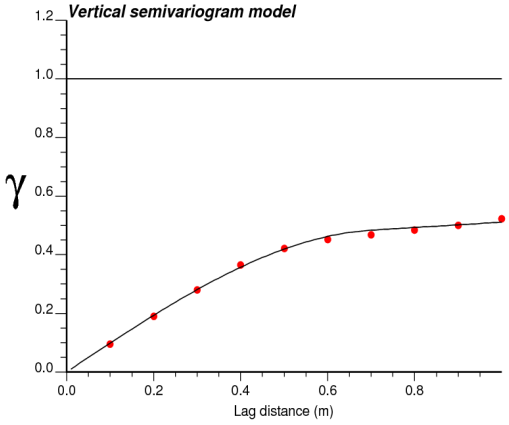

Fig. 8. Semivariogram model in the vertical direction.

2.4. Sequential Gaussian Simulation of Porosity

In this part, porosity of sandy IHS facies is simulated. Two kinds of Gaussian simulation are done on the porosity values, both of them based on unconditional data. One is carried out with no transformation and no reference distribution. The other one is performed with the reference distribution and transformation. The former, is named P-field simulation and its results include the normal scores. In the latter, the transformation is set as the transformation table created in producing the normal scores. Also, the reference distribution is set as the porosity values of facies 2. The results of the latter simulation are in original scale of porosity values. In both kinds of simulation, 100 realizations with grid size of 0.1 m by 0.1 m by 0.1 m along X, Y, and Z directions within the cube of 1m by 1m by 1m are set; therefore there will be 10 grid cells along each direction. Figs. 9 and 10 show the 3-D view of Gaussian simulation of porosity with transformation in original scale after using POSTSIM command of GSLIB for averaging the values of 100 realizations.

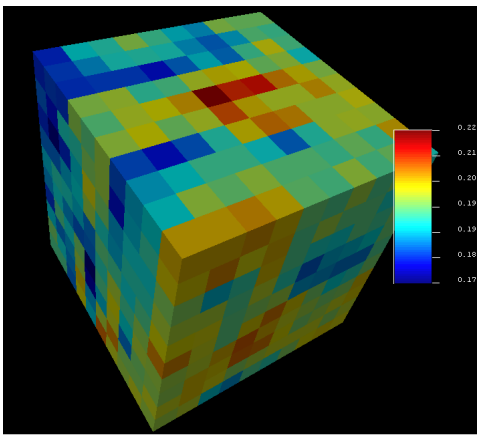

Fig. 9. 3-D view of simulated porosity.

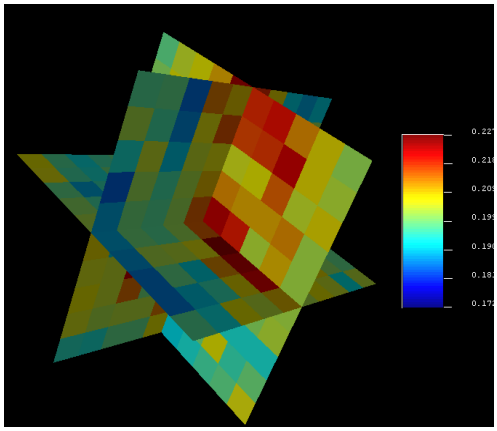

Fig. 10. Typical 2-D views of simulated porosity.

Table 5 indicates the statistics of POSTSIM results.

Table 5. Statistics of results of simulation after using POSTSIM.

Number of lines of the input data	1000
Mean	0.202
Standard deviation	0.007
Minimum	0.185
Maximum	0.22

2.5. Bivariate distribution

In order to model the permeability values related to the micro-modeling results, a bivariate distribution of porosity-permeability is required. Using the Bimodel program of GSLIB, the bivariate distribution of porosity and permeability is modeled. Bimodel program quantifies a bivariate distribution at a user-defined discretization for K_H and Ø (McLennan *et al.*, 2006). The K_H and Ø were extracted from the flow simulation output of micro-modeling. Fig. 11 indicates the bivariate distribution of porosity and horizontal permeability values.

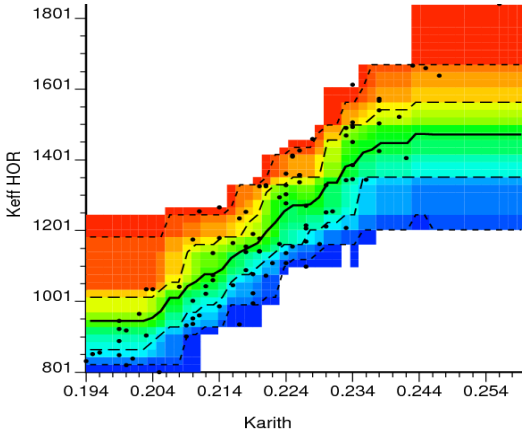

Fig. 11. Bivariate distribution of porosity and horizontal permeability.

2.6. Cloud transformation

In this step, to find the horizontal permeability values for the mini-modeling grid cells, the Cltrn program of GSLIB is used. Cloud transformation technique is used to populate the permeability values for the given porosity values from the simulation output. The cloud transformation technique uses the bivariate distribution of porosity and horizontal permeability from micro-modeling results and porosity values of mini-modeling from the sequential Gaussian simulation outputs to assign permeability values to the mini-modeling grid cells. Therefore, three input files for cloud transformation are: the bivariate model of porosity and horizontal permeability from section 2.5 and output files of the 2 types of simulation performed in section 2.4. The output of the cloud transform has three columns: porosity values, probabilities, and K values assigned to the mini-modeling grid cells as the result of cloud transformation. The cloud transform will preserve the uncertainty in the bivariate relationship between porosity and permeability. This technique will use the probability field simulation (p-field) to sample the permeability cumulative distribution function (CDF) to ensure the spatial continuity in the neighboring model cells (Waite *et al.*, 2004). Table 6 represents the statistics for permeability values of cloud transformation results. The output file of cloud transformation includes 100 realizations. Using POSTSIM command, the average of these realizations is obtained. Fig. 12 and Fig. 13 show the output of POSTSIM.

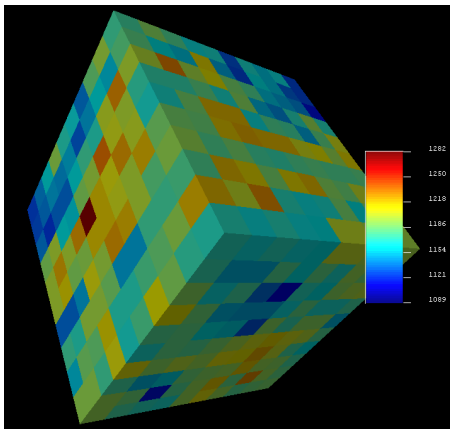

Fig. 12. 3-D view of horizontal permeability from cloud transform.

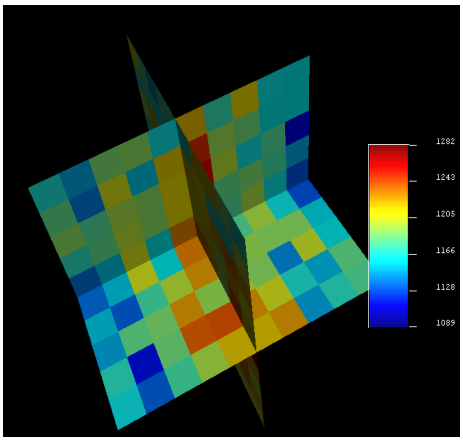

Fig. 13. 2-D views of horizontal permeability from cloud transform.

So far, the bivariate distribution of horizontal permeability and porosity are calculated and drawn. Also, using cloud transformation, the values of horizontal permeability are simulated. There are some ways to calculate the vertical permeability. One way which is applied here is to use the ratio of vertical permeability and horizontal permeability from the flow model done in the macro-modeling. This ratio equals to 1.653. Then, the value of this ratio is multiplied to the values of horizontal permeability outputted from the cloud transform. The results for the vertical permeability are shown in Figs. 14 and 15.

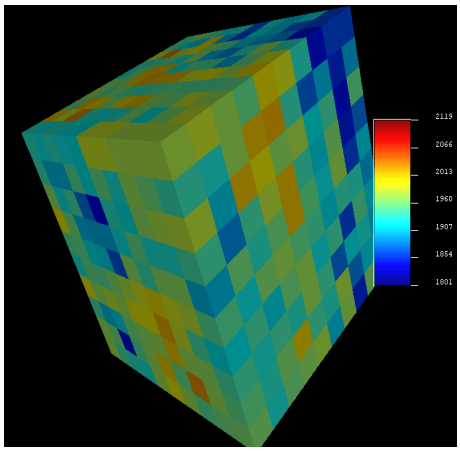

Fig. 14. 3-D view of vertical permeability.

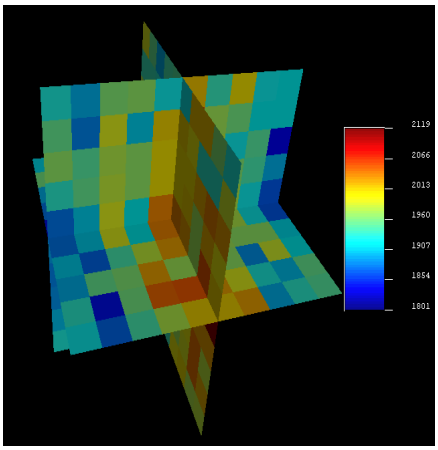

Fig. 15. 2-D views of vertical permeability.

2.7. Flow modeling and analysis

Using the porosity, horizontal permeability and vertical permeability from the cloud transformation output, the flow simulation can be done to upscale the data from decimeter scale to the meter scale. The flow simulation calculates the effective horizontal and vertical permeability values and the effective porosity values for the mini-modeling grid cells. Here, using FLOWSIM program of GSLIB, the flow of porosity and permeability in the domain is modeled. The porosity of the domain is calculated as the arithmetic average of porosity of grid cells. The arithmetic average cannot be applied for permeability. The summary statistics of porosity, vertical and horizontal permeability are presented in Table 6.

Table 6. Summary statistics of flow simulation results.

Variable	Min.	Max.	Mean	Standard deviation
Porosity	0.086	0.307	0.1988	0.0449
Vertical permeability (mD)	1554.317	2284.027	1883.0311	176.961
Horizontal permeability (mD)	946.073	1401.500	1161.628	110.856
Vertical/horizontal permeability (mD)	1.592	1.643	1.621	0.0103

Fig. 16 shows the diagram of change of average porosity between 100 realizations of FLOWSIM.

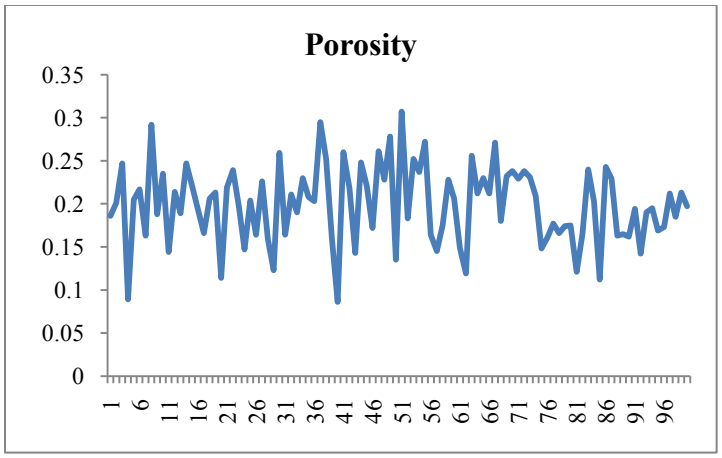

Fig. 16. Diagram of changes of porosity through realizations.

Also, the histograms of porosity, vertical and horizontal permeability are shown in Figs. 17 to 19.

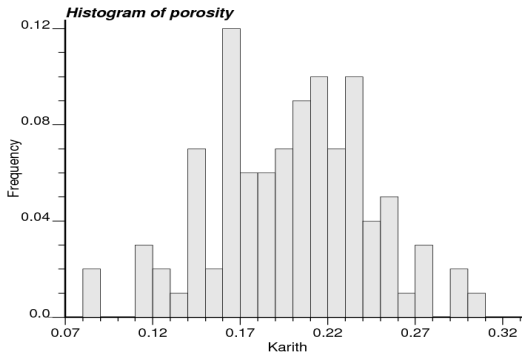

Fig. 17. Histogram plot of porosity.

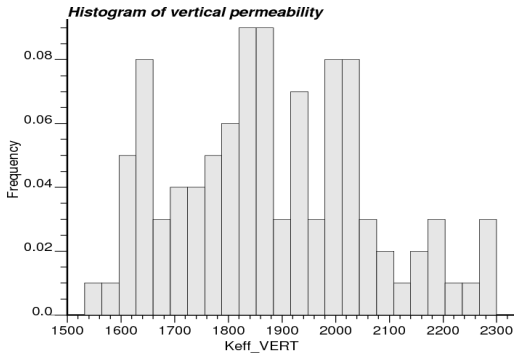

Fig. 18. Histogram plot of vertical permeability.

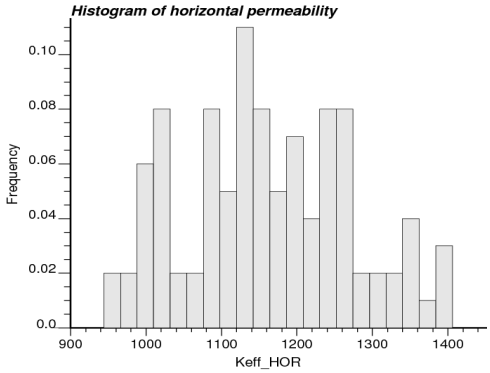

Fig. 19. Histogram plot of horizontal permeability.

Fig. 20 shows the scatter plot of horizontal permeability versus porosity. The correlation is 0.998.

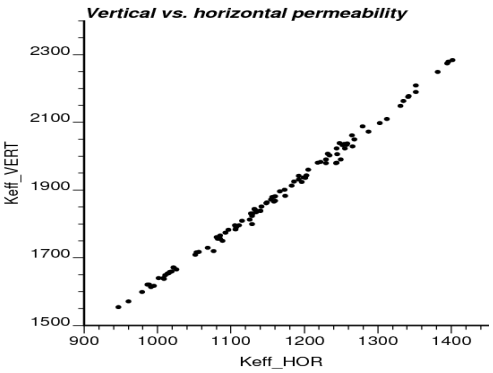

Fig. 20. Scatter plot of vertical permeability versus horizontal permeability.

Fig. 21 shows the scatter plot of the ratio of vertical to horizontal permeability versus horizontal permeability. The corresponding correlation is -0.314.

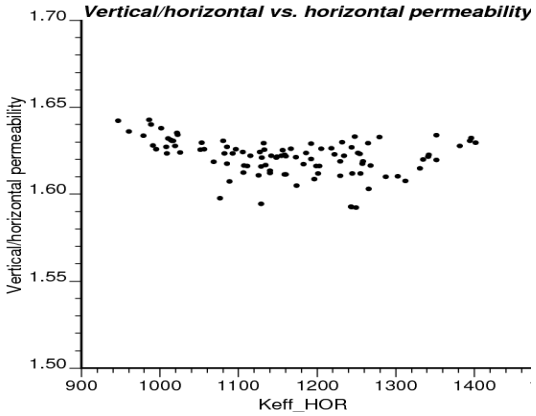

Fig. 21. Scatter plot of ratio of vertical permeability to horizontal permeability versus horizontal permeability.

3. 3D conventional modeling

The 3D conventional modeling of an exploration data within the McMurray formation is presented here. Therefore, the general information about the data and the related statistics are the same as in section 2. The steps of the 3D conventional modeling are presented in this section. These steps include facies modeling, porosity modeling and merging the models.

3.1. Facies modeling

The main tasks involved in the facies modeling are as follows: 1) Trend modeling 2) Semivariogram modeling 3) Kriging and 4) Sequential Indicator Simulation (SIS).

3.1.1 Trend modeling

Areal proportions of the facies are summarized by calculating the proportion of each facies in the 37 wells. This gives the facies proportions in all the wells categorized by well ID. Fig. 22 shows the areal proportion of each facies in the vertical direction.

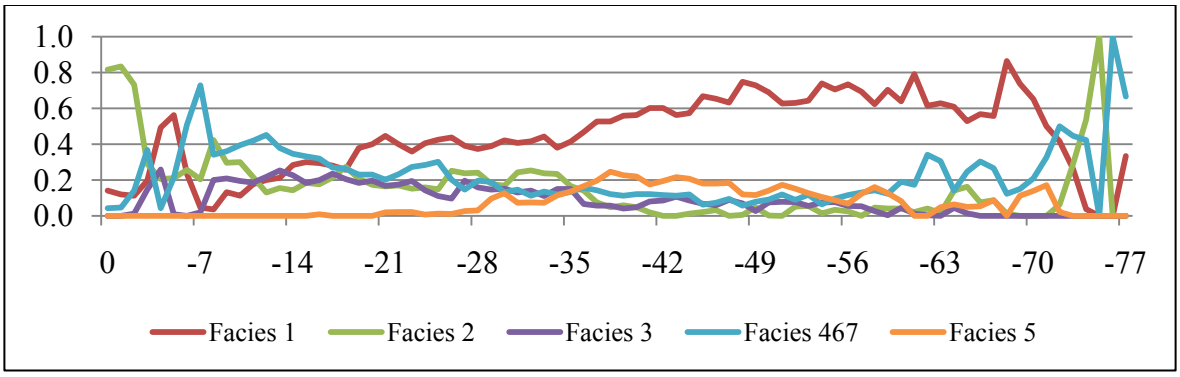

Fig. 22. Areal proportion of each facies in the vertical direction.

Then, in order to estimate the facies trend in 2D at all locations, the facies data are kriged. Ordinary kriging with a variogram that has 40% nugget effect and a range of 1/3 of the domain size is used. This is known as the horizontal trend. The horizontal trend statistics from kriging is summarized in Table 7 for all the facies. Also, Fig. 23 to Fig. 27 show the horizontal trend maps for each facies.

Table 7. Horizontal trend statistics from kriging of all facies.

Parameter \ Statistic	Minimum	Maximum	Mean	Std. deviation
Facies 1	0.264	0.685	0.471	0.095
Facies 2	0.047	0.273	0.134	0.045
Facies 3	0.013	0.283	0.116	0.062
Facies 467	0.066	0.501	0.216	0.089
Facies 5	0.029	0.144	0.064	0.020

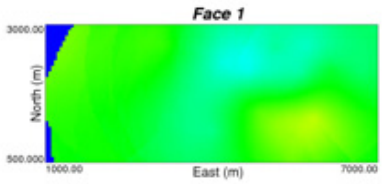

Fig. 23. Horizontal trend map of facies 1.

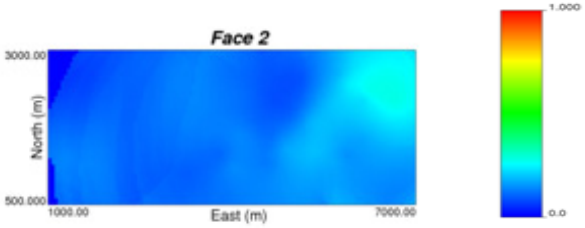

Fig. 24. Horizontal trend map of facies 2.

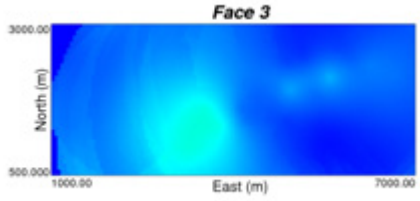

Fig. 25. Horizontal trend map of facies 3.

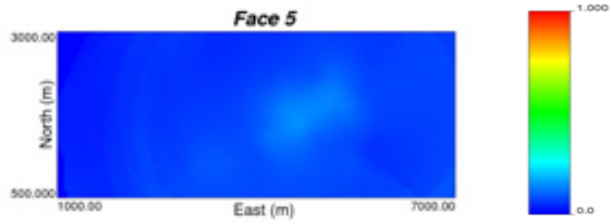

Fig. 26. Horizontal trend map of facies 5.

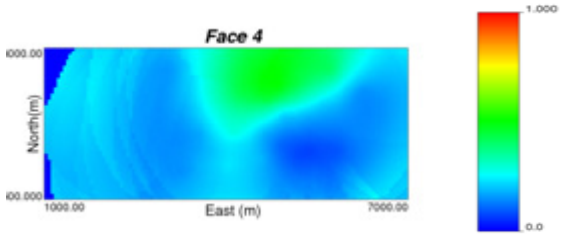

Fig. 27. Horizontal trend map of facies 467.

A vertical trend model is calculated from the data by subsetting the data by slices of SZ. The original vertical data spacing is 0.1m and this is regrouped in SZ slices of 1m which is the target grid dimension. A graph of facies proportion in every 1m depth is plotted to visualize the vertical trend. Fig. 28 to Fig. 32 show the plots of the vertical trend for all of the facies.

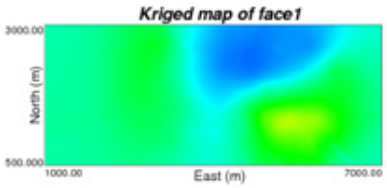

Fig. 28. Vertical trend map of facies 1.

Fig. 29. Vertical trend map of facies 2.

Fig. 30. Vertical trend map of facies 3.

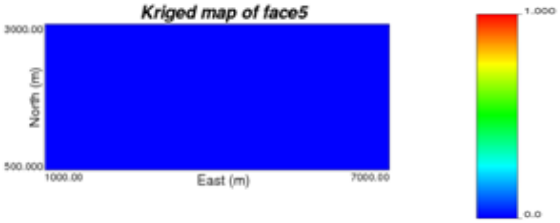

Fig. 31. Vertical trend map of facies 5.

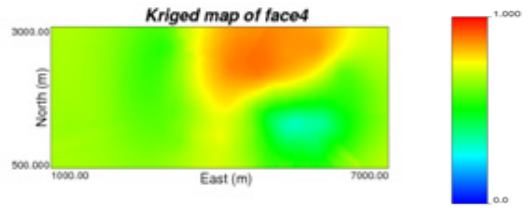

Fig. 32. Vertical trend map of facies 467.

The horizontal and vertical trend models are merged to get a 3-D trend model which will be used to control kriging and simulation of the facies proportion in the grid. The 3-D trend model is calculated based on Eq. (1) (Hong and Deutsch, 2009):

$$m(x,y,z) = \frac{m_z(z).m_{x,y}(x,y)}{m_{global}} \quad (1)$$

Where $m_z(z)$: mean from the vertical trend,

$m_{x,y}(x,y)$: mean from the areal trend,

m_{global} : global mean from histogram,

m(x,y,z): mean at location (x,y,z).

This equation is based on the assumption of conditional independence of vertical and areal trends. Use of this equation amounts to scaling the vertical trend curve, m_z, by the areal trend, m_x and m_y. Maps of facies of the same slice in the 3D trend model are comparable to that from the 2D trend model.

3.1.2 Semivariogram modeling

The original 3-D data is used to calculate the indicator experimental semivariogram for each of the facies in the vertical and horizontal directions. All the vertical semivariograms are modeled from the experimental semivariogram. The horizontal semivariograms for facies 1 and 4 are modeled whilst anisotropy ratio is used to obtain the horizontal semivariogram models for facies 2, 3, and 5. Vertical to horizontal anisotropy ratio is considered to be 1:80. The semivariograms for facies 1 to 5 are shown by Eqs. (2) to (6), respectively. The modeled semivariogram plots are shown in Fig. 33 to Fig. 39.

$$\gamma(h) = 0.0 + 0.125Exp_{\substack{av=2.2 \\ ah1=1.0 \\ ah2=1.0}}(h) + 0.103Sph_{\substack{av=24.0 \\ ah1=1200.0 \\ ah2=1200.0}}(h) + 0.020Sph_{\substack{av=24.0 \\ ah1=20000.0 \\ ah2=20000.0}}(h) \quad (2)$$

$$\gamma(h) = 0.0 + 0.0780Exp_{\substack{av=2.5 \\ ah1=200.0 \\ ah2=200.0}}(h) + 0.0487Sph_{\substack{av=24.0 \\ ah1=1920.0 \\ ah2=1920.0}}(h) \quad (3)$$

$$\gamma(h) = 0.0 + 0.0500Exp_{\substack{av=2.3 \\ ah1=1.0 \\ ah2=1.0}}(h) + 0.0350Sph_{\substack{av=10.0 \\ ah1=800.0 \\ ah2=800.0}}(h) + 0.0125Sph_{\substack{av=50.0 \\ ah1=4000.0 \\ ah2=4000.0}}(h) \quad (4)$$

$$\gamma(h) = 0.0 + 0.060Exp_{\substack{av=1.5 \\ ah1=1.0 \\ ah2=1.0}}(h) + 0.047Sph_{\substack{av=7.5 \\ ah1=500.0 \\ ah2=500.0}}(h) + 0.055Sph_{\substack{av=60.0 \\ ah1=1400.0 \\ ah2=1400.0}}(h) \quad (5)$$

$$\gamma(h) = 0.0 + 0.0553Exp_{\substack{av=2.5 \\ ah1=200.0 \\ ah2=200.0}}(h) + 0.0180Sph_{\substack{av=12.0 \\ ah1=960.0 \\ ah2=960.0}}(h) \quad (6)$$

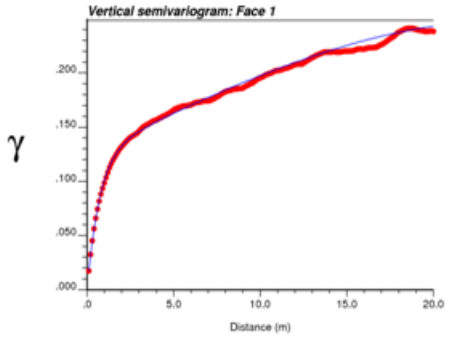

Fig. 33. Vertical semivariogram model of facies 1.

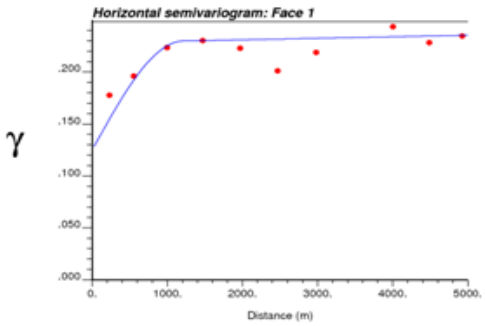

Fig. 34. Horizontal semivariogram model of facies 1.

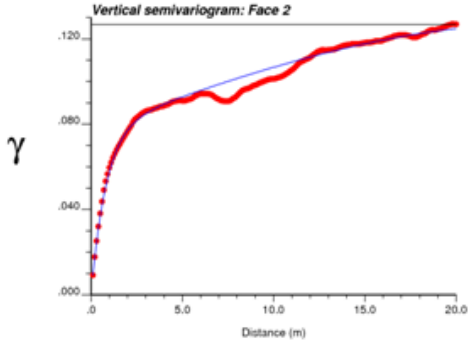

Fig. 35. Vertical semivariogram model of facies 2.

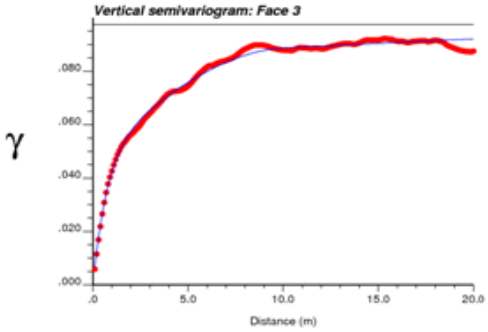

Fig. 36. Vertical semivariogram model of facies 3.

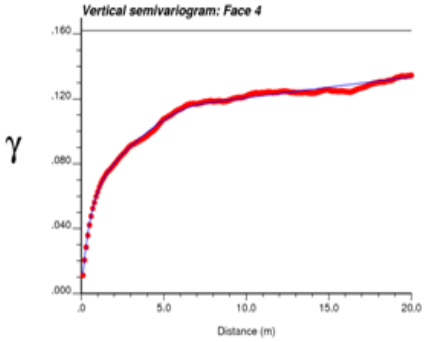

Fig. 37. Vertical semivariogram model of facies 467.

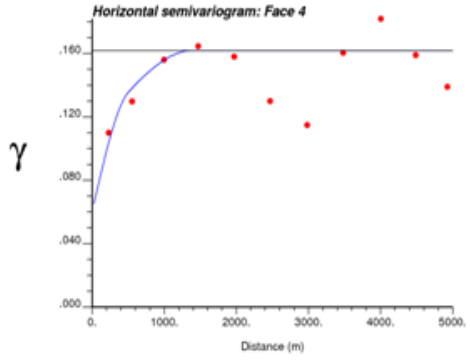

Fig. 38. Horizontal semivariogram model of facies 467.

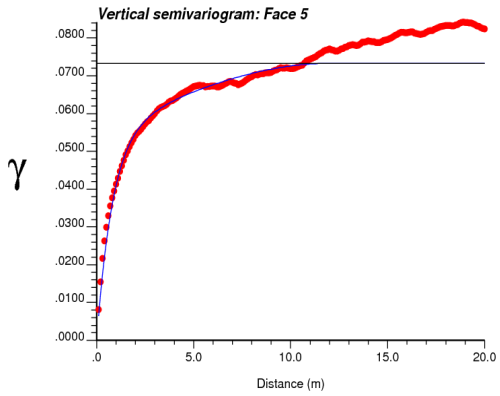

Fig. 39. Vertical semivariogram model of facies 5.

3.1.3 Kriging

Using simple kriging, facies kriged model is validated and estimated from the data using the semivariogram models and the 3-D trend model on a grid of blocks, 120 x 50 x 78 with block sizes of 50m in x-y direction and 1m in z direction. The use of the trend model is to guide the kriging process as various facies proportions in the grid. The cross validation of the facies showed good results with high correlation coefficients and a regression slope of 1 in all facies. After kriging 468000 blocks, the estimated mean and standard deviation for the facies have been summarized in Table 8. Figs. 40 to 44 show the kriged maps of the facies.

Table 8. Summary statistics from the kriged facies models

Parameter \ Statistic	Minimum	Maximum	Mean	Std. deviation
Facies 1	0	0.995	0.468	0.224
Facies 2	0	1.000	0.158	0.187
Facies 3	0	0.550	0.099	0.103
Facies 467	0	1.000	0.247	0.182
Facies 5	0	0.376	0.065	0.068

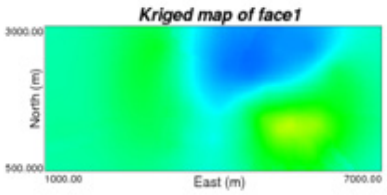

Fig. 40. Kriged map of facies 1.

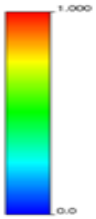

Fig. 41. Kriged map of facies 2.

Fig. 42. Kriged map of facies 3.

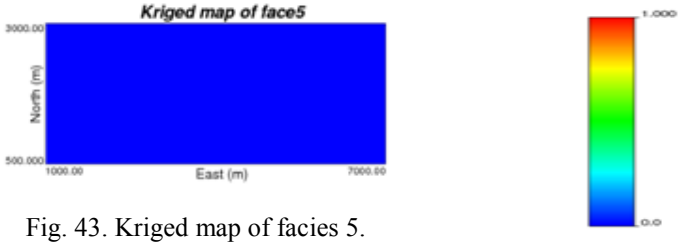

Fig. 43. Kriged map of facies 5.

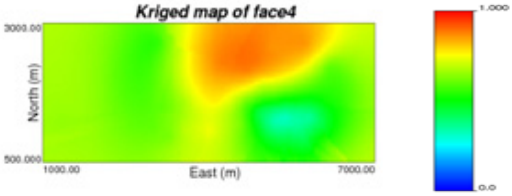

Fig. 44. Kriged map of facies 467.

3.1.4 Sequential indicator simulation (SIS)

Using simple kriging with locally varying means (LVM), a facies SIS is performed using the original 3-D well data, the 3-D trend model data and the semivariogram models. The use of the trend model is to guide the simulation process as to the various facies proportions in the grid. 100 realizations are simulated with light cleaning and the results summarized for comparison with the kriged data. The mean and standard deviation of the facies from SIS are shown in Table 9 and compares well with kriged results and the original data statistics. Fig. 45 shows a 2D view of 100 realization from the SIS data which shows the dominance of facies 467 at the upper portion of the formation.

Table 9. Statistics of SIS for each facies.

Parameter	Mean	Std. deviation
Facies 1	0.492	0.480
Facies 2	0.133	0.339
Facies 3	0.086	0.281
Facies 467	0.249	0.432
Facies 5	0.040	0.196

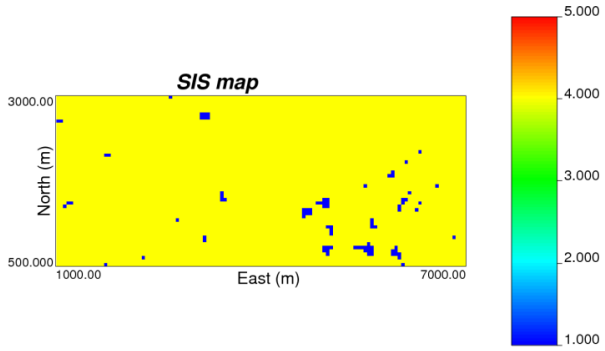

Fig. 45. 2D view of facies model from simulation.

3.2. Porosity modeling

The tasks involved in porosity modeling are: 1) declustering and normal score transform 2) semivariogram modeling 3) kriging and 4) Sequential Gaussian Simulation (SGS).

3.2.1 Declustering and normal score transform

The subset porosity data are declustered to quantify the impact of irregular drillhole spacing on the porosity statistics. The results from the declustered data compared with the equal weighted statistics data for each facies is shown in Table 10.There are no significant differences in the two results. The data are then transformed to normal scores without declustered weights to be used in semivariogram and kriging calculations.

Table 10. Statistics of porosity in the facies from equal weighted and declustered data.

Statistic / Parameter	Minimum	Maximum	Equal weighted		Declustered	
			Mean	Std. dev.	Mean	Std. dev.
Porosity of facies 1	0	0.647	0.327	0.074	0.311	0.090
Porosity of facies 2	0	0.400	0.197	0.099	0.181	0.103
Porosity of facies 3	0	0.380	0.108	0.089	0.108	0.089
Porosity of facies 467	0	0.644	0.024	0.065	0.024	0.065
Porosity of facies 5	0	0.410	0.203	0.091	0.203	0.091

3.2.2 Semivariogram modeling

The normal score data without declustering weights is used in calculating the experimental semivariograms for each of the facies porosity in the vertical and horizontal directions. All the vertical semivariograms are modeled from the experimental semivariograms. The horizontal semivariograms for porosity of facies 467 is modeled whilst anisotropy ratio is used to obtain the horizontal semivariogram models for porosity of facies 1, 2, 3, and 5. Vertical to horizontal anisotropy ratio of 1:80 is used. The porosity semivariograms for the five facies are modeled by Eq. (7) to (11), respectively. The modeled porosity semivariogram plots are presented in Figs. 46 to 51.

$$\gamma(h) = 0.0 + 0.47\,Exp_{\substack{av=1.2\\ah1=96.0\\ah2=96.0}}(h) + 0.53\,Sph_{\substack{av=22.0\\ah1=1760.0\\ah2=1760.0}}(h) \quad (7)$$

$$\gamma(h) = 0.0 + 0.53\,Exp_{\substack{av=1.1\\ah1=88.0\\ah2=88.0}}(h) + 0.47\,Sph_{\substack{av=24.0\\ah1=1920.0\\ah2=1920.0}}(h) \quad (8)$$

$$\gamma(h) = 0.0 + 0.51\,Exp_{\substack{av=1.1\\ah1=88.0\\ah2=88.0}}(h) + 0.49\,Sph_{\substack{av=40.0\\ah1=3200.0\\ah2=3200.0}}(h) \quad (9)$$

$$\gamma(h) = 0.4 + 0.13\,Exp_{\substack{av=0.1\\ah1=1.0\\ah2=1.0}}(h) + 0.17\,Sph_{\substack{av=4.0\\ah1=1900.0\\ah2=1900.0}}(h) + 0.30\,Sph_{\substack{av=40.0\\ah1=1900.0\\ah2=1900.0}}(h) \quad (10)$$

$$\gamma(h) = 0.0 + 0.8\,Exp_{\substack{av=1.0\\ah1=80.0\\ah2=80.0}}(h) + 0.2\,Sph_{\substack{av=60.0\\ah1=4800.0\\ah2=4800.0}}(h) \quad (11)$$

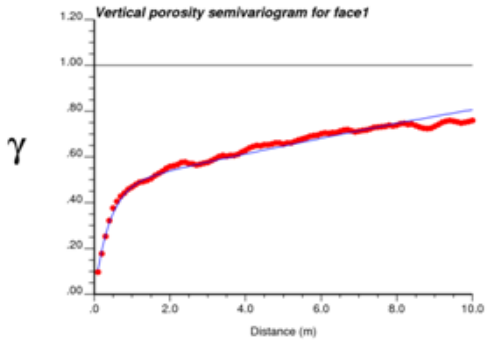

Fig. 46. Vertical semivariogram of porosity for facies 1.

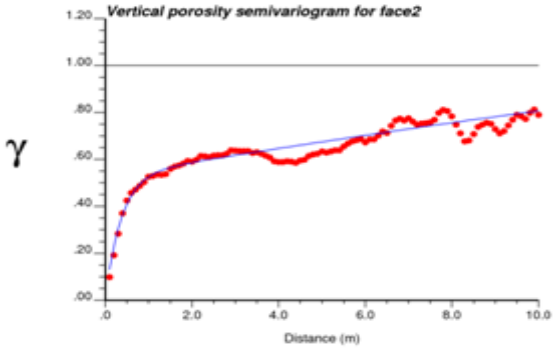

Fig. 47. Vertical semivariogram of porosity for facies 2.

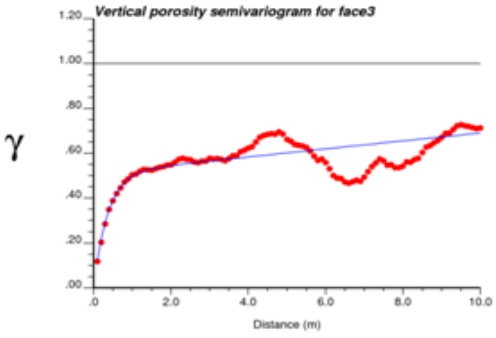

Fig. 48. Vertical semivariogram of porosity for facies 3.

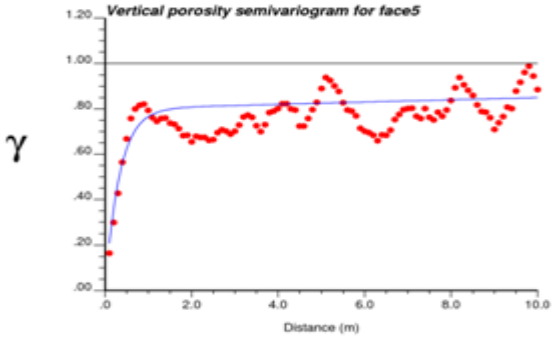

Fig. 49. Horizontal semivariogram of porosity for facies 5.

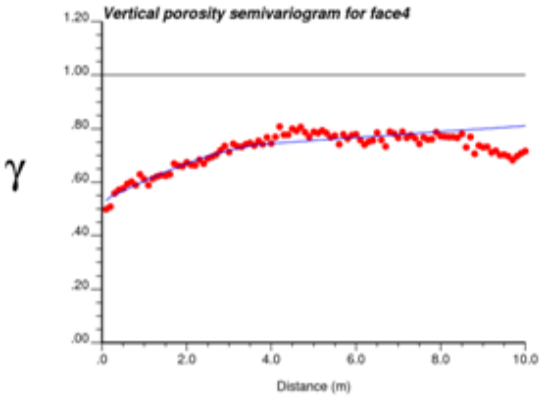

Fig. 50. Vertical semivariogram of porosity for facies 467.

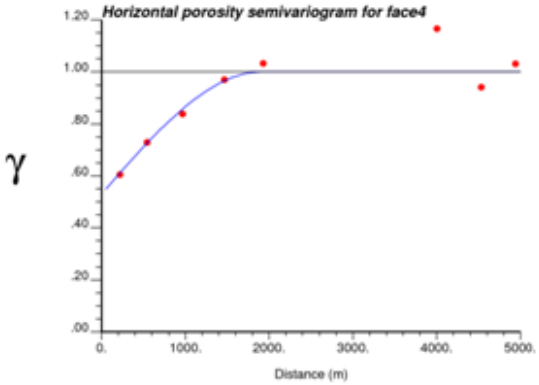

Fig. 51. Vertical semivariogram of porosity for facies 467.

3.2.3 Kriging

Using simple kriging, a porosity kriged model is validated and estimated from the normal score data of each facies using the variogram models on a grid of blocks, 120 x 50 x 78 with block sizes of 50m in x-y direction and 1m in z direction. The cross validation of porosity of the facies shows good results with high correlation coefficients and a slope of regression of 1 in all facies. After kriging 468000 blocks and back-transforming, the estimated mean and variance for porosity of the facies is summarized in Table 11. Figs. 52 to 56 show the cross validation results of porosity of the facies from kriging.

Table 11. Summary statistics from the porosity kriged model of the facies.

Parameter	Minimum	Maximum	Mean	Std. deviation
Kriged porosity of facies1	0.278	0.347	0.344	0.005
Kriged porosity of facies 2	0.000	0.209	0.192	0.013
Kriged porosity of facies 3	0.056	0.151	0.098	0.006
Kriged porosity of facies 467	0.000	0.113	0.011	0.025
Kriged porosity of facies 5	0.000	0.223	0.176	0.068

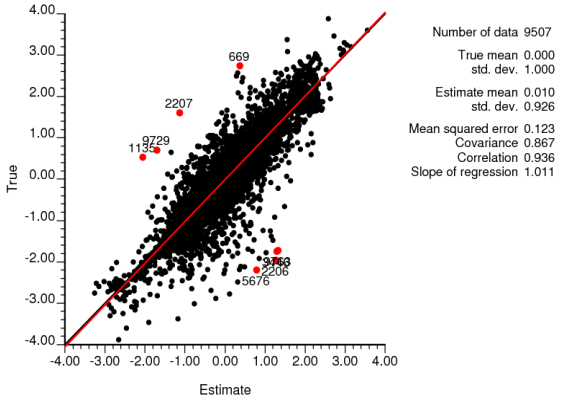

Fig. 52. Cross validation for facies 1.

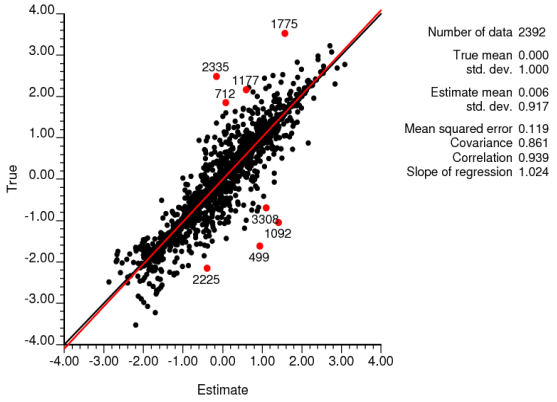

Fig. 53. Cross validation for facies 2.

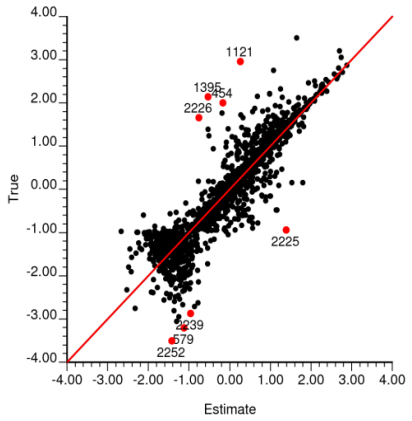

Fig. 54. Cross validation for facies 3.

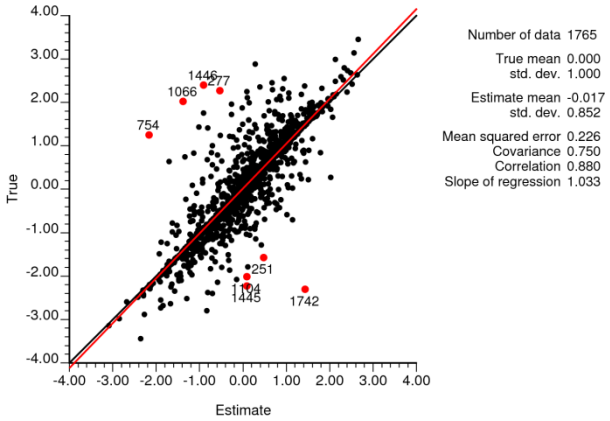

Fig. 55. Cross validation for facies 467.

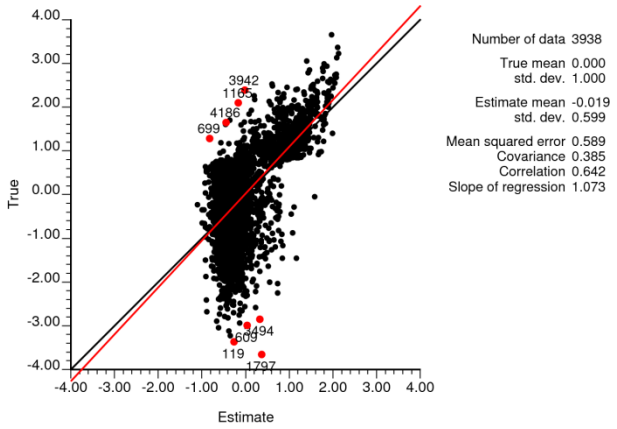

Fig. 56. Cross validation for facies 5.

3.2.4 Sequential Gaussian Simulation (SGS)

Using simple kriging a SGS of porosity is performed using the declustered porosity data of each facies and the semivariogram models. The grid system is simulated through 100 realizations and the results are summarized for comparison with the kriged data. The mean and standard deviation of porosity of the facies from SGS are presented in Table 12 and compares well with the kriged results and the original data statistics. Figs. 57 to 61 show the map of porosity of the facies from the SGS data which shows the dominance of porosity of facies 1.

Table 12. Statistics of porosity of the facies from SGS.

Parameter	Minimum	Maximum	Mean	Std. deviation
SGS porosity of facies 1	0	0.364	0.307	0.015
SGS porosity of facies 2	0	0.300	0.177	0.016
SGS porosity of facies 3	0	0.259	0.098	0.015
SGS porosity of facies 467	0	0.210	0.018	0.008
SGS porosity of facies 5	0	0.400	0.202	0.009

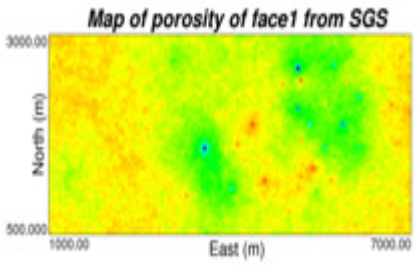

Fig. 57. Simulation map of porosity for facies 1.

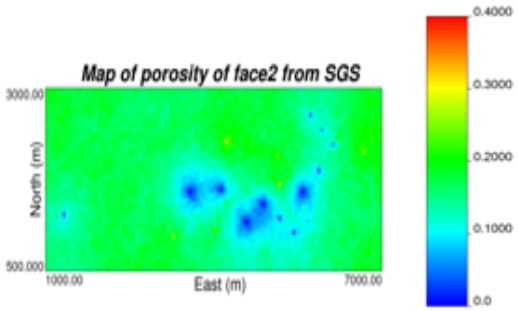

Fig. 58. Simulation map of porosity for facies 2.

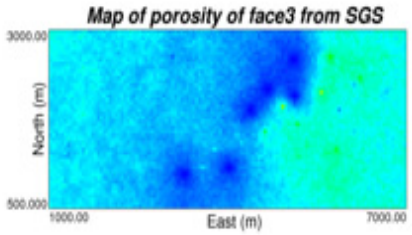

Fig. 59. Simulation map of porosity for facies 3.

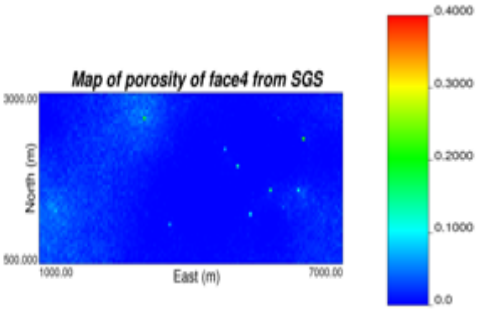

Fig. 60. Simulation map of porosity for facies 5.

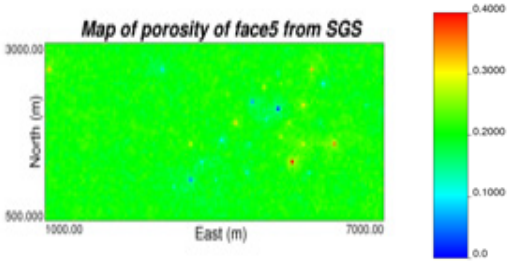

Fig. 61. Simulation map of porosity for facies 467.

3.3. Merging models

The facies simulation output from SIS and the five porosity simulation outputs of the facies are merged to get the final 100 porosity models. This is done by matching the different porosity data of the facies with the facies data from simulation and drawing the appropriate porosity value that matches the simulated facies. Statistics from the merged porosity models are summarized in Table 13. The histogram plot of the merged porosity models is shown in Fig. 62. Maps of slice 1 and 78 of 100th realization in the merged porosity models are shown in Fig. 63. This shows the dominance of facies 467 with low porosity values in the upper portion of the formation and facies 1, 2 and 5 with high porosity values in the lower portion of the formation.

Table 13. Statistics from merged porosity models.

Parameter	Minimum	Maximum	Mean	Std. deviation
Porosity of merged model	0	0.647	0.179	0.155

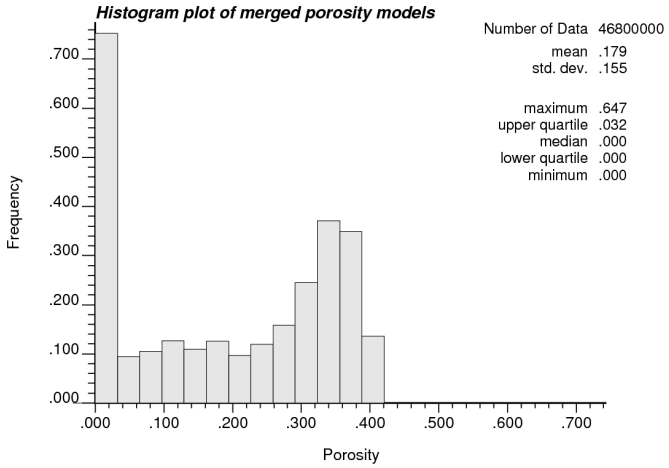

Fig. 62. Histogram plot of the merged porosity models.

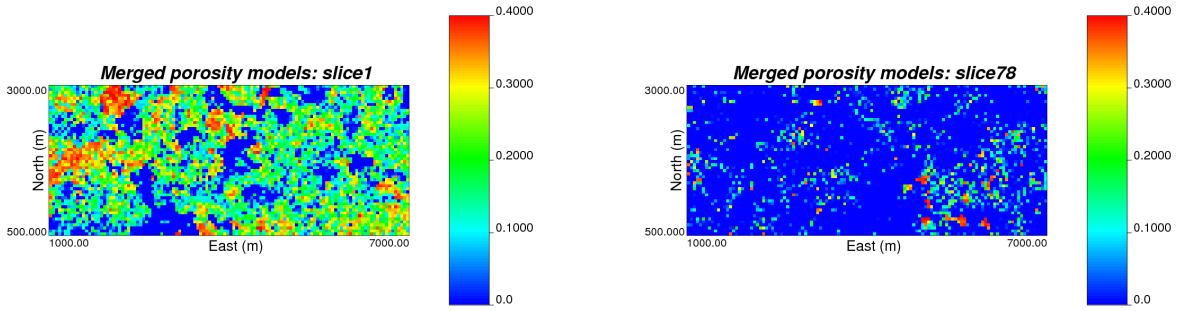

Fig. 63. Maps of slice 1 and 78 of realization 100 in the merged porosity models.

4. Conclusions

In this paper, two main modeling at the scale of regional modeling are performed. The data related to geological features of a domain in Fort McMurray formation are used for these modeling works. Mini-modeling considers the results of micro-modeling and the well log data. The resolution scale is dm^3 within a m^3 volume. Bivariate distribution of porosity-horizontal permeability from the micro-modeling results are extracted. Then, using cloud transformation technique, horizontal permeability values are assigned to the mini-modeling grid cells. In order to find the vertical permeability, the average Kv/K_H ratio of micro-modeling is used. The correlation between K_v/K_H ratio and K_H is very low which is reasonable. On the other hand, the 3-D conventional data modeling enables us to estimate porosity of a deposit at a resolution of about 103m. The five facies in the study area under consideration are: 1) sand, 2) sandy Inclined Heterolithic Strata (IHS), 3) muddy IHS, 4) mud, and 5) breccia. The most dominant facies are 1 and 467. Facies 1 has the most

dominant porosity value of 0.3 and facies 467 is the least porous with a value approximately zero. After merging the facies model and the porosity models, 100 final models of porosity are obtained.

5. References

[1] Deutsch, C. V. (2009). Geostatistical methods for modeling earth sciences data. Edmonton, University of Alberta,

[2] Deutsch, C. V. and Journel, A. G. (1997). *GSLIB: Geostatistical Software Library and Users Guide.* Oxford University Press, New York, Second ed,

[3] Hong, S. and Deutsch, C. V. (2009). 3D trend modeling by combining lower order trends. CCG Annual Report 11, University of Alberta, Edmonton,

[4] McLennan, J. A., Deutsch, C. V., Garner, D., Wheeler, T. J., Richy, J. F., and Mus, E. (2006). Permeability Modeling for SAGD Precess Using Minimodels. *Society of Petroleum Enigineers*,

[5] Waite, M., Johanson, S., and Betancourt, D. (2004). *Modeling of Scale-Dependent Permeability Using Single-Well Micro-Models: Application to Hamaca Field, Venezuela*, in Proceedings of SPE International Thermal Operations and Heavy Oil Symposium and Western Regional Meeting, Society of Petroleum Engineers, Bakersfield, California,

Hierarchical mine production scheduling using discrete-event simulation

Eugene Ben-Awuah, Samira Kalantari
Yashar Pourrahimian, and Hooman Askari-Nasab
Mining Optimization Laboratory (MOL)
University of Alberta, Edmonton, Canada

Abstract

Mine planning involves different levels of decision-making depending on the time horizon under consideration. Long-term production plans determine the optimal sequence of mining and allocation of resources over a yearly time horizon, whereas short-term scheduling provides the feasible production schedules for every day operations. The main goal of this study is to develop a discrete-event simulation model to link long-term predictive mine plans with short-term production schedules in the presence of uncertainty. We have developed, verified and validated a discrete-event simulation model for open pit production scheduling with the SLAM simulation language. The simulation model proved to bridge the gap between a deterministic long-term yearly plan and a daily dynamic short-term schedule. The simulation model takes into consideration the constraints and uncertainties associated with mining and processing capacities, crusher availability, stockpiling strategy and blending requirements. The results of an iron ore open pit mine case study show that discrete-event simulation is a powerful tool in minimizing the discrepancies between long and short-term mine plans.

1. Introduction

Mine planning traditionally is categorized based on the time horizon of the planning periods or the acceptable ranges of accuracy for project evaluation. The conceptual mine plan establishes a basis for the main variables of the project and economic analysis of the potential viability of the mineral resource. If the project looks promising, a prefeasibility and feasibility study will follow to confirm the economic viability of the mineral project by selecting the effective mining and mineral processing methods and enough details to make a well-informed decision. Subsequently, a bankable feasibility study will obtain the capital required to bring the mine into production and this is followed by the operational planning stage, which is aimed at specifying the details about how the overall plan should be executed.

Life-of-mine production schedules define the complex strategy of ore, waste and overburden displacement over the mine life. The objective of long-term production scheduling is to determine the sequence of extraction and displacement of material in order to fulfill managements' goal within the existing economic and technical constraints. Pit optimization and cut-off analysis lead to definition of reserves and the subsequent long-term production scheduling is the backbone of short-term planning and day to day mining operations. The long-term production schedules resolve mine and processing plant capacity and their expansion potential.

There are well developed long-term mine planning techniques based on operations research and heuristic methods. These techniques aim at maximizing shareholder values by quantitative

modeling of the primary drivers influencing project value. The main variables driving the mine plans are not limited to but can be categorized as: (i) economic factors such as market commodity price and costs, (ii) metallurgical and processing factors such as recoveries and throughput, (iii) mining parameters such as capacity, productivity, equipment performance, stockpiles, cut-offs and dilution, (iv) geotechnical factors such as overall pit slopes, batter angles, and hydrology, and (v) geological parameters such as tonnes, grades, continuity, and geological structures. In the mine planning context, many of these variables and their relationships are estimated and quantified. These deterministic estimations are used to optimize a life-of-mine schedule and are the basis of short-term plans. However, the main mine planning parameters articulated above are either stochastic processes that would add up to a sequence of random variables over time or are random fields, whose domain is a random function. These variables may be independent random variables, or exhibit complicated statistical correlations.

One of the major shortcomings of the mine planning methods mostly used in industry is treatment of stochastic input variables as deterministic parameters, which in turn results in over or underestimation of project value, impractical mine plans, and significant discrepancies between long and short-term predictive models with the actual outcomes. In mining the relationship between these parameters, decision variables and the physical and economic outcomes are complex and often non- linear. Models that are used for optimization must therefore capture the dynamics of the economic system in question as well as anticipate changes to the relationships between these variables.

The main purpose of this study is to develop, verify and validate a discrete-event simulation model to link long-term and short-term open pit production scheduling. The simulation model intends to bridge the gap between a deterministic long-term yearly plan and a daily dynamic short-term schedule. The simulation model takes into consideration the constraints and uncertainties associated with mining and processing capacities, crusher availability, stockpiling strategy and blending requirements. The objective of this project is to use simulation to minimize ore production variation and idling time of the crusher while satisfying all the mining, processing, stockpiling and grade constraints. To achieve the goals, the following tasks are followed: (i) optimal final pit limit design using Lerchs and Grossmann (1965) algorithm; (ii) long-term production scheduling with the objective of providing a uniform feed to the processing plant. Milawa balanced tool in Whittle software (Gemcom Software International, 2008) is used to generate a deterministic production schedule; (iii) development of a simulation model in Visual Slam (Pritsker and O'Reilly 1999). The deterministic long-term schedule developed in stage two is the input into the simulation model. We simulate the deterministic long-term schedule with uncertain variables such as mining capacity, crusher availability and downtimes, and stockpiling and blending requirements; (iv) comparison and analysis of the deterministic production schedule against the simulated schedule after introduction of production and processing uncertainties into the model.

The simulation model developed is to be used as a linkage between the strategic mine plans and the short-term schedule. The simulation tool will assist mine planers to simulate the developed deterministic long-term schedule with uncertain input variables. Simulation of the long-term schedule over the short-term discrete time periods (days or weeks) with stochastic variables will reveal the discrepancies between the targeted long-term plan and the possible outcomes in the real world. This information is very valuable since the long-term plans could be revised until practical and robust schedules are developed at the early stages of the mine life.

The results show that discrete-event simulation is a powerful tool in minimizing the discrepancies between long and short-term plans. The simulation model also could assess different scenarios of long-term mine plans where multiple elements, multiple processing paths, various blending constraints and complex stockpiling strategies are required. Simulation allows the analyst to capture both the positive or negative swings in the operations for all possible values of the

uncertain variables and to experiment with several scenarios to get a better understanding of the system.

The next section of the paper covers the relevant literature to open pit production scheduling problem and utilization of discrete-event simulation in mining. Section 3 presents problem definition and assumptions, while Section 4 presents the simulation model description and the logic flow diagrams of the model. Section 5 presents the experimental design and the next section represents the discussion of results with the iron ore mining case study. Finally, Section 7 presents the conclusions followed by the list of references.

2. Relevant literature

Current production scheduling methods in the literature are not just limited to, but can be divided into heuristic methods, applications of artificial intelligence techniques, and operations research methods. Some of these algorithms are embedded into available commercial software packages.

One of the heuristic methods used in mine production scheduling was proposed by Gershon. XPAC AutoScheduler , a commercial mine scheduling software is based on Gershon's (1987) proposed heuristic approach. Gershon's (1987) algorithm generates cones upward from each block to approximate the shape of a pit and to determine whether or not the block in question could be part of the schedule. A list of exposed blocks and a ranking of those blocks based on what makes an exposed block more or less desirable to mine at the present time is updated through the algorithm with an index called the positional weight. This weighted function is used to determine the removal sequence.

Another popular heuristic used in strategic mine planning software, such as Whittle (Gemcom Software International, 2008) and NPV Scheduler (Datamine Corporate Limited, 2008) is based on the concept of parametric analysis introduced by Lerchs and Grossmann (LG). The LG algorithm provides an optimal solution to the final pit outline. There are unlimited numbers of strategies to reach the final pit. Each has a different discounted cash-flow. The optimal production schedule is the strategy that would maximize the discounted cash-flow and meets all the physical and economical constraints. The parametric analysis generates a series of nested pits based on varying the price of the product (revenue factor) and finding an optimal pit layout using LG algorithm. These nested pits then are used as a guideline to identify clusters of high grade ore and to determine the production schedule. The main disadvantage of heuristic algorithms are that the solution may be far from optimal and in mega mining projects, this is equal to huge financial losses.

Various models based on a combination of artificial intelligence techniques have been developed (Denby and Schofield, 1994; Denby et al., 1996; Tolwinski and Underwood, 1996; Askari-Nasab et al., 2005; Askari-Nasab, 2006; Askari-Nasab et al., 2007; Askari-Nasab and Szymanski, 2007; Askari-Nasab et al., 2008; Askari-Nasab and Awuah-Offei, 2009). In a sequence of publications we developed and tested the intelligent agent-based theoretical framework for open pit mine planning (Askari-Nasab et al., 2005; Askari-Nasab, 2006; Askari-Nasab et al., 2007; Askari-Nasab and Szymanski, 2007; Askari-Nasab et al., 2008) comprising algorithms based on reinforcement learning (Sutton and Barto, 1998) and stochastic simulation. This intelligent open pit simulator (IOPS) (Askari-Nasab, 2006) has a component that simulates practical mining push-backs over the mine life. An intelligent agent interacts with the push-back simulator to learn the optimal push-back schedule using reinforcement learning. The intelligent agent-based mine planning simulator, IOPS, was successfully used to determine the optimal push-back schedule of an open pit mine with a geological block model containing 883 200 blocks (Askari-Nasab and Awuah-Offei, 2009). A number of the artificial intelligence techniques, such as IOPS are based on frameworks that theoretically will converge to the optimal solution, given sufficient number of simulation iterations.

The main disadvantage however, is that there is no criteria to compare the solutions provided against the theoretical optimum.

Mixed integer linear programming (MILP) mathematical optimization have been used by different researchers to tackle the long-term open-pit scheduling problem (Caccetta and Hill, 2003; Ramazan and Dimitrakopoulos, 2004; Dagdelen and Kawahata, 2007). The MILP models theoretically have the capability to consider diverse mining constraints such as multiple ore processors, multiple material stockpiles, and blending strategies. The applications of MILP models result in production schedules generating near theoretical optimal net present values for mining ventures. The number of binary variables required in formulations presented by Caccetta and Hill (2003) and Ramazan and Dimitrakopoulos (2004) is equal to the number of blocks in the block model multiplied by the total number of scheduling periods. For a typical real size open pit scheduling problem, number of blocks is in the order of couple of hundred thousand to millions and the number of scheduling periods usually varies between twenty to thirty years for a life-of-mine schedule. Evidently, a problem of this size is numerically intractable with current state of hardware and commercial optimization solvers. Ramazan and Dimitrakopoulos (2004) presented a method to reduce the number of binary integer variables by setting waste blocks as linear variables. Setting waste blocks as linear variables will cause a block to be extracted in multiple periods, generating a schedule which is not feasible from practical equipment access point of view. Also, notable is the work by Dagdelen and Kawahata (2007), who applied the Lagrangian relaxation technique and sub-gradient methods to solve the mine production scheduling MILP problem.

Boland et al. (2007) extended the formulation of Caccetta and Hill (2003) based on strict temporal sequence of blocks rather than assigning blocks to periods of extraction. Boland et al. (2007) reduced the number of decision variables by eliminating a number of variables presented in Caccetta and Hill (2003) formulation prior to optimization. This was achieved by combining the block precedence constraints with the production constraints, aggregated over a sequence of time periods. The numerical results illustrated a decrease in computational requirements to obtain the optimal integer solution. Boland et al. (2009) have demonstrated an iterative disaggregation approach to using a finer spatial resolution for processing decisions to be made based on the small blocks, while allowing the order of extraction decisions to be made at an aggregate level. Boland et al. (2009) reported notable improvements on the convergence time of their algorithm. Boland et al. (2009) did not present enough information on their method of aggregation and assumed that some aggregation technique already exists.

Simulation has become established as one of the powerful techniques that can handle complex mining systems, which are stochastic in nature, change dynamically over time and space and operate within a variable economic environment (Panagiotou, 1999). Computer simulation is typically defined as either continuous or discrete-event simulation. Continuous simulation is concerned with modeling a system over time by representation of state variables changing continuously. However, discrete-event simulation deals with the modeling of systems that change their state based on the occurrence of events. The simulator changes the state variables at discrete time intervals and sets in motion new events at discrete points in time as each event is processed (Banks et al., 2010).

One of the first published work of discrete-event simulation of a mining operation is by Rist (1961). His model was about determination of the optimum number of trains to have on a haulage level in an underground molybdenum mine. Harvey (1964) expanded on Rist (1961) model by specifically using the GPSS language. During the 1960's other investigators were attempting to build computer simulation models of mining systems with GPSS. Bauer and Calder (1973) pointed out the advantages of using the GPSS simulation languages for open pit operations. Steiker (1982) simulated an underground train haulage system using GPSS language. Sturgul and Smith (1993) simulated complex underground mining operations with GPSS/H software. Simulation has been applied in different areas of mining, mainly in connection with transportation systems, mining

operation, mine planning and production scheduling (Basu and Baafi, 1999; Knights and Bonates, 1999; Konyukh et al., 1999; Panagiotou, 1999; Turner, 1999; Vegenas, 1999). Suglo et al. (2003) modeled three mining operations using Visual SLAM with AweSim software. These operations included a continuous surface miner-truck mining system in a strip coal mine, a continuous miner-shuttle car system, and hoist scheduling system both in an underground coal mine. Suglo et al. (2009) also studied the prospect of using at face slurry and continuous mining systems in oil sands. Interested readers are referred to Raj et al. (2009) for a detailed literature review on simulation models used in mining industry.

3. Problem definition

Long-term production schedule optimization is usually carried out with deterministic geological block models and estimated input parameters for mining and processing capacities, costs, prices, and recoveries. The generated schedules are optimized based on a fixed mining rate and processing plant availability and utilization with a constant production level. In reality, the mining rate is subject to deviations from the set target during the mine life. The processing plant availability and utilization is subject to plant breakdowns. These deviations from the optimized long-term production targets result in significant losses throughout the mine life, thereby deviating from the optimized net present value (NPV) of the operation.

Simulation models are major tools used to quantify uncertainties associated with production operations. The simulation model developed in this study seeks to address the problem of quantifying the effect of uncertainties associated with production and plant operations. The simulation model is to be used as a linkage between the strategic mine plan developed by Whittle software and the daily short-term schedule. The simulation tool developed will assist mine planers to simulate the developed deterministic long-term schedule with uncertain variables such as mining and processing capacities, equipment availability and utilization, crusher availability and downtimes, and stockpiling and blending requirements. Simulation of the long-term schedule over the short-term discrete time periods (days or weeks) with stochastic variables will reveal the discrepancies between the targeted long-term plan and the possible outcomes in the real world. This information is very valuable since the long-term plans could be revised until practical and robust schedules are developed at the early stages of the mine life.

After generating the long-term production plan, the resulting schedule and economic block values are used as the input source data for the simulation model where production and processing plant uncertainties are introduced and their resulting effect on the schedules and NPV are analyzed and compared to the original results from long-term schedule. The objective of this project is to use simulation to minimize ore production variation and idling time of the crusher while satisfying all the mining, processing, stockpiling and grade constraints.

Fig. 1 is a schematic diagram of the proposed mining operation circuit. The circuit starts from the pit operation where the material is being mined and transported to the crusher. The material is dumped directly into the crusher and no waiting time is allowed at the crusher. Hence, when the crusher is busy, the ore is sent to a stockpile where it is kept until the stockpile reaches the minimum required capacity and then crushing starts. The ore has two main rock-types which cannot be processed at the same time; therefore these rock-types have separate stockpiles. One rock-type is processed at a time, and the two rock-types after processing are blended together to achieve the requirement of the processing plant. As a result of this crushing requirement, a Visual SLAM sub-network is built to simulate the crushing schedule which runs with the main production network model processing one rock-type at a time with a change over time and requirement based on stockpile capacity and the rock type being mined. Another Visual SLAM sub-network is built to implement the stockpile management system required to run with the crushing schedule sub-network.

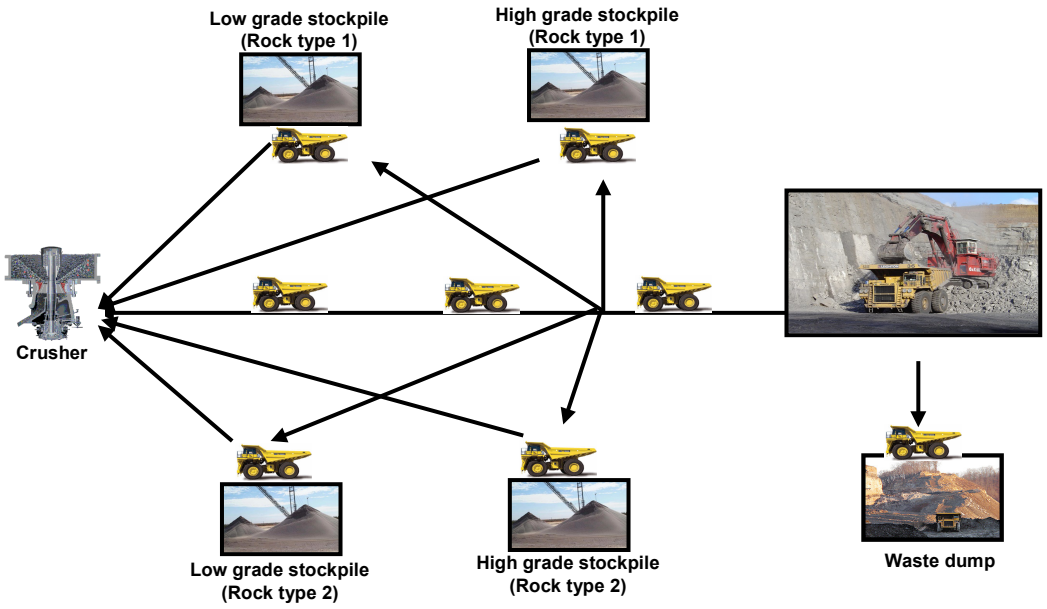

Fig. 1. Schematic diagram of proposed mining operation.

The simulation model will analyze the following variables in each period of the long-term schedule.

- The tonnage of ore and waste,
- The tonnage and average grade of MWT at the crusher,
- The tonnage and average grade of MWT directly sent to the crusher,
- The tonnage and average grade of MWT sent to stockpile 1 and stockpile 2,
- The tonnage and average grade of MWT sent from stockpile 1 and stockpile 2 to the crusher,
- How the crusher alternates between stockpile 1 and stockpile 2,
- The downtime (including idling time) of the crusher,
- The utilization of the crusher,
- The net present value,
- The appropriate mining and crushing rate for the blocks,
- The mine life.

4. Model description

The summary of the proposed mining operation process is as follows:

- One rock-type is milled at a time.
- The other rock-type is sent to the stockpile.
- The mill is fed directly from the mine and the stockpile.
- There is some downtime for the crusher to switch between rock-types.

In developing the model the following factors were considered: (i) the time used in hauling material from the pit to the crusher was not considered in the analysis; (ii) the production and crushing rate was considered to be very important in the analysis; (iii) the data from the blocks are carried by an entity as its attributes, and using the Visual SLAM with AweSim these attributes are employed to obtain the final production statistics; (iv) it is assumed that the crusher cannot process the two rock types at the same time; therefore a change over time is required which also takes care

of crusher breakdowns; (v) the crushing change over depends on the stockpile level and the rock type being mined; (vi) the whole system consisting of the mining and crushing facilities is analyzed as a single system with the assumption that the crusher can start processing as soon as it is turned on with the same capacity as steady state conditions.

The mining blocks are contained in a user-defined file (BM102.dat) which is read by the read node in the network. The parameters in the user-defined file includes the block tonnages (BlockTonnage, blockP, blockS, and blockMWT), the block grades (pGrade, sGrade, and mwtGrade), the period (Period), fraction of extraction (Fraction), the economic block value (EBV), the rock type (RockType) and the ore value (oreValue). The Visual SLAM network for the read and documentation nodes which represents the mining system is shown with a schematic network diagram in Fig. 2.

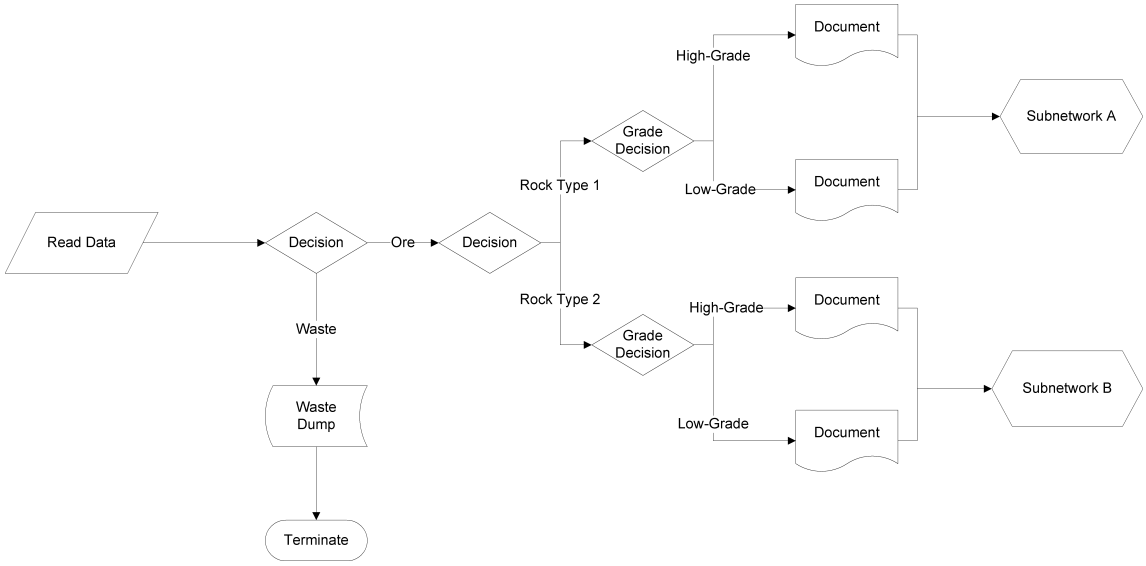

Fig. 2. Schematic network diagram for the read node which represents the mining system and the documentation of the various rock type tonnages and ore grades mined.

The production and processing rates used in the Whittle optimization will be used as the mean production and processing rates in the simulation model. These are further modified systematically to reduce the idling time of the mining operation in the later part of the mine life in line with our objective.

From the read node the daily production from year 1 to 8 is sampled from a normal distribution with a mean of 109,500 tonnes and a standard deviation of 10,000 tonnes from the user defined file, and this is stored by AweSim in the variable, LL[0]. Subsequently, the daily production from year 9 to 14 is sampled from a normal distribution with a mean of 47,000 tonnes and a standard deviation of 10,000 tonnes. When LL[0] becomes zero, the end of the file is reached. The blocks are sent to three different destinations in the network according to their rock types. The waste blocks will go to the waste dump. Rock type one is separated into high-grade and low-grade and the cut-off grade between high-grade and low-grade is 60%. The same rule applies for separating rock type two. The various statistics required from the block model are assigned to entities using Awesim global variables. These statistics are of interest in the simulation and are extracted with collect nodes. The Visual SLAM network for the collect nodes which represents the compilation of various statistics from the mining and crushing system is shown in the schematic network diagram in Fig. 2 and Fig. 3. Collect nodes are used to calculate the average grade of magnetic weight recovery, sulphur, and phosphor. Similarly the ore, sulphur and phosphor tonnages are calculated respectively.

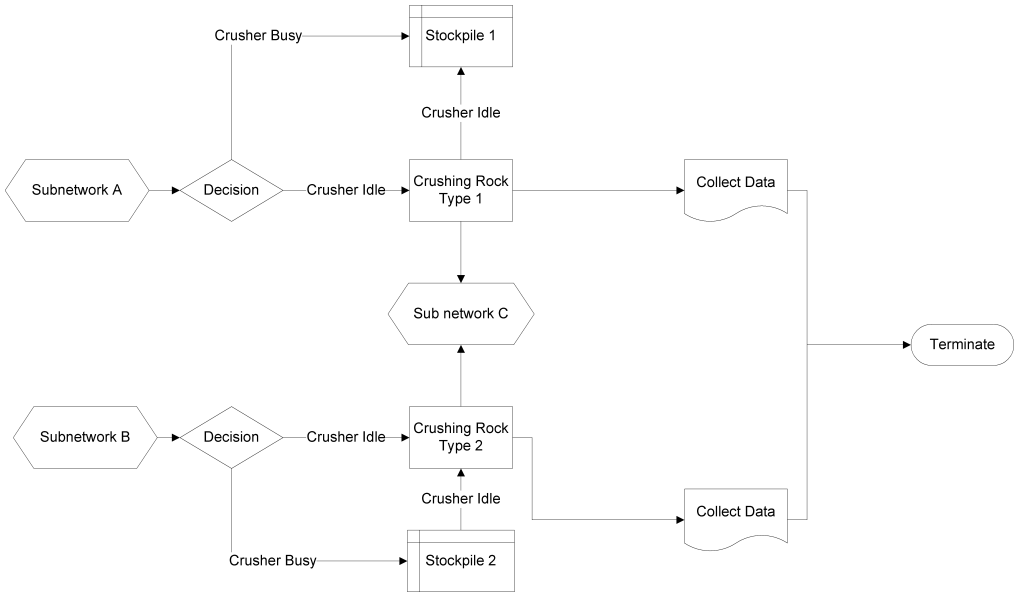

Fig. 3. Schematic network diagram for the crushing and stockpiling system.

The crusher is modeled as two separate resources, however only one of them is in operation at any point in time, so that it will mimic the presence of one crusher in the model. The rock type one material are sent to crusher one and rock type two are sent to crusher two. The crusher breakdowns and changeover time from one rock type to another is sampled from a normal distribution with a mean of 1 day and a standard deviation of 0.5 day. To enforce pre-stripping the crusher is not present in the first two years. From year three to five the crusher can process 22,000 tonnes a day, and any other material that arrives at the crusher during processing, is sent to the appropriate stockpile. The crushing capacity is increased to 33,500 tonnes a day from the sixth year of operation till the end of the mine life. After processing all the material coming directly from the pit to the crusher, the material from the stockpiles will be sent to the crusher for processing.

The change over from one rock type to the other is controlled by the rock type being mined and the stockpile capacities. A sub network is used to monitor the stockpile level and the rock type and once the required capacity is reached, the crushing on the other stockpile is stopped and a changeover is initiated. After the change over, the crusher is turned on again to attend to the stockpile that has reached its required capacity. The crusher will remain with this stockpile until the capacity of the other stockpile initiates another change over. This required stockpile capacity is seven times the daily production target. In cases where both stockpiles are above the required level, a three day excess production capacity of one stockpile over the other is needed to initiate a crusher change. This is to ensure that both stockpiles are fed on a uniform basis as required by the processing plant. This crushing schedule, which is implemented by a sub-network in the model, is utilized until the end of the simulation time. The Visual SLAM network for the crushing system and the stockpile management system are shown with the schematic network diagrams in Fig. 3 and Fig. 4 respectively.

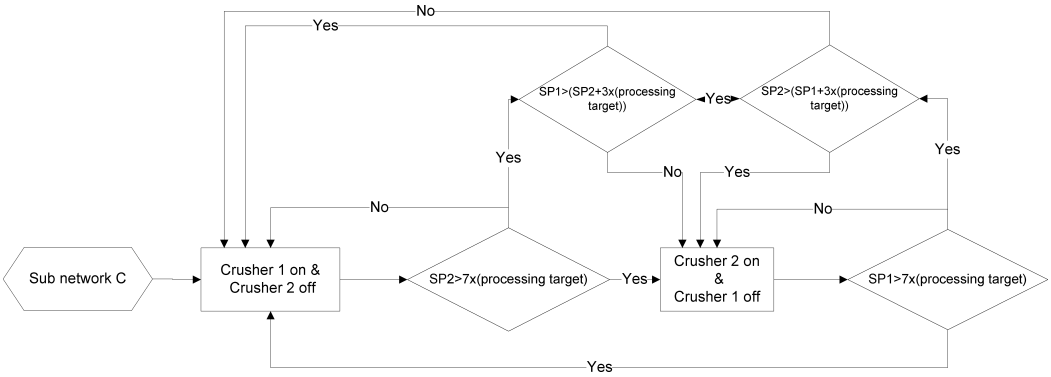

Fig. 4. Schematic network diagram for the stockpile management system.

5. Experimental design

An important aspect in simulation projects is to run the models effectively and try to understand the results in the context of your objective. This involves a careful planning of the simulation experiment to assess the performance of the system with an estimated prescribed set of conditions (Pritsker and O'Reilly 1999; Kelton, 2000).

In this paper, the simulation model was designed with an input mine schedule from Whittle software as per our objective. This contains information such as the block tonnage, grade and rock-type to be mined in each period. A crushing and stockpiling system was introduced with uncertainties to enable the quantification of real operational uncertainties on the mining operation. All simulation functions were tested using simple entity flow tests to determine if they are working properly and as expected.

The choice of the production and crushing rate was based on their corresponding values used in Whittle production scheduling optimization. These were further adjusted systematically based on the objective of minimizing operational idling time. It was decided to combine the crusher changeover time and downtime to reduce the number of variables and nodes that are used in the simulation project. The uncertainties associated with production and crushing rate and crusher changeover and downtime were based on the experience of the researchers. However, for production simulation runs, the statistical distribution for each process need to be calibrated based on the historical data gathered from the site. The general simulation model linking the long-term production schedule to a short-term production schedule under resource availability uncertainty is valid and applicable to different scenarios.

The length of the simulation run was based on the mine life. Once the scheduled blocks in the optimal pit are depleted, the simulation is terminated. For the number of replications, assuming that the sample mean, $\overline{X}_I$ is unbiased and that the sample variance, $Var\left[\overline{X}_I\right] = \sigma_X^2 / I$, then the number of replications, I required to obtain a $(1-\alpha)$ confidence that the population mean, μ_X is contained in a prescribed interval can be calculated using standard statistical formulas as demonstrated by Pritsker and O'Reilly (1999). σ_X^2 is the population variance and α is the significance level. In this paper, it was decided to quantify the simulation output uncertainties based on a 95% confidence interval of the input expected values ± 0.5 of their standard deviation. This required 15 runs of the simulation model for each scenario of one production year (Kelton et al., 1998; Pritsker and O'Reilly 1999).

In analyzing the output results, a comparison between the Whittle schedule and the simulated schedule was done. Some specific variables for comparison were the life of mine and the net

present value of the mine that has been impacted upon by the uncertainties and the complex operational strategies introduced in the simulated schedule.

6. Results and discussion

6.1. Deterministic schedule from Whittle

In the first stage of the study, the long-term production schedule of the iron ore open pit was developed using Whittle software . The block model contains the estimated magnetic weight recovery (MWT%) of iron ore and the contaminants in the model are phosphor (P%) and sulphur (S%). The blocks in the original geological model represent a volume of rock equal to $25m \times 25m \times 15m$, which were reblocked for simulation. The final pit includes 412.99 million tonnes of rock where 124.09 million tonnes is iron ore with an average magnetic weight recovery grade of 70.3%. Initially a capacity of 109,500 tonnes per day was considered as the upper bound of mining. The objective was to maximize the NPV while providing a constant feed to the mill throughout the mine life. Two years of pre-stripping was considered to open up the mine. The processing capacity gradually ramped up to 33,500 tonnes per day, with year's three to five at 22,000 tonnes per day capacity. There are two rock types (with varying densities) rock type one and rock type two which have been modeled with the code 101 and 102. The two rock types have different stockpiles. Other information such as block tonnage, ore tonnage, economic block value (EBV), magnetic weight recovery, grade of sulphur and grade of phosphor are used as inputs into the simulation model. Fig. 5 illustrates the long-term production schedule modeled by Whittle software . This is the target long-term production goals that we need to meet through the day to day operation. The long-term schedule is not achievable most of the times because the uncertainties of many input factors are not taken into consideration in long-term planning. Fig. 6 illustrates the same schedule with highlighting the portion of ore types one and two in the feed. Fig. 7 shows cross section 600500m looking east of the final pit. The extraction period of each block is labeled based on the Whittle long term schedule.

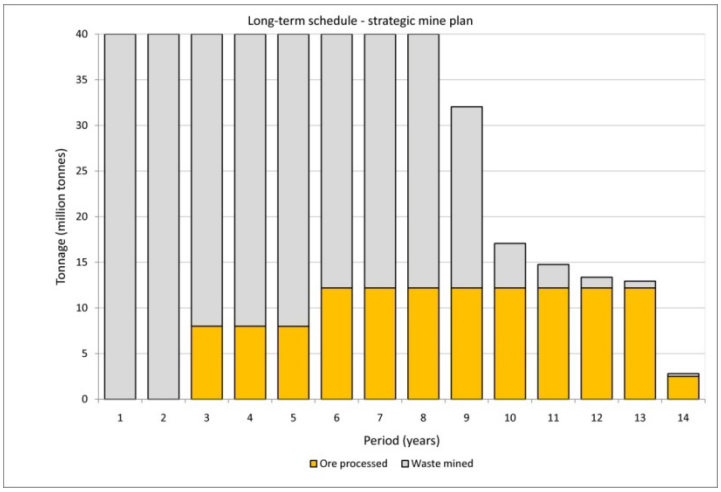

Fig. 5. Long-term production schedule generated based on deterministic input values.

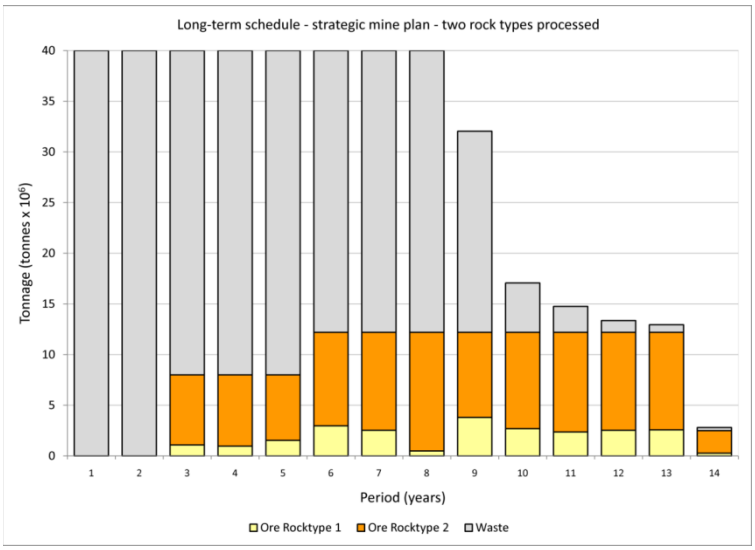

Fig. 6. Long-term production schedule, with the portion of two different ore types in feed.

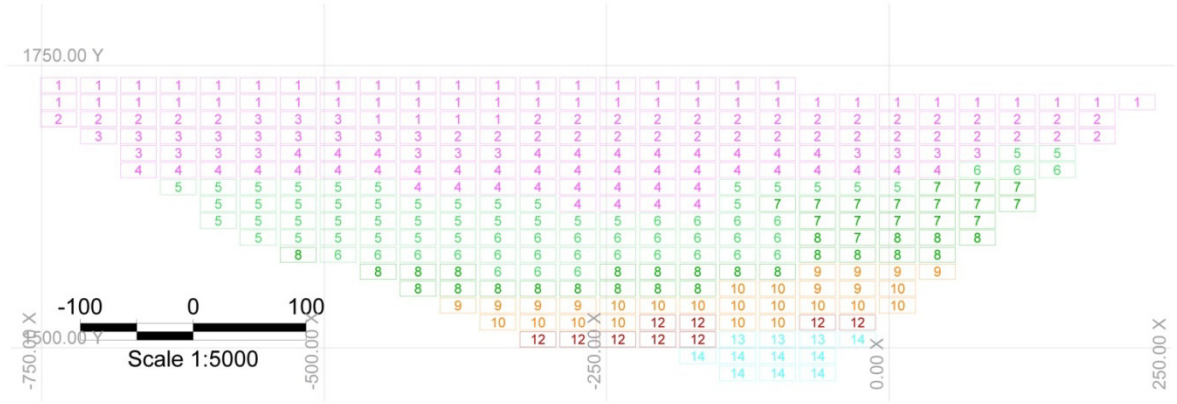

Fig. 7. Cross section 600500m looking east, the extraction period of each block is labeled based on the long term schedule.

6.2. Simulation model results

6.2.1 Tonnage mined and NPV

The long-term schedule presented in Fig. 5 to Fig. 7 is the input into the Visual Slam simulation model to mimic the block extraction sequence with uncertain mining and processing rate and changeover of the crusher. At this stage the stockpiling strategy is simulated as well. The mining rate is set to 109,500±10,000 tonnes per day for the first 8 years and 47,000±10,000 tonnes per day for the remaining years. The crushing rate is 22,000 tonnes per day from year 3 to 5 and 33,500 tonnes for the remaining years. In the first two years only pre-stripping occurred. The stockpile capacities are a minimum of seven times of the daily processing target which is 154,000 tonnes from year 3 to 5 and 234,500 tonnes for the remaining years. Above the minimum stockpile capacity, 3 days excess processing capacity of one stockpile over the other is required as the minimum stockpile capacity. The change over time from rock type one to rock type two is 1±0.5 days and the reverse is true for the other rock type. The simulation was run on annual bases to ascertain the details of what will happen to the mining operation within each production year with our objective of minimizing mining and processing variations.

Fig. 8 illustrates the simulation result of the long-term schedule based on short-term uncertain input variables. The dashed straight line shows the 12 million tonnes per year target set up by the long-term schedule. The amount actually processed after simulation of the mining sequence is shown by

the black solid line. Evidently, there is a considerable feed shortfall in years nine and ten. This is due to the unpredicted uncertainties in mining and processing capacities as well as crusher downtimes and ore availability. This shows how the effects of constraints and uncertainties on the mining operation can be quantified. Fig. 9 illustrates the same simulated schedule with high-grade and low-grade material distinguished by rock type. From the simulation, the mine will have an operating life of 14.5 years, which is extended by sixteen months comparing to the long-term schedule. Mining rate will be at an average of 39.6M tonnes of material every period of one year for the first 8 years and then reduced to 15.9M tonnes from year 9 to the end of the mine life. The simulation result is a great assist in choosing the proper truck-shovel fleet to be purchased or the mining capacity that needs to be acquired through contract mining. During the first two periods, only waste material will be available for mining to enable the exposure of ore which will become available in the third period. From this period, the mine will operate at an average stripping ratio of 2.83 till the end of year 10. From year 11, when little waste is left to mine, the stripping ratio reduces to 0.20. The average ore tonnage processed by the crusher from year 3 to 5 is 7.12M tonnes and that from year 6 to the end of the mine life is 10.18M tonnes.

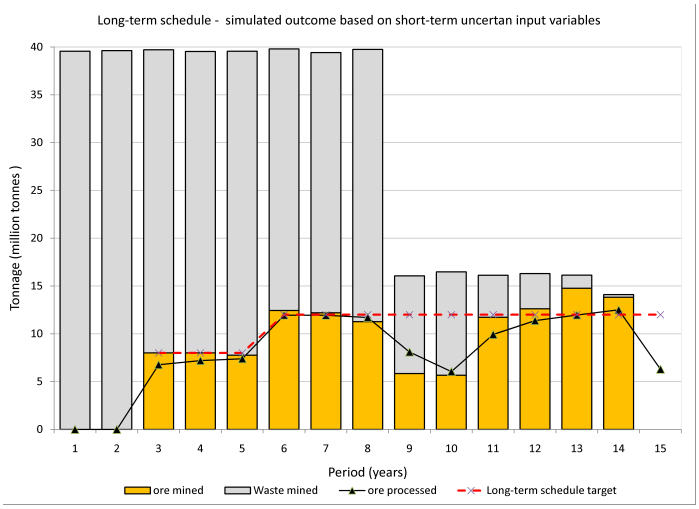

Fig. 8. Long term schedule simulated outcome based on short-term uncertain input variables.

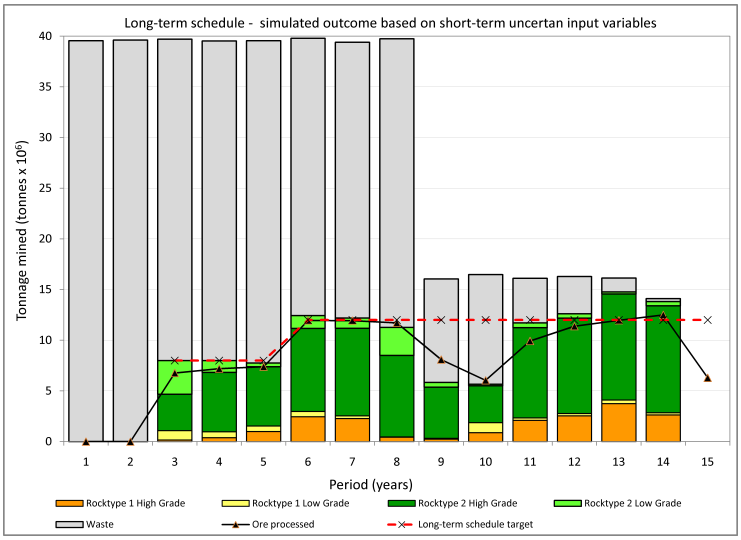

Fig. 9. Simulated long-term schedule with high-grade and low-grade material.

Fig. 10 shows the cumulative progression of the NPV values from one period to another obtained from simulation (dashed line) compared to Whittle results (solid line). This shows a reduction in NPV as a result of the mining and processing rate constraints and uncertainties. The net present value of the operation at a discount rate of 10%, starts from -$76.23M in period 1 due to the waste being mined and cumulatively decreases to -$145.64M in period 2. When processing of ore starts from period 3, the NPV increases to $79.90M and cumulatively increases to $3175.70M in period 15 when the life of mine is reached. With the operational constraints and uncertainties, the total NPV at the end of the mine life with 10% discount rate is $3175.70M as compared to $3251.79M obtained from Whittle with no uncertainty modeling.

Further assessment of mine production uncertainty from the results of the simulation model shows an output mean daily production of 108543 tonnes with a standard deviation of 354 tonnes from year 1 to 8. From year 9 to 14, the mean daily production is 43471 tonnes with a standard deviation of 2399 tonnes. This high standard deviation is as a result of lack of material in year 14 for mining. Excluding year 14, the mean daily production from year 9 to 13 will be 44435 tonnes with a standard deviation of 470 tonnes. These results are consistent with the target set in the experimental design.

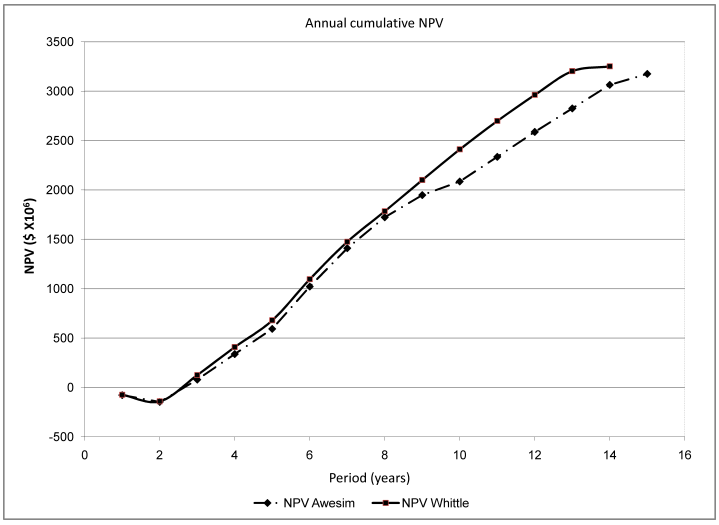

Fig. 10. Cumulative progression of the net present value during the mine life.

6.2.2 Ore tonnage and grade of Fe mined

Fig. 11 and Fig. 12 show the graphical relationship of the different rock types and grades of Fe mined during different periods from simulation and from Whittle respectively. The simulation can provide us the details of the mining operation by rock type and grade on any time scale throughout the mine life as well as the effects of production constraints and uncertainties. The simulation shows that (Fig. 11) with a magnetic weight recovery cut-off of 60% between high grade and low grade for both rock types one and two, the tonnage of ore mined for rock type one high grade starts from 0.16M tonnes at a magnetic weight recovery of 66.2% in period 3 and continues until period 14 when 2.64M tonnes of ore at a magnetic weight recovery of 72.6% is mined. In all a total of 18.86M tonnes of rock type one high grade ore at a magnetic weight recovery of 72.4% was mined as at the end of the fourteenth period. The mining of low grade ore of rock type one also starts in period 3 with a value of 0.93M tonnes at a magnetic weight recovery of 54.1% and continues until period 14 where 0.21M tonnes are mined at a magnetic weight recovery of 49.3%. In all a total of 4.97M tonnes of low grade ore of rock type 1 was mined at a magnetic weight recovery of 49.7%.

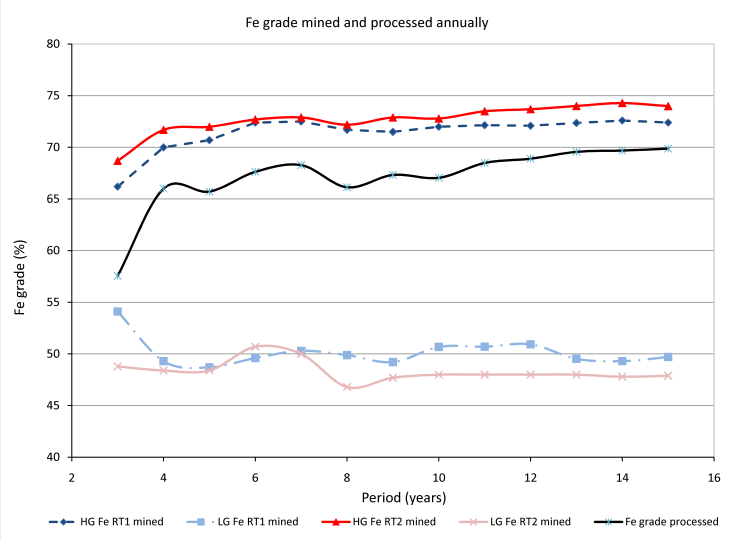

Fig. 11. Graphical relationship of the different rock types and grades of Fe mined and processed from simulation model.

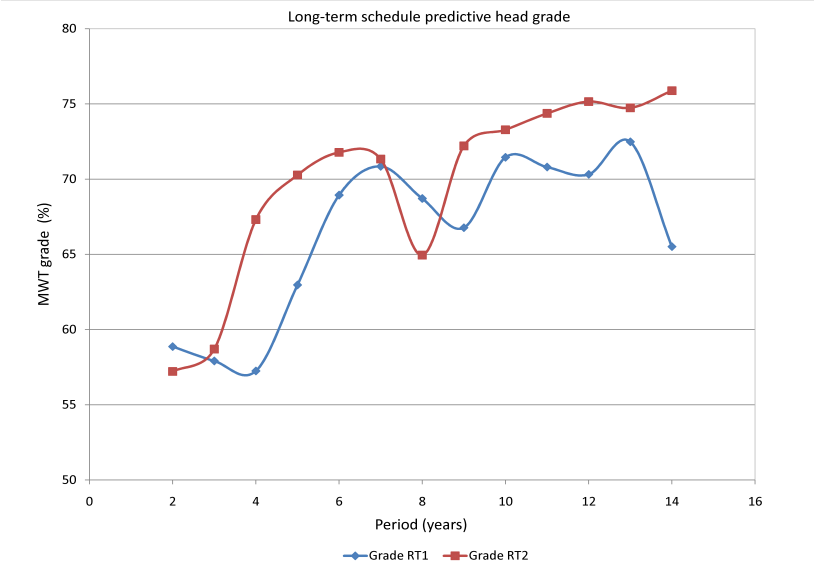

Fig. 12. Graphical relationship of the different rock types and grades of Fe mined from Whittle.

6.2.3 Ore tonnage mined and processed by the crusher directly and from stockpile

The tonnage of ore mined from the pit is either processed directly by the crusher or it is processed from the stockpile by the crusher. The ore is sent to the stockpile depending on whether the crusher is available or it is being utilized. No waiting is allowed at the crusher head, therefore any material that arrives at the crusher when the crusher is busy is sent to the stockpile. Also since the crusher is managing the capacity of the two stockpiles of different rock types, it is available to process one stockpile at a time depending on the stockpile capacity and rock type being mined and hence all material for the other rock type is sent to the stockpile.

Fig. 13 shows the graphical relationship of ore processed directly and processed from the stockpiles. It also shows the cumulative stockpile level changes used to support plant processing throughout the mine life. The total amount of ore of both rock types processed during the mine life is 123.18M tonnes at a magnetic weight recovery of 69.6%. 0.91M tonnes of ore remain at the stockpiles as at the end of the simulation. The tonnage of ore from the pit processed directly by the

crusher is 2.57M tonnes in period 3. Crushing continues until period 14 when 9.27M tonnes of material is processed directly, making up a total of 65.00M tonnes of ore throughout the mine life. Similarly, 4.20M tonnes of ore were processed from the stockpile by the crusher in period 3 and processing continued until period 15 when 6.29M tonnes of material were processed. A total of 58.18M tonnes of ore were processed from the stockpile throughout the mine life.

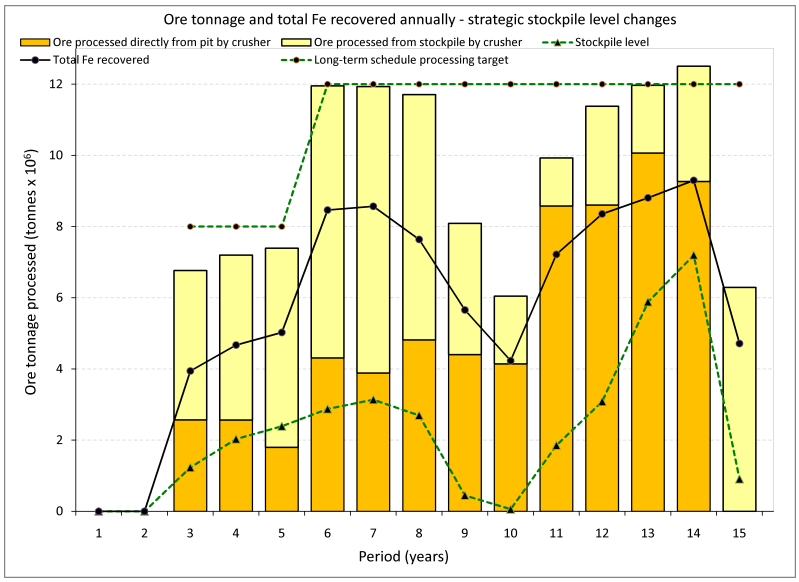

Fig. 13. Graphical relationship of ore tonnage processed directly and from stockpile.

6.2.4 Crusher utilization

During the first two periods the crusher was idle due to the waste being mined. From period 3, crushing of rock type 1 and 2 started with a cumulative crusher utilization of 28%. The cumulative crusher utilization continues to increase steadily as more material becomes readily available for crushing directly from the pit and from the stockpiles. At the end of the mine life in period 15, the cumulative crusher utilization will be 14% for rock type 1 and 62% for rock type 2, totaling 76%. 1±0.5 days are required in setting up the crusher from crushing one rock type to the other as well as crusher downtimes. This together with the crusher idling time during the initial stages of the operation, accounts for the non utilization of the crusher during the mine life and is referred to in this project as the shutdown time. The average crusher utilization excluding the idling time in the initial stages of the operation is 88%. Fig. 14 shows the graphical relationship of the progressive utilization of the crusher during the mine life.

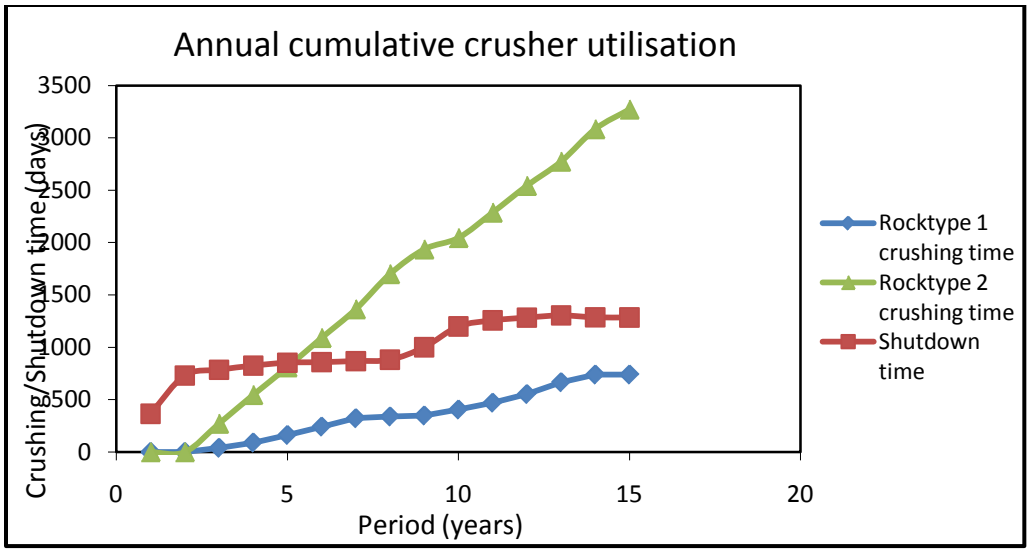

Fig. 14. Graphical relationship of the utilization of the crusher during the mine life.

7. Conclusions

One of the major shortcomings of the current mine planning methods is treatment of stochastic input variables as deterministic parameters, which in turn results in over or underestimation of project value, impractical mine plans, and significant discrepancies between long and short-term predictive models with the actual outcomes. In mining, the relationship between these parameters, decision variables and the physical and economic outcomes are complex and often non- linear. Models that are used for optimization must therefore capture the dynamics of the economic system in question as well as anticipate changes to the relationships between these variables.

We have developed, verified and validated a discrete-event simulation model for open pit production scheduling with the SLAM simulation language. The simulation model proved to bridge the gap between a deterministic long-term yearly plan and a daily dynamic short-term schedule. The simulation model takes into consideration the constraints and uncertainties associated with mining and processing capacities, crusher availability, stockpiling strategy and blending requirements. The results show that discrete-event simulation is a useful tool in minimizing the discrepancies between long and short-term plans.

An iron ore mine case study was carried out by generating the long-term schedule with Whittle software and then simulating the block sequence extraction with the discrete-event simulation. 65.00M tonnes of ore were processed directly by the crusher and 58.18M tonnes of ore were processed from the stockpile throughout the mine life. In all, a total of 123.18M tonnes of ore with a magnetic weight recovery of 69.6% were processed by the crusher with a utilization of 88% while 288.1M tonnes of waste were sent to the waste dump. 0.91M tonnes of ore remain at the stockpiles as at the end of the simulation. With the operational constraints and uncertainties, the total NPV at the end of the mine life with 10% discount rate is $3175.70M as compared to $3251.79M obtained from Whittle with no constraints and uncertainties. The results of the simulation show that for the deposit of 412M tonnes of material, at 95% confidence interval, a duration of 14.5 years is required to mine at a production rate of 109,500±5,000 tonnes per day for the first 8 years and 47,000±5,000 tonnes per day for the remaining years. The ore processing rate was 22,000 tonnes from year 3 to 5 and 33,500 tonnes from year 6 to 14.5. No ore was processed in years 1 and 2. The results show that discrete-event simulation is a powerful tool in assessing different scenarios of long-term mine plans, where multiple elements, multiple processing paths, various blending constraints and complex stockpiling strategies are required.

8. References

[1] Askari-Nasab, H. (2006). Intelligent 3D interactive open pit mine planning and optimization. PhD Thesis, University of Alberta, Edmonton, Canada, Pages 167.

[2] Askari-Nasab, H. and Awuah-Offei, K. (2009). Open pit optimization using discounted economic block value. *Transactions of the Institution of Mining and Metallurgy. Section A, Mining industry*, *118*,(1), 1-12.

[3] Askari-Nasab, H., Frimpong, S., and Awuah-Offei, K. (2005). *Intelligent optimal production scheduling estimator*. Paper presented at 32nd Application of Computers and Operation Research in the Mineral Industry, Tucson, Arizona, USA.

[4] Askari-Nasab, H., Frimpong, S., and Szymanski, J. (2007). Modeling open pit dynamics using discrete simulation. *International Journal of Mining, Reclamation and Environment*, *21*,(1), 35-49.

[5] Askari-Nasab, H., Frimpong, S., and Szymanski, J. (2008). Investigating the continuous time open pit dynamics. *The Journal of the South African Institute of Mining and Metallurgy*, *108*,(2), 61-73.

[6] Askari-Nasab, H. and Szymanski, J. (2007). *Open pit production scheduling using reinforcement learning*. Paper presented at 33rd International Symposium on Computer Application in the Minerals Industry (APCOM), Santiago, Chile.

[7] Banks, J., Carson, J. S., Nelson, B. L., and Nicol, D. M. (2010). *Discrete-event system simulation.* Upper Saddle River, N.J. ; Singapore : Prentice Hall, c2010, 5th ed,

[8] Basu, A. J. and Baafi, E. Y. (1999). Discrete event simulation of mining systems: current practice in Australia. *International Journal of Surface Mining, Reclamation and Environmental*, *13*,(2), 77-78.

[9] Bauer, A. and Calder, P. (1973). *Planning open pit mining operations using simulation*. Paper presented at Application of Computers and Operations Research in the Mineral Industry (APCOM), South African Institute of Mining and Metallurgy, Johannesburg, South Africa. pp. 273-298.

[10] Boland, N., Dumitrescu, I., Froyland, G., and Gleixner, A. M. (2009). LP-based disaggregation approaches to solving the open pit mining production scheduling problem with block processing selectivity. *Computers and Operations Research*, *36*,(4), 1064-1089.

[11] Boland, N., Fricke, C., and Froyland, G. (2007). A strengthened formulation for the open pit mine production scheduling problem. *Optimization Online,* Retrieved Jan. 9, 2009 from: http://www.optimization-online.org/

[12] Caccetta, L. and Hill, S. P. (2003). An application of branch and cut to open pit mine scheduling. *Journal of Global Optimization*, *27*,(2-3), 349-365.

[13] Dagdelen, K. and Kawahata, K. (2007). *Oppurtunities in multi-mine planning through large scale mixed integer linear programming optimization*. Paper presented at 33rd International Symposium on Computer Application in the Minerals Industry (APCOM), Santiago, Chile.

[14] DatamineCorporateLimited (2008). NPV Scheduler. Ver. 4, Beckenham, United Kingdom.

[15] Denby, B. and Schofield, D. (1994). Open-pit design and scheduling by use of genetic algorithms. *Transactions of the IMM Section A*, *103*,(1), A21-A26.

[16] Denby, B., Schofield, D., and Hunter, G. (1996). *Genetic algorithms for open pit scheduling - extension into 3-dimensions*. Paper presented at 5th International Symposium on Mine Planning and Equipment Selection, Sao Paulo, Brazil.

[17] GemcomSoftwareInternational (2008). Whittle strategic mine planning software. Ver. 4.2, Vancouver, B.C.

[18] Gershon, M. (1987). Heuristic approaches for mine planning and production scheduling. *Geotechnical and Geological Engineering*, *5*,(1), 1-13.

[19] Harvey, P. R. (1964). *Analysis of production capabilities*. Paper presented at Application of Computers and Operations Research in the Mineral Industry (APCOM), Colorado School of Mines, Colorado, USA. pp. 713-726.

[20] Kelton, W. D. (2000). *Experimental design for simulation*. Paper presented at Winter Simulation Conference, Orlando, USA.

[21] Kelton, W. D., Sadowski, R. P., and Sadowski, D. A. (1998). *Simulation with Arena.* McGraw-Hill, New York.

[22] Knights, P. F. and Bonates, E. J. L. (1999). Application of discrete mine simulation modeling in South America. *International Journal of Surface Mining, Reclamation and Environmental*, *13*,(2), 69-72.

[23] Konyukh, V., Galiyev, S., and Li, Z. (1999). Mine simulation in Asia. *International Journal of Surface Mining, Reclamation and Environmental*, *13*,(2), 57-67.

[24] Lerchs, H. and Grossmann, I. F. (1965). Optimum design of open-pit mines. *The Canadian Mining and Metallurgical Bulletin, Transactions*, *LXVIII*, 17-24.

[25] Panagiotou, G. N. (1999). Discrete mine system simulation in Europe. *International Journal of Surface Mining, Reclamation and Environmental*, *13*,(2), 43-46.

[26] Pritsker, A. A. B. and O'Reilly , J. J. (1999). *Simulation with Visual SLAM and AweSim.* WILEY, 2nd ed, Pages 852.

[27] Raj, M. G., Vardhan, H., and Rao, Y. V. (2009). Production optimisation using simulation models in mines: a critical review. *International Journal of Operational Research*, *6*,(3), 330-359.

[28] Ramazan, S. and Dimitrakopoulos, R. (2004). Traditional and new MIP models for production scheduling with in-situ grade variability. *International Journal of Surface Mining, Reclamation & Environment*, *18*,(2), 85-98.

[29] Rist, K. (1961). *The solution of a transportation problem by use of a Monte Carlo technique*. Paper presented at Application of Computers and Operations Research in the Mineral Industry (APCOM), Unversity of Arizona, Tucson, Arizona, USA. pp. L2-1 to L2-15.

[30] Steiker, A. B. (1982). *Simulation of an underground haulage systems*. Paper presented at Application of Computers and Operations Research in the Mineral Industry (APCOM), Denver. pp. 599-613.

[31] Sturgul, J. R. and Smith, M. L. (1993). *Using GPSS/H to simulate complex underground mining operations.* Paper presented at 2nd International Symposium on Mine Mechanization and Automation, Lulea, Sweden. pp. 827.

[32] Suglo, R. S., Szymanski, J., Booth, D., and Frimpong, S. (2003). *Simulation analysis of mining models*. Paper presented at IASTED International Conference on Applied Simulation and Modelling(ASM2003), Marbella, Spain. pp. 267-272.

[33] Suglo, R. S., Szymanski, J., and Planeta, S. (2009). Simulaiton of at face slurrying method and continuous miner truck system in an open pit mine. in *Transport*, vol. 1, pp. 2-8.

[34] Sutton, R. S. and Barto, A. G. (1998). *Reinforcement learning : an introduction.* MIT Press, Cambridge, Mass. Pages 322.

[35] Tolwinski, B. and Underwood, R. (1996). A scheduling algorithm for open pit mines. *IMA Journal of Mathematics Applied in Business & Industry*,(7), 247-270.

[36] Turner, R. J. (1999). Simulation in the mining industry of South Africa. *International Journal of Surface Mining, Reclamation and Environmental*, *13*,(2), 47-56.

[37] Vegenas, N. (1999). Application of discrete mine simulation in Canadian mining operations in the nineties. *International Journal of Surface Mining, Reclamation and Environmental*, *13*,(2), 77-78.

Simulation-optimization of the short-term open pit mine planning problem

Hesameddin Eivazy and Hooman Askari-Nasab
Mining Optimization Laboratory (MOL)
University of Alberta, Edmonton, Canada

Abstract

In this paper, the simulation-optimization approach is applied to solve the short-term mine planning problem in a stochastic environment. First, a mixed integer linear programming model for short-term scheduling of open pit mines is formulated, which includes a buffer stock-pile. The role of buffer stock-pile is to assure a uniform feed to the processing plant. Due to the stochastic nature of the input parameters such as estimated grade of ore, simulation optimization approach is applied to solve the problem. The numerical experiments are performed on a typical problem and results are illustrated.

1. Introduction

One of the most important aspects of mine production planning is the short-term production planning/scheduling (Dimitrakopoulos and Ramazan, 2004). The objective of the short-term production scheduling is to determine the optimum sequence of extraction of blocks to meet the goals imposed by the long-term scheduling in each short-term period (output of long term scheduling). In fact, the open pit mine short-term production scheduling problem is the sequencing of each block's removal from the mine with respect to a variety of physical and economic constraints (Caccetta and Hill, 2003). Typically, these limitations are: the mining extraction sequence, mining, milling and refinery capacities, mill feed and concentrates grades, and different operational requirements like minimum mining width (Caccetta and Hill, 2003).

On the other hand, one of the most challenging issues in the mine scheduling problems is the choice of solution methods. Typically, the short-term mine scheduling problems are complex. The complexities arise from the involvement of several continuous and binary variables and the large number of blocks to be extracted in the real-world problems. There are many research related to solution methods of the mine scheduling problems in the literature. These methods are not limited to but include:

1. Heuristics methods: Caccetta *et al.* (1998) developed and implemented a graph-theoretic technique. They implement a strategy including the application of a dynamic programming technique to "bound" the optimum solution. Also, Gershon (1987) propose two heuristic methods: the first method is applicable to surface and underground mining with decision on blending issues. Another is applicable to general situations but mostly efficient in open pit mining problem.
2. Dynamic programming techniques: Tolwinski and Underwood (1996) propose a model for the mine scheduling problem as sequential optimization. They developed an

algorithm based on dynamic programming approach. Dynamic programming assisted to overcome the difficulty related to the large number of states in the problem.

3. Mixed integer linear programming (MILP): Caccetta and Hill (2003) propose a mixed integer programming model for open pit mine scheduling problem. Also, Gershon (1983) develop a mixed-integer model for the mine scheduling problem to optimize both the mine production sequencing and the mill blending and processing problems, simultaneously. Carlyle and Eaves (2001) formulate a maximization integer programming model for mining platinum and palladium at Stillwater Mining Company which is able to reach near-optimal solutions without applying any special methods to reduce solution time.
4. Artificial intelligence algorithms: these algorithms include simulated annealing, genetic algorithms, and neural networks. For example, Denby and Schefield (1995) apply the neural network algorithm to the mine scheduling. In addition, Denby *et al.* (1991) implement the genetic algorithm in the underground mine scheduling.

Classical methods are not successful to consider the risk of not meeting production targets caused by the uncertainty in estimated grades (Dimitrakopoulos and Ramazan, 2004). Vallee (2000) reports that 60% of examined mines had an average rate of production that is less than 70% of the nominal capacity in early years because of uncertainties in planning. Also, Rossi and Parker (1994) report shortcomings against predictions of mine production in later steps of the production.

A simulation-optimization approach is applied to handle ore grade uncertainty and its effect on short-term mine scheduling. If ore grade risk is not handled properly, it can create considerable error in mine planning. The simulation-optimization approach briefly includes the following steps:

- Setting a Probability Distribution Function (PDF) for the stochastic parameters such as ore grade.
- Generating a random number based on the set PDF.
- Solving the short-term scheduling problem with these random numbers in a deterministic form.
- Repeating the above three steps for sufficient number of runs.

As the stochastic parameter has the distribution for its values, the results will have a distribution too. Fig. 1 shows the schematic view of this approach for one stochastic parameter and *n* output variables.

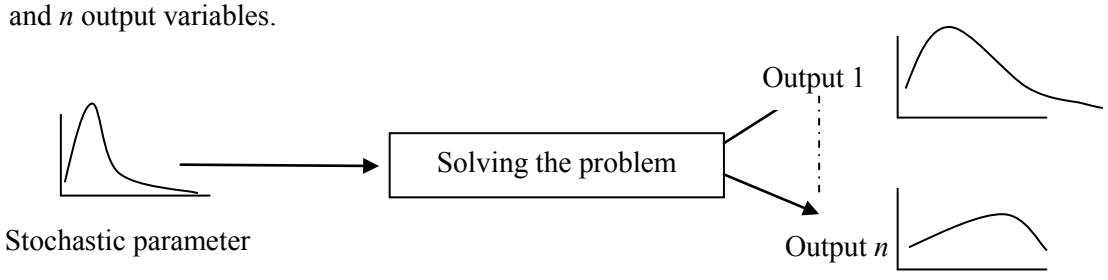

Fig. 1. Schematic view of simulation-optimization solving approach.

Managers, having access to the obtained distribution for output variables, can make more accurate decisions with high confidence than when they decide deterministically.

The structure of this paper is as follows: section 2 presents the problem definition. In this section the general description of the problem is presented. In section 3, the formulation of the mixed integer programming model for the problem is presented. The parameters and decision variables

are defined first. Then, the operational research formulation of the problem with description of specific notations is presented. In section 4, the methodology of solving the MILP model is elaborated. In section 5, a typical simple example is briefly explained and the different specifications of this example are defined. In section 6, the numerical results of applying the simulation-optimization method to solve the defined example are presented. Finally in section 7, the conclusions and future research lines are highlighted.

2. Problem definition

As mentioned in the introduction section, the problem is the short-term scheduling of an open pit mine. Fig. 2 shows the general schematic view of the problem. According to this figure, there is an open pit mine and a buffer stock-pile. The total rock tonnage in the mine is divided among a specific number of blocks. The mine has *E* elements such as copper, silver, gold, etc. Some open pit mines just have one element of interest, which is economical to be extracted, while other deposits include multi-elements. The role of buffer stock-pile is to hold the excess amount of ore extracted from the mine. In periods that the amount of extracted ore is less than the minimum acceptable processing plant's feed, the required amount of ore is reclaimed from the stock-pile to balance the processing plant feed. In fact, in each period, ore is extracted from the mine with respect to various physical and economic constraints. A portion of the extracted ore is delivered to the processing plant directly. The ore extra to the processing plant capacity is stacked onto the stock-pile. In the long-term scheduling phase, it has been determined that in each period *t* which blocks must be extracted from the mine to achieve the maximum net present value (NPV). Each long-term period t is divided into *k* short periods in the short-term scheduling.

Therefore, the short-term scheduling of open pit mine is making a decision about: 1) what portion of which blocks should be extracted in each period of time, 2) amount of ore that should be extracted from the mine in each period, and the respective amount of ore sent to the stockpiles and processing plant.

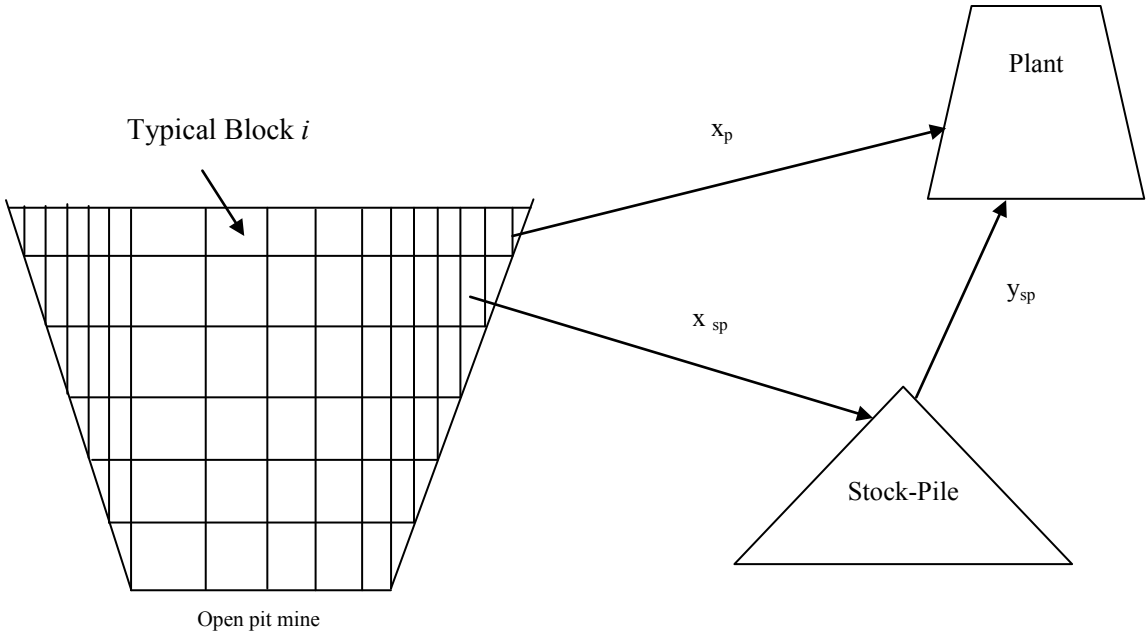

Fig. 2. Schematic view of the problem.

The proposed model for the short-term mine planning minimizes the mining cost subject to some physical and technical constraints.

3. Theoretical framework and models

In this section, the defined problem is presented as an MILP model. First, the parameters and decision variables are defined. Section 3.1 explains the parameters and variables in the model. Afterward , in section 3.2, the MILP formulation is presented.

3.1. Parameters and Decision Variables

3.1.1 Parameters

The parameters are as follows:

t	period of scheduling ($t=1,...,k$).
e	element e ($e=1,...,E$).
J	set of blocks to be extracted during k periods. This set is defined by the long-term schedule (this is the input from long-term schedule).
C_m^t	unit cost of mining in period t.
M_u^t	upper bound on usage of capacity of mining in period t.
M_l^t	lower bound on usage of capacity of mining in period t.
P_u^t	upper bound on usage of capacity of processing plant in period t.
P_l^t	lower bound on usage of capacity of processing plant in period t.
O_n	ore tonnage within block n.
R_n	rock tonnage of block n.
g_n^e	grade of element e in block n.
gu_e^t	upper bound on acceptable average head grade of element e in period t.
gl_e^t	lower bound on acceptable average head grade of element e in period t.
me	lower bound of tonnage extracted from each block in each period.
$N(J)$	number of blocks in set J.
$C_n(L)$	set of immediate predecessor blocks placed just above block n that must be extracted completely prior to extraction of block n.
$N_{C_n(l)}$	number of blocks in $C_n(L)$.

3.1.2 Decision variables

Decision variables are as follows:

$u_n^t \in [0,1]$ continuous variable which determines the portion of block n to be extracted in period t.

X_p^t amount of ore to be delivered directly from mine to the plant in period *t*.

X_{sp}^t amount of ore to be delivered from mine to the stock-pile in period *t*.

y_{SP}^t amount of ore to be charged into the plant from the stock-pile in period .

I^t amount of inventory of stock-pile at the end of period *t*.

b_n^t binary variable; 1 when block *n* is to be extracted in period t, 0 otherwise.

3.2. MILP Formulation

After defining the parameters and variables of the model, the mathematical formulation of the proposed model is presented as follows:

$$\text{Min } Z = \sum_{\forall n \in J} \sum_{t=1}^{k} R_n . u_n^t . C_m^t \tag{1}$$

Subject to:

$$\sum_{t=1}^{k} u_n^t = 1 \ , \ \forall n \in J \tag{2}$$

$$u_n^t \le b_n^t , \quad \forall t = 1,2,\ldots,k \ , \ \forall n \in J \tag{3}$$

$$me.b_n^t \le u_n^t \quad \forall t = 1,2,\ldots,k \text{ and } \forall n \in J \tag{4}$$

$$\sum_{n \in J} O_n . u_n^t = X_{SP}^t + X_p^t , \quad \forall t = 1,2,..,k \tag{5}$$

$$P_l^t \le X_p^t + y_{SP}^t \le P_u^t \quad \forall t = 1,2,..,k \tag{6}$$

$$M_l^t \le \sum_{n \in J} R_n . u_n^t \le M_u^t \quad \forall t = 1,2,..,k \tag{7}$$

$$N_{C_n(l)} . b_n^t \le \sum_{\forall l \in C_n(l)} \sum_{i=1}^{t} u_l^i \ , \ \forall n \in J \ , \ \forall t = 1,2,..,k \tag{8}$$

$$gl_e^t \le \frac{\sum_{n \in J} g_n^e . O_n . u_n^t}{X_P^t + y_{SP}^t} \le gu_e^t \quad \forall t = 1,2,\ldots,k, \ e \in \{1,..,E\} \tag{9}$$

$$I^t = I^{t-1} + X_{SP}^t - y_{SP}^t \quad \forall t = 1,2,..,k \tag{10}$$

$$b_n^t = 0,1 \ \forall t = 1,\ldots,k; \quad \text{all other variables are} \ge 0 \tag{11}$$

The objective function is minimization of mining costs including drilling, blasting, loading and hauling costs. Eqs. (2) to (11) present the constraints. Eq. (2) indicates that each block should be extracted completely during k periods according to long term schedule.

Eq. (3) defines the relation between binary variable b_n^t and continuous variable u_n^t. Based on this equation, whenever a portion of a block u_n^t is extracted, the binary variable b_n^t obtains a value of 1. Otherwise, it gets 0. Eq. (4) indicates that a minimum amount of material from each block should be extracted. This constraint is due to the physical constraints enforced by shovels. In fact, it is not economically or physically possible to extract a small portion of a block. Eq. (5) indicates that the amount of ore extracted is delivered to the plant or stock-pile. Eq. (6) controls the capacity of the processing plant. Based on the limitation of the plant, it is essential that in each period, the total tonnage of ore delivered to the plant from both mine and stock-pile be in an acceptable range. Eq. (7) indicates the limitation of mining equipments' capacity. The amount of rock extracted in each period should be in a certain range. Eq. (8) represents the precedence relationships between blocks. Fig. 3 illustrates the precedence of extraction of 4 blocks:

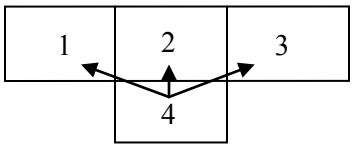

Fig. 3. Precedence relationship between 4 blocks.

To extract block 4, first blocks 1, 2, and 3 have to be extracted completely. In other words, block 4 cannot be extracted unless these three blocks have been extracted completely. Therefore, to extract block 4 in period t ($b_4^t = 0$), sum of the portions of each of the three blocks 1, 2, and 3 should be equal to 3. If this summation is less than 3, then $b_4^t = 0$. Eq. (9) indicates that the average grade of element *e* in the ore delivered to the plant should be in a certain range acceptable for the plant. Eq. (10) shows the balance of inventory in stock-pile. Based on this constraint, the value of inventory at the end of each period is the summation of inventory value at the end of the previous period and the ore received from the mine, minus the amount of ore sent to the plant. Finally, Eq. (11) indicates the sign constraints.

4. Methodology

The methodology of applying the simulation-optimization to this problem is a follows:

1. Setting a PDF for the value of ore grade of each block: there are several PDFs like Gaussian, triangle, etc. that can be considered.
2. Generating a series of random numbers based on the set PDF: to generate a random number, there are different known methods. Here, inverse transform method (ITM) is used.
3. Solving the problem with these random numbers in the deterministic form: setting the parameters of the MILP and solving it with mathematical programming solvers. in this study we used LPSolve.
4. Repeating steps 1 to 3 for a large number of runs.

5. Illustrative example

As mentioned before, mixed-integer linear programming is used to formulate the problem. These problems naturally are complex problems (NP-hard problems), especially when the size of the problem grows. Therefore, a small typical problem is considered for running the numerical experiments. The essence of the model and the solution approach in this paper can be applied to the large size problems without any changes. This problem includes 7 blocks that have configurations sketched in Fig. 4:

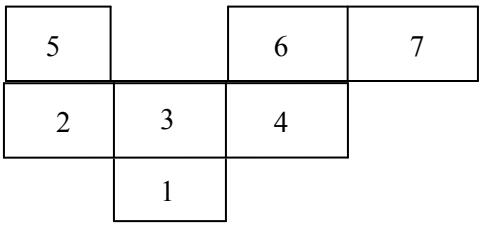

Fig. 4. Configuration of blocks.

The precedent relations between blocks are shown in Table 1:

Table 1. Precedent relations between blocks for extraction.

Blocks	Block 1	Block 2	Block 3	Block 4	Block 5	Block 6	Block 7
Precedent blocks	2-3-4	5	5-6	6-7	-	-	-

In fact, the precedence of blocks shown in Table 1 represent the $C_n(L)$ set. Different specifications of each block, including ore tonnage, rock tonnage and average grade are presented in Table 2:

Table 2. Specifications of each block.

	Block 1	Block 2	Block 3	Block 4	Block 5	Block 6	Block 7
Ore (ton)	200	220	100	150	400	330	300
Average Grade	0.08	0.04	0.05	0.07	0.05	0.05	0.04
Rock (ton)	1000	1000	1200	700	700	1000	1000

For this small problem only two time periods are considered. Also, the mine has only one main element such as copper and the value of I_0 is 0 (zero initial inventory). Other parameters considered in the problem are set as shown in Table 3:

Table 3. Set of parameters set in the problem.

	M_u^t (ton)	M_l^t (ton)	P_u^t (ton)	P_l^t (ton)	gu_l^t	gl_l^t	me
Period 1 (t=1)	4200	700	1000	200 (ton)	0.08	0.05	0.05
Period 2 (t=2)	4200	700	1000	200 (ton)	0.08	0.05	0.05

Also, the mining cost for each block in each period is indicated in Table 4:

Table 4. Mining cost (R_n*C_m^n -$) for each block in each period.

	Block 1	Block 2	Block 3	Block 4	Block 5	Block 6	Block 7
Period 1 (t=1)	1000	1000	1200	700	700	1000	1000
Period 2 (t=2)	1100	1100	1320	770	770	1100	1100

C_m^1=$1 and C_m^2=$1.1

In this paper we assume, the uncertainty only lies in the estimated values of grades of blocks. To quantify this uncertainty, for simplicity, the value of grade for each block is considered to have the symmetric triangle PDF. The triangle probability distribution has a shape presented in Fig. 5 with three independent parameters a, b, and c.

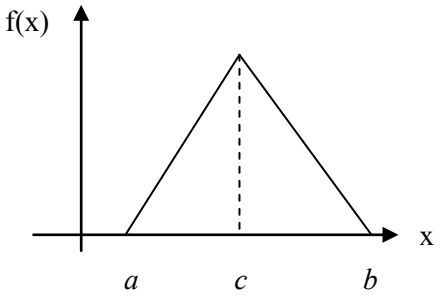

Fig. 5. Triangle probability distribution function diagram.

In the symmetric triangle distribution, $c-a=b-c$. Assuming symmetric triangle PDF for the ore grade of each block, c represents the average grade (Table 2). Table 5 indicates the three parameters a, b, and c for grade of each block:

Table 5. Specifications of triangle PDF of grade for each block.

	Block 1	Block 2	Block 3	Block 4	Block 5	Block 6	Block 7
a	0.02	0.01	0.0125	0.0175	0.0125	0.0125	0.01
c	0.08	0.04	0.05	0.07	0.05	0.05	0.04
b	0.14	0.07	0.0875	0.1225	0.0875	0.0875	0.07

As mentioned before, to generate the triangle PDF number for each block's ore grade, ITM is applied. First, separate uniform random numbers (*U(0,1)*) are produced for each block. Then, they are converted to respected triangle PDF numbers based on Eq. (12):

$$X_n = \begin{cases} \sqrt{U_n \bullet (b-a) \bullet (c-a)} & if\ 0 \le U_n \le \dfrac{c-a}{b-a} \\ b - \sqrt{(1-U_n) \bullet (b-a) \bullet (b-c)} & if\ \dfrac{c-a}{b-a} < U_n \le 1 \end{cases} \quad (12)$$

In Eq. (12), X_n and U_n indicate the triangle random number of block *n* and uniform random number related to block *n*, respectively.

6. Results and discussion

After setting the parameters of the model, 50 runs are performed by using LPSolve IDE-5.5.0.5 software (the typical code for average grade values for blocks is presented in the appendix). In each run, the values of grade for each block changes based on the symmetric triangle distribution. Among these 50 runs, only 31 runs have feasible and optimal solution. The remaining 19 runs show no feasible solution. Thus, it is expected that the problem has not any solution with probability of 19/50=0.38. Fig. 6 shows this ratio:

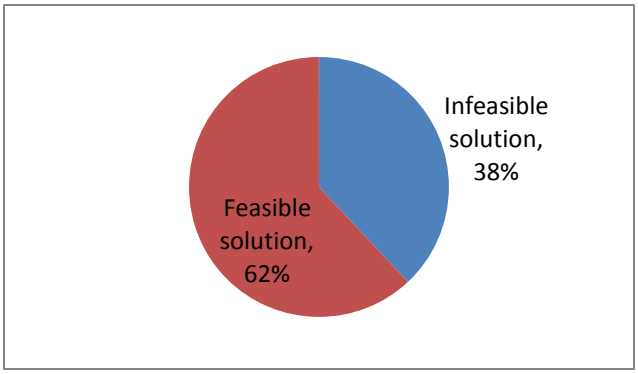

Fig. 6. Feasible/Infeasible solution ratio.

Table 6 indicates the values of mean and standard deviation of decision variables (u_n^t):

Table 6. Mean and standard deviation of decision variables.

Mean	0	0.27	0.64	0.67	1	0.94	0.92	1	0.72	0.35	0.32	0	0.05	0.07
Standard deviation (SD)	0	0.42	0.31	0.42	0	0.22	0.19	0	0.42	0.31	0.42	0	0.22	0.19

Table 7 shows the mean of rock tonnage extracted in each period resulted from numerical experiment. This table can assist in managing the mining equipment better. For example, based on this table the value of rock tonnage to be extracted in period 2 is about half of period 1. Thus, they can assign the remaining mining capacity of equipment in period 2 to other sites.

Table 7. Mean values of rock extraction in each period.

	Mean
Rock extracted in period 1 (ton)	4091.14
Rock extracted in period 2 (ton)	2508.85

Finally, the following figure shows how the value of objective function (mining cost) changes through different runs. Based on Fig. 7, the value of mining cost has almost a constant value of $6840. In some runs this value goes higher than 6840. The values of mean and standard deviation of mining cost are $6850.9 and $36.4, respectively. Thus, it is expected that the optimal mining cost is around $6850.

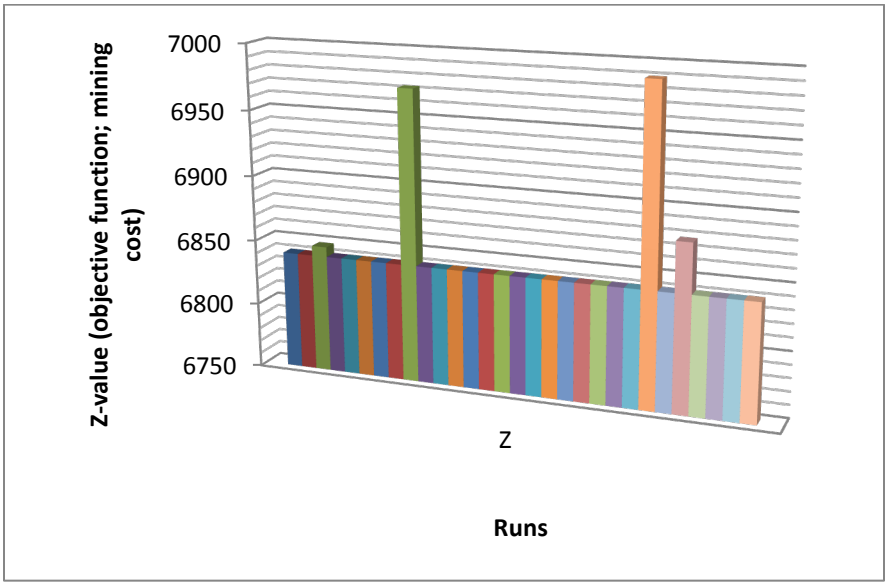

Fig. 7. Optimal mining cost through different runs.

7. Conclusions and future work

In this paper, a simulation-optimization approach has been used to solve a short-term mine scheduling problem. An MILP has been formulated for modeling the problem. Different steps of simulation-optimization method have been elaborated. It has been assumed that the value of grade of each block is based on the triangle distribution function. The solving method has been run for 50 iterations. In each iteration, different values for grade of each block have been set. The results of numerical experiment show that the optimal value (mining cost) is almost constant. As the future research work, developing an MILP model, considering more realistic constraints and solving with the simulation-optimization approach that is applied in this paper, seems to be of much of interest.

8. References

[1] Caccetta, L., Giannini, L. M., and Kelsey, P. (1998). *Application of Optimization Techniques in Open Pit Mining*, in Proceedings of Fourth International Conference on Optimization Techniques and Applications (ICOTA'98), Curtin University of Technology: Perth, Australia, pp. 414-422.

[2] Caccetta, L. and Hill, S. P. (2003). An Application of Branch and Cut to Open Pit Mine Scheduling. *Journal of Global Optimization*, *27*, 349-365.

[3] Carlyle, M. and Eaves, B. (2001). Underground planning at stillwater mining company. *Interfaces*, *31*,(4), 50-60.

[4] Denby, B. and Schefield, D. (1995). *The Use of Genetic Algorithms in Underground Mine Scheduling*, in Proceedings of 25th APCOM Symposium of the Society of Mining Engineers, New York, pp. 389-394.

[5] Denby, B., Schefield, D., and Bradford, S. (1991). Neural Network Applications in Mining Engineering. in *Department of Mineral Resources Engineering Magazine,University of Nottingham*, pp. 13-23.

[6] Dimitrakopoulos, R. and Ramazan, S. (2004). Uncertainty based production scheduling in open pit mining. *SME Transactions*, *316*, 1-9.

[7] Gershon, M. (1983). Mine Scheduling Optimization with Mixed Integer Programming. *Mining Engineering*, *35*, 351-354.

[8] Gershon, M. (1987). Heuristic Approaches for Mine Planning and Production Scheduling. *International Journal of Mining and Geological Engineering*, *5*, 1-13.

[9] Rossi, M. and Parker, H. M. (1994). Estimating recoverable reserves - Is it Hopeless? in Geostatistics for the Next Century. in *Kluwer Academic*, pp. 259-276.

[10] Tolwinski, B. and Underwood, R. (1996). A Scheduling Algorithm for Open Pit Mines. *IMA Journal of Mathematics Applied in Business and Industry*, *7*, 247-270.

[11] Vallee, M. (2000). Mineral resource + engineering, economic and legal feasibility = ore reserve. in *CIM Bulletin*, vol. 90, pp. 53-61.

9. Appendix

In this appendix, the respected LPSolve code used in the paper is presented. The code is regarding to the average grade values for each block. However before going through code, Table 8 and

Table 9 show the definition of equivalent variables used in the code.

Table 8. List of variables used in the LPSolve code.

x1	**x2**	**x3**	**x4**	**x5**	**x6**	**x7**	**x8**	**x9**	**x10**	**x11**	**x12**	**x13**	**x14**	**x15**	**x16**	**x17**	**x18**	**x19**	**x20**	**x21**	**x22**	**x23**	**x24**

Table 9. List of variables used in the LPSolve code.

										I^0	I^1	I^2
x25	**x26**	**x27**	**x28**	**x29**	**x30**	**x31**	**x32**	**x33**	**x34**	**x35**	**x36**	**x37**

```
/* Objective function (Eq. (1))*/
min:1000*x1+1000*x2+1200*x3+700*x4+700*x5+1000*x6+1000*x7+1100*x8+1100*x9+1320*x10+770
*x11+770*x12+1100*x13+1100*x14;
 /*   constraint 1 ((Eq. (2))*/
  x1+x8=1;
  x2+x9=1;
  x3+x10=1;
  x4+x11=1;
  x5+x12=1;
  x6+x13=1;
  x7+x14=1;
 /*   constraint 2 (Eq. (3))*/
  x1-x21<=0;
  x2-x22<=0;
  x3-x23<=0;
  x4-x24<=0;
  x5-x25<=0;
  x6-x26<=0;
  x7-x27<=0;
  x8-x28<=0;
  x9-x29<=0;
  x10-x30<=0;
  x11-x31<=0;
  x12-x32<=0;
  x13-x33<=0;
  x14-x34<=0;
 /*   constraint 3 (Eq. (4)) */
  0<=x1-0.05*x21;
  0<=x2-0.05*x22;
  0<=x3-0.05*x23;
  0<=x4-0.05*x24;
  0<=x5-0.05*x25;
  0<=x6-0.05*x26;
  0<=x7-0.05*x27;
  0<=x8-0.05*x28;
  0<=x9-0.05*x29;
  0<=x10-0.05*x30;
  0<=x11-0.05*x31;
  0<=x12-0.05*x32;
  0<=x13-0.05*x33;
```

```
0<=x14-0.05*x34;
/*   constraint 4 (Eq. (5))*/
200*x1+220*x2+100*x3+150*x4+400*x5+330*x6+300*x7-x15-x16=0;
200*x8+220*x9+100*x10+150*x11+400*x12+330*x13+300*x14-x17-x18=0;
/*   constraint 5 (Eq. (6))*/
 200<=x15+x19;
 200<=x17+x20;
x15+x19<=1000;
x17+x20<=1000;
/*   constraint 6 (Eq. (7))*/
700<=1000*x1+1000*x2+1200*x3+700*x4+700*x5+1000*x6+1000*x7;
700<=1000*x8+1000*x9+1200*x10+700*x11+700*x12+1000*x13+1000*x14;
1000*x1+1000*x2+1200*x3+700*x4+700*x5+1000*x6+1000*x7<=4200;
1000*x8+1000*x9+1200*x10+700*x11+700*x12+1000*x13+1000*x14<=4200;
    /*   constraint 7 (Eq. (8))*/
3*x21-x2-x3-x4<=0;
3*x28-x2-x3-x4-x9-x10-x11<=0;
x22-x5<=0;
x29-x5-x12<=0;
2*x23-x5-x6<=0;
2*x23-x5-x6-x12-x13<=0;
2*x24-x6-x7<=0;
2*x31-x6-x7-x13-x14<=0;
/*   constraint 8 (Eq. (9))*/
0<=16*x1+8.8*x2+5*x3+10.5*x4+20*x5+16.5*x6+12*x7-0.05*x15-0.05*x16;
16*x1+8.8*x2+5*x3+10.5*x4+20*x5+16.5*x6+12*x7-0.08*x15-0.08*x16<=0;

0<=16*x8+8.8*x9+5*x10+10.5*x11+20*x12+16.5*x13+12*x14-0.05*x17-0.05*x18;
16*x8+8.8*x9+5*x10+10.5*x11+20*x12+16.5*x13+12*x14-0.08*x17-0.08*x18<=0;
/*   constraint 9 (Eq. (10)) */
x16+x35-x19-x36=0;
x36+x18-x20-x37=0

  /*   other constraint (sign constraints-Eq. (11)) */
Sign constraints;

/* Variable bounds */
```

Aggregate cost minimization in hot-mix asphalt design

Kwame Awuah-Offei and Hooman Askari-Nasab
Mining Optimization Laboratory (MOL)
University of Alberta, Edmonton, Canada

Abstract

Hot-mix asphalt (HMA) is a mixture of aggregates and asphalt binder in appropriate ratios to produce a high performing material for asphalt pavements. The aggregate structure, which depends on the gradation, is an important factor in determining the volumetric properties of HMA. The design process of determining the optimal aggregate blend is currently iterative and engineers rely almost exclusively on past experience. This approach is time consuming and often results in sub-optimal HMA mixtures. This work presents linear programming (LP) optimization models, and attendant solution procedures, that minimize the HMA aggregate cost while producing high quality HMA. The models have been validated with real-life examples. The results indicate that the models can be used to replicate HMA mixes during field modifications, reduce the aggregate cost in a mixture and manage stockpile inventory. It is believed that the application of optimization models will increase the application of the Bailey method in the United States.

1. Introduction

Hot-mix asphalt (HMA) is a mixture of aggregate and asphalt binder with specific performance characteristics for pavement construction. Aggregate is the major structural (load bearing) component of HMA. Modern HMA production involves: (i) the use of different size distribution (gradation) aggregate stockpiles introduced into the plant through a set of feed bins or directly fed from the stockpiles, (ii) blending and drying in a drum dryer, and (iii) blending the hot aggregate with asphalt and storing in insulated silos for use in pavement construction. If desired, recycle asphalt product (RAP) can be introduced into the aggregate mixture after heating the aggregate to elevated temperatures. The use of quality materials (aggregates and asphalt binder), in optimal proportions, is the key to producing optimally performing HMA.

Researchers have long recognized the significance of aggregate gradation in producing high performing HMA (Richardson 1912, Goode and Lufsey 1962, Huber and Shuler 1992). The aggregate size distribution (or gradation) affects the volumetric properties such as air voids, voids in mineral aggregate (VMA), and voids filled with asphalt (VFA) of the mixture and consequently, the HMA performance. Despite this recognition, mix design methods in the United States (US) prior to the 1990s had no guidance for aggregate structure selection to achieve optimal HMA performance. The introduction of the Superior Performance Asphalt Pavement System

(SUPERPAVE) mix design standard in the US marked the introduction of specific volumetric property requirements in HMA design (Kennedy, et al. 1994). The SUPERPAVE mix design criteria for aggregate structure focuses on: (i) maximum aggregate size for the application; (ii) VMA; and (iii) aggregate skeleton. These objectives are achieved by controlling the nominal maximum particle size (NMPS) and the percent passing the 2.36 mm (US #8) and 0.075 mm (US #200) sieves (Vavrik 2000).

Even with the introduction of the SUPERPAVE mix design standards, engineers and lab technicians have largely relied on trial and error to achieve the volumetric requirements. The Bailey method is the only technique that provides a procedure to achieve the volumetric requirements of the SUPERPAVE standard (Vavrik 2000; Vavrik et al. 2002b). However, the Bailey method does not take into account the cost of the aggregate mixture. The method involves some trial and error to achieve a mixture with the desired aggregate ratios. Consequently, the first mix that meets the specified aggregate ratios is selected with no regard to the proportion of expensive or scarce aggregate stockpiles that are included in the design. This leads to sub-optimal (with regards to aggregate cost) mixes which are unacceptable in an industry where competitive bidding is the norm.

The objective of this work is to account for aggregate cost in HMA mix design through the application of optimization theory. This is done by modeling the HMA mix design problem as a linear programming (LP) optimization problem using the principles of the Bailey method. The optimization problem is then solved using LINDO API 6.0 (Lindo Systems, Inc. 2008) in MATLAB 7.7 (Mathworks, Inc. 2008). The optimization model is validated with a real life example and the practical applications of the work are illustrated with some further real-life mix design examples. The models included in this work are limited to dense-graded HMA mixes even though the principles could be applied to other HMA mixes. This work will help engineers and lab technicians design low cost HMA mixes by controlling aggregate cost in the mix. The optimisation algorithm ensures the least cost aggregate blend that meets the performance criteria is used in the mix. Also, aggregate plant managers can use the models to control stockpile inventory by including as little as possible of *scarce* stockpiles in the HMA mix. The trial and error involved in HMA mix design is significantly reduced by using the optimization modeling. Finally, this approach will increase the application of the Bailey method principles for aggregate blending during HMA mix design.

The next section of the paper covers a review of the relevant literature. Next section presents the LP models while Section 4 presents the numerical solution algorithm. The next two sections present the numerical examples used for validation and the results and discussions, respectively. Finally, Section 6 presents the conclusions followed by the list of references.

2. Relevant Literature

The objective of HMA mix design is to determine the proportions of each available component (aggregate stockpiles and asphalt binder) that will provide optimal HMA performance. The aggregates portion is the key structural component and is typically, over 94% by weight of the mix. For durable aggregate, the literature recognizes the significance of the aggregate gradation (size distribution) in producing high performing HMA (Richardson 1912, Goode and Lufsey 1962, Vavrik 2000). Different transportation authorities use different methods to design HMA mixes, for a comprehensive review of mix design methods see Vavrik (2000). Prior to the introduction of the SUPERPAVE mix design methodology in the US, the Hveem and Marshall methods were the predominant methods (Kandhal and Keohler 1985). The SUPERPAVE standards require the control of the nominal maximum particle size, voids in mineral aggregate (VMA), restricted gradation zone, and the percent passing the 2.36 mm (US #8) and 0.075 mm (US #200) sieves (Kennedy et al. 1994; McGennis et al. 1995).

The Bailey method is a systematic approach to blending aggregates to achieve the desired mixture properties (Vavrik 2000; Vavrik et al. 2002a,b). The method has been used since the early 1980s throughout the state of Illinois. The Bailey method can be used with any mix design method but the method itself is not a mix design method. The Bailey method, as discussed here, is suitable for dense-graded mixtures but can be applied to stone matrix asphalt (SMA) and fine graded mixes with some modification (Vavrik et al. 2002a,b). The Bailey method rests on two basic principles - aggregate packing, and coarse and fine aggregate definition. The degree of aggregate packing in a mixture is a function of the type and amount of compactive effort, particle shape, particle surface texture, gradation, and particle strength and durability. The Bailey method proposes an alternate definition of coarse and fine aggregate in HMA mixtures based on the mixture packing and interlock characteristics. Coarse aggregates are defined as those particles that will create voids in a unit volume and fine aggregate are the particles that fill the created voids. A particle ratio of 0.22 is used in the Bailey method to break the mixture into different fractions via control sieves (Vavrik 2000; Vavrik et al. 2002a,b). Equation (1) shows the Bailey method definition of primary, secondary and tertiary control sieves. NMPS is defined as one sieve larger than the first sieve that retains more than 10% as per SUPERPAVE terminology; and PCS, SCS and TCS are the primary, secondary and tertiary control sieves, respectively. The half sieve is defined in the Bailey method as shown in Equation (2). Using the standardized set of sieves in Table 1, and Equations (1) and (2), results in the control sieves shown in Table 2. Further to the control sieves, the method defines three aggregate ratios (Equation 3) to characterize the coarse, the coarse portion of the fine, and the fine portion of the fine aggregate in the mixture. These aggregate ratios have been shown to correlate well with the volumetric properties of the HMA mix (Vavrik et al. 2002a,b; Mohammad and Shamsi 2007). The Bailey method is based on volumetric blending of aggregate to achieve the desired aggregate ratios and hence the desired HMA volumetric properties (see Vavrik, et al. (2002a) for recommended aggregate ratios for different HMA mixes).

$$PCS = 0.22NMPS$$
$$SCS = 0.22PCS \quad (1)$$
$$TCS = 0.22SCS$$

$$\text{Half sieve} = 0.5NMPS \quad (1)$$

$$\text{CA ratio} = \frac{\%\text{ passing half sieve - }\%\text{ passing PCS}}{100\%\text{ - }\%\text{ passing half sieve}} \quad (2a)$$

$$\text{FA}_c = \frac{\%\text{ passing SCS}}{\%\text{ passing PCS}} \quad (3b)$$

$$\text{FA}_f = \frac{\%\text{ passing TCS}}{\%\text{ passing SCS}} \quad (3c)$$

3. Aggregate Blending Optimization

We formulated the aggregate blending problem during HMA mix design as a LP problem. The objective was to minimize the aggregate cost while producing high performing HMA that meets all the production specifications. The approach ensures the production specifications were met by taking advantage of the correlation between the specifications and the Bailey method aggregate ratios. A typical asphalt plant has a finite number of aggregate stockpiles. The aggregate blending problem is to determine the ratio of each stockpile that needs to be used in the HMA mix to produce a high performance mixture. Therefore, the percentages of each stockpile are the decision variables in this problem.

Table 1 US standard sieve sizes for HMA analysis

Sieve #	***Sieve Size***	
	US Standard	*(mm)*
1	1 1/2"	37.5
2	1"	25.0
3	3/4"	19.0
4	1/2"	12.5
5	3/8"	9.5
6	#4	4.75
7	#8	2.36
8	#16	1.18
9	#30	0.600
10	#50	0.300
11	#100	0.150
12	#200	0.075

Table 2 Bailey method control sieves

	NMPS (mm)					
	37.5	*25.0*	*19.0*	*12.5*	*9.5*	*4.75*
Half sieve	19.0	12.5	9.5	4.75	4.75	2.36
PCS	9.5	4.75	4.75	2.36	2.36	1.18
SCS	2.36	1.18	1.18	0.60	0.60	0.30
TCS	0.60	0.30	0.30	0.15	0.15	0.075

3.1. Objective Function

The objective of aggregate blending should be to minimize the cost of the aggregate used in the HMA mix. Equation (4) shows the objective function. c_j is the unit cost ($/ton) of stockpile *j*, x_j is the percentage of stockpile *j* in the mix (decision variables), and n is the number of bins/stockpiles.

$$Min \quad z = \frac{1}{100}\sum_{j=1}^{n} c_j x_j \tag{3}$$

3.2. Constraints

3.2.1 *Percentage Constraint*

This constraint is an equality constraint to ensure that the sum of the decision variables is equal to 100% (Equation 5).

$$\sum_{j=1}^{n} x_j = 100 \tag{4}$$

3.2.2 *Gradation Constraints*

Equation (6) represents the gradation constraints. g_{ij} is the percent passing sieve *i* of stockpile *j*, *m* is the number of sieve sizes included in the model, l_i is the lower gradation limit for sieve *i*, and u_i is the upper gradation limit for sieve *i*. This results in *2m* constraints which is typically equal to 24 constraints in the US (Table 1). l_i and u_i must be 0 and 100% for all sieves except on sieves that the agency has a specification for the mix.

$$l_i \le \sum_{j=1}^{n} g_{ij} x_j \le u_i \quad \text{for i} = 1, 2, \cdots \text{m} \tag{5}$$

3.2.3 *Maximum Particle Size (MPS) Constraint*

Equation (7) represents the constraint to ensure the intended HMA maximum particle size is maintained by the solution. The maximum particle size is ensured by using the nominal maximum particle size as defined earlier. This is done by changing the upper bound of the next sieve below the NMPS sieve to 90%. Equation (7) uses the assigned sieve numbers in Table 1.

$$u_{(nmps+1)} = 90 \tag{6}$$

3.2.4 *Bailey Method Aggregate Ratios*

The Bailey method applies three aggregate size ratios (CA, FA_c and FA_f ratios) to control the volumetric properties of the HMA mix (Equation 3). We used two modeling approaches to model the CA ratio constraint – modeling as a range or a specific value. Equation (8) represents the constraint, if the CA ratio is modeled as a range. *a* is the sieve number for the half-sieve, *b* is the sieve number for the PCS, CA_l and CA_u are the lower and upper bounds of the CA ratio, respectively. The half-sieve and PCS are determined from Table 2 and the given NMPS. Equation (8) results in two constraints.

$$CA_l \le \frac{\sum_{j=1}^{n}\left(g_{aj} - g_{bj}\right)x_j}{100 - \sum_{j=1}^{n} g_{aj}x_j} \le CA_u \tag{7}$$

Alternatively, the CA ratio constraint can be modeled as a specific value (Equation 9). This is useful, for instance, in cases where the engineer is trying to correct for field deviation and therefore has a specific CA ratio value for the mix.

$$\frac{\sum_{j=1}^{n}\left(g_{aj} - g_{bj}\right)x_j}{100 - \sum_{j=1}^{n} g_{aj}x_j} = CA \tag{9}$$

We used a similar approach (modeling for a range and a specific value) for the FA_c constraint modeling. Equations (10) and (11) represent the inequality and equality constraints, respectively. FA_{cl} and FA_{cu} are the lower and upper bounds of the FA_c ratio, respectively, and *c* is the sieve number for the SCS.

$$FA_{cl} \le \frac{\sum_{j=1}^{n} g_{cj}x_j}{\sum_{j=1}^{n} g_{bj}x_j} \le FA_{cu} \tag{10}$$

$$\frac{\sum_{j=1}^{n} g_{cj}x_j}{\sum_{j=1}^{n} g_{bj}x_j} \le FA_c \tag{11}$$

Similarly, Equations (12) and (13) represent the inequality and equality FA_f constraints, respectively. FA_{fl} and FA_{fu} are the lower and upper bounds of the FA_f ratio, respectively, *d* is the sieve number for the TCS and the previously defined terms apply.

$$FA_{fl} \le \frac{\sum_{j=1}^{n} g_{dj} x_j}{\sum_{j=1}^{n} g_{cj} x_j} \le FA_{fu} \tag{12}$$

$$\frac{\sum_{j=1}^{n} g_{dj} x_j}{\sum_{j=1}^{n} g_{cj} x_j} \le FA_{f} \tag{13}$$

There can be three to six Bailey method aggregate ratio constraints. However, in order not to over constrain the model, the four constraints are recommended for a problem (two equality and a tight range for the third).

3.2.5 *Lower and Upper Bound Constraints*

There are technological and regulatory reasons why an engineer will require lower and upper limits on the percentage from a particular stockpile. For instance, many transportation authorities have a maximum percentage of recycle asphalt product (RAP) that can be used in a mix. Also, a mix design that requires 2% of a particular stockpile may be difficult to achieve since it requires a very low conveyor belt speed for regular production rates. Equation (14) represents the constraint for the lower and upper bounds imposed on the solution. l_i and u_i are the lower and upper bounds on the decision variable x_i, respectively. By ensuring that all l_i are greater than or equal to zero, the non-negativity constraint of an LP problem is satisfied by the lower bound constraint. Hence the non-negativity constraint is not explicitly built into the LP model in this work.

$$\begin{aligned} & l_j \le x_j \le u_j \quad \text{for } j = 1, 2, \cdots n \\ & l_i \ge 0 \\ & u_i \le 100 \end{aligned} \tag{14}$$

These constraints are the preferred way to manage stockpile inventory using these models. Provided the engineer can estimate the amount of stockpile *i*, that will be available in the production period, he can then convert that to the maximum percentage of stockpile *i*, that can be included in the mix. Alternatively, the engineer could arbitrarily make the unit cost of stockpile *i* high so that as little as possible is used in the mix. This alternative is not the best since it discourages the use of the particular material and may result in less than the inventory being used over the production period.

4. Numerical Solution Procedure

LINDO is designed to solve a wide range of optimization problems, including linear programs, mixed integer programs, quadratic programs, and general nonlinear non-convex programs (Lindo Systems, 2009a,b). The linear programming solvers in LINDO are designed to solve the LP problem in Equation (15). The solvers return the optimal solution, $\mathbf{x}^*$, and the optimal slack/surplus values as well as the optimal solution and slack/surplus values for the dual problem. LINDO also includes algorithms to conduct sensitivity analysis of the objective function coefficients, **c**, and the right-hand side (RHS) coefficients, **b**. There are three linear solvers in LINDO - the Primal Simplex, Dual Simplex, and the Barrier Methods (Lindo Systems, 2009b). The nature of the LP problem determines which of the three algorithms will be the most efficient. The LP problems discussed in this paper are not exceptionally complicated in themselves. We used the Dual Simplex

because it tends to do well on sparse models with fewer columns than rows or models that are primal and/or dual degenerate (Lindo Systems, 2009b).

$$\begin{aligned} &\text{minimize } \mathbf{c}^T\mathbf{x} \\ &\text{subject to } \mathbf{A}\mathbf{x} \geq \mathbf{b} \\ &\mathbf{u} \geq \mathbf{x} \geq \mathbf{l} \end{aligned} \tag{15}$$

LINDO API is an interface that allows software developers to incorporate LINDO's optimization algorithms into their own application programs. It allows a person to access the LINDO solvers from the MATLAB environment through the MATLAB executable file (MEX-file), mxLINDO. In this work, we developed MATLAB routines to read the input data from Excel files and formulate the vectors and matrices that describe the mix design LP problem. We then accessed the LINDO solution algorithms by issuing calls to mxLINDO with these matrices and vectors, and other mxLINDO input. These calls to LINDO returned the optimal solutions to both the primal and dual problem and the ranges of the objective function coefficients and RHS coefficient for which the optimal basis will remain the same.

5. Practical Applications

5.1. Case Study

We used a real-life mix design problem from Washington State to illustrate the practical applications of the work as well as to verify and validate the models and solution procedures. The contractor had to design a 12.5 mm HMA mix for a Washington State Department of Transportation (WSDOT) project. The contractor submitted an aggregate blend of 74%, 16% and 10% respectively of the 1/2" × 0, 1/2" × 1/4" and RAP (Table 3). The 1/2" × 0 and 1/2" × 1/4" crushed rock were purchased at $ 7.00 and $8.50 per ton, respectively. The value of the recycled asphalt product (RAP) is difficult to estimate since this contractor will usually not sell it to a third party. Other companies are charged a fee to dump their asphalt concrete removed from highways. The company then crushes this recycled pavement into acceptable gradation for use as RAP. The asphalt in the RAP offers an additional value to using this product in the HMA mix (RAP reduces the amount of *new* asphalt necessary). Hence, the cost (to the contractor) of using RAP is the crushing cost less the revenue from receiving and the cost savings from reduced asphalt consumption during HMA production. For the purposes of this work, the value of the RAP was estimated at $2.00/ton. Consequently, the cost of the aggregate blend in the designed mix is $ 6.74/ton.

The designed mix resulted in a VMA of 13.1% (less than the recommended 14% but above the minimum 12.5%. The designed VFA was 67% which is within the specified 65-75%. The designed mix also met all the gradation specifications of the WSDOT 12.5 mm HMA mix. Using the designed aggregate blend, the CA, FA_c and FA_f ratios were calculated to be 0.260, 0.468 and 0.371, respectively. The FA_c and FA_f ratios are within the ranges recommended by Vavrik et al. (2002a) for a 12.5 mm mix (0.35 to 0.5). Vavrik et al. (2002a) recommends that the CA ratio for a 12.5 mm mix should be between 0.5 and 0.65. However, data from the contractor and other successful mixes suggests that a CA ratio between 0.25 and 0.4 gives good results for these stockpiles.

First, we set up the LP problem, based on the models presented in prior, with the stockpile data and the ratios set to the exact same ratios of the contractor's design (the FA_f ratio was set to a range in order not to over constrain the problem due to round-off errors). The problem results in a LP problem with three decision variables and 29 constraints (the percentage constraint, 24 gradation constraints and four Bailey method ratio constraints). We set the lower and upper bounds of the decision variables to zero and 100, respectively, except for the upper bound of the RAP which was set to 20% per WSDOT specifications. The purpose of this scenario was to evaluate the existence

of multiple solutions to obtaining the contractor's designed mix. Also, this scenario allows one to evaluate the ability of the models to reproduce a particular blend.

Table 3 Stockpile material gradations

Sieve Size	*Stockpile Gradation (% Passing)*			*Gradation Limits (% passing)*	
(mm)	*1/2" × 0*	*1/2" × 1/4"*	*RAP*	*Min*	*Max*
37.55	100.00	100.00	100.00		
25.00	100.00	100.00	100.00		
19.00	100.00	100.00	100.00	100	100
12.50	95.93	95.98	98.20	90	100
9.50	82.38	59.76	88.20		90
4.75	54.49	3.34	71.30		
2.36	38.19	1.40	60.00	28	58
1.18	24.95	1.27	44.00		
0.60	18.12	1.21	25.50		
0.30	10.30	1.17	22.30		
0.15	6.39	1.16	10.80		
0.075	4.76	1.14	8.50	2	7

Further, we prepared another problem with the same data but by setting CA ratio to be between 0.25 and 0.4 while the FA_c and FA_f ratios were set to be between 0.35 and 0.5 each. This problem results in a problem with three decision variables and 31 constraints (the percentage constraint, 24 gradation constraints and six Bailey method ratio constraints). The lower and upper bounds of the decision variables were the same as the first problem. This will be the ideal input for an initial design if the contractor were to do the design with the approach presented here. These two problems were solved using the LINDO solution algorithms through the LINDO API 6.0. We also conducted sensitivity analysis of the optimal solution. The results are discussed in the next section.

5.2. Results & Discussions

Table 4 shows the optimal solutions, x_i^*, (mix design) of the two problems, the Bailey method ratios for the optimal mix design and the optimal value (cost/ton). We obtained the same solution as the contractor's design for the first problem. Thus, one can conclude that there is no *better* (cheaper) solution that will result in a blend with the same ratios as the contractor's design. In fact, the range of acceptable changes of unit costs (Table 7) suggests that the unit costs may be irrelevant in obtaining that solution. The solution, however, shows that one could reproduce a mix of the same properties (Bailey method ratios) using the proposed approach. The ability to reproduce a blend of the same characteristics is crucial in making field modifications to a particular mix design. For instance, if samples of the stockpile gradations show a consistent deviation, one can easily correct for the mix by obtaining a solution of the LP problem with the new gradations but the same aggregate ratios. Since the volumetric properties of the HMA mix are a function of the Bailey method ratios of the aggregate blend, the volumetric properties of such a modified mix should be close to the original.

Table 4 Optimal solution and aggregate ratios

	Mix 1	Mix 2
1/2" × 0 Ratio (%)	74	80
1/2" × 1/4" Ratio (%)	16	0
RAP Ratio (%)	10	20
CA ratio	0.260	0.363
FA_c ratio	0.468	0.461
FA_f ratio	0.371	0.371
Cost/ton ($/ton)	6.74	6.00

Mix 2 is the optimal solution to the design problem. The solution shows that it is possible to obtain a mix with acceptable volumetric properties without using any material of the most expensive stockpile (1/2" × 1/4"). This illustrates the benefit of using the proposed approach for aggregate blending during HMA mix design. Even though this results in an apparently marginal reduction ($ 0.74/ton) in the aggregate cost, this might be the difference between two contractors in an industry that is fiercely dependent on the cost at bid time. Of course, the overall reduction in cost of an asphalt paving job may be significant depending on the amount of asphalt to be used on the project. Furthermore, the environmental benefits of using more RAP is not captured in this analysis.

Table 5 shows the slack or surplus variable optimal solutions for constraints used to model the aggregate specifications. Even though the LINDO solution reports the optimal values of the slack/surplus variables for all the constraints, all except the ones reported in Table 5 were found to convey meaningful information. The percentage constraint will always have a slack of zero. The slack/surplus optimal values of the Bailey method aggregate ration constraints cannot be used to make any conclusions about the Bailey method ratios because the ratios appear in both the right-hand side (RHS) and left-hand side (LHS) of the constraints. Interestingly, Table 5 shows that none of the agency specifications are controlling constraints on the optimal solution.

Table 5 Slack/surplus values for gradation specification constraints

	Mix 1 (%)	Mix 2 (%)
12.5-mm sieve lower bound surplus	6.2	6.4
9.5-mm sieve upper bound slack	10.7	6.5
2.36-mm sieve upper bound slack	23.5	15.5
2.36-mm sieve lower bound surplus	6.5	14.5
0.075-mm sieve upper bound slack	2.4	1.5
0.075-mm sieve lower bound surplus	2.6	3.5

Table 6 and Figure 1 show the gradations of the two mixes. Both mixes respect all the gradation limits as modeled by the constraints. Mix 2 is coarser than Mix 1, with a CA ratio of 0.363 (an increase of 0.103). Also, the FA_c ratio is slightly lower than the contractor's design (Table 4). As CA ratio increases or FA_c ratio decreases, the VMA increases (Vavrik et al. 2002; Mohammad and Shamsi, 2007). Also, an increase CA ratio or a decrease in FA_c ratio will cause the VFA to increase (Mohammad and Shamsi 2007). Consequently, Mix 2 is likely to produce a mix with higher VMA and VFA than Mix 1 which had a VMA lower than the recommended 14%. The amount of material passing the 0.075 mm sieve is also slightly higher for Mix 2. Higher proportions of material of this size is known to increase the stiffness of the HMA mix. This is, however, not considered to be a significant issue given the slight increase in the material of this size.

Table 6 Gradation of optimal mixes

Sieve Size (mm)	***Gradation (% Passing)***	
(mm)	*Mix 1*	*Mix 2*
37.5	100.0	100.0
25.0	100.0	100.0
19.0	100.0	100.0
12.5	96.2	96.4
9.5	79.3	83.5
4.75	48.0	57.9
2.36	34.5	42.5
1.18	23.1	28.8
0.600	16.2	19.6
0.300	10.0	12.7
0.150	6.0	7.3
0.075	4.6	5.5

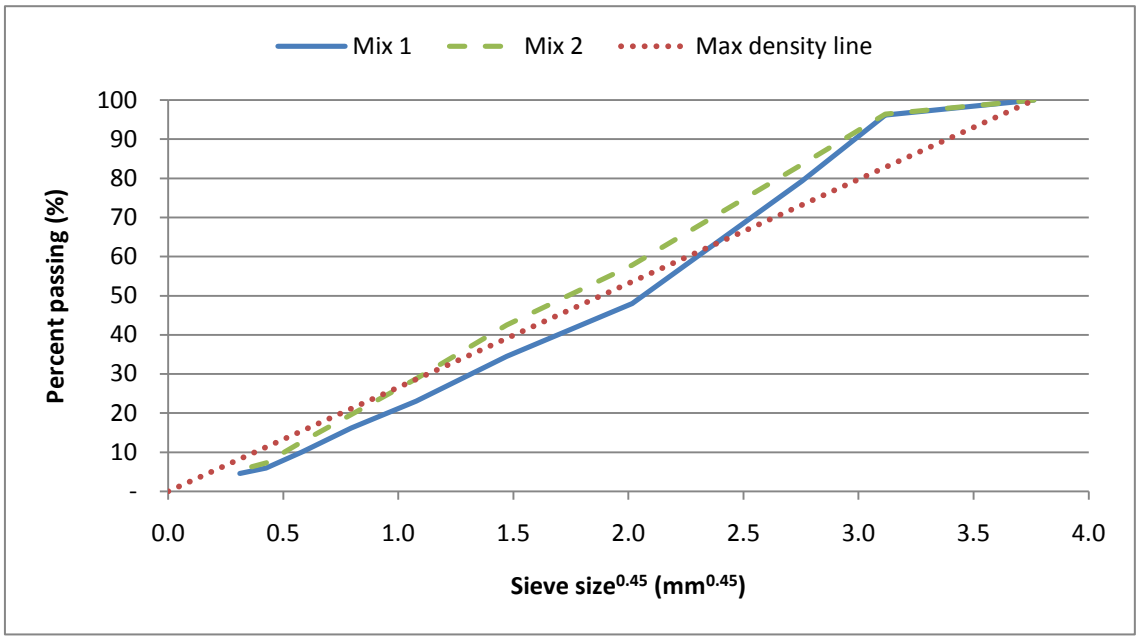

Figure 1 Gradation of optimal mixes.

It should be noted that the amount of material passing the 0.075 mm sieve is still within the WSDOT specification.

Table 7 shows the results of the sensitivity analysis on the coefficients of the objective function (unit costs of aggregate stockpiles). The ranges shown in Table 7 are the ranges for which the solution basis will remain unchanged. Sensitivity analysis of the RHS values is not reported here because it does not provide any meaningful information. The sensitivity analysis of the gradation constraint RHS values does not provide any information that cannot be inferred from the slack/surplus variables. The Bailey method ratio constraint RHS values do not provide any useful for the same reason the slack/surplus values are not useful. The sensitivity analysis shows that Mix 1, the contractor's design, does not change with changes in the unit cost. The basis solution in Mix 2, on the other hand, is sensitive to the unit price. The basis solution will remain the same (i.e. engineer can use only aggregates and RAP in the mix) so long as 1/2" × 0" aggregate is cheaper than 1/2" × 1/4" and RAP is cheaper than both. This is particularly important since the design will require no purchase of aggregates.

Table 7 Sensitivity analysis of optimal solutions

Parameter	Mix 1			Mix 2		
	Input	Min.	Max	Input	Min.	Max.
1/2" × 0 cost ($/ton)	7.00	-Infinity	Infinity	7.00	2.00	8.50
1/2" × 1/4" cost ($/ton)	8.50	-Infinity	Infinity	8.50	7.00	Infinity
RAP cost ($/ton)	2.00	-Infinity	Infinity	2.00	-Infinity	7.0

The models presented in this work have significant benefits in asphalt mix design. Firstly, the program can quickly and accurately produce aggregate blends that meet specific Bailey method ratios and agency specifications without the trial and error normally involved in such exercises. Secondly, the application of LP optimization techniques assures users that the design is the least cost option that meets all their performance measures. This allows an engineer to manage cost or control stockpile inventories. Finally, this approach, especially if incorporated into a commercial software package (see Awuah-Offei and Askari-Nasab 2009), is likely to encourage the widespread use of the Bailey method in aggregate blending during HMA mix design.

6. Conclusions

HMA mix design is a process of determining the proportions of aggregates and asphalt that will constitute an optimally performing mixture. The role of the aggregate gradation, and consequently the aggregate blend, in HMA mix design is well recognized. The Bailey method provides a structured guideline for developing an aggregate blend which results in HMA mixes that have optimal volumetric properties. This is done through control of three aggregate ratios defined by the method. However, the Bailey method on its own does not remove the trial and error inherent in current mix design techniques. Also, the method does not allow for any means of aggregate cost control or inventory management during HMA mix design. The work presented in this paper applies optimization techniques to the aggregate blending process in HMA mix design and production. HMA aggregate blending has been modeled as a linear programming problem. The models have been verified and validated with real-world examples using Washington State specifications.

The results show that for a 12.5-mm HMA mix designed by a contractor for a WSDOT project, a cheaper aggregate mix could have been obtained using this approach. The optimal mix obtained using this approach is $ 0.74/ton cheaper than the contractor's original mix. The resulting mix is coarser than the original mix with a higher coarse aggregate (CA) ratio (0.103 higher) and a lower ratio of the coarse portion of the fine aggregate (FAc). The increase in CA ratio and decrease in FAc ratio is likely to result in an increase in the voids in mineral aggregate (VMA) and the voids filled with asphalt (VFA) of the HMA. In fact, the VMA of the original HMA was below the recommended 14%. The optimal aggregate mix meets all the WSDOT specifications. The application of these models will allow engineers to quickly develop aggregate mixes for optimal HMA performance without going through the trial and error usually associated with aggregate blending in HMA design. Secondly, this approach provides a means to control HMA aggregate cost and/or aggregate stockpile inventories. It allows engineers to use stockpiles that are abundant and limit the use of those that are limited without sacrificing the performance of the HMA they can produce. Finally, this work will help increase the use of the Bailey method in HMA design and production in the US.

7. Notations

7.1. Symbols

NMPS	NMPS sieve, defined as one sieve larger than the first sieve that retains more than 10% as per SUPERPAVE terminology
PCS	Primary control sieves
SCS	Secondary control sieves
TCS	Tertiary control sieves
CA	Coarse aggregate ratio
FA_c	Coarse portion of the fine aggregate ratio
FA_f	Fine portion of the fine aggregate ratio
c_j	Unit cost ($/ton) of stockpile *j*
x_j	The percentage of stockpile *j* in the mix
n	The number of bins/stockpiles
g_{ij}	The percent passing sieve *i* of stockpile *j*

m	The number of sieve sizes included in the model
l_i	The lower gradation limit for sieve i
u_i	The upper gradation limit for sieve i
a	The sieve number for the half-sieve, b is
b	The sieve number for the primary control sieve
c	The sieve number for the secondary control sieve
d	The sieve number for the tertiary control sieve
i	Sieve number
j	Stockpile number
u	Upper limit
l	Lower limit

8. References

1. AASHTO; FAA; FHA; NAPA; USACE; APWA; NACE. (2000) *Hot-Mix Asphalt Paving Handbook*, Washington, DC: U. S. Army Corps of Engineers.
2. Awuah-Offei, K., and Askari-Nasab, H., (2009). "Asphalt Mix Optimization for Efficient Plant Management", *Transportation Research Record: Journal of the Transportation Research Board, No. 2098,* 105-112.
3. Goode, J. F., and Lufsey, L. A. (1962). "A New Graphical Chart for Evaluating Aggregate." *Proceedings of the Association of Asphalt Paving Technologists,* MN, 176-207.
4. Huber, G. A., and Shuler, T. S. (1992). "Providing Sufficient Void Space for Asphalt Cement: Relationship of Mineral Aggregate Voids and Aggregate Gradation." *Symposium on Effects of Aggregates and Mineral Fillers on Asphalt Mixture Performance: ASTM Special Technical Publication 1147.* Philadelphia, PA, 225-251.
5. Kandhal, P. S., and Keohler, W. S. (1985). "Marshall Mix Design Method: Current Practices." *Proceedings of The Association of Asphalt Paving Technologists,* MN, 284-303.
6. Kennedy, T. W., et al. (1994) *Superior Performing Asphalt Pavements (SUPERPAVE): The Product of the SHRP Asphalt Research Program, Report No. SHRP-A-410*, Transportation Research Board, Washington, DC, 156 pp.
7. Lindo Systems, Inc. (2009a). *LINDO API 6.0 Software*, Lindo Systems, Inc., Chicago, IL.
8. Lindo Systems, Inc. (2009b). *LINDO API 6.0 User Manual*, Lindo Systems, Inc., Chicago, IL.
9. Mathworks, Inc. (2007). *MATLAB 7.4 (R2007a) Software,* The Mathworks, Inc.
10. McGennis, R. B., Anderson, R.M., Kennedy, T.W. and Solaimanian, M. (1995). *Background of SUPERPAVE Asphalt Mixture Design and Analysis. Report No. FHWA-SA-95-003*, Federal Highway Administration, Washington, DC, 172 pp.
11. Mohammad, L. N., and Shamsi, K. A. (2007). "A Look at the Bailey Method and Locking Point Concept in SUPERPAVE Mixture Design", *Practical Approaches to Hot-Mix Asphalt*

Mix Design and Production Quality Control Testing, Transportation Research Circular, Circular No. E-C124, Transportation Research Board, Washington, DC, 24-32.

12. Richardson, C. (1912). *The Modern Asphalt Pavement*, 2nd Edition, New York, NY: John Wiley & Sons.
13. Vavrik, W. R. (2000). *Asphalt Mixture Design Concepts to Develop Aggregate Interlock.* PhD Dissertation. University of Illinois at Urbana-Champaign, Urbana-Champaign, IL, USA.
14. Vavrik, W. R., Huber, G., Pine, W. J., Carpenter, S. H. and Bailey, R. (2002a) *Bailey Method for Gradation Selection in Hot-Mix Asphalt Mixture Design, Transportation Research Circular*, No. E-C044, DC, USA: Transportation Research Board, 33pp.
15. Vavrik, W. R., Pine, W. J. and Carpenter, S. H. (2002b). "Aggregate Blending for Asphalt Mix Design: Bailey Method", *Transportation Research Record,* Vol. 1789, pp. 146-153.

Using simulation in determining the storage capacity of a coal terminal

Mohammad Mahdi Badiozamani and Hooman Askari-Nasab
Mining Optimization Laboratory (MOL)
University of Alberta, Edmonton, Canada

Abstract

In this project, the mining industry is looked from the logistic network point of view. It is assumed that in order to ship the metallurgical coal to the final demand destinations (steel manufacturers), the commodity should be shipped from different mine plants (coal mines) to a number of intermediate transshipment points (coal terminals), stored there and then, shipped to the final destinations, the manufacturing plants, via some connecting routes. One of the critical decisions in such logistics networks is the stockpile capacity of the coal terminal. In this study, the network is considered to have only one coal terminal (single depot) and the proper storage capacity of the terminal is estimated using simulation techniques. It is assumed that the rate of supply (as the input to the inventory system), and demand (as the output) are known and determined by some polynomial and oscillatory functions. It is also assumed that there are two ore types with different characteristics which cannot be mixed in the stockpile to avoid dilution. The governing equations of the system are presented and solved, using SIMULINK toolbox in MATLAB. Two scenarios are proposed, representing the different sets of supply and demand functions. For each scenario, more than 15600 runs are executed to identify the optimized parameters.

1. Introduction

From the overall perspective, designing a proper logistics network that facilitates the shipment and storage of the mined materials is considered to be an important issue. This network is consisted of two main elements; the nodes and the arcs. The nodes represent all of the facilities in the network such as stockpiles, mining and processing plants (the supply side), the steel manufacturer blast furnace as the final destination of the materials (the demand side) and finally, some transshipment points (coal terminal) that balance the demand and supply flows through the network. The arcs are the routes that connect different nodes together. One of the critical decisions that should be made among decision making problems of the network is the number, location and the size of transshipment points. The importance of such transshipment points is from the network balancing point of view, optimization, and cost reduction aspects as well. Transshipment point's capacity mostly depends on the input rate of commodity (from suppliers) and the output rate (from demand points). Both supply and demand may have deterministic or probabilistic rates that can be linear or non linear.

In the literature, this issue is discussed in logistics and inventory management context. A number of different supply and demand patterns are considered in literature. The decision making problem is solved either using exact solution methods using operations research techniques, or with some heuristic or meta-heuristic methods which provide near optimal solutions.

Urban (2005) reviews the available literature about several demand functions that are considered as inventory-dependant in the inventory management models. In these models, the inventory is assumed to have a motivation effect on the customer's demand. According to Urban (2005), all of these models can be classified into two main groups; models in which the demand rate of an item is a function of the initial inventory level and those in which it depends on the instantaneous inventory level.

Urban (1995) considers an inventory with both linear and power demand function. The demand dependency to the inventory in his work is classified into three different patterns as; initial, instantaneous or two-staged. The objective function is maximization of the profit and he assumes an infinite planning time horizon. Teng (1996) proposes a computationally efficient optimal method for determining the time and number of replenishment points at each replenishment order size. He considers a deterministic linear demand and presents an objective function that minimizes the total inventory, shortage and ordering costs. Bhunia and Maiti (1997) consider the instantaneous dependency of demand to the inventory level. They build their model with both linear and power demand functions and the objective function is cost minimization. They also assume infinite planning time horizon. Liao *et al.* (2000) consider a polynomial demand function with an initial dependency to the inventory level. Their objective function is cost minimization and they assume that the planning time horizon is finite. Kar *et al.* (2001) develop a deterministic inventory model for a single item. They assume that there are two storage facilities, i.e. owned and rented warehouses, and the demand has a linear time-dependant increasing function. The planning time horizon in their model is considered to be fixed and finite. Balkhi and Benkherouf (2004) considers an instantaneous dependency of demand to the inventory level, with a demand power function. They assume a finite planning time horizon and their objective function is cost minimization. Begum *et al.* (2009) propose an order-level inventory model with a demand rate as a function of time. They introduce an exponential demand rate and their presented objective function minimizes the total average cost.

In addition to the demand rate, the supply rate can be assumed to have several patterns. Chao *et al.* (2008) study a joint optimization problem of replenishment and pricing for a periodic-review inventory system. They consider a random supply capacity. In their model, they assume that the firm only knows the supplier's available capacity in the current period and do not know about the available supply capacity in future periods. In addition, the random supply capacities for different periods are considered to be dependent. They assume several stochastic dependency structures for the supply capacity sequence, including the one-lag and the multi-lag dependency.

In most of the reviewed literature, the demand and supply are considered to be either deterministic, which an exact or heuristic solution is proposed to solve it, or stochastic which in some cases are solved with simulation techniques. In this project, the deterministic supply and demand are assumed and the model is analyzed, using simulation techniques. It is also assumed that the planning time horizon is infinite.

Problem definition, mathematical notations, and governing equations are presented in the second section of the paper. Two scenarios that are considered in modeling and simulating the problem are proposed in the third section. The result of the simulation, corresponding to each scenario, is reported in the third section as well. The conclusion from simulations is discussed in the forth section. Finally, the MATLAB m.file and commands are presented in the fifth section in the appendix.

2. Problem definition

A logistics network with three coal mines (suppliers) and three steel manufacturers (demand points) is considered. The supply and demand of each plant is assumed to be deterministic and the supply and demand functions are known. It is also assumed that there is one coal terminal

(transshipment point) in the network that receives the commodity from the coal mines, stores it if required and sends it to the steel manufacturers. Each coal mine can produce two types of ore, type "A" and type "B". Since the specifications of the ore types are different, they should not be mixed together in order to avoid the dilution. As the result in the coal terminal stockpile, it is required to assign a specific and separate capacity for storage and handling of each ore type. On the demand side, each of the steel manufacturers is able to process both ore types as well.

The capacity of the stockpile for each type of ore, which is the maximum inventory level of that ore type in the terminal, depends on the proportions of ore types that are produced by coal mines and consumed by steel manufacturers. Since the holding cost of the inventory is considerably high and there is not any back order or lost sale costs, the goal is to find the minimum inventory level of each ore type in the terminal. So, the question is "what is the best proportion for ore type production by each coal mine, and on the other hand, the best proportion of ore type required by each steel manufacturer that minimizes the total inventory level of the terminal's stockpile?" In addition, "what is the required capacity for the storage of each ore type?" The problem is presented schematically in Fig. 1.

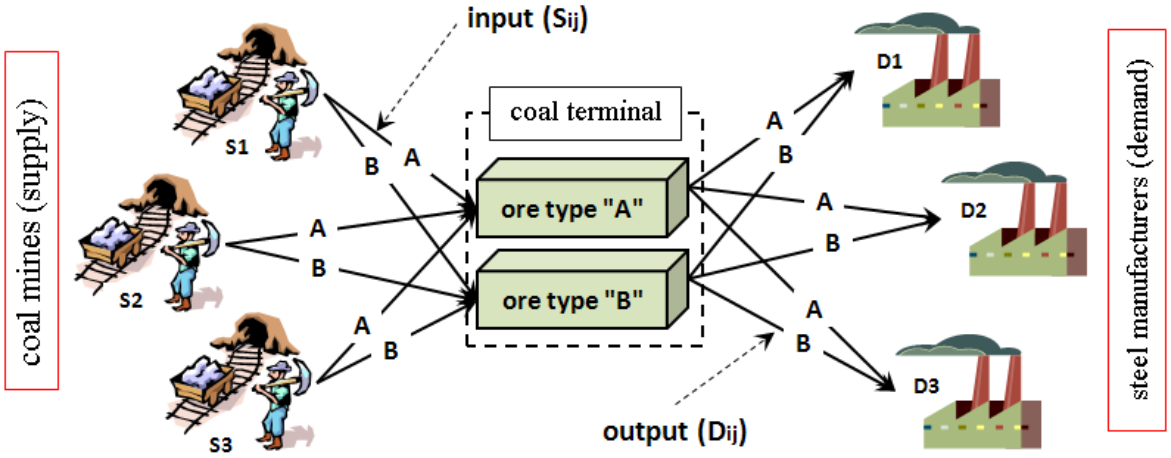

Fig. 1. Schematic presentation of the problem.

In order to present the model in mathematical format, the following notations are used:

$S_i(t)$ the supply of coal mine i (determines the input to the system)

S_{ij} the amount of ore type j that goes from coal mine i to the coal terminal

$s_i(t)$ the supply rate for coal mine i

p_i the proportion of S_i that is ore type A

$D_j(t)$ the demand of steel manufacturer j (determines the output of the system)

D_{ij} the amount of ore type i that goes from the coal terminal to the steel manufacturer j

$d_j(t)$ the demand rate for steel manufacturer j

q_j the proportion of D_j that is ore type A

$I_A(t)$ the inventory of the ore type A at time t

$i_A(t)$ the inventory rate for ore type A

$I_B(t)$ the inventory of the ore type B at time t

$i_B(t)$ the inventory rate for ore type B

The combination of the ore types that can be produced by each coal mine is as the relationship presented by Eq. (1).

$$S_i = p_i.S_i + (1-p_i).S_i = S_{iA} + S_{iB} \qquad i = 1,2,3 \tag{1}$$

On the other hand, each steel manufacturer requires both types of ore with the combination that is presented by Eq. (2).

$$D_j = q_j.D_j + (1-q_j).D_j = D_{Aj} + D_{Bj} \qquad j = 1,2,3 \tag{2}$$

It is assumed that the supply and demand have continuous functions, are very sensitive to the changes in price (high price elasticity of demand and supply) and so they vary in time. For the rates of demand, supply and inventory, we have Eqs. (3) to (6) as follows:

$$s_i(t) = \frac{dS_i(t)}{dt} = \dot{S}_i(t) \tag{3}$$

$$d_j(t) = \frac{dD_j(t)}{dt} = \dot{D}_j(t) \tag{4}$$

$$i_A(t) = \frac{dI_A(t)}{dt} = \dot{I}_A(t) \tag{5}$$

$$i_B(t) = \frac{dI_B(t)}{dt} = \dot{I}_B(t) \tag{6}$$

The inventory level for each type of ore, that determines the required stockpile capacity of the coal terminal, is calculated, using Eq. (7) and Eq. (8):

$$\frac{dI_A(t)}{dt} = \sum_{i=1}^{3} p_i \frac{dS_i(t)}{dt} - \sum_{j=1}^{3} q_j \frac{dD_j(t)}{dt} \tag{7}$$

$$\frac{dI_B(t)}{dt} = \sum_{i=1}^{3} (1-p_i) \frac{dS_i(t)}{dt} - \sum_{j=1}^{3} (1-q_j) \frac{dD_j(t)}{dt} \tag{8}$$

Eq. (7) and Eq. (8) are considered to be the governing equations, which determine the inventory level for ore types A and B, respectively. The total required capacity for the mine terminal can be determined from the inventory level behavior of each ore type.

According to Eqs. (7) and (8), in order to determine the stockpile capacity for each ore type, two groups of input data to the problem that have effect on the problem solution are important; (1) the supply and demand functions and (2) the proportions; p_i and q_j.

For the supply and demand functions, two types of functions are considered, representing various typical families of functions; (1) polynomial functions for supply and demand, as it is assumed in many relaxed versions of inventory management models (special case: linear functions), and (2) oscillatory functions, which represent the seasonal behavior of supply and demand in the mining industry. The combination of these function families are considered as well.

The proportions, p_i and q_j, are practically determined from the operational considerations, such as the available machinery for production and processing of each ore type the grades. In this project, it is assumed that the proportions are not constrained by the operational issues; instead, they should be determined in a way to minimize the overall inventory at the coal terminal. In order to consider all of the assumptions and provide a means to assist the decision making process, two scenarios are considered.

3. Proposed scenarios

Since in practice, two types of supply and demand functions are more common, which are oscillatory and polynomial functions, two scenarios are considered in this project. In the first scenario, all six coal mines and steel manufacturers are assumed to have periodic oscillatory supply and demand functions. In the second scenario, a combination of oscillatory and polynomial functions is considered for the supply and demand functions. In each of these two cases, a full range of values for all p_i and q_j proportions is tested, in order to find the best proportion of ore types "A" and "B" to be assigned to each plant which minimizes the maximum total inventory level as the required stockpile capacity of the coal terminal.

3.1. Scenario 1: oscillatory functions

In the first scenario, it is assumed that all of coal mines (S_1, S_2 and S_3) have oscillatory supply function. On the other hand, all of steel manufacturers (D_1, D_2 and D_3) have oscillatory demand functions as well. The SIMULINK model of the first scenario is illustrated in Fig. 2. Specifically, the supply and demand functions are presented through Eq. (9) to Eq. (14).

$$S_1 = 200\cos(0.25t) \quad (9)$$

$$S_2 = 20\cos(0.15t) \quad (10)$$

$$S_3 = 300\cos(0.1t) \quad (11)$$

$$D_1 = 15\cos(0.15t) \quad (12)$$

$$D_2 = 20\sin(0.35t) \quad (13)$$

$$D_3 = 500\cos(0.05t) \quad (14)$$

In this model, it is assumed that the manufacturing plants may ask penalty from the coal terminal when receive a load. This may happen due to the bad quality of ore that is received, or other reasons that are mentioned in their contracts with the coal terminal head office, e.g. the market

demand for the ore types. This phenomenon is translated as a negative demand rate in the model. Thus, the demand functions may oscillate or take a negative value for polynomial functions. The same scenario might happen vice versa about the coal mines, when their supply rate becomes negative.

According to Eq. (7) and Eq. (8), the proportions p_i and q_j are required to build the governing equations. In this scenario, all possible combinations for proportions p_i and q_j are considered in the range of 0.2 to 1 with the increments of 0.2. This has resulted in 15625 runs $[(1/0.2)^6]$. The simulations are performed from t=0 to t=100.

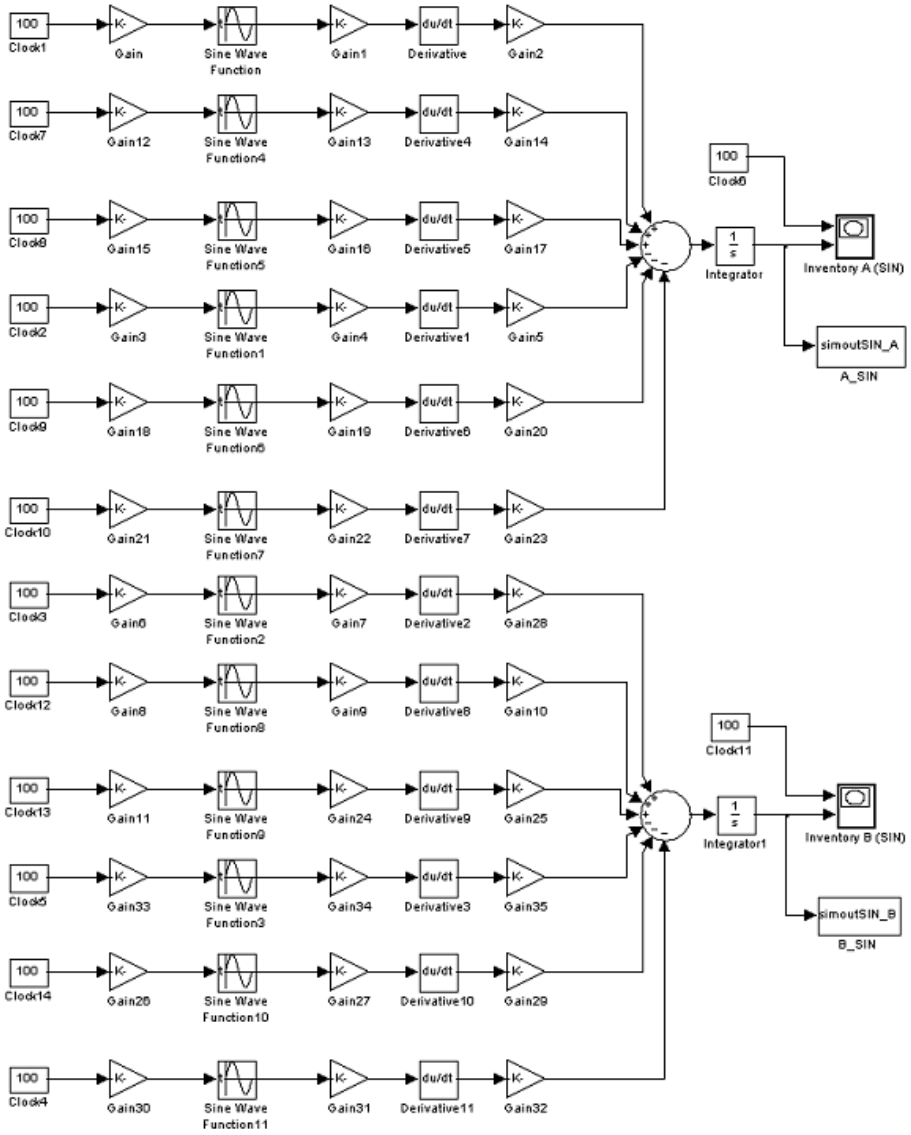

Fig. 2. SIMULINK model for the first scenario.

The sets of proportions that minimize and maximize the inventory of ore types “A” and “B” separately are reported in Table 1. The total inventory at the stockyard, “A+B”, and the corresponding proportions are reported in Table 1 as well. The inventory resulting behaviors for ore types “A” and “B”, corresponding to the optimum set of proportions, are illustrated in Fig. 3 and Fig. 4, respectively. The trend for the total inventory at the stockyard is illustrated in Fig. 5.

Table 1. Simulation results (first scenario).

Ore type	coal terminal storage capacity (units)		Proportions					
			p_1	p_2	p_3	q_1	q_2	q_3
A (separately)	Min (among maxs)	**270.9**	0.2	1.0	0.2	0.2	0.2	0.2
	Max (among maxs)	**1392.2**	1.0	0.2	1.0	0.8	1.0	1.0
B (separately)	Min (among maxs)	**0.0**	1.0	1.0	1.0	1.0	1.0	1.0
	Max (among maxs)	**1181.7**	0.2	1.0	0.2	0.2	0.2	0.2
A+B	Min (maxs)	**1336.6**	**1.0**	**0.8**	**1.0**	**0.8**	**0.8**	**1.0**
	Max (among maxs)	**1549.3**	0.2	0.2	1.0	0.2	0.2	0.2

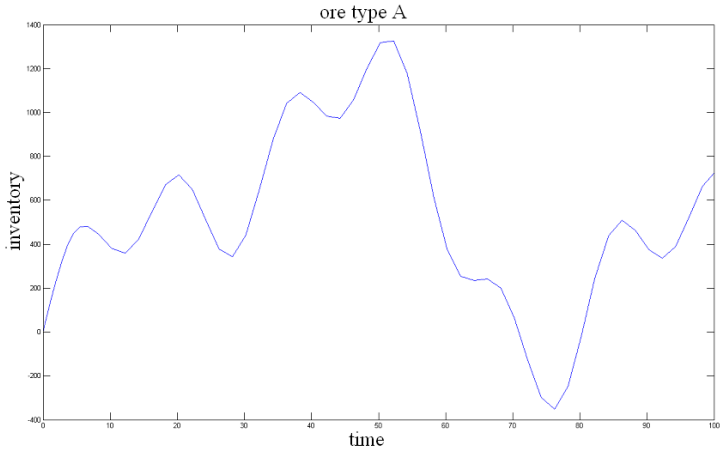

Fig. 3. Period number versus units of inventory for ore type A
The inventory of ore type "A" for [p1 p2 p3 q1 q2 q3]=(1.0 0.8 1.0 0.8 0.8 1.0).

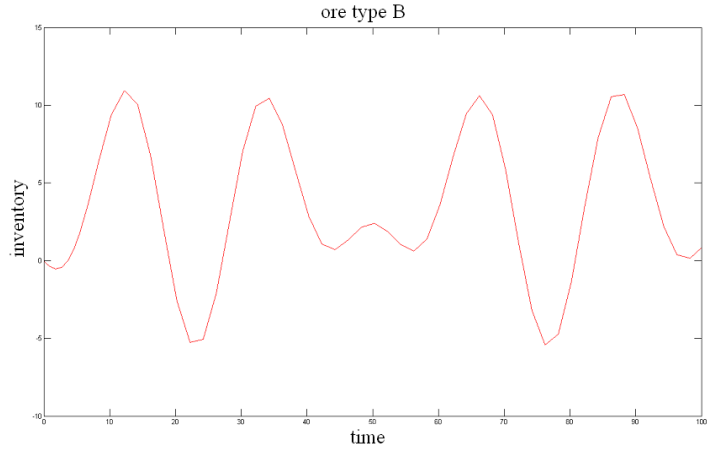

Fig. 4. Period number versus units of inventory for ore type B
The inventory for ore type "B" for [p1 p2 p3 q1 q2 q3]=(1.0 0.8 1.0 0.8 0.8 1.0).

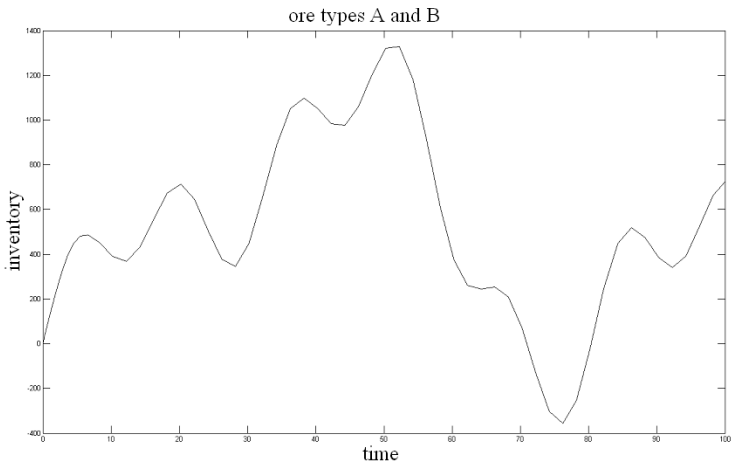

Fig. 5. Period number versus units of inventory for ore types A& B
Total inventory (A+B) for [p1 p2 p3 q1 q2 q3]=(1.0 0.8 1.0 0.8 0.8 1.0).

3.2. Scenario 2: combination of oscillatory and polynomial functions

In the second scenario, it is assumed that one of coal mines (S_2) has polynomial supply function. The other two mines, S_1 and S_3, follow the same oscillatory supply functions, as in the first scenario. On the other hand, two of steel manufacturing plants, D_1 and D_2, have polynomial demand functions. The other manufacturing plant (D_3) has the same oscillatory demand function, as in the first scenario. The SIMULINK model of the second scenario is illustrated in Fig. 6. Specifically, the supply and demand functions are presented by Eq. (15) to Eq. (20).

$$S_1 = 200\cos(0.25t) \quad (15)$$

$$S_2 = 0.00015x^3 - 0.06x^2 + 30x + 3 \quad (16)$$

$$S_3 = 300\cos(0.1t) \quad (17)$$

$$D_1 = 0.00015x^3 - 0.03x^2 + 0.4x + 2 \quad (18)$$

$$D_2 = 0.003x^3 - 0.002x^2 + 0.25x + 1 \quad (19)$$

$$D_3 = 500\cos(0.05t) \quad (20)$$

According to Eq. (7) and Eq.(8), the proportions p_i and q_j are required to build the governing equations. In this scenario, again all of possible combinations for proportions p_i and q_j are considered in the range of 0.2 to 1 with the increments of 0.2. It has resulted in 15625 runs $[(1/0.2)^6]$. The simulations are performed from t=0 to t=100, the same as the first scenario.

Same description about the negative values for supply and demand rates in the first scenario applies about the supply and demand rates in the second scenario.

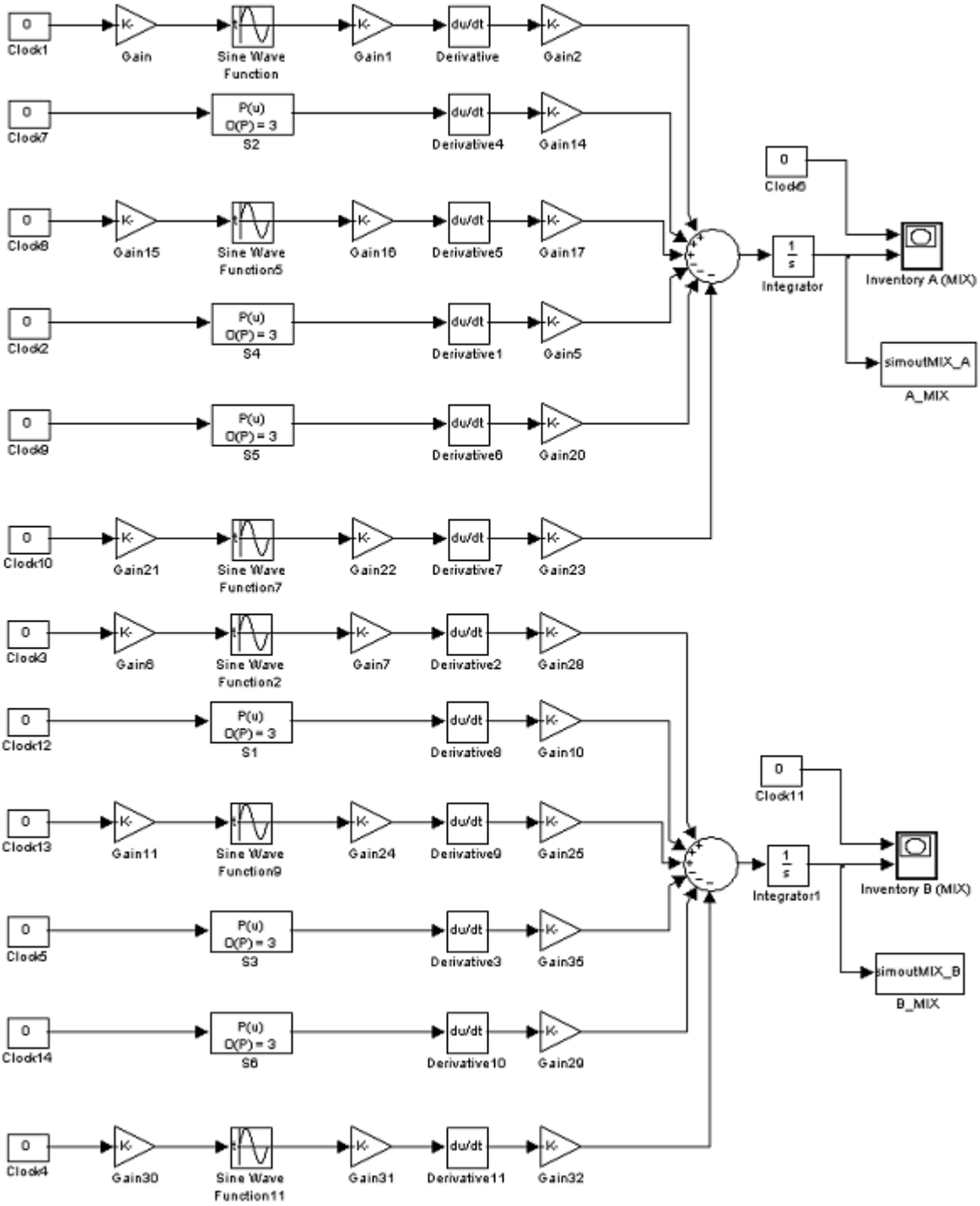

Fig. 6. SIMULINK model for the second scenario.

The sets of proportions that minimize and maximize the inventory of ore types “A” and “B” separately are reported in Table 2. The total inventory at the terminal, “A+B”, and the corresponding proportions are reported in Table 2 as well. The inventory resulting behaviors for ore types “A” and “B”, corresponding to the optimum set of proportions, are illustrated in Fig. 7 and Fig. 8, respectively. The trend for the total inventory at the terminal’s stockyard is illustrated in Fig. 9.

Table 2. Simulation results (second scenario).

Ore type	coal terminal storage capacity (units)		Proportions					
			p_1	p_2	p_3	q_1	q_2	q_3
A (separately)	Min (among maxs)	**257.8**	0.2	0.2	0.4	0.2	1.0	0.2
	Max (among maxs)	**2837.8**	1.0	1.0	1.0	1.0	0.2	1.0
B (separately)	Min (among maxs)	**0.0**	1.0	1.0	1.0	1.0	1.0	1.0
	Max (among maxs)	**2805.3**	0.2	0.2	0.2	0.2	1.0	0.2
A+B	Min (among maxs)	**2378.8**	**1.0**	**1.0**	**1.0**	**0.2**	**0.8**	**0.8**
	Max (among maxs)	**3491.4**	1.0	0.2	0.2	0.2	1.0	1.0

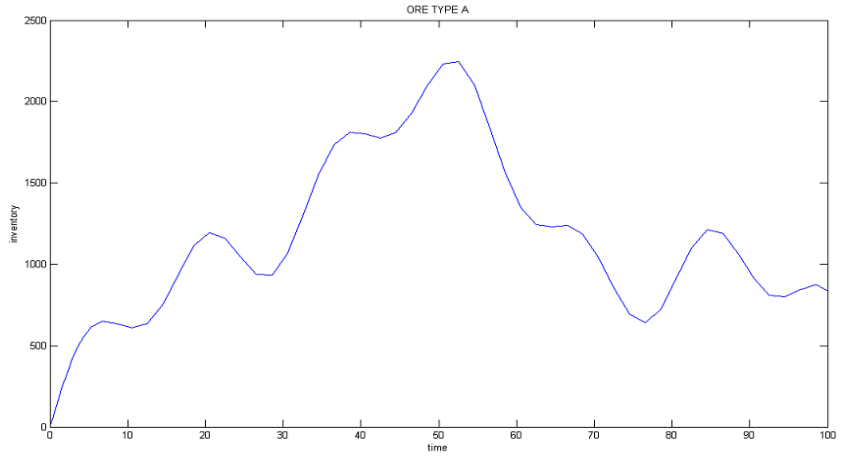

Fig. 7. Period number versus units of inventory for ore type A
The inventory of ore type "A" for [p1 p2 p3 q1 q2 q3]=(1.0 1.0 1.0 0.2 0.8 0.8).

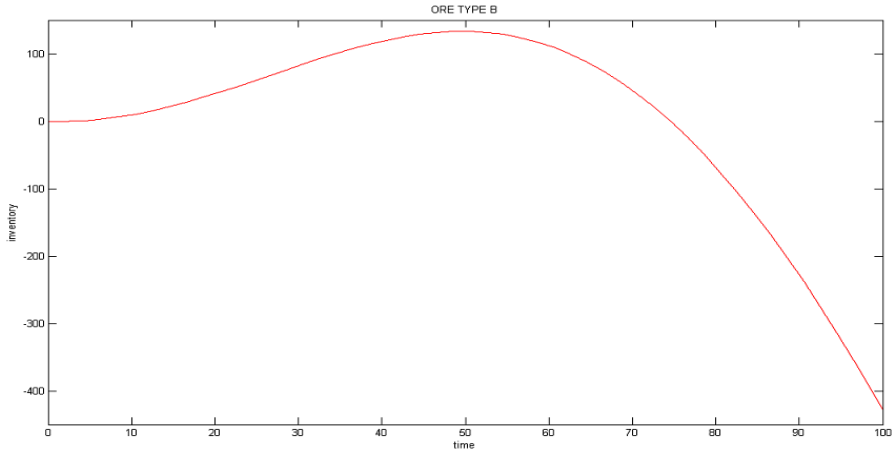

Fig. 8. Period number versus units of inventory for ore type B
The inventory of ore type "B" for [p1 p2 p3 q1 q2 q3]=(1.0 1.0 1.0 0.2 0.8 0.8).

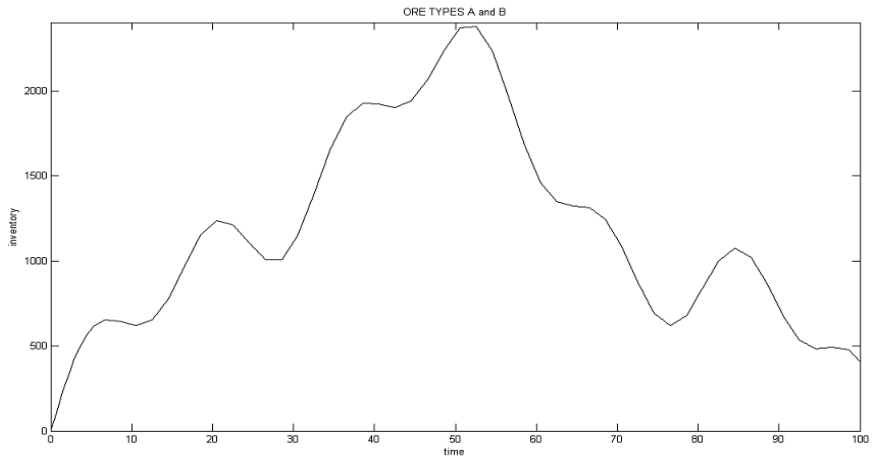

Fig. 9. Period number versus units of inventory for ore types A& B
Total inventory (A+B) for [p1 p2 p3 q1 q2 q3]=(1.0 1.0 1.0 0.2 0.8 0.8).

4. Conclusion

In general, two types of supply and demand functions are among the important patterns in the mining industry, the polynomial and the oscillatory functions. Accordingly in this paper, two scenarios are proposed, each considering different combination of polynomial and oscillatory supply and demand functions. In reality, there exist some minimum acceptance criteria for the ore, specified in contracts between coal mines, coal terminal and manufacturing plants. It may happen that the conditions have not been met in a specific load. In such cases, proper penalty applies to one contract side. To cover such real conditions, i.e. the penalties, it is assumed that negative supply and demand rates are possible.

The goal of this simulation is to identify the optimal proportion of ore types “A” and “B” that each mine sends to the coal terminal, as well as the optimal proportion of ore types “A” and “B” that each steel manufacturer receives from the terminal, in a way that minimize the overall inventory in the terminal’s stockyard.

As the result of more than 15600 runs for the first scenario, the best proportions is determined to be $[p_1\ \ p_2\ \ p_3\ \ q_1\ \ q_2\ \ q_3]$ = (1.0 0.8 1.0 0.8 0.8 1.0), that results in a total inventory level of 1336.6 units, as the required stockyard capacity for the coal terminal. The same number of runs are executed for the second scenario and have resulted in $[p_1\ \ p_2\ \ p_3\ \ q_1\ \ q_2\ \ q_3]$ = (1.0 1.0 1.0 0.2 0.8 0.8) as the optimum proportions, that results in a total inventory level of 2378.8 units as the required stockyard capacity for the coal terminal.

In general, if the supply and demand functions follow the combination of polynomial and oscillatory patterns, it is recommended to consider the capacity of approximately 2380 units of inventory. On the other hand, if according to the production and processing conditions, all supply and demand functions show oscillatory patterns, the stockyard should have the capacity equal to approximately 1340 units.

5. Appendix

5.1. The MATLAB m.file for simulation loop

Note: the following m.file is for the second scenario. The m.file for the first scenario is the same, with different model name (MIX.mdl instead of SIN.mdl)

```
for p1=1:5
PQ(1,1)=0.2*p1
      for p2=1:5
      PQ(2,1)=0.2*p2
            for p3=1:5
            PQ(3,1)=0.2*p3
                  for q1=1:5
                  PQ(1,2)=0.2*q1
                        for q2=1:5
                        PQ(2,2)=0.2*q2
                              for q3=1:5
                              PQ(3,2)=0.2*q3
                              sim SIN.mdl
                               MAX_A(p1,p2,p3,q1,q2,q3)=max(simoutS
                               IN_A.signals.values)
                               MAX_B(p1,p2,p3,q1,q2,q3)=max(simoutS
                               IN_B.signals.values)
                              end
                        end
                  end
            end
      end
end
```

5.2. The MATLAB codes for plotting the results

Note: the following MATLAB codes are for the second scenario. The codes for the first scenario are the same, with different names. (simoutMIX instead of simoutSIN)

```
>> plot(tout,simoutSIN_A.signals.values,'b'), axis([0 100 -400 1400])
>> title('ORE TYPE A')
>> xlabel('time')
>> ylabel('inventory')
>> plot(tout,simoutSIN_B.signals.values,'r'), axis([0 100 -10 15])
>> title('ORE TYPE B')
>> xlabel('time')
>> ylabel('inventory')
>> plot(tout,simoutSIN_TOTAL,'k'), axis([0 100 -400 1400])
>> title('ORE TYPEs A and B')
>> xlabel('time')
>> ylabel('inventory')
```

6. References

[1] Balkhi, Z. T. and Benkherouf, L. (2004). An inventory model for deteriorating items with stock dependent and time-varying demands. *Computers & Operations Research*, *31*,(*2*), 223-240.

[2] Begum, R., Sahu, S.K. and Sahoo, R. R. (2009). An inventory model with exponential demand rate, finite production rate and shortages. *Journal of Scientific Research*, *1*,(3), 473-483.

[3] Bhunia, A. K. and Maiti, M. (1997). A deterministic inventory model with inventory level-dependent consumption rate for two warehouses. *Bulletin of the Calcutta Mathematical Society*, *89*,(2), 105-114.

[4] Chao, X., , and Chen, H., Zheng, S. (2008). Joint replenishment and pricing decisions in inventory systems with stochastically dependent supply capacity. *European Journal of Operational Research*, *191*, 142-155.

[5] Kar, S., , and Bhunia, A. K., Maiti, M. (2001). Deterministic inventory model with two levels of storage, a linear trend in demand and a fixed time horizon. *Computers & Operations Research*, *28*, 1315-1331.

[6] Liao, H. C., , and Tsai, C. H., Su, C.T. (2000). An inventory model with deteriorating items under inflation when a delay in payment is permissible. *International Journal of Production Economics*, *63*,(2), 207-214.

[7] Teng, J. T. (1996). A deterministic inventory replenishment model with a linear trend in demand. *Operations Research Letters*, *19*, 33-41.

[8] Urban, T. L. (1995). Inventory models with the demand rate dependent on stock and shortage levels. *International Journal of Production Economics*, *40*,(1), 21-28.

[9] Urban, T. L. (2005). Inventory models with inventory-level-dependent demand: A comprehensive review and unifying theory. *European Journal of Operational Research*, *162*, 792-804.